

# **Design, Synthesis & Biophysical Investigations of Ant-Pro Based Peptidomimetics**

Thesis Submitted to AcSIR For the Award of  
the Degree of  
**DOCTOR OF PHILOSOPHY**  
In  
Chemical Sciences



By  
**AMOL S. KOTMALE**  
10CC11J26015

Under the guidance of  
**Dr. P. R. Rajamohanan**  
and  
**Dr. G. J. Sanjayan**

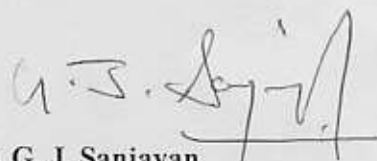
CSIR-National Chemical Laboratory, Pune

## CERTIFICATE

Certified that the work incorporated in the thesis entitled “**Design, Synthesis & Biophysical Investigations of Ant-Pro Based Peptidomimetics**”, submitted by **Mr. Amol S. Kotmale** to the Academy of Scientific and Innovative Research (AcSIR) in fulfillment of the requirements for the award of the degree of **Doctor of Philosophy**, embodies original research work carried out by the candidate under our supervision. We further certify that this work has not been submitted to any other university or institution in part or full for the award of any degree or diploma. Research materials obtained from other sources has been duly acknowledged in the thesis. Any text, illustration, table etc., used in the thesis from other sources, have been duly cited and acknowledged.



**Dr. P R Rajamohanan**  
(Research Guide)



**Dr. G. J. Sanjayan**  
(Research Co-Guide)



**Amol S. Kotmale**  
(Research Student)

Date: 22 June 2017  
Place: Pune

## CANDIDATE'S STATEMENT

I hereby declare that the thesis entitled "**Design, Synthesis & Biophysical Investigations of Ant-Pro Based Peptidomimetics**" submitted for the Degree of Doctor of Philosophy in Chemical Sciences to the Academy of Scientific and Innovative Research (AcSIR) has not been submitted by me to any other university or institution. This work has been carried out at Central NMR Facility and Division of Organic Chemistry, CSIR-National Chemical Laboratory, Pune under the supervision of Dr. P. R. Rajamohanan (Research Guide) and Dr. G. J. Sanjayan (Research Co-Guide).

Date: 22/06/2017



**Amol Suresh Kotmale**  
(Research Student)

*Dedicated to my family*



## ***Acknowledgement***

*First and foremost I am indebted to my **parents** who have always supported under all circumstances and believing me.*

*It is my privilege to express my gratitude to my research supervisors **Dr. P. R. Rajamohanam** and **Dr. G. J. Sanjayan** for the guidance, suitable suggestions and support during the course of my Ph.D. work. They taught me each and every aspect of research, from working table to formulation of ideas to presentation of results. I'm deeply thankful to them for introducing me to this fascinating area of science, which I enjoyed learning profoundly.*

*I would like to thank my DAC member **Dr. T. G. Ajithkumar**, **Dr. A. T. Biju**, **Dr. K. Kulkarni**, **Dr. C. G. Suresh**, for their guidance, timely advice and support in all matters.*

*I am also thankful to **Dr. Pradeep K. Tripathi**, Head of the Organic Chemistry Division, and **Dr. Ashwinikumar Nangia**, Director, for providing the infrastructure to work in this prestigious research institute.*

*I thank **Dr. Rajesh Gonade** for solving the single crystal X-ray structures. Special thanks to **Dr. Rupesh Gawade**, **Debha**, **Shridhar**, **Samir** and **Ektha** for their help in solving crystal structures.*

*My sincere thank to **Dr. Shantakumari**, **Dr. B. Senthilkumar** and **Dr. V. K. Gumaste** for their help in performing mass analyses. I thank to **Dr. Sushma Gaikwad**, **Dr. K. B. Sonawane**, **Mrs. S. S Kunte** and **Mr. Revan Katte** for help in HPLC analysis.*

*I thank to **Dr. S. Ganapthy** **Dr. S. Ravindranathan**, **Dr. Uday Kiran**, for their valuable guidance in understanding of NMR spectroscopy. I take this opportunity to express my heartfelt gratitude to my teachers **Dr. B. P. Bandagar**, **Dr. H. V. Chavan**, **Dr. Padwal**, **Dr. A. H. Manikshette**, **Prof. Battin**, **Dr. A. Shaikh** for their motivation and encouragement who helped me to learn basics of chemistry starting from school days to M. Sc studies.*

*I would like to thank my past and present labmates **Dr. Arup**, **Dr. Ramesh**, **Dr. Gowri**, **Dr. Sangram**, **Dr. Roshna**, **Dr. Vijaydas**, **Dr. Tukaram**, **Dr. Ganesh**, **Dr. Chaitanya**, **Vijay**, **Dr. Sanjeev**, **Dr. Sachin**, **R. Suresh**, **M. Suresh**, **Dr. Shiva**,*

*Krishnaprasad, Rashid, Mahendra, Bibhishan, Mridul and all project trainees for their cheerful company, support and made the working atmosphere healthy.*

*I had strong bonding with my tablemates during lunch time Mr. Prashant Mane, Suhas Dev Sir, Umesh Katamkar and Sachin Kate, I thank all of them for their brotherly love.*

*I would like to thank my past and present labmates Dr. Eldho, Hilda, Dr. Deepak Patil, Dr. Sumesh, Dr. Anny, Dr. Rupali, Dr. Bindu, Dr. Anjali, Shrikant, Snehal, Mayur, Dinesh, Pramod, Kavya, Minakshi, and Varsha from NMR lab.*

*Special thanks to our beloved cook Mrs. Dhagale mausi for providing excellent food during my stay in Sutarwadi, I also thanks to all my roommates especially Shahaji, Shivaji, Uttam, Sandip, Pravin, Samadhan, Nitin, Sachin, Manoj, Dilip, Parshuram, Krishna and Dhiraj for their constant supports.*

*I owe my deepest gratitude to my grandfather, grandmother, parents, uncle, aunty, brother Sunil, sister Ujwala and wife Sharmila for their care, constant encouragement, support and timely advice during my studies. Without their support, my ambition to pursue my research in NCL can be hardly realized.*

*I thank UGC, New Delhi, for the financial support.*

*Finally, I would like to thank all those who have contributed to the successful realization of this dissertation as well as expressing my apology that I could not mention personally one by one.*

*This chain of my gratitude only is completed if I would thank the Almighty.*

***Amol S. Kotmale***

## Table of Contents

Abbreviations.....	I
Abstract.....	II
General remarks.....	VII
NMR Experimental Conditions.....	VIII
List of publications.....	IX

### Chapter 1

#### *Synthesis & conformational investigation of “Ant-Pro” incorporated Gramicidin S and Avellanin mimics*

1.1 Introduction.....	3
1.1.1 Secondary structure elements in the peptides and proteins.....	4
1.1.2 Reverse turn mimics.....	5
1.1.3 Reverse turn mimics containing unnatural amino acid residues.....	6
1.1.4 Importance of foldamer based mimics.....	8
1.1.5 Reverse turn mimics for peptide therapeutics.....	9
1.1.6 Gramicidin S .....	9
1.1.7 Gramicidin S Mimics.....	10
1.1.8 Avellanin.....	13
1.2 Objective of the present work.....	13
1.3 Design strategy.....	13
1.4 Synthesis.....	15
1.5 Conformational Analyses.....	18

1.5.1 Single crystal X-ray diffraction studies.....	18
1.5.2 NMR studies.....	18
1.5.2.1 Variable Temperature Studies of 1.....	19
1.5.2.2 Variable Temperature Studies of 2.....	20
1.5.2.3 ROESY and CD spectra analysis of 1.....	21
1.5.2.4 MD Simulation study of 1.....	21
1.5.2.5 2D ROESY, CD analysis and MD Simulation of 2.....	22
1.6 Antibacterial studies of 1 and 2.....	23
1.7 Attempts for syntheses of cyclic <sup>L</sup> Pro analogs 15 and 17.....	23
1.7.1 Comparative CD studies of linear peptides 8, 9, 15 and 16.....	24
1.8 Conclusions.....	24
1.9 Experimental Section.....	25
1.10 References and notes.....	65

## Chapter 2

### *Design, synthesis & conformational investigation of Ant-Pro urea based foldamers*

2.1 Introduction.....	71
2.1.1 Reverse turn, $\beta$ -hairpin and $\beta$ -Sheet.....	71
2.1.2 Urea based templates for parallel $\beta$ -sheet structures.....	73
2.2 Objective and design strategy .....	74



<b>2.3 Synthesis</b> .....	75
<b>2.4 Results and discussion</b> .....	78
<b>2.4.1 Crystal structure analysis</b> .....	78
<b>2.4.2 NMR Study</b> .....	78
<b>2.4.2.1 Variable temperature studies of 1-4</b> .....	79
<b>2.4.2.2 DMSO-<i>d</i><sub>6</sub> titration studies of 1-4</b> .....	79
<b>2.4.2.3: NOESY/ROESY analysis and MD simulated structures</b> .....	79
<b>2.4.3 Solution state conformational investigation of 5 and 6</b> .....	81
<b>2.5 Conclusions</b> .....	82
<b>2.6 Experimental Section</b> .....	83
<b>2.7 References and notes</b> .....	122

## Chapter 3

### Part A

#### *Self assembly in designed $\beta$ -lactam antibiotics*

<b>3.1 Introduction</b> .....	127
<b>3.1.1 <math>\beta</math>-lactam antibiotics</b> .....	127
<b>3.1.2 Mode of action</b> .....	127
<b>3.1.3 Catagories of Beta-lactam antibiotics</b> .....	128
<b>3.1.4 Resistance</b> .....	129
<b>3.1.5 Ureidopenicillins</b> .....	129
<b>3.1.7 Ureidopyrimidones</b> .....	130
<b>3.1.8 Tautomeric and dimeric forms of ureidopyrimidinones</b> .....	130

<b>3.2 Objective of present work.....</b>	<b>131</b>
<b>3.3 Design strategy.....</b>	<b>131</b>
<b>3.4 Synthesis.....</b>	<b>131</b>
<b>3.5 Result and Discussion.....</b>	<b>132</b>
<b>3.6 Antibacterial studies.....</b>	<b>134</b>
<b>3.7 Conclusions.....</b>	<b>134</b>
<b>3.8 Experimental Section.....</b>	<b>134</b>
<b>3.9 References and Notes.....</b>	<b>142</b>

## **Chapter 3**

### **Part B**

#### *Unusual three residual cyclization in the AVPI peptides*

<b>3.10 Preamble.....</b>	<b>147</b>
<b>3.10.1 Apoptosis.....</b>	<b>147</b>
<b>3.10.2 Inhibitor of Apoptosis Proteins (IAP).....</b>	<b>148</b>
<b>3.10.3 Smac/DIABLO.....</b>	<b>148</b>
<b>3.10.4 Structure Activity Relationship of Smac mimetics.....</b>	<b>149</b>
<b>3.10.5 Smac mimetics and their binding affinities to XIAP protein.....</b>	<b>150</b>
<b>3.10.6 Examples of Smac mimetics which are in clinical trial.....</b>	<b>152</b>
<b>3.11 Objective of the present work.....</b>	<b>152</b>
<b>3.12 Design and strategy.....</b>	<b>153</b>
<b>3.13 Syntheses.....</b>	<b>153</b>
<b>3.14 Conclusions.....</b>	<b>155</b>
<b>3.15 Experimental Section.....</b>	<b>155</b>
<b>3.16 References and Notes.....</b>	<b>176</b>

## Chapter 4

### *Detailed NMR studies of Zipper peptides*

<b>4.1 Introduction.....</b>	<b>181</b>
<b>4.1.1 Structure Determination.....</b>	<b>181</b>
<b>4.1.2 One dimensional NMR spectroscopy .....</b>	<b>181</b>
<b>4.1.3 Two dimensional NMR spectroscopy.....</b>	<b>182</b>
<b>4.1.4 Types of 2D NMR spectroscopy.....</b>	<b>183</b>
<b>4.1.5 Correlation Spectroscopy.....</b>	<b>184</b>
<b>4.1.7 Heteronuclear Correlation Spectroscopy.....</b>	<b>184</b>
<b>4.1.6 Nuclear Overhauser Effect Spectroscopy (NOESY).....</b>	<b>185</b>
<b>4.1.7 Rotating-frame Overhauser Spectroscopy (ROESY).....</b>	<b>185</b>
<b>4.1.8 Molecular Weight and Maximum NOE/ ROE.....</b>	<b>185</b>
<b>4.1.9 Constraints Generation.....</b>	<b>186</b>
<b>4.1.10 Hydrogen bonding.....</b>	<b>188</b>
<b>4.1.11 Molecular Dynamics.....</b>	<b>188</b>
<b>4.1.12 Ant-Pro zipper peptides.....</b>	<b>189</b>
<b>4.2 Objective.....</b>	<b>190</b>
<b>4.3 NMR studies of 1, 2 and 3.....</b>	<b>191</b>
<b>4.3.1 Titration studies.....</b>	<b>191</b>
<b>4.3.2 Temperature variation study .....</b>	<b>193</b>
<b>4.3.3 H/D exchange studies study in Methanol-<i>d</i><sub>4</sub>.....</b>	<b>194</b>
<b>4.3.4 2D NOESY/ ROESY analysis.....</b>	<b>196</b>
<b>4.4 MD simulation studies of 2 and 3 .....</b>	<b>200</b>
<b>4.5 Conclusion of NMR studies of 1, 2 and 3.....</b>	<b>201</b>
<b>4.6 NMR studies of 4 and 5.....</b>	<b>202</b>
<b>4.6.1 Titration studies.....</b>	<b>202</b>

<b>4.6.2 H/D exchange studies study in Methanol-<i>d</i><sub>4</sub></b> .....	203
<b>4.6.3 2D NOESY analysis</b> .....	204
<b>4.7 MD simulation studies of 4 and 5</b> .....	205
<b>4.8 Conclusions</b> .....	206
<b>4.9 Experimental section</b> .....	207
<b>4.10 References and Notes</b> .....	228
<b>Erratum</b> .....	230

## Abbreviations

<b>A</b>			
Å	Ångström	HPLC	Spectrometry High-Pressure Liquid Chromatography
$\alpha$	Alpha	<b>K</b>	
ACN	Acetonitrile	$K_{dim}$	Dimerization constant
AcOH	Acetic acid	$K_{taut}$	Tautomeric constant
AcOEt	Ethyl acetate	<b>L</b>	
Aib	$\alpha$ -amino isobutyric acid	Leu	Leucine
Ala	Alanine	LCMS	Liquid chromatography– mass spectrometry
Ant	Anthranilic acid	<b>M</b>	
<b>B</b>		m	Multiplet (NMR)
$\beta$	beta	Me	Methyl
Boc	tert-Butyloxycarbonyl	MHz	Megahertz
<b>C</b>		mp	Melting point
Calcd	Calculated	MS	Mass spectrometry
CDCl <sub>3</sub>	Chloroform- <i>d</i>	ms	millisecond
COSY	Correlated spectroscopy	<b>N</b>	
Cbz	Benzyl carbamate	NOESY	Nuclear Overhauser Effect Spectroscopy
<b>D</b>		<b>O</b>	
d	doublet (NMR)	Orn	Ornithine
$\delta$	Chemical shift (NMR)	<b>P</b>	
DBU	1,8-Diazabicycloundec-7- ene	Piv	Pivaloyl
DCM	Dichloromethane	Pd/C	palladium 10 % on activated carbon
DMF	Dimethylformamide	Pro	Proline
DIPEA	N,N- Diisopropylethylamine	Pet ether	Petroleum ether
DMSO	Dimethyl sulfoxide	<b>R</b>	
DMAP	4-Dimethylaminopyridine	r.f.	Radio frequency
<b>E</b>		<b>S</b>	
ESI	Electron spray ionization	s	Singlet (NMR)
EDC	1-Ethyl-3(3-dimethylamino Propyl) carbodiimide	S	second
<b>G</b>		<b>T</b>	
$\gamma$	Gamma	t	Triplet (NMR)
Gly	Glycine	TFA	Trifluoroacetic acid
<b>H</b>		TEA	Triethyl amine
H-bond	Hydrogen bond	THF	Tetrahydrofuran
HMBC	Heteronuclear Multiple Bond Correlation	TOCSY	Total Correlation Spectroscopy
HBTU	O-benzotriazol-1-yl-N,N, N',N'-tetramethyluronium hexafluorophosphate	$\tau$	Tau
HOBt	1-Hydroxybenzotriazole	<b>V</b>	
HSQC	Hetero Nuclear Single Quantum Coherence	Val	Valine
Hz	Hertz	$\omega$	Omega
HRMS	High Resolution Mass		

## ABSTRACT

Name of the Candidate	<b>Amol Suresh Kotmale</b>
Research Supervisors	<b>Dr. P. R. Rajamohanam and Dr. G. J. Sanjayan</b>
Title of the Ph. D. thesis	<b>Design, synthesis &amp; biophysical investigations of <i>Ant-Pro</i> based peptidomimetics</b>

**Preamble:** Synthetic peptide analogues are now widely recognized as important lead compounds, both for the development of new materials and also for the generation of therapeutic agents. Our focus in the area of peptidomimetics is directed towards determination of structural conformation and biological activity of molecules resulting from incorporation of a known robust synthetic structural motif in selected oligopeptides such as gramicidin S, avellanin,  $\beta$ -lactam antibiotics like ampicillin, amoxicillin & cefalexine etc. Ultimately, we aim to attain tailor-made peptidomimetic building blocks with desired secondary structure.

**Contents:** This thesis is divided into four chapters. The first chapter describes the synthesis and investigation on the conformational preferences of “Ant-Pro” C9 turn motif incorporated gramicidin S and avellanin.<sup>1</sup> The second chapter discusses about design of “Ant-Pro urea” based foldamers, which exhibit C9 and C11 bifurcated hydrogen bonding.<sup>2</sup> Chapter three is divided into two parts; first part deals with synthesis of novel self-assembling system containing  $\beta$  lactam moiety. The second part of this chapter describes the unusual cyclization of the anticancer tetrapeptide AVPI. Fourth chapter deals with investigations of conformational changes of zipper architecture peptides by using solution state NMR and MD simulation studies.

### **Chapter 1: Synthesis & conformational investigation of “Ant-Pro” incorporated gramicidin S mimic**

This chapter describes the synthesis of gramicidin S mimic (**GS-1**) and avellanin mimic (**2**), incorporated with conformationally constrained  $\beta$ -amino acid *i.e.* anthranilic acid (Ant) and D-Proline (<sup>D</sup>Pro) dipeptide unit (a well known pseudo  $\beta$  *i.e.* C9 turn motif).<sup>1</sup> The D-Phe and L-Pro dipeptide unit of natural gramicidin S

were replaced by a robust “Ant-Pro” motif, to improve its efficacy as an antimicrobial agent, while the truncated form of GS mimic was synthesized as one of avellanin analog (cyclic penta peptide). We have also investigated the conformational preferences of synthetic gramicidin S mimics as well as avellanin analog by solution-state NMR spectroscopy and MD simulation studies. We carried out extensive solution-state NMR experiments such as variable temperature studies, 2D COSY, TOCSY, NOESY/ROESY, HSQC & HMBC experiments to validate the pleated antiparallel  $\beta$ -sheet conformation of synthetic GS mimic, while the truncated form disturbs the  $\beta$ -sheet conformation. Antibacterial studies of synthetic gramicidin S mimic show equipotent activity similar to that of natural gramicidin S.

**Gramicidin S mimic: Cyclo(-Val-(D)Pro-Ant-leu-Orn-)<sub>2</sub>**

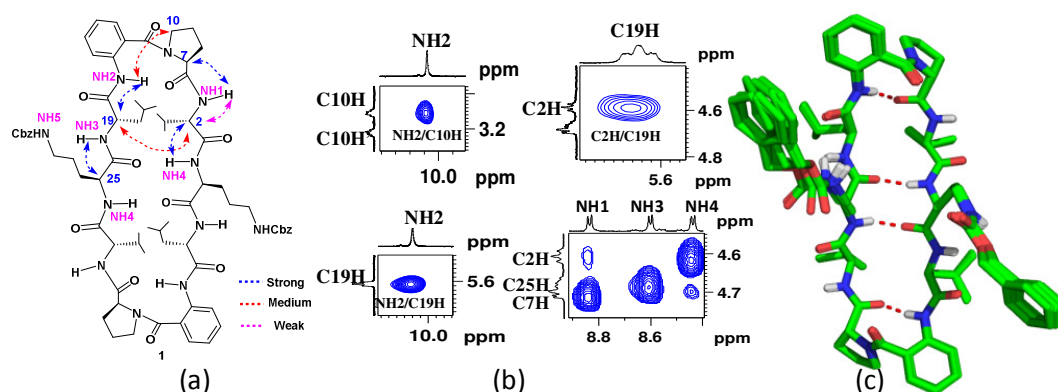


Figure 1.1a) Structure of modified gramicidin S containing “Ant-<sup>D</sup>pro” unit, b) characteristic nOe’s and c) 20 minimized MD simulated structures of synthetic gramicidin S mimic.

**Avellanin mimic: Cyclo(-Val-(D)Pro-Ant-leu-Orn-)**

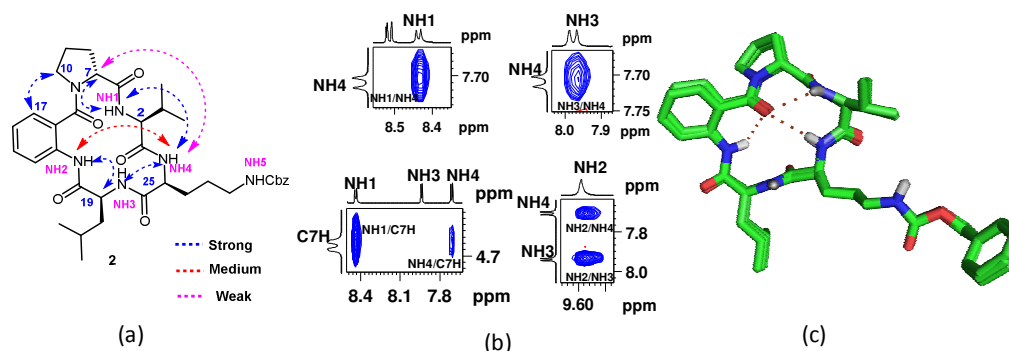
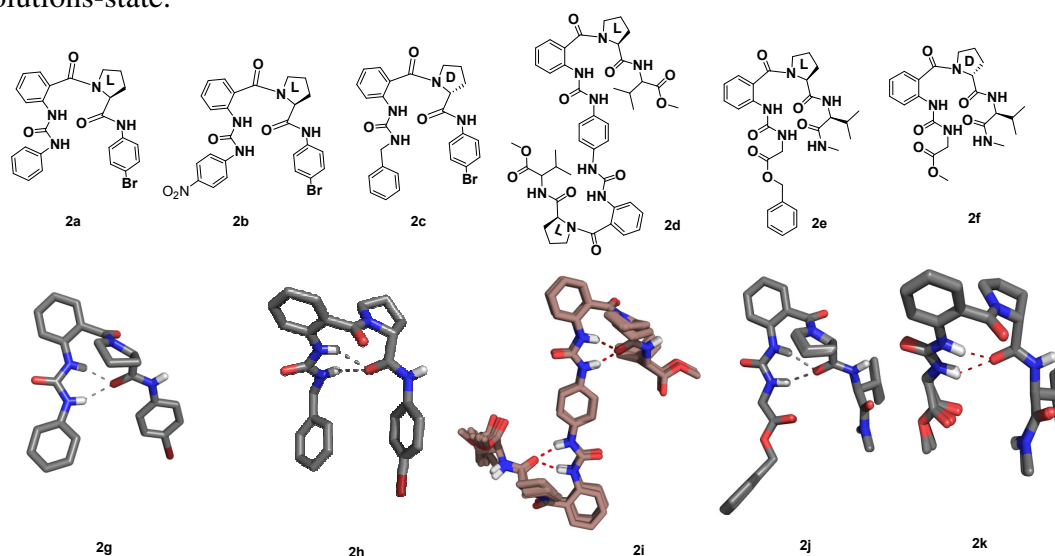


Figure 1.2a) Structure of modified avellanin analog containing “Ant-<sup>D</sup>pro” unit, b) characteristic nOe’s and c) 20 minimized MD simulated structures of synthetic avellanin analog.

## Chapter 2: Design, synthesis & conformational investigation of “Ant-Pro urea” based foldamers

The field of foldamer has helped chemists to create a large collection of structural assemblies and also understanding of the structural intricacy of biopolymers. In this chapter, we designed and investigated novel “Ant-Pro urea” based building blocks which exhibit C9 & C11 bifurcated hydrogen bond in solid as well as in solutions-state.



**Fig.2.** 2a-f) Molecular structures of “Ant-Pro urea” foldamers prepared; 2g 2h are crystal structures of 2a and 2c; 2i-k are MD simulated structures of 2d-f analogs respectively.

Analogs 2a-d were synthesized using corresponding isocyanates, while analog 2e & 2f were synthesized using active carbamate strategy *i.e* using *p*-nitrophenylchloroformate. All analogues were extensively analysed by solution-state NMR experiments and solid-state crystal structure.

## Chapter 3: Synthesis of novel antibacterial & anticancer agents

### Part A: Self assembly in designed $\beta$ -lactam antibiotics

This part deals with the design and synthesis of novel self-assembling systems incorporated with  $\beta$ -lactam antibiotics such as ampicillin, amoxicillin & cefalexine. The duplex formation of novel self-assembling system was confirmed by its characteristic 2M+H peak in ESI-HRMS..



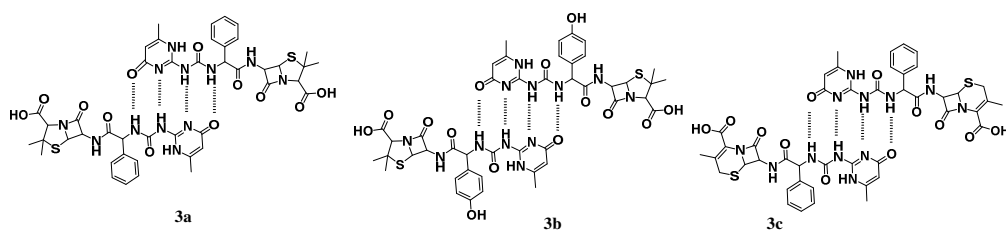


**Fig 3a-c** Molecular structures of self assemblies of ampicillin, amoxicillin & cefalexin respectively.

All synthetic ureidopenicillin analogues showed equipotent antibacterial activity with parent penicillins against tested bacteria.

### Part B: Unusual three residual cyclization in AVPI tetra peptides

The part B of this chapter describes structural studies on the tetrapeptide AVPI, which undergo unusual three residual cyclization when exposed to EDC.HCl. This unusual cyclization was confirmed by spectroscopic methods such as NMR and HRMS. Different analogues were synthesized to explore the unusual three residual cyclization.<sup>4</sup>

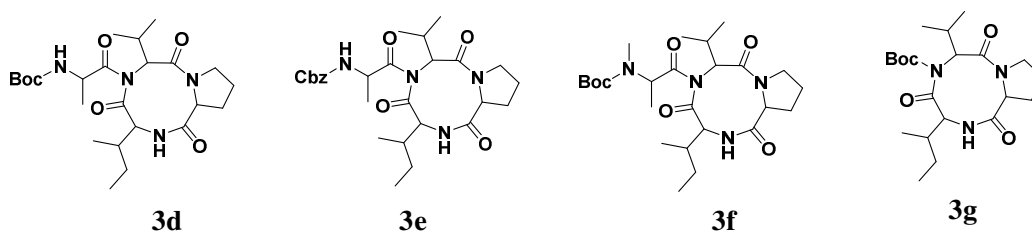


**Fig.3. 3d-g** Molecular structures of synthetic cyclic AVPI analogues

### Chapter 4: Detailed NMR studies of zipper peptides

In this chapter, a thorough investigation of the conformation of zipper peptides featuring long range terminal hydrogen bonding, pi-pi stacking, chirality modulated and terminal residue specificity, was carried out using solution-state NMR and MD simulation studies.

The part A of this chapter describes solution state conformational investigation of novel heterochiral hybrid peptides **4a** (n=2) and **4b** (n = 4) of the general sequence  $L\alpha\beta_n^D\alpha\beta_n$ , featuring proline (Pro, a constrained  $\alpha$ -amino acid) and anthranilic acid (Ant, a constrained  $\beta$ -amino acid) as building blocks exhibited a unique zipper like folded architecture featuring a large inter-residual hydrogen

bond spanning 26 and 42 atoms respectively (Figure 4f and 4g). While in the absence of terminal hydrogen bond donor (4c) folded architecture remains unchanged but fraying of the termini occurs (Figure 4h).

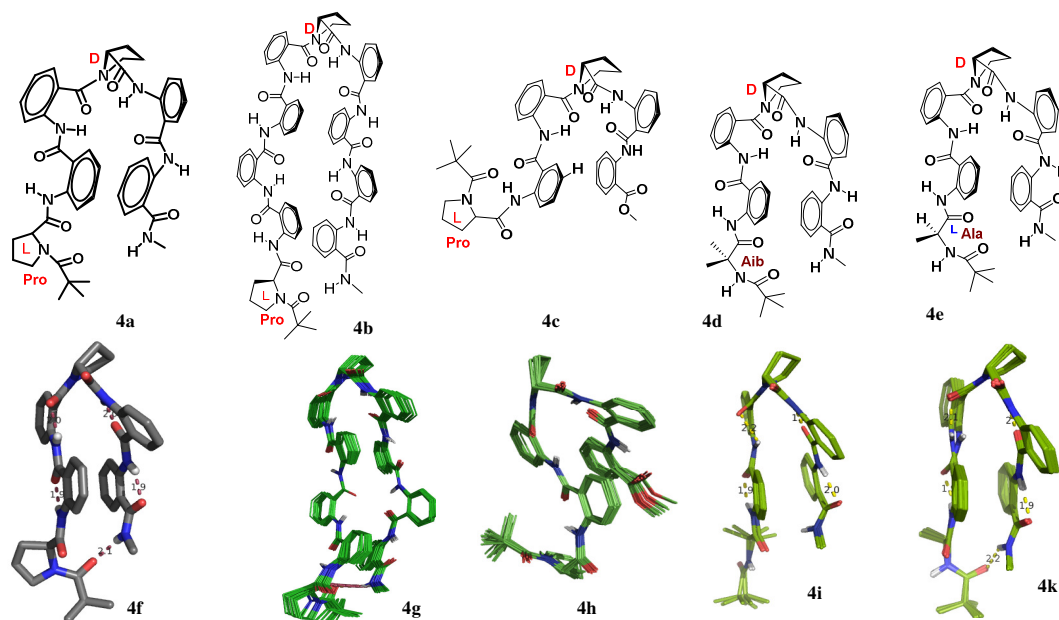


**Fig.4** 4a-e Molecular structures of zipper peptides, 4f is crystal structure of 4a whereas 4g-k are MD simulated structures 4b-k of zipper peptides.

The part B of this chapter describes the substitution alterations at the N-terminus of the zipper motif and their consequent influences on its structure and stability. The N-terminus Pro residue of the zipper motif was substituted with a flexible amino acid - alanine (4d) and a constrained acyclic amino acid - 2-aminoisobutyric acid (4e) to investigate the role of N-terminus proline in stabilizing Ant-Pro zipper motif, and their stabilities were assessed by employing solution-state NMR, MD simulation studies. The results suggested that the conformationally arrested residue like Pro fulfills all the requirements for the stable zipper architecture. Comparatively, substitutions at the N-terminus with Aib (Figure 4i) or <sup>L</sup>Ala (Figure 4k) support zipper architecture, but considerably weaker terminal H-bonding interaction indicated the interplay of dihedral constraints in stability of these unique structures.

### ***General Remarks***

- Unless otherwise stated, all the chemicals and reagents were obtained commercially.
- Required dry solvents and reagents were prepared using the standard procedures.
- All the reactions were monitored by thin layer chromatography (TLC) on precoated silica gel plates (Kieselgel 60F254, Merck) with UV, I<sub>2</sub> or ninhydrin solution as the developing reagents in the concerned cases.
- Column chromatographic purifications were done with 100-200 Mesh silica gel or with flash silica gel (230-400 mesh) in special cases.
- Melting points were determined on a Buchi Melting Point B-540 and are uncorrected.
- IR spectra were recorded in nujol or CHCl<sub>3</sub> using Shimadzu FTIR-8400 spectrophotometer.
- NMR spectra were recorded on AV 400 MHz, AV 500 MHz and AV 700 MHz Bruker NMR spectrometers. All chemical shifts are reported in  $\delta$  ppm downfield to TMS and peak multiplicities as singlet (s), doublet (d), quartet (q), broad (br), broad singlet (bs) and multiplet (m).
- MALDI-TOF/TOF mass spectrometric measurements were done on ABSCIEX TOF/TOF<sup>TM</sup> 5800 mass spectrometer and high-resolution mass spectrometric analyses (HRMS) were carried out using a Thermo Scientific Q-Exactive, Accela 1250 pump mass spectrometer.
- nOe-restrained molecular modeling studies were carried out using Insight II (97.0)/Discover program on a Silicon Graphics Octane workstation and MacroModel, Maestro version from Schrodinger software.
- Single crystal X-ray data were collected on a Bruker SMART APEX CCD Area diffractometer.
- Circular dichroism (CD) was performed using JASCO 2000 spectrometer and Spectra were smoothed and plotted using Origin Pro 6.0 software.

## ***NMR Experimental Conditions***

All the solution state NMR measurements were carried out on a Bruker AV 400 (resonating at 400.13, 100.62 MHz for  $^1\text{H}$  and  $^{13}\text{C}$ , respectively), AV500 (500.13, 125.75 MHz for  $^1\text{H}$  and  $^{13}\text{C}$  nuclei, respectively), AV 700 (resonating at 700.13, 176.04 MHz for  $^1\text{H}$ ,  $^{13}\text{C}$ , respectively). The measurements were performed in a standard 5 mm NMR tube and  $^1\text{H}$ , COSY, NOESY,  $^{13}\text{C}$ ,  $^{13}\text{C}$  DEPT,  $^1\text{H}$ - $^{13}\text{C}$  HSQC, and  $^1\text{H}$ - $^{13}\text{C}$  HMBC experiments were done on 5 mm broad band observe (BBO) gradient probe at ambient temperature ( $\sim 28^\circ\text{C}$ ). Gradient spectroscopic techniques were employed for all the 2D experiments. In general, 256 experiments ( $t_1$  increments) of 8 to 24 scans were used for COSY, TOCSY and NOESY measurements. The COSY and the  $^1\text{H}$ - $^{13}\text{C}$  HMBC spectra were collected in a magnitude mode while a phase sensitive (States-Time Proportionate Phase Increment (TPPI)) mode was used for HSQC and NOESY measurements. A mixing time of 1 s was employed for NOESY experiment. A pulse train of  $\sim 300$  ms, was used for ROESY spin lock. The number of scans used for each  $t_1$  increment for other 2D experiments were 16 to 24 for  $^1\text{H}$ - $^{13}\text{C}$  HSQC and  $^1\text{H}$ - $^{13}\text{C}$  HMBC.  $^1\text{H}$ - $^{13}\text{C}$  HMBC collected with polarization transfer delay corresponding to long-range coupling constant of 7 Hz whereas the corresponding. The HMBC spectra were acquired without proton decoupling during detection. Appropriate window functions, viz. sine squared bell with no phase shift for all magnitude modes and phase shifted (ssb = 2) sine-squared bell for phase sensitive mode were used for data processing. In general a 1 K $\times$ 1 K data matrix size was used for the 2-D experiments.  $^1\text{H}$  chemical shifts were referred to the residual solvent peak ( $\delta = 7.27$  ppm for  $\text{CHCl}_3$ ) and for  $^{13}\text{C}$  the central signals of the solvent multiplet is used for referencing ( $\delta = 77.0$  ppm for  $\text{CDCl}_3$ ).

## *List of Publications*

- 1) Multifaceted folding in a foldamer featuring highly cooperative folds, V. V. E. Ramesh , G. Priya, **A. S. Kotmale**, R. G. Gonnade, P. R. Rajamohanan, G. J. Sanjayan, *Chem. Commun.*, 2012, 48, 11205.
- 2) An unusual conformational similarity of two peptide folds featuring sulfonamide and carboxamide on the backbone, K. N Vijayadas, H.C Davis, **A. S. Kotmale**, R. L Gawade, Ve. G Puranik, P. R Rajamohanan, G. J Sanjayan, *Chem. Commun.*, 2012, 48, 9747
- 3) Helical folding in heterogeneous foldamers without inter-residual backbone hydrogen-bonding, G.Priya, **A.S Kotmale**, R. L Gawade, D. Mishra, S. Pal, V.G Puranik, P. R Rajamohanan, G. J Sanjayan, *Chem. Commun.*, 2012, 48, 8922.
- 4) Conformational modulation of Ant-Pro oligomers using chirality alteration of proline residues, S. S Kale, **A. S Kotmale**, A. Kumar Dutta, S. Pal, P. R Rajamohanan, G. J Sanjayan, *Org. Biomol. Chem.*, 2012, 10, 8426.
- 5) Orthanilic acid-promoted reverse turn formation in peptides, S, S Kale, G, Priya, **A. S Kotmale**, R. L Gawade, V. G Puranik, P. R Rajamohanan, G. J Sanjayan, *Chem. Commun.*, 2013, 49, 2222.
- 6) Ester vs. amide on folding: a case study with a 2-residue synthetic peptide, K. N Vijayadas, R. V Nair, R. L Gawade, **A. S Kotmale**, P. Prabhakaran, R. G Gonnade, V. G Puranik, P. R Rajamohanan, G. J Sanjayan, *Org. Biomol. Chem.*, 2013, 11, 8348-8356.
- 7) Carboxamide versus sulfonamide in peptide backbone folding: a case study with a hetero foldamer, V. VE Ramesh, S. S Kale, **A. S Kotmale**, R. L Gawade, V. G Puranik, P. R Rajamohanan, G. J Sanjayan, *Org. Lett.*, 2013, 15, 1504.
- 8) A Synthetic Zipper Peptide Motif Orchestrated via Co-operative Interplay of Hydrogen Bonding, Aromatic Stacking, and Backbone Chirality, R.V.

- Nair, S. Kheria, S. Rayavarapu, **A. S. Kotmale**, B. Jagadeesh, R. G. Gonnade, V. G. Puranik, P. R. Rajamohanam G. J. Sanjayan *J. Am. Chem. Soc.* 2013, *135*, 11477-11480.
- 9) Formation of a pseudo- $\beta$ -hairpin motif utilizing the Ant-Pro reverse turn: consequences of stereochemical reordering, R. V Nair, **A. S Kotmale**, S. A Dhokale, R. L Gawade, V. G Puranik, P. R Rajamohanam, G. J Sanjayan, *Org. Biomol. Chem.*, 2014, *12*, 774.
- 10) Probing the folding induction ability of orthanilic acid in peptides: some observations, A. Roy, **A. S Kotmale**, R. L Gawade, V. G Puranik, P. R Rajamohanam, G. J Sanjayan, *RSC Advances* 2014, *4*, 13018.
- 11) Conformational modulation of peptides using  $\beta$ -amino benzenesulfonic acid (S Ant), G. Priya, **A. S Kotmale**, D. Chakravarty, V. G Puranik, P. R. Rajamohanam, G. J. Sanjayan, *Org. Biomol. Chem.*, 2015, *13*, 2087.
- 12) Reversal of H-bonding direction by N-sulfonation in a synthetic reverse-turn peptide motif, K. N Vijayadas, **A. S Kotmale**, S. H Thorat, R. G Gonnade, R. V Nair, P. R Rajamohanam, G. J Sanjayan, *Org. Biomol. Chem.*, 2015, *13*, 3064.
- 13) The role of N-terminal proline in stabilizing the Ant-Pro zipper motif, S. Kheria, R. V. Nair, **A. S. Kotmale**, P. R. Rajamohanam, Gangadhar J. Sanjayan *New J. Chem.* 2015, *39*, 3327-3332.
- 14) Angiotensin II analogs comprised of Pro-Amb ( $\gamma$ -turn scaffold) as angiotensin II type 2 (AT 2) receptor agonists, G. S Jedhe, **A. S. Kotmale**, P. R Rajamohanam, S. Pasha, G. J Sanjayan, *Chem. Commun.*, 2016, *52*, 1645.
- 15) Residue dependent hydrogen-bonding preferences in orthanilic acid-based short peptide  $\beta$ -turn motifs, G. S Jedhe, K. N Vijayadas, **A. S. Kotmale**, E. Sangtani, D. R Shinde, R. G Gonnade, P. R Rajamohanam, G. J Sanjayan, *RSC Advances*, 2016, *6*, 35328.

- 16) 3-Aminothiophenecarboxylic acid (3-Atc)-induced folding in peptides, T. S Ingole, **A. S Kotmale**, R. L Gawade, R. G Gonnade, P. R Rajamohanam, G. J Sanjayan, *New J. Chem.*, 2016, 40, 9205.
- 17) Disruption of Native  $\beta$ -Turns: Consequence of Folding Competition between Native and Orphanic Acid Proline-Based Pseudo  $\beta$ -Turn, T.S Ingole, K. N Vijayadas, K. N Chaitanya, **A. S Kotmale**, R. L Gawade, R. G Gonnade, P. R Rajamohanam, G. J Sanjayan *Eur. J. Org. Chem.* 2016, 7, 1380.
- 18) Additive Mediated Syn-Anti Conformational Tuning at Nucleation to Capture Elusive Polymorphs: Remarkable Role of Extended  $\pi$ -Stacking Interactions in Driving the Self-Assembly, R.L Gawade, D. K Chakravarty, **A. S. Kotmale**, E. Sangtani, P. V Joshi, A. Ahmed, M. V Mane, S.a Das, K. Vanka, P. R Rajamohanam, V. G Puranik, R. G Gonnade, *Cryst. Growth Des.*, 2016, 16, 2416.
- 19) 'Triazine-based Highly Stable AADD-type Self-complementary Quadruple Hydrogen-bonded Systems Devoid of Prototropy', S. Kheria, S. Rayavarapu, **A. S. Kotmale**, R. G. Gonnade G.J. Sanjayan, *Chem. Eur. J.* 2017, 23, 783.
- 20) Three in One: Prototropy-free Highly Stable AADD-type Self-Complementary Quadruple Hydrogen-Bonded Molecular Duplexes with Built-in Fluorophore, S. Kheria, S. Rayavarapu, **A. S. Kotmale**, G. J. Sanjayan *Chem. Commun.* 2017, 53, 2689-2692.
- 21) Structural Insights into the Hydrogen-Bonding and Folding Pattern in Ant-Ant-Pro-Gly Tetrapeptides, S. B Baravkar, **A. S Kotmale**, S. R Shaikh, R. G Gonnade, G. J Sanjayan, *Eur. J. Org. Chem.* 2017, 20, 2944.
- 22) Coumarin-appended Stable Fluorescent Self-complementary Quadruple Hydrogen-bonded Molecular Duplexes, S. Kheria, S. Rayavarapu, **A. S. Kotmale**, D. R. Shinde, R. G. Gonnade, G. J. Sanjayan, *J. Org. Chem.*, Article ASAP.

23) Conformational studies of Ant-Pro motif-incorporated cyclic peptides such as gramicidin S and Avellanin, **A. S. Kotmale**, E. Sangtani, R. G. Gonnade, D. Sarkar, S. Burade, P. R. Rajamohanan, G. J. Sanjayan  
(*Manuscript under preparation*)



# *Chapter 1*

*Synthesis & conformational investigation of “Ant-Pro”  
incorporated Gramicidin S and Avellanin mimics*



## 1.1 Introduction#

Natural peptides and proteins are fundamental components of organism that carry out important biological and physiological functions. These proteins and natural polypeptides are mainly composed of twenty  $\alpha$ -amino acids and a few relatively rare amino acids. Different combinations and proper sequences of these amino acids lead to enormous structural diversity in the proteins. Protein structures are divided into four levels of polypeptide chain (Figure 1.1). The primary structure represents a linear array of amino acids (linear strand) held together by covalent bonds. The secondary structures are referred to conformations resulting from the primary sequences with well-defined geometry.<sup>1</sup> The common secondary structures are helices ( $\alpha$ -helix,  $3_{10}$ -helix and  $\pi$ -helix),  $\beta$ -sheets and turns. The tertiary structure is composed with well-defined spatial arrangement of many secondary structures like helices,  $\beta$ -sheet, turns and loops,<sup>2</sup> while the quaternary structure is the three-dimensional arrangement of multiple protein subunits or tertiary structures, comprising different peptide strands stabilized by non-covalent interactions.<sup>3</sup>

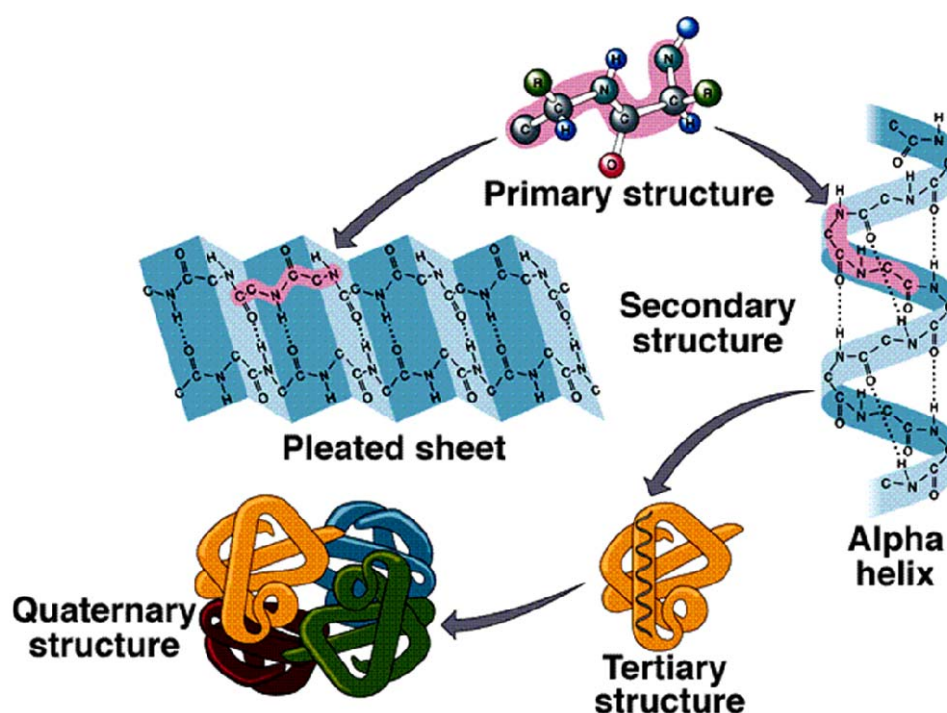


**Figure 1.1** Four levels of hierarchical organization in protein (Image source: internet)<sup>44</sup>

### 1.1.1 Secondary structure elements in the peptides and proteins

The backbone dihedral angles of  $\alpha$  amino acids ( $\psi$  and  $\phi$ ) play an essential role in determining the secondary structure of peptides. The distribution of dihedral angles given by the Ramachandran plot provides information about the possible secondary structures of the polypeptides.<sup>4</sup> The regular secondary structural elements of proteins are the following.

**$\alpha$ -helix:** This is most stable motif in the secondary structure of proteins and is a right hand-coiled or spiral conformation (helix) in which every backbone N-H is involved in hydrogen bonding with the backbone C=O group of the amino acid located three or four residues earlier along the protein sequence. It involves 13 member hydrogen bond rings and it is generally denoted as 3.6<sub>13</sub>-helix (the average number of residues per helical turn, with 13 atoms are involved in the ring formation).

**$\beta$ -sheet:** This is a common secondary structure motif of protein in which two polypeptide chains ( $\beta$ -strands) run alongside each other and are linked together by hydrogen bonds to form a  $\beta$ -sheet. Green fluorescent proteins and immunoglobulins are two proteins which contain predominantly  $\beta$ -sheet structures (Figure 1.2a). They are of two types; (a) parallel and (b) anti parallel. Parallel  $\beta$ -sheets are less prevalent and less stable where as anti-parallel  $\beta$ -sheets occur frequently and are highly stable.

**$\beta$ -hairpins:** The  $\beta$ -hairpin ( $\beta$ - $\beta$  unit or  $\beta$ -ribbon) is the simple protein structural motif involving two  $\beta$ -strands that look like a hairpin.

**Loops:** These are the connectors of two secondary structures which are often located at the surface of folded protein. Loops varying in length and shapes are important structural entity in biological recognition process.

**Turns:** Turns are regions in peptide chain where a chain reversal occurs.<sup>5-7</sup> They can be classified into  $\alpha$ ,  $\beta$ ,  $\gamma$ ,  $\pi$  etc.<sup>8</sup> and are represented by the following diagram (Figure 1.2b).

**$\gamma$ -turn:** If the carbonyl of first amino acid forms a 7-membered ring hydrogen bond with NH of third amino acid, then it is called a  $\gamma$ -turn.<sup>9-11</sup>

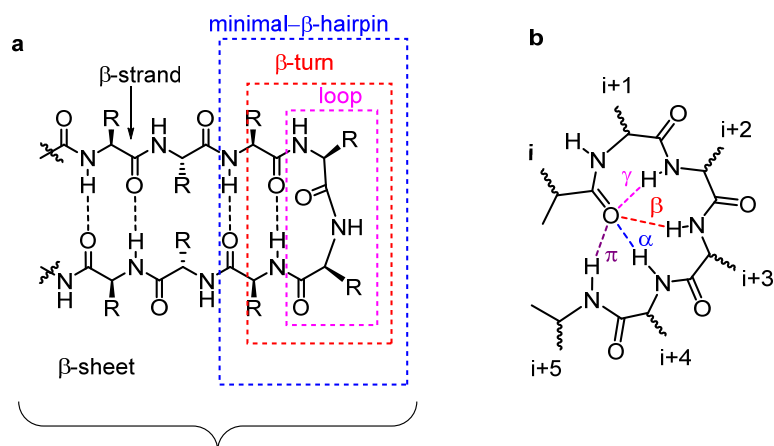


**Figure 1.2** Schematic representation of a typical  $\beta$ -hairpin secondary structure detailing the components of its structure:  $\beta$ -strand,  $\beta$ -turn, and loop (a); Different types of reverse turns (b).

**$\beta$ -turn:** The most common turn motif, where the carbonyl of first amino acid forms a 10-membered ring hydrogen bond with NH of fourth amino acid, is the  $\beta$ -turn.  $\beta$ -turns are found abundantly in biological systems<sup>12,13</sup> and are further classified into type-I, type-II (Figure 1.3) and so on, depending on their dihedral angle preferences ( $\psi$  and  $\phi$ ).

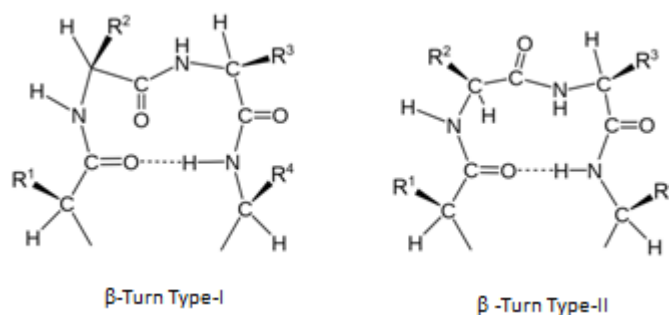


**Figure 1.3** Two types of  $\beta$ -turn

**$\alpha$ -turn:** Here, the carbonyl of first amino acid forms a 13-membered ring hydrogen bond with NH of fifth amino acid.<sup>14-16</sup>

**$\pi$ -turn:** A 16-membered ring hydrogen bonded ring formed between the carbonyl of first amino acid and the NH of sixth amino acid.

### 1.1.2 Reverse turn mimics

Reverse turns in proteins are the sites, where the polypeptide chain totally reverses on itself causing proteins to adopt a globular shape. Reverse turns exhibit multi-faceted functions in biological systems. For example, the  $\beta$ -turns, which act as recognition sites

for the initiation of complex metabolic, hematological, immunological, and endocrinological reactions.<sup>17</sup> Many of the synthetic three-dimensionally ordered reverse turn mimics although imitate the structural topology of natural bioactive peptides but, at the same time can interfere in the biological pathways of their natural analogs. The incorporation of reverse turn mimics into functional bioactive core increasingly ameliorate the understanding of interactions of small molecules with biological targets such as enzymes or receptors, besides tackling different ‘peptides as drugs’ related concerns. Rigidification of reverse turn can be accomplished by use of various backbone modifications or by making reverse turn mimics.

### **1.2.3 Reverse turn mimics containing unnatural amino acid residues**

To confine the reverse turn architecture, the easiest way is to incorporate torsionally constrained amino acids into the peptide backbone (Figure 1.4). The common examples include geminal constraints or constrained  $\alpha$ -amino acids, such as  $\alpha$ -amino butyric acid (Aib) (gem-dimethyl substituted amino acid)<sup>18</sup> and *N*-aminoproline (cyclically constrained).<sup>19</sup> Another significant category is insertion of modified *homo*-analogues i.e.  $\beta$ -amino acids like 2-aminocyclopropanecarboxylic acid (ACC),<sup>20</sup> 2-aminocyclopentanecarboxylic acid (ACPC),<sup>21</sup> 2-aminocyclohexanecarboxylic acid (ACHC),<sup>22</sup> and 2-aminobenzoic acid (anthranilic acid, Ant)<sup>23</sup> or  $\gamma$ -amino acids like nipecotic acid, a hetero-chiral dinipeptic acid segment promotes antiparallel sheet structure,<sup>24</sup> 1-aminomethylcyclohexanecarboxylic acid (gabapentin, Gpn), *etc.*<sup>25, 26, 27</sup>

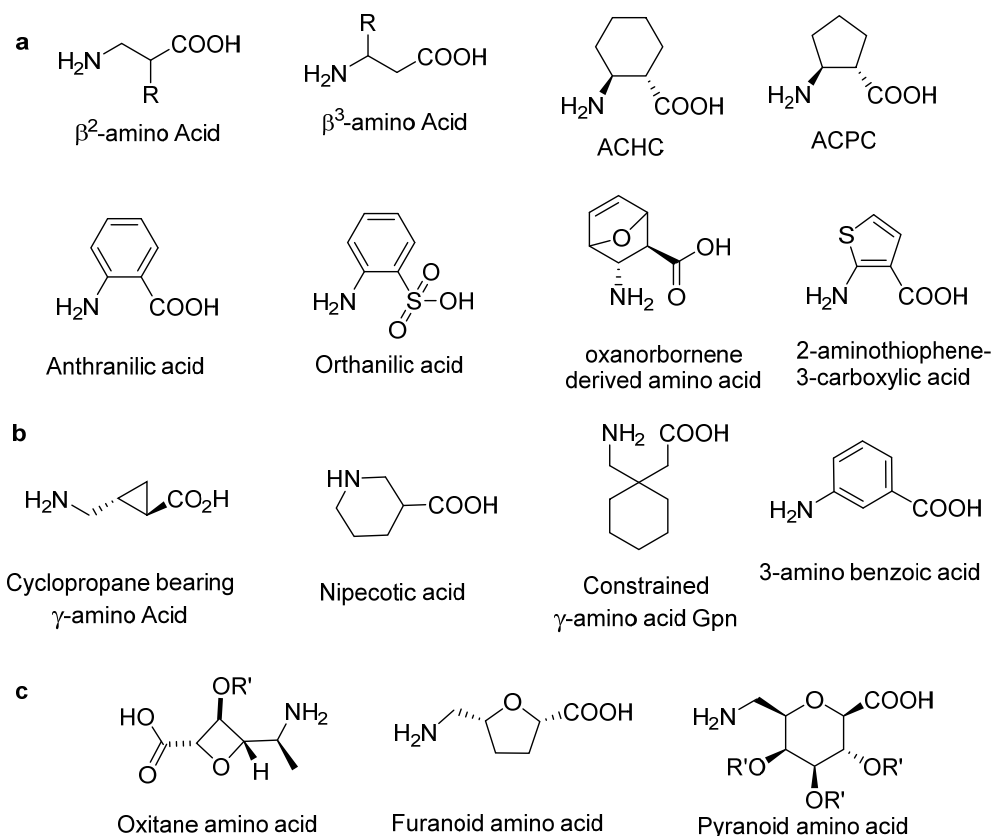


**Figure 1.4** Some examples of peptide building blocks: (a)  $\beta$ -amino acids, (b)  $\gamma$ -amino acids, and (c)  $\delta$ -amino acids.

The use of aliphatic-aromatic hybrid building block is a recent practise in the locale of heterogeneous peptide design. These hybrid building blocks offer the combined local conformational preferences of the  $\alpha$ -amino acid and rigidity of the conjoining aromatic residue.<sup>28</sup>

Another significant aliphatic-aromatic amino acid based reverse turn motif reported from our group is the anthranilic acid ( $\beta$ -amino acid) –proline ( $\alpha$ -amino acid) conjugated pseudo beta turn mimic (Figure 1.5).<sup>23</sup> The effect of the steric and dihedral angle constraints offered by proline on the anthranilic acid (Ant) residue evades the formation of much anticipated 6-membered H-bond (which causes the Ant repeats to adopt sheet structure<sup>29</sup>) to establish a 9-membered H-bond between Ant-NH and Pro-CO (Figure 1.5). Extensive studies confirmed that the proline and six-membered constrained ring structure of Ant are essential for the formation of pseudo- $\beta$ -turn structure.<sup>23</sup> Further analysis of the robustness of this motif when it incorporated in cyclic peptides will be discussed in this chapter.

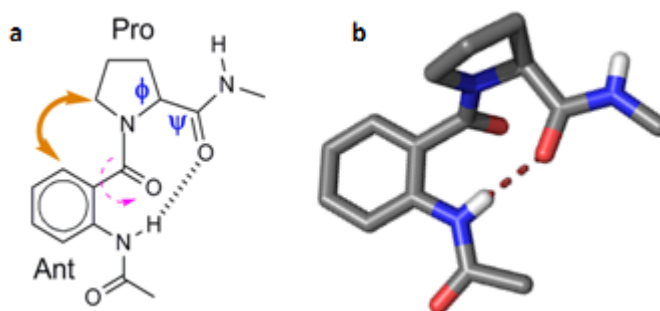


**Figure 1.5** Molecular structure and corresponding crystal structure of Ant-Pro motif.<sup>23</sup>

### 1.1.3 Importance of foldamer based mimics

Peptides face an inherent problem of large degree of conformational freedom rendering the biologically active conformations to be feebly populated in solution state. Also, they possess the tendency to form unintended hydrogen bonds, thus they face difficulties in crossing membranes leading to poor transportation into cells. However, the modified bioactive peptides are one of the most preferred drug candidates because of their high potency, specificity and biological & chemical diversity. They are better than the peptide based therapeutics which possess short half-life (prone to proteolysis), poor solubility or aggregate and cumbersome synthesis. Peptide-based drugs are biocompatible to greater extents with lesser toxicity, reaching the site of action after an easy administration with minimized drug-drug interactions and reduced accumulation in tissues. There has been great development in the area of peptide based drug research, with various technologies meant for improvement in their activity and bioavailability.

### 1.1.4 Application of foldamer-based reverse turn mimics

Foldamer-based mimics maintain stable three-dimensional compact architecture in both solid- and solution state. These robust turn mimics successfully retain the desired conformation for biological receptor recognition by enzymes or peptides. Besides medicinal relevance, it also has established its forte in organic asymmetric synthesis by providing the proper orientation and site selectivity over long distances meant to bring reactants closer or activate the functional groups.



### **1.1.5 Reverse turn mimics for peptide therapeutics**

Bioactive peptides are present in all forms of life and many physiological processes in living systems is an outcome of their interactions with the receptor molecules. Several peptides have been identified for carrying out specific functions. A few examples are angiotensin that causes vasoconstrictor effects, vasopressin that brings vasodilator effects, enkephalins and neurotensin that directs central nervous mechanisms like respiratory, cardiovascular, temperature pain and sensory controls *etc.* This knowledge significantly stimulated the development of peptide emulating drugs or structural analogs in form of their agonists (which mimic the parent peptide) and antagonists (that occupies peptide receptor) as they are non-toxic.

Reverse turns form an integral part in many antibiotics, toxins, antitoxins, ionophores, antimicrobial decapeptide sequences like gramicidin S and tyrocidines A-E, antibiotic viomycin and cyclic dodecadepsipeptide valinomycin, octapeptide amatoxins and the heptapeptide phallotoxins.

Many of these bioactive peptides possess turn structure at the site of molecular recognition. Even a small peptide can acquire the turn conformation, triggering physiological process through peptide-receptor interaction. Turn mimics are one of the most thoroughly investigated secondary structure mimics. These motifs are having implications in recognition of elements in structure-activity studies of the peptide hormones, angiotensin II, bradykinin, GnRH, somatostatin, gramicidin S, and many others.

#### **1.1.6 Gramicidin S:**

Gramicidin S (GS) is a cationic cyclic decapeptide (Cationic antibacterial peptides: CAP)<sup>30</sup> and has a structure of an anti-parallel beta-sheet conformation. Gramicidin S molecule is amphiphilic, with hydrophobic amino acids (D-Phe, Val, Leu side chains) and hydrophilic (charged) amino acid (L-Orn). GS exhibits strong antibiotic activity towards Gram- positive and Gram- negative and even several pathogenic fungi.<sup>31</sup> The mode of action of gramicidin S is by disruption of the lipid membrane and enhancement of permeability of the bacterial cytoplasmic membrane. Unfortunately, being hemolytic at even low concentrations, it cannot be administered internally, and hence it is used as topical medication.

### 1.1.7 Gramicidin S Mimics:

Structurally, gramicidin S is a C<sub>2</sub> symmetric cyclo (-Val-Orn-Leu-D-Phe-Pro-)2 antiparallel pleated  $\beta$ - sheet conformation with two D-Phe-Pro dipeptide units (type II'  $\beta$ -turn) at the loop region (Figure 1.6).<sup>32</sup> Native gramicidin S is a broadly utilized cyclic peptide scaffold for the study of the effects of turn inducers and peptide mimetics.<sup>33-42</sup>

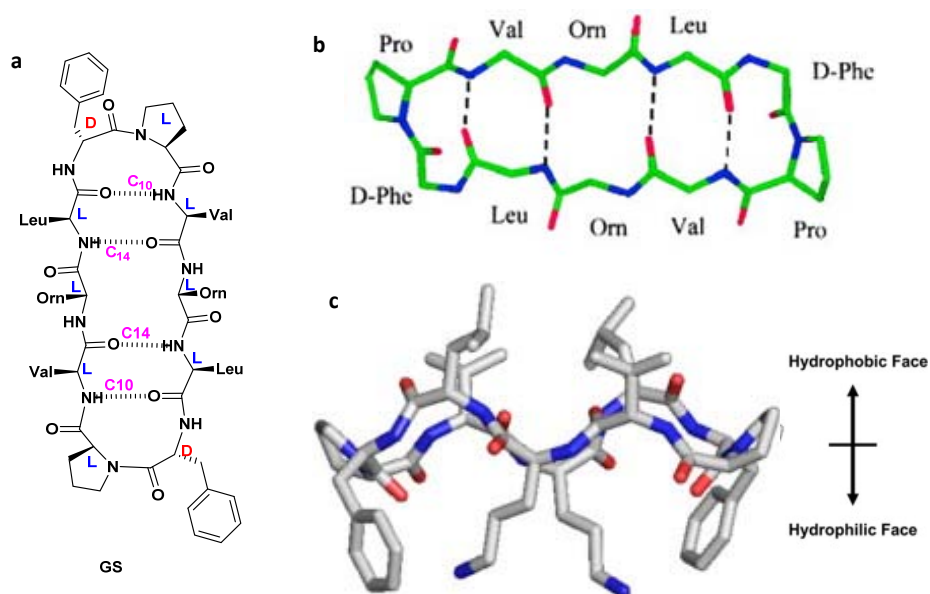


**Figure 1.6** a) Structure of native gramicidin S, b) Native gramicidin S with possible *intra* molecular hydrogen bonding (side chain hydrogens are omitted for clarity), c) Crystal structure of gramicidin S (horizontal view) where, hydrophobic and hydrophilic faces are in opposite direction.

Various groups have been working on incorporating turn mimics into GS. Peter Wipf & Co-worker introduced trisubstituted (E)-alkene to peptide bond as replacements in the loop region of GS (Figure.7).<sup>33</sup> Hruby and co-workers developed a bicyclic -leu-enkephalin analogue incorporating 4-phenyl indolizidinone.<sup>34</sup> Similarly, Jurzak and group used (2*S*,6*S*,8*S*)-indolidin-9-one amino ester as BTD.<sup>35</sup>

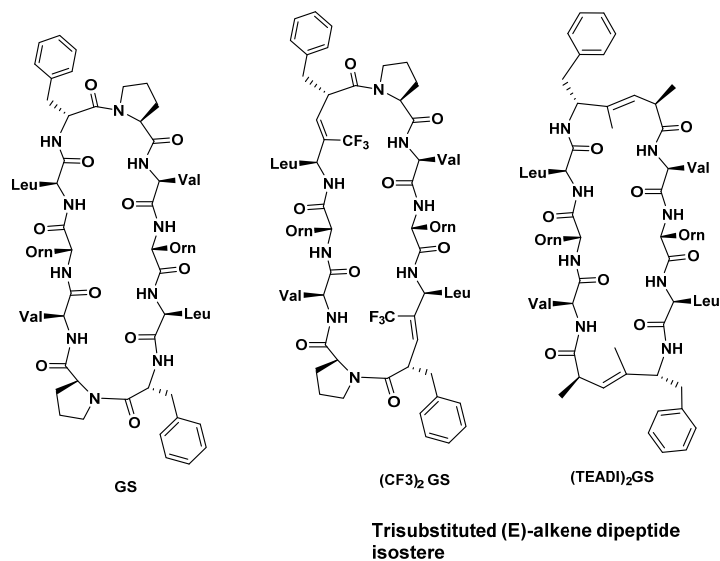


**Figure 1.7** Trisubstituted alkene  $\beta$ -turn mimic of Gramicidin S from P. Wipf *et al.*<sup>33</sup>

Sugar-based reverse turn mimetic has been shown to mimic GS structure (Figure 1.8).<sup>36</sup>

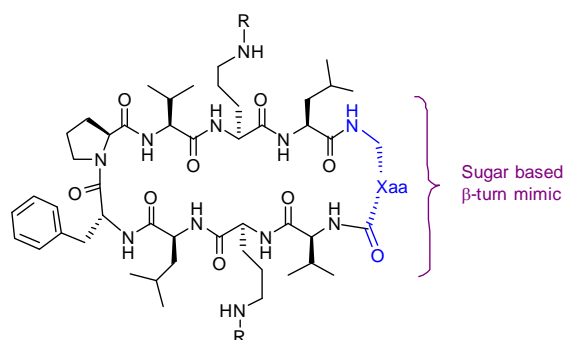


**Figure 1.8** Sugar based GS mimics designed by Overhand *et al.*<sup>36</sup>

Recently, T. K. Chakraborty and co-workers introduced tetrahydrofuran amino acid in the GS to improve biological profiles (figure 9).<sup>20</sup>

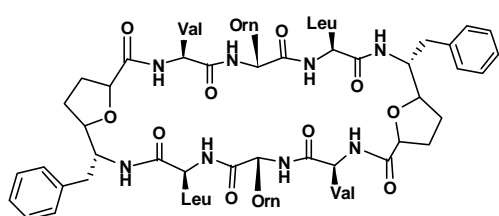


**Figure 1.9** Tetrahydrofuran amino acid  $\beta$ -turn region of Gramicidin S published by Chakraborty *et al.*<sup>37</sup>

Carlos Cativiela and his group showed that sequence inversion and phenylalanine surrogates (Figure 1.10) at the  $\beta$ -turn which enhances the antibiotic activity of gramicidin S.<sup>38</sup>

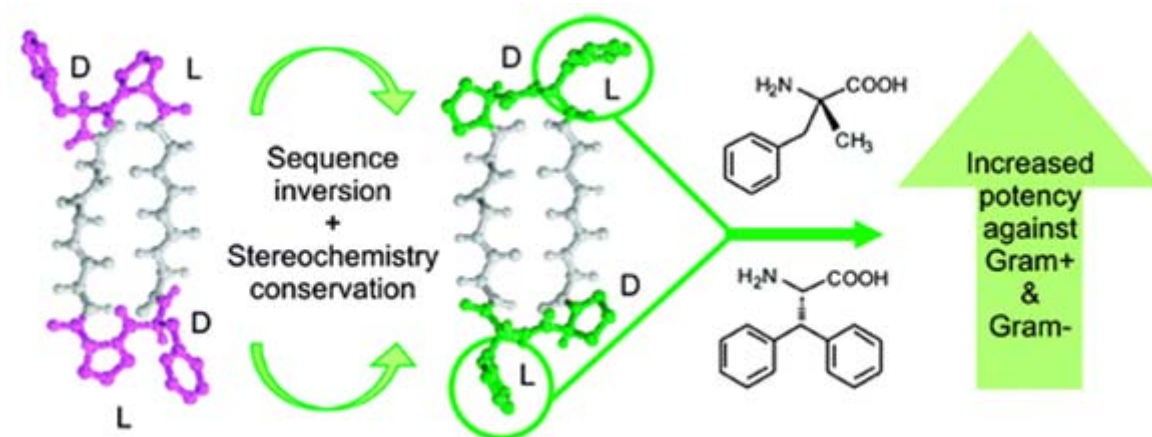


**Figure 1.10** Sequence inversion and phenylalanine surrogates in the GS taken from C. Cativiela and group.<sup>38</sup>

Thiazole-based  $\gamma$ -building block incorporated in GS (Figure 1.11) was studied by Ludovic T. Maillard and his group.<sup>39</sup>

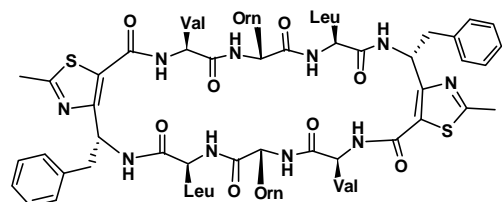


**Figure 1.11** Thiazole-based  $\gamma$ -building block in the  $\beta$ -turn region of Gramicidin S published by Maillard *et al.*<sup>39</sup>

Komarov, and co-workers reported a biological active peptidomimetic containing a reversibly photoisomerizable diarylethene scaffold (Figure 1.12) which is effectively controlled by ultraviolet/visible light and illustrated it by a bacterial lawn treated with the modified gramicidin S and illuminated through a mask.<sup>40</sup>

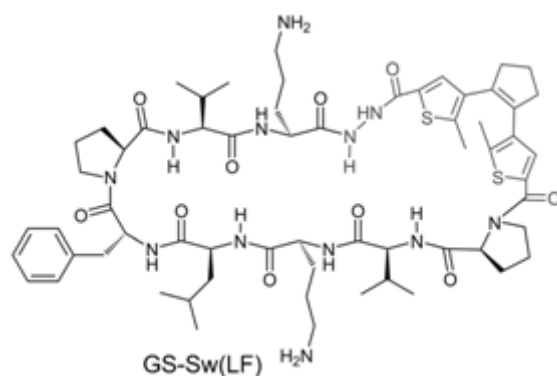


**Figure 1.12** Photoswitch gramicidine S by Komarov *et al.*<sup>40</sup>

### 1.1.8. Avellanin:

Avellanins are the fungal metabolites isolated from Hamigera family.<sup>41</sup> They are cyclic pentapeptides containing Ant-L-Pro dipeptide unit, as well as NMe-D-Phe and D-Ala residues (Figure 1.13).

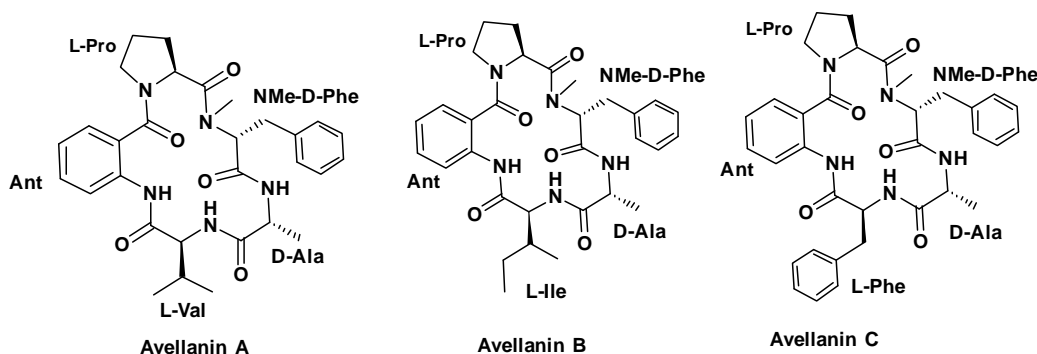


**Figure 1.13** Different types of avellanins and their structures.

Natural avellins differ in their structure at one residue. Avellanin A contains L-Val residue, Avellanin B contains L-Ile residue while Avellanin C contains L-Phe residue respectively. Avellanin C was inactive in antimicrobial or cytotoxic assay but displayed inhibitory effects on the quorum-sensing signalling in *Staphylococcus aureus*.<sup>42</sup>

## 1.2 Objective of the present work

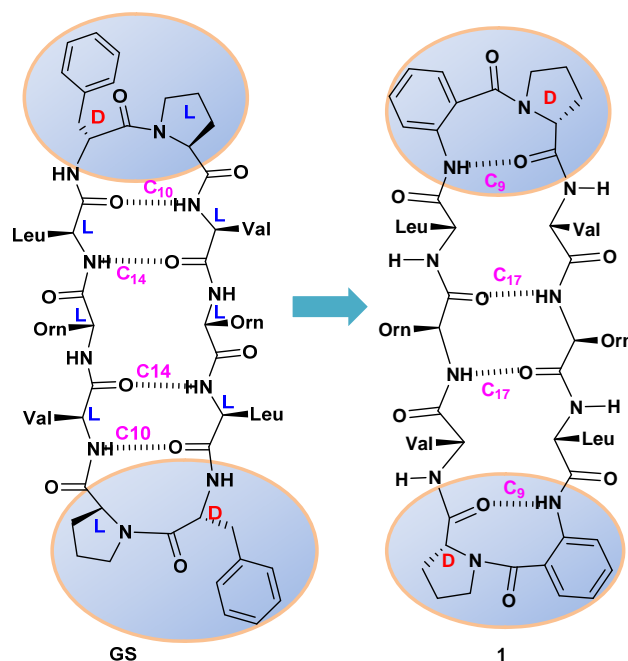
The aim of the studies reported in this chapter is to incorporate Ant-Pro (a robust C9-pseudo  $\beta$ -turn inducer) dipeptide unit<sup>23</sup> in natural cyclic peptides such as gramicidin S (GS) and avellanin. We also aim to investigate the conformation as well as to determine the bioactivity of synthetic mimics.

## 1.3 Design strategy

The synthesis and conformational investigation of gramicidin S (GS) analogues **1** (Figure 1.14a) containing Ant-Pro (a robust C9-pseudo  $\beta$ -turn) dipeptide unit<sup>23</sup> as a replacement of the two D-Phe-Pro  $\beta$ -turn regions of natural gramicidin S is described in this section. The cyclic, gramicidin S analogue assumed to adopt a  $\beta$ -sheet conformation featuring pseudo  $\beta$  reverse (C9) turn induced by the Ant-Pro and C17 type hydrogen bonding network between two ornithine residues. The altered turn region induces a similar antiparallel pleated  $\beta$ -sheet conformation as that of natural GS and the overall

geometry closely resembles GS. This GS mimic **1** is also shown to be antibacterial agent as active as the parent GS. We also aim to modify the Ant Pro based cyclic peptide i.e avellanin analogue **2** (Figure 1.14b) and investigate its conformation as well as its bioactivity.

a) Gramicidin S mimic



b) Avellanin mimic

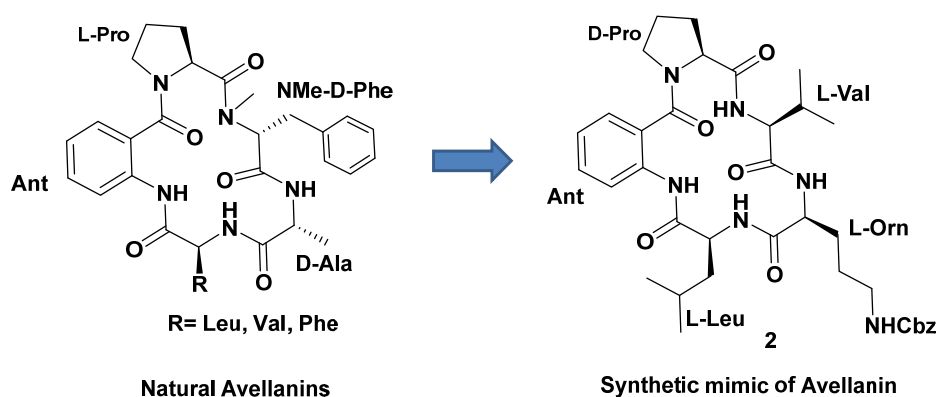


**Figure 1.14** Native cyclic peptides i.e gramicidin S and avellanin and designed modified analogues containing Ant-<sup>D</sup>Pro dipeptide unit.

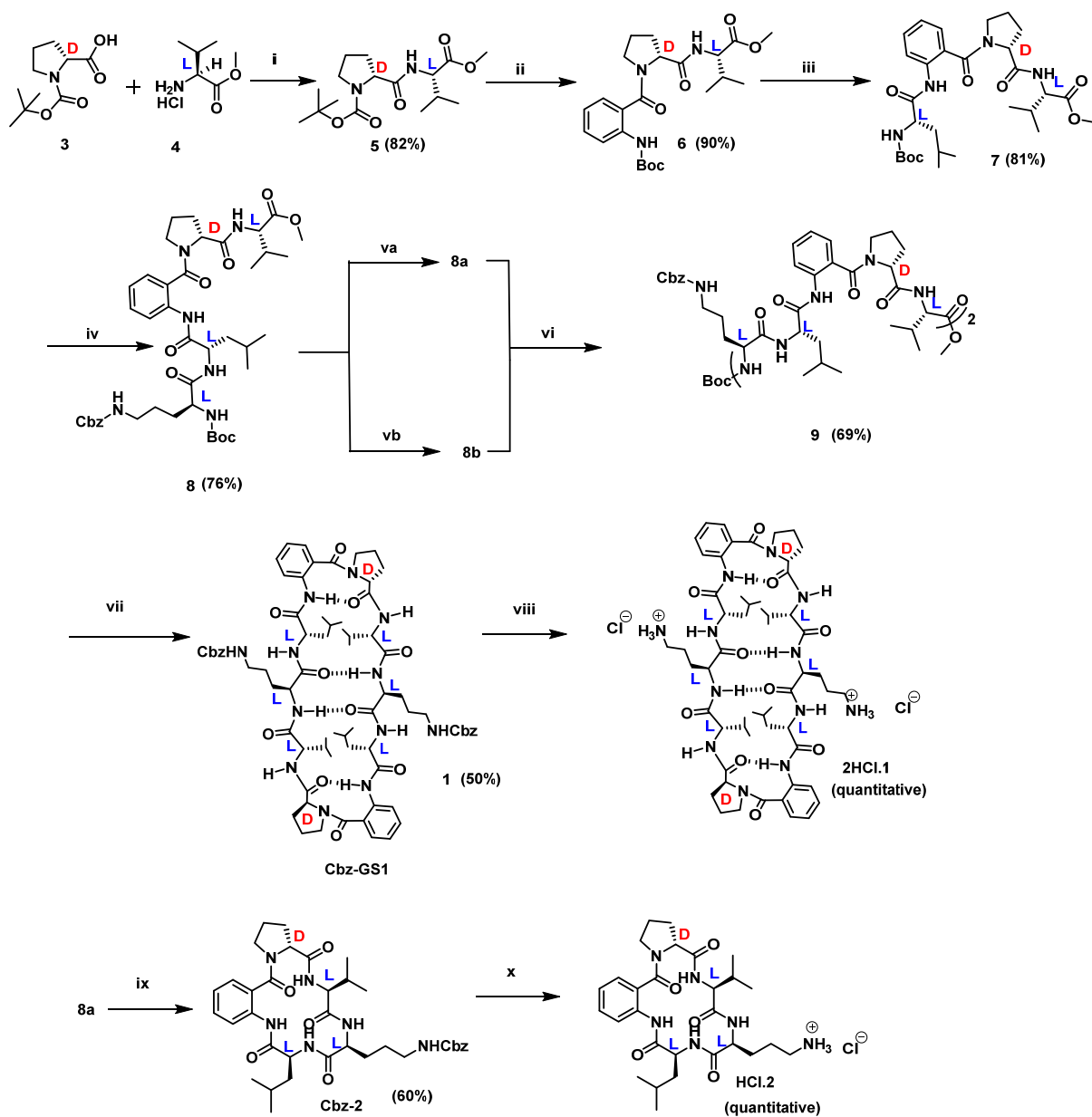
## 1.4 Synthesis

Synthesis of cyclic peptides **1** and **2** was done by solution phase coupling strategy using suitable coupling reagent and suitable solvent in each coupling reaction. Initially, HCl.<sup>L</sup>Val-OMe was coupled with Boc-<sup>D</sup>Pro-OH in the presence of EDC.HCl, DIEA, HOBt (cat.) in DCM to get dipeptide Boc-<sup>D</sup>Pro<sup>L</sup>Val-OMe (**5**). This dipeptide on deprotection with TFA:DCM resulted the TFA salt which was neutralized by sat. NaHCO<sub>3</sub> to get free amine, H-<sup>D</sup>Pro<sup>L</sup>Val-OMe. This free amine, H-<sup>D</sup>Pro<sup>L</sup>Val-OMe, was coupled with Boc-Ant-OH in presence of HBTU, DIEA in ACN to produce Boc-Ant-<sup>D</sup>Pro<sup>L</sup>Val-OMe (**6**). This tripeptide was deprotected and coupled with Boc-<sup>L</sup>Leu-OH in presence of EDC.HCl, HOBt (cat) in DCM to get Boc-<sup>L</sup>Leu-Ant-<sup>D</sup>Pro<sup>L</sup>Val-OMe (**7**). This tetrapeptide on deprotection and coupling with Boc(Z)-Orn-OH, in presence of HBTU, DIEA gave the pentapeptide Boc(Z)-Orn-<sup>L</sup>Leu-Ant-<sup>D</sup>Pro<sup>L</sup>Val-OMe (**8**). For the synthesis of **1**, we used segment strategy, in which one part is acid of pentapeptide i.e. Boc(Z)-Orn-<sup>L</sup>Leu-Ant-<sup>D</sup>Pro<sup>L</sup>Val-OH and other part was amine i.e. H-(Z)-Orn-<sup>L</sup>Leu-Ant-<sup>D</sup>Pro<sup>L</sup>Val-OMe. They were coupled in the presence of HBTU, DIEA in ACN to get the decapeptide i.e. Boc(Z)-Orn-<sup>L</sup>Leu-Ant-<sup>D</sup>Pro<sup>L</sup>Val-(Z)-Orn-<sup>L</sup>Leu-Ant-<sup>D</sup>Pro<sup>L</sup>Val-OMe (**9**). This decapeptide sequentially hydrolysed and deprotected to get TFA. H-(Z)-Orn-<sup>L</sup>Leu-Ant-<sup>D</sup>Pro<sup>L</sup>Val-(Z)-Orn-<sup>L</sup>Leu-Ant-<sup>D</sup>Pro<sup>L</sup>Val-OH. This on cyclization by using HBTU, DIEA in DCM yielded to Cbz-**1**. All NMR characterization was done at this stage and finally, Cbz-**1** was deprotected using H<sub>2</sub>, Pd/C, 10 mol% in 0.02M HCl solution and the HCl.**1**, salt was directly used for bio-activity.

For synthesis of compound **2**, Boc(Z)-Orn-<sup>L</sup>Leu-Ant-<sup>D</sup>Pro<sup>L</sup>Val-OH was deprotected to get TFA. H-(Z)-Orn-<sup>L</sup>Leu-Ant-<sup>D</sup>Pro<sup>L</sup>Val-OH, and this was cyclised under dilute condition using HBTU, DIEA in DCM to produce Cbz-**2**, and was used for conformational investigation using NMR and other characterization techniques. Cbz-**2** was deprotected using H<sub>2</sub>, Pd/C, 10 mol% in 0.01M HCl solution and the resultant salt was directly used for bio-activity.

The detailed schematic representation of the synthesis is shown in Scheme-1.1

Scheme 1.1 Synthesis of modified analogous 1 and 2



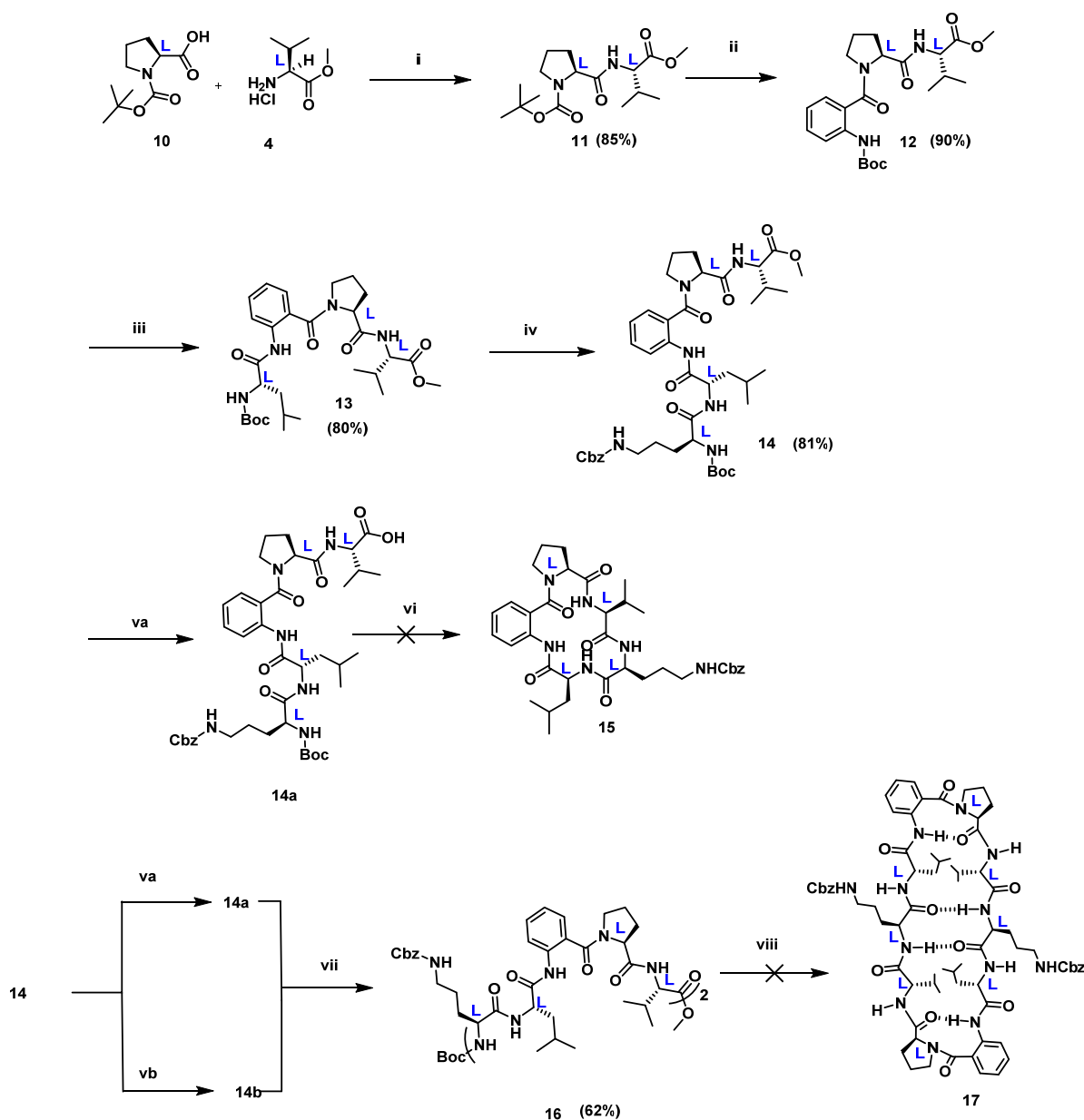
**Reagents and conditions:** (i) EDC.HCl, DIEA, HOBT, DCM, RT, 8 h; (ii) a) TFA:DCM; b) Boc-Ant-OH, HBTU, DIEA, ACN, RT, 6 h; (iii) a) TFA:DCM; b) Boc-Leu-OH, EDC.HCl, HOBT, DCM, RT, 8 h; (iv) a) TFA:DCM; b) Boc-(Cbz)-Orn-OH, HBTU, DIEA, ACN, RT, 12 h; (v) a) LiOH:H<sub>2</sub>O; b) TFA:DCM; (vi) HBTU, DIEA, ACN, RT, 12 h; (vii) a) LiOH : H<sub>2</sub>O; b) TFA:DCM; c) HBTU, DCM, RT, 12 h; (viii) H<sub>2</sub>, 10 mol% Pd/C, 0.02M HCl in MeOH, 12 h; (ix) a)TFA:DCM; b) HBTU, DIEA, DCM, RT, 12 h, (x) H<sub>2</sub>, 10 mol% Pd/C, 0.01M HCl in MeOH, RT,12 h.



Attempts for synthesis of <sup>L</sup>Pro containing cyclic analogues **15** and **17**:

We also attempted the syntheses of cyclic peptide **15** and **17**, by similar synthetic procedures used for syntheses of **1** and **2**, shown in Scheme-1.2.

Scheme 1.2 Synthesis of <sup>L</sup>Pro analogues **15** and **17**



**Reagents and Conditions:** (i) EDC.HCl, DIEA, HOBt, DCM, RT, 8 h; (ii) a) TFA:DCM; b) Boc-Ant-OH, HBTU, DIEA, ACN, RT, 6h; (iii) a) TFA:DCM; b) Boc-Leu-OH, EDC.HCl, HOBt, DCM, RT, 8h; (iv) a) TFA:DCM; b) Boc-(Cbz)-Orn-OH, HBTU, DIEA, ACN, RT, 12h; (va) LiOH:H<sub>2</sub>O; (vb) TFA:DCM; (vi) a) TFA:DCM; b) HBTU, DIEA, ACN, RT, 12h. (vii) HBTU, DIEA, ACN, RT, 12h, (vii) a) LiOH:H<sub>2</sub>O b) TFA:DCM; b) HBTU, DIEA, ACN, RT, 12h.

## 1.5 Conformational analyses

The conformational features of the synthetic peptides were investigated by X-ray crystallography, solution state NMR and CD studies.

### 1.5.1 Single crystal X-ray diffraction studies

We could crystallize two tripeptide units **6** (Boc-Ant-<sup>D</sup>Pro-<sup>L</sup>Val-OMe) and **12** (Boc-Ant-<sup>L</sup>Pro-<sup>L</sup>Val-OMe) in the mixture of solvents pet. ether and ethyl acetate. The solid-state conformation of both tripeptides **6** and **12** revealed that the nine-membered hydrogen-bonding pattern of Ant-Pro reverse-turn clearly prevailed in both the cases, regardless of chirality alteration in the proline residue (Figure 1.15). But, it is found that the termini of D-Pro analogue **6** were quite closer than that the termini of L-Pro analogue **12**.

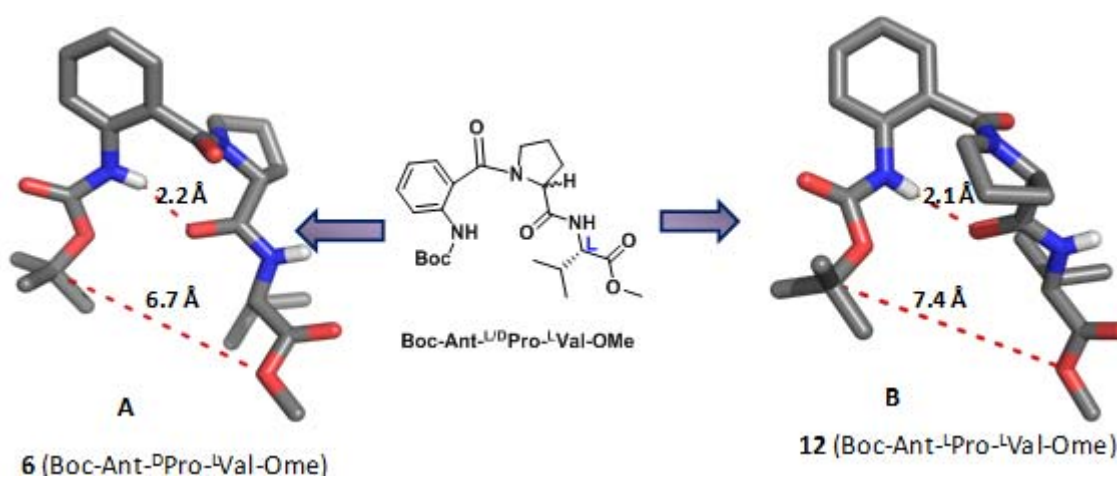


**Figure 1.15** Crystal structures of tripeptides **6** (Boc-Ant-<sup>D</sup>Pro-<sup>L</sup>Val-OMe) and **12** (Boc-Ant-<sup>L</sup>Pro-<sup>L</sup>Val-OMe). Note, hydrogens other than the polar amide hydrogens have been removed for clarity.

### 1.5.2 NMR studies

In order to investigate the solution-state conformation of the two cyclic peptides **1** and **2** containing Ant-<sup>D</sup>Pro (C9) reverse turn segment, we performed 2D ROESY NMR study of analogue **1** (10 mM, 700 MHz) in DMSO-*d*<sub>6</sub>. The signal assignments were carried out with a combination of 2D COSY, TOCSY, HSQC and HMBC.

### 1.5.2.1 Variable Temperature Studies

Variable temperature NMR experiment (Figure 1.16, Table 1.1) was used to probe the strength of *intra* molecular hydrogen bonding in **1**. The amide NH protons of Ant and Orn residues had temperature coefficients -2.36 and -2.31 ppb/K, respectively, which supported *intra* molecular hydrogen bonding at these sites. Whereas, the other amide NH of Val, Leu and side chain of Orn showed temperature coefficient more than 4.5 ppb/K which indicates non involvement in *intra* molecular hydrogen bonding at these sites.

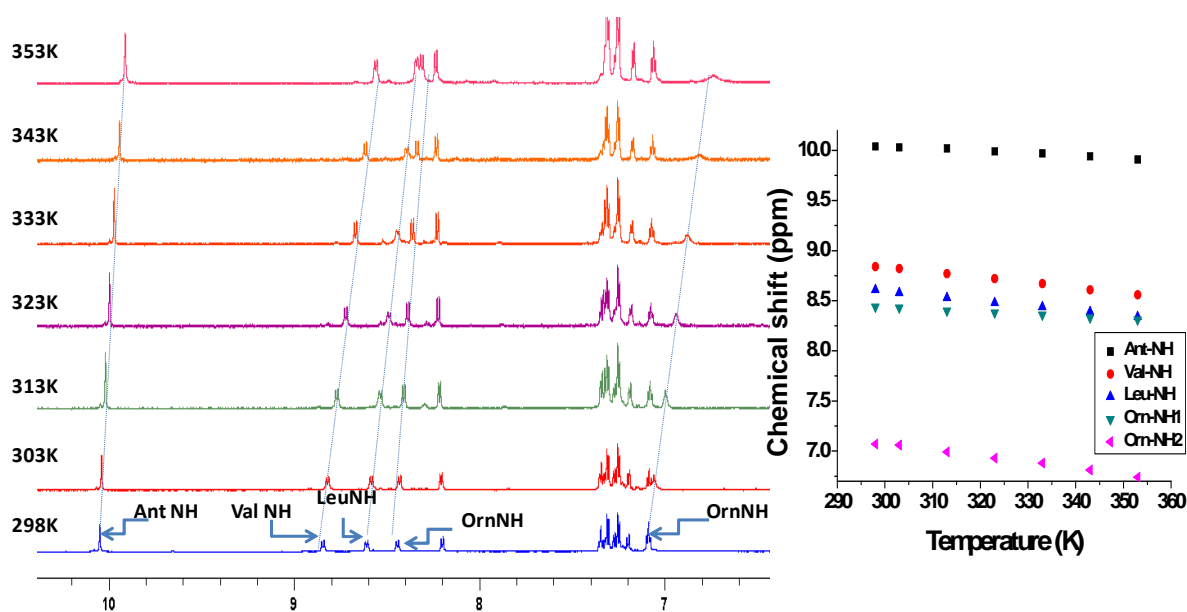
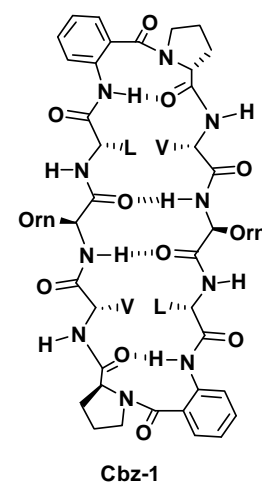


**Figure 1.16** Stacked partial  $^1\text{H}$  NMR spectra at different temperature) of **1** (2 mM, 700 MHz) in  $\text{DMSO-}d_6$ .

**Table 1.1** Variable temperature study of **1** (2 mM, 700 MHz,  $\text{DMSO-}d_6$ )

Temperature (K)	Chemical shift (in ppm)				
	$\delta_{\text{Ant-NH}}$	$\delta_{\text{Val-NH}}$	$\delta_{\text{Leu-NH}}$	$\delta_{\text{Orn-NH1}}$	$\delta_{\text{Orn-NH2}}$
298	10.04	8.84	8.61	8.44	7.07
303	10.03	8.82	8.58	8.43	7.06
313	10.02	8.77	8.53	8.4	6.99
323	9.99	8.72	8.48	8.38	6.93
333	9.97	8.67	8.44	8.36	6.88
343	9.94	8.61	8.39	8.33	6.81
353	9.91	8.56	8.34	8.31	6.74
<b>Temperature Coefficient in ppb/K</b>	<b>-2.36</b>	<b>-5.09</b>	<b>-4.9</b>	<b>-2.31</b>	<b>-6.0</b>



### 1.5.2.2 Variable Temperature Studies of 2:

The difference in hydrogen bonding pattern of two macro cyclic compounds incorporated with Ant<sup>D</sup>Pro units i.e. cyclic deca peptide **1** and its truncated form cyclic penta peptide **2** was observed in variable temperature NMR experiment (Figure 1.17, Table 1.2). The Val NH, Ant NH and Orn NH showed temperature coefficients -1.81, -4.36 and -3.09, ppb/K respectively, which supported *intra* molecular hydrogen bonding at these sites. The Leu NH and side chain Orn NH, on the other hand, showed temperature coefficients more than -5 ppb/K, indicating their non involvement in *intra* molecular hydrogen bonding.

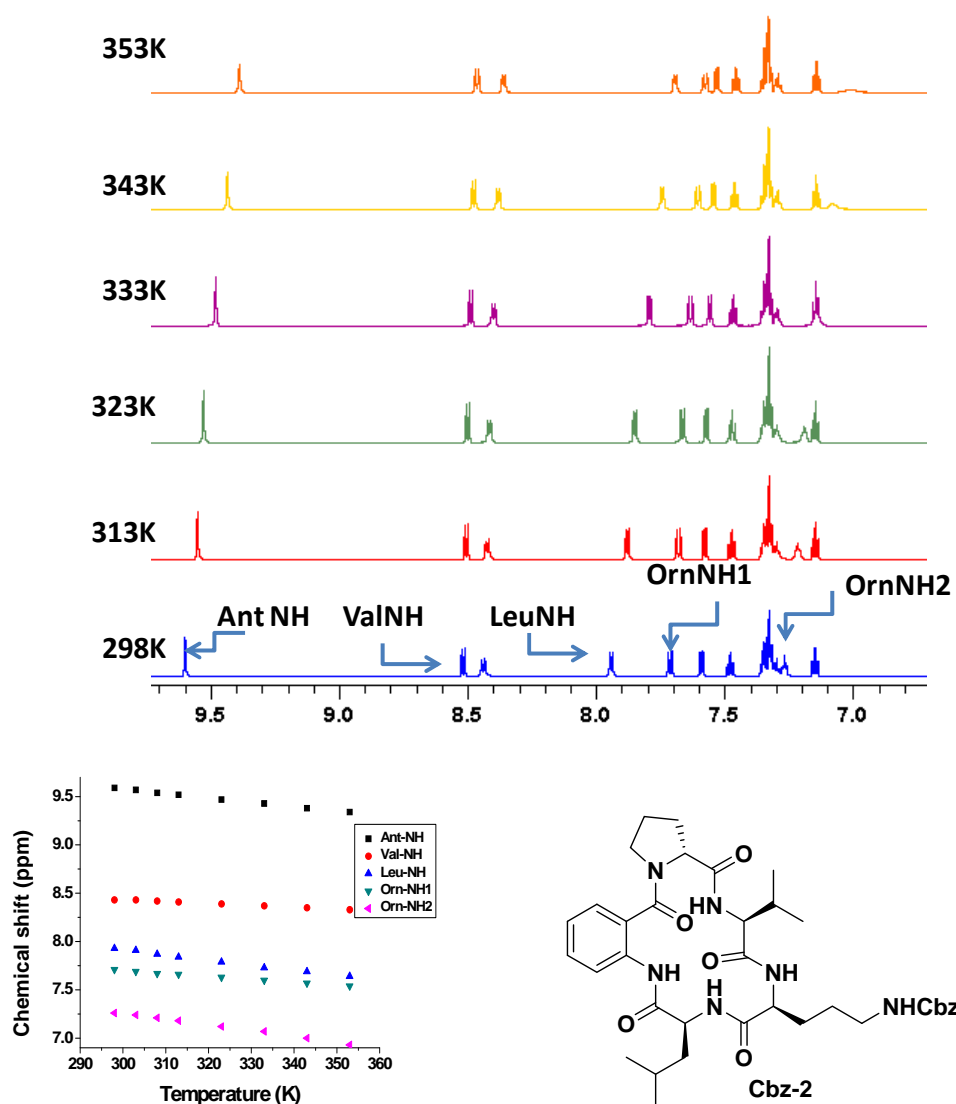
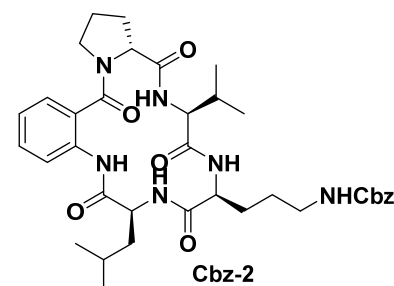


**Figure 1.17** Stacked plot of partial <sup>1</sup>H NMR spectra of **2** at different temperature (5 mM, 700 MHz) in DMSO-*d*<sub>6</sub>

**Table 1.2** Variable temperature study of **2** (5 mM, 700 MHz, DMSO-*d*<sub>6</sub>)

Temperature (K)	Chemical shift (in ppm)				
	$\delta_{\text{Ant-NH}}$	$\delta_{\text{Val-NH}}$	$\delta_{\text{Leu-NH}}$	$\delta_{\text{Orn-NH1}}$	$\delta_{\text{Orn-NH2}}$
298	9.59	8.43	7.93	7.71	7.26
303	9.57	8.43	7.91	7.69	7.24
308	9.54	8.42	7.87	7.67	7.21
313	9.52	8.41	7.84	7.66	7.18
323	9.47	8.39	7.79	7.63	7.12
333	9.43	8.37	7.73	7.6	7.07
343	9.38	8.35	7.69	7.57	7
353	9.34	8.33	7.64	7.54	6.93
<b>Temperature Coefficient in ppb/K</b>	<b>-4.36</b>	<b>-1.81</b>	<b>-5.27</b>	<b>-3.09</b>	<b>-6.0</b>



### 1.5.2.3 ROESY and CD spectra analysis of **1**

2D ROESY NMR reveals inter-strand C19H ( $\alpha$ H of Leu)-C2H ( $\alpha$ H of Val) medium nOe, while *intra* -( $\beta$ ) strand strong nOe's are observed for C7H ( $\alpha$ H of <sup>D</sup>Pro)-NH1 (NH of Val), C2H ( $\alpha$ H of Val)-NH4 (NH of Orn), C19H ( $\alpha$ H of Leu)-NH2 (NH of Ant), C25H ( $\alpha$ H of Orn)-NH3 (NH of Leu). The medium nOe in the loop region (turn segment) viz. C10H ( $\delta$ H of <sup>D</sup>Pro)-NH2 (NH of Ant), C10'H ( $\delta$ H of <sup>D</sup>Pro)-C17H (C4H of Ant) (Figures 1.18a and 1.18b) suggests  $\beta$  sheet conformation for compound **1** in solution state.

The minima at 220 nm and maxima at 200 nm in CD spectra (Figure 19a) of **1** in methanol clearly indicate the presence of  $\beta$  sheet conformation for compound **1** in methanol.

### 1.5.2.4 MD Simulation study of **1**

The MD-simulated structures were generated for compound **1**, using the quantitative restraints obtained from the ROESY spectra of **1** in DMSO-*d*<sub>6</sub> (Table 1.5). The 20 superimposed minimum energy structures derived from MD simulations show a perspicuous antiparallel  $\beta$ -sheet conformation for compound **1** with orthogonal ornithine side chains (Figure 1.20).

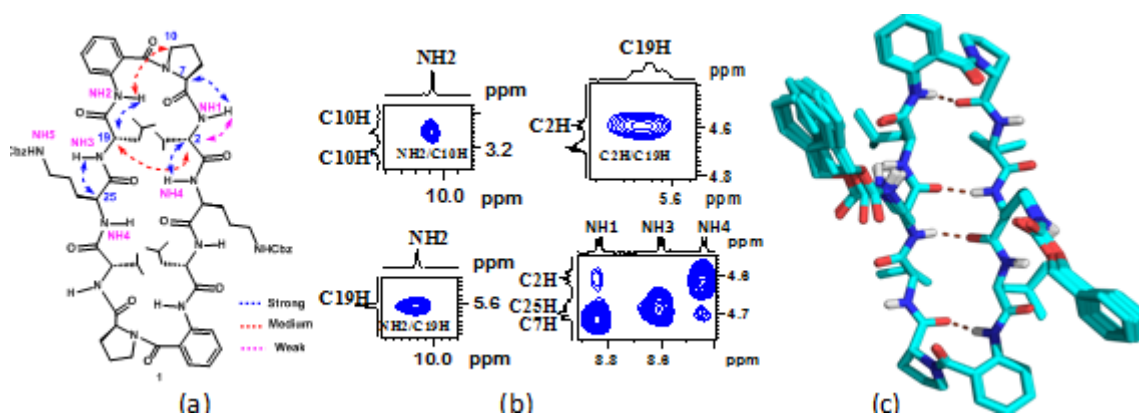


**Figure 1.18** (a) Structure of **1** highlighting nOe’s with dotted double headed arrows; (b) Diagnostic nOe’s and (c) Overlay of MD simulated 20 minimized structures calculated using nOe distance restraints.

### 1.5.2.5 2D ROESY and CD analysis of **2**

Compound **2** showed different nOe pattern than compound **1** (Figure 1.20). The strong nOe between NH1 (Val NH) and NH4 (Orn NH), NH1(Val NH) and C7H (( $\alpha$ H of DPro), weak nOe between NH4(Orn NH) and C7H (( $\alpha$ H of DPro), as well as medium nOe between NH4 (Orn NH) and NH2 (Ant NH) suggesting three NH’s i.e. NH1, NH2 and NH4 are involved in *intra* molecular hydrogen bonding with same carbonyl group (carbonyl of Ant).

The CD studies of compound **2** in methanol showed two minima at 235 nm and 195 nm (Figure 1.19.b) and suggested a completely different conformation than compound **1**, which exhibited minima at 220 nm and maxima near 200 nm for the  $\beta$  sheet conformation.

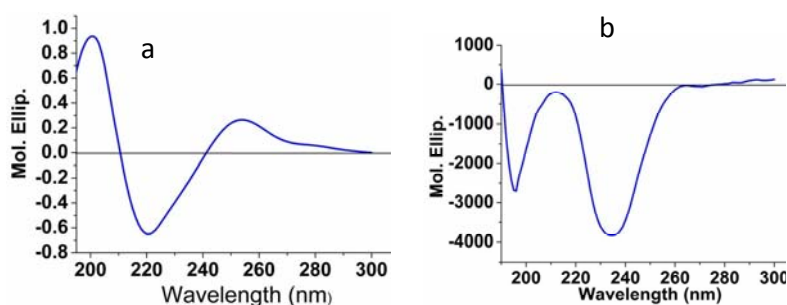


**Figure 1.19** Circular Dichroism spectra of **1** (0.1 mM) and **2** (0.2 mM) in MeOH (a and b respectively)

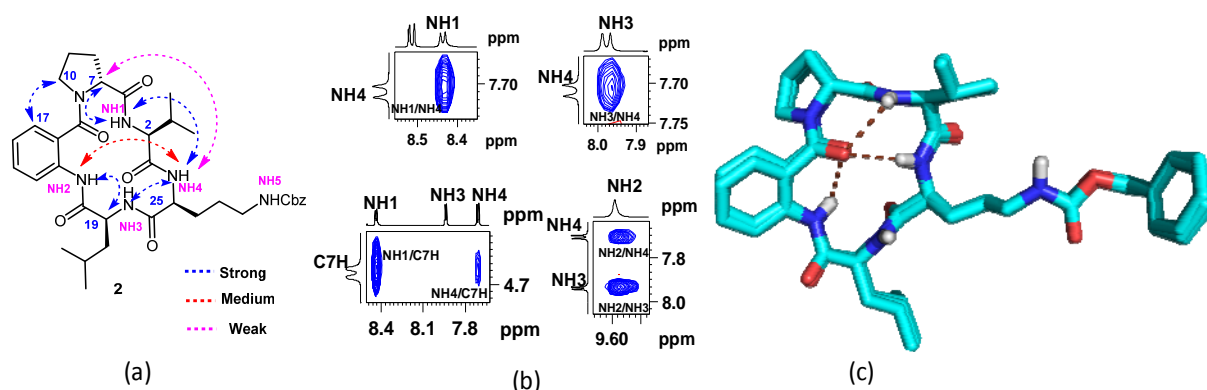


**Figure 1.20** (a) Structure of **2** highlighting nOe's with dotted double headed arrows, (b) Characteristic nOe's and (c) Overlay of MD simulated 20 minimized structures calculated using nOe distance restraints (rTable 1.6).

### 1.6 Antibacterial studies of **1** and **2**:

Synthetic analogs of gramicidin S i.e Cbz deprotected, HCl salt of **1** & **2** were tested against bacteria such as *Bacillus subtilis*, *Escherichia coli*, *Pseudomonas aeruginosa* and *Staphylococcus aureus*. The antibacterial studies of this modified cyclic deca peptide **1** showed 3-15  $\mu\text{g/mL}$  MIC values which is equipotent to natural gramicidin S, while in the case of cyclic penta peptide **2** it doesn't reach to 100  $\mu\text{g/mL}$   $\text{IC}_{50}$  value against all the tested bacteria. This reveals that  $\beta$  sheet conformation with two orthogonal side chains of ornithine residue is essential for antibacterial activity. The cyclic penta peptide **2** does not possess both these requirements which was confirmed from CD and NMR studies, hence it didn't show effect on bacteria.

### 1.7 Attempts for syntheses of cyclic $^L$ Pro analogs **15** and **17**:

We made efforts to cyclise the deprotected penta peptide **14** and deca peptide **16** incorporated with Ant $^L$ Pro segment, using similar condition for cyclization of **8** and **9** but it didn't give cyclic products **15** and **17** respectively, probably due to the conformational restriction for cyclization of the peptides, created by Ant $^L$ Pro turn segment in these systems, and which lead to fraying the termini.

### 1.7.1 Comparative CD studies of linear <sup>D</sup>Pro analogs 8 and 9 with <sup>L</sup>Pro analogs 14 and 16:

The linear compounds 8, 9, 14 and 16 are the precursors of cyclic peptides. We find conformational difference between <sup>D</sup>Pro and <sup>L</sup>Pro linear analogs in CD studies. Figure 1.21 describes the CD spectra of linear <sup>D</sup>Pro analogs i.e D-Penta 8 and D- Deca peptide 9 showing minima near 210 and maxima near 237 while <sup>L</sup>Pro analogs L-penta 14 and L-Deca 16 maxima near 210 and minima near 240 nm suggesting that difference in conformation with altering the chirality of proline residue.

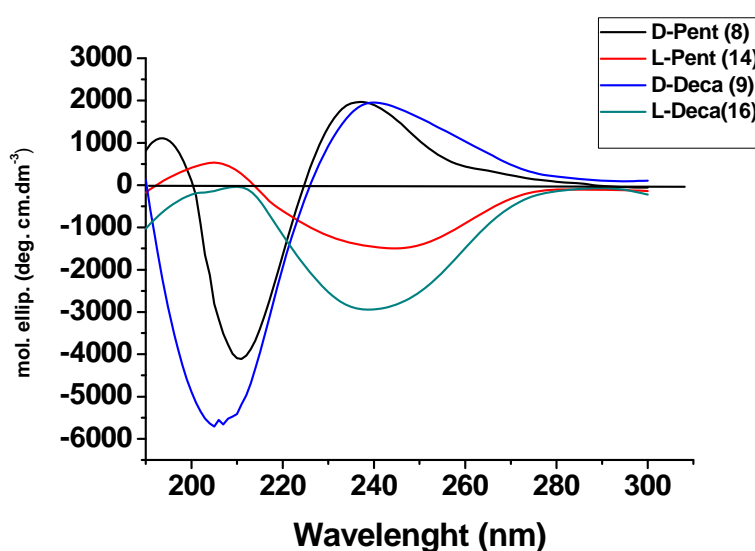


**Figure 1.21** Circular dichroism spectra of 8, 9, 14 and 16 (0.2 mM) in methanol.

From the CD spectra of linear analogues, it could be conclude that, in this case study <sup>D</sup>Pro sequence preorganizes the conformation for the cyclization while <sup>L</sup>Pro sequences resist the cyclization.

## 1.8 Conclusions

In conclusion, we successfully demonstrated the synthesis of gramicidin S mimic 1 with Ant<sup>D</sup>Pro a pseudo  $\beta$ -turn segment in the loop region. The solution state conformational analysis using CD studies as well as NMR studies approves the  $\beta$  sheet conformation for gramicidin S mimic 1 with orthogonal (to backbone)



side chain of ornithine residues. The cyclic penta peptide **2** shows perturbation from  $\beta$  sheet conformation and three of its NHs were involved in *intra* molecular hydrogen bonding with single carbonyl of Ant residue. The antibacterial studies of these modified cyclic peptides showed that **1** is as active as its natural analogue GS, while **2** is not active. We anticipate that this study will be beneficial in developing the new cyclic peptidomimetics with hetero chiral residues.

## 1.9 Experimental Section

### X-ray Crystallography:

Single crystals of **6** and **12** were obtained by slow evaporation of the solution of ethyl acetate and pet ether. X-ray intensity data measurement of compounds **LDTRI** and **LLTRI** were carried out on a Bruker D8 VENTURE Kappa Duo PHOTON II CPAD diffractometer equipped with Incoatech multilayer mirrors optics. The intensity measurements were carried out with Cu ( $\text{CuK}_\alpha = 1.54178 \text{ \AA}$ ) and Mo ( $\text{MoK}_\alpha = 0.71073 \text{ \AA}$ ) micro-focus sealed tube diffraction source at 100(2) K temperature respectively. The X-ray generator was operated at 50 kV and 1.1 mA for Cu radiation and 1.4 mA for Mo radiation. A preliminary set of cell constants and an orientation matrix were calculated from two sets of 40 frames for Cu source and three sets of 36 frames for Mo source. Data were collected for both radiations with  $\omega$  scan width of  $0.5^\circ$  at different settings of  $\varphi$  and  $2\theta$  with a frame time of 10 secs keeping the sample-to-detector distance fixed at 5.00 cm. The X-ray data collection was monitored by APEX3 program (Bruker, 2016).<sup>43</sup> All the data were corrected for Lorentzian, polarization and absorption effects using SAINT and SADABS programs (Bruker, 2006). SHELX-97 was used for structure solution and full matrix least-squares refinement on  $F^2$ .<sup>2</sup> All the hydrogen atoms were placed in geometrically idealized positions and constrained to ride on their parent atoms except H atoms attached to N atoms which were located in difference Fourier map and refined isotropically.

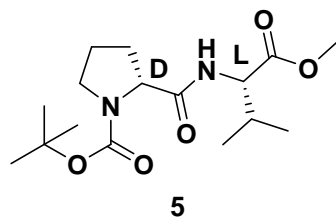
Crystal data of **LDTRI**  $\text{C}_{23}\text{H}_{33}\text{N}_3\text{O}_6$ ,  $M = 447.52$ , colorless plate,  $0.12 \times 0.11 \times 0.07 \text{ mm}^3$ , tetragonal, space group  $P4_12_12$ ,  $a = 9.6856(3) \text{ \AA}$ ,  $b = 9.6856(3) \text{ \AA}$ ,  $c = 51.0690(16) \text{ \AA}$ ,  $V = 4790.8(3) \text{ \AA}^3$ ,  $Z = 8$ ,  $T = 100(2) \text{ K}$ , Cu radiation ( $\text{CuK}_\alpha = 1.54178 \text{ \AA}$ ),  $2\theta_{\text{max}} = 145.71^\circ$ ,  $D_{\text{calc}} (\text{g cm}^{-3}) = 1.241$ ,  $F(000) = 1920$ ,  $\mu (\text{mm}^{-1}) =$

0.740, 33857 reflections collected, 4731 unique reflections ( $R_{\text{int}}=0.0497$ ), 4378 observed ( $I > 2\sigma(I)$ ) reflections, multi-scan absorption correction,  $T_{\text{min}} = 0.916$ ,  $T_{\text{max}} = 0.950$ , 295 refined parameters,  $S = 1.022$ ,  $R1 = 0.0384$ ,  $wR2 = 0.0844$  (all data  $R = 0.0432$ ,  $wR2 = 0.0869$ ), maximum and minimum residual electron densities;  $\Delta\rho_{\text{max}} = 0.159$ ,  $\Delta\rho_{\text{min}} = -0.232$  ( $\text{e}\text{\AA}^{-3}$ ).

Crystal data of LLTRI  $\text{C}_{23}\text{H}_{33}\text{N}_3\text{O}_6$ ,  $M = 447.52$ , colorless plate,  $0.34 \times 0.21 \times 0.10 \text{ mm}^3$ , monoclinic, space group  $P2_1$ ,  $a = 13.3238(5) \text{ \AA}$ ,  $b = 7.2153(3) \text{ \AA}$ ,  $c = 13.5409(6) \text{ \AA}$ ,  $\beta = 114.1870(10)^\circ$ ,  $V = 1187.48(9) \text{ \AA}^3$ ,  $Z = 2$ ,  $T = 100(2) \text{ K}$ , Mo radiation ( $\text{MoK}\alpha = 0.71073 \text{ \AA}$ ),  $2\theta_{\text{max}} = 61.062^\circ$ ,  $D_{\text{calc}} (\text{g cm}^{-3}) = 1.252$ ,  $F(000) = 480$ ,  $\mu (\text{mm}^{-1}) = 0.091$ , 41983 reflections collected, 7203 unique reflections ( $R_{\text{int}}=0.0595$ ), 6847 observed ( $I > 2\sigma(I)$ ) reflections, multi-scan absorption correction,  $T_{\text{min}} = 0.970$ ,  $T_{\text{max}} = 0.991$ , 303 refined parameters,  $S = 1.038$ ,  $R1 = 0.0352$ ,  $wR2 = 0.0856$  (all data  $R = 0.0382$ ,  $wR2 = 0.0872$ ), maximum and minimum residual electron densities;  $\Delta\rho_{\text{max}} = 0.330$ ,  $\Delta\rho_{\text{min}} = -0.191$  ( $\text{e}\text{\AA}^{-3}$ ).

### Synthetic procedures and data:

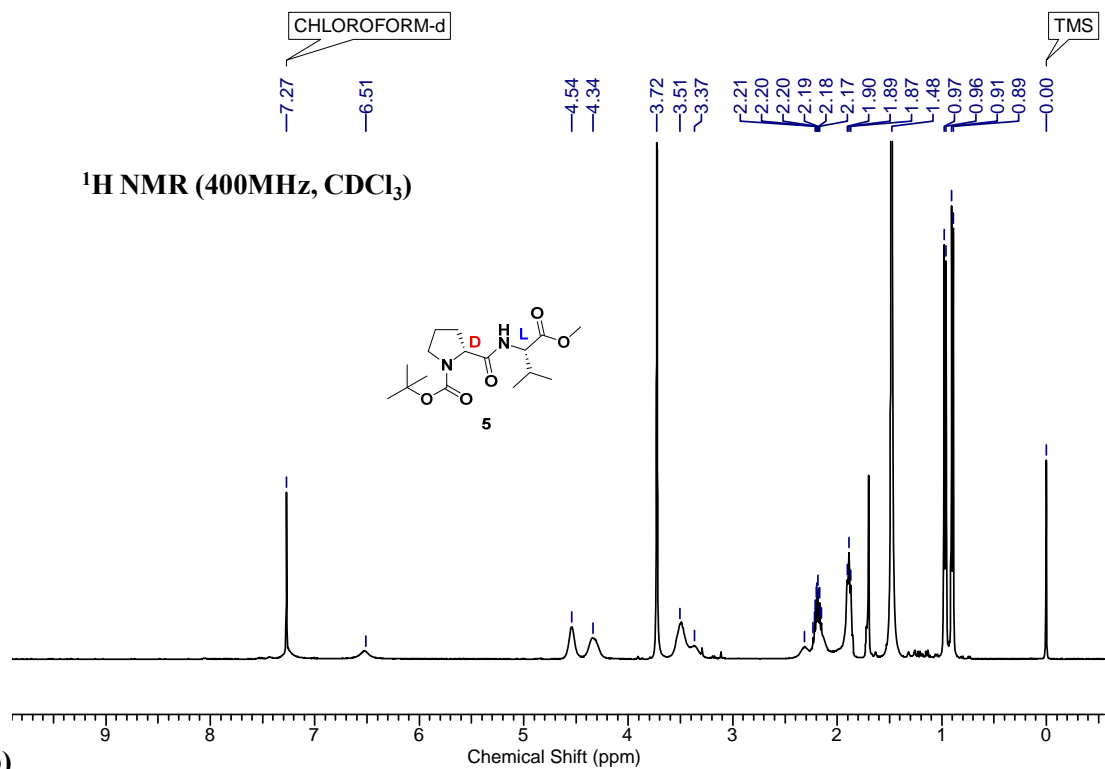
**Compound 5 (Boc-<sup>D</sup>Pro<sup>L</sup>Val-OMe):** To a solution of HCl.<sup>L</sup>Val-OMe **4** (6.523 g, 34.88 mmol, 1.5 equiv.) in DCM (60 mL) at 0°C, DIEA (12.12 mL, 69.75 mmol, 3 equiv.) was added slowly and the reaction mixture stirred for 5 minutes. Later Boc-<sup>D</sup>Pro-OH **3** (5g, 23.25, 1 equiv.), EDC.HCl (8.88 g, 46.5mmol, 2 equiv.) & HOBT (catalytic amount) were added sequentially and the



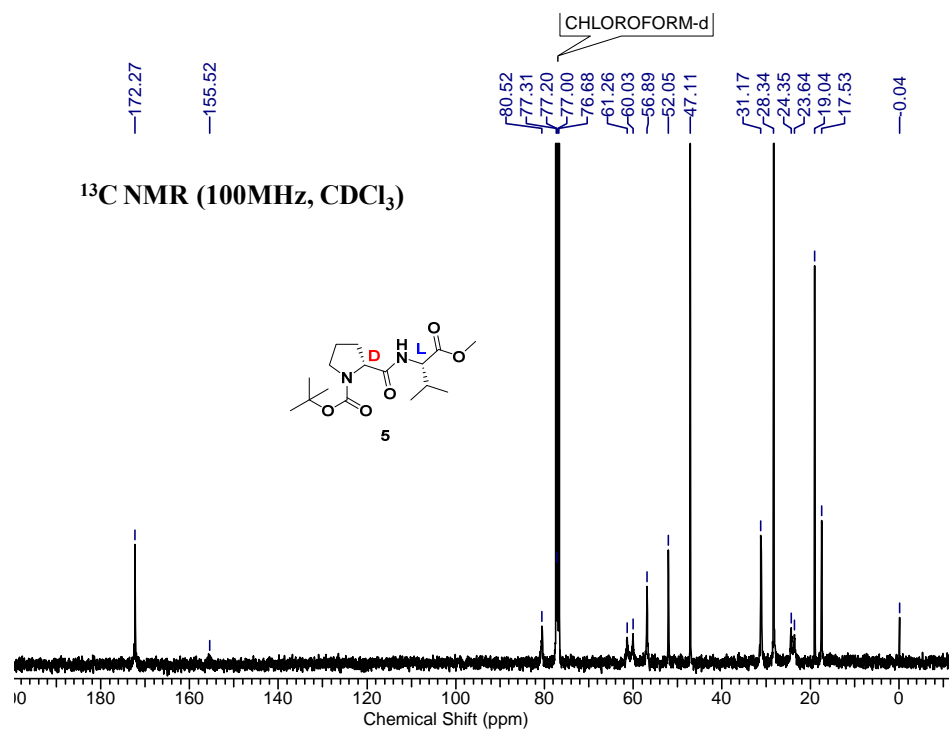
reaction mixture was stirred for 8 h at rt. After completion of reaction, the reaction mixture was diluted with DCM and washed sequentially with solutions of  $\text{KHSO}_4$ ,  $\text{NaHCO}_3$  and brine. The organic layer was dried over  $\text{Na}_2\text{SO}_4$  and evaporated under vacuum. The crude product was purified by column chromatography (eluent: 20% AcOEt/Pet. ether,  $R_f$ : 0.3) afforded **5** (6.25 g, 82%) as a white fluffy solid material. mp: 102-104 °C;  $[\alpha]^{25.97}_{\text{D}} = 105.39^\circ$  ( $c = 0.122$ ,  $\text{CHCl}_3$ ); IR ( $\text{CHCl}_3$ )  $\nu$  ( $\text{cm}^{-1}$ ): 3294, 2967, 2358, 1741, 1691, 1658, 1442, 1209, 766;  $^1\text{H NMR}$  (400MHz,  $\text{CDCl}_3$ )  $\delta$ : 6.51 (bs, 1H), 4.54 (bs, 1H), 4.34 (bs, 1H), 3.72 (s, 3H), 3.60 (m, 1H), 3.44-3.27 (m, 1H), 3.49 (bs, 2H), 2.31 (bs, 1H), 2.26-2.11 (m, 2H), 1.89 (t,  $J = 6.6 \text{ Hz}$ , 2H), 1.48 (s, 9H), 0.97 (d,  $J = 6.8 \text{ Hz}$ , 3H), 0.90 (d,  $J = 6.8 \text{ Hz}$ , 3H);  $^{13}\text{C NMR}$  (100 MHz,  $\text{CDCl}_3$ )  $\delta$ : 172.3, 155.5, 80.5,

61.3, 60.0, 56.9, 52.1, 47.1, 31.2, 28.3, 24.3, 23.6, 19.0, 17.5; HRMS (ESI)  $C_{16}H_{30}N_2O_5$  calculated  $[M+H]^+$ : 329.1998, found 329.2061,  $C_{16}H_{28}N_2NaO_5$  calculated  $[M+Na]^+$  351.1896, found 351.1880.

a)



b)



c)

D-DL\_151202141937 #104 RT: 0.46 AV: 1 NL: 2.41E9  
T: FTMS + p ESI Full ms [100.00-1500.00]

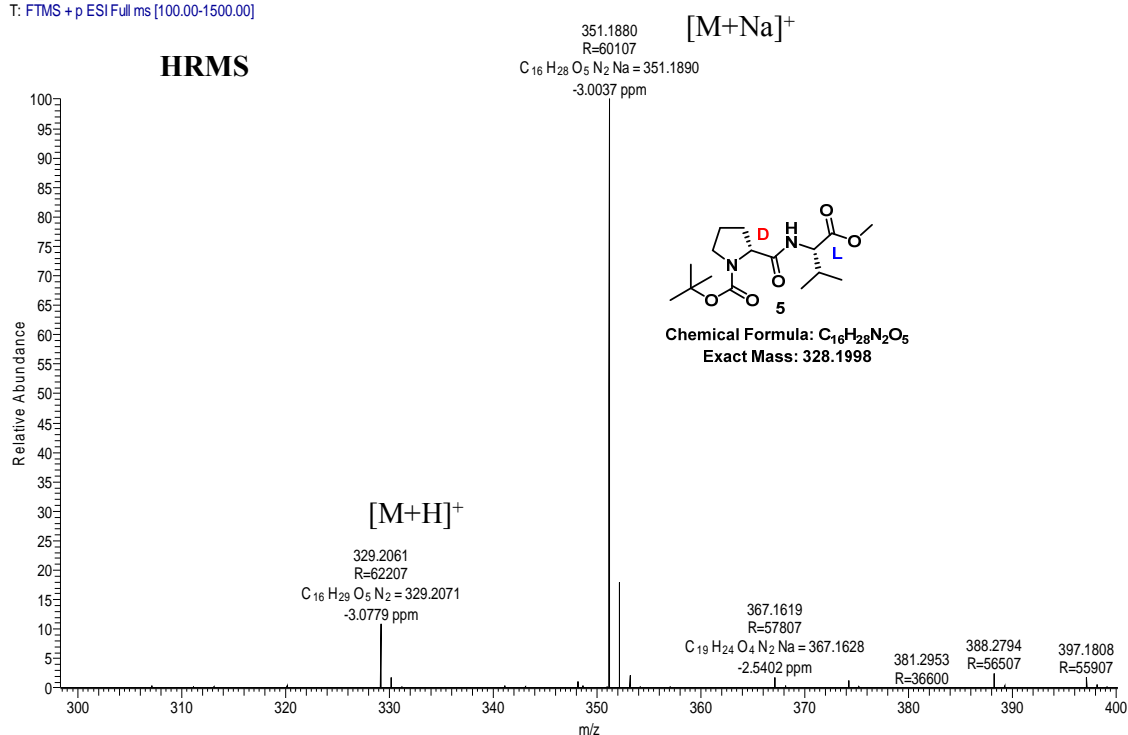
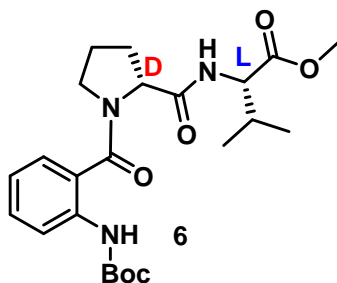


Figure 1.22 a) <sup>1</sup>H NMR, b) <sup>13</sup>C NMR and c) HRMS of compound 5

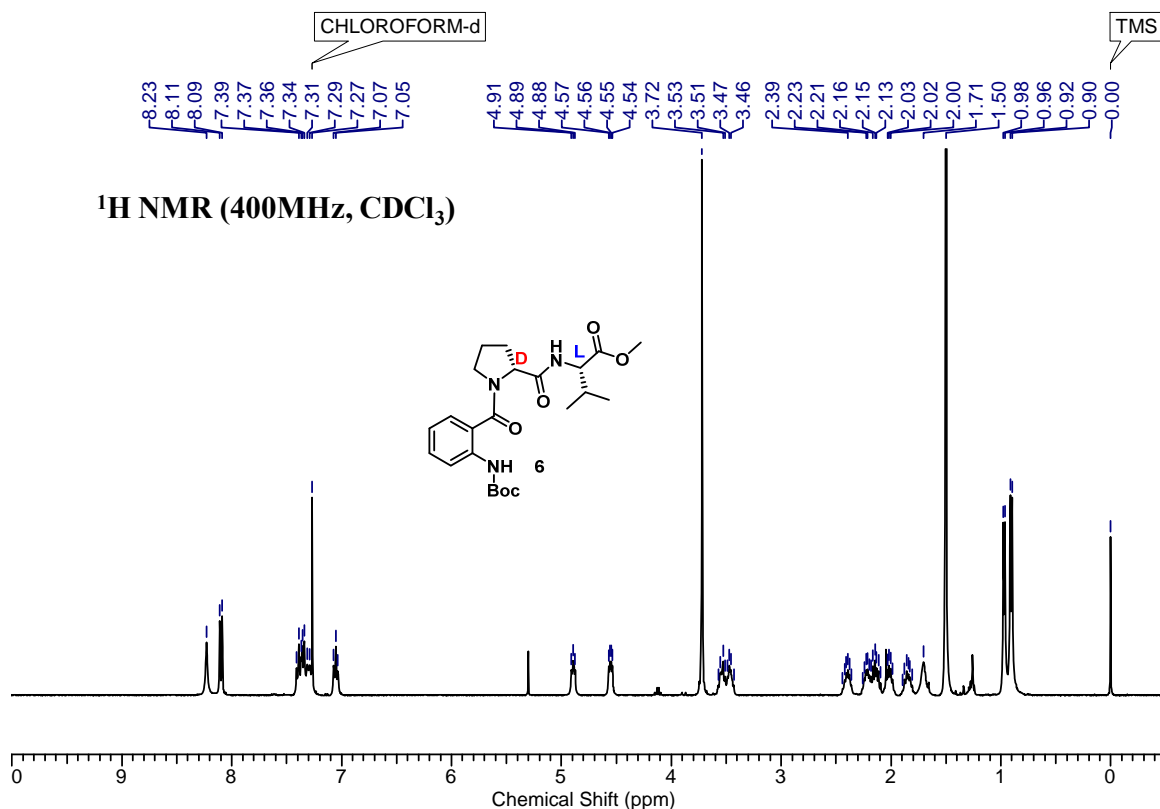
**General Boc-deprotection procedure:** Peptide compound stirred in TFA:DCM (1:1) solution for 30 min. After deprotection, DCM was evaporated under reduced vacuum and TFA salt was neutralized by NaHCO<sub>3</sub> solution and compound was extracted with ethyl acetate and washed with water and brine. The resulting ethyl acetate solution dried over Na<sub>2</sub>SO<sub>4</sub> and evaporated under vacuum. The crude product (free amine) was used for next reaction without further purification.

**Compound 6 (Boc-Ant<sup>D</sup>Pro<sup>L</sup>Val-OMe):** To a solution of BocAnt-OH (2.495 g, 10.52 mmol, 1.2 equiv.) and DIEA (4.57 mL, 26.31 mmol, 3 equiv.) in 30mL of ACN, the amine (H-ProVal-OMe) (2 g, 8.77 mmol, 1 equiv.), HBTU (6.653 g, 17.54 mmol, 2 equiv.) & catalytic amount of HOBt were added sequentially at 0 °C. This reaction mixture was then stirred for 6 h at rt. After completion of reaction, ACN was removed under reduced pressure and the compound was taken into ethyl acetate. The combined organic layers were washed sequentially with saturated solutions of KHSO<sub>4</sub>, NaHCO<sub>3</sub> and brine. Organic layer was then dried over Na<sub>2</sub>SO<sub>4</sub> and was evaporated under

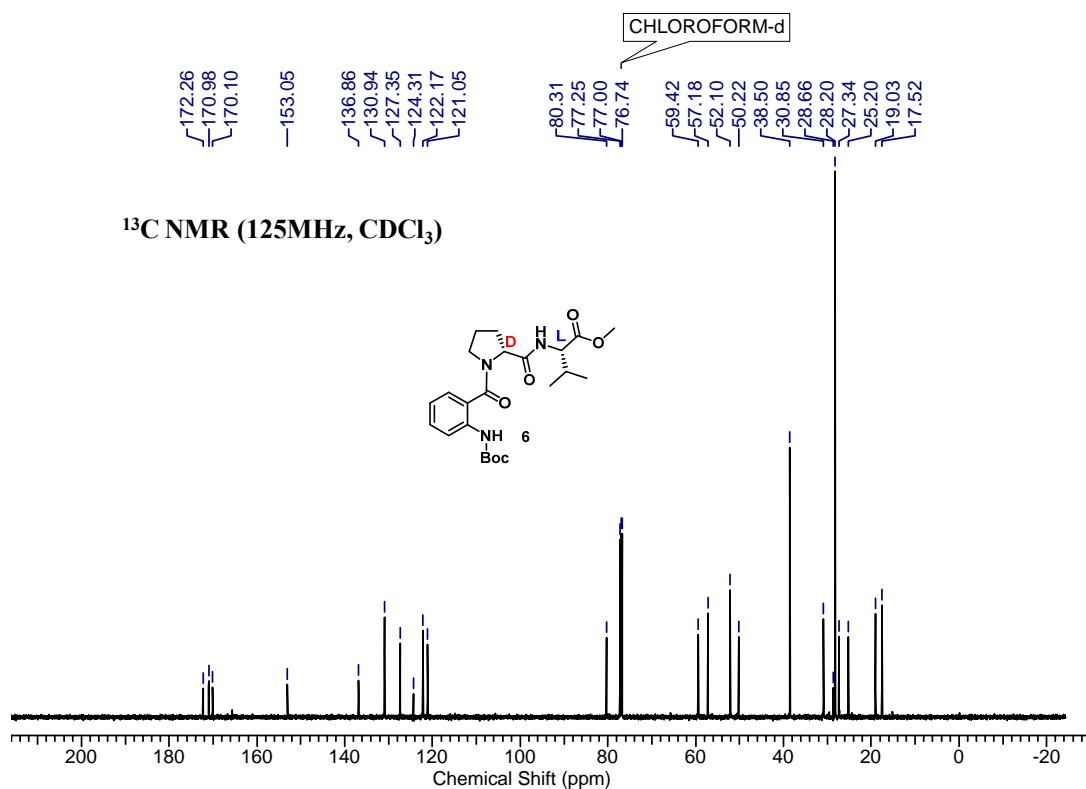


vacuum. The crude product was purified by column chromatography (eluent 40% AcOEt/pet. Ether,  $R_f$ : 0.3) to furnish compound **6** (3.51 g, 90%) as a white solid. mp: 144-146°C;  $[\alpha]^{25.97}_D = 156.08^\circ$  ( $c = 0.11$ ,  $\text{CHCl}_3$ ); IR ( $\text{CHCl}_3$ )  $\nu$  ( $\text{cm}^{-1}$ ) 3315, 2971, 2358, 1731, 1676, 1525, 1160, 761;  $^1\text{H}$  NMR (400MHz,  $\text{CDCl}_3$ )  $\delta$  ppm 8.23 (bs, 3H), 8.10 (d,  $J = 8.3$  Hz, 1H), 7.40 (m, 1H), 7.37 - 7.28 (m, 2H), 7.05 (t,  $J = 7.5$  Hz, 1H), 4.90 (d,  $J = 5.6$  Hz, 1H), 4.66 - 4.45 (m, 1H), 3.72 (s, 3H), 3.60 - 3.39 (m, 2H), 2.48 - 2.32 (m, 1H), 2.29 - 2.18 (m, 1H), 2.18 - 2.08 (m, 1H), 2.04 - 1.93 (m, 1H), 1.91 - 1.78 (m, 1H), 1.50 (s, 9H), 0.98 (s, 3H), 0.91 (d,  $J = 6.8$  Hz, 3H)  $^{13}\text{C}$  NMR (125MHz,  $\text{CDCl}_3$ )  $\delta = 172.3$ , 171.1, 170.2, 153.1, 137.0, 131.0, 127.4, 124.4, 122.3, 121.1, 80.4, 59.5, 57.3, 50.3, 38.6, 30.9, 28.3, 27.4, 25.3, 19.1, 17.6; HRMS (ESI)  $\text{C}_{23}\text{H}_{34}\text{N}_3\text{O}_6$  calculated  $[\text{M}+\text{H}]^+$ : 448.2369, found 448.2431,  $\text{C}_{23}\text{H}_{33}\text{N}_3\text{NaO}_6$  calculated  $[\text{M}+\text{Na}]^+$  470.2267, found 470.2249.

a)



b)



c)

D-TRI\_151202142249 #110 RT: 0.49 AV: 1 NL: 3.72E9  
T: FTMS + p ESI Full ms [100.00-1500.00]

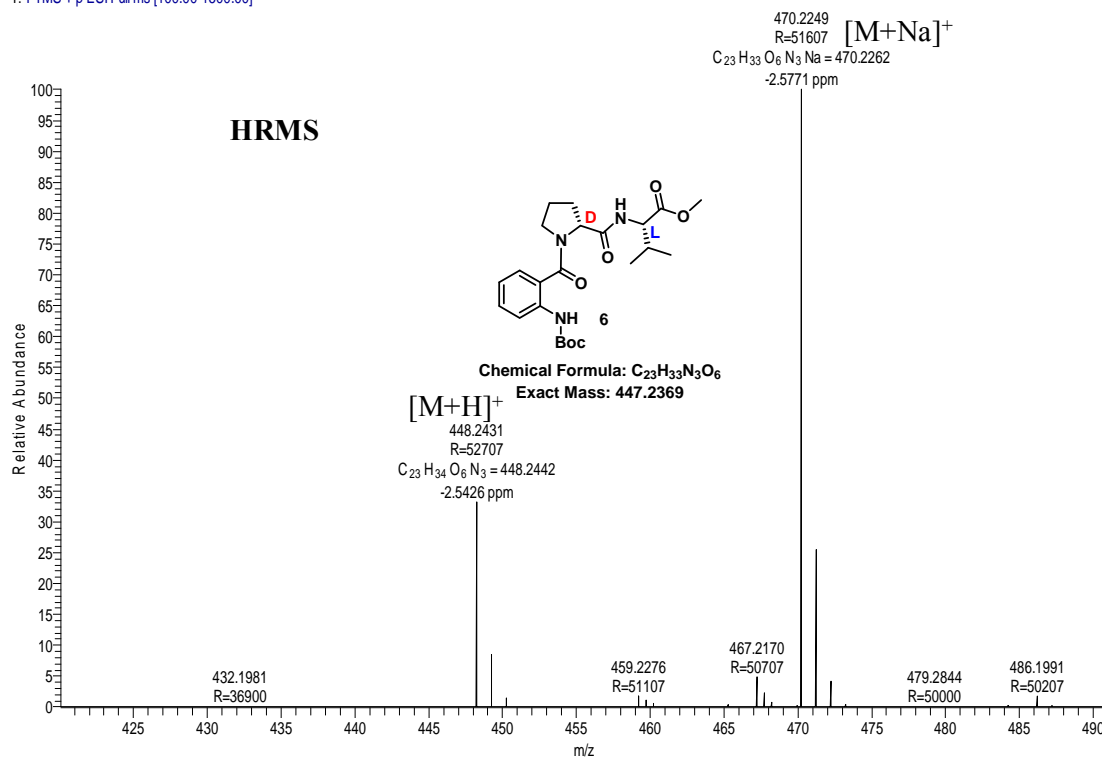
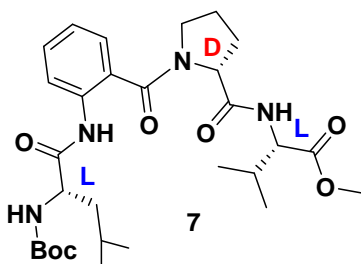


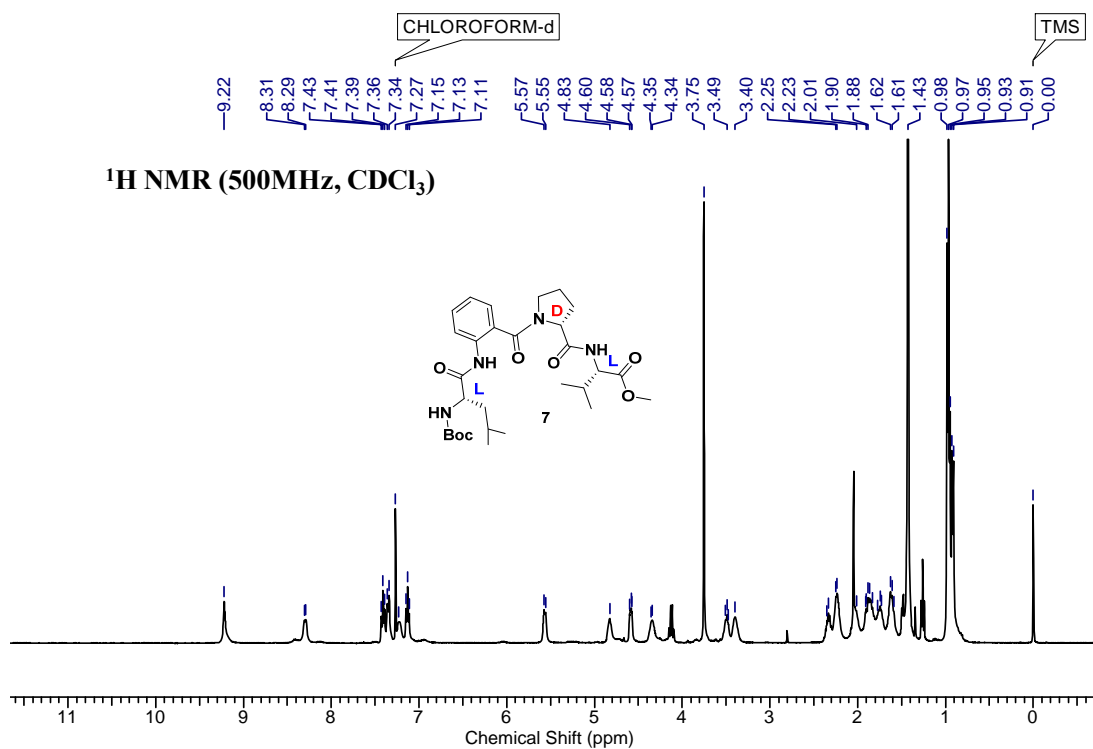
Figure 1.23 a) <sup>1</sup>H NMR, b) <sup>13</sup>C NMR and c) HRMS spectra of compound 6

Compound 7 (Boc <sup>L</sup>LeuAnt <sup>D</sup>Pro <sup>L</sup>Val-OMe):

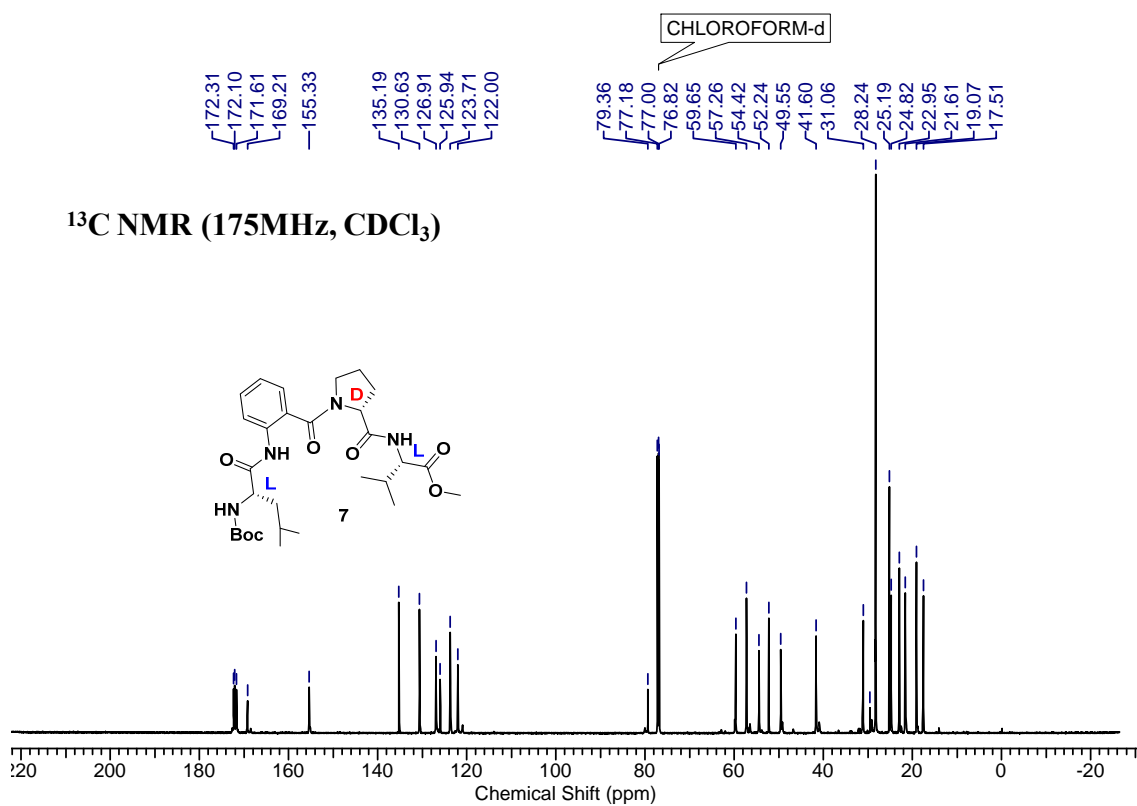


To a solution of Boc-<sup>L</sup>Leu-OH (1.33 g, 5.76 mmol, 2 equiv.) in 20 mL DCM, EDC.HCl(1.1 g, 5.763 mmol, 2 equiv.) & catalytic amount of HOBt were added and reaction mixture was stirred at 0 °C for 30 min., the solution of amine (H-Ant<sup>D</sup>Pro<sup>L</sup>Val-OMe) (1 g, 2.88 mmol, 1equiv.) in 10mL DCM was added slowly to the reaction mixture at 0 °C. This reaction mixture was then stirred for 4 h at rt. After completion of reaction, solution was diluted with DCM. The organic layer was washed sequentially with saturated solutions of KHSO<sub>4</sub>, NaHCO<sub>3</sub> and brine. Organic layer was then dried over Na<sub>2</sub>SO<sub>4</sub> and was evaporated under vacuum. The crude product was purified by column chromatography (eluent 50% AcOEt/pet. Ether, R<sub>f</sub>: 0.3) afforded **7** (1.3 g, 81%) as a white fluffy solid. mp: 82-84°C; [α]<sup>25.97</sup><sub>D</sub> = 84.44° (*c* = 0.046, CHCl<sub>3</sub>); IR (CHCl<sub>3</sub>) ν (cm<sup>-1</sup>) 3343, 3020, 2970, 2357, 1674, 1590, 1217, 764; <sup>1</sup>H NMR (400MHz, CDCl<sub>3</sub>) δ ppm 9.22 (bs, 1H), 8.30 (d, *J* = 6.6 Hz, 1H), 7.41 (t, *J* = 7.3 Hz 1H), 7.34 (d., *J* = 7.3 Hz, 1H), 7.23 (bs, 1H), 7.13 (t, *J* = 7.3 Hz, 1H), 5.56 (d, *J* = 7.1 Hz, 1H), 4.83 (m., 1H), 4.60 (m, 1H), 4.42 - 4.25 (m, 1H), 3.75 (s, 3 H), 3.49 (m, 1H), 3.40 (m., 1H), 2.30 (m, 3H), 2.01 (m., 1H), 1.94 - 1.69 (m, 3H), 1.67 - 1.56 (m, 1H), 1.43 (s, 9H), 1.00 - 0.94 (m, 9H), 0.92 (d, *J* = 6.8 Hz, 3H); <sup>13</sup>C NMR (100 MHz , CDCl<sub>3</sub>) δ ppm 172.3, 172.1, 171.6, 169.2, 155.3, 135.2, 130.6, 126.9, 125.9, 123.7, 79.4, 59.6, 57.3, 54.4, 52.2, 49.6, 41.6, 31.1, 28.2, 25.2, 24.8, 23.0, 21.6, 21.6, 19.1, 17.5; HRMS (ESI) C<sub>29</sub>H<sub>45</sub>N<sub>4</sub>O<sub>7</sub> calculated [M+H]<sup>+</sup>: 561.3210, found 560.3273, C<sub>29</sub>H<sub>44</sub>N<sub>4</sub>NaO<sub>7</sub> calculated [M+Na]<sup>+</sup> 583.3108, found 583.3091.

a)



b)





c)

D-TETRA\_151202142558 #115 RT: 0.51 AV: 1 NL: 1.40E9  
T: FTMS +p ESI Full ms [100.00-1500.00]

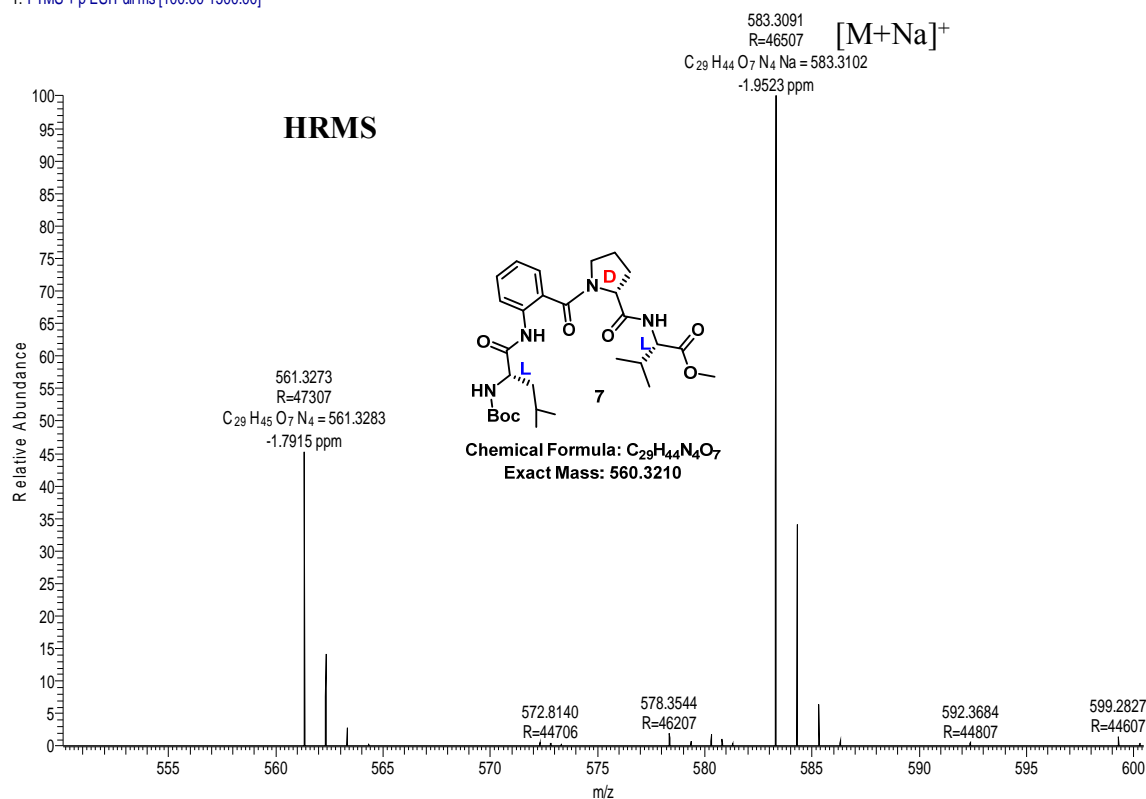
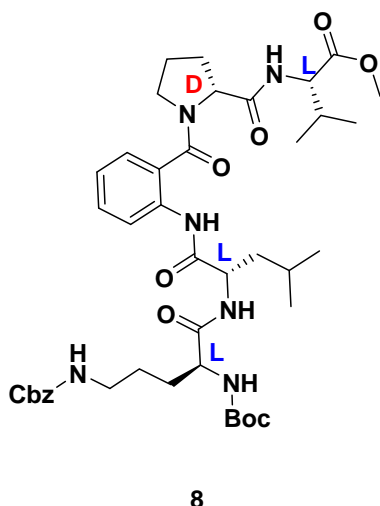


Figure 1.24 a) <sup>1</sup>H NMR, b) <sup>13</sup>C NMR and c) HRMS spectra of compound 7

### Compound 8 Boc-(z)<sup>L</sup>Orni<sup>L</sup>LeuAnt<sup>D</sup>ProVal-OMe:

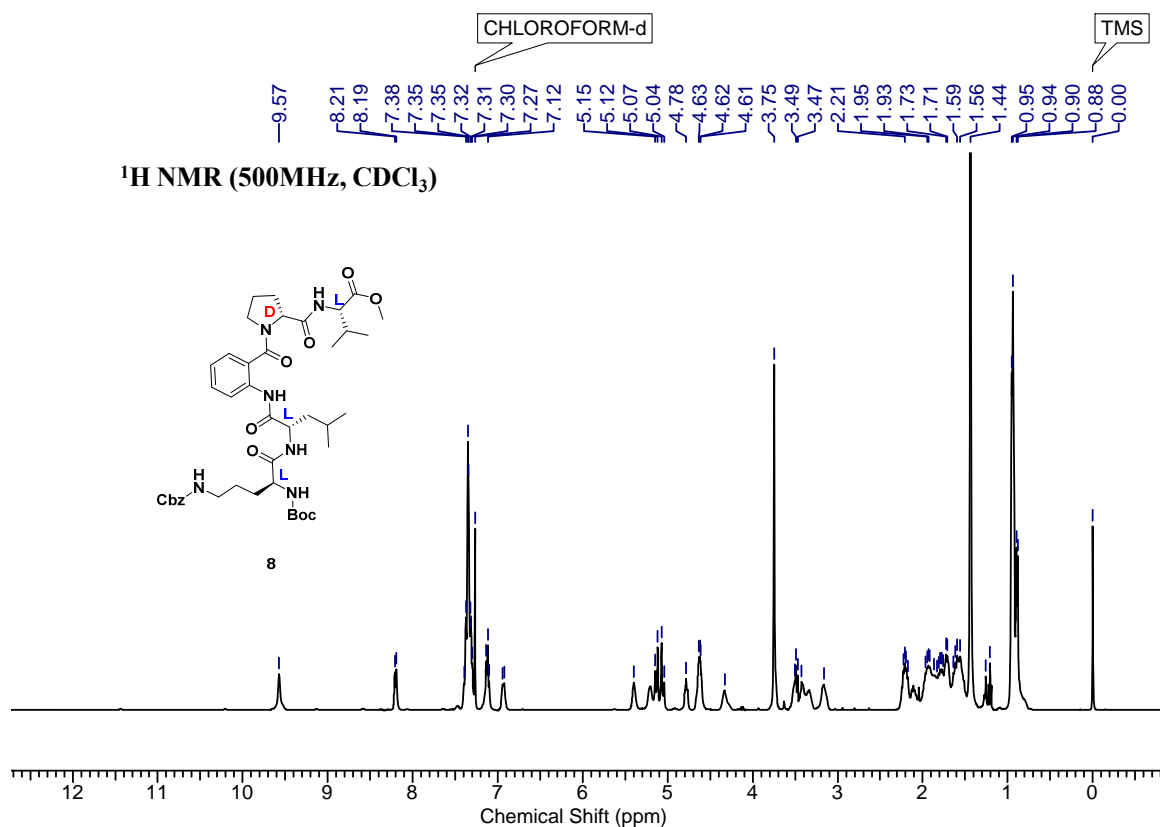


To a stirred solution of tetra-amine (H-<sup>L</sup>LeuAnt<sup>D</sup>ProVal-OMe) (1 g, 2.17 mmol, 1equiv.), and DIEA (1.33 mL, 4.34 mmol, 3 equiv.) in 20mL ACN, Boc-(z)<sup>L</sup>Orn-OH (0.96 g, 2.60 mmol, 1.2 equiv.) HBTU (1.643 g, 4.34 mmol, 2 equiv.) & catalytic amount of HOBT were added sequentially at 0 °C. This reaction mixture was then stirred for 8 h at rt. After completion of reaction, ACN was removed under reduced pressure and then the mixture was taken into ethyl acetate. The organic layer was washed sequentially with saturated solutions of

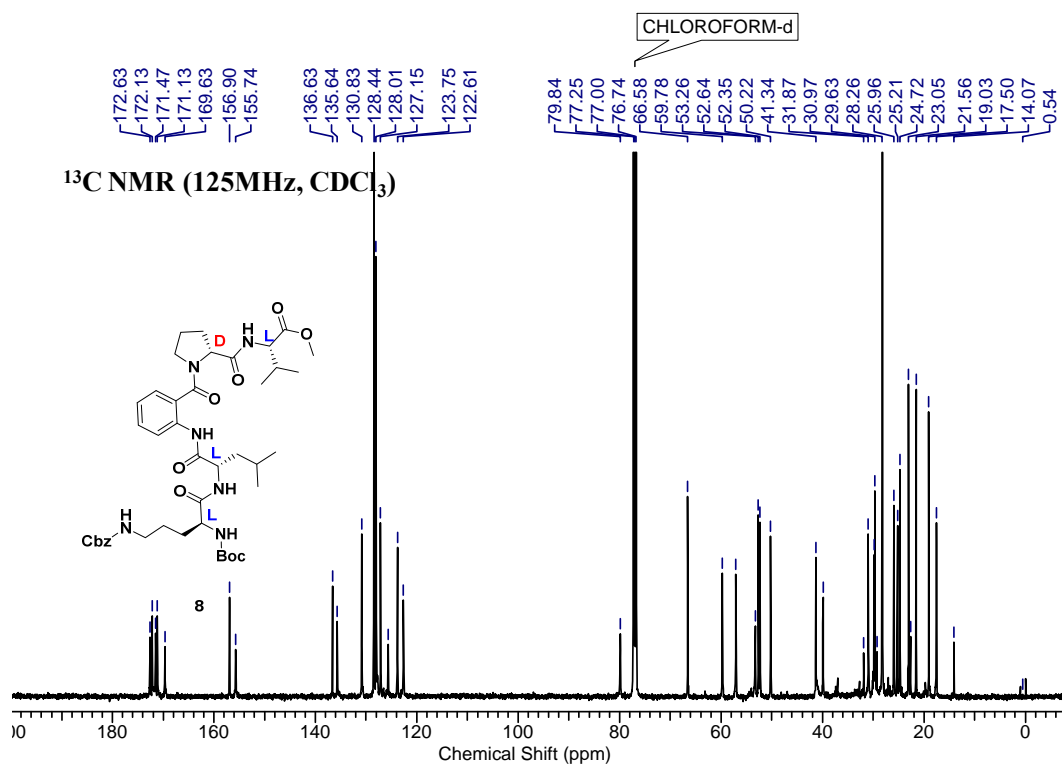
KHSO<sub>4</sub>, NaHCO<sub>3</sub> and brine. The organic layer was dried over Na<sub>2</sub>SO<sub>4</sub> and was evaporated under vacuum. The crude product was purified by column chromatography (eluent 60% AcOEt/pet. Ether, R<sub>f</sub>: 0.3) to furnish **9** (1.33 g, 76%) as a white fluffy solid.

mp: 90-92°C;  $[\alpha]^{25.60}_D = 52.59^\circ$  ( $c = 0.043$ ,  $\text{CHCl}_3$ ); IR ( $\text{CHCl}_3$ )  $\nu$  ( $\text{cm}^{-1}$ ): 3422, 3331, 3020, 2970, 2405, 2357, 1679, 1217, 764;  $^1\text{H}$  NMR (400MHz,  $\text{CDCl}_3$ )  $\delta$  ppm 9.57 (bs, 1H), 8.20 (d,  $J = 7.9$  Hz, 1H), 7.43 - 7.28 (m, 8H), 7.17 - 7.07 (m, 2H), 6.93 (d,  $J = 6.4$  Hz, 1H), 5.40 (bs, 1H), 5.20 (bs, 1H), 5.16 - 5.01 (dd, 11.90 Hz, 2H), 4.78 (m., 1H), 4.65 (m, 2H), 4.33 (m., 1H), 3.75 (s, 3H), 3.58 - 3.38 (m, 2H), 3.37 - 3.28 (m, 1H), 3.16 (m., 1H), 2.31 - 2.15 (m, 3H), 2.11 (m, 1H), 2.02 - 1.67 (m, 3H), 1.67 - 1.55 (m, 3H), 1.44 (s, 9), 0.95 (m, 9H), 0.89 (d,  $J = 6.7$  Hz, 3H);  $^{13}\text{C}$  NMR (125MHz,  $\text{CDCl}_3$ )  $\delta$  ppm 172.6, 172.1, 171.5, 171.1, 169.6, 156.9, 155.7, 136.6, 135.6, 130.8, 128.4, 128.0, 127.1, 125.6, 123.8, 122.6, 79.8, 66.6, 59.8, 57.1, 53.3, 52.6, 52.3, 50.2, 41.3, 39.9, 31.0, 29.8, 29.6, 28.3, 26.0, 25.2, 24.7, 23.1, 21.6, 19.0, 17.5; HRMS (ESI)  $\text{C}_{42}\text{H}_{60}\text{N}_6\text{O}_{10}$  calculated  $[\text{M}+\text{H}]^+$ : 809.4371, found 809.4429,  $\text{C}_{42}\text{H}_{60}\text{N}_6\text{NaO}_{10}$  calculated  $[\text{M}+\text{Na}]^+$  831.4269, found 831.4244.

a)



b)



c)

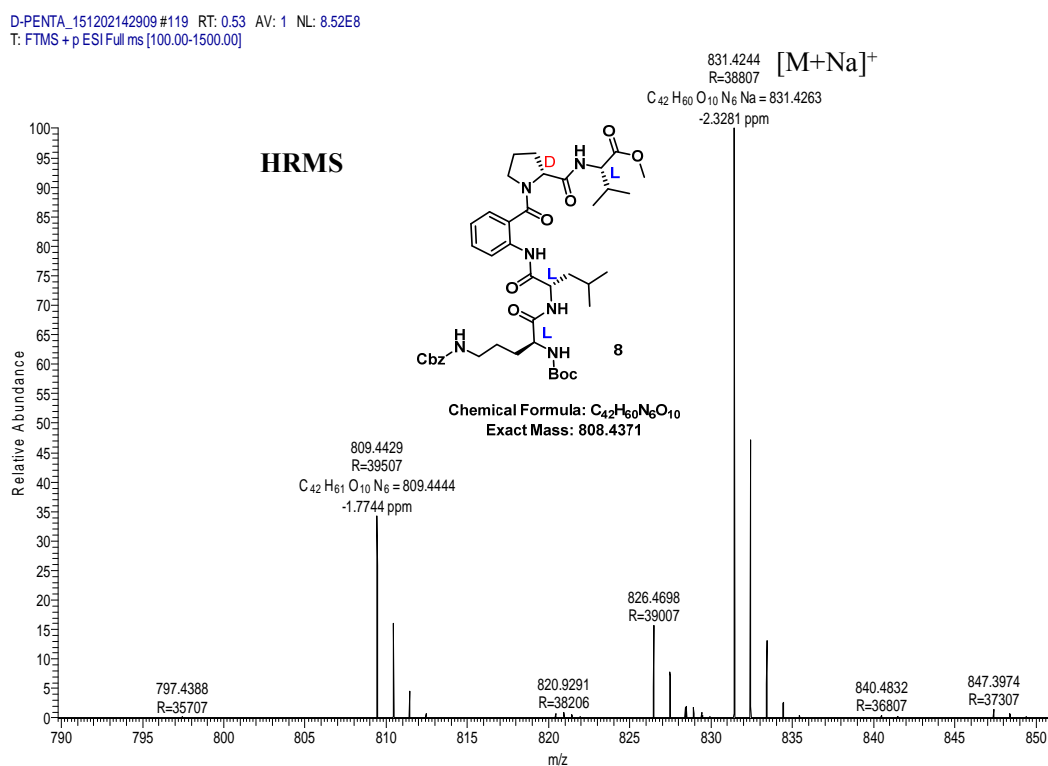
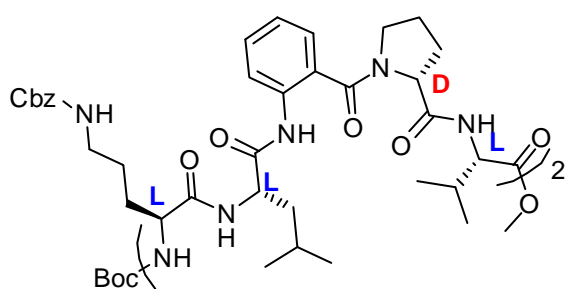


Figure 1.25 a) <sup>1</sup>H NMR, b) <sup>13</sup>C NMR and c) HRMS spectra of compound 8

**Hydrolysis of 8:** To a stirred solution of **8** in MeOH, LiOH:H<sub>2</sub>O (2 equiv.) in water, was added and reaction mixture was stirred for 8h. After complete consumption of starting material, MeOH was evaporated under vacuum and then mixture was acidified with KHSO<sub>4</sub> solution. The compound was then extracted with ethyl acetate and washed with water and brine. The ethyl acetate layer was dried over Na<sub>2</sub>SO<sub>4</sub> and was evaporated under reduced pressure. The penta-peptide acid (Boc-(z)<sup>L</sup>Orni<sup>L</sup>LeuAnt<sup>D</sup>ProVal-OH) **8a** was used for next reaction without further purification.

**Compound 9 Boc-((z)<sup>L</sup>Orni<sup>L</sup>LeuAnt<sup>D</sup>ProVal)<sub>2</sub>-OMe (Deca-peptide):** The deca-peptide



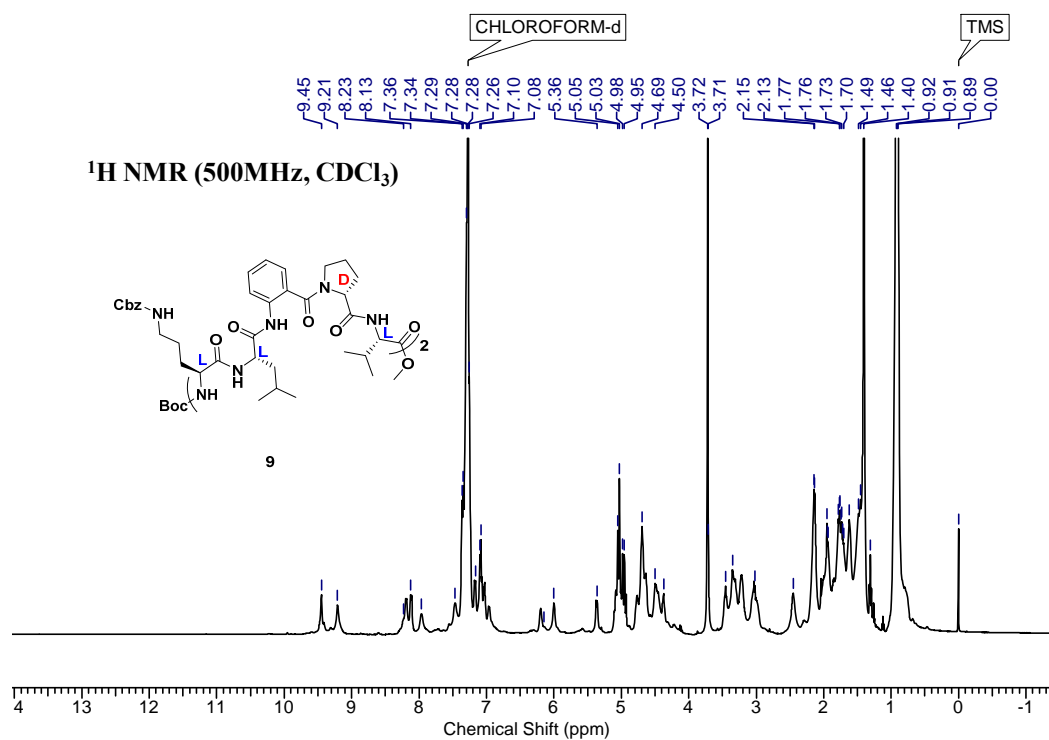
**9**

**9** was synthesized by segment doubling strategy from penta-peptide. To a stirred solution of **8a** (0.41 g, 0.56 mmol, 1 equiv.) and **8b** (0.4 g, 0.56 mmol, 1 equiv.) in 15 mL of ACN, HBTU (0.43 g, 1.16 mmol, 2 equiv.) & DIEA (0.3 mL, 1.6 mmol, 3 equiv.) were added at 0 °C. The reaction mixture was then stirred for 8 h at

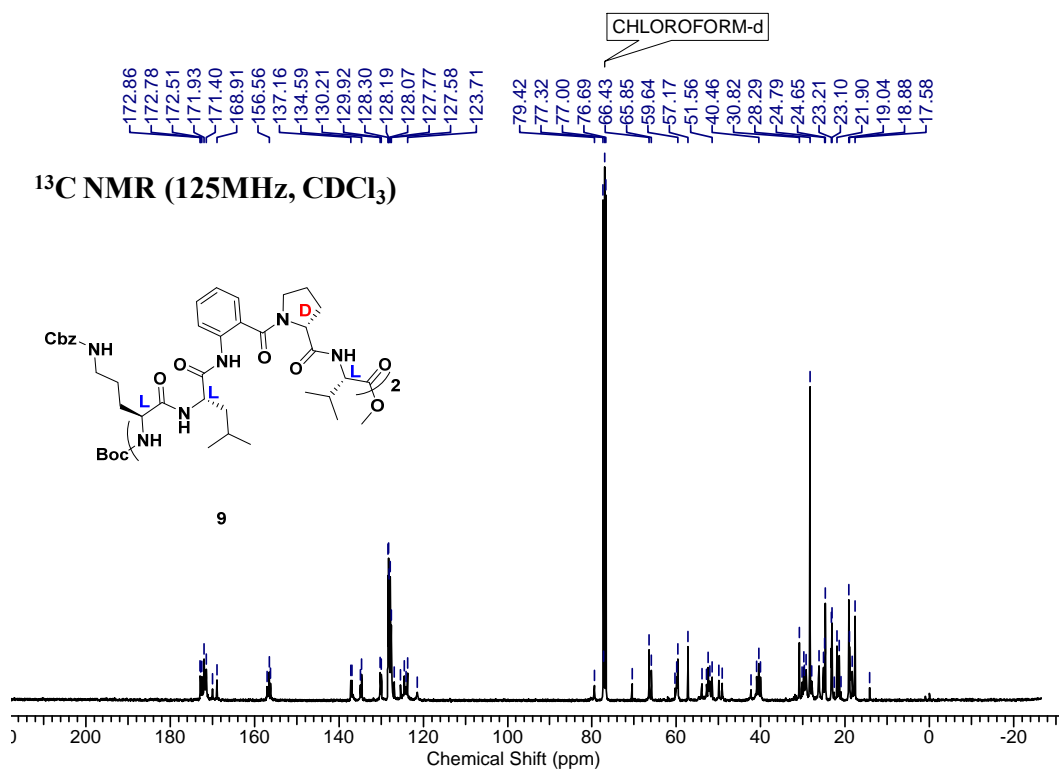
room temperature. After completion of reaction, ACN was removed under reduced pressure and then the mixture was taken into ethyl acetate. The organic layer was washed sequentially with saturated solutions of KHSO<sub>4</sub>, NaHCO<sub>3</sub> and brine. The organic layer was dried over Na<sub>2</sub>SO<sub>4</sub> and was evaporated under vacuum. The crude product was purified by column chromatography (eluent 70% AcOEt/pet. Ether, R<sub>f</sub>: 0.3) to furnish **9** (0.57 g, 69%) as a white fluffy solid. mp: 126-128°C; [ $\alpha$ ]<sup>25.64</sup><sub>D</sub> = 33.4824° (*c* = 0.012, CHCl<sub>3</sub>); IR (CHCl<sub>3</sub>)  $\nu$  (cm<sup>-1</sup>) 3297, 3071, 2962, 2357, 1646, 1538, 1252, 1160, 761; <sup>1</sup>H NMR (500 MHz, CDCl<sub>3</sub>)  $\delta$  ppm 9.45 (bs, 1H), 9.21 (bs, 1H), 8.19 (d, *J* = 6.7 Hz, 1H), 8.13 (d, *J* = 7.6 Hz., 1H), 7.96 (bs, 1H), 7.46 (t, *J* = 6.7 Hz, 1H), 7.41 - 7.19 (m, 14H), 7.17 (d, *J* = 7.0 Hz, 1H), 7.12 - 7.05 (m, 2H), 7.03 (d, *J* = 7.0 Hz, 1H), 6.96 (d, *J* = 6.1 Hz, 1H), 6.20 (bs, 1H), 6.00 (bs, 1H), 5.36 (dd, *J* = 8.54 Hz, 1H), 5.16 - 4.90 (m, 5H), 4.77 (m., 1H), 4.72 - 4.60 (m, 3H), 4.48 (m, 2H), 4.37 (m., 1H), 3.71 (s., 3H), 3.45 (m., 1H), 3.35 (m., 3H), 3.22 (m, 2H), 3.02 (m, 2H), 2.45 (bs, 2H), 2.14 (m, 5H), 2.03 - 1.88 (m, 8H), 1.62 (m, 4H), 1.49-1.46 (m, 5H), 1.43 (S, 9H), 0.97 - 0.84 (m, 24H). <sup>13</sup>C NMR (101 MHz, CDCl<sub>3</sub>)  $\delta$  ppm 172.9, 172.8, 172.5, 171.9, 171.5, 171.4, 170.0, 168.9, 157.0, 156.6, 156.2, 137.2, 136.9, 135.0, 134.6, 130.2, 129.9, 128.3, 128.2, 128.1, 127.8, 127.7, 127.6,

126.8, 125.4, 124.5, 124.1, 123.7, 121.4, 79.4, 70.5, 66.4, 65.8, 60.3, 59.9, 59.6, 53.9, 52.8, 52.2, 51.8, 51.6, 50.0, 49.1, 42.3, 40.9, 40.5, 40.0, 30.8, 30.2, 29.7, 29.2, 28.3, 27.8, 26.3, 26.2, 25.1, 24.8, 24.7, 23.2, 23.1, 21.9, 21.4, 19.0, 18.9, 18.3, 17.6. HRMS (ESI)  $C_{78}H_{108}N_{12}O_{17}$  calculated  $[M+H]^+$ : 1485.7955, found 1485.8007.

a)



b)



c)

D-DECA #152 RT: 0.67 AV: 1 NL: 2.48E7  
T: FTMS + p ESI Full ms [100.00-1500.00]

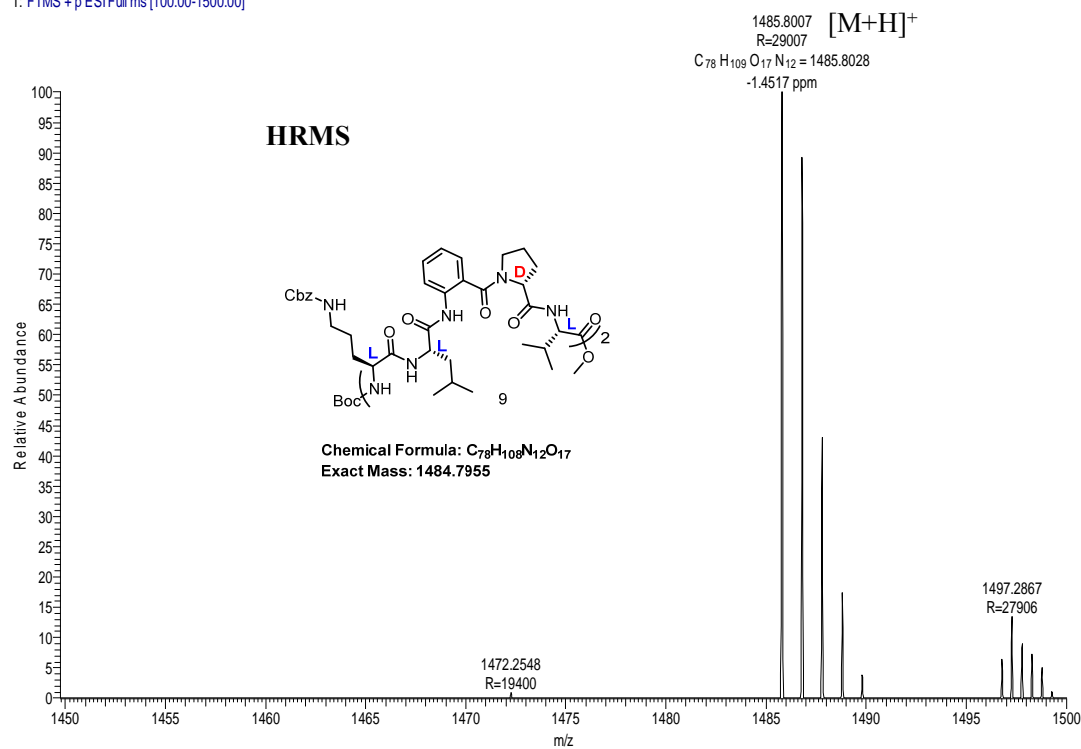
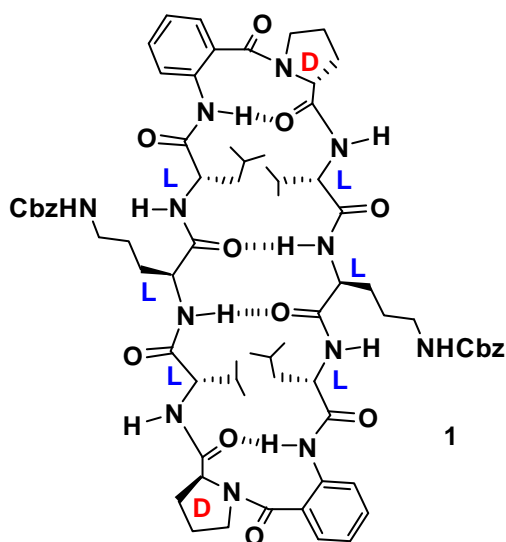


Figure 1.26 a) <sup>1</sup>H NMR, b) <sup>13</sup>C NMR and c) HRMS spectra of compound 9

**Hydrolysis of 9:** Following the hydrolysis procedure of **8**, compound **9** was hydrolyzed to Boc-((z)<sup>L</sup>Orn<sup>L</sup>LeuAnt<sup>D</sup>ProVal)<sub>2</sub>-OH (i.e. Boc-Deca-OH).

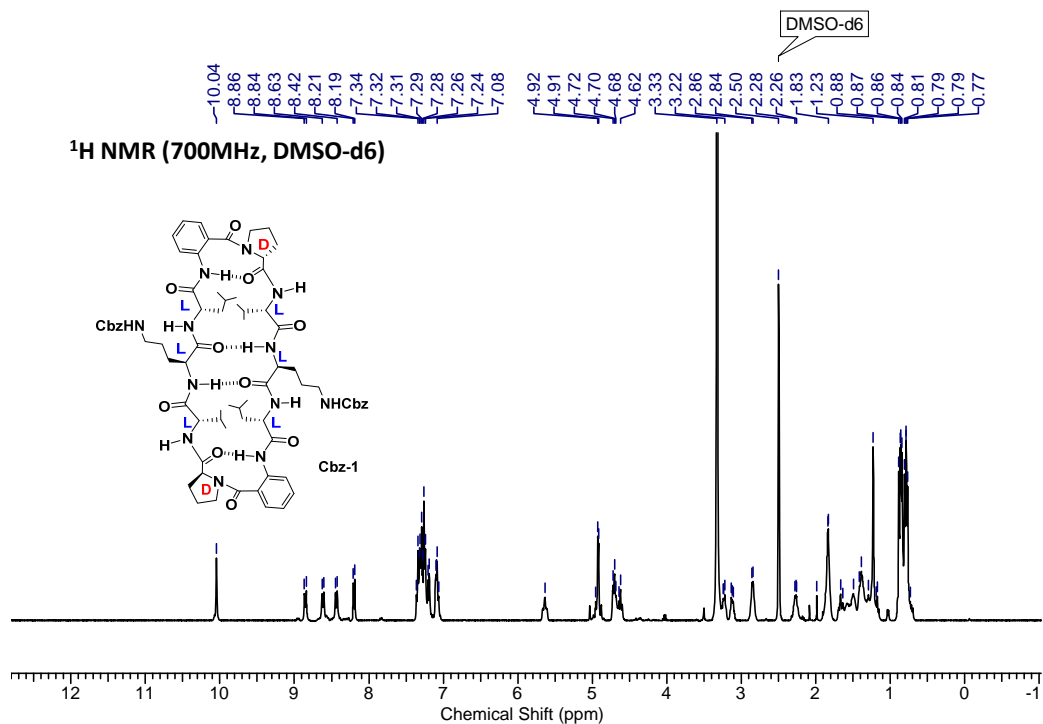
**Compound 1 (Cbz-GS1):** Cyclo-((z)<sup>L</sup>Orn<sup>L</sup>LeuAnt<sup>D</sup>ProVal)<sub>2</sub>; Boc-Deca-OH was



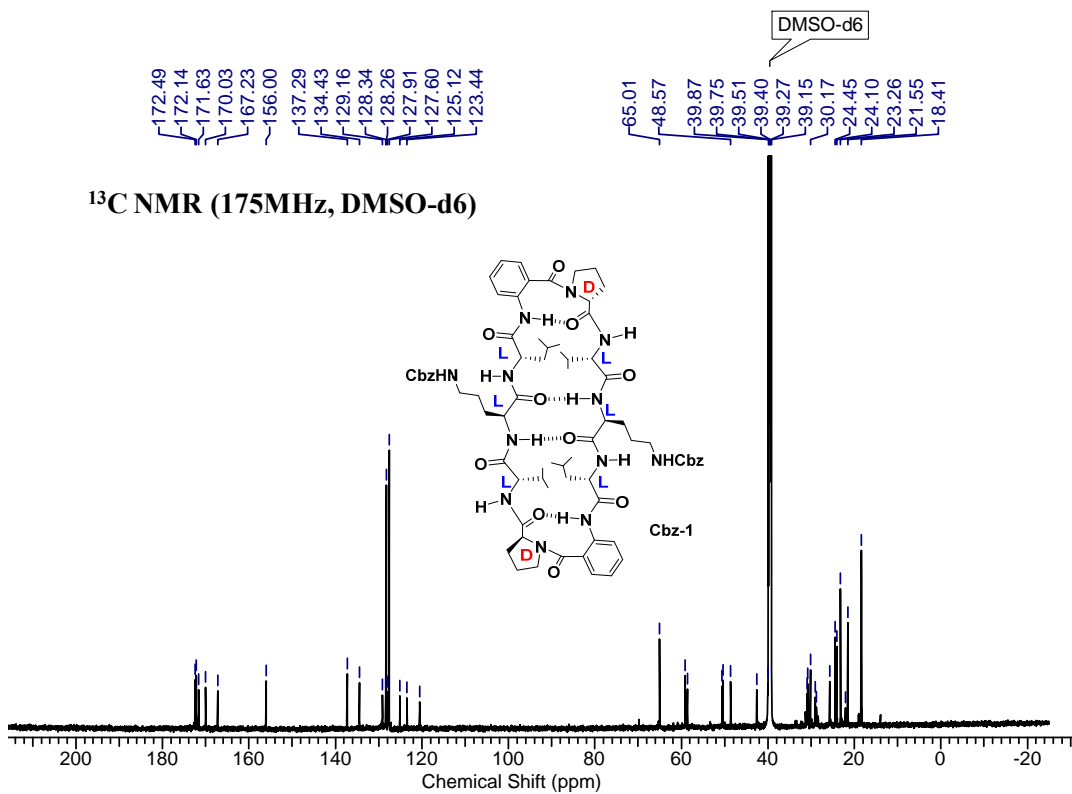
stirred in TFA:DCM (1:1) solution for 30 minutes. After deprotection, solution was evaporated under reduced vacuum and resulted solid TFA salt of H-Deca-OH which was then dried under high vacuum pump. This TFA salt of H-Deca-OH (0.08 g, 0.055 mmol, 1 equiv.) was taken in 10 mL DCM and stirred for 5 min at 0 °C, to this reaction mixture DIEA (0.04mL, 0.033 mmol, 4 equiv.) was added. Later, HBTU (0.042 g, 0.011, 2 equiv.) and HOBT (catalytic amount) were added into the reaction mixture

and then reaction mixture was stirred for overnight at room temperature. After completion of reaction, the reaction mixture was diluted with DCM and washed with saturated solutions of KHSO<sub>4</sub>, NaHCO<sub>3</sub> and brine. The organic layer was dried over Na<sub>2</sub>SO<sub>4</sub> and was evaporated under vacuum. The crude product was purified by column chromatography (eluent 2% methanol/DCM, R<sub>f</sub>: 0.3) to furnish compound **1** (0.037 g, 50%) as a white fluffy solid. mp: 284-286°C; [ $\alpha$ ]<sup>25.64</sup><sub>D</sub> - 87.08° (*c* = 0.007, CHCl<sub>3</sub>); IR (CHCl<sub>3</sub>)  $\nu$  (cm<sup>-1</sup>) 3418, 3022, 2966, 2930, 2869, 2405, 2357, 1641, 1544, 1421, 1216, 765, 670; <sup>1</sup>H NMR (700MHz, DMSO-d<sub>6</sub>)  $\delta$  ppm 10.04 (s, 2H), 8.85 (d, *J* = 9.3 Hz, 2H), 8.62 (d, *J* = 9.5 Hz, 2H), 8.44 (d, *J* = 9.5 Hz, 2H), 8.20 (d, *J* = 8.3 Hz, 2H), 7.38 - 7.22 (m, 14H), 7.20 (d, *J* = 7.6 Hz, 2H), 7.12 (m, 2H), 7.10 (t, *J* = 7.6 Hz, 2H), 5.70 (m, 2H), 5.01 (m, 2H), 4.75 - 4.66 (m, 4H), 4.62 (m, 2H), 3.23(m, 2H), 3.17(m, 2H), 2.85 (m, 4H), 2.35 (m, 2H), 1.90-1.80(m, 8H), 1.72 (m, 2H), 1.60- 1.45 (m., 5H), 1.44-1.33 (m, 5H), 1.29 (m, 2H), 0.88 (d, *J* = 6.6 Hz, 6H), 0.85 (d, *J* = 6.6 Hz, 6H), 0.80 (d, *J* = 7.3 Hz, 6H), 0.78 (d, *J* = 7.3 Hz, 6H); <sup>13</sup>C NMR (175 MHz, DMSO-d<sub>6</sub>)  $\delta$  ppm 172.5, 172.2, 171.6, 170.0, 167.23, 156.0, 137.2, 134.4, 129.2, 128.3, 128.2, 127.9, 127.6, 125.1, 123.4, 120.5, 65.0, 59.3, 58.6, 50.6, 50.3, 48.6, 42.5, 31.3, 31.0, 30.8, 30.2, 29.0, 25.7, 24.4, 24.1, 23.3, 21.5, 18.41; HRMS (ESI) C<sub>72</sub>H<sub>96</sub>N<sub>12</sub>O<sub>14</sub> calculated [M+H]<sup>+</sup> 1353.7169 found 1353.7225, C<sub>72</sub>H<sub>96</sub>N<sub>12</sub>NaO<sub>14</sub> calculated [M+Na]<sup>+</sup> 1375.7067, found 1375.7036.

a)



b)





c)

GS-1 #205 RT: 0.91 AV: 1 NL: 5.10E7  
T: FTMS +p ESI Full ms [100.00-1500.00]

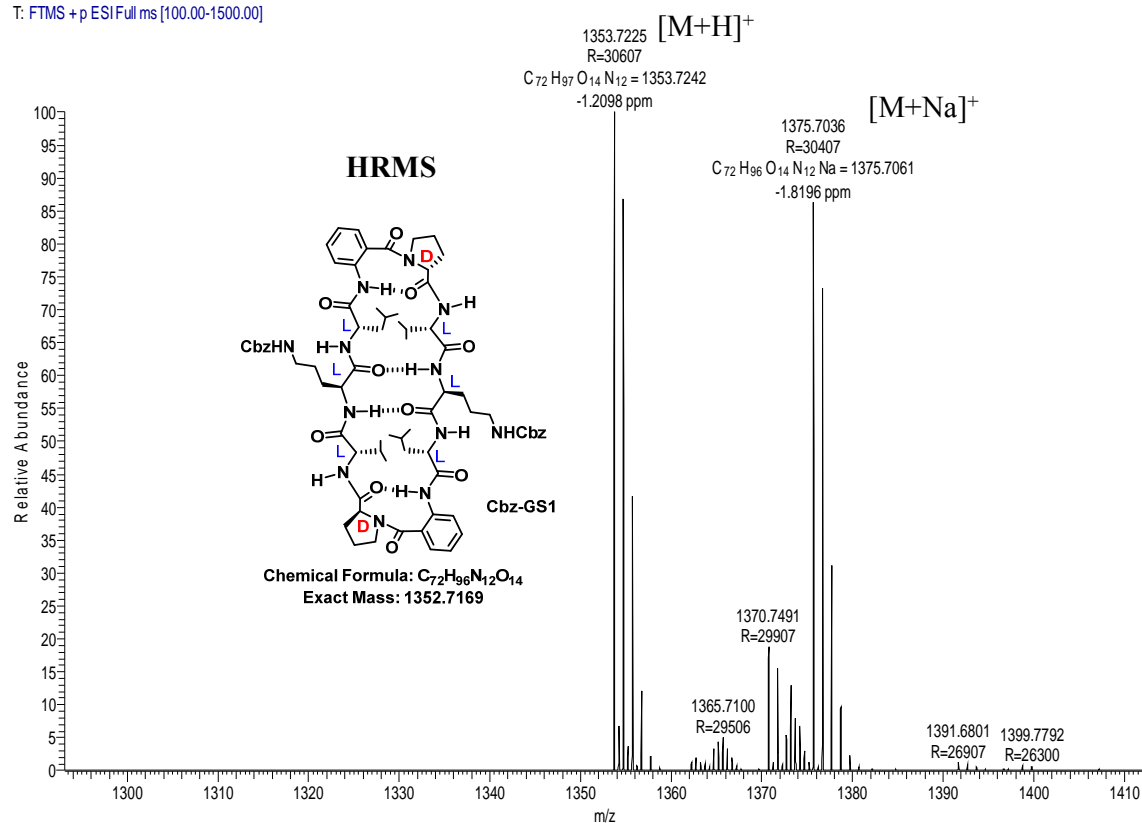


Figure 1.27 a)  $^1H$  NMR, b)  $^{13}C$  NMR and c) HRMS spectra of compound 1

**Procedure for Cbz deprotection and HCl salt formation of 1:** The Cbz protecting groups in **Cbz-1** was successfully removed by hydrogenolysis in the presence of 10% Pd/C in a 0.02 M HCl/MeOH solution. After deprotection, reaction mixture was filtered through celite pad and then filtrate was evaporated under vacuum which resulted to a colorless solid; HRMS (ESI)  $C_{72}H_{96}N_{12}O_{14}$  calculated  $[M]^+$  1084.6433 found 1084.6481,  $C_{72}H_{97}N_{12}O_{14}$  calculated  $[M+H]^+$  1085.6433, found 1085.6553.

H2GS-1 #119 RT: 0.53 AV: 1 NL: 8.40E6  
T: FTMS + p ESI Full ms [100.00-1500.00]

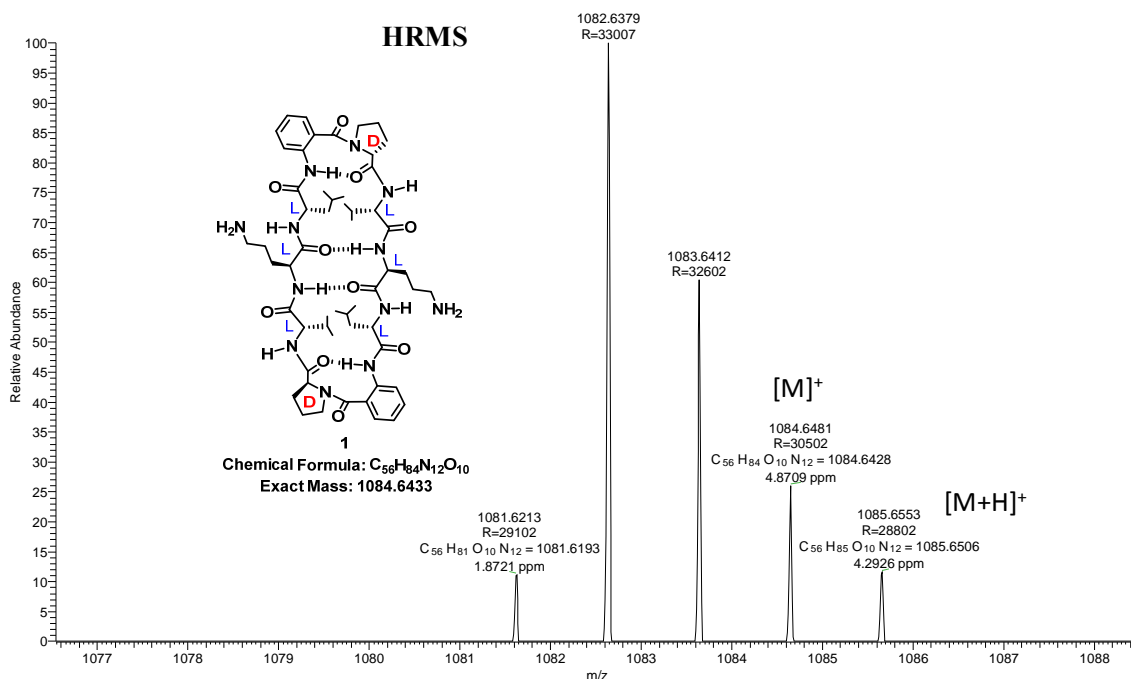
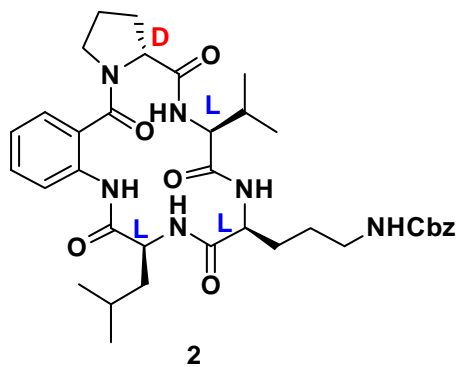


Figure 1.28) HRMS spectrum of free amine **1**

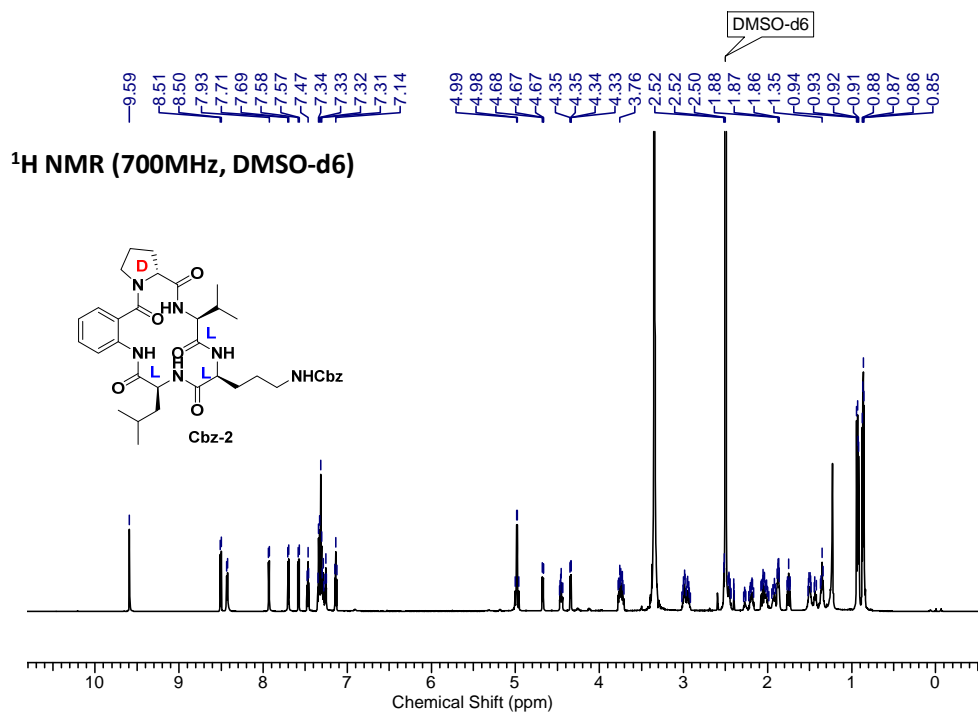
**Compound 2** Cyclo-((z)<sup>L</sup>Orni<sup>L</sup>LeuAnt<sup>D</sup>ProVal); Cyclic compound **2** was prepared using



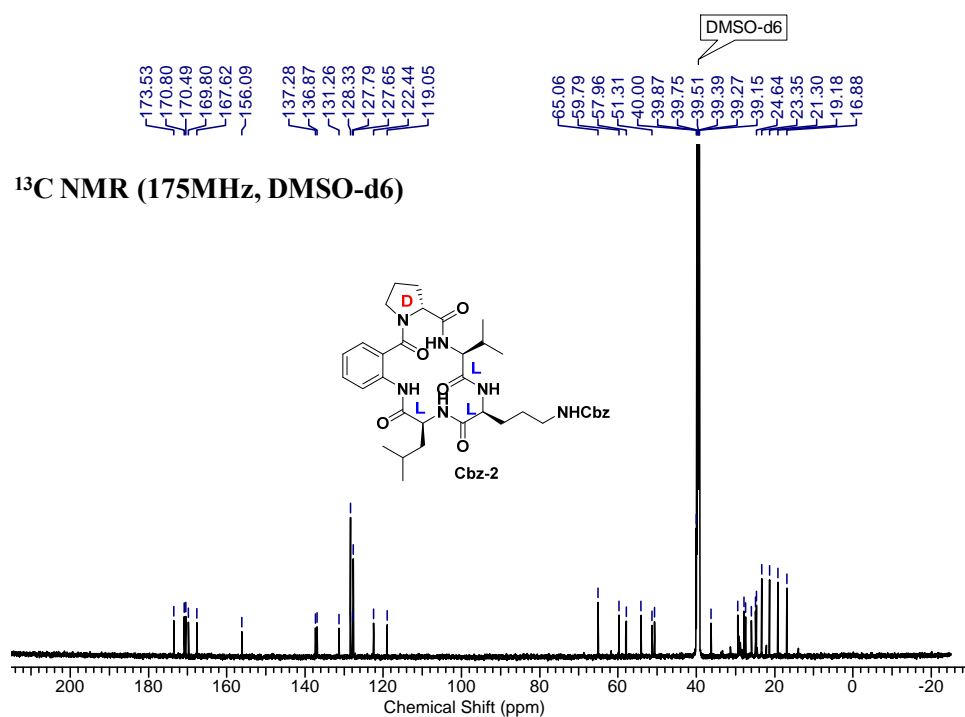
same procedure of **1**, which purified by column chromatography (eluent 60% AcOEt/pet. Ether, R<sub>f</sub>: 0.3) to furnish compound **1** yielded (60%) as a white fluffy solid. mp: 138-140°C;  $[\alpha]^{25.64}_D - 162.6^\circ$  ( $c = 0.01$ , CHCl<sub>3</sub>); IR (CHCl<sub>3</sub>)  $\nu$  (cm<sup>-1</sup>) 3331, 2959, 2874, 2357, 1668, 1591, 1532, 1421, 763; <sup>1</sup>H NMR (700 MHz, DMSO-*d*<sub>6</sub>)  $\delta$  ppm 9.59 (s, 1H), 8.52 (d,  $J = 7.9$  Hz, 1H), 8.43 (d,  $J = 8.4$  Hz, 1H), 7.70 (d,  $J = 9.5$  Hz, 1H), 7.58 (dd,  $J = 1.4, 7.6$  Hz, 1H), 7.47 (dt,  $J = 1.1, 8.6$  Hz, 1H), 7.36 - 7.27 (m, 3H), 7.26 (t,  $J = 5.7$  Hz, 1H), 7.14 (dt,  $J = 1.1, 7.5$  Hz, 1H), 4.91 (m, 2H), 4.67 (m, 1H), 4.46 (m, 2H), 4.34 (dd,  $J = 3.7$  Hz, 8.4 Hz, 1H), 3.79 (m, 2H), 3.06 (m, 2H), 2.48 (m, 1H), 2.30 - 2.15 (m, 2H), 2.10 - 1.98 (m, 2H), 1.95 (m, 1H), 1.90 - 1.85 (m, 2H), 1.75 (m, 1H), 1.56 (m, 2H), 1.47 (m, 1H), 0.94 (d,  $J = 7.1$  Hz, 3H), 0.92 (d,  $J = 7.1$  Hz, 3H), 0.87 (d,  $J = 6.7$  Hz, 3H), 0.86 (d,  $J = 6.7$  Hz, 3H); <sup>13</sup>C NMR (175MHz, DMSO-*d*<sub>6</sub>)  $\delta$  ppm 173.5, 170.8, 170.5, 169.8, 167.6, 156.1, 137.3, 136.9, 131.3, 128.3, 127.8, 127.7, 127.7, 122.5, 122.4, 119.1, 65.1, 59.9, 58.0, 54.1, 51.3, 50.7, 36.2, 29.4,

29.0, 27.8, 27.4, 25.9, 24.9, 23.3, 21.3, 19.2, 16.9; HRMS (ESI)  $C_{36}H_{48}N_6O_7$  calculated  $[M+H]^+$  676.3584, found 676.3647,  $C_{36}H_{48}N_6NaO_7$  calculated  $[M+Na]^+$  699.3482, found 699.3450

a)



b)



c)

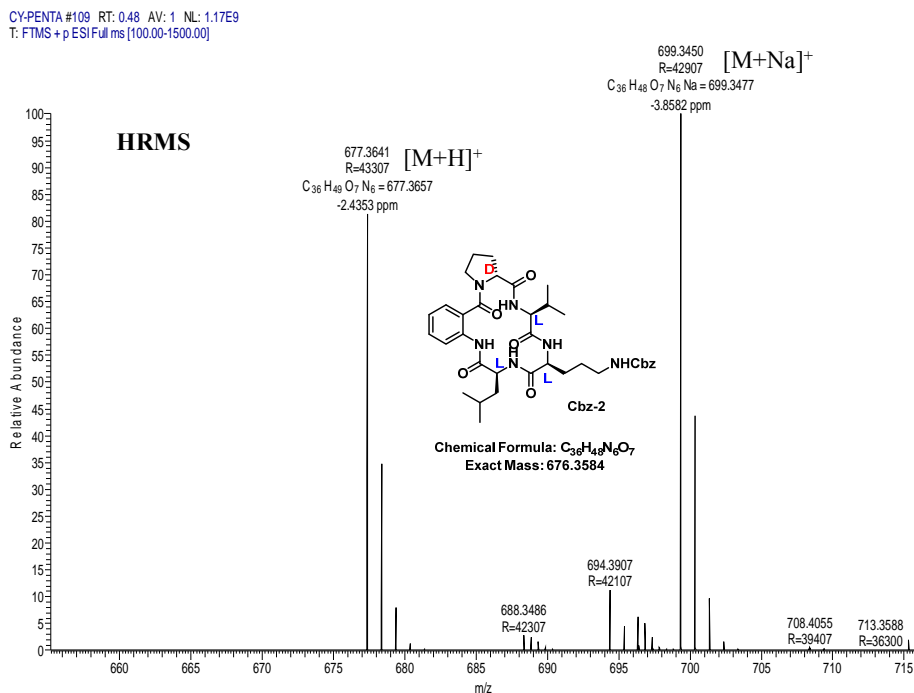


Figure 1.29 a) <sup>1</sup>H NMR, b) <sup>13</sup>C NMR and c) HRMS spectra of compound 2

**Cbz deprotection procedure and HCl salt formation of 2:** Following the same procedure Cbz deprotection of 1, compound 2 was deprotected and HCl salt of 2 was formed as a colorless solid; HRMS (ESI) C<sub>28</sub>H<sub>42</sub>N<sub>6</sub>O<sub>5</sub> calculated [M]<sup>+</sup> 542.3217 found 542.2968, C<sub>28</sub>H<sub>43</sub>N<sub>6</sub>O<sub>5</sub> calculated [M+H]<sup>+</sup> 542.3217, found 542.3283.

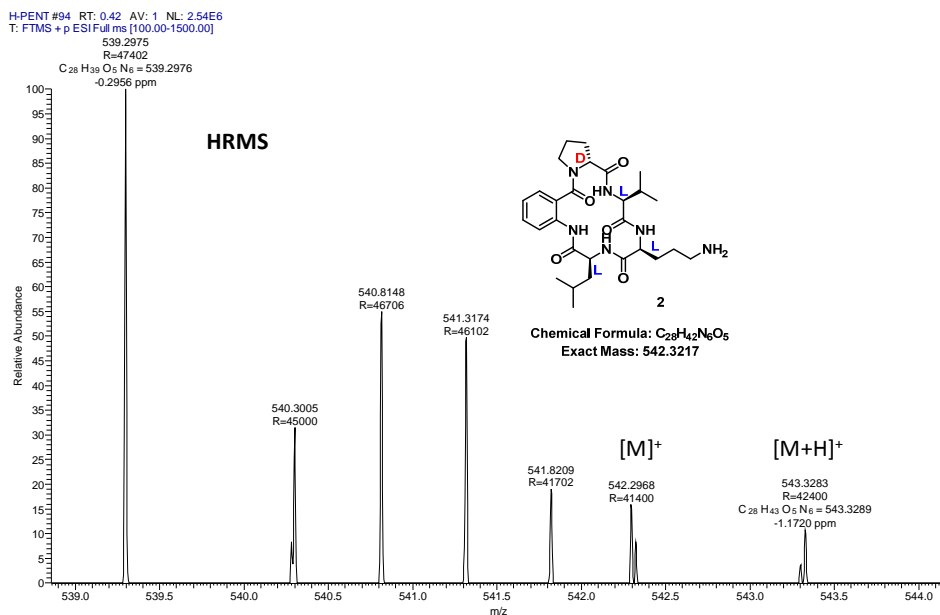
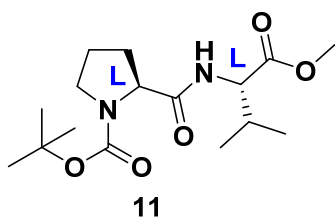


Figure 1.30 HRMS spectra of free amine 2

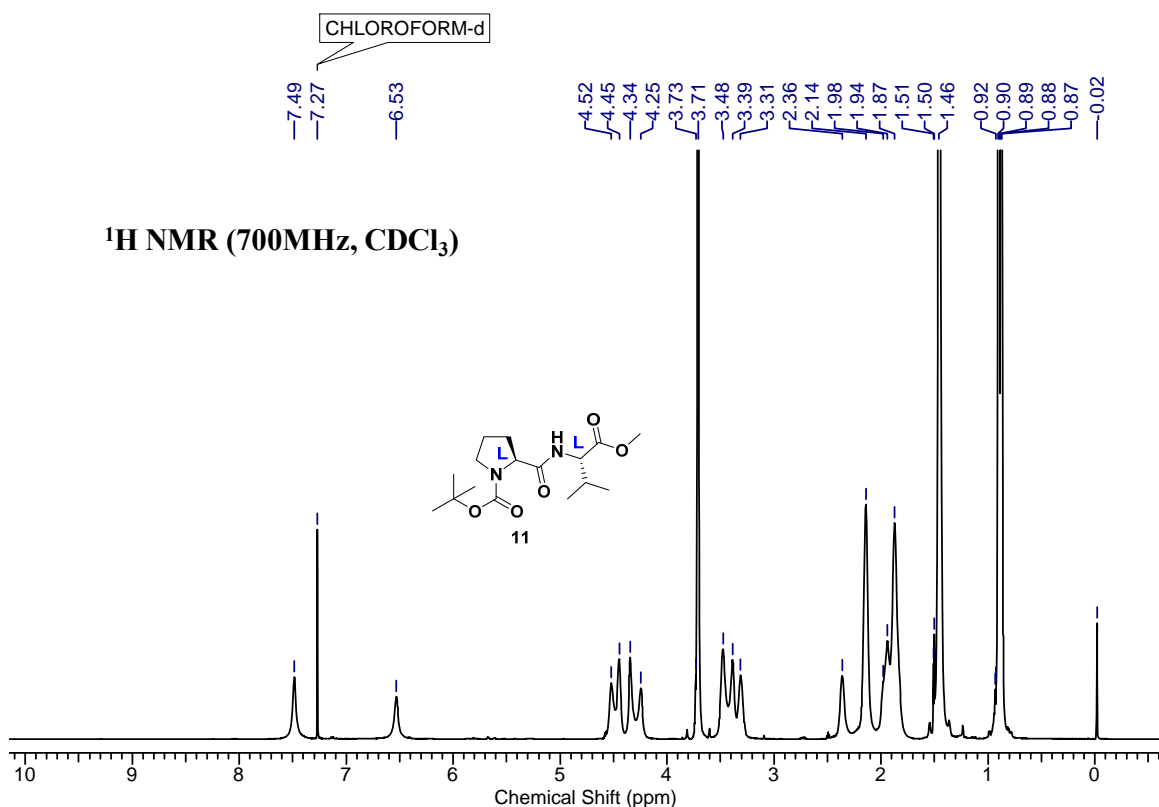
**Compound 11 (Boc-L-Pro<sup>L</sup>-Val-OMe):** Following the same procedure for synthesis of



compound **5**, compound **11** was synthesized. Purification was done by column chromatography (eluent 20% AcOEt/Pet. Ether, R<sub>f</sub>: 0.3) afforded **11** (6.4 g, 85%) as a white fluffy solid material; Mp: 66-68°C [ $\alpha$ ]<sup>25.97</sup><sub>D</sub> = -85.09° (*c* = 0.09, CHCl<sub>3</sub>; IR (CHCl<sub>3</sub>)  $\nu$  (cm<sup>-1</sup>): 3324, 2970, 2884, 2357, 1743, 1689, 1534,

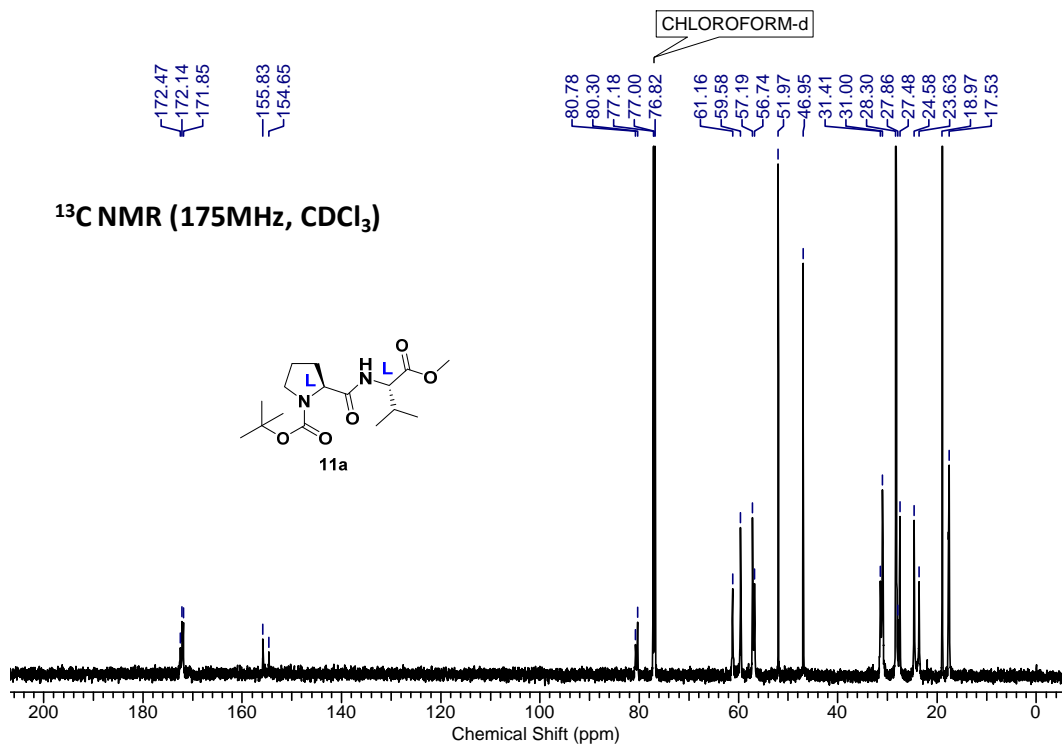
1398, 1166, 761; <sup>1</sup>H NMR (700MHz, CDCl<sub>3</sub>)  $\delta$  ppm 7.49 (bs, rota. NH), 6.53 (bs, rota. NH), 4.60 (m, 1 H), 4.37 (m, 1 H), 3.71 (s, 3 H), 3.52 - 3.24 (m, 2 H), 2.36 (bs, rota. H), 2.14 (bs, rota. 2 H), 2.02 - 1.75 (m, 3H), 1.46 (bs, 9 H), 0.90 (d, *J* = 6.7 Hz, 3 H), 0.87 (d, *J* = 6.4 Hz, 3 H); <sup>13</sup>C NMR (175 MHz, CDCl<sub>3</sub>)  $\delta$  ppm 172.5 (rota), 172.0, 172.1 (rota), 171.8, 155.8, 154.6 (rota), 80.8 (rota), 80.3, 61.2 (rota), 59.6, 57.2, 56.7 (rota), 52.0, 46.9 (rota), 31.4 (rota), 31.2, 28.3, 27.5 (rota), 24.6, 23.6 (rota), 19.0, 17.6 (rota), 17.5. HRMS (ESI) C<sub>16</sub>H<sub>30</sub>N<sub>2</sub>O<sub>5</sub> calculated [M+H]<sup>+</sup>: 329.1998, found 329.2062, C<sub>16</sub>H<sub>28</sub>N<sub>2</sub>NaO<sub>5</sub> calculated [M+Na]<sup>+</sup> 351.1896, found 351.1881.

a)



Note: Extra signals or signal broadening are seen due to rotamer (minor conformer) formation at N-terminus of proline residue (*Chem. Eur. J.* 2008, **14**, 6192).

b)



c)

L-DI\_151202144813 #105 RT: 0.46 AV: 1 NL: 3.30E9  
T: FTMS + p ESI Full ms [100.00-1500.00]

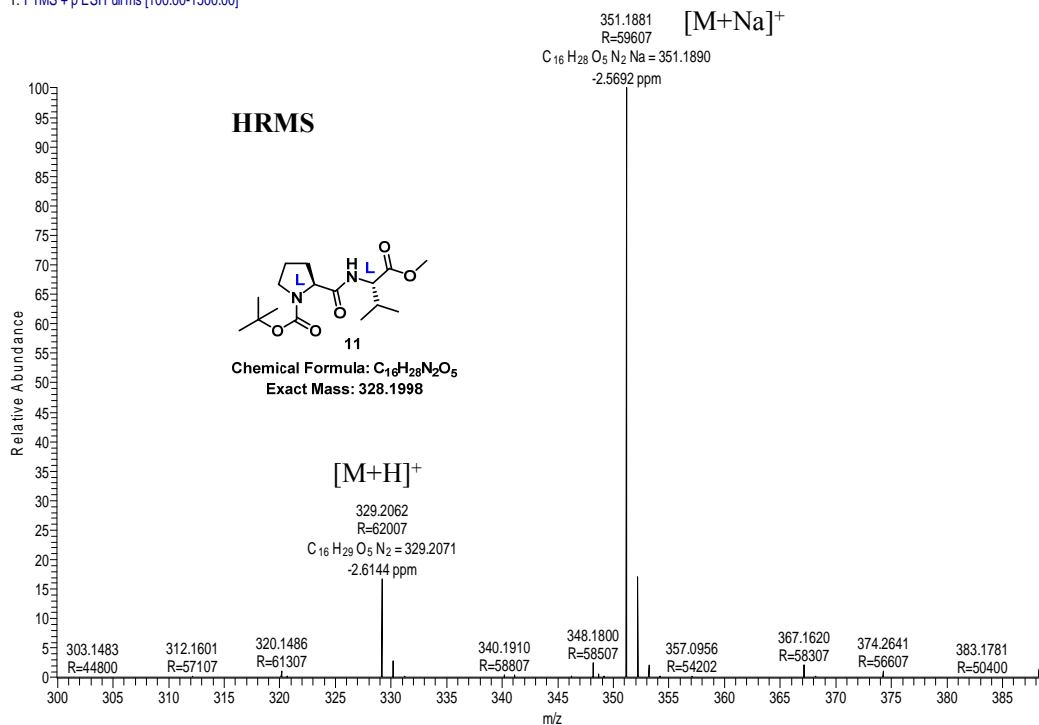
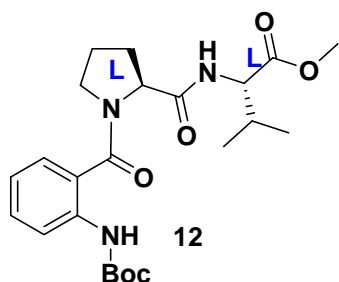


Figure 1.31 a) <sup>1</sup>H NMR, b) <sup>13</sup>C NMR and c) HRMS spectra of compound 11

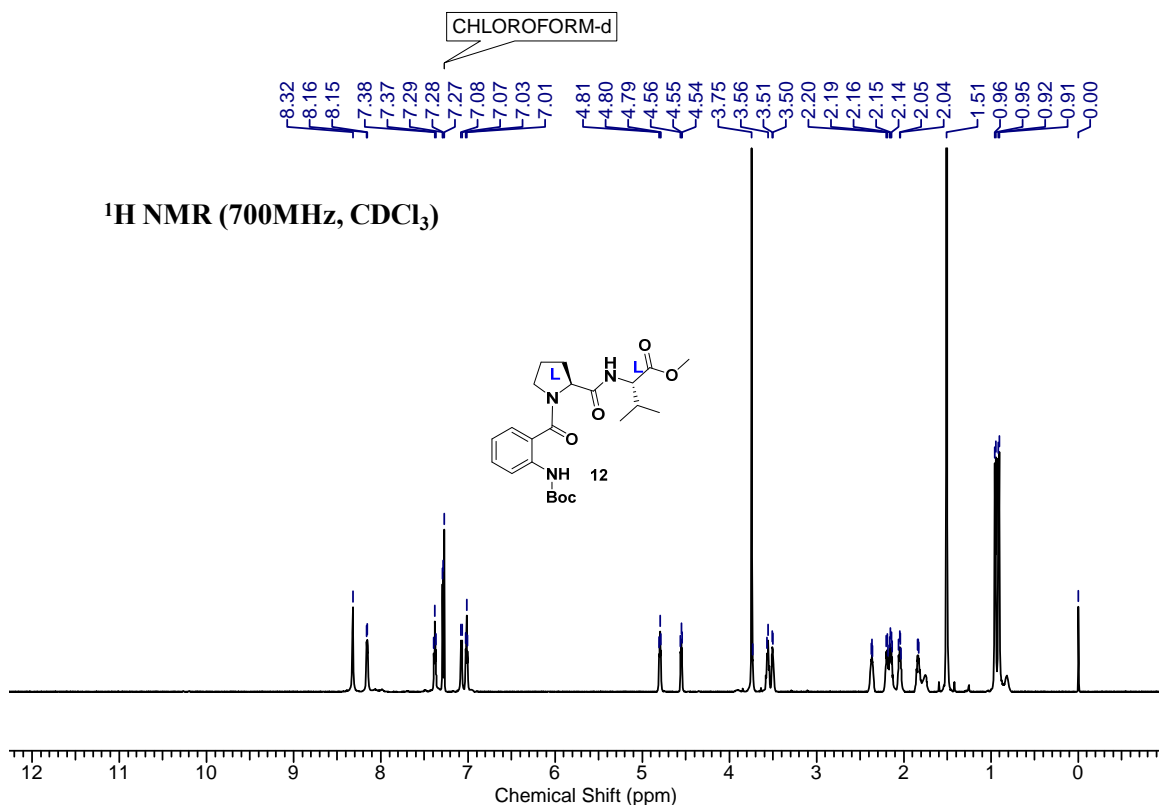
**Compound 12 (Boc-Ant<sup>L</sup>Pro<sup>L</sup>Val-OMe):** Following the same synthetic procedure of **6**,



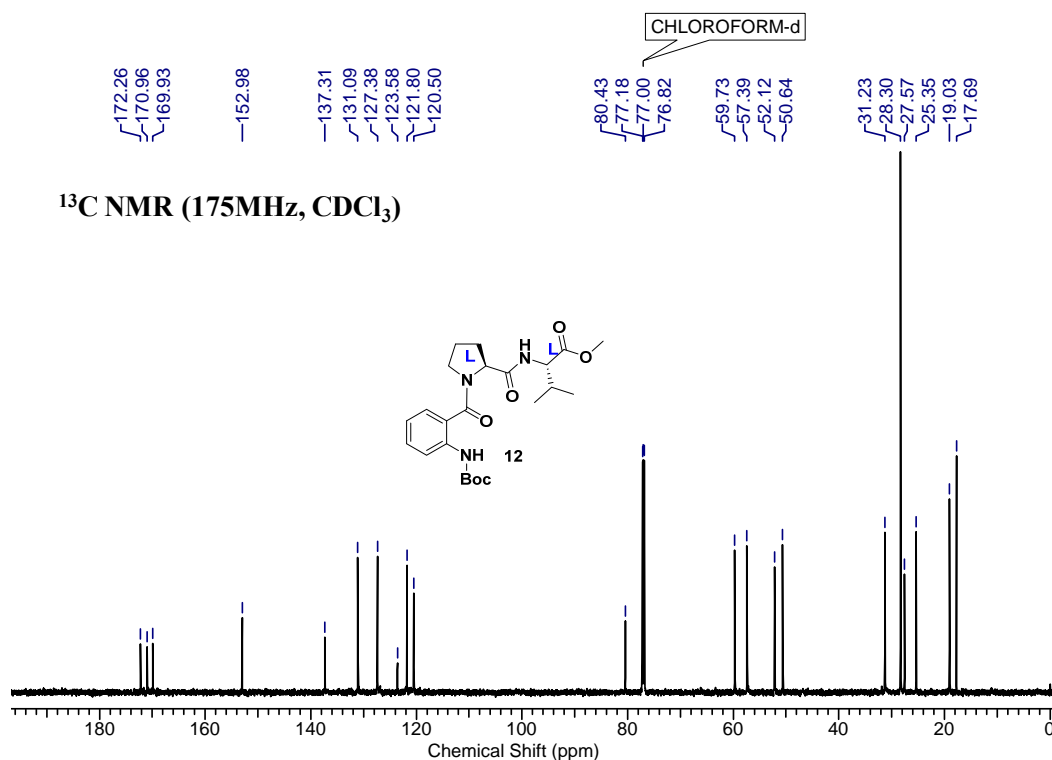
compound **12** was synthesized and purification was done by column chromatography (eluent 15-20% AcOEt/Pet. Ether,  $R_f$ : 0.3) afforded **12** (3.5 g, 90%) as a white fluffy solid material; Mp: 110-112°C  $[\alpha]^{25.95}_D = -106.1^\circ$  ( $c = 0.03$ ,  $\text{CHCl}_3$ ); IR ( $\text{CHCl}_3$ )  $\nu$  ( $\text{cm}^{-1}$ ): 3331, 2971, 2888, 2357, 1820, 1728, 1675, 1623, 1595, 1160, 779;  $^1\text{H}$  NMR (700MHz,  $\text{CDCl}_3$ )  $\delta$  ppm 8.32 (bs, 1H), 8.16 (d,  $J = 7.7$  Hz, 1H), 7.38

(t,  $J = 7.7$  Hz, 1H), 7.29 (d,  $J = 7.5$  Hz, 1H), 7.08 (d,  $J = 8.4$  Hz, 1H), 7.01 (t,  $J = 7.3$  Hz, 1H), 4.80 (t,  $J = 6.6$  Hz, 1H), 4.55 (dd,  $J = 5.2, 7.7$  Hz, 1H), 3.75 (s, 3H), 3.56 (m, 1H), 3.51 (m, 1H), 2.44 (m, 1H), 2.20 (m, 1H), 2.17 (m, 1H), 2.04 (m, 1H), 1.90 (m, 1H), 1.51 (s, 9H), 0.95 (d,  $J = 6.7$  Hz, 3H), 0.91 (d,  $J = 6.7$  Hz, 3H);  $^{13}\text{C}$  NMR (175MHz,  $\text{CDCl}_3$ )  $\delta$  ppm 172.3, 171.0, 169.9, 153.0, 137.3, 131.1, 127.4, 123.6, 121.8, 120.5, 80.4, 59.7, 57.4, 52.1, 50.6, 31.2, 28.3, 27.6, 25.4, 19.0, 17.7; HRMS (ESI)  $\text{C}_{23}\text{H}_{33}\text{N}_3\text{O}_6$  calculated  $[\text{M}+\text{H}]^+$ : 448.2369, found 448.2433,  $\text{C}_{23}\text{H}_{33}\text{N}_3\text{NaO}_6$  calculated  $[\text{M}+\text{Na}]^+$  470.2267, found 470.2252.

a)



b)



c)

L-TRI\_151202143841 #106 RT: 0.47 AV: 1 NL: 1.11E9  
T: FTMS +p ESI Full ms [100.00-1500.00]

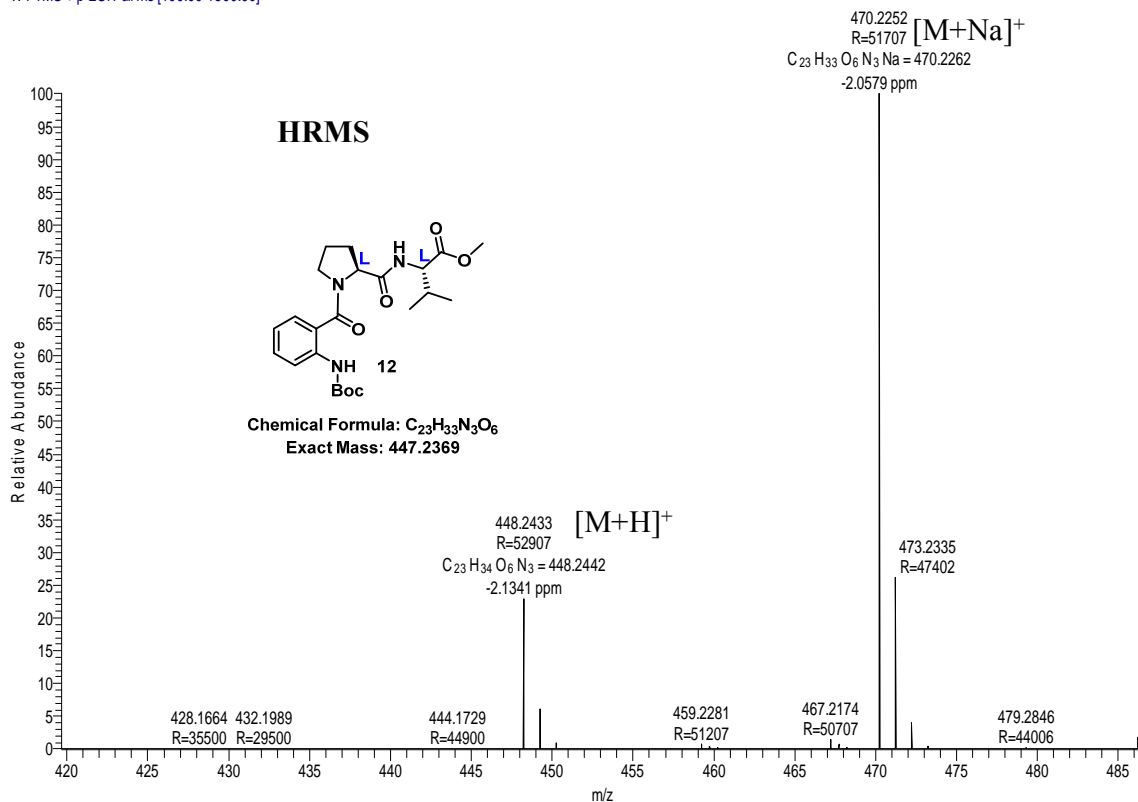
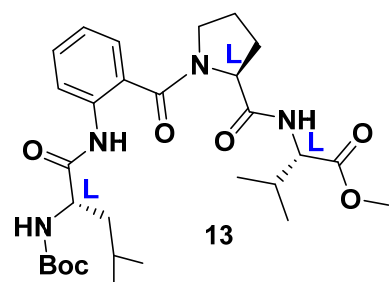


Figure 1.32 a) <sup>1</sup>H NMR, b) <sup>13</sup>C NMR and c) HRMS spectra of compound 11



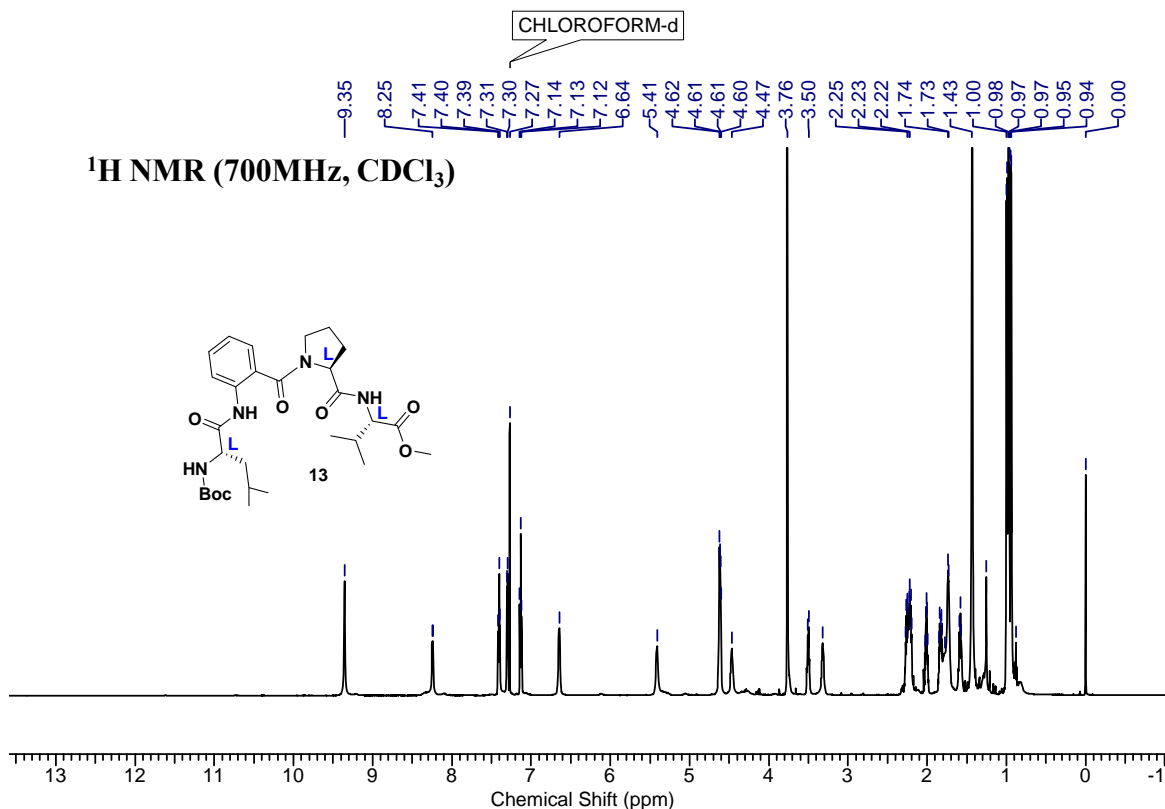
**Compound 13 (Boc<sup>L</sup>LeuAnt<sup>L</sup>Pro<sup>L</sup>Val-OMe):** Following the same synthetic procedure



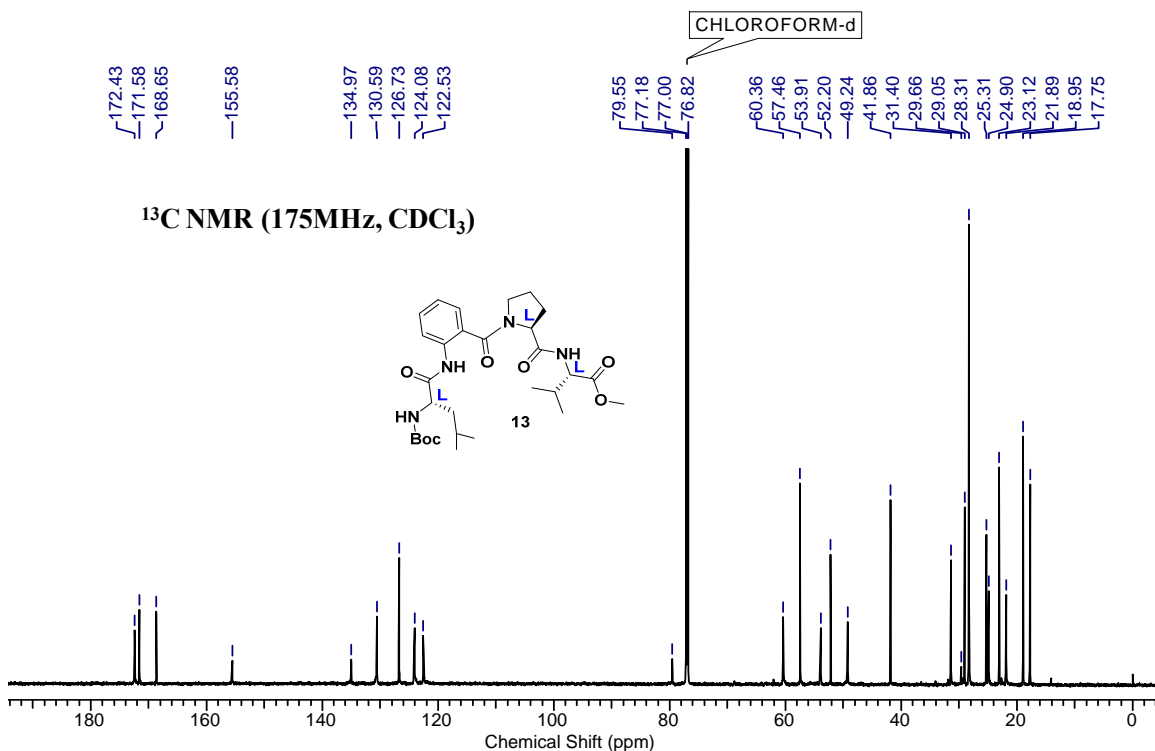
of **7**, compound **13** was synthesized. The crude product was purified by column chromatography (eluent 50% AcOEt/pet. Ether,  $R_f$ : 0.3) afforded **7** (1.03 g, 80%) as a white fluffy solid. Mp: 83-85°C;  $[\alpha]^{25.87}_D = -84.10^\circ$  ( $c = 0.035$ , CHCl<sub>3</sub>); IR (CHCl<sub>3</sub>)  $\nu$  (cm<sup>-1</sup>): 3318, 2966, 2357, 1670, 1625, 1535, 1455, 1166, 760; <sup>1</sup>H NMR (700 MHz,

CDCl<sub>3</sub>)  $\delta$  ppm= 9.35 (bs, 1H), 8.24 (d,  $J = 7.1$  Hz, 1H), 7.40 (t,  $J = 7.9$  Hz, 1H), 7.30 (d,  $J = 7.3$  Hz, 1H), 7.13 (t,  $J = 7.5$  Hz, 1H), 6.65 (d,  $J = 4.5$  Hz, 1H), 5.41 (bs, 1H), 4.67 (m, 2H), 4.47 (bs, 1H), 3.76 (s, 3H), 3.50 (m, 1H), 3.32 (m, 1H), 2.34 (m, 3H), 2.01 (m, 1H), 1.78 (m, 1H), 1.73 (m, 2H), 1.62 (m, 1H), 1.43 (s, 9H), 1.00 (d,  $J = 6.9$  Hz, 3H), 0.97 (dd,  $J = 5.8$  Hz, 6H), 0.94 (d,  $J = 6.9$  Hz, 3H); <sup>13</sup>C NMR (175 MHz, CDCl<sub>3</sub>)  $\delta = 172.5, 172.4, 171.6, 168.6, 155.6, 135.0, 130.6, 126.7, 124.1, 122.5, 79.5, 60.4, 57.5, 53.9, 52.2, 49.2, 41.9, 31.4, 29.0, 28.3, 25.3, 24.9, 23.1, 21.9, 19.0, 17.7$ ; HRMS (ESI) C<sub>29</sub>H<sub>45</sub>N<sub>4</sub>O<sub>7</sub> calculated  $[M+H]^+$ : 561.3210, found 561.3271, C<sub>29</sub>H<sub>44</sub>N<sub>4</sub>NaO<sub>7</sub> calculated  $[M+Na]^+$  583.3108, found 583.3088.

a)



b)



c)

L-TETRA\_151202144150 #111 RT: 0.49 AV: 1 NL: 2.28E9  
T: FTMS + p ESI Full ms [100.00-1500.00]

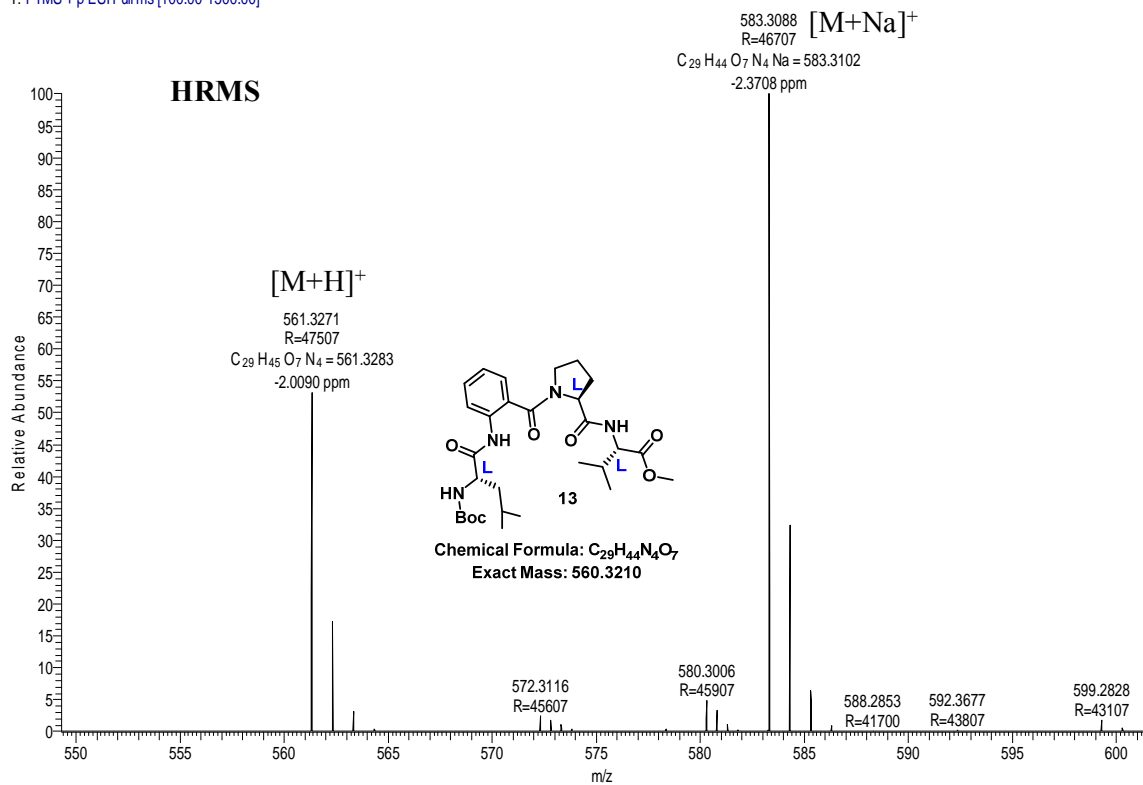
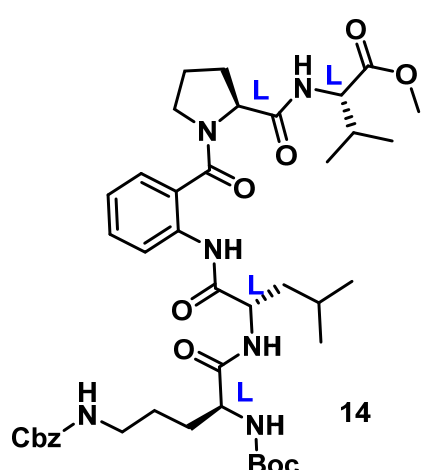


Figure 1.33 a) <sup>1</sup>H NMR, b) <sup>13</sup>C NMR and c) HRMS spectra of compound 13

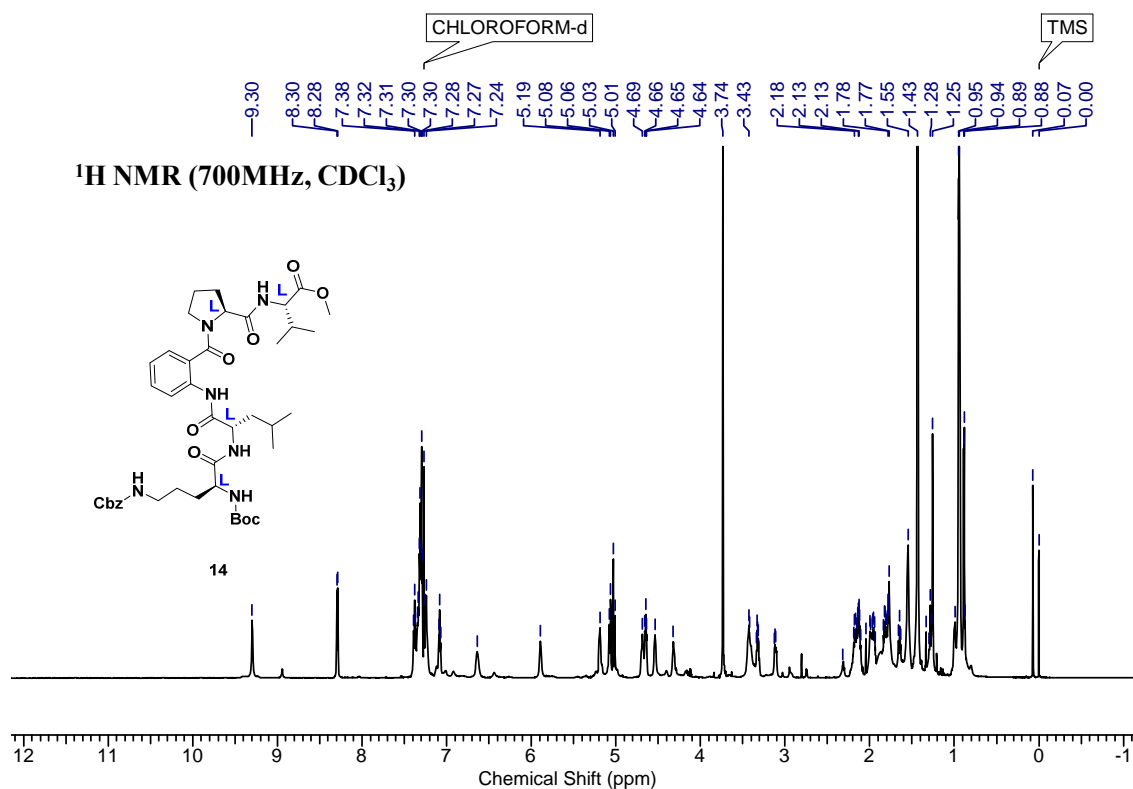


**Compound 14 Boc-(z)<sup>L</sup>Orni<sup>L</sup>LeuAnt<sup>D</sup>ProVal-OMe:**

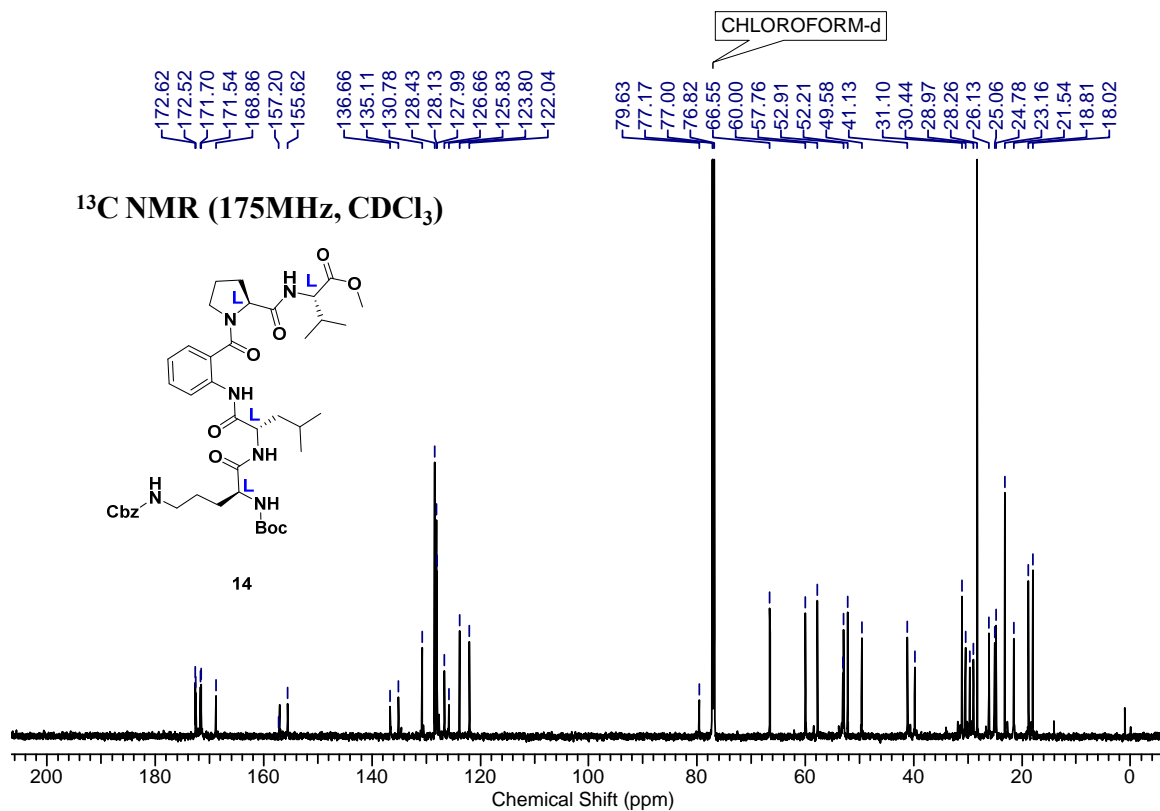
**(Penta-peptide):** Following the same synthetic procedure of **8**, compound **14** was synthesized. The crude product purified by column chromatography (eluent 60% AcOEt/Pet. Ether,  $R_f$ : 0.3) afforded **14** (0.71g, 81%) as a white fluffy hygroscopic solid. Mp: 74-78°C;  $[\alpha]^{25.87}_D = -52.26^\circ$  ( $c = 0.03$ ,  $\text{CHCl}_3$ ); IR ( $\text{CHCl}_3$ )  $\nu$  ( $\text{cm}^{-1}$ ): 3422, 3334, 3019, 2408, 1675, 1217, 763;  $^1\text{H}$  NMR (700 MHz,  $\text{CDCl}_3$ )  $\delta$  ppm 9.30 (bs, 1H),

8.29 (d,  $J = 8.4$  Hz, 1H), 7.38 (t,  $J = 7.9$  Hz, 1H), 7.36 - 7.27 (m, 6H), 7.25 (m, 2H), 7.08 (t,  $J = 7.3$  Hz, 1H), 6.64 (bs, 1H), 5.89 (bs, 1H), 5.19 (d,  $J = 12.5$  Hz, 1H), 5.07 (d,  $J = 12.5$  Hz, 1H), 5.04 - 5.00 (m, 1H), 4.69 (bs, 1H), 4.65 (t,  $J = 6.7$  Hz, 1H), 4.54 (bs, 1H), 4.32 (bs, 1H), 3.74 (s, 3H), 3.43 (m, 2H), 3.36 (m, 1H), 3.18 (m, 1H), 2.2 (m, 3H), 2.0 (m, 2H), 1.95 (m, 2H), 1.85 (m, 4H), 1.65 (m, 1H), 1.43 (s, 9H), 0.94 (m, 9H), 0.89 (d,  $J = 6.7$  Hz, 3H);  $^{13}\text{C}$  NMR (175MHz,  $\text{CDCl}_3$ )  $\delta$  ppm 172.6, 172.5, 171.7, 171.5, 168.9, 157.2, 155.6, 136.7, 135.1, 130.8, 128.4, 128.1, 128.0, 126.7, 125.8, 123.8, 122.0, 79.6, 66.5, 60.0, 57.8, 53.1, 52.9, 52.2, 49.6, 41.1, 39.8, 31.1, 30.4, 29.0, 28.3, 26.1, 25.1, 24.8, 23.2, 21.5, 18.8, 18.0; HRMS (ESI)  $\text{C}_{42}\text{H}_{60}\text{N}_6\text{O}_{10}$  calculated  $[\text{M}+\text{H}]^+$ : 809.4371, found 809.4432,  $\text{C}_{42}\text{H}_{60}\text{N}_6\text{NaO}_{10}$  calculated  $[\text{M}+\text{Na}]^+$  831.4269, found 831.4244.

a)



b)



c)

L-PENTA\_151202145433 #116 RT: 0.51 AV: 1 NL: 1.52E9  
T: FTMS +p ESI Fullms [100.00-1500.00]

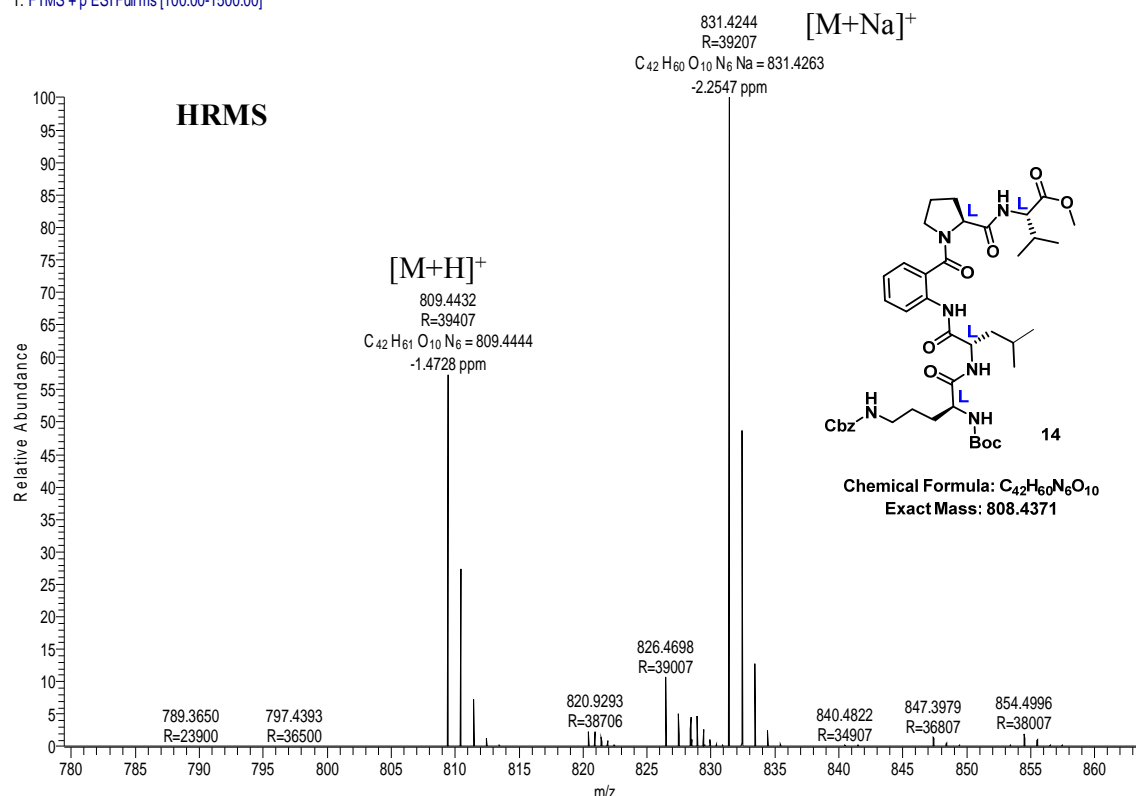
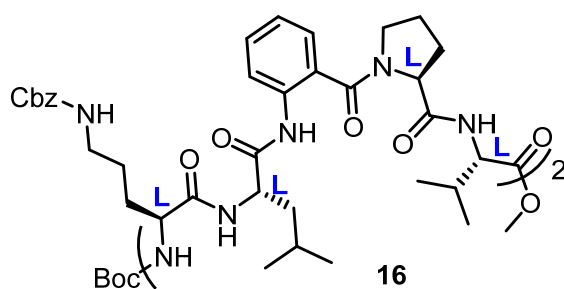


**Figure 1.34** a) <sup>1</sup>H NMR, b) <sup>13</sup>C NMR and c) HRMS spectra of compound **14**

**Compound 14a Boc-(z)<sup>L</sup>Orni<sup>L</sup>LeuAnt<sup>L</sup>ProVal-OH:** Following the same hydrolysis procedure of **8**, compound **14** hydrolyzed to compound **14a** (Boc-(z)<sup>L</sup>Orni<sup>L</sup>LeuAnt<sup>L</sup>ProVal-OH or Boc-Penta-OH).

**Attempt for synthesis of cyclic compound 15:** Following the same synthetic procedure of **2**, for the synthesis of compound **15**; reaction does not give desired product **15**. Later, trials using various coupling agents but reaction did not offered cyclic compound **15**.

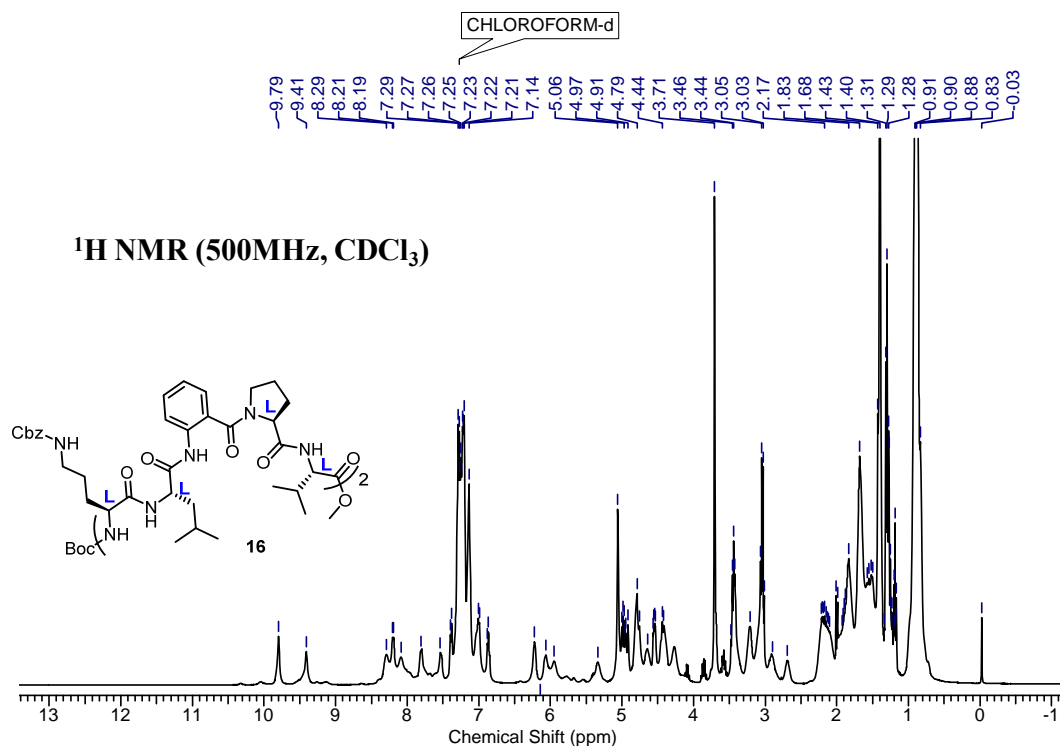
**Compound 16 Boc-((z)<sup>L</sup>Orni<sup>L</sup>LeuAnt<sup>L</sup>ProVal)<sub>2</sub>-OMe (Deca-peptide):** Following the



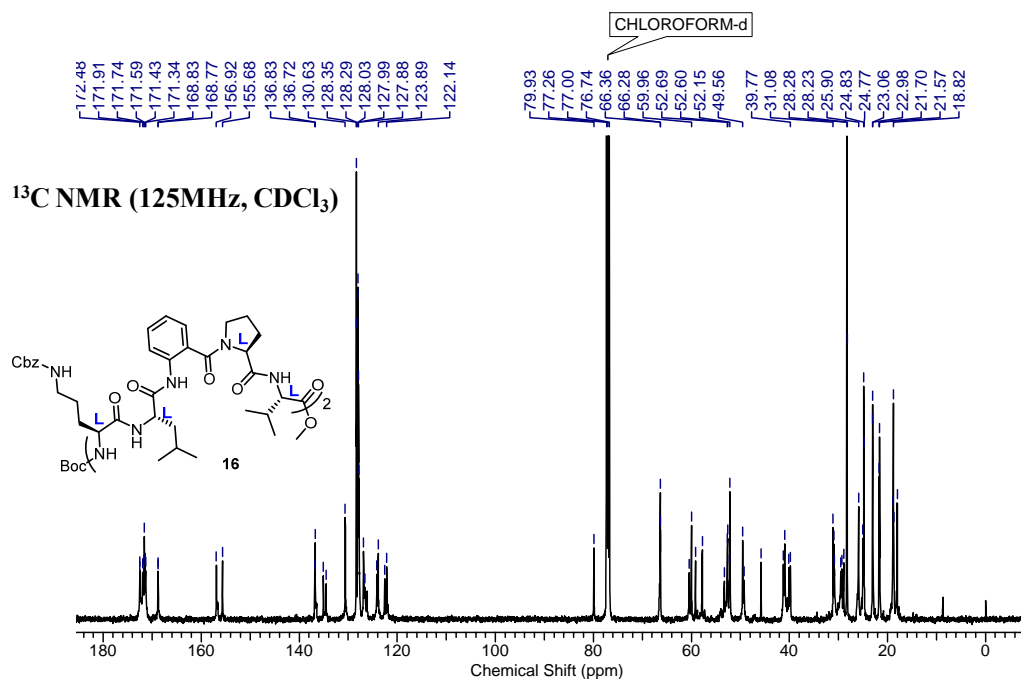
same synthetic procedure of **9**, compound **16** was synthesized and the crude product purified by column chromatography (eluent: 70% AcOEt/pet. Ether, R<sub>f</sub>: 0.3) to furnish **16** (0.57 g, 62%) as a white fluffy solid. Mp: 128-130°C; [α]<sub>D</sub><sup>26</sup> = -755° (c =

0.014, CHCl<sub>3</sub>); IR (CHCl<sub>3</sub>)  $\nu$  (cm<sup>-1</sup>) 3324, 3021, 2969, 1674, 1519, 1422, 1217, 1039, 766, 670; <sup>1</sup>H NMR (500MHz, CDCl<sub>3</sub>)  $\delta$  ppm 9.82 (bs, 1H), 9.44 (bs, 1H), 8.39 (bs, 1H), 8.17 (d, *J* = 6.9 Hz 1H), 7.84 (d, *J* = 5.9 Hz 1H), 7.56 (bs, 1H), 7.42 (d, *J* = 7.1 Hz, 1H), 7.31 (m., 3H), 7.29 (m, 7 H), 7.16 (m, 3H), 7.03 (m, 2H), 6.96 (t, *J* = 6.9 Hz 1H), 6.25 (bs, 1H), 6.09 (bs, 1H), 5.42 (m, 1H), 5.09 (m, 2H), 5.04 (m, 2H), 4.87 (m, 3H), 4.67 (m., 1H), 4.58 (dd, *J* = 4.4, 8.6 Hz, 1H), 4.45 (m, 2H), 4.30 (m., 1H), 3.74 (s, 3H), 3.67 (m, 1H), 3.54 (m, 2H), 3.24 (m., 1H), 2.94 (m, 2H), 2.81 (m, 2H), 2.35 (m, 4H), 2.0 (m, 1H), 1.95 (m, 5H), 1.7(m, 4H) 1.64 (m, 6H), 1.43 (bs, 9H), 1.08 (m, 24H); <sup>13</sup>C NMR (125 MHz, CDCl<sub>3</sub>)  $\delta$  ppm 172.6, 172.5, 171.9, 171.7, 171.6, 171.4, 171.3, 168.8, 168.8, 156.9, 156.9, 155.7, 136.8, 136.7, 135.1, 134.5, 130.6, 128.3, 128.3, 128.0, 128.0, 127.9, 127.9, 127.8, 127.7, 126.9, 126.8, 126.6, 126.1, 122.6, 122.1, 79.9, 66.4, 66.3, 60.5, 60.0, 57.8, 53.3, 52.7, 52.6, 52.2, 52.1, 49.6, 49.3, 45.8, 41.2, 40.1, 39.8, 31.1, 30.9, 30.8, 29.5, 29.3, 28.9, 28.3, 28.2, 25.9, 25.1, 24.8, 24.8, 23.1, 23.0, 21.7, 21.6, 18.9, 18.8, 18.7, 18.0; HRMS (ESI) C<sub>78</sub>H<sub>108</sub>N<sub>12</sub>O<sub>17</sub> calculated [M+H]<sup>+</sup>: 1485.7955, found 1485.8011.

a)



b)



c)

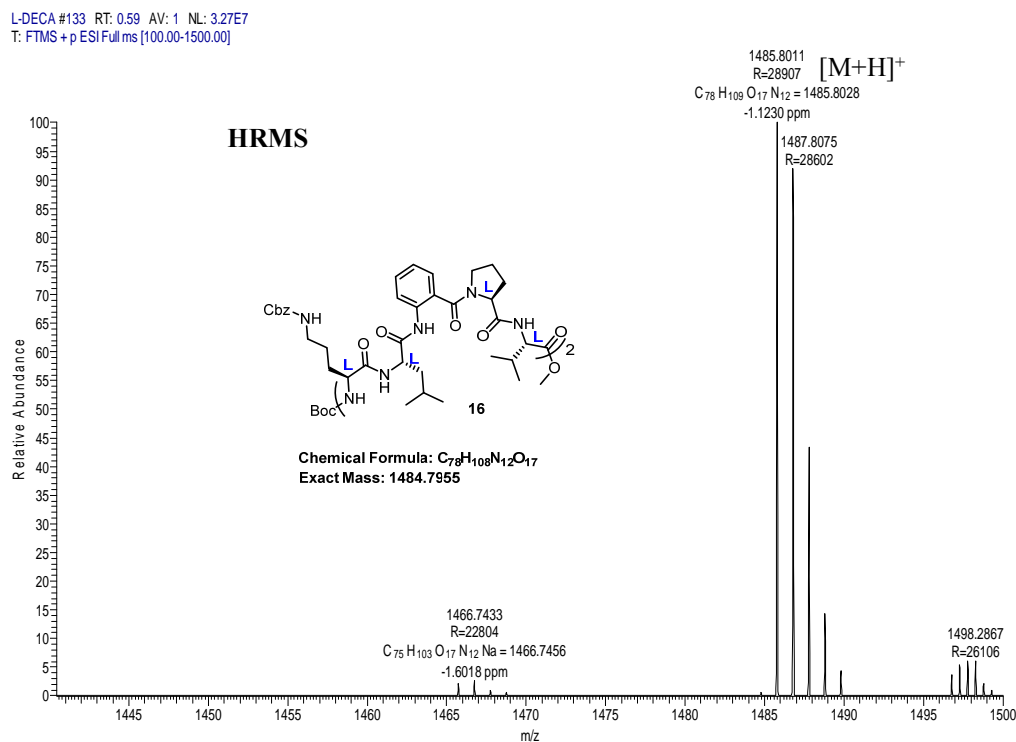


Figure 1.35 a) <sup>1</sup>H NMR, b) <sup>13</sup>C NMR and c) HRMS spectra of compound 14

**Attempt for synthesis of cyclic compound 17:** Following the same synthetic procedure of 1, attempted to synthesis 17, but the reaction did not produce the desired cyclic product 17.

2D- NMR spectra

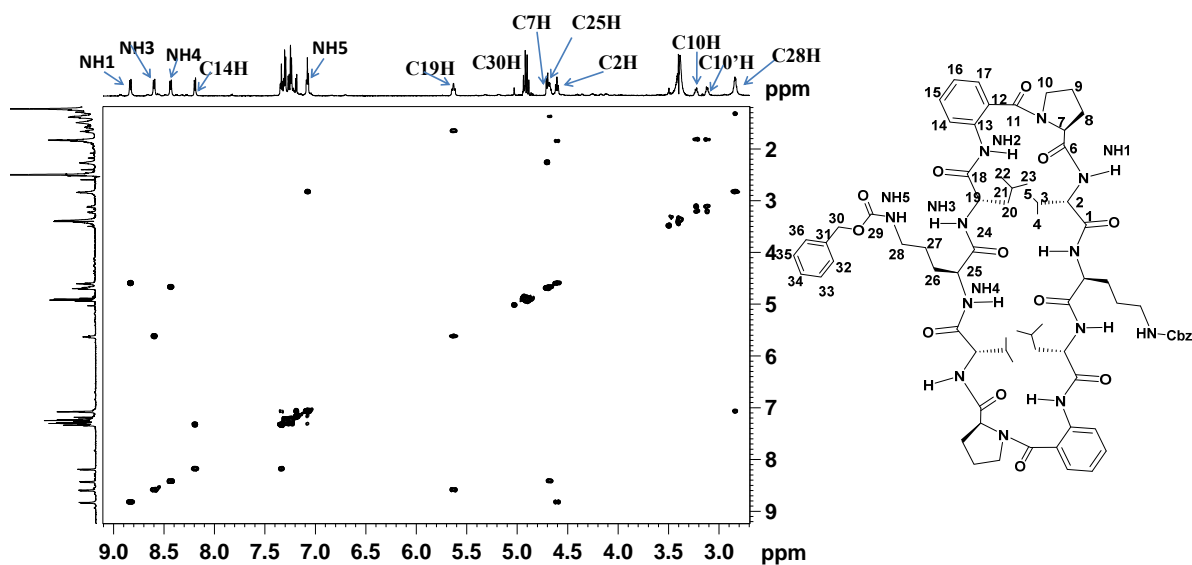


Figure 1.36 COSY spectrum of **1** (10 mM, 700 MHz) in DMSO-*d*<sub>6</sub>

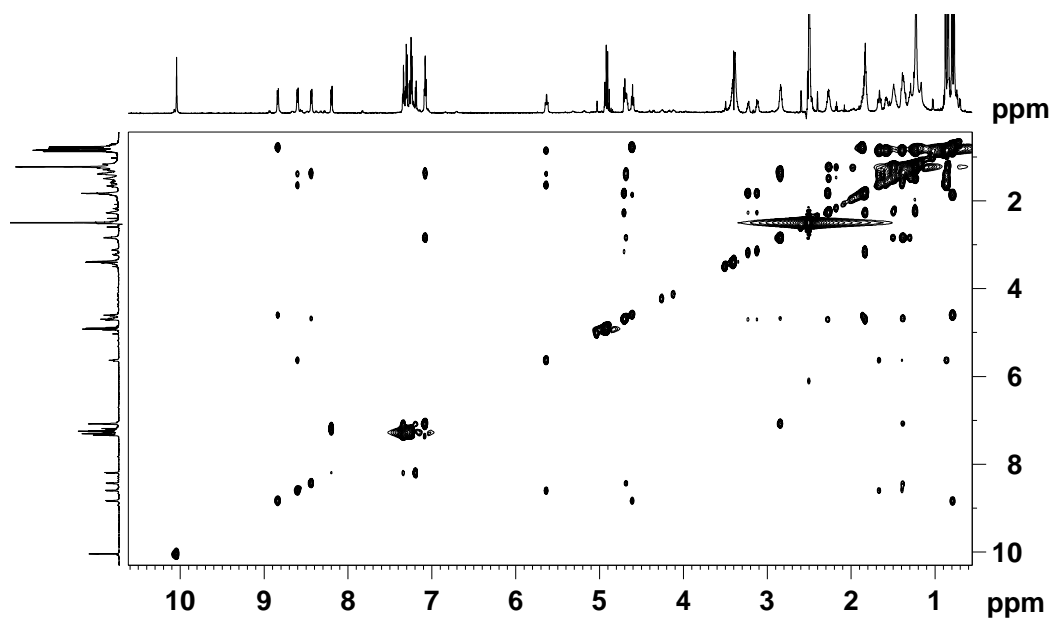


Figure 1.37 TOCSY spectrum of **1** ((10 mM, 700 MHz) in DMSO-*d*<sub>6</sub>



Table 1.3 Signal assignment of Cbz-1 from TOCSY Spectra

Proton Vs chemical shift	NH1	$\alpha$ H/1H	$\beta$ H/2H	$\gamma$ H/3H	$\delta$ H/4H	NH2
Val	8.86(d) NH1	4.61(t) C1H	1.86(m) C2H	0.77(d)C3H 0.79(d)C3'H		
Pro		4.70(dd) C7H	2.25(m) C8H	1.82(m) C9H	3.11(m)C10H 3.22(m)C10'H	
Ant	10.04(s) NH2	8.18(d) C14H	7.33(t) C15H	7.08(t) C16H	7.19(d) C17H	
Leu	8.58(d) NH3	5.63(t) C19H	1.65(m)C20H 1.38(m)C20'H	1.58(m) C21H	0.83(d)C22H 0.87(d)C23H	
Orn	8.43(d) NH4	4.66(m) C25H	1.66(m) C26H	1.37(m) C27H	2.85(m) 28CH	7.08(t) NH5

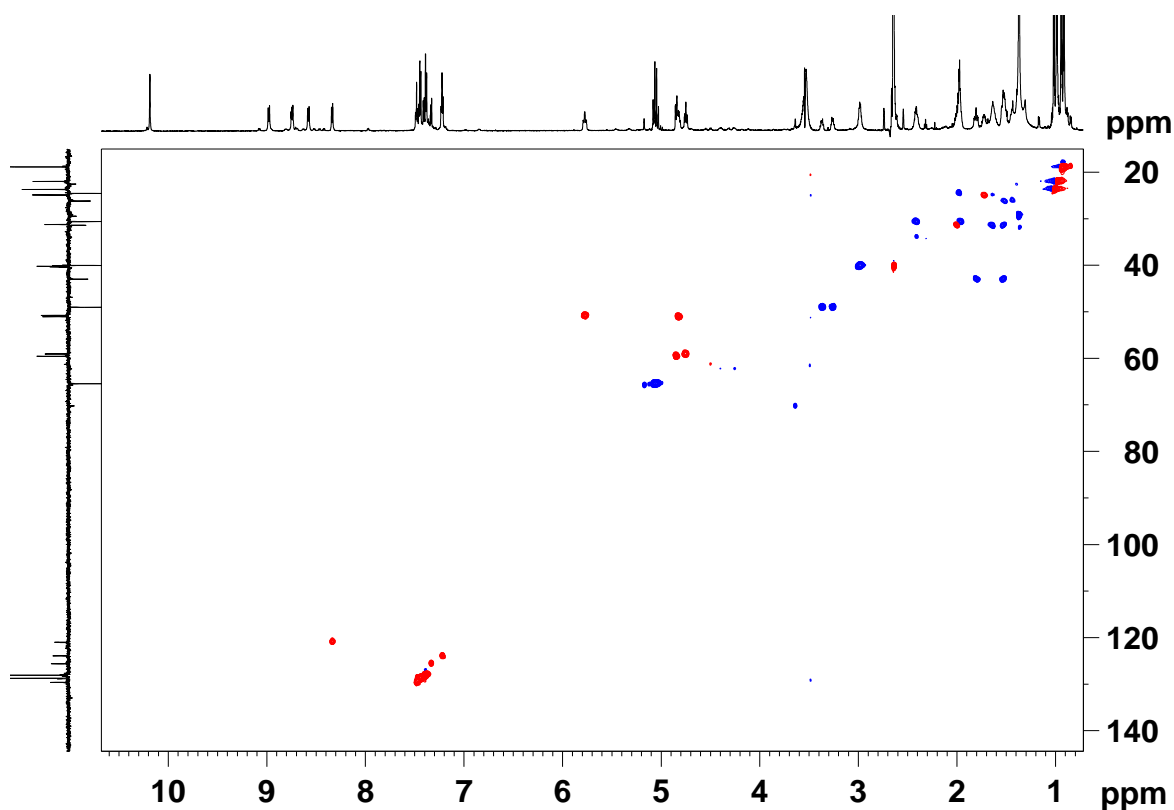


Figure 1.38 HSQC spectrum of **1** (10 mM, 700 MHz) in DMSO- $d_6$

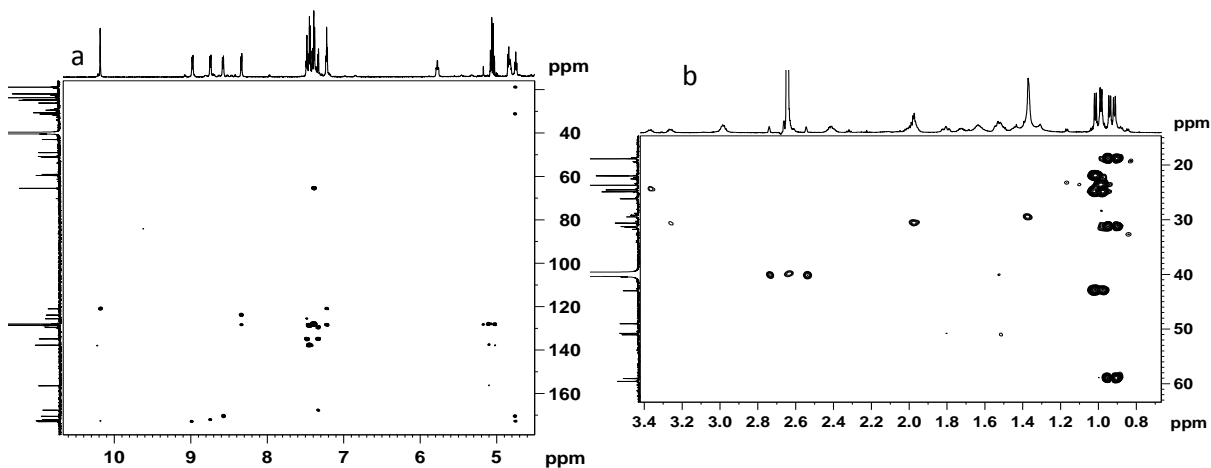


Figure 1.39 Partial HMBC spectrum of **1** (10 mM, 700 MHz) in DMSO-*d*<sub>6</sub>

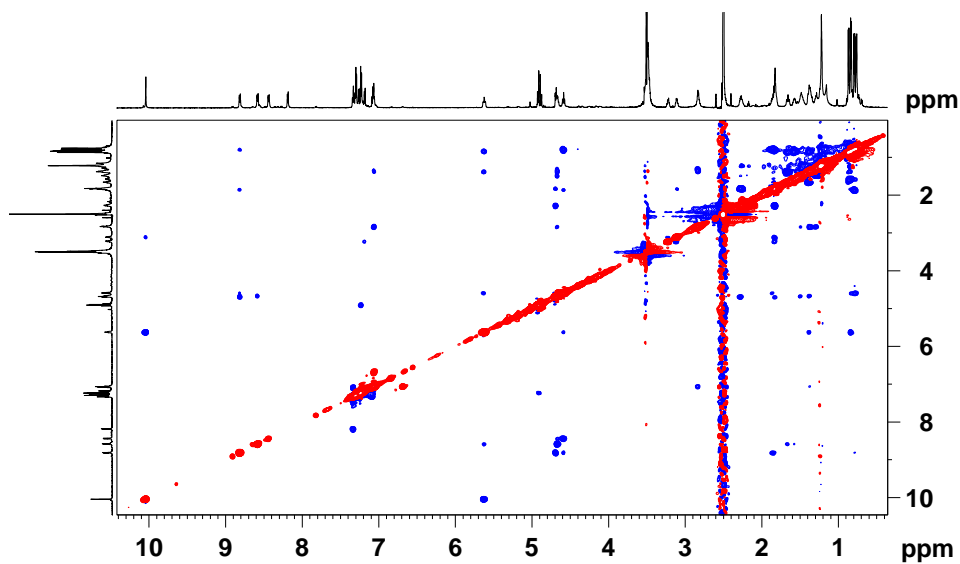
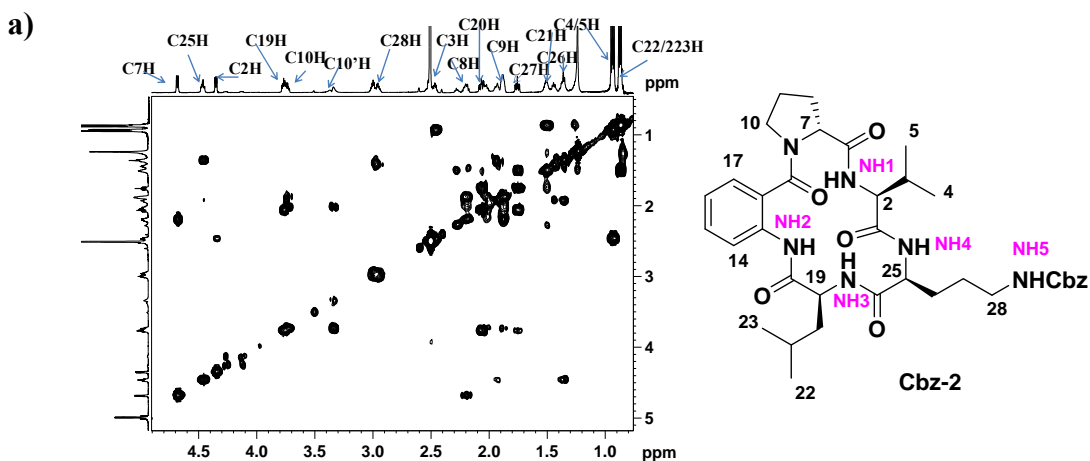
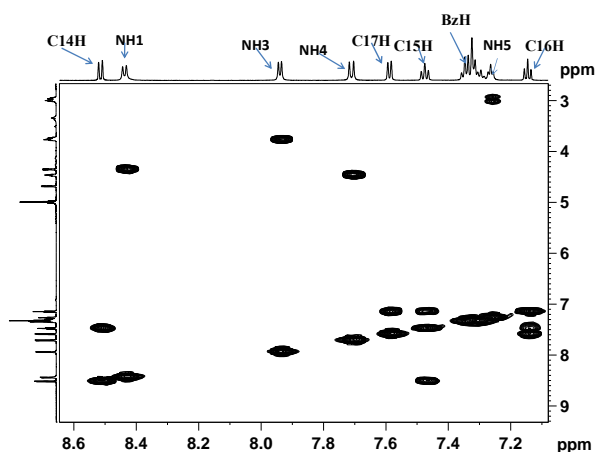


Figure 1.40 Full ROESY spectrum of **1** (10 mM, 700 MHz) in DMSO-*d*<sub>6</sub>

## 2D NMR spectra of **2**:



b)



**Figure 1.41** Partial COSY spectra of **2** (15 mM, 700 MHz) in DMSO-*d*<sub>6</sub>, a) aliphatic region, b) aromatic region.

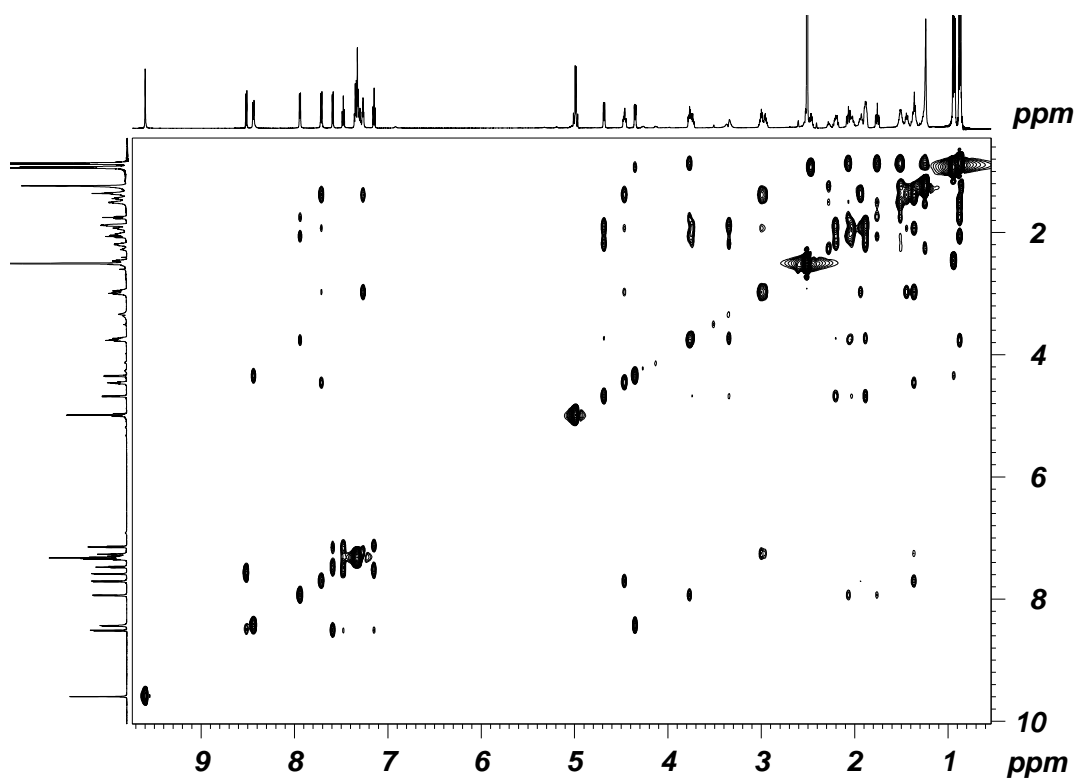


**Figure 1.42** TOCSY spectrum of **2** (15 mM, 700 MHz) in DMSO-*d*<sub>6</sub>

Table 1.4 Signal assignment of Cbz-2 from TOCSY Spectra.

Proton Vs chemical shift	NH1	$\alpha$ H/1H	$\beta$ H/2H	$\gamma$ H/3H	$\delta$ H/4H	NH2
Val	8.83(d) NH1	4.34(dd) C2H	2.47(m) C3H	0.94(d)C4H 0.93(d)C5H		
Pro		4.68(br. d) C7H	2.20(m) C8H	1.88(m) C9H	3.75(m)C10H 3.34(m)C10'H	
Ant	9.59(s) NH2	8.51(d) C14H	7.49(t) C15H	7.14(t) C16H	7.50(d) C17H	
Leu	7.94(d) NH3	3.76(m) C19H	2.07(m) C20H 1.92 (m) C20'H	1.51(m) C21H	0.88(d)C22H 0.86(d)C23H	
Orn	7.71(d) NH4	4.46(m) C25H	1.91(m) C26H	1.35(m) C27H	2.96(m) 28CH	7.26(t) NH5

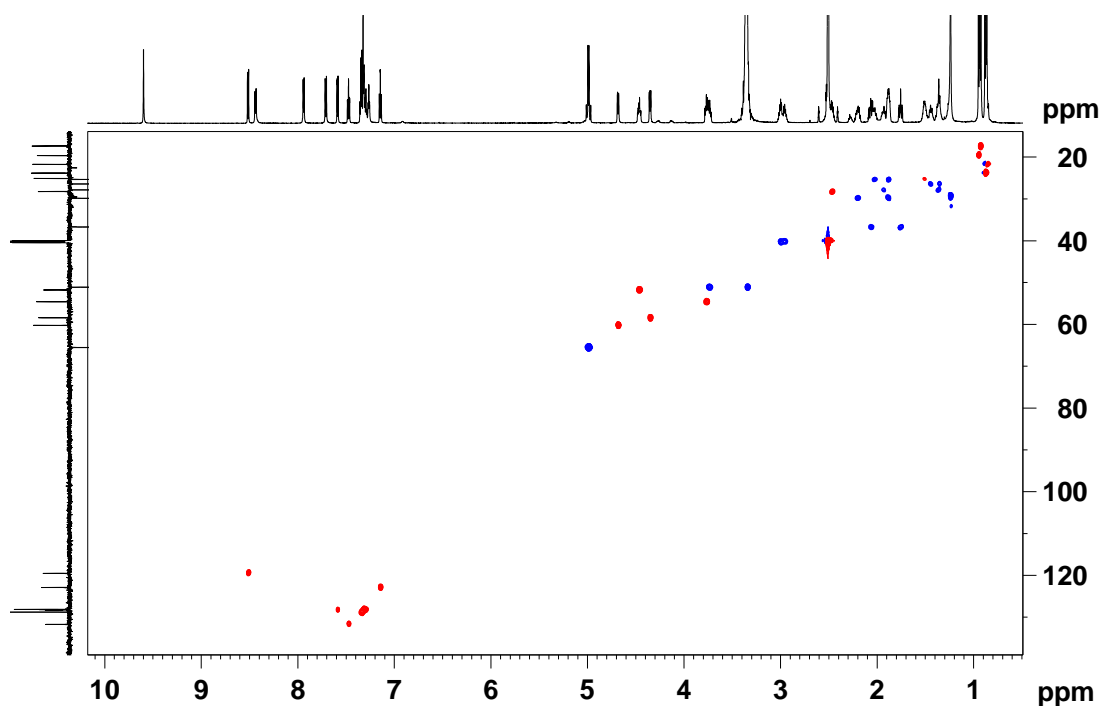


Figure 1.43 HSQC spectrum of 2 (15 mM, 700 MHz) in DMSO- $d_6$

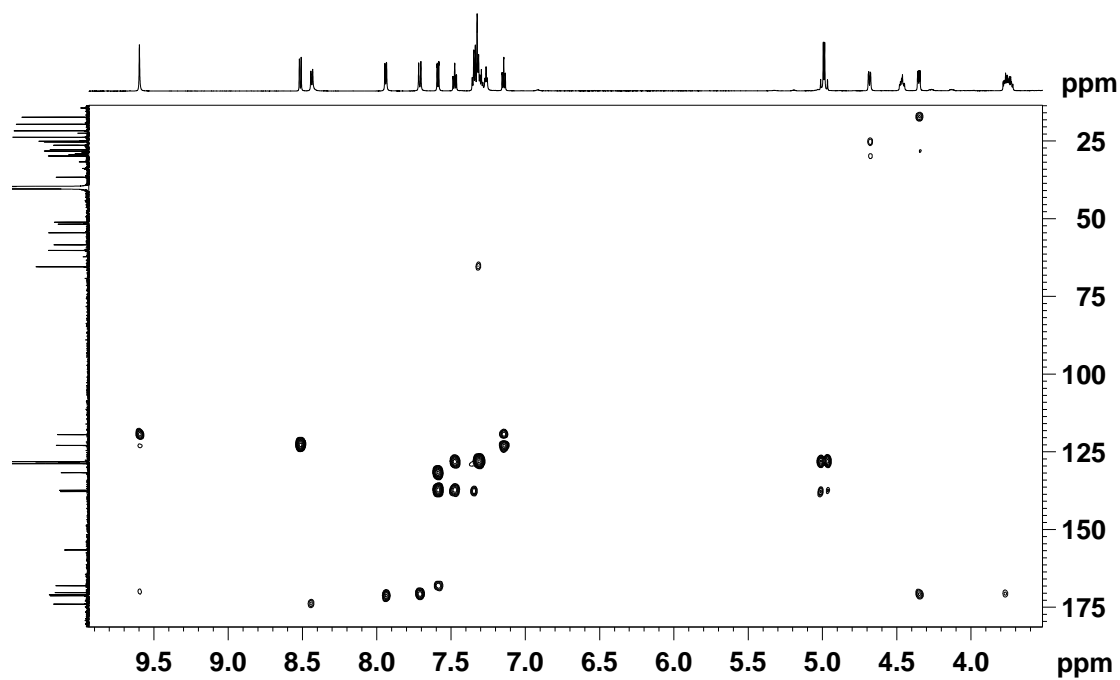


Figure 1.44 a) HMBC spectrum of **2** (15 mM, 700 MHz) in DMSO- $d_6$

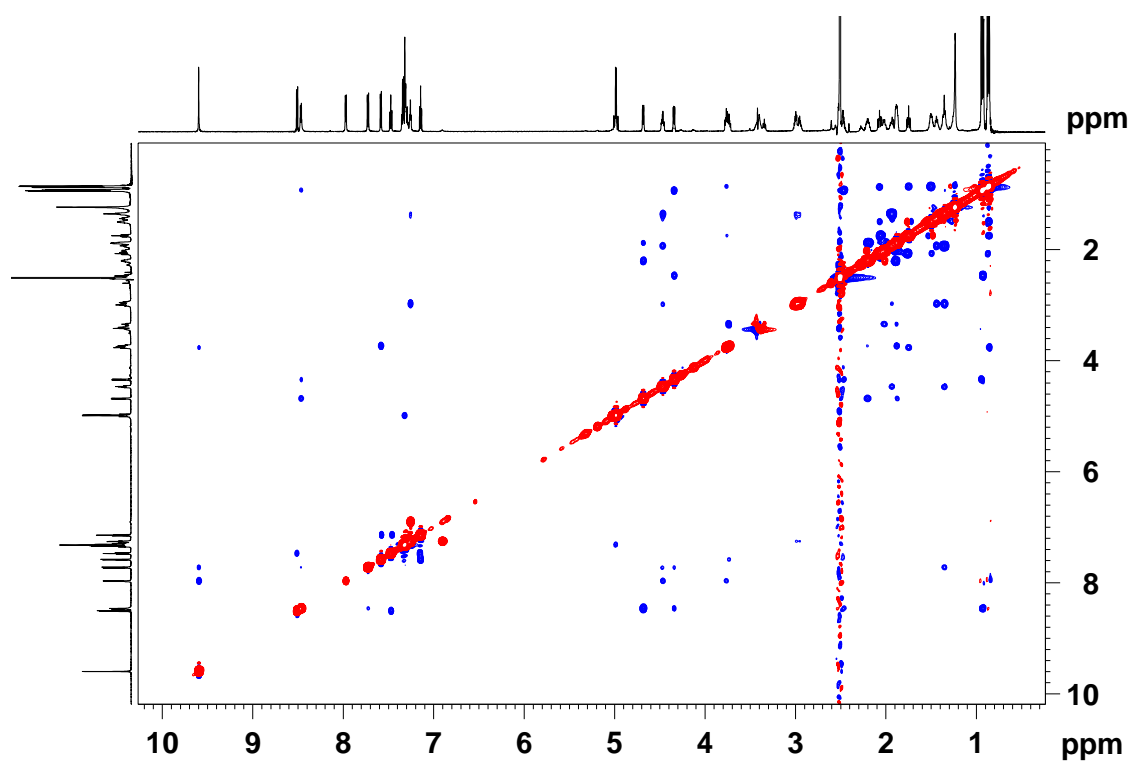


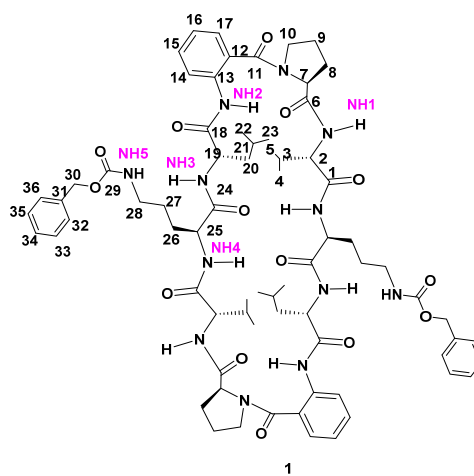
Figure 1.45 ROESY spectrum of **2** (15 mM, 700 MHz) in DMSO- $d_6$

### Molecular Dynamic Studies

The molecular dynamic study was carried out on MacroModel, version 10.8 program from Schrodinger software with OPLS\_2005 Force Field, using the quantitative restraints obtained from the ROESY spectra calculating the relativity of cross-peak intensities of the volume integrals. The 20 superimposed minimum energy of **1** (RMSD <0.15Å) and **2** (RMSD <0.2 Å).

**Table 1.5** ROESY restraints used for MD simulation studies of **1**

Atom1	Atom2	Upper Bound(Å)	Lower Bound(Å)
14H	15H	2.68	2.2
NH2	19H	2.43	1.99
NH2	10aH	3.75	3.07
NH1	4H/5H	3.79	3.1
NH1	3H	3.09	2.53
NH1	2H	3.48	2.85
NH1	7H	2.6	2.12
NH3	21H	3.57	2.92
NH3	20H	3.25	2.66
NH3	25H	2.49	2.03
NH3	19H	3.43	2.81
NH4	2H	2.5	2.05
NH4	25H	3.69	3.02
NH5	27aH	3.76	3.08
NH5	27bH	4.79	3.92
NH5	28H	2.83	2.31
30H	32H/36H	2.91	2.38
2H	19H	3.23	2.64
19H	22H/23H	2.75	2.25
19H	20H	3.06	2.5
19H	21H	3.62	2.97
2H	4H/5H	2.46	2.01
25H	27H	3.32	2.72
25H	26aH	2.95	2.41
25H	26bH	3.08	2.52
7H	9aH	3.2	2.62
2H	3H	3.2	2.61
7H	8H	2.63	2.15



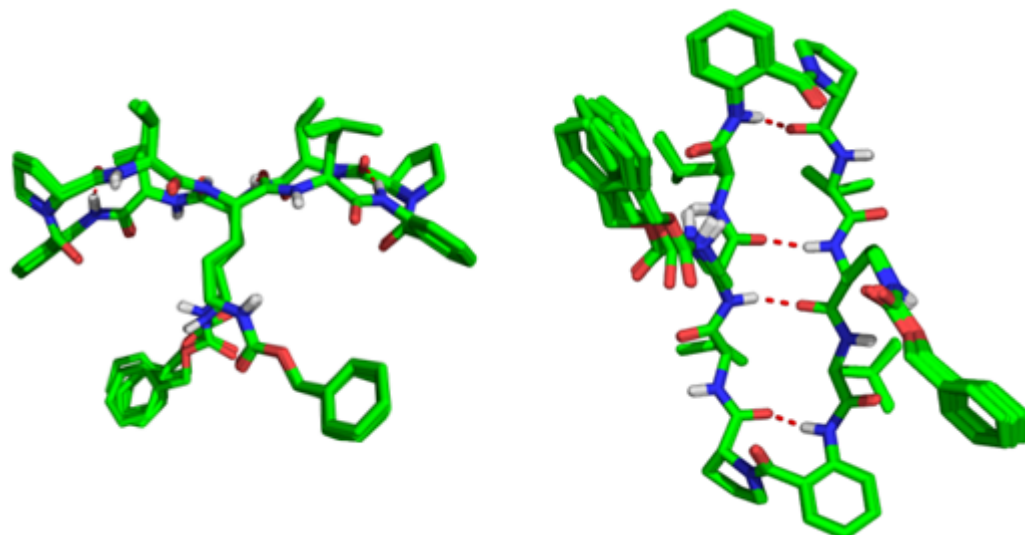
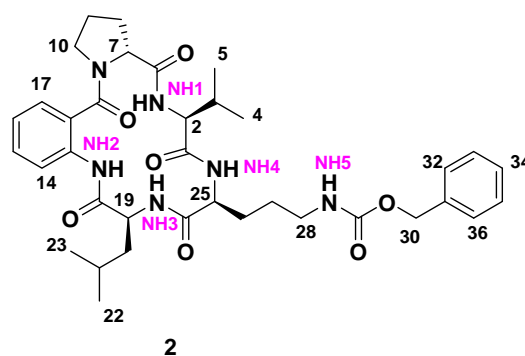


**Figure 1.46** Different stereo views of 20 superimposed minimum energy structures for peptide 1. Note-hydrogens, other than the polar amide hydrogens have been removed for clarity.

**Table 1.6** ROESY restraints used for MD simulation studies of 2

Atom I	Atom II	Upper Bound	Lower Bound
14H	15H	2.68	2.2
NH2	NH3	2.88	2.36
NH2	NH4	3.3	2.7
NH2	14H	4.32	3.54
NH2	19H	3.34	2.73
NH1	3H	3.78	3.09
NH1	2H	3.35	2.74
NH1	7H	2.41	1.97
NH1	NH4	2.88	2.36
NH3	21H	3.57	2.92
NH3	26aH	3.64	2.98
NH3	20AH	3.77	3.08
NH3	25H	3.07	2.51
NH3	2H	4.18	3.42
NH4	4H/5H	4.07	3.33
NH4	27aH	3.05	2.49
NH4	27bH	3.53	2.88
NH4	2H	3.43	2.81
NH4	25H	3.25	2.66
17H	10bH	3.44	2.82
17H	10aH	2.49	2.04
30H	32H/36H	2.88	2.36
NH5	28H	2.72	2.23



---

NH5	26aH	3.57	2.92
NH5	27aH	3.72	3.05
NH5	27bH	3.45	2.82
7H	9aH	3.11	2.54
7H	8aH	2.65	2.17
25H	28aH	3.12	2.56
2H	4H/5H	2.59	2.12
19H	22H/23H	2.64	2.16
19H	21H	3.26	2.67
NH1	4H/5H	2.65	2.17
NH3	22H/23H	3.64	2.98
7H	10aH	4	3.28
NH3	NH4	3.07	2.51
NH4	7H	4.08	3.34

---

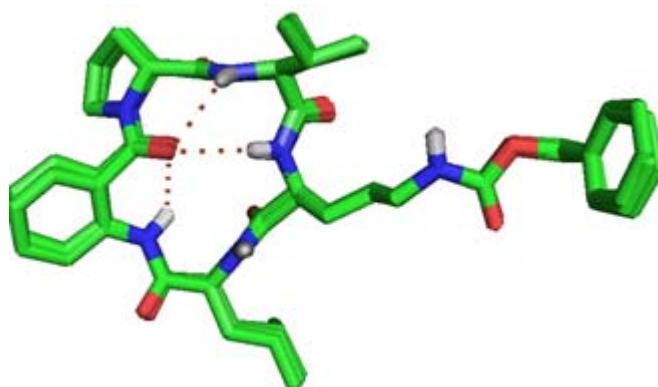


**Figure 1.47** Stereo view of 10 superimposed minimum energy structures for peptide **2**. Note-hydrogens, other than the polar amide have been removed for clarity.



### 1.10 References and Notes:

1. (a) C. Branden, J. Tooze, *Introduction to Protein Structure edn 2<sup>nd</sup>* Ed. New York, NY: Garland, 1998. (b) L. G. Presta, G. D. Rose, *Nature* 1988, **240**, 1632. (c) D. C. Richardson, J. S. Richardson, *Proc. Natl. Acad. Sci.* 2002, **99**, 2754. (d) M. Fandrich, M. A. Fletcher, C. M. Dobson, *Nature* 2001, **410**, 165.
2. (a) M. Bajaj, T. Blundell, *Annu. Rev. Biophys. Bioeng.* 1984, **13**, 453. (b) J. Meiler, D. Baker, *Proc. Natl. Acad. Sci. USA* 2003, **100**, 12105.
3. (a) I. M. Klotz, N. R. Langerman, *Annu. Rev. Biochem.* 1970, **39**, 25. (b) M. F. Perutz, A. J. Wilkinson, M. Paoli, G. G. Dadson, *Annu. Rev. Biophys. Biomol. Struct.* 1998, **27**, 1.
4. (a) G. N. Ramachandran, C. Ramakrishnan, V. Sasisekharan, *J. Mol. Biol.* 1963, **7**, 95. (b) C. Ramakrishnan, G. N. Ramachandran, *Biophys. J.* 1965, **5**, 909. (c) G. N. Ramachandran, V. Sasisekharan, *Adv. Protein Chem.* **1968**, *23*, 283.
5. C. M. Wilmot, J. M. Thornton, *J. Mol. Biol.* 1988, **203**, 221.
6. P. G. Vasudev, S. Chatterjee, N. Shamala, P. Balaram, *Chem. Rev.* 2010, **111**, 657.
7. S. Chatterjee, R. S. Roy, P. Balaram, *J. R. Soc. Interface* 2007, **4**, 587.
8. K. C. Chou, *Anal. Biochem.* 2000, **286**, 1.
9. (a) Baruah, P. K.; Sreedevi, N. K.; Gonnade, R.; Ravindranathan, S.; Damodaran, K.; Hofmann, H.-J.; Sanjayan, G. J. *J. Org. Chem.* 2006, **72**, 636, (b) G. S. Jedhe, A.S. Kotmale, P. R. Rajamohanan, S. Pasha and G. J. Sanjayan, *Chem. Commun.*, 2016, **52**, 1645.
10. D. Frishman, Argos, P. *Proteins* 1995, **23**, 566.
11. E. J. Milner-White, *J. Mol. Biol.* 1990, **216**, 386.
12. G. D. Rose, L. M. Gierasch, J. A. Smith, *Adv. Protein Chem.* 1985, **37**, 1
13. S. R. Raghothama, S. K. Awasthi, P. Balaram, *J. Chem. Soc., Perkin Trans.* 1998, **2**, 137.
14. D. V. Nataraj, N. Srinivasan, R. Sowdhamini, C. Ramakrishnan *Curr. Sci.* **1995**, *69*, 434.

15. V. Pavone, G. Geata, A. Lombardi, F. Nastri, O. Maglio, C. Isernia, M. Saviano, *Biopolymers* 1996, **38**, 705.
16. L. A. Cavacini, R. L. Stanfield, D. R. Burton, I. A. Wilson, *J. Mol. Biol.* **2008**, 375, 969.
17. (a) G. Ruiz-Gómez, J. D. A. Tyndall, B. Pfeiffer, G. Abbenante, D. P. Fairlie, *Chem. Rev.* 2010, **110**, PR1. (b) J. D. A. Tyndall, B. Pfeiffer, G. Abbenante, D. P. Fairlie, *Chem. Rev.* 2005, **105**, 793.
18. C. Toniolo, G. M. Bonora, A. Bavoso, E. Benedetti, B. Diblasio, V. Pavone, C. Pedone, *Biopolymers* 1983, **22**, 205.
19. S. Zerkout, V. Dupont, A. Aubry, J. Vidal, A. Collet, A. Vicherat, M. Marraud, *Int. J. Pept. Protein Res.* 1994, **44**, 378.
20. S. D. Pol, C. Zorn, C. D. Klein, O. Zerbe, O. Reiser, *Angew. Chem., Int. Ed.*, 2004, **43**, 511.
21. S. H. Gellman, *Acc. Chem. Res.*, 1998, **31**, 173.
22. (a) I. M. Mandity, L. Fulop, E. Vass, G. K. Toth, T. A. Martinek and F. Fulop, *Org. Lett.*, 2010, **12**, 5584. (b) W. Seth Horne and S. H. Gellman, *Acc. Chem. Res.* 2008, **41**, 1399.
23. (a) P. Prabhakaran, S. S. Kale, V. G. Puranik, P. R. Rajamohanam, O. Chetina, J. A. K. Howard, H. J. Hofmann, G. J. Sanjayan, *J. Am. Chem. Soc.* 2008, **130**, 17743. (b) S. S. Kale, A. S. Kotmale, A. K. Dutta, S. Pal, P. R. Rajamohanam, G. J. Sanjayan, *Org. Biomol. Chem.* 2012, **10**, 8426. (c) K. N. Vijayadas, R. V. Nair, R. L. Gawade, A. S. Kotmale, P. Prabhakaran, R. G. Gonnade, V. G. Puranik, P. R. Rajamohanam and G. J. Sanjayan, *Org. Biomol. Chem.*, 2015, **13**, 3064. (d) K. N. Vijayadas, H. C. Davis, A. S. Kotmale, R. L. Gawade, V. G. Puranik, P. R. Rajamohanam and G. J. Sanjayan, *Chem. Commun.*, 2012, **48**, 9747. (e) V. H. Thorat, T. S. Ingole, K. N. Vijayadas, R. V. Nair, S. S. Kale, V. V. E. Ramesh, H. C. Davis, P. Prabhakaran, R. G. Gonnade, R. L. Gawade, V. G.

- Puranik, P. R. Rajamohanam and G. J. Sanjayan, *Eur. J. Org. Chem.* 2013, **17**, 3529.
24. (a) Huck, B. R.; Fisk, J. D.; Gellman, S. H. *Organic Letters* 2000, **2**, 2607.(b) Chung, Y. J.; Christianson, L. A.; Stanger, H. E.; Powell, D. R.; Gellman, S. H. *J. Am. Chem. Soc.* 1998, **120**, 10555.
25. P. G. Vasudev, K. Ananda, S. Chatterjee, S. Aravinda, N. Shamala, P. J. Balaram, *Am. Chem. Soc.* 2007, **129**, 4039.
26. (a) P. Schramm, H.-J. r. Hofmann, *J. Mol. Struct.: THEOCHEM* 2009, **907**, 109. (b) B. W. Matthews, *Macromolecules* 1972, **5**, 818.
27. (a) G. W. J Fleet, S. W. Johnson, J. H. Jones, *J. Pept. Sci.*, 2006, **12**, 559. (b) T. K. Chakraborty, V. R. Reddy, G. Sudhakar, S. U. Kumar, T. J. Reddy, S. K. Kuran, A. C. Kunwar, A. Mathur, R. Sharma, N. Gupta, S. Prasad, *Tetrahedron*, 2004, **60**, 8329. (c) E. -F Fuchs, J. Lehmann, *Chem. Ber.*, 1975, **108**, 2254.
28. R. V. Nair, K. N. Vijayadas, A. Roy, G. J. Sanjayan, *Eur. J. Org. Chem.*, 2014, **35**, 7763.
29. Y. Hamuro, S. J. Geib, A. D. Hamilton, *J. Am. Chem. Soc.*, 1997, **119**, 10587.
30. G. G. Gauge M. G. Brazhnikova, *Nature*, 1944, **154**, 703.
31. L. H. Kondejewski, S. W. Farmer, D. S. Wishart, C. M. Kay, R. E. Hancock, R. S. Hodges, *The Journal of Biological Chemistry*, 1996, **271**, 25261.
32. (a) K. Yamada, M. Unno, K. Kobayashi, H. Oku, H. Yamamura, S. Araki, H. Matsumoto, R. Katakai, and M.Kawai, *J. AM. CHEM. SOC.* 2002, **124**, 12684, (b) A. Stern, W. A. Gibbons,. and L. C. Craig, *Proc. Natl. Acad. Sci. U.S.A.* 1968, **61**, 734. (c) A. C. Gibbs, T. C. Bjorndahl, R. S. Hodges, D. S . Wishart,. *J. Am. Chem. Soc.* 2002, **124**, 1203.
33. a) J. Xiao, B. Weisblum, and P. Wipf, *J. Am. Chem. Soc.*, 2005, **127**, 5742. b)J. Xiao, B. Weisblum, and P. Wipf, *Org. Lett.*, 2006 8, **21**, 4731.
34. a) W. Qiu, X. Gu, V. A. Soloshonok, M. D. Carducci, V. J. Hruby, *Tetrahedron Lett.* 2001, **42**, 145. (b) C. Xiong, J. Zhang, P. Davis, W. Wang, J. Ying, F. Porreca, V. J. Hruby, *Chem. Comm.* 2003, **13**, 1598
35. Gosselin, F.; Lubell, W. D.; Tourwe', D.; Ceusters, M.; Meert, T.; Heylen, L.; Jurzak, M. *J Pept Res* 2001, **57**, 337.

36. a) Grotenbreg, G. M.; Timmer, M. S. M.; Llamas-Saiz, A. L.; Verdoes, M.; van der Marel, G. A.; van Raaij, M. J.; Overkleeft, H. S.; Overhand, M. *J. Am. Chem. Soc.* 2004 , **126**, 3444 b) A. D. Knijnenburg, A. W. Tuin, E. Spalburg, A. J. de Neeling, R. H. M. Groenendijk, D. Noort, J. M. Otero, A. L. Llamas-Saiz, M. J. V. Raaij, G. A. V. Marel, H. S. Overkleeft and M. Overhand, *Chem. Eur. J.*, 2011, **17**, 3995 (c) J. Swierstra, V. Kapoerchan A. Knijnenburg, A. van Belkum and M. Overhand, *Eur J Clin Microbiol Infect Dis*, 2016, **35**, 763. (d) G.M. Grotenbreg, A. E. M. Buizert, A. L. Llamas-Saiz, E. Spalburg, P. A. V. van Hooft, A. J. de Neeling, D. Noort, M. J. van Raaij, G. A. V. Marel, H. S. Overkleeft, and M. Overhand, *J. Am. Chem. Soc.*, 2006, **128**, 7559.
37. S. Pal, G. Singh, S. Singh, J. Tripathi, J. K. Ghosh, S. Sinha, R. S. Ampapathi and T. K. Chakraborty, *Org. Biomol. Chem.*, 2015, **13**, 6789.
38. C. Solanas, B. G. de la Torre, M. Fernández-Reyes, C. M. Santiveri, M. Á. Jiménez, L. Rivas, A. I. Jiménez, D. Andreu,, and C.s Cativiela, *J Med Chem.* 2010; **53**, 4119.
39. B. Legrand, L. Mathieu, A. Lebrun, S. Andriamanarivo, V. Lisowski, N. Masurier, S. Zirah, Y. K. Kang, J. Martinez and L. T. Maillard, *Chem. Eur. J.* 2014, **20**, 6713.
40. O. Babii, S. Afonin, M. Berditsch, S. Reiber, P. K. Mykhailiuk, V. S. Kubyshkin, T. Steinbrecher, A. S. Ulrich, and I. V. Komarov, *Angew. Chem. Int. Ed.* 2014, **53**, 3392.
41. M. Yamazaki, Y. Horie, K. Bae, Y. Maebayashi, Y. Jisai, and H. Fujimoto, *Chem. Pharm. Bull.* 1987, **35**, 2122.
42. Y. Igarashi, F. Gohda<sup>1</sup>, T. Kadoshima, T. Fukud, T. Hanafusa, A. Shojima, J. Nakayama, G. F Bills and S. Peterson, *The Journal of Antibiotics* , 2015, **68**, 707.
43. (a) Bruker (2016). *APEX3*, *SAINT* and *SADABS*. Bruker AXS Inc., Madison, Wisconsin, USA. (b) G. M. Sheldrick, *Acta Crystallogr.*, 2008, **A64**, 112. (c) L. J. Farrugia, *J. Appl. Cryst.* 1997, **30**, 565–565.
44. <http://www.mhhe.com/biosci/pae/botany/uno/graphics/uno01pob/vrl/images/0031.gif>

## *Chapter 2*

*Design, Synthesis & Conformational Investigation  
of Ant-Pro Urea Based Foldamers*



## 2.1 Introduction

### 2.1.1 Reverse turn, $\beta$ -hairpin and $\beta$ -Sheet:

Reverse turn and  $\beta$ -hairpin scaffolds are integral part of proteins and polypeptides which are playing a vital role in several fundamental biological processes and also instrumental for the three dimensional structure.<sup>1, 2</sup> Due to significant biological properties, the reverse turn and  $\beta$ -hairpin structures have attracted much attention in the research field. Several research groups have developed model systems by making use of synthetically modified backbones, which mimic intriguing structures and functions of these protein subunits. With intensive research, chemists and biologists have shown that synthetically modified novel peptide mimetic systems possess potential applications in the interdisciplinary fields such as medicinal chemistry,<sup>2</sup> organocatalysis<sup>3</sup> and material chemistry.<sup>4</sup> The  $\beta$ -hairpin is a simple protein structural motif involving two beta strands that look like a hairpin. The  $\beta$ -sheet is divided into two major types **a**) antiparallel  $\beta$ -sheet and **b**) Parallel  $\beta$ -sheet (Figure 2.1).

**a) Antiparallel  $\beta$ -sheet:** This type is characterized by two peptide strands running in opposite directions held together by hydrogen bonding between the strands.

**b) Parallel  $\beta$ -sheet:** This type is characterized by two peptide strands running in the same direction held together by hydrogen bonding between the strands.

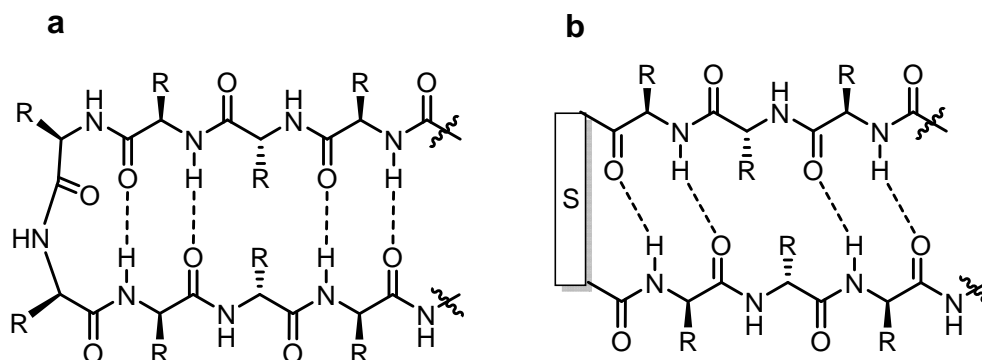


**Figure 2.1** a) General schematic representation antiparallel  $\beta$ -sheet, b) parallel  $\beta$ -Sheet (S = Spacer).

Antiparallel  $\beta$ -sheets can be constructed by attaching two adjacent antiparallel peptide strands to a peptidic or nonpeptidic-based linker, most often, a short loop or turn segment (Figure 2.1a).<sup>5</sup> Parallel  $\beta$ -sheets can be constructed by using nonpeptidic turn motifs such as diamine (Figure 2.2a) or diacid (Figure 2.2b) linker, which can connect

adjacent peptide strands through the C-terminus to C-terminus or N-terminus to N-terminus connection respectively.<sup>6-16</sup>

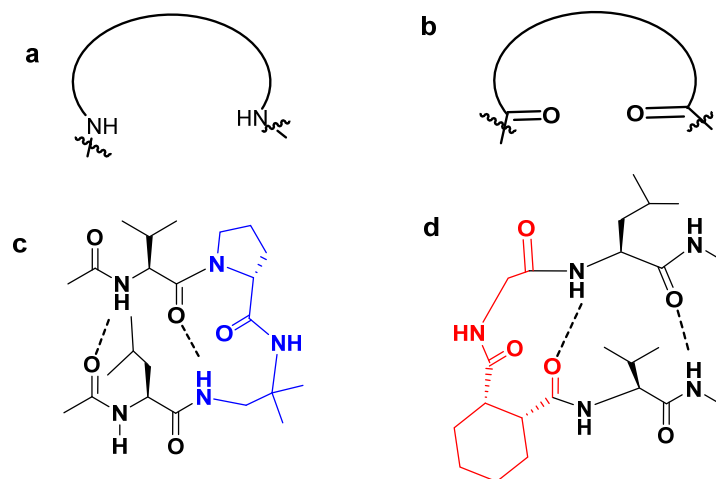


**Figure 2.2** Parallel  $\beta$ -sheet promoting linkers: diamine (a) and diacid (b). Examples of parallel  $\beta$ -sheet in the short peptides containing C to C linker DPro-DAMDE (c) and N to N linker CHDA-Gly (d).

Herein, we discuss the  $\beta$ -turn mimetics, in particular, that finds application in generating parallel  $\beta$ -sheet models. In this context, Feigel's group reported parallel  $\beta$ -sheet macrocycles using phenoxathiin-4,6-dicarboxylic acid and 2,8-dimethyl-4,6-bis(aminomethyl)phenoxathiin-10,10-dioxide moieties.<sup>6</sup> Sogah's group showed the parallel  $\beta$ -sheet models that contain 2,8-dimethylphenoxathiin 4,6-dicarboxylic acid motif as a turn inducing scaffold.<sup>7</sup> Kelly's group developed the dibenzofuran moiety-based diacid linker that promote parallel  $\beta$ -sheet conformation in peptides.<sup>8</sup> Nowick's group prepared artificial parallel  $\beta$ -sheet models utilizing urea-based reverse turn mimetics.<sup>9</sup> Karle and co-workers constructed the norbornene-based reverse turn scaffold to induce parallel  $\beta$ -sheet structures.<sup>10</sup> Gellman *et.al.* reported the reverse turn scaffold such as D-prolyl-(1,1-dimethyl)-1,2-diaminoethyl linker (D-Pro-DADME) to induce parallel  $\beta$ -sheet conformation (Figure 2.2c).<sup>11</sup> Subsequently, Gellman's group also utilized diacid linker-based reverse turn mimetics such as *cis*-1,2-cyclohexanedicarboxylic acid-Gly [(*S,R*)-CHDA-Gly, (Figure 2.2d) to create parallel  $\beta$ -sheet structures, wherein they attached adjacent peptide strands to nonpeptidic reverse turn scaffold *via* N-terminus to N-terminus connection.<sup>12</sup> Further, Gellman *et.al* also reported a small, stable, parallel  $\beta$ -sheet macrocyclic scaffold using N to N and C to C linker.<sup>13</sup> Kraatz and coworkers developed



ferrocene diacid linker which acts as a reverse turn scaffold to induce parallel sheet conformation in peptides.<sup>14</sup>

### 2.1.2. Urea based templates for parallel $\beta$ sheet structures:

$\beta$ -Sheets consist of extended polypeptide strands ( $\beta$ -strands) connected by a network of hydrogen bonds and occur widely in proteins. Although the importance of  $\beta$ -sheets in the folded structures of proteins has long been recognized, there is a growing recognition of the importance of intermolecular interactions among  $\beta$ -sheets. Intermolecular interactions between the hydrogen-bonding edges of  $\beta$ -sheets constitute a fundamental form of biomolecular recognition (like DNA base pairing) and are involved protein quaternary structure, protein-protein interactions, and peptide and protein aggregation. The importance of  $\beta$ -sheet interactions in biological processes makes them potential targets for intervention in diseases such as AIDS, cancer, and Alzheimer’s syndrome.

Lee’s group introduced D-Prolyl- *cis*-1,2-diaminocyclohexane (D-Pro-DACH); a conformationally constrained turn scaffold, which can find application in the generation of parallel  $\beta$ -sheet structures (Figure 2.3a).<sup>15</sup> An intriguing example of urea-based nonpeptidic reverse turn scaffold was developed by Smith *et.al.*, which can promote parallel  $\beta$ -sheet conformation in a cyclopropane-based  $\delta$ -amino acid-containing peptide (Figure 2.3b).<sup>16</sup> They further showed that synthetically modified urea-based analogues efficiently catalyze the asymmetric Mukaiyama-Mannich reaction (Figure 2.3c).<sup>17</sup>

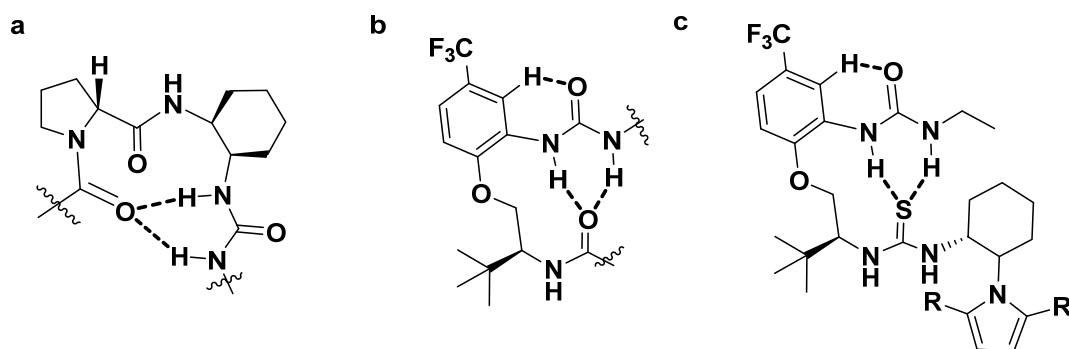


**Figure 2.3** Templates for the induction of parallel  $\beta$ -sheet structures (a and b), and dual hydrogen-bonded urea-based organocatalyst for Mukaiyama-Mannich reaction (c).

Nowick’s group developed many artificial  $\beta$ -sheet structures which are urea based foldamer (Figure 2.4a) containing parallel  $\beta$ -sheet (Figure 2.4b) anti parallel  $\beta$ -sheet (Figure 2.4c) three-stranded  $\beta$ -sheets containing parallel as well as anti parallel strands.

The group of D.S Kemp developed symmetrical  $\beta$ -sheet using 2, 8-diaminoepindolidione template (Figure 2.4d).

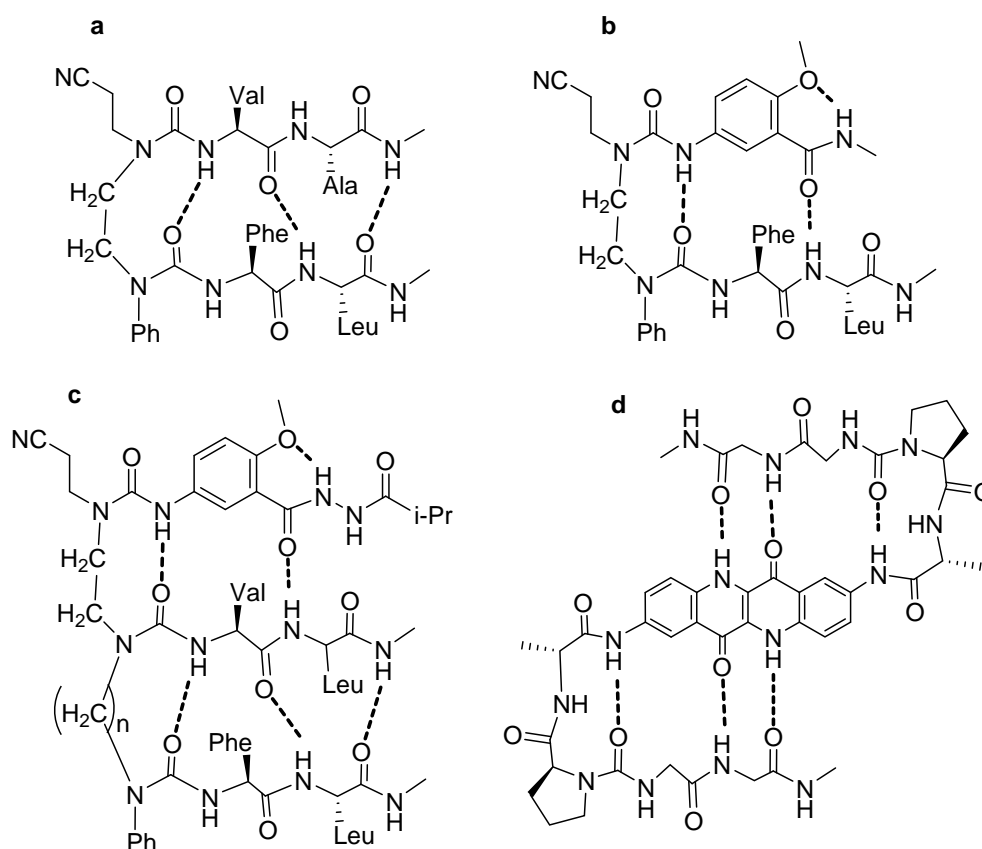


**Figure 2.4** Urea based foldamer containing (a) parallel  $\beta$ - sheet (b) anti parallel  $\beta$ - sheet (c) three-stranded  $\beta$ -sheets containing parallel as well as anti parallel  $\beta$ - sheet (d) symmetrical  $\beta$ -sheet contain 2,8-diaminoepindolidione template.

In summary, the studies in the development of  $\beta$ -sheet models revealed that in addition to the non covalent interactions, there are two more factors which substantially determine the stability of  $\beta$ -sheet structures: **a**) the turn scaffold which holds adjacent peptide strands and **b**) its precise position in the peptide sequence.

## 2.2 Objective and design strategy:

Herein, we have designed the urea-based foldamer of H-X-H three centred dual hydrogen bonding stabilized reverse turn scaffold containing a Ant-Pro (C9) reverse turn (developed in our laboratory)<sup>18</sup> and a urea moiety at the N-terminus of the turn motif (Figure 2.5). We anticipated that the urea NHs would form *intra* molecular dual hydrogen

bonding with the C=O of proline. In this regard, the urea moiety can be installed at the N-terminus of Ant-Pro reverse turn scaffold<sup>18</sup> by reacting H<sub>2</sub>N-Ant-Pro with various isocyanates. In the present study, various isocyanates used to generate the unsymmetrical as well as symmetrical urea analogues (1-4) shown in (Figure 2. 5). This urea-based dual hydrogen-bonded reverse turn scaffold can be linked to the peptide strands via N-terminus to N-terminus connection and thus can promote parallel  $\beta$ -sheet structures in the peptides.

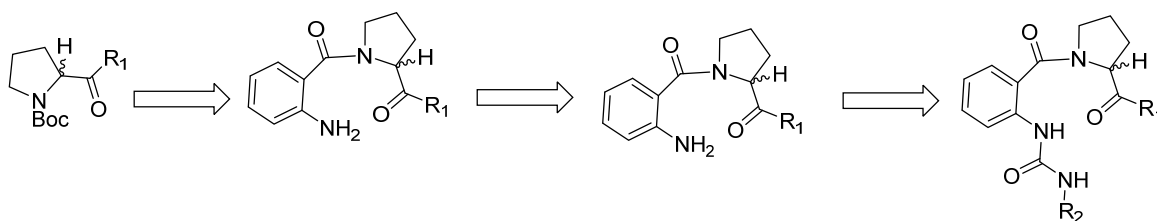


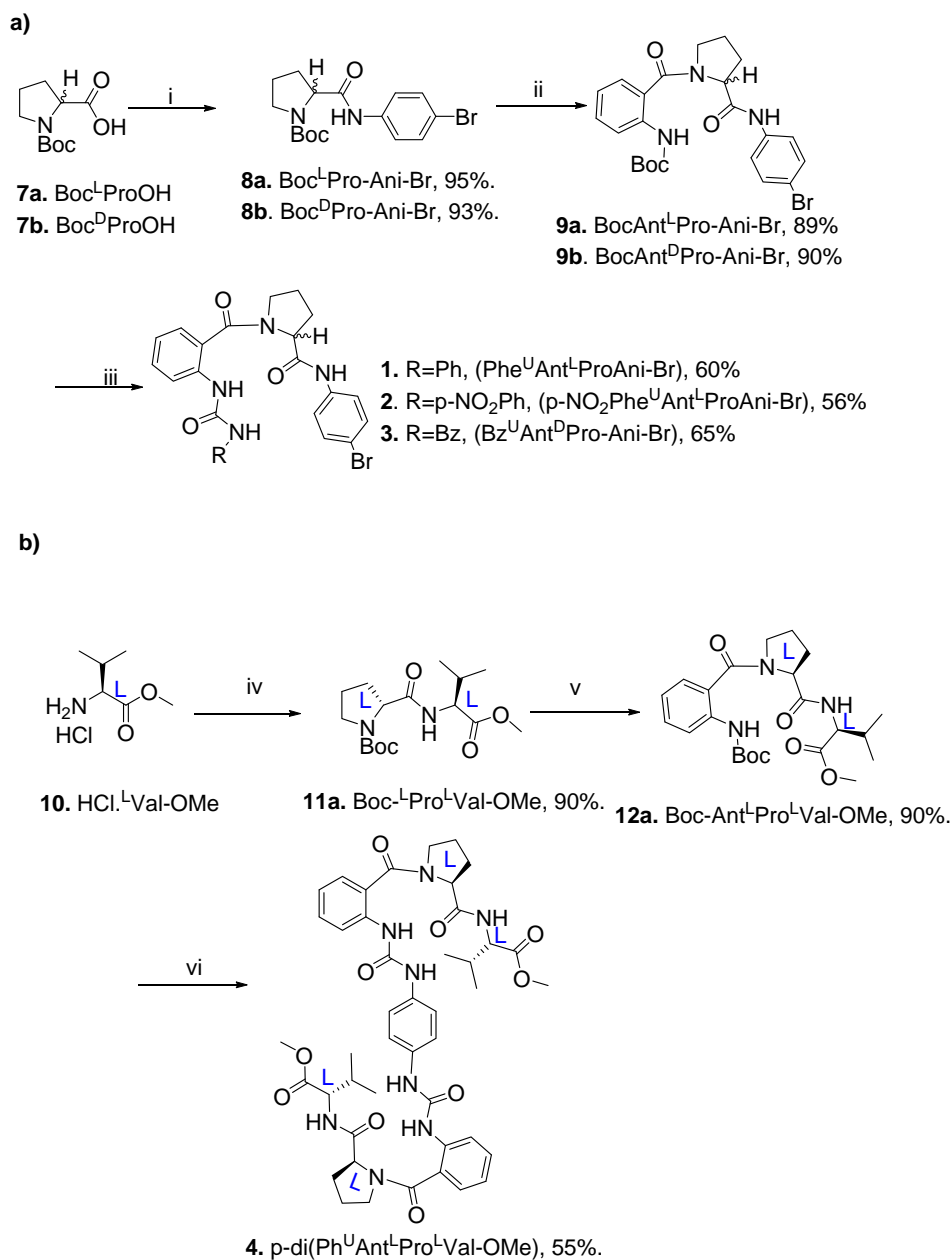
**Figure 2.5** Design strategy for the H-X-H three centered dual hydrogen bonding stabilized reverse turn (Ant Pro) scaffold.

### 2.3 Synthesis

The unsymmetrical urea analogues were synthesized from amine NH<sub>2</sub>- Ant-Pro-Ani-Br building block as shown in the Scheme 2.1a. The synthesis started by coupling of H-Pro-Ani-Br (Deprotected **8a/8b**) with Boc-Ant-OH in presence of HBTU, HOBT and DIEA which resulted in Boc-Ant-Pro-Ani-Br **9a/9b**. Next step was deprotection of Boc of **9a/9b** using TFA:DCM, to get the free amine H- Ant-Pro-Ani-Br, which was used for next coupling with different isocyanates to produces urea analogs **1** to **3**.

The symmetrical urea analogue was synthesized from amine NH<sub>2</sub>- Ant-Pro-Val-OMe building block as given in Scheme 2.1b. The synthesis started from coupling of Boc-<sup>L</sup>Pro-OH and HCl.H-<sup>L</sup>Val-OMe in presence of EDC.HCl, HOBT, DIEA, DCM, to get the dipeptide Boc-<sup>L</sup>Pro-<sup>L</sup>Val-OMe (**11a**). This dipeptide on Boc deprotection using TFA:DCM, resulted in free amine H-<sup>L</sup>Pro-<sup>L</sup>Val-OMe, which was used for next coupling reaction with Boc-Ant-OH in the presence of HBTU, HOBT and DIEA to get Boc-Ant-<sup>L</sup>Pro-<sup>L</sup>Val-OMe (**12a**). The tripeptide on deprotection with TFA:DCM, gave the free amine H-Ant-<sup>L</sup>Pro-<sup>L</sup>Val-OMe, which on coupling with 1,4-Phenylene diisocyanate, in Pyridine formed a symmetric urea analogue **4**. Formation of this symmetric urea is further confirmed by its <sup>1</sup>H and <sup>13</sup>C NMR spectra.

Scheme-2.1:

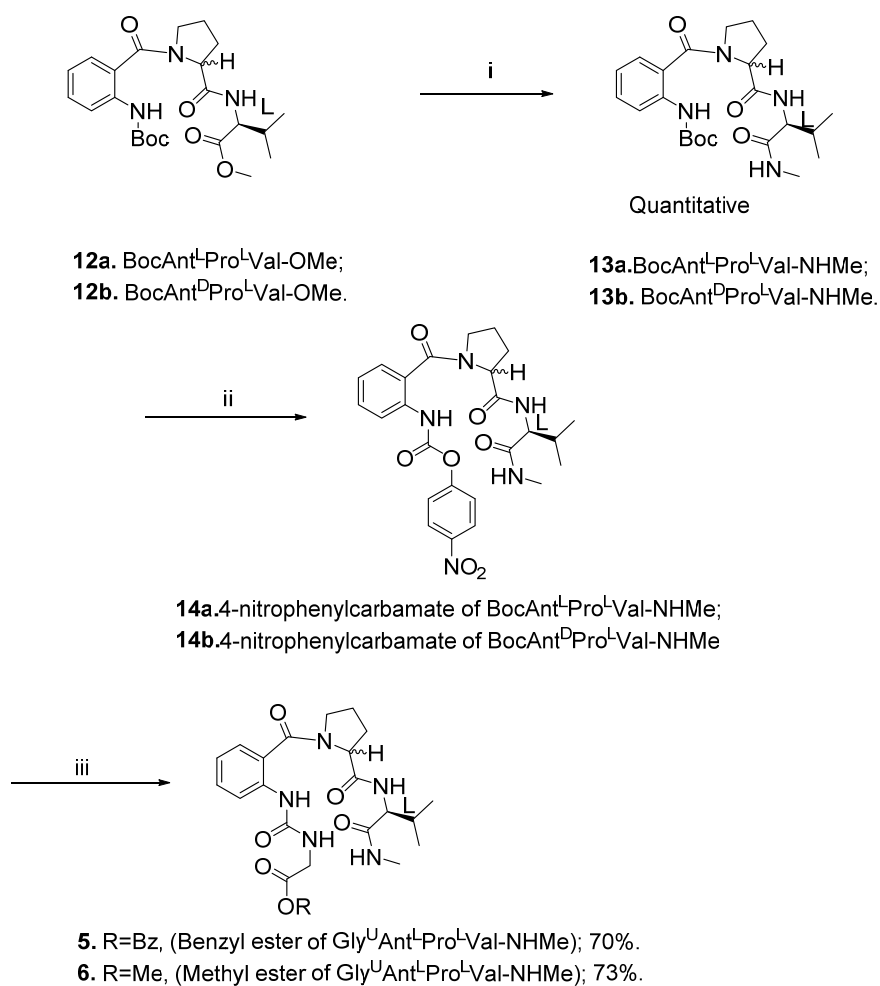


**Reagent & conditions:** (i) p-bromoaniline, EDC.HCl, DMAP, DCM, rt, 6h; (ii) TFA:DCM; (iib) BocAnt-OH, HBTU, ACN, rt, 8h; (iiia) TFA:DCM; (iiib) RNCO, Pyridine, rt, 5h. (iv). Boc<sup>L</sup>Pro-OH, EDC.HCl, HOBt, DIEA, DCM, rt, 8h; (va) TFA:DCM; (vb) BocAnt-OH, HBTU, ACN, rt, 6h; (via) TFA:DCM; (vib) 1,4-Phenylene diisocyanate, Pyridine, rt, 5h.

### Installation of N terminal amino acid

The synthetic root for the N-terminal amino acid incorporation into the designed urea-based foldamer is given in the following Scheme 2.2

Scheme-2.2:



**Reagent & conditions:** (i) MeNH<sub>2</sub> in MeOH, rt, 12h; (ii) TFA:DCM; (iib) 4-nitrophenyl chloroformate, NaHCO<sub>3</sub>, ACN, rt, 1h; (iii) PTSA salt of Gly-Bz/ HCl salt of Gly-OMe, DIEA, DMF, rt, 1h.

## 2.4 Results and discussion

### 2.4.1 Crystal structure analysis:

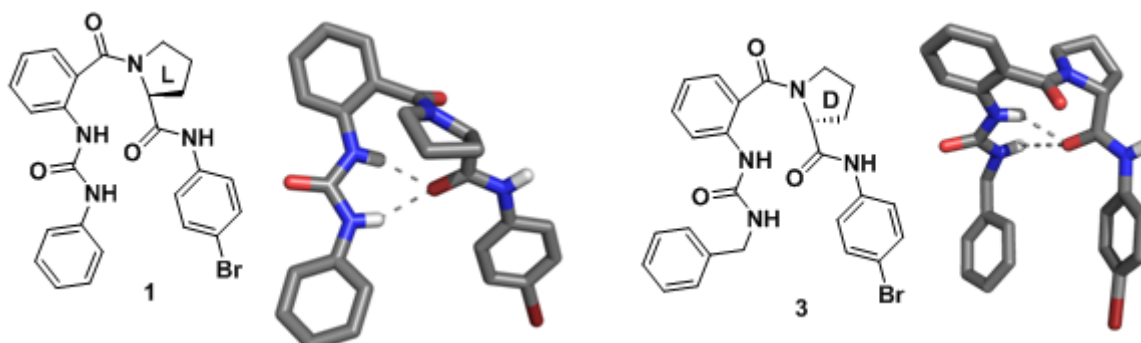


**Figure 2.6** Molecular structures (left) of **1** and **3** displaying observed hydrogen bonding and crystal structures (right).

After extensive crystallization trials, we could grow good quality crystals of an analogue **1** in a mixture of ethyl acetate and toluene while analogue **3**, crystals were grown in ethyl acetate and pet ether mixture. The crystal structure (Figure 2.6) analysis of **1** and **3** revealed that the distance between NH1 and NH2 is 2.0 Å for **1** and 2.1 Å for **3** which indicated the trans-trans configuration of the urea-NH'S and planar orientation of urea moiety in the solid-state. The hydrogen bonding distances were found to be [d(NH1---O) = 2.1 Å] and [d(NH2---O) = 2.1 Å] for **1**, while for **3**, [d(NH1---O) = 2.5 Å] and [d(NH2---O) = 2.1 Å], which clearly suggested participation of urea NH's in the strong *intra* molecular hydrogen bonding with carbonyl of proline. Crystal structure also revealed that on alteration of chirality of proline residue doesn't affect the hydrogen bonding pattern of urea NHs.

### 2.4.2 NMR Studies of 1-4

We have undertaken detailed 2D NMR studies of all synthetic urea analogues (**1-4**) to gain insights into solution-state conformation of urea-based scaffolds (see experimental section 2.5). The involvement of urea-NHs in an *intra* molecular hydrogen bonding was confirmed by variable temperature (VT) experiments and DMSO- $d_6$  titration studies in  $CDCl_3$ .

#### 2.4.2.1 Variable temperature studies of 1-4

The values of temperature coefficients obtained for urea-NHs of **1-4** (*vide infra* Table 2.1) were found to be very negligible [ $\Delta\delta/\Delta T$  (NH1 or NH2) < -3 ppb/K] which clearly indicated their participation in strong *intra* molecular hydrogen bonding, while, on the contrary, larger value of temperature coefficient for NH3 [ $\Delta\delta/\Delta T$  (NH3) > -5 ppb/K] suggested its solvent exposed nature or non involvement of *intra* molecular hydrogen bonding.

**Table 2.1** Temperature coefficients and chemical shift change in DMSO-*d*<sub>6</sub> titration studies of compounds **1-4**.

Urea analogues	Temp coefficients <sup>a</sup> $\Delta\delta/\Delta T$ (ppb/K)			Chemical shifts <sup>b</sup> $\Delta\delta$ (ppm)		
	NH1	NH2	NH3	NH1	NH2	NH3
1	-3.79	-4.5	-8.36	0.24	0.09	0.44
2	-1.81	-4.1	-8.0	0.23	0.30	0.42
3	-2.9	-4.36	-6.18	0.12	0.09	0.35
4	-3.23	-2.92	-3.80	0.20	0.1	1.23

Note: <sup>a</sup> Variable temperature studies carried out in CDCl<sub>3</sub> (2 mM, 700 MHz) and <sup>b</sup> Values of chemical shifts obtained from DMSO-*d*<sub>6</sub> titration studies in CDCl<sub>3</sub> (2 mM, 700 MHz, 298 K). See tables 2.3 to 2.6 in the experimental section.

#### 2.4.2.2 DMSO-*d*<sub>6</sub> titration studies of 1-4

We carried out DMSO-*d*<sub>6</sub> titration studies of all in CDCl<sub>3</sub>, the values of chemical shifts change for urea-NHs of **1-4** (*vide supra* Table. 2.1) were found to be very negligible [ $\Delta\delta$  (NH1 or NH2) < 0.3 ppm] which clearly indicated their involvement in strong *intra* molecular hydrogen bonding. On the contrary larger value of chemical shifts change seen for NH3 [ $\Delta\delta$  (NH3) > 0.3 ppm] suggested its non involvement in *intra* molecular hydrogen bonding.

#### 2.4.2.3 NOESY/ROESY analysis and MD simulated structures

Solution state conformational investigation of **1-4** was done using 2D NOESY/ROESY experiment in CDCl<sub>3</sub>. The noticeable inter-residual nOes were observed in the compound **1-4**, such as NH2/C12Ha and C4H/C12Hb (Figure 2.7), which suggested that compound **1-4** adopted well-defined folded conformation (C9 turn). The appropriately positioned





### 2.4.3 Solution state conformational investigation of **5** and **6**

#### 2.4.3.1 Variable temperature studies and DMSO-*d*<sub>6</sub> titration studies.

The values of temperature coefficients for urea-NHs of **5** and **6** (*vide infra* Table 2.2 and also see tables 2.7 and 2.8 in the experimental section) were found to be very negligible [ $\Delta\delta/\Delta T$  (NH1 or NH2) < -3 ppb/K] (except NH2 of **6**) which clearly indicated their participation in strong *intra* molecular hydrogen bonding, while larger value of temperature coefficient for NH3 and NH4 [ $\Delta\delta/\Delta T$  (NH3 or NH4) > -5 ppb/K] suggested its solvent exposed nature or non involvement of *intra* molecular hydrogen bonding.

In the DMSO-*d*<sub>6</sub> titration studies, the values of chemical shift changes for urea-NHs of **5** and **6** (*vide infra* Table 2.2) were found to be very negligible [ $\Delta\delta$  (NH1 or NH2) < 0.3 ppm] which clearly indicated their involvement in strong *intra* molecular hydrogen bonding. The larger value of chemical shifts change for NH3 and NH4 [ $\Delta\delta$  (NH3 or NH4) > 0.3 ppm] suggested its non involvement in *intra* molecular hydrogen bonding.

**Table 2.2** Temperature coefficients and chemical shift change in DMSO-*d*<sub>6</sub> titration studies of compounds **5** and **6**.

Urea analogues	Temp coefficients <sup>a</sup> $\Delta\delta/\Delta T$ (ppb/K)				Chemical shifts <sup>b</sup> $\Delta\delta$ (ppm)			
	NH1	NH2	NH3	NH4	NH1	NH2	NH3	NH4
<b>5</b>	-3.33	-3.33	-9.5	-9.6	0.14	0.01	0.17	0.68
<b>6</b>	-3.09	-7.81	-6.72	-9.63	0.15	0.05	0.67	0.45

Note: <sup>a</sup> Variable temperature studies carried out in CDCl<sub>3</sub> (5 mM, 700 MHz) and <sup>b</sup> Values of chemical shifts obtained from DMSO-*d*<sub>6</sub> titration studies in CDCl<sub>3</sub> (5 mM, 700 MHz, 298 K). Also see tables 2.7 and 2.8, in the experimental section.

#### 2.4.3.2: NOESY analysis and MD simulation of **5** and **6**.

The noticeable inter-residual nOes were observed in the compound **5** and **4**, such as NH2/C14Ha and C6H/C14Hb, which suggested that compound **5** and **6** adopted well-defined folded conformation (C9 turn). The appropriately positioned C=O group of proline and trans-trans conformation of urea can form the dual hydrogen bonding effectively. The significant nOe C11H/NH3 and weak nOe C16H/NH3 confirmed projection of C=O group of proline towards urea-NHs while strong nOe: NH2/NH1

confirmed the trans-trans conformation of urea and hence the hydrogen bonding sites facilitated participation of C=O of proline in the dual hydrogen bonding with urea-NHs in compound **5** and **6** shown in Figure 2.9.

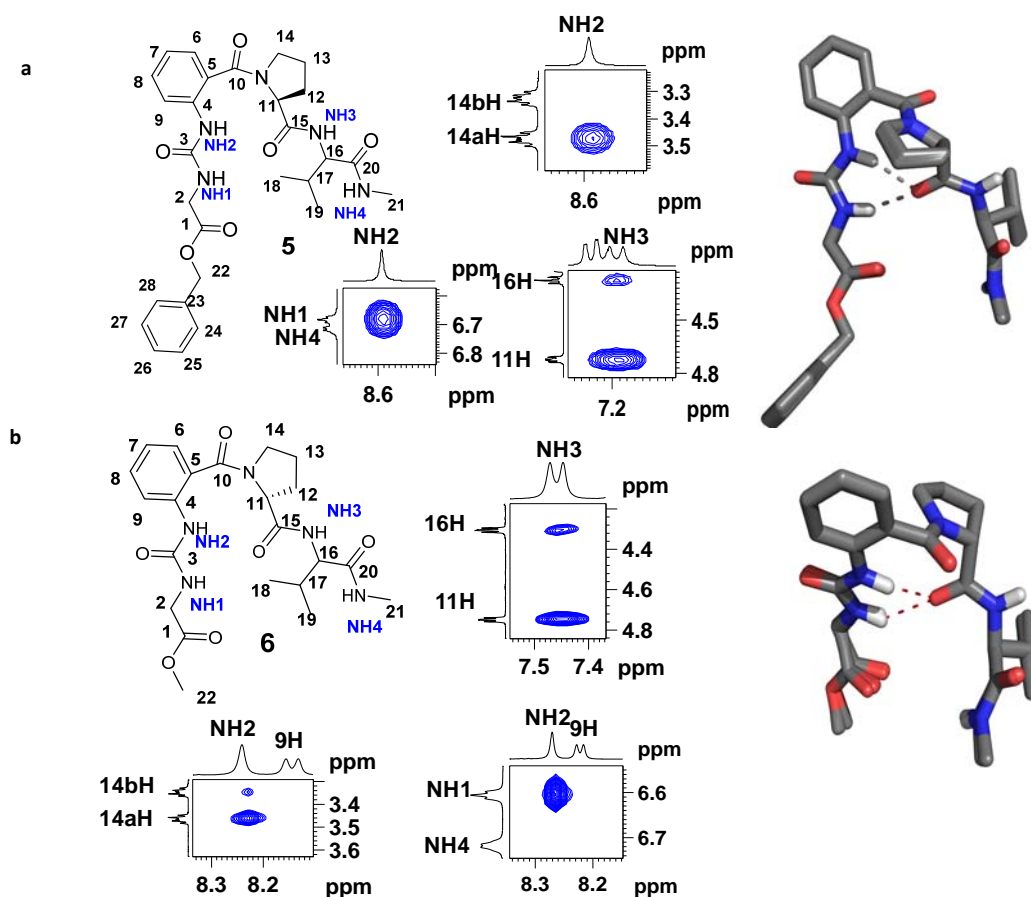
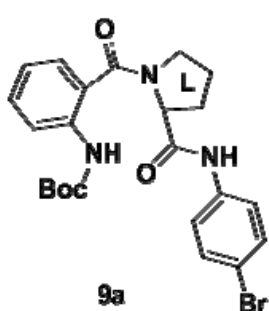


**Figure 2.9 (a) and (b)** Structure of **5** and **6** with characteristic nOe's and overly of MD simulated 20 minimized structures calculated using nOe restraints given in Table 2.10 and 2.11 respectively..

## 2.5 Conclusions

Conformational investigations of designed urea derivatives (unsymmetrical as well as symmetrical urea) in the solid and solution-state by single crystal X-ray crystallography and detailed 2D NMR studies, respectively, revealed that these scaffolds adopt well-defined conformation featuring robust urea-based H-X-H three-centered C9 and C11 dual hydrogen bonding. We also standardized the protocol for this urea scaffold attached to peptide strands through N-terminus as well as C- terminus, and thus it can serve as a template to promote parallel  $\beta$ -sheet structures.

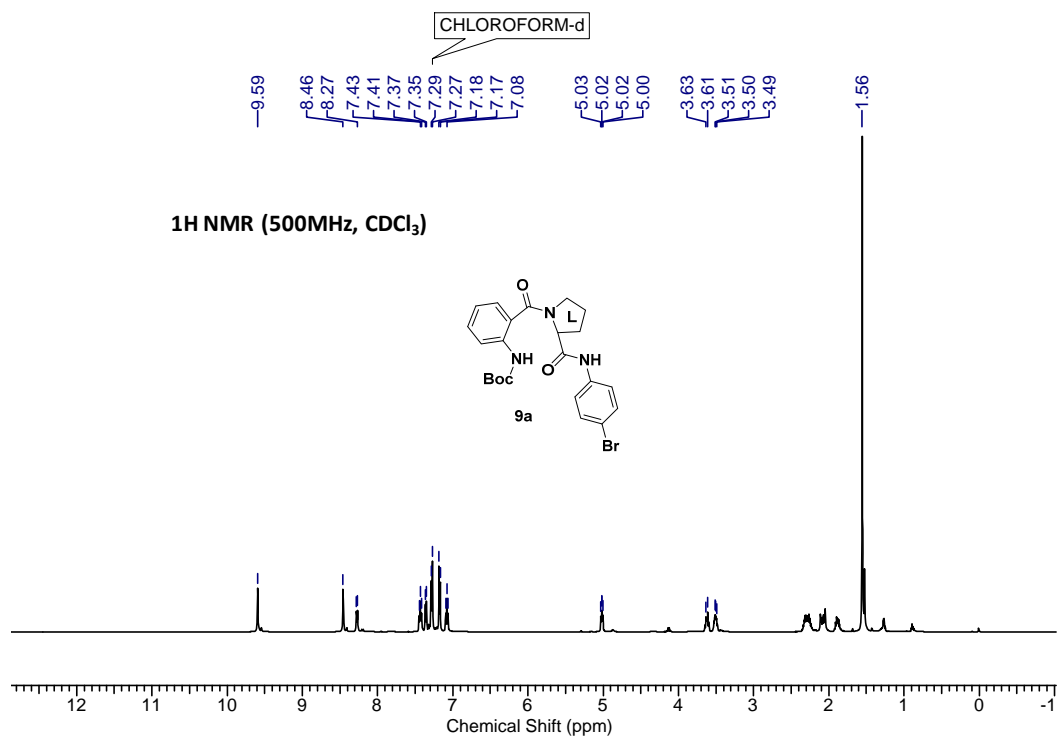
## 2.6 Experimental Section: Experimental Procedure and data



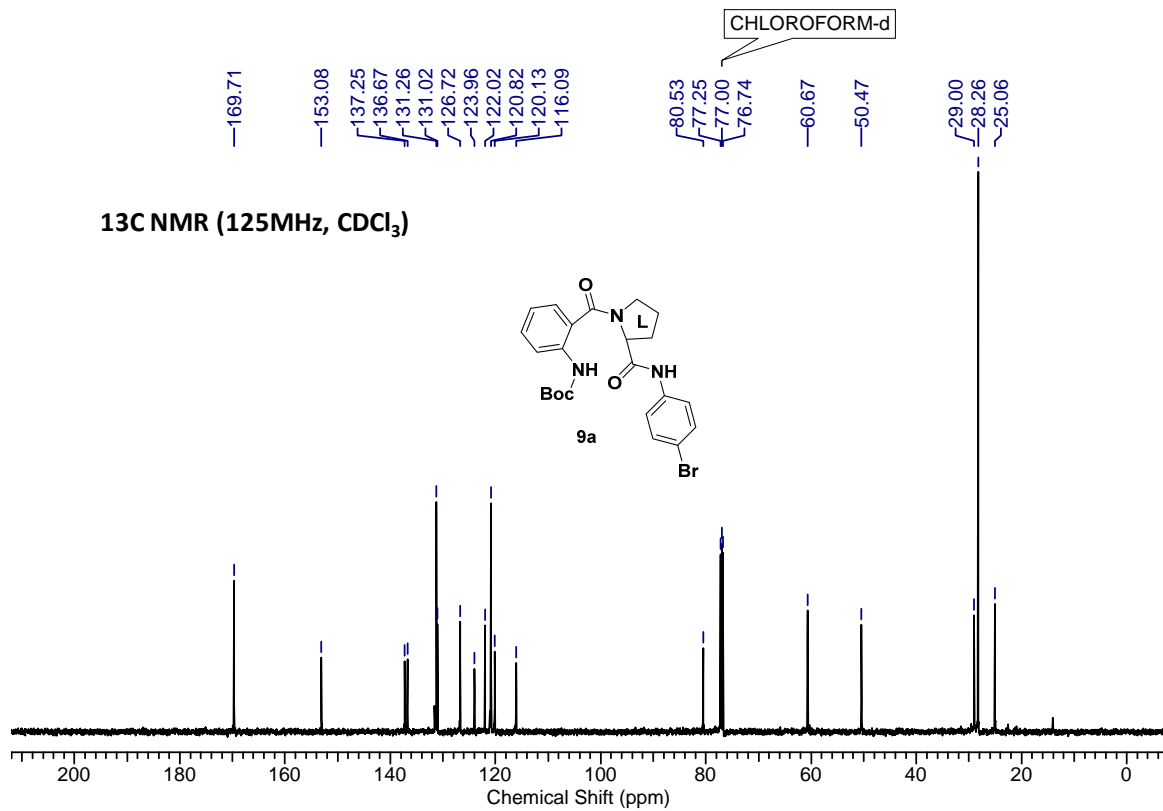
**Compound 9a: (Boc-Ant-<sup>L</sup>Pro-Ani-Br):** To a solution of H-Pro-Ani-Br (1.3 g, 4.85 mmol, 1 equiv.) and DIEA (2.53 mL, 1.45 mmol, 3 equiv.) in ACN (15 mL), Boc-Ant-OH (1.2 g, 5.3 mmol, 1.1 equiv.) was added, followed by addition of HBTU (2.75 g, 7.27 mmol, 1.3 equiv.) and HOBT (catalytic amount). The reaction mixture was stirred at room temperature for 8 h. After completion of reaction, ACN was removed under reduced pressure and the product was taken into ethyl acetate. The combined organic layers were washed sequentially with saturated solutions of KHSO<sub>4</sub>, NaHCO<sub>3</sub> and brine. Organic layer was then dried over Na<sub>2</sub>SO<sub>4</sub> and was evaporated under vacuum. The crude product was purified by column chromatography (eluent 35% AcOEt/pet. Ether, R<sub>f</sub>: 0.3) to furnish **9a** (2.05 g, 89%) as a white solid. Mp: 193-195 °C;  $[\alpha]_{D}^{26.16} = -52.12$  ( $c = 0.16$ , CHCl<sub>3</sub>); IR (CHCl<sub>3</sub>)  $\nu$  (cm<sup>-1</sup>), 3314.17, 3282.46, 3020.05, 1724.04, 1690.52, 1615.25, 1536.18, 1158.76; <sup>1</sup>H NMR (500 MHz, CDCl<sub>3</sub>-d)  $\delta$  ppm = 9.59 (s, 1H), 8.46 (s, 1H), 8.27 (d,  $J = 8.4$  Hz, 1H), 7.43 (t,  $J = 7.8$  Hz, 1H), 7.36 (d,  $J = 7.2$  Hz, 1H), 7.28 (d,  $J = 8.8$  Hz, 2H), 7.18 (d,  $J = 8.8$  Hz, 2H), 7.08 (t,  $J = 7.4$  Hz, 1H), 5.02 (dd,  $J = 5.9, 7.8$  Hz, 1H), 3.71 - 3.58 (m, 1H), 3.55 - 3.45 (m, 1H), 2.39 - 2.18 (m, 2H), 2.14 - 1.99 (m, 2H), 1.94 - 1.83 (m, 1H), 1.56 (s, 9H); <sup>13</sup>C NMR (125 MHz, CDCl<sub>3</sub>)  $\delta$  ppm = 169.7, 153.1, 137.3, 136.7, 131.5, 131.3, 131.0, 126.7, 124.0, 122.0, 120.8, 120.1, 116.1, 80.5, 60.7, 50.5, 29.0, 28.3, 25.1; HR-MS C<sub>23</sub>H<sub>27</sub>BrN<sub>3</sub>O<sub>4</sub> calculated: 487.1185, Found: 488.1185; C<sub>23</sub>H<sub>26</sub>BrN<sub>3</sub>NaO<sub>4</sub> calculated: 510.1004, Found: 512.0982.

## Chapter II: Design, Synthesis & Conformational Investigation of “Ant-Pro Urea” Based Foldamers

a)



b)



c)

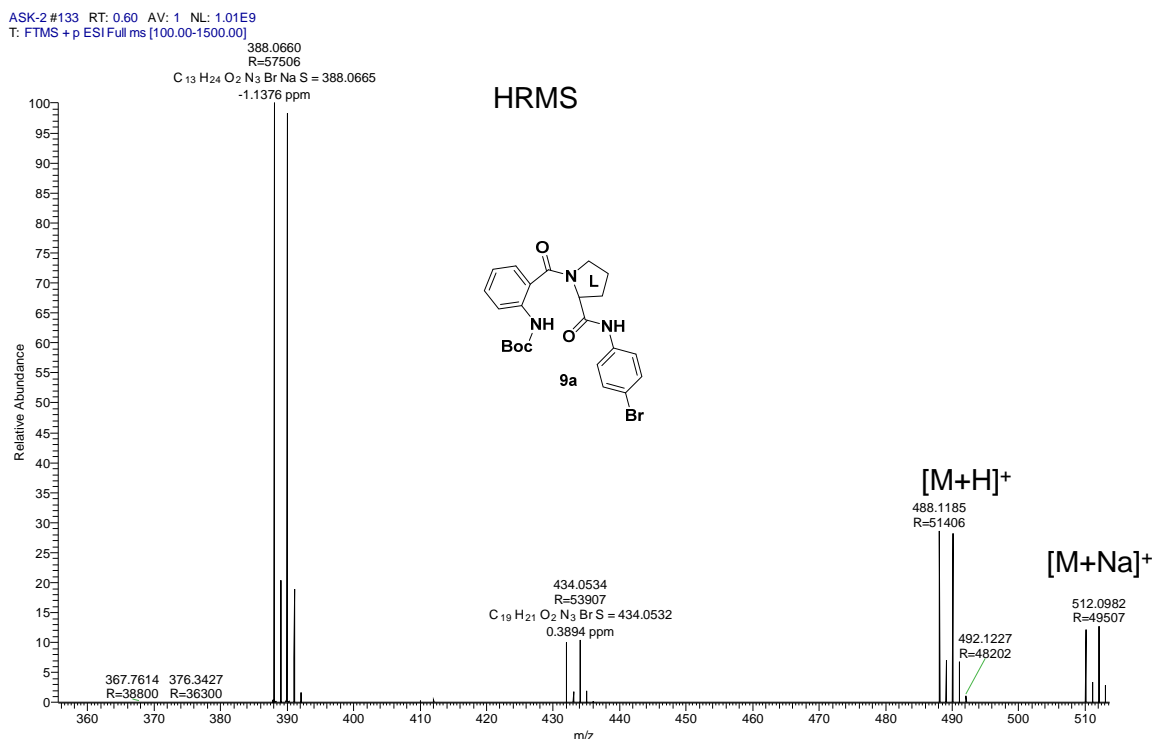
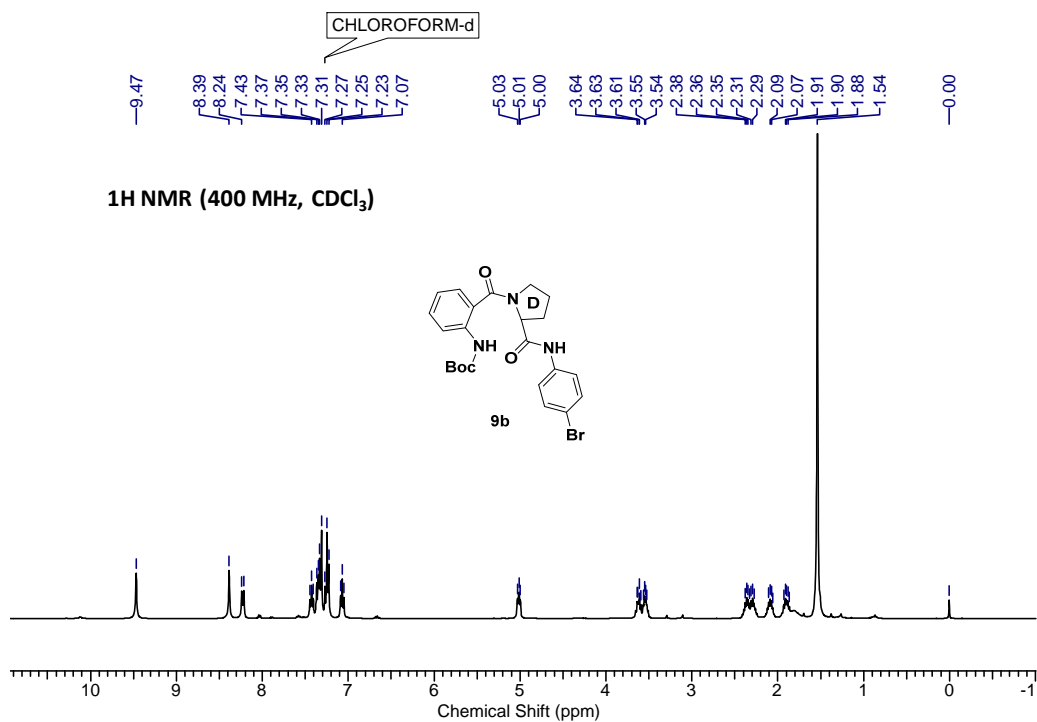


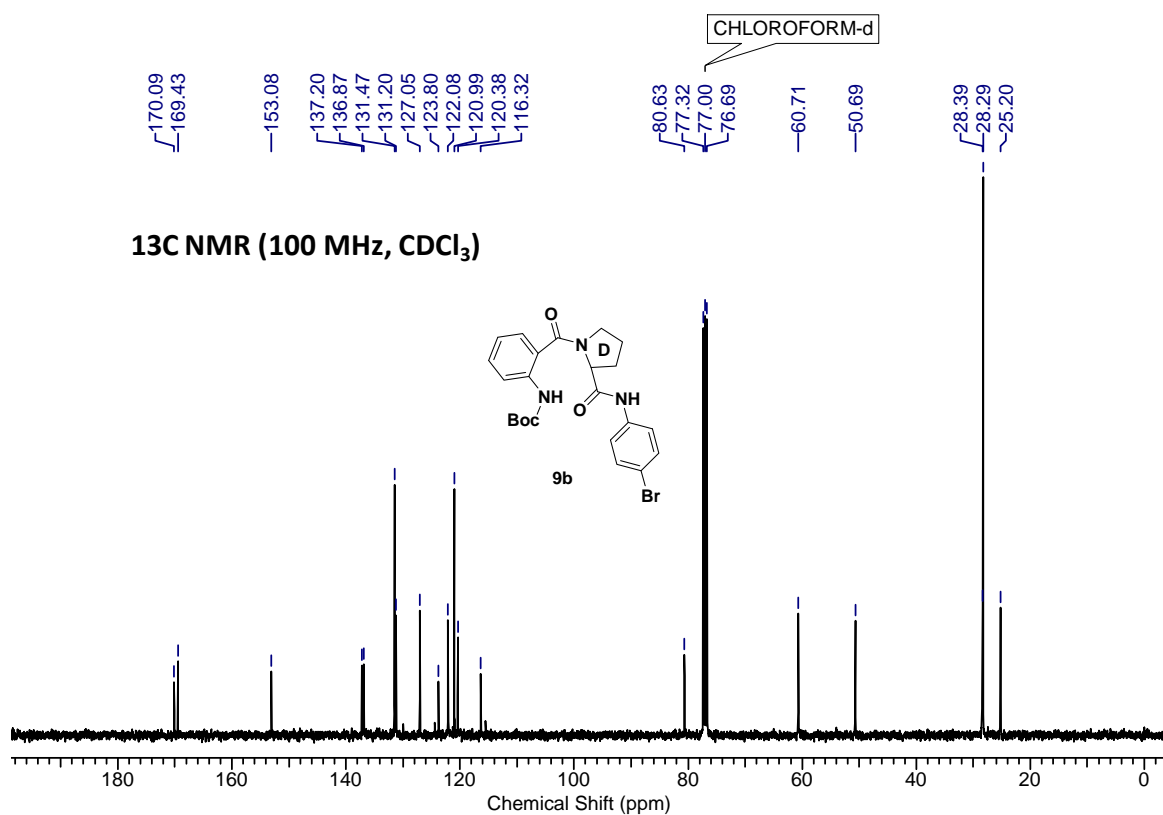
Figure 2.10 a) <sup>1</sup>H NMR, b) <sup>13</sup>C NMR and c) HRMS spectra of compound **9a**

**Compound 9b (Boc-Ant-<sup>D</sup>Pro-Ani-Br):** Compound **9b** was prepared using same procedure of **9a**. **9b** is a white solid. Mp:195-197 °C;  $[\alpha]_D^{26.28} = 86.96$  ( $c = 0.15$ , CHCl<sub>3</sub>); IR (CHCl<sub>3</sub>)  $\nu$  (cm<sup>-1</sup>) 3312.78, 3305.08, 3019.22, 2982.05, 1723.58, 1688.93, 1615.57, 1523.37, 1458.53, 1158.55, <sup>1</sup>H NMR (400MHz, CDCl<sub>3</sub>)  $\delta$  ppm : 9.47 (s, 1H), 8.39 (s, 1H), 8.23 (d,  $J = 7.9$  Hz, 1H), 7.43 (t,  $J = 7.6$  Hz, 1H), 7.36 (d,  $J = 7.9$  Hz, 1H), 7.32 (d,  $J = 8.5$  Hz, 2H), 7.26 - 7.20 (m, 2H), 7.07 (t,  $J = 7.6$  Hz, 1H), 5.06 - 4.96 (m, 1H), 3.67 - 3.58 (m, 1H), 3.58 - 3.48 (m, 1H), 2.45 - 2.21 (m, 2H), 2.17 - 2.01 (m, 1H), 1.98 - 1.85 (m, 1H), 1.54 (s, 9H); <sup>13</sup>C NMR (100MHz, CDCl<sub>3</sub>)  $\delta$  ppm : 170.1, 169.4, 153.1, 137.2, 136.9, 131.5, 131.2, 127.0, 123.8, 122.1, 121.0, 120.4, 116.3, 80.6, 60.7, 50.7, 28.3, 28.2, 25.2; HR-MS C<sub>23</sub>H<sub>27</sub>BrN<sub>3</sub>O<sub>4</sub> Calculated: 487.1107, Found: 490.1161; C<sub>23</sub>H<sub>26</sub>BrN<sub>3</sub>NaO<sub>4</sub> Calculated: 510.1004, Found: 510.1003.

a)



b)



c)

ASK-12 #149 RT: 0.66 AV: 1 NL: 1.34E9  
T: FTMS + p ESI Full ms [100.00-1500.00]

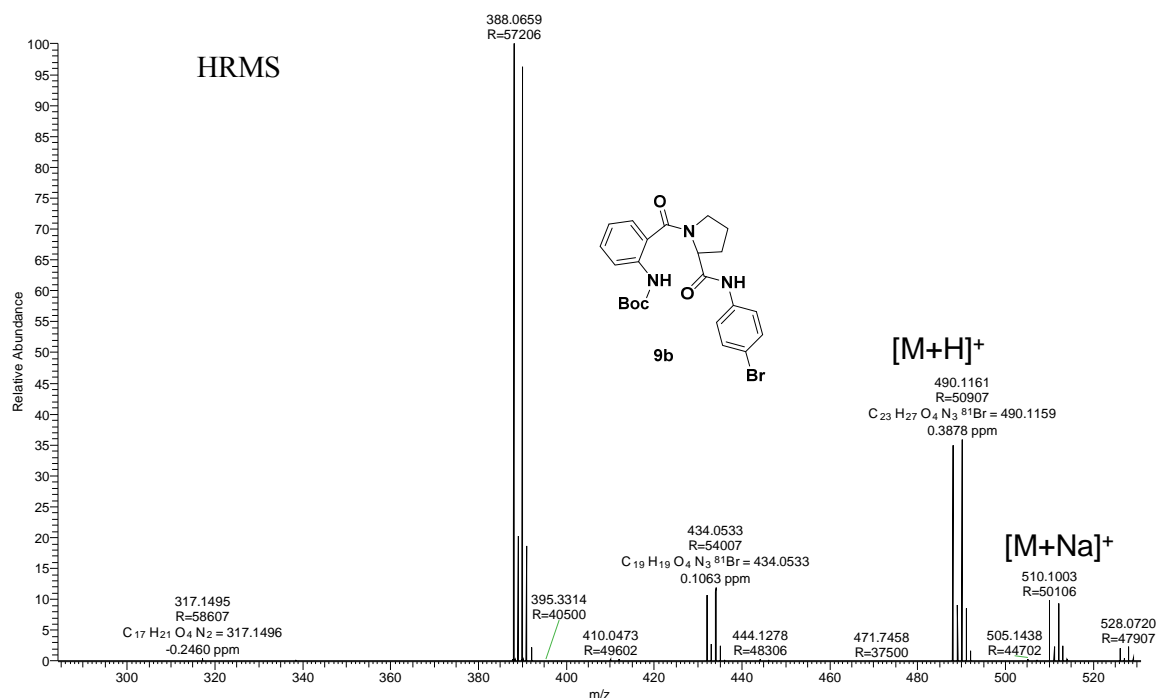


Figure 2.11 a) <sup>1</sup>H NMR, b) <sup>13</sup>C NMR and c) HRMS spectra of compound 9b

### Boc Deprotection:

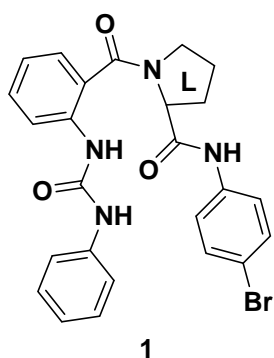
Boc-9a or 9b was deprotected with TFA:DCM and DCM was evaporated under vacuum, to get the TFA salt which was neutralized by solution of NaHCO<sub>3</sub> and extracted with DCM. The organic layer was washed with water and brine and dried over Na<sub>2</sub>SO<sub>4</sub> and was evaporated under vacuum. The crude product (free amine i.e. H-AntProAni-Br) was used for next reactions, without further purification.

### Synthetic procedure for compounds 1, 2, & 3:

The amine (H-AntProAni-Br, 1equiv.) was taken into 2 mL of dry pyridine and the solution was stirred for 5 min at 0 °C, isocyanate (1 equiv.) and activated molecular sieves were added to the reaction mixture. This reaction was stirred at room temperature for 4-5 h. After completion of reaction, the reaction mixture was diluted with ethyl acetate (20 mL). Pyridine from mixture was removed by washing several times with CuSO<sub>4</sub> solution. Organic layer was dried over Na<sub>2</sub>SO<sub>4</sub> and was evaporated under vacuum. The crude product was purified by column chromatography (eluent 30% AcOEt/pet. Ether, R<sub>f</sub>: 0.3).

Chapter II: Design, Synthesis & Conformational Investigation of “Ant-Pro Urea”  
Based Foldamers

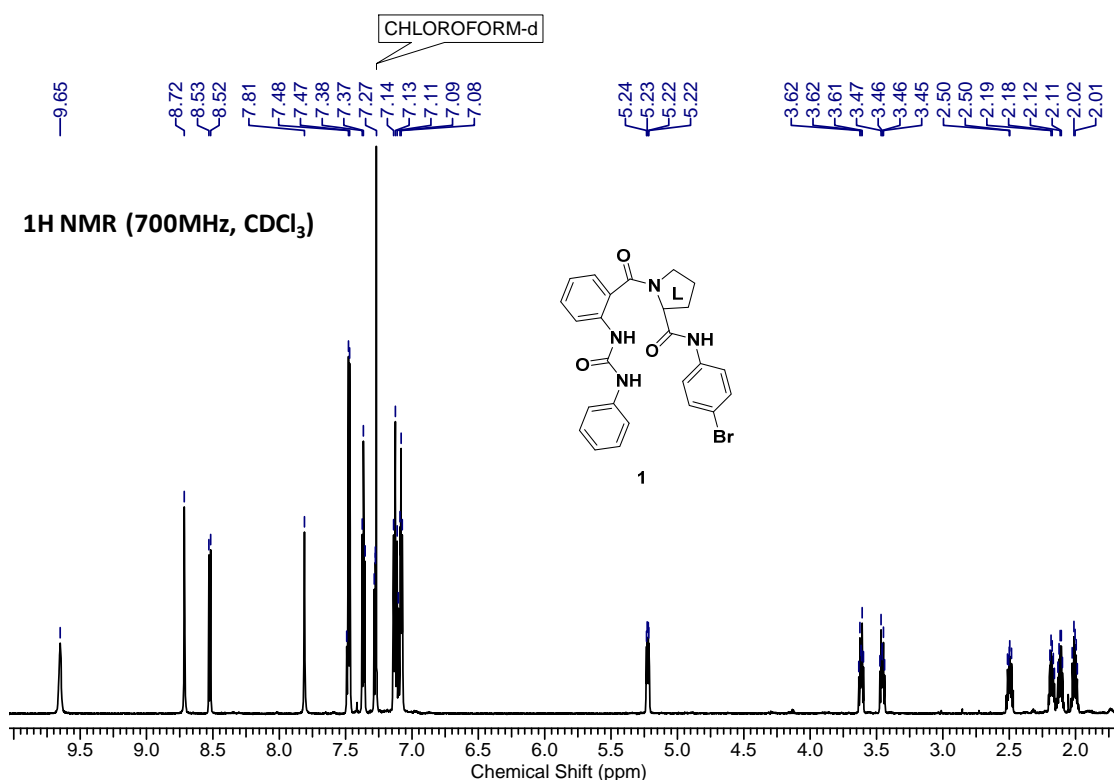
**Compound 1:** Compound 1 was yielded as a white solid (60 %), mp: 168-170 °C;



$[\alpha]^{26.54}_D = 17.54.96$  ( $c = 0.1$ ,  $\text{CHCl}_3$ ); IR ( $\text{CHCl}_3$ )  $\nu$  ( $\text{cm}^{-1}$ ) 3385.50, 3299.87, 3129.43, 1716.33, 1545.77, 1216.51.  $^1\text{H}$  NMR (700MHz,  $\text{CDCl}_3$ )  $\delta$  ppm : 9.65 (bs, 1 H), 8.72 (s, 1 H), 8.52 (d,  $J = 8.4$  Hz, 1 H), 7.81 (s, 1 H), 7.48 (m, 3 H), 7.37 (t,  $J = 7.9$  Hz, 2 H), 7.13 (t,  $J = 9.4$  Hz, 3 H), 7.28 (dd,  $J = 1.1, 7.53$  Hz, 1 H), 7.14 - 7.07 (m, 6 H), 5.23 (dd,  $J = 5.1, 8.9$  Hz, 1 H), 3.62 (m, 1 H), 3.46 (m, 1 H), 2.53 (m, 1 H), 2.18 (m, 1 H), 2.12 (m, 1 H), 2.01 (m, 1 H);  $^{13}\text{C}$

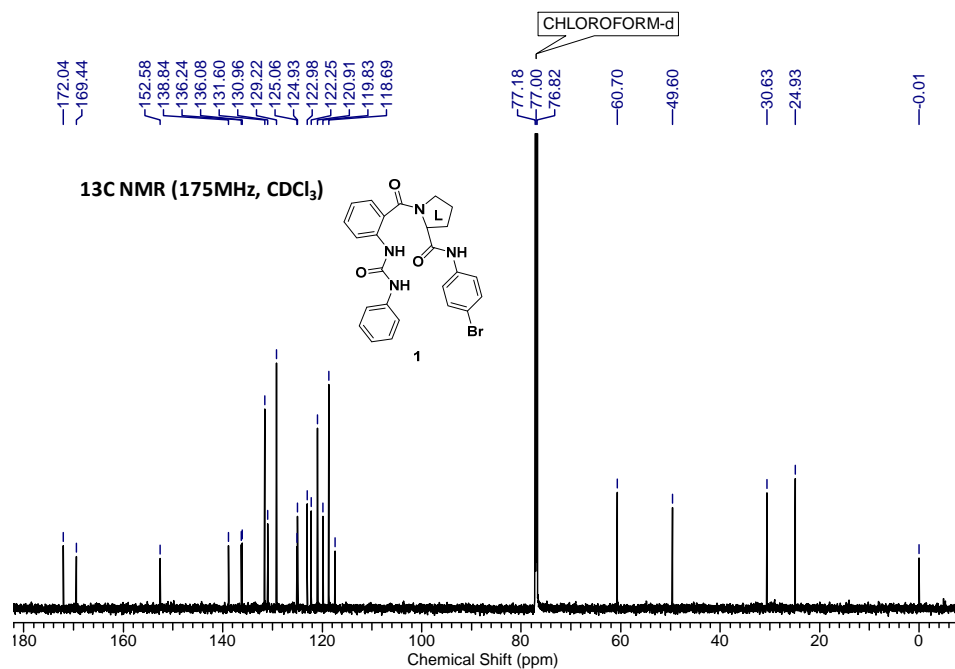
NMR (175 MHz,  $\text{CDCl}_3$ )  $\delta$  ppm : 172.0, 169.4, 152.6, 138.8, 136.2, 136.1, 131.6, 131.0, 129.2, 125.1, 124.9, 123.0, 122.2, 120.9, 119.8, 118.7, 117.4, 60.7, 49.6, 30.6, 24.9; HRMS  $[\text{M}+\text{H}]^+$   $\text{C}_{25}\text{H}_{24}\text{BrN}_4\text{O}_3$  Calculated: 507.0954, Found: 507.1033,  $[\text{M}+\text{Na}]^+$   $\text{C}_{25}\text{H}_{23}\text{BrN}_4\text{NaO}_3$  Calculated: 529.0851, Found: 529.0850.

a)





b)



c)

ASK-3 #141 RT: 0.63 AV: 1 NL: 1.80E8  
T: FTMS + p ESI Full ms [100.00-1500.00]

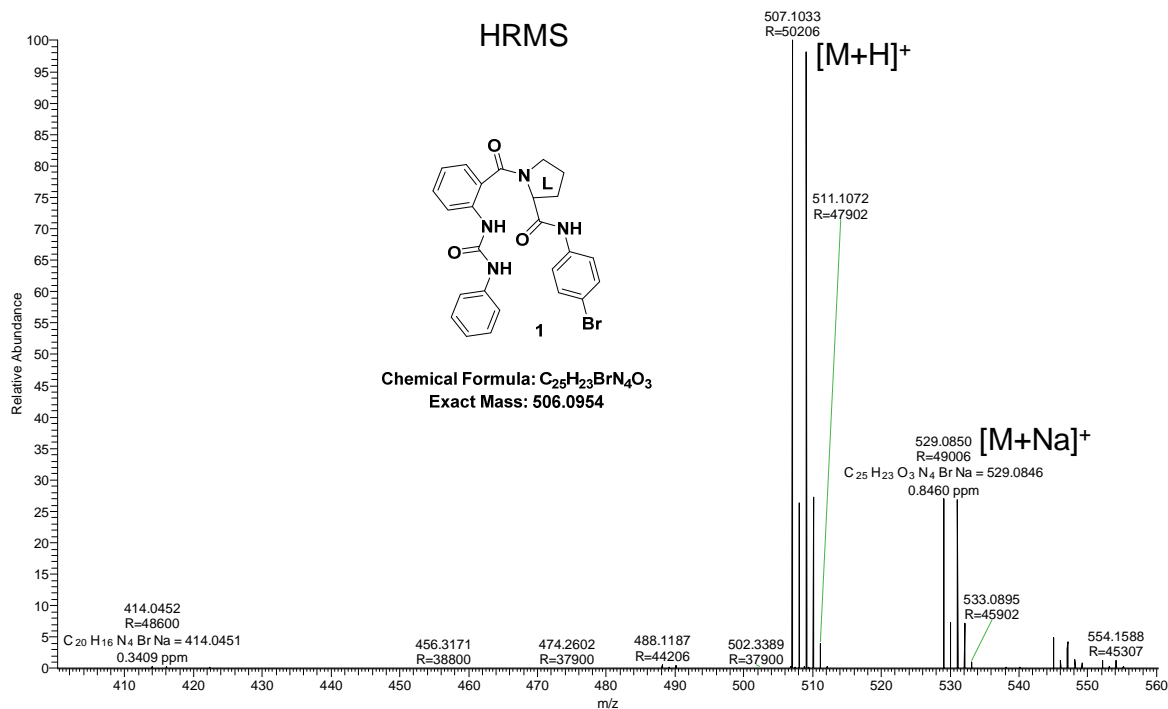


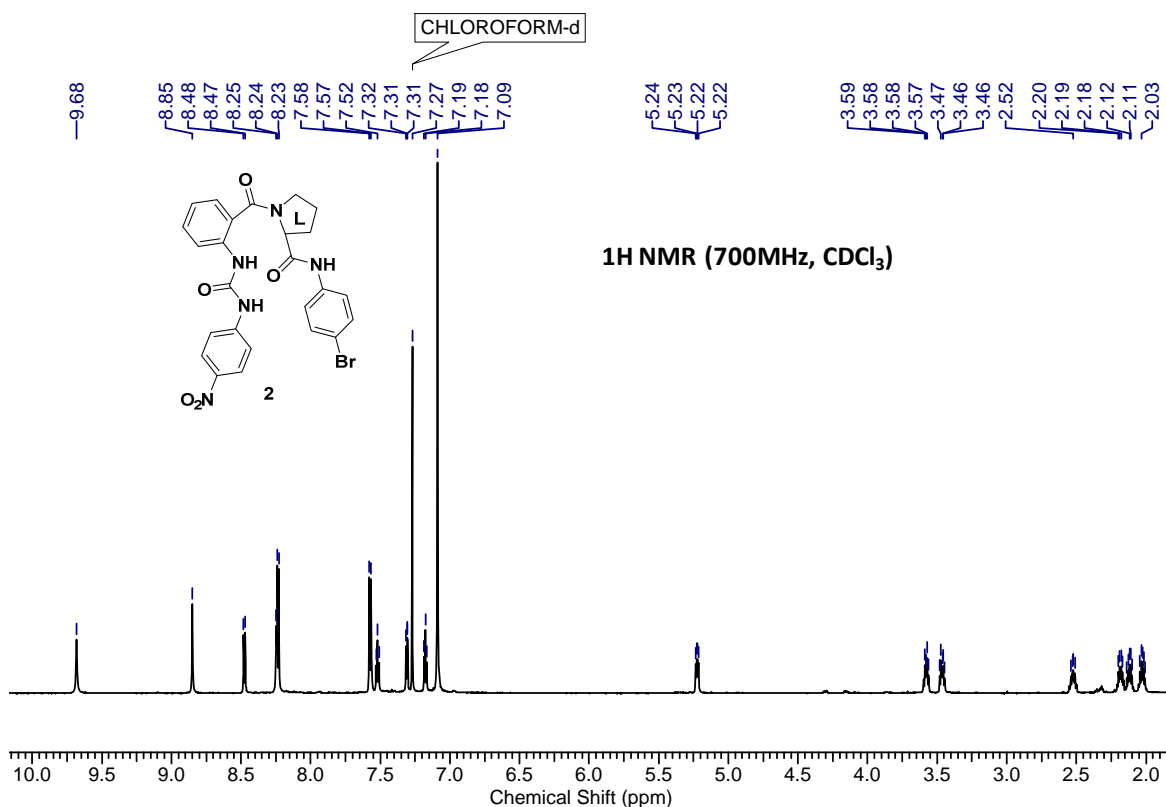
Figure 2.12 a) <sup>1</sup>H NMR, b) <sup>13</sup>C NMR and c) HRMS spectra of compound 1.

Chapter II: Design, Synthesis & Conformational Investigation of “Ant-Pro Urea”  
Based Foldamers

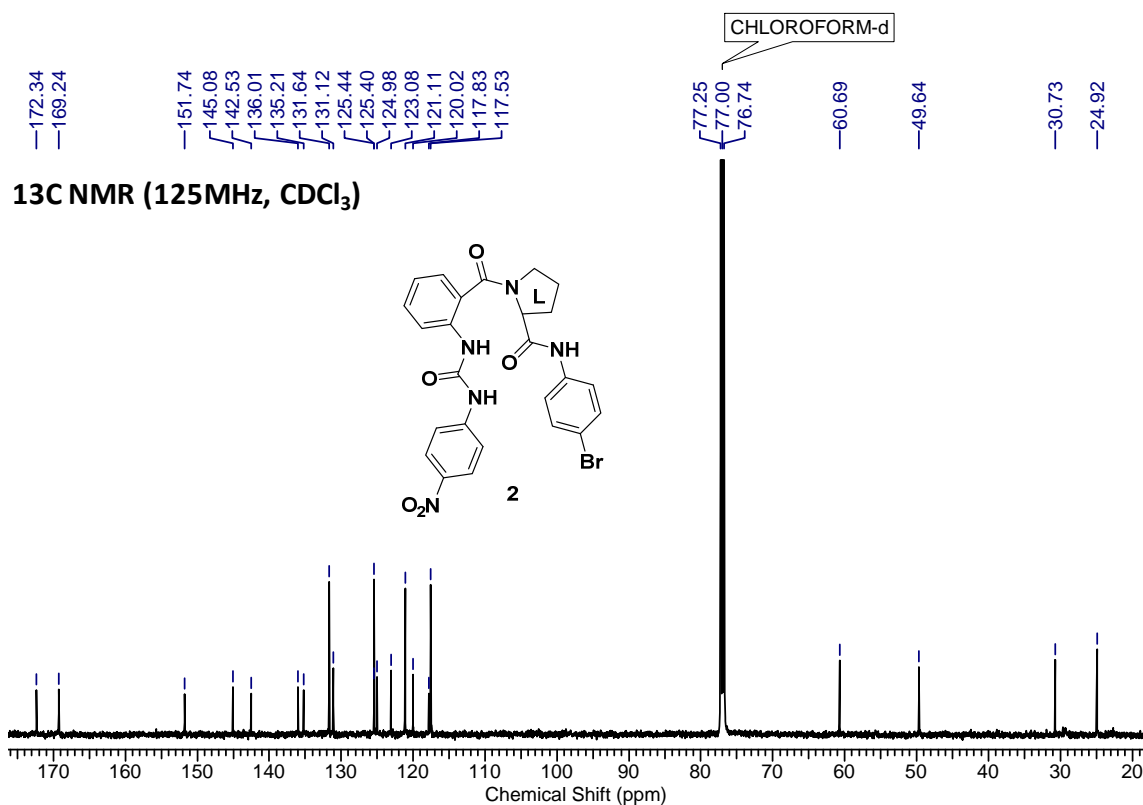
**Compound 2:** Compound 2 was yielded (56 %) as a white solid; mp: 222-224 °C;

$[\alpha]_{26.48}^D = 13.96$  ( $c = 0.05$ ,  $\text{CHCl}_3$ ); IR ( $\text{CHCl}_3$ )  $\nu$  ( $\text{cm}^{-1}$ ) 3682.72, 3378.61, 3020.29, 2933.21, 1601.63, 1546.82, 1514.57, 1215.96, 1034.04;  $^1\text{H}$  NMR (700MHz,  $\text{CDCl}_3$ )  $\delta = 9.68$  (bs, 1 H), 8.85 (s, 1 H), 8.48 (d,  $J = 8.4$  Hz, 1 H), 8.25 (bs, 1 H), 8.23 (d,  $J = 9.03$  Hz, 2 H), 7.57 (d,  $J = 9.0$  Hz, 2 H), 7.53 (td,  $J = 1.08, 8.4$  Hz, 1 H), 7.31 (dd,  $J = 1.08, 7.53$  Hz, 1 H), 7.18 (t,  $J = 7.3$  Hz, 1 H), 7.09 (s, 4 H), 5.23 (dd,  $J = 5.1, 8.9$  Hz, 1 H), 3.59 (m, 1 H), 3.47 (m, 1 H), 2.53 (m, 1 H), 2.18 (m, 1 H), 2.12 (m, 1 H), 2.02 (m, 1 H);  $^{13}\text{C}$  NMR (125 MHz,  $\text{CDCl}_3$ )  $\delta = 172.3, 169.2, 151.7, 145.1, 142.5, 136.0, 135.2, 131.6, 131.1, 125.5, 125.4, 125.0, 123.1, 121.1, 120.0, 117.8, 117.5, 60.7, 49.6, 30.7, 24.9$ ; HRMS  $[\text{M}+\text{H}]^+$   $\text{C}_{25}\text{H}_{23}\text{BrN}_5\text{O}_5$  Calculated: 552.0804, Found: 552.0886,  $[\text{M}+\text{Na}]^+$   $\text{C}_{25}\text{H}_{22}\text{BrN}_5\text{NaO}_5$  Calculated: 576.0702, Found: 576.0681.

a)



b)



c)

ASK-4 #154 RT: 0.68 AV: 1 NL: 3.32E7  
T: FTMS + p ESI Full ms [100.00-1500.00]

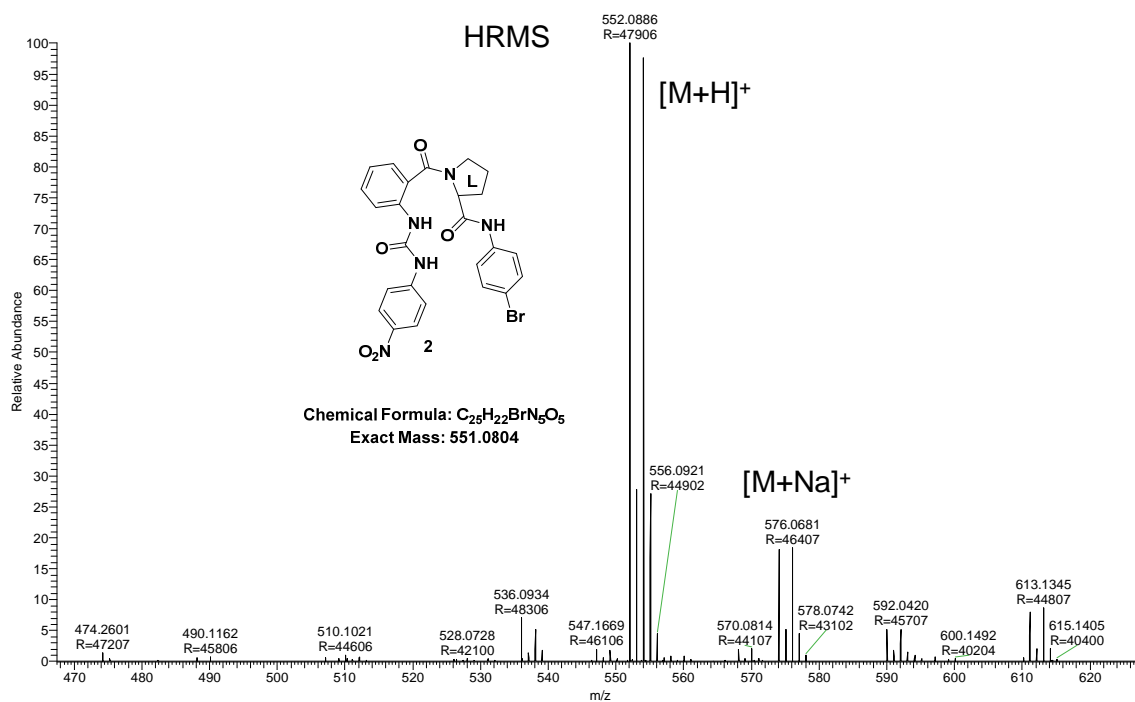
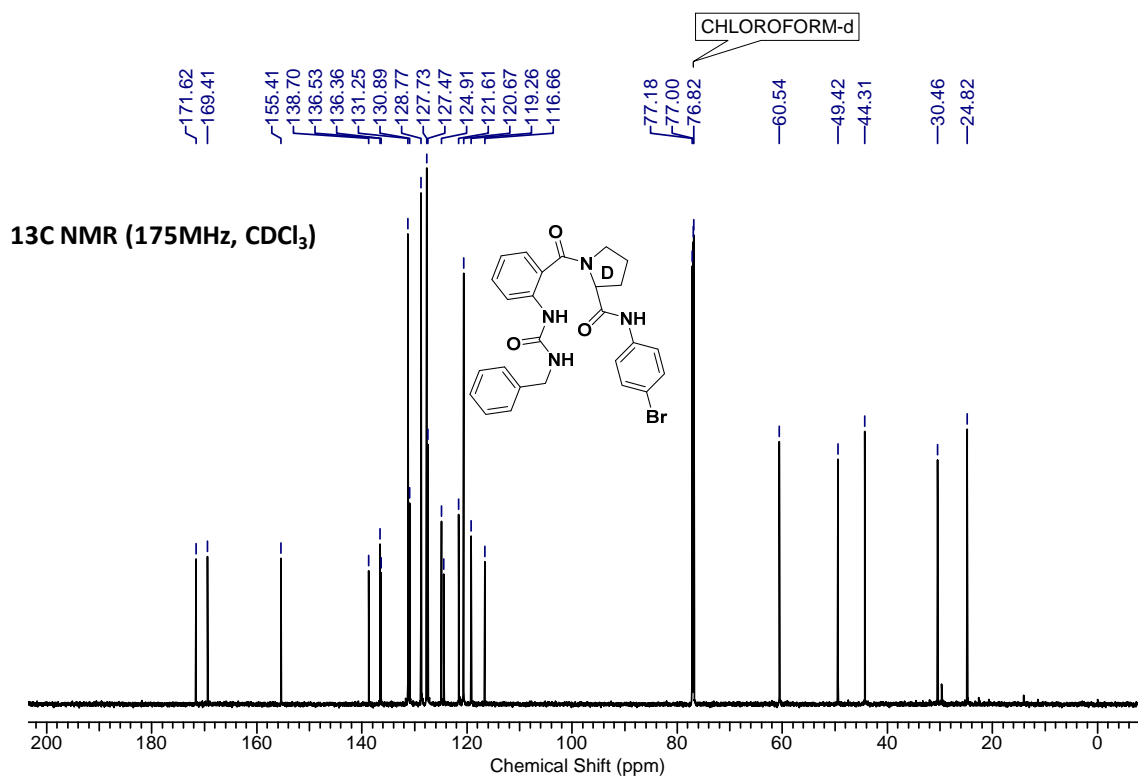


**Figure 2.13** a) <sup>1</sup>H NMR, b) <sup>13</sup>C NMR and c) HRMS spectra of compound **2**.



b)



c)

ASK-13 #140 RT: 0.62 AV: 1 NL: 4.57E8  
T: FTMS + p ESI Full ms [100.00-1500.00]

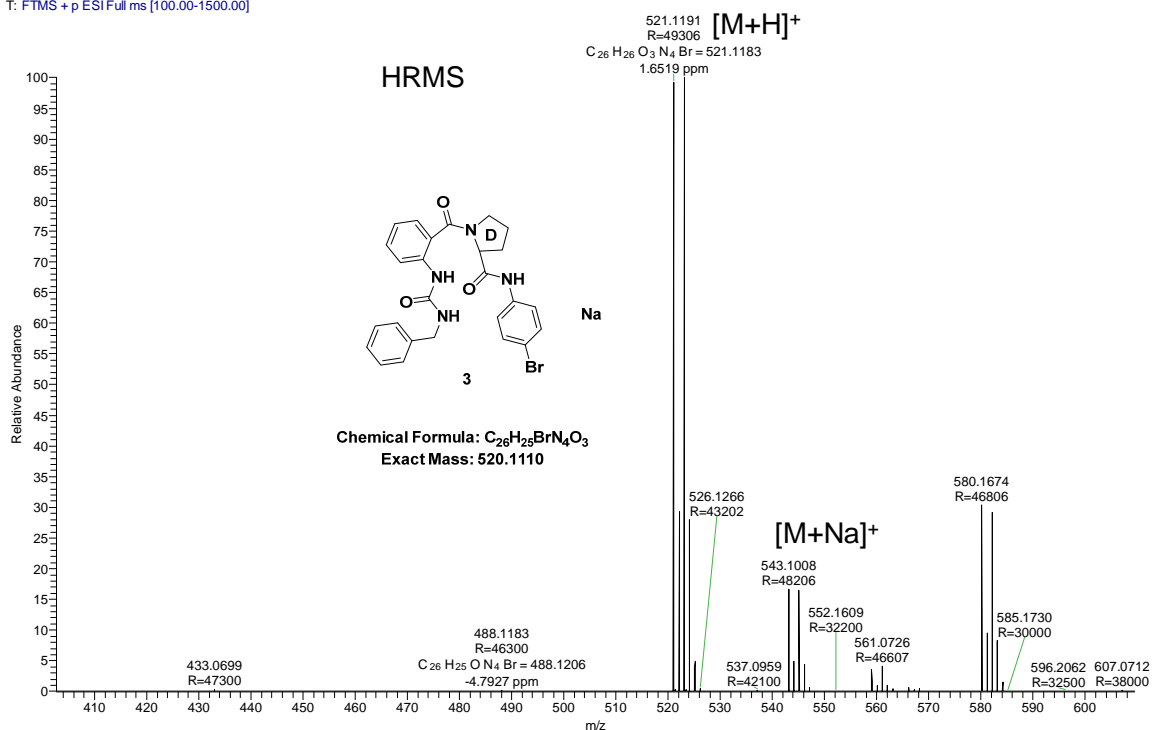
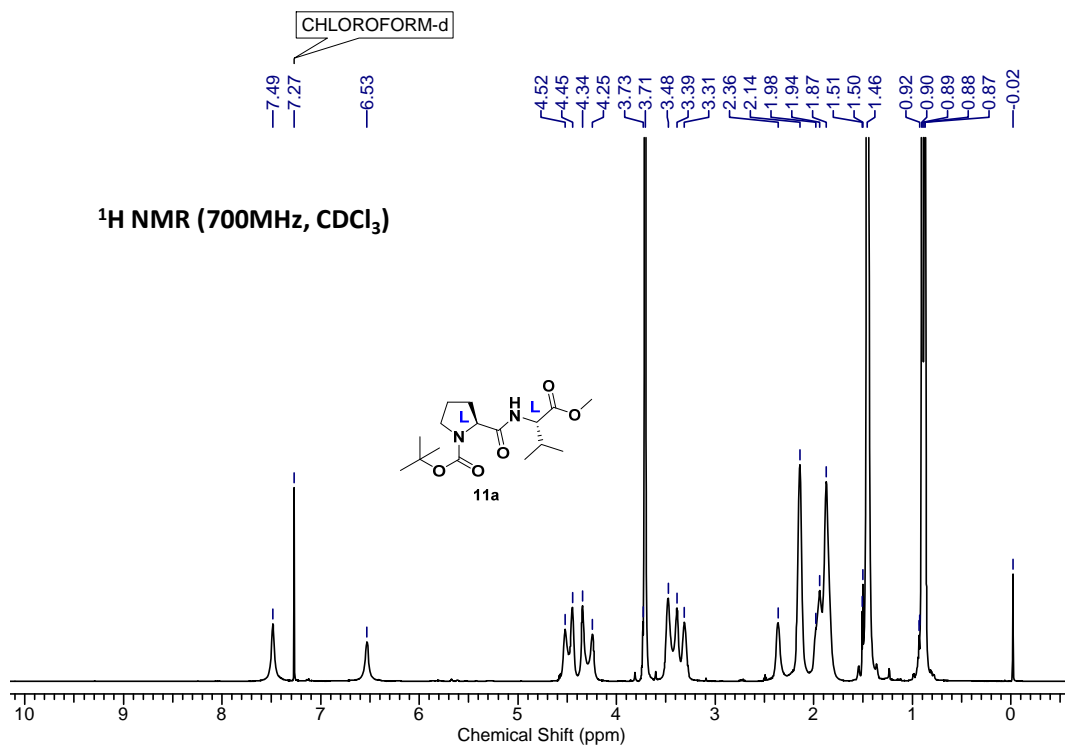


Figure 2.14 a) <sup>1</sup>H NMR, b) <sup>13</sup>C NMR and c) HRMS spectra of compound 3

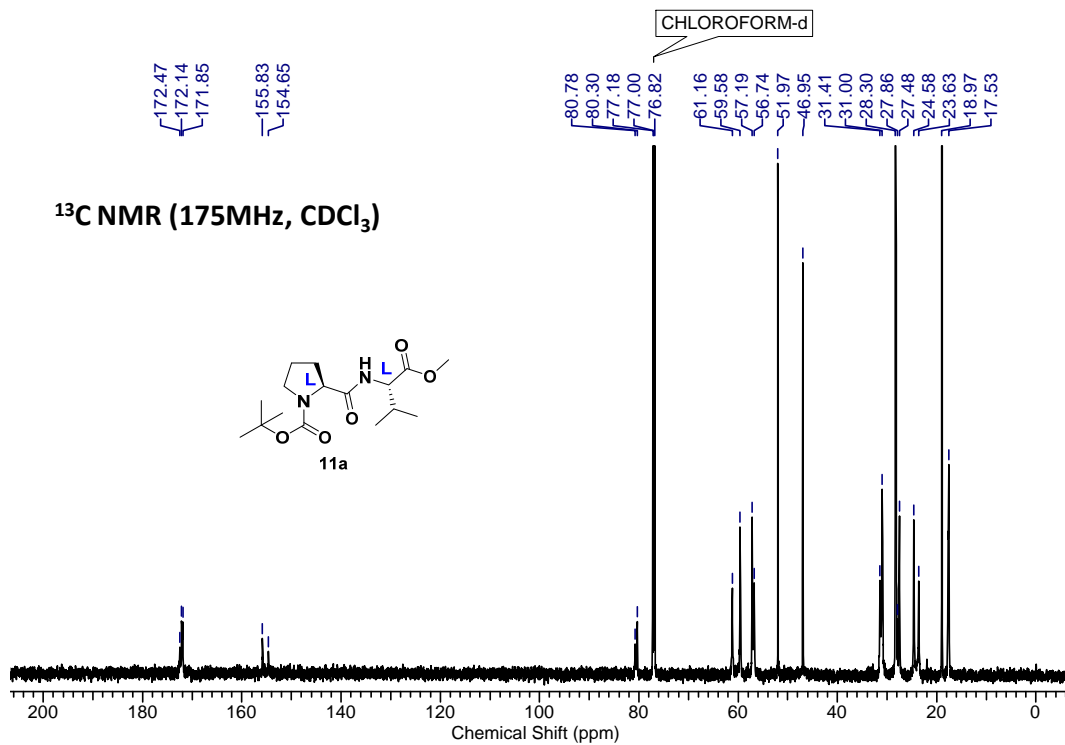


a)



NOTE: Extra signals or signal broadening are seen due to rotamer (minor conformer) formation at N-terminus of proline residue (*Chem. Eur. J.* 2008, **14**, 6192).

b)



c)

L-DL\_151202144813 #105 RT: 0.46 AV: 1 NL: 3.30E9  
T: FTMS +p ESI Full ms [100.00-1500.00]

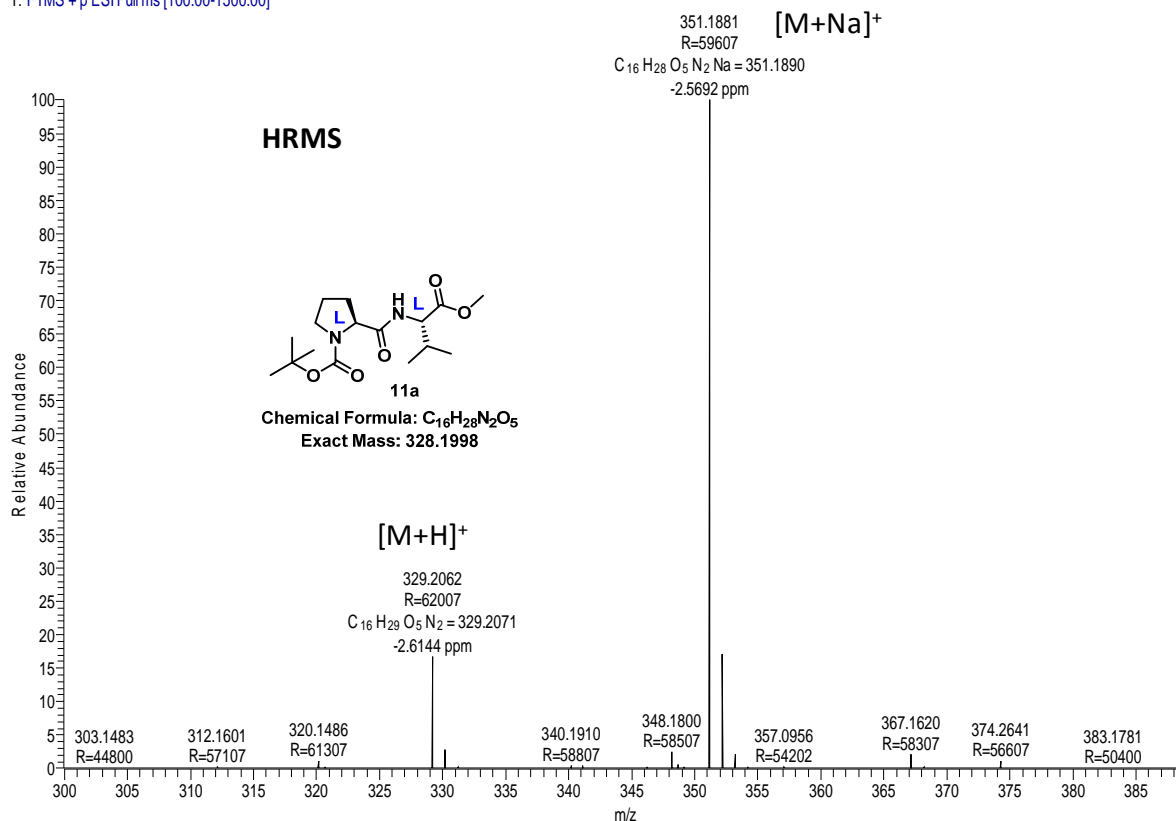
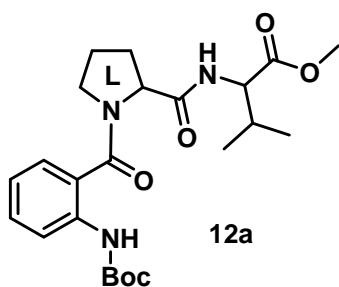


**Figure 2.15 a)**  $^1H$  NMR, **b)**  $^{13}C$  NMR and **c)** HRMS spectra of compound **11a**

**Compound 12a:** Methyl (2-((tert-butoxycarbonyl)amino)benzoyl)-L-prolyl-L-valinate;  
Boc deprotection of **11a** was achieved by stirring it with TFA:DCM (50:50) mixture for 30 minutes. The solution obtained was evaporated under vacuum, the TFA salt obtained was neutralized by saturated  $NaHCO_3$  and the product was extracted with ethyl acetate. The organic layer was washed by water and brine. The resulting ethyl acetate solution was dried over  $Na_2SO_4$  and evaporated under vacuum. The crude product (free amine i.e. H- $^L$ Pro $^L$ Val-OMe) was used for next reaction without purification.

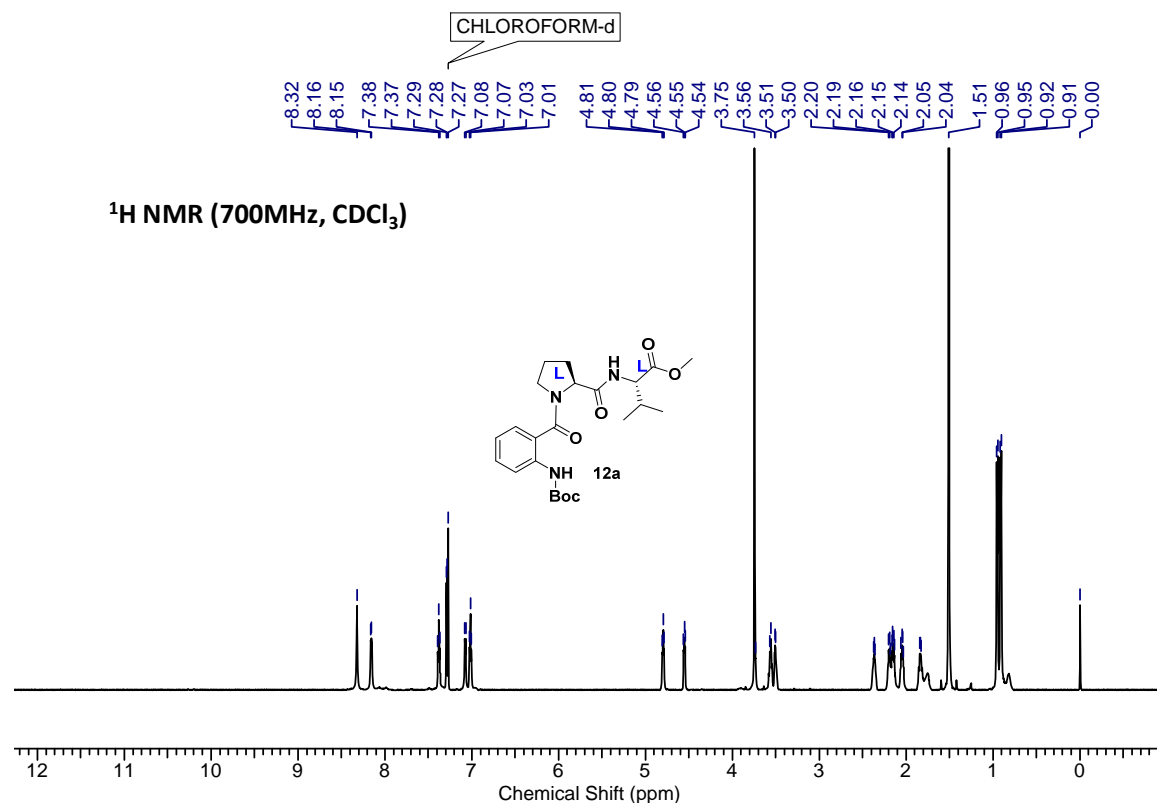


To a solution of BocAnt-OH ( 2.495g, 10.52mmol, 1.2 equi.) and DIEA (4.57mL, 26.31 mmol, 3 equi.) in 30mL of ACN, free amine (H-ProVal-OMe) (2 g, 8.77 mmol, 1equiv.), HBTU (6.653 g, 17.54 mmol, 2 equiv.) & catalytic amount of HOBt were added sequentially at 0 °C and the reaction

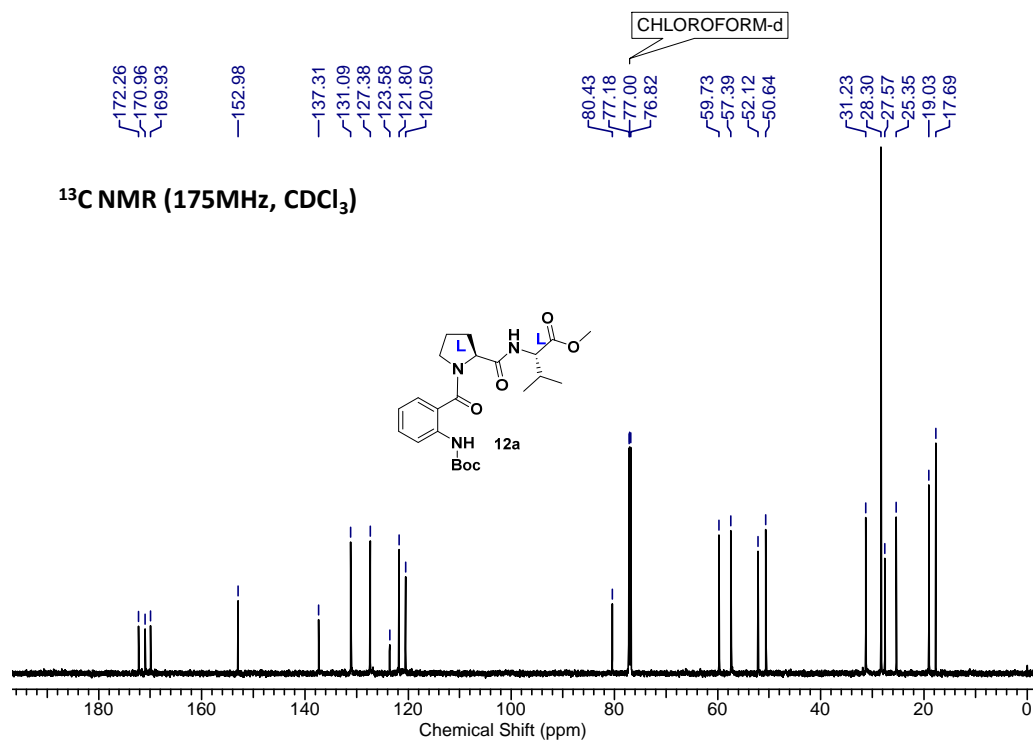


mixture was stirred for 6 h at room temperature. ACN was evaporated and the compound was diluted with ethyl acetate. The combined organic layer was washed sequentially with solutions of  $\text{KHSO}_4$ ,  $\text{NaHCO}_3$  and brine. Organic layer was then dried over  $\text{Na}_2\text{SO}_4$  and was evaporated under vacuum. The crude product was purified by column chromatography (eluent 40% AcOEt/pet. Ether,  $R_f$ : 0.3) to furnish **12a** (3.51 g, 90%) as a white solid. mp: 100-102 °C;  $[\alpha]^{25.97}_D = -106.11$  ( $c = 0.03$ ,  $\text{CHCl}_3$ ); IR ( $\text{CHCl}_3$ )  $\nu$  ( $\text{cm}^{-1}$ ): 3331, 2971, 2888, 2357, 1820, 1728, 1675, 1623, 1595, 1160, 779;  $^1\text{H}$  NMR (700MHz,  $\text{CDCl}_3$ )  $\delta$  ppm 8.32 (bs, 1H), 8.16 (d,  $J = 7.7$  Hz, 1H), 7.38 (t,  $J = 7.7$  Hz, 1H), 7.29 (d,  $J = 7.5$  Hz, 1H), 7.08 (d,  $J = 8.4$  Hz, 1H), 7.01 (t,  $J = 7.3$  Hz, 1H), 4.80 (t,  $J = 6.6$  Hz, 1H), 4.55 (dd,  $J = 5.2, 7.7$  Hz, 1H), 3.75 (s, 3H), 3.56 (m, 1H), 3.51 (m, 1H), 2.44 (m, 1H), 2.20 (m, 1H), 2.17 (m, 1H), 2.04 (m, 1H), 1.90 (m, 1H), 1.51 (s, 9H), 0.95 (d,  $J = 6.7$  Hz, 3H), 0.91 (d,  $J = 6.7$  Hz, 3H);  $^{13}\text{C}$  NMR (175MHz,  $\text{CDCl}_3$ )  $\delta$  ppm 172.3, 171.0, 169.9, 153.0, 137.3, 131.1, 127.4, 123.6, 121.8, 120.5, 80.4, 59.7, 57.4, 52.1, 50.6, 31.2, 28.3, 27.6, 25.4, 19.0, 17.7; HRMS (ESI)  $\text{C}_{23}\text{H}_{33}\text{N}_3\text{O}_6$  calculated  $[\text{M}+\text{H}]^+$ : 448.2369, found 448.2433,  $\text{C}_{23}\text{H}_{33}\text{N}_3\text{NaO}_6$  calculated  $[\text{M}+\text{Na}]^+$  470.2267, found 470.2252.

a)



b)



c)

L-TRI\_151202143841 #106 RT: 0.47 AV: 1 NL: 1.11E9  
T: FTMS + p ESI/Full ms [100.00-1500.00]

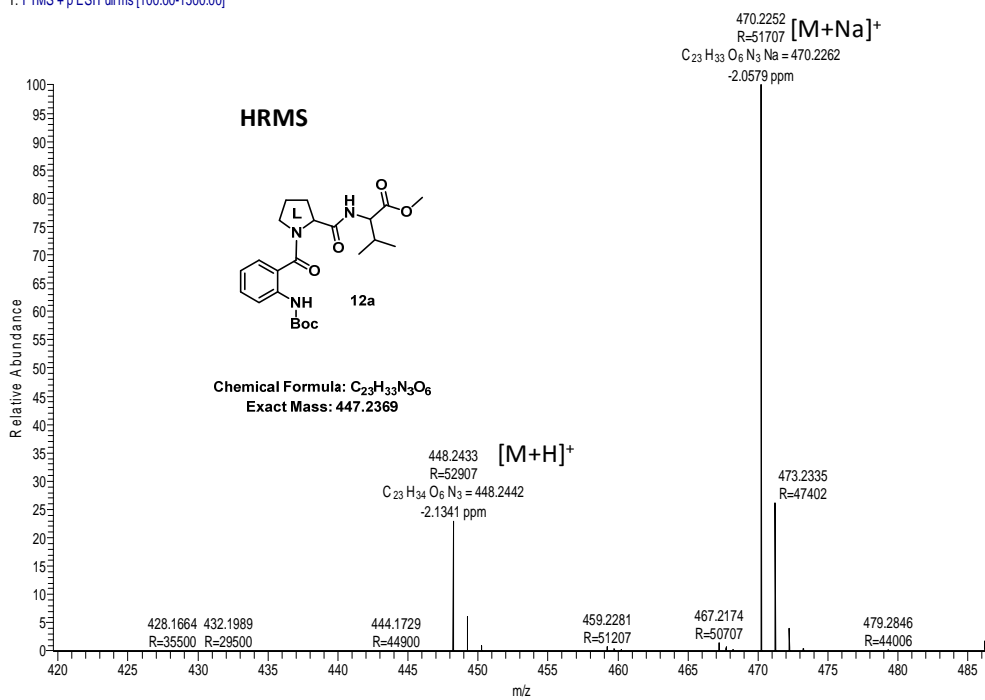
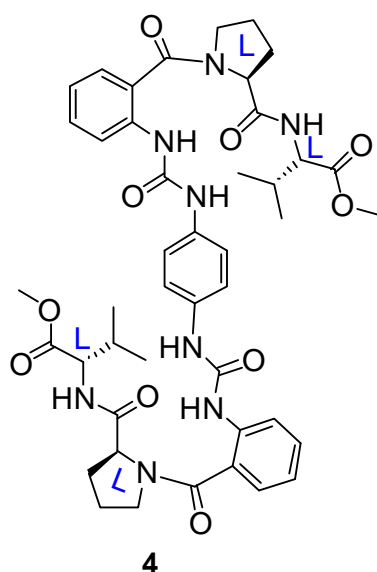


Figure 2.16 a) <sup>1</sup>H NMR, b) <sup>13</sup>C NMR and c) HRMS spectra of compound 12a.

**Compound 4:** The compound **12a** was deprotected using TFA:DCM and the resultant solution was evaporated under vacuum. The TFA salt obtained was then neutralized to

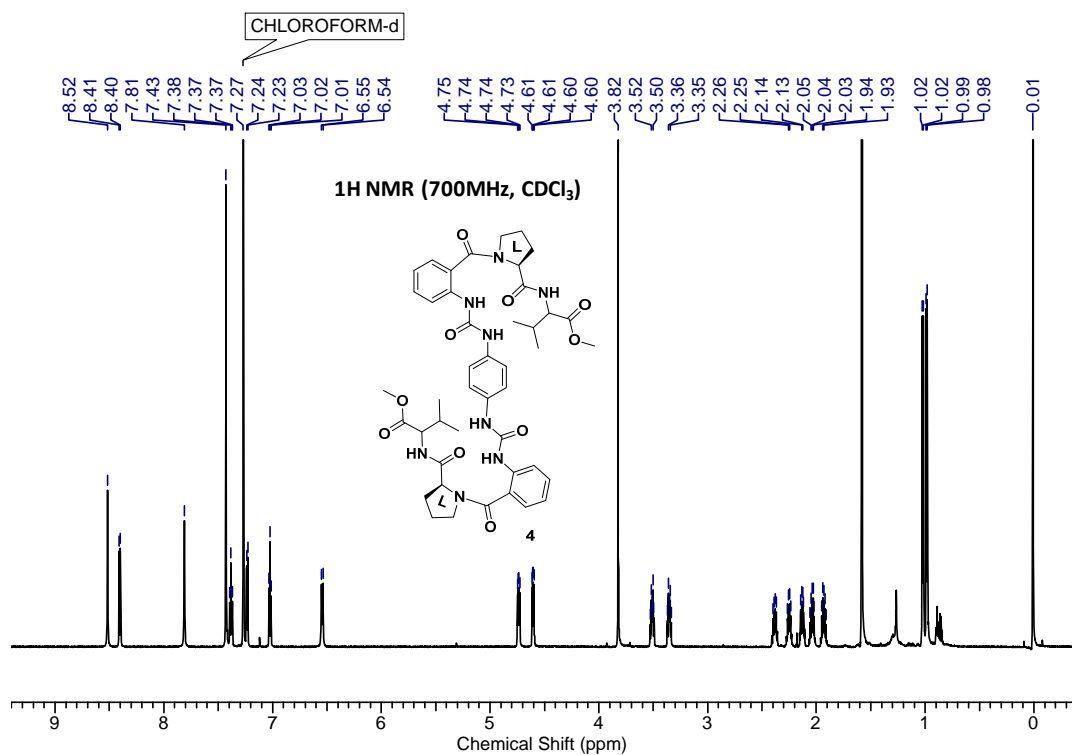


free amine by NaHCO<sub>3</sub> solution and extracted with ethyl acetate. The organic layer was washed by water and brine. The resulting ethyl acetate solution dried over Na<sub>2</sub>SO<sub>4</sub> and was evaporated under vacuum. The crude product (free amine i.e. H-<sup>L</sup>Pro<sup>L</sup>Val-OMe) was used for next reaction without further purification.

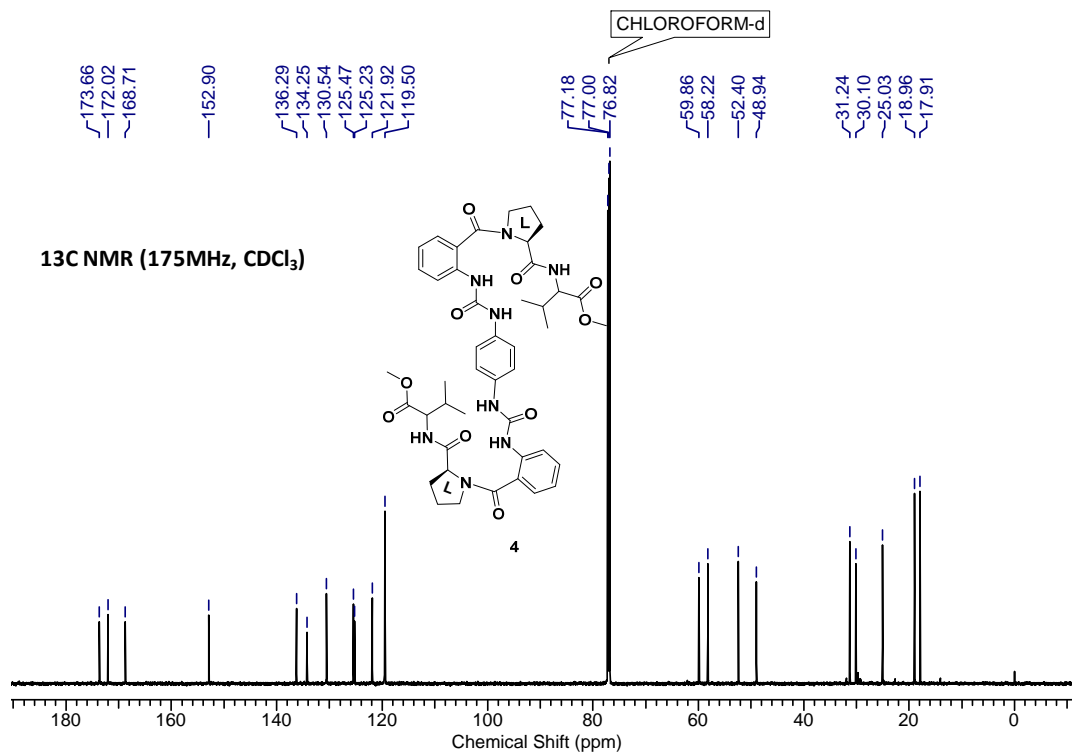
The free amine (H-Ant-<sup>L</sup>Pro<sup>L</sup>Val-OMe), (0.066 g, 0.19 mmol, 1equi.) was taken into 1 mL of dry pyridine and stirred for 5 min at 0 °C followed by addition of 1,4-Phenylene diisocyanate (0.018 g, 0.114 mmol, 0.6 equi.) and activated molecular sieves. This reaction mixture was stirred at room temperature for 5 h. After completion of reaction, the reaction mixture was diluted with ethyl acetate and washed with CuSO<sub>4</sub> solution to remove pyridine from reaction mixture. Organic layer was dried over Na<sub>2</sub>SO<sub>4</sub> and was evaporated under vacuum. The crude product was purified by column chromatography (eluent 50% AcOEt/pet. Ether, R<sub>f</sub>: 0.4) to furnish **4** (0.046 g, 55%) as a white solid; mp: 224-226 °C; [α]<sup>26.65</sup><sub>D</sub> = 3.00 (*c* = 0.05, CHCl<sub>3</sub>); IR (CHCl<sub>3</sub>) ν (cm<sup>-1</sup>) 3377.99, 3302.40, 2971.73, 2933.97, 1738.75, 1661.84, 1547.09, 1460.42, 1215.62, 1032.11, 770.36; <sup>1</sup>H NMR (700 MHz CDCl<sub>3</sub>) δ = 8.52 (s, 2 H), 8.40 (d, *J* = 8.2 Hz, 2 H), 7.81 (s, 2 H), 7.43 (s, 4 H), 7.38(t, *J* = 8.2 Hz, 2 H), 7.23 (dd, *J* = 1.0, 7.4 Hz, 2 H), 7.02 (t, *J* = 7.4 Hz, 2 H), 6.54 (d, *J* = 8.6 Hz, 2 H), 4.74 (dd, *J* = 5.1, 8.7 Hz, 2 H), 4.60 (dd, *J* = 4.8, 8.5 Hz, 2 H), 3.82 (s, 6 H), 3.51 (m, 2 H), 3.35 (m, 2 H), 2.38 (m, 2 H), 2.25 (m, 2 H), 2.13 (m, 2 H), 2.04 (m, 2 H), 1.93 (m, 2 H), 1.02 (d, *J* = 6.9 Hz, 6 H), 0.98 (d, *J* = 6.9 Hz, 7 H); <sup>13</sup>C NMR (175 MHz, CDCl<sub>3</sub>) δ = 173.7, 172.0, 168.7, 152.9, 136.3, 134.3, 130.5, 125.5, 125.2, 121.9, 119.5, 119.5, 59.9, 58.2, 52.4, 48.9, 31.2, 30.1, 25.0, 19.0, 17.9; HRMS (ESI) C<sub>44</sub>H<sub>54</sub>N<sub>8</sub>O<sub>10</sub> calculated [M+H]<sup>+</sup>: 855.3963, found 855.4042, C<sub>44</sub>H<sub>54</sub>N<sub>8</sub>NaO<sub>10</sub> calculated [M+Na]<sup>+</sup> 877.3861, found 877.3909.

## Chapter II: Design, Synthesis & Conformational Investigation of “Ant-Pro Urea” Based Foldamers

a)



b)



C)

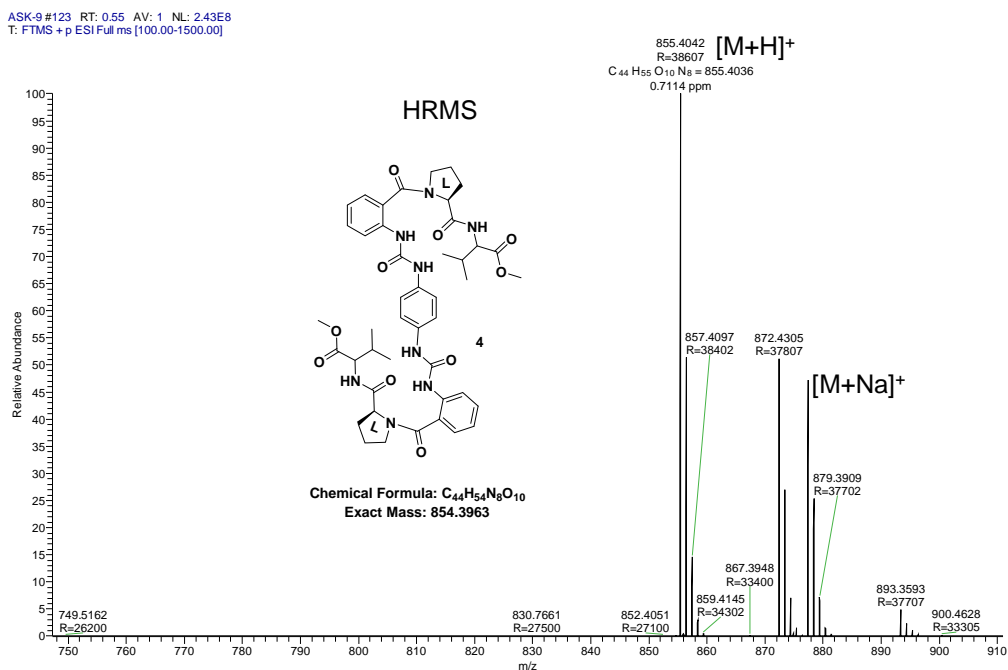
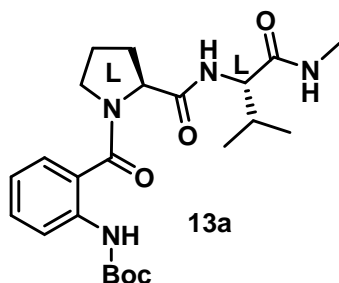


Figure 2.17 a)  $^1\text{H}$  NMR, b)  $^{13}\text{C}$  NMR and c) HRMS spectra of compound **4**

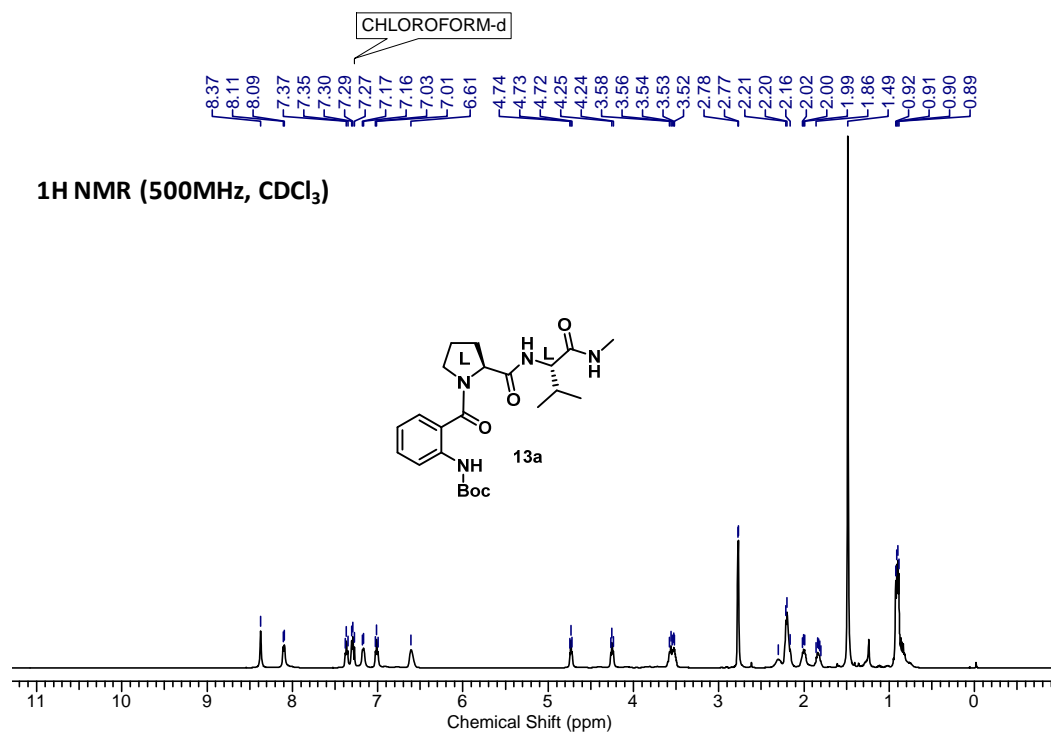
**Compound 13a:** The compound **12a** was taken in saturated methanolic methyl amine



solution and stirred for 12h at room temperature. After complete consumption of ester **12a**, methanolic methyl amine solution was evaporated under vacuum and compound was purified by column chromatography (eluent 70% AcOEt/pet. Ether,  $R_f$ : 0.3) to furnish quantitative yield of **13a**;  $^1\text{H}$  NMR (500MHz,  $\text{CDCl}_3$ )  $\delta$  = 8.37 (bs, 1 H), 8.10

(d,  $J$  = 8.0 Hz, 1 H), 7.37 (t,  $J$  = 7.6 Hz, 1 H), 7.30 (d,  $J$  = 7.2 Hz, 1 H), 7.17 (d,  $J$  = 6.1 Hz, 1 H), 7.01 (t,  $J$  = 7.2 Hz, 1 H), 6.61 (bs, 1 H), 4.73 (t,  $J$  = 6.9 Hz, 1 H), 4.25 (t,  $J$  = 7.2 Hz, 1 H), 3.62 - 3.47 (m, 2 H), 2.77 (d,  $J$  = 4.2 Hz, 3 H), 2.30 (bs, 1 H), 2.20 (m, 2 H), 2.00 (m, 1 H), 1.84 (m, 1 H), 1.49 (s, 9 H), 0.91 (d,  $J$  = 6.5, 3 H), 0.90 (d,  $J$  = 6.5, 3 H);  $^{13}\text{C}$  NMR (125 MHz,  $\text{CDCl}_3$ )  $\delta$  = 171.6, 171.4, 170.0, 153.0, 137.3, 131.1, 127.4, 123.6, 121.9, 120.7, 80.4, 60.2, 58.8, 50.7, 30.6, 28.4, 28.2, 26.1, 25.4, 19.3, 17.9.

a)



b)

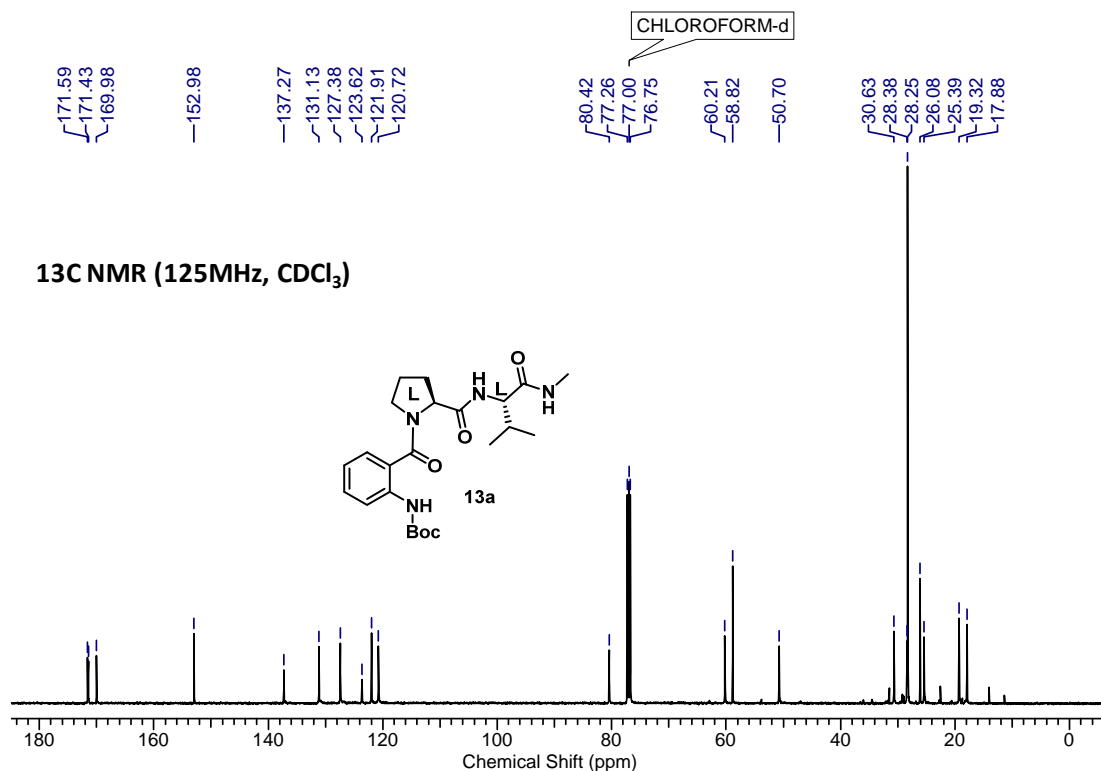
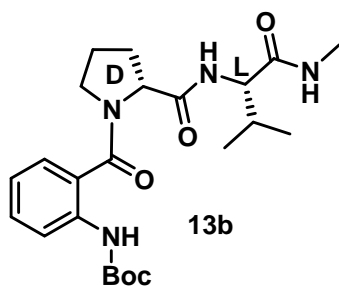


Figure 2.18 a) <sup>1</sup>H NMR and b) <sup>13</sup>C NMR spectra of compound **13a**.

**Compound 13b:** Following same synthetic procedure of compound **13a** and using **12b**,

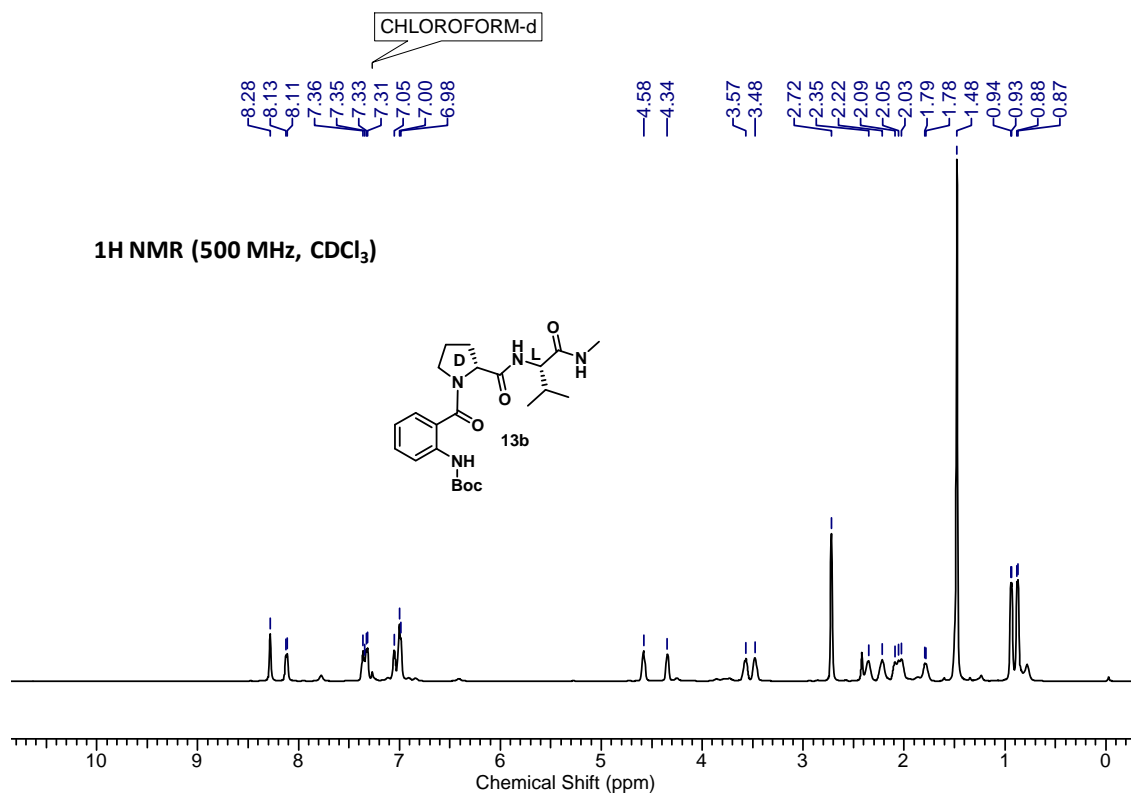


compound **13b** was prepared.  $^1\text{H}$  NMR (500 MHz,  $\text{CDCl}_3$ )

$\delta$  = 8.28 (bs, 1 H), 8.12 (d,  $J$  = 7.2 Hz, 1 H), 7.34 (m, 2 H),  
7.05 (bs., 1 H), 6.99 (d,  $J$  = 7.2 Hz, 2 H), 4.58 (bs, 1 H),  
4.34 (bs, 1 H), 3.57 (bs, 1 H), 3.48 (bs, 1 H), 2.72 (bs, 3 H),  
2.35 (m, 1 H), 2.22 (m, 1 H), 2.12 - 1.96 (m, 2 H), 1.79 (m,  
1 H), 1.48 (bs, 9 H), 0.94 (d,  $J$  = 4.6 Hz, 3 H), 0.88 (d,  $J$  =

4.6 Hz, 3 H);  $^{13}\text{C}$  NMR (125 MHz,  $\text{CDCl}_3$ )  $\delta$  = 172.2, 171.4, 169.5, 153.0, 137.1, 131.1,  
127.1, 123.6, 121.8, 120.5, 80.5, 60.6, 58.4, 50.6, 29.6, 29.3, 28.2, 26.1, 25.4, 19.4, 17.3.

a)



b)

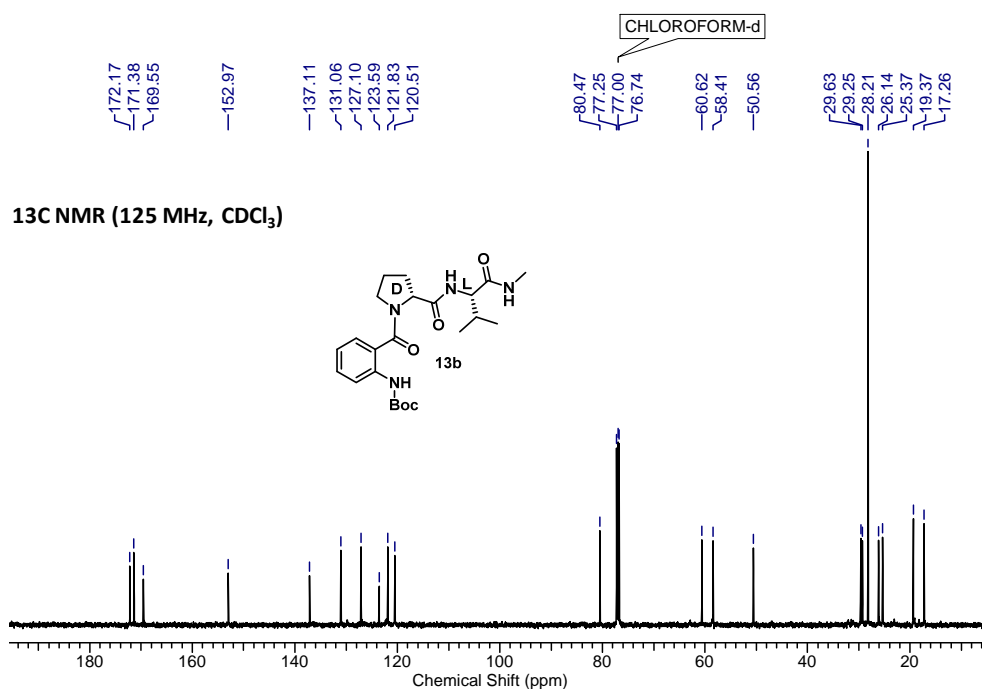
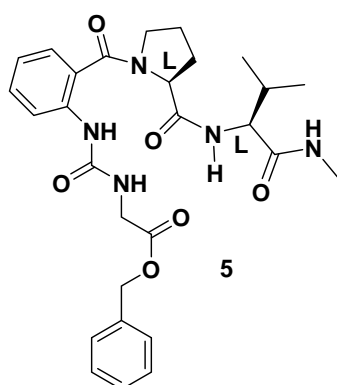


**Figure 2.19** a) <sup>1</sup>H NMR and b) <sup>13</sup>C NMR spectra of compound **13b**.

**Compound 14a & 14b:** To a solution of free amine of **13a/13b** (H-AntProVal-NHMe, 1equiv.) in ACN, NaHCO<sub>3</sub> (2equiv.) and 4-Nitrophenyl chloroformate (1.5 equiv.) were added and reaction mixture was stirred at 0 °C for 1h or until the appearance of a white precipitate. This precipitate was filtered out under suction pump and washed with chilled ACN to get rid of impurities. This results in a white solid which was dried over high vacuum pump and used for next reaction without further purification.

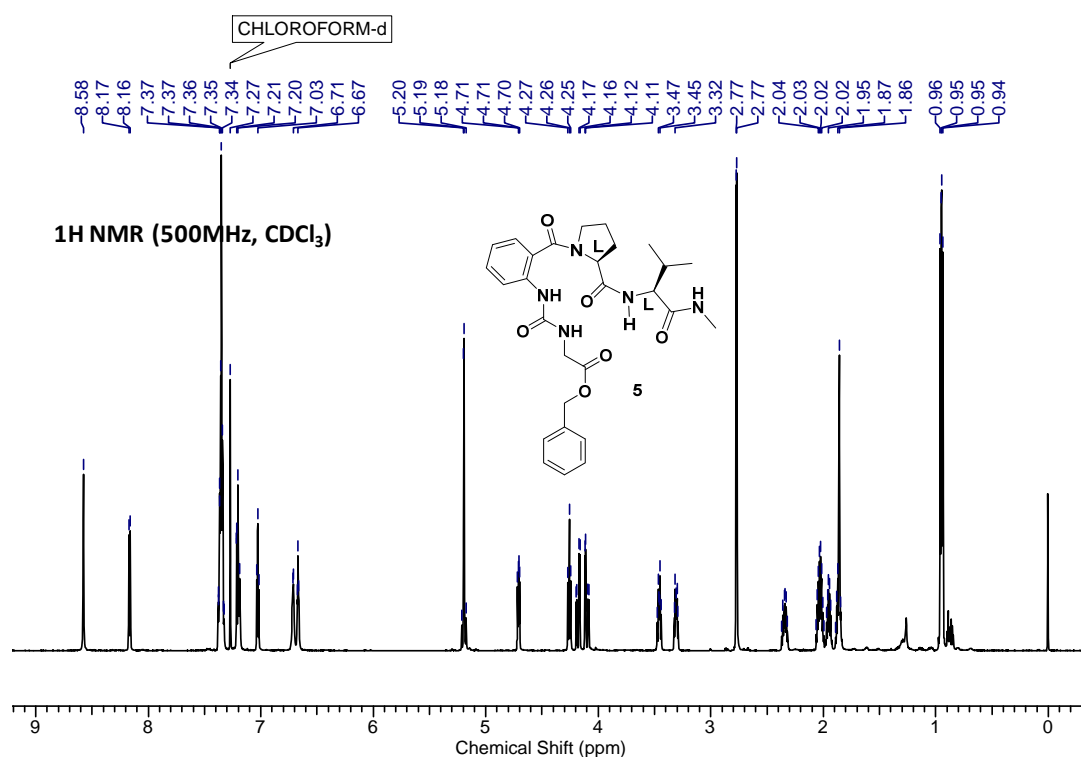


**Compound 5:** To a solution of H-Gly-OBz (0.143 g, 0.867 mmol, 2 equiv.) and DIEA (0.15 mL, 0.867 mmol, 2 equiv.) in ACN at 0 °C, a solution of **14a** in ACN was added drop wise and stirred at room temperature for 2h. After completion of reaction, ACN was evaporated under vacuum and the reaction mixture was taken into DCM. The combined organic layer was sequentially washed with solution of KHSO<sub>4</sub>, NaHCO<sub>3</sub> and brine. The organic layer was dried over Na<sub>2</sub>SO<sub>4</sub>, and was evaporated under vacuum. The crude product was purified by column

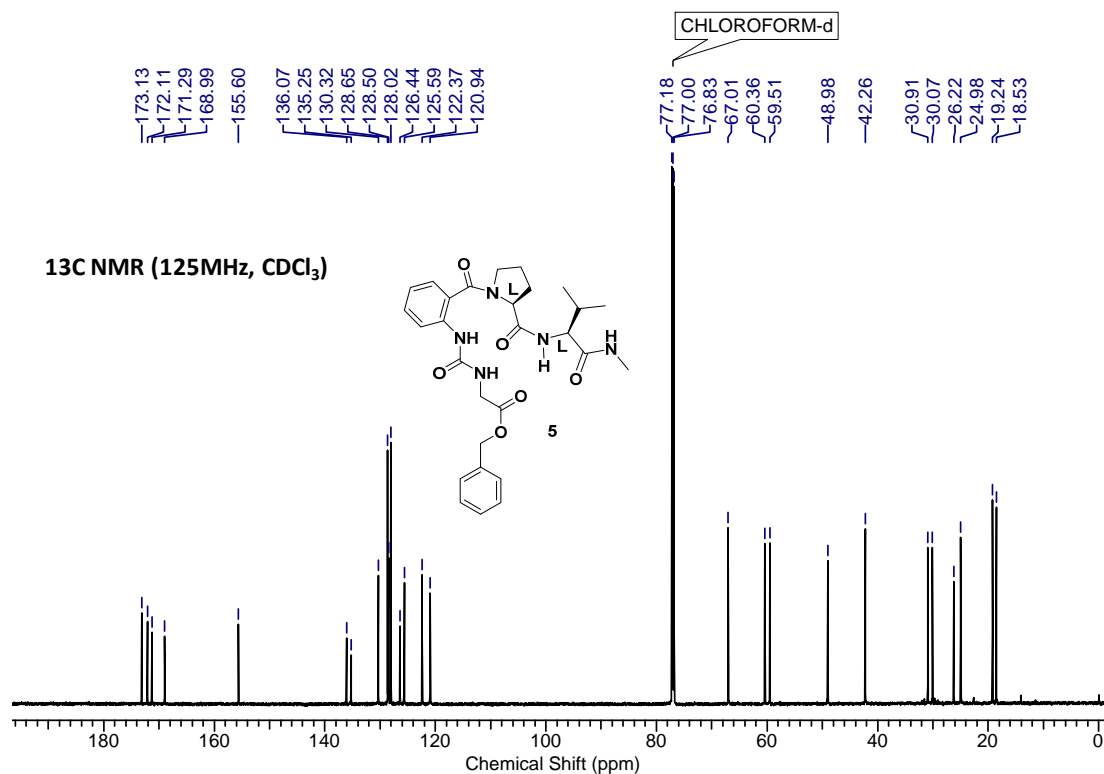


chromatography (eluent 70% AcOEt/pet. Ether,  $R_f$ : 0.3) to furnish pure compound **5**; mp.101-103 °C,  $[\alpha]^{26.65}_D = -23.62$  ( $c = 0.135$ ,  $\text{CHCl}_3$ ); IR ( $\text{CHCl}_3$ )  $\nu$  ( $\text{cm}^{-1}$ )3362.20, 3301.38, 3069.93, 2968.38, 1742.06, 1645.06, 1552.78, 1449.93, 1391.73;  $^1\text{H}$  NMR (700 MHz,  $\text{CDCl}_3$ )  $\delta = 8.58$  (s, 1 H), 8.17 (d,  $J = 8.4$  Hz, 1 H), 7.39 - 7.31 (m, 6 H), 7.20 (m, 2 H), 7.03 (t,  $J = 7.4$  Hz, 1 H), 6.71 (d,  $J = 4.3$  Hz, 1 H), 6.67 (t,  $J = 4.7$  Hz, 1 H), 5.19 (m, 2 H), 4.71 (dd,  $J = 5.5, 8.5$  Hz, 1 H), 4.26 (t,  $J = 8.6$  Hz, 1 H), 4.21 - 4.06 (m, 2 H), 3.46 (m, 1 H), 3.31 (m, 1 H), 2.77 (d,  $J = 4.7$  Hz, 3 H), 2.34(m, 1 H), 2.04(m, 2 H), 1.95 (m, 1 H), 1.87 (m, 1 H), 0.96 (d,  $J = 6.7$  Hz, 3 H), 0.94 (d,  $J = 6.7$  Hz, 3 H);  $^{13}\text{C}$  NMR (175 MHz,  $\text{CDCl}_3$ )  $\delta = 173.1, 172.1, 171.3, 169.0, 155.6, 136.1, 135.3, 130.3, 128.7, 128.5, 128.0, 126.4, 125.6, 122.4, 120.9, 67.0, 60.4, 59.5, 49.0, 42.3, 30.9, 30.1, 26.2, 25.0, 19.2, 18.5$  HRMS (ESI)  $\text{C}_{28}\text{H}_{36}\text{N}_5\text{O}_6$  calculated  $[\text{M}+\text{H}]^+$ : 538.2587, found 538.2668,  $\text{C}_{28}\text{H}_{35}\text{N}_5\text{NaO}_6$  calculated  $[\text{M}+\text{Na}]^+$  560.2485, found 560.2482.

a)



b)



c)

ASK-10 #118 RT: 0.53 AV: 1 NL: 1.88E9  
T: FTMS + p ESI Full ms [100.00-1500.00]

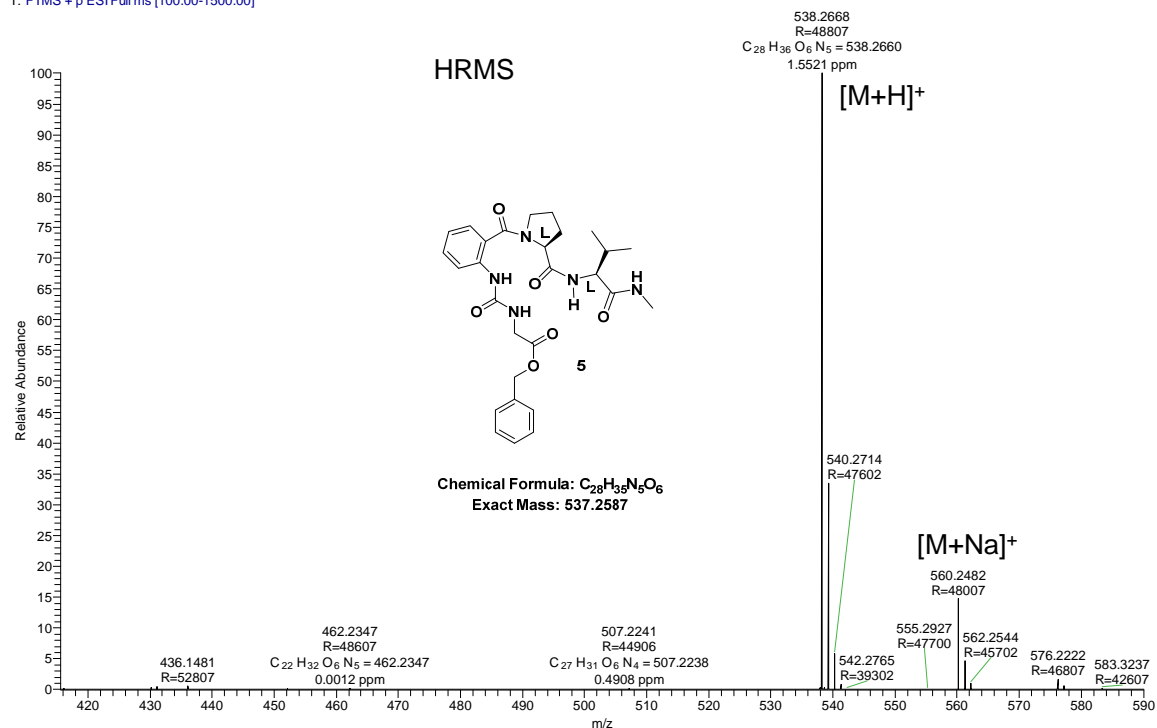
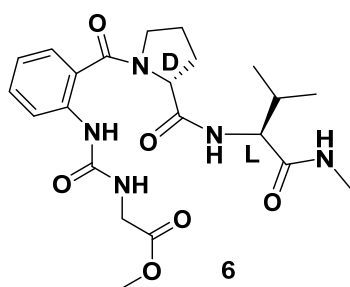


Figure 2.20 a) <sup>1</sup>H NMR, b) <sup>13</sup>C NMR and c) HRMS spectra of compound 5.

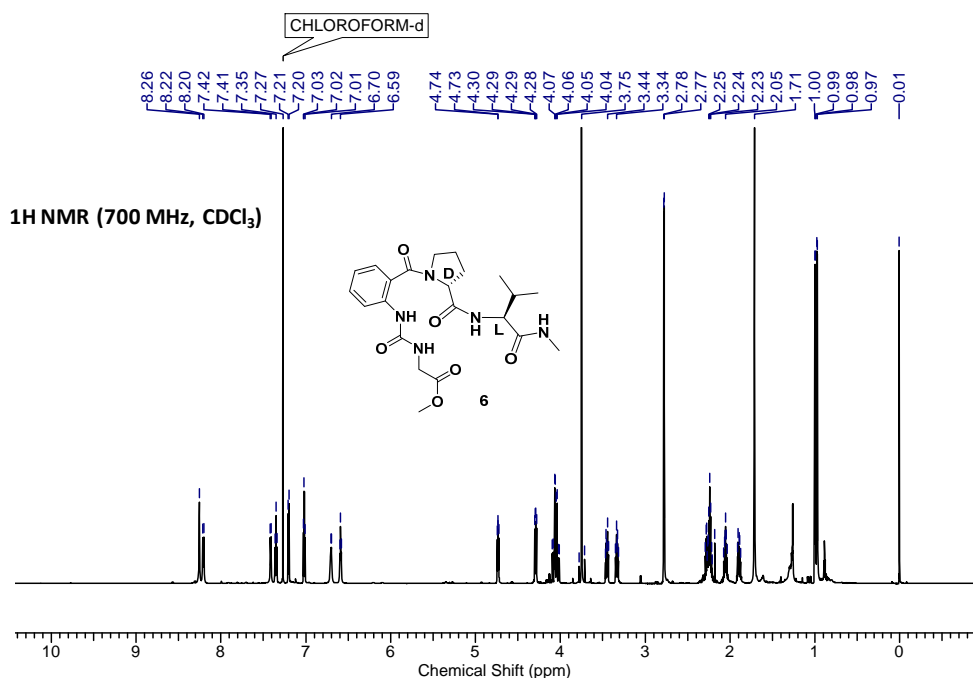
**Compound 6:** Following the same synthetic procedure of **5**, compound **6** was prepared



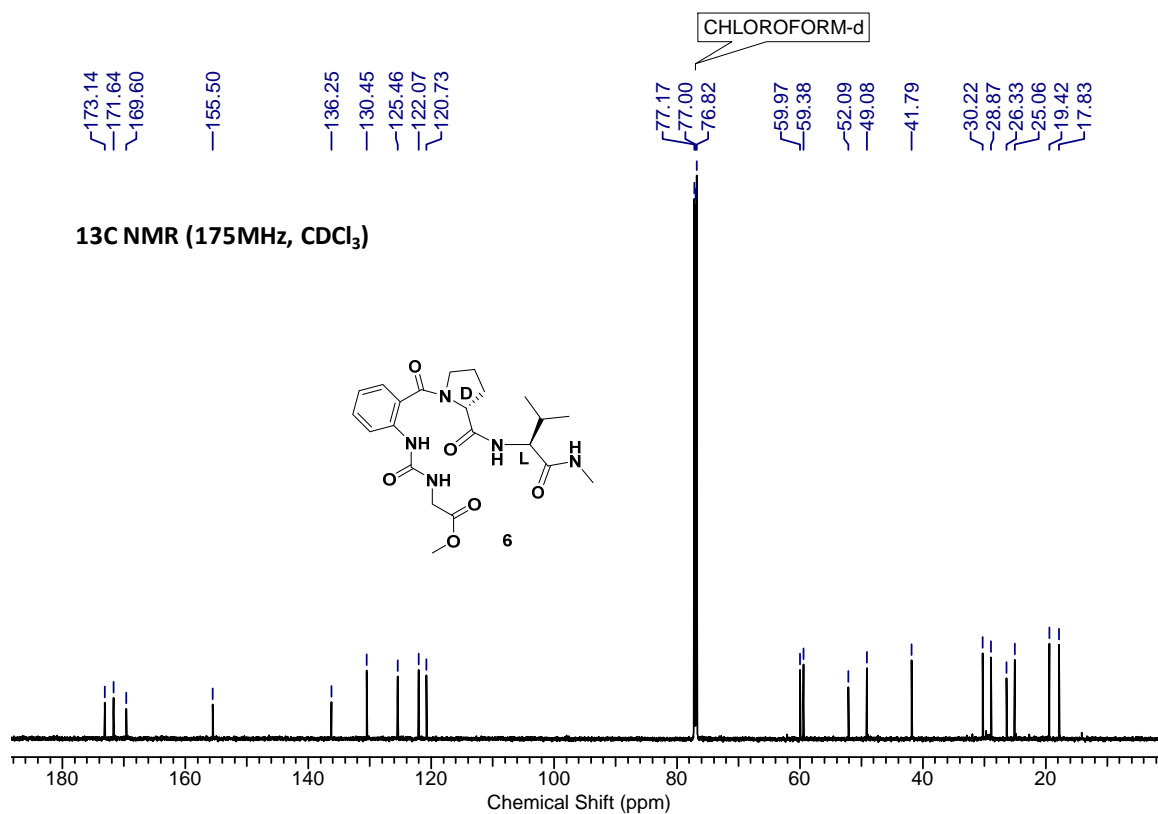
using HCl.Gly-OMe (0.118 g, 0.9393 mmol, 2.5 equiv.), **14b** (0.191 g, 0.375 mmol, 1 equiv.) and DIEA (0.26 mL, 1.5 mmol, 1 equiv.). Compound **6** yielded as a pasty material after purification using column chromatography (eluent 80% AcOEt/pet. Ether,  $R_f$ : 0.3) to furnish pure compound **6**;  $[\alpha]^{26.77}_D = 15.98$  ( $c = 0.1$ ,  $\text{CHCl}_3$ ); IR

( $\text{CHCl}_3$ )  $\nu$  ( $\text{cm}^{-1}$ ) 3300.74, 3015, 2966.10, 1747.55, 1648.93, 1591.12, 1553.36, 1461.23, 1370.79;  $^1\text{H}$  NMR (700 MHz,  $\text{CDCl}_3$ )  $\delta = 8.26$  (s, 1 H), 8.21 (d,  $J = 8.4$  Hz, 1 H), 7.41 (d,  $J = 8.4$  Hz, 1 H), 7.35 (t,  $J = 8.6$  Hz, 1 H), 7.20 (dd,  $J = 1.4, 7.6$  Hz, 1 H), 7.02 (td,  $J = 0.9, 7.5$  Hz, 1 H), 6.70 (m, 1 H), 6.59 (t,  $J = 5.4$  Hz, 1 H), 4.73 (dd,  $J = 5.4, 8.0$  Hz, 1 H), 4.29 (dd,  $J = 6.0, 8.6$  Hz, 1 H), 4.10 - 4.01 (m, 2 H), 3.75 (s, 3 H), 3.45 (m, 1 H), 3.33 (m, 1 H), 2.78 (d,  $J = 4.7$  Hz, 3 H), 2.26 (m, 3 H), 2.05 (m, 1 H), 1.89 (m, 1 H), 1.00 (d,  $J = 6.7$  Hz, 3 H), 0.97 (d,  $J = 6.9$  Hz, 3 H);  $^{13}\text{C}$  NMR (175 MHz,  $\text{CDCl}_3$ )  $\delta = 173.1, 171.6, 171.6, 169.6, 155.5, 136.3, 130.4, 125.5, 125.4, 122.1, 120.7, 60.0, 59.4, 52.1, 49.1, 41.8, 30.2, 28.9, 26.3, 25.1, 19.4, 17.8$ ; HRMS (ESI)  $\text{C}_{22}\text{H}_{32}\text{N}_5\text{O}_6$  calculated  $[\text{M}+\text{H}]^+$ : 462.2274 found 462.2350,  $\text{C}_{22}\text{H}_{31}\text{N}_5\text{NaO}_6$  calculated  $[\text{M}+\text{Na}]^+$  484.2172, found 484.2168.

a)



b)



c)

ASK-14 #107 RT: 0.47 AV: 1 NL: 1.54E9  
T: FTMS +p ESI Full ms [100.00-1500.00]

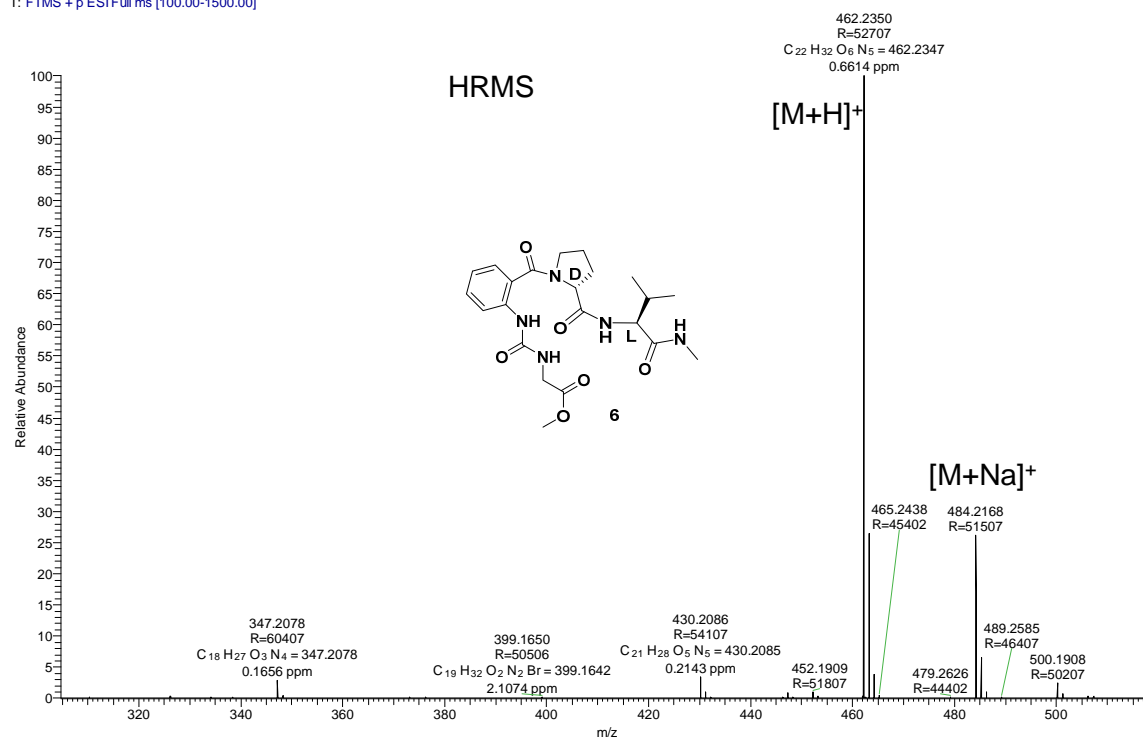


Figure 2.21 a) <sup>1</sup>H NMR, b) <sup>13</sup>C NMR and c) HRMS spectra of compound 6

**Table 2.3** a) Titration study of **1** in CDCl<sub>3</sub> (5mM) with DMSO-d<sub>6</sub> b) Temperature variation study of **1**(5 mM, 700 MHz, CDCl<sub>3</sub>)

a)

V <sub>DMSO-d6</sub> added (in μl)	Chemical shift (in ppm)		
	δ <sub>NH1</sub> (ppm)	δ <sub>NH2</sub> (ppm)	δ <sub>NH3</sub> (ppm)
0	7.82	8.73	9.68
5	7.88	8.72	9.74
10	7.95	8.71	9.86
15	7.98	8.7	9.95
20	8.01	8.69	10.01
25	8.03	8.68	10.05
30	8.04	8.67	10.08
35	8.05	8.66	10.09
40	8.06	8.66	10.1
45	8.06	8.65	10.11
50	8.06	8.64	10.12

b)

Temperature (K)	Chemical shift (in ppm)		
	δ <sub>NH1</sub> (ppm)	δ <sub>NH2</sub> (ppm)	δ <sub>NH3</sub> (ppm)
268	7.9	8.85	9.87
273	7.89	8.83	9.85
278	7.88	8.81	9.82
283	7.87	8.79	9.79
288	7.86	8.78	9.76
293	7.84	8.75	9.71
298	7.82	8.72	9.66
303	7.8	8.7	9.62
308	7.78	8.68	9.57
313	7.76	8.65	9.52
318	7.74	8.63	9.48
323	7.72	8.6	9.41

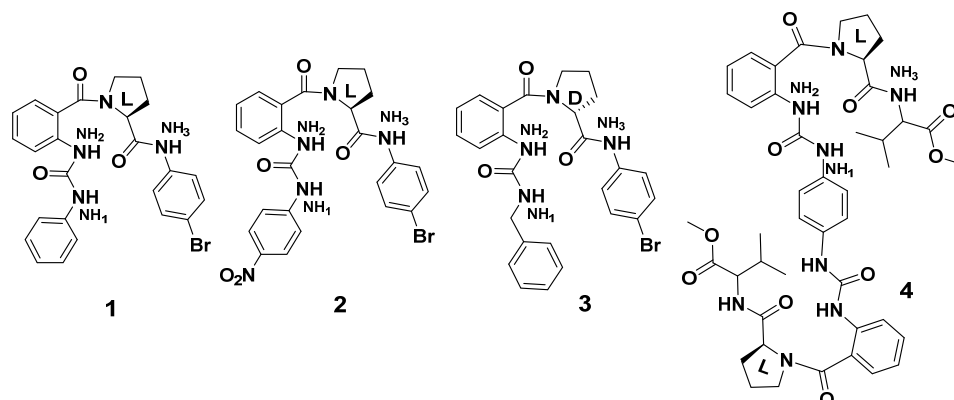


**Table 2.4** a) Titration study of **2** (5mM) in CDCl<sub>3</sub> with DMSO-d<sub>6</sub>, b) Temperature variation study of **2**(5 mM, 700 MHz, CDCl<sub>3</sub>)

a)

V <sub>DMSO-d6</sub> added (in μl)	Chemical shift (in ppm)		
	δ <sub>NH1</sub> (ppm)	δ <sub>NH2</sub> (ppm)	δ <sub>NH3</sub> (ppm)
0	8.26	8.86	9.7
5	8.24	8.87	9.85
10	8.22	8.87	9.92
15	8.19	8.87	10.01
20	8.17	8.87	10.07
25	8.15	8.86	10.11
30	8.13	8.85	10.12
35	8.1	8.85	10.12
40	8.09	8.85	10.12
45	8.05	8.84	10.12
50	8.03	8.83	10.12

b)

Temperature (K)	Chemical shift (in ppm)		
	δ <sub>NH1</sub> (ppm)	δ <sub>NH2</sub> (ppm)	δ <sub>NH3</sub> (ppm)
268	8.31	8.98	9.9
273	8.2	8.96	9.88
278	8.29	8.94	9.84
283	8.29	8.92	9.81
288	8.28	8.91	9.81
293	8.27	8.89	9.79
298	8.26	8.86	9.74
303	8.25	8.84	9.69
308	8.24	8.82	9.64
313	8.23	8.8	9.61
318	8.22	8.77	9.55
323	8.21	8.75	9.51

**Chapter II: Design, Synthesis & Conformational Investigation of “Ant-Pro Urea”  
Based Foldamers**

**Table 2.5** a) Titration study of **3** (5mM) in CDCl<sub>3</sub> with DMSO-d<sub>6</sub>, b) Temperature variation study of **3**(5 mM, 700 MHz, CDCl<sub>3</sub>)

V <sub>DMSO-d6</sub> added (in μl)	Chemical shift (in ppm)		
	δ <sub>NH1</sub> (ppm)	δ <sub>NH2</sub> (ppm)	δ <sub>NH3</sub> (ppm)
0	5.98	8.57	9.64
5	6.01	8.56	9.7
10	6.03	8.55	9.76
15	6.05	8.54	9.8
20	6.06	8.53	9.84
25	6.08	8.52	9.89
30	6.09	8.51	9.92
35	6.09	8.5	9.94
40	6.09	8.5	9.96
45	6.09	8.49	9.97
50	6.1	8.48	9.9

Temperature (K)	Chemical shift (in ppm)		
	δ <sub>NH1</sub> (ppm)	δ <sub>NH2</sub> (ppm)	δ <sub>NH3</sub> (ppm)
268	6.06	8.7	9.82
273	6.05	8.68	9.79
278	6.04	8.66	9.77
283	6.04	8.64	9.75
288	6.02	8.62	9.72
293	6	8.6	9.7
298	5.98	8.52	9.67
303	5.97	8.56	9.63
308	5.97	8.53	9.59
313	5.94	8.51	9.56
318	5.92	8.4	9.52
323	5.9	8.46	9.48

**Table 2.6** a) Titration study of **4** (2mM) in CDCl<sub>3</sub> with DMSO-d<sub>6</sub>, b) Temperature variation study of **4** (2 mM, 700 MHz, CDCl<sub>3</sub>)

V <sub>DMSO-d6</sub> added (in μl)	Chemical shift (in ppm)		
	δ <sub>NH1</sub> (ppm)	δ <sub>NH2</sub> (ppm)	δ <sub>NH3</sub> (ppm)
0	7.82	8.53	6.56
5	7.83	8.53	6.64
10	7.86	8.54	6.75
15	7.92	8.57	6.89
20	7.95	8.58	7
25	7.98	8.6	7.1
30	8	8.61	7.25
35	8.01	8.61	7.38
40	8.01	8.62	7.5
45	8.01	8.62	7.65
50	8.02	8.63	7.79

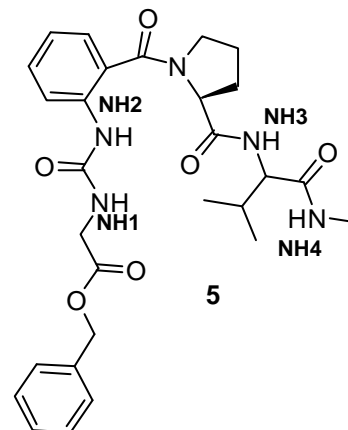
Temperature (K)	Chemical shift (in ppm)		
	δ <sub>NH1</sub> (ppm)	δ <sub>NH2</sub> (ppm)	δ <sub>NH3</sub> (ppm)
268	7.92	8.62	6.69
273	7.90	8.60	6.66
278	7.89	8.59	6.64
283	7.87	8.57	6.61
288	7.85	8.55	6.59
293	7.84	8.54	6.57
298	7.82	8.53	6.56
303	7.81	8.51	6.54
308	7.79	8.50	6.52
313	7.78	8.48	6.51
318	7.76	8.47	6.50
323	7.74	8.46	6.49

**Chapter II: Design, Synthesis & Conformational Investigation of “Ant-Pro Urea”  
Based Foldamers**

**Table 2.7** a) Titration study of **5** (5 mM) in CDCl<sub>3</sub> with DMSO-d<sub>6</sub>, b) Temperature variation study of **5** (5 mM, 700 MHz, CDCl<sub>3</sub>)

a)

V <sub>DMSO-d<sub>6</sub></sub> added (in μl)	Chemical shift (in ppm)			
	δ <sub>NH1</sub> (ppm)	δ <sub>NH2</sub> (ppm)	δ <sub>NH3</sub> (ppm)	δ <sub>NH4</sub> (ppm)
0	6.69	8.59	7.22	6.74
5	6.68	8.59	7.21	6.79
10	6.66	8.6	7.19	6.84
15	6.64	8.61	7.17	6.89
20	6.63	8.61	7.14	6.95
25	6.61	8.6	7.13	6.98
30	6.6	8.6	7.11	7.02
35	6.58	8.6	7.1	7.04
40	6.57	8.59	7.09	7.04
45	6.56	8.59	7.06	7.05
50	6.55	8.58	7.05	7.06



b)

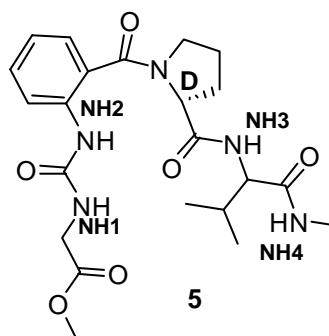
Temperature (K)	Chemical shift (in ppm)			
	δ <sub>NH1</sub> (ppm)	δ <sub>NH2</sub> (ppm)	δ <sub>NH3</sub> (ppm)	δ <sub>NH4</sub> (ppm)
268	6.78	8.69	7.54	7.04
273	6.77	8.68	7.48	6.99
278	6.75	8.66	7.42	6.94
283	6.73	8.64	7.37	6.89
288	6.72	8.63	7.32	6.84
293	6.7	8.61	7.26	6.78
298	6.68	8.59	7.21	6.73
303	6.66	8.57	7.17	6.68
308	6.65	8.56	7.14	6.65
313	6.63	8.54	7.09	6.59
318	6.61	8.52	7.05	6.55
323	6.59	8.51	7.02	6.51

**Chapter II: Design, Synthesis & Conformational Investigation of “Ant-Pro Urea”  
Based Foldamers**

**Table 2.8** a) Titration study of **6** (5 mM) in CDCl<sub>3</sub> with DMSO-d<sub>6</sub> b) Temperature variation study of **6** (5 mM, 700 MHz, CDCl<sub>3</sub>)

a)

V <sub>DMSO-d<sub>6</sub></sub> added (in μl)	Chemical shift (in ppm)			
	δ <sub>NH1</sub> (ppm)	δ <sub>NH2</sub> (ppm)	δ <sub>NH3</sub> (ppm)	δ <sub>NH4</sub> (ppm)
0	6.61	8.28	7.45	6.72
5	6.59	8.31	7.7	6.9
10	6.58	8.33	7.82	6.98
15	6.56	8.34	7.94	7
20	6.54	8.35	8	7.1
25	6.53	8.35	8.04	7.13
30	6.52	8.35	8.06	7.143
35	6.5	8.34	8.09	7.16
40	6.49	8.34	8.11	7.17
45	6.47	8.33	8.11	7.18
50	6.46	8.33	8.12	7.18



b)

Temperature (K)	Chemical shift (in ppm)			
	δ <sub>NH1</sub> (ppm)	δ <sub>NH2</sub> (ppm)	δ <sub>NH3</sub> (ppm)	δ <sub>NH4</sub> (ppm)
268	6.69	8.55	7.67	7.06
273	6.67	8.49	7.63	6.99
278	6.66	8.44	7.58	6.93
283	6.65	8.4	7.54	6.88
288	6.63	8.34	7.49	6.81
293	6.62	8.3	7.46	6.77
298	6.6	8.27	7.42	6.72
303	6.58	8.23	7.39	6.67
308	6.57	8.2	7.37	6.63
313	6.59	8.17	7.34	6.59
318	6.54	8.15	7.32	6.55
323	6.52	8.12	7.3	6.53



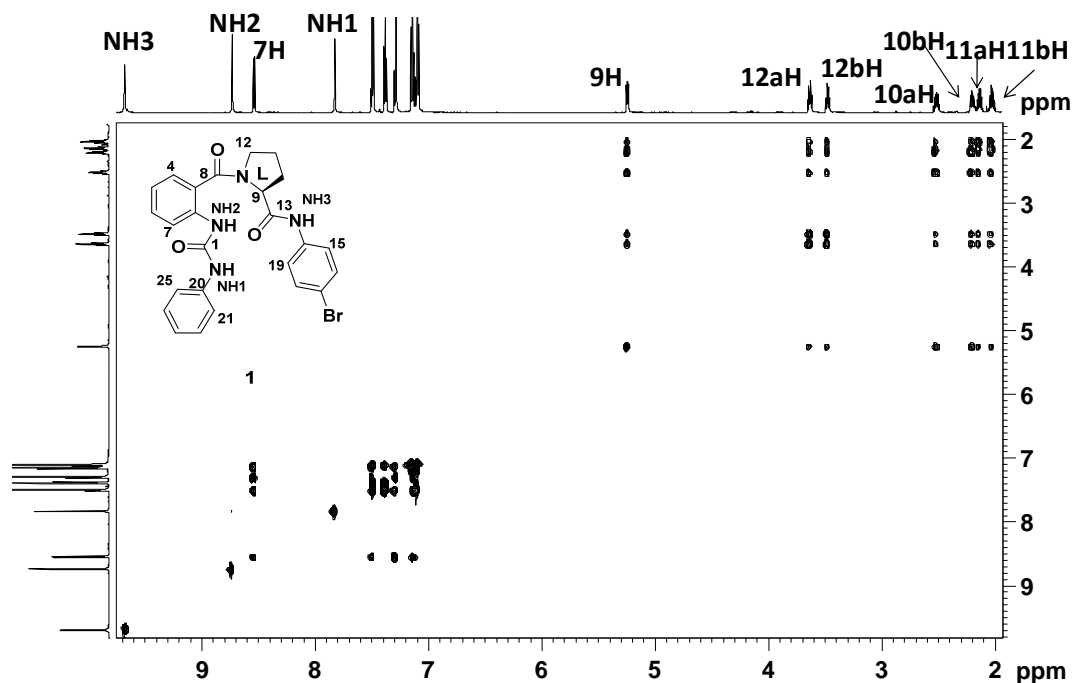


Figure 2.22 TOCSY spectrum of **1** (10 mM, CDCl<sub>3</sub>, 700MHz)

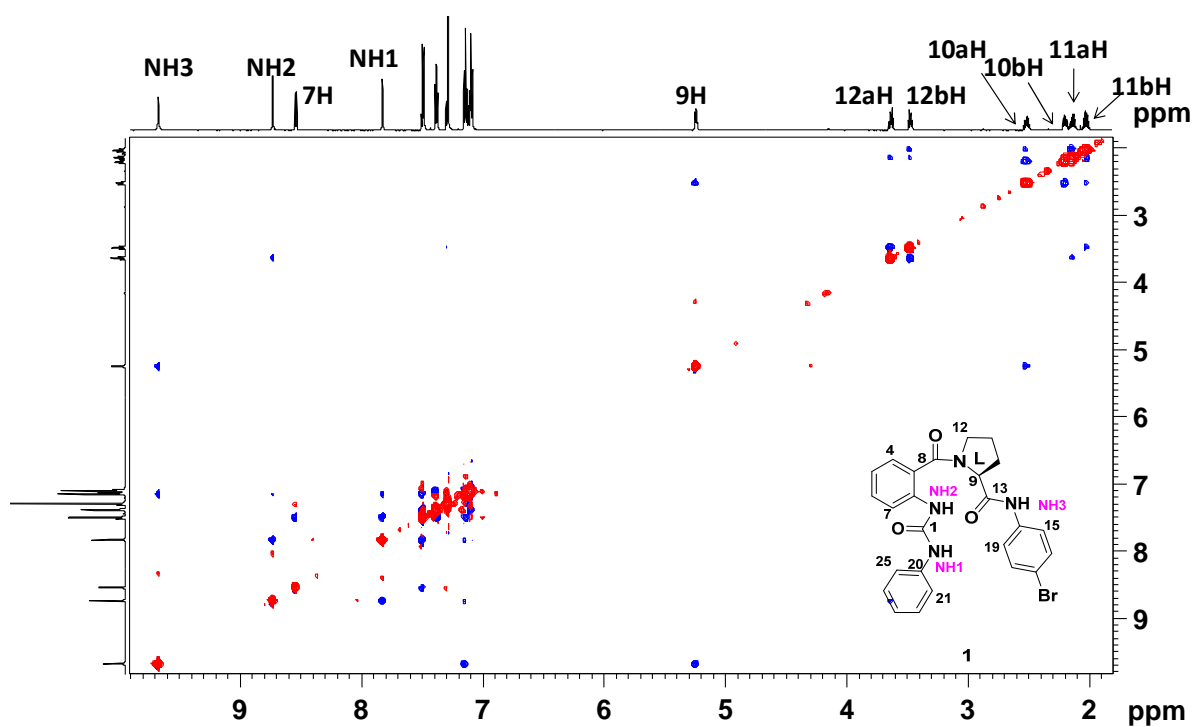


Figure 2.23 NOESY spectrum of **1** (10 mM, CDCl<sub>3</sub>, 700MHz)

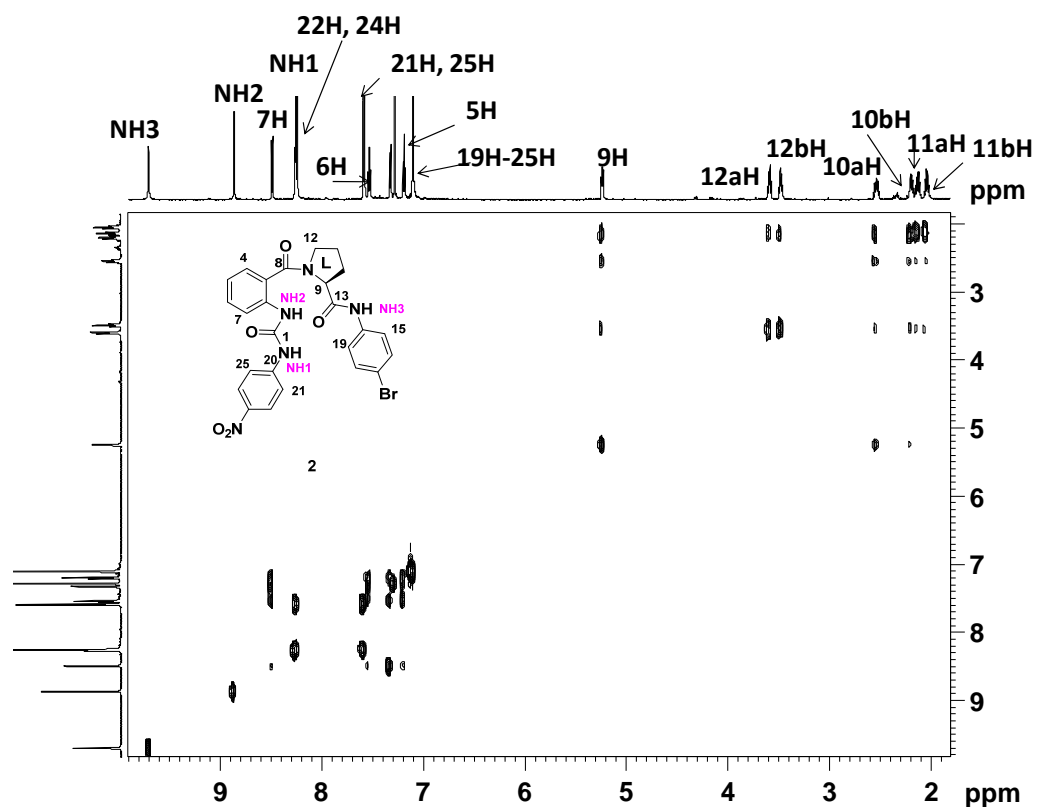


Figure 2.24 TOCSY spectrum of **2** (10 mM, CDCl<sub>3</sub>, 500MHz)

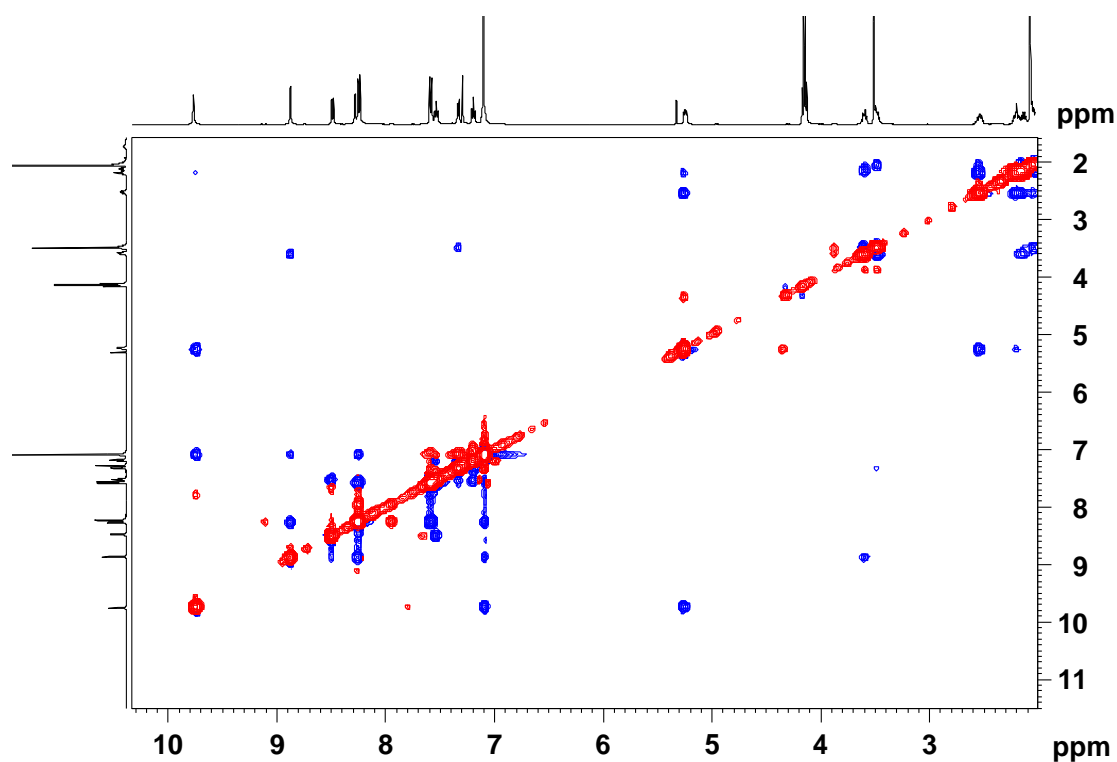


Figure 2.25 NOESY spectrum of **2** (10 mM, CDCl<sub>3</sub>, 500MHz)

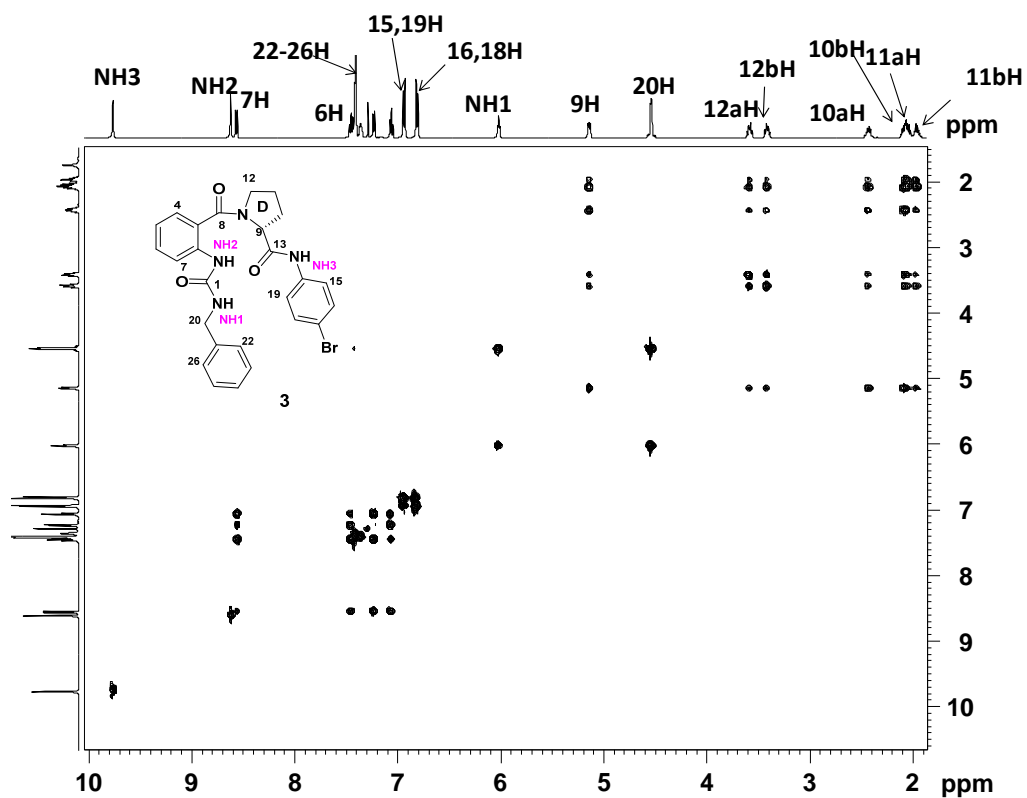


Figure 2.26 TOCSY spectrum of **3** (20 mM, CDCl<sub>3</sub>, 500MHz)

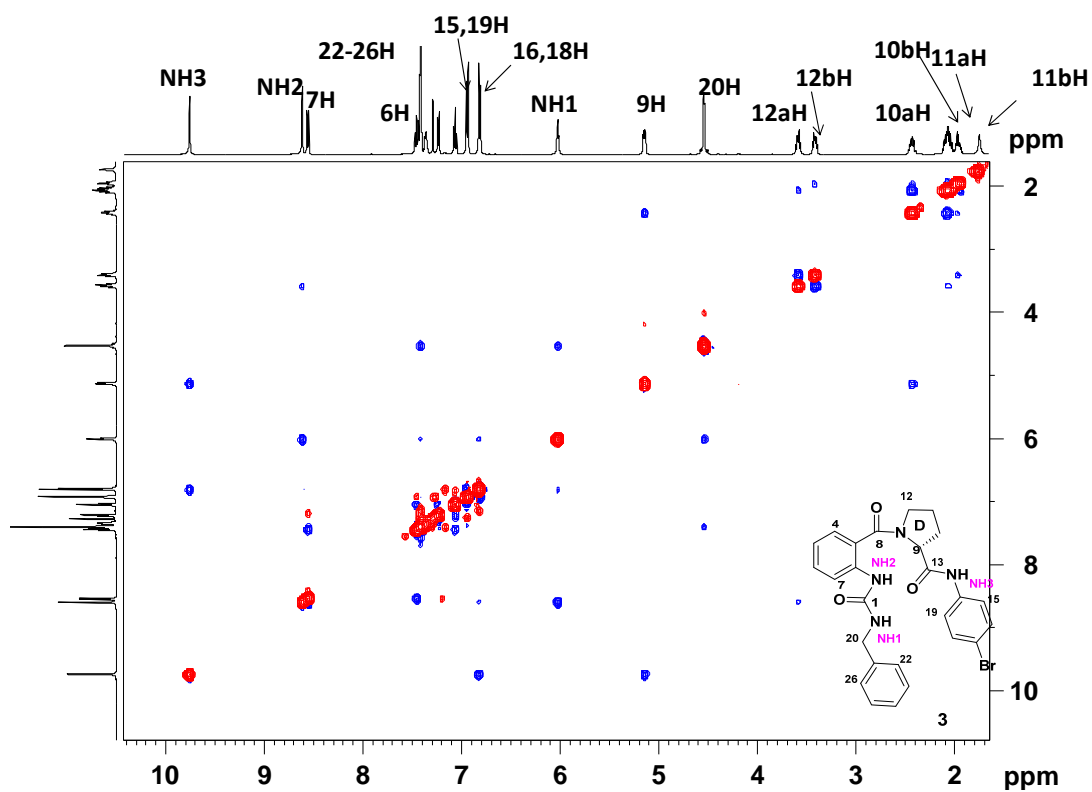


Figure 2.27 NOESY spectrum of **3** (20 mM, CDCl<sub>3</sub>, 500MHz)

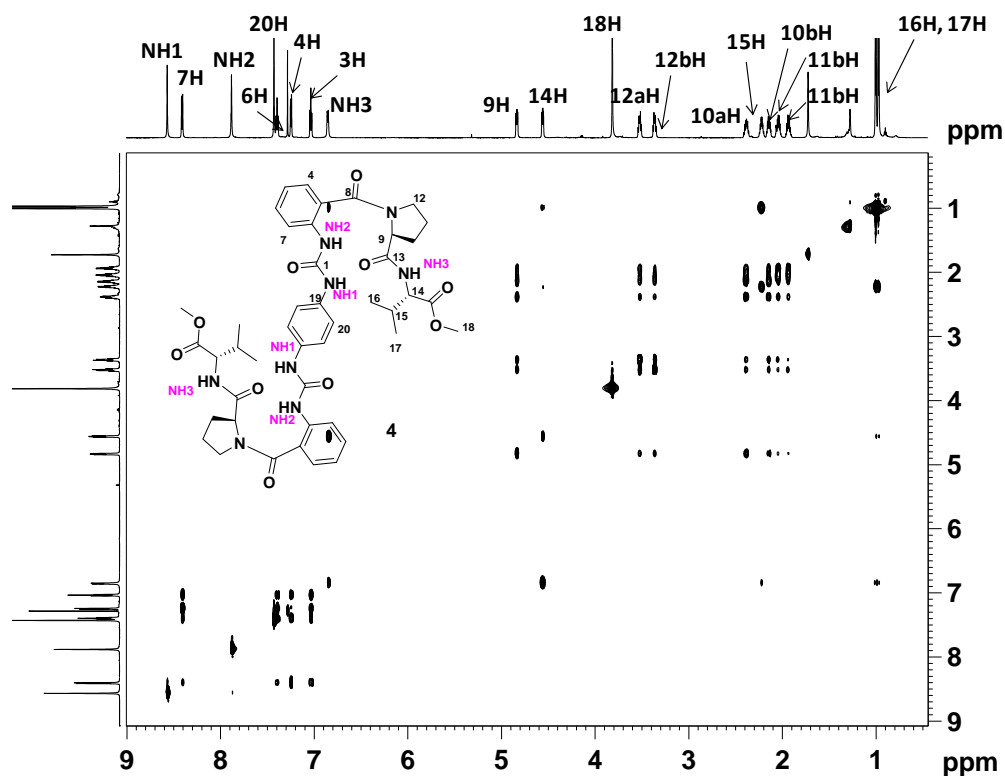


Figure 2.28 TOCSY spectrum of **4** (10 mM, CDCl<sub>3</sub>, 700MHz)

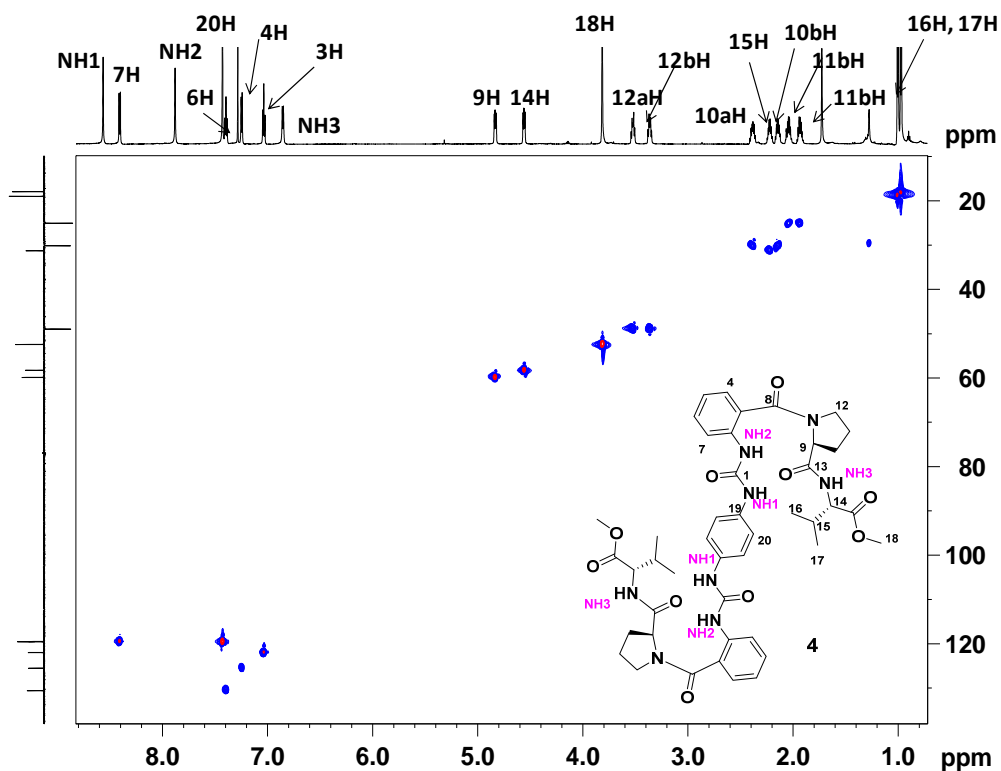


Figure 2.29 HSQC spectrum of **4** (10 mM, CDCl<sub>3</sub>, 700MHz)

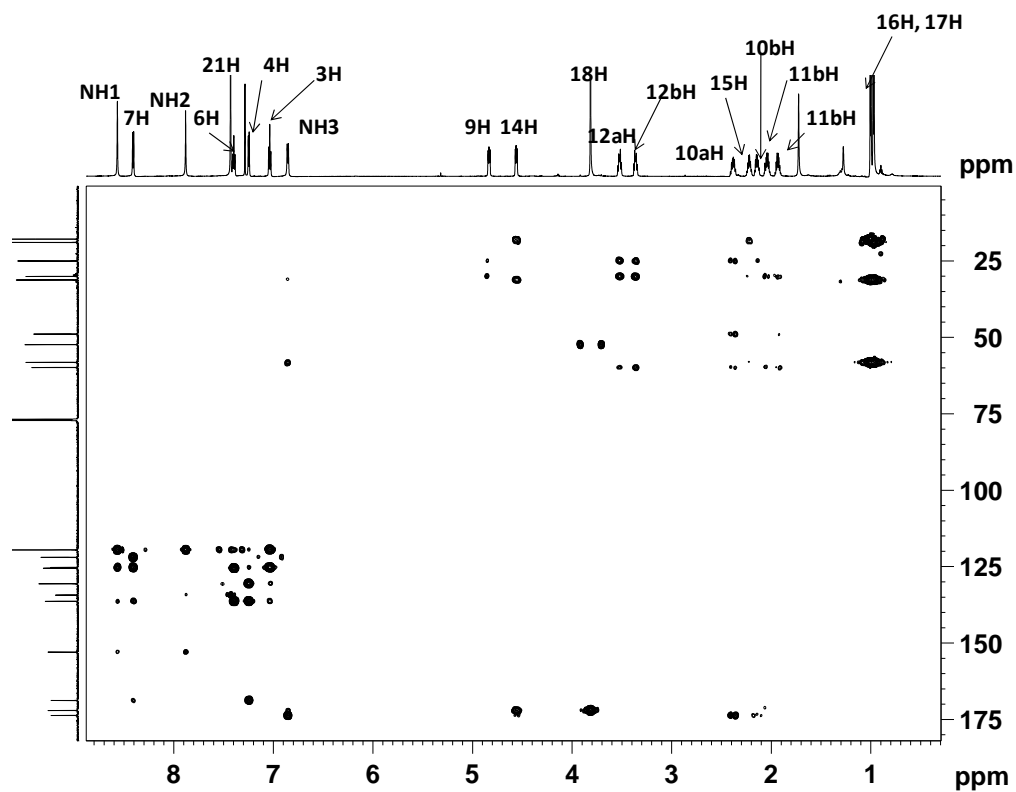


Figure 2.30 HMBC spectrum of **4** (10 mM, CDCl<sub>3</sub>, 700MHz)

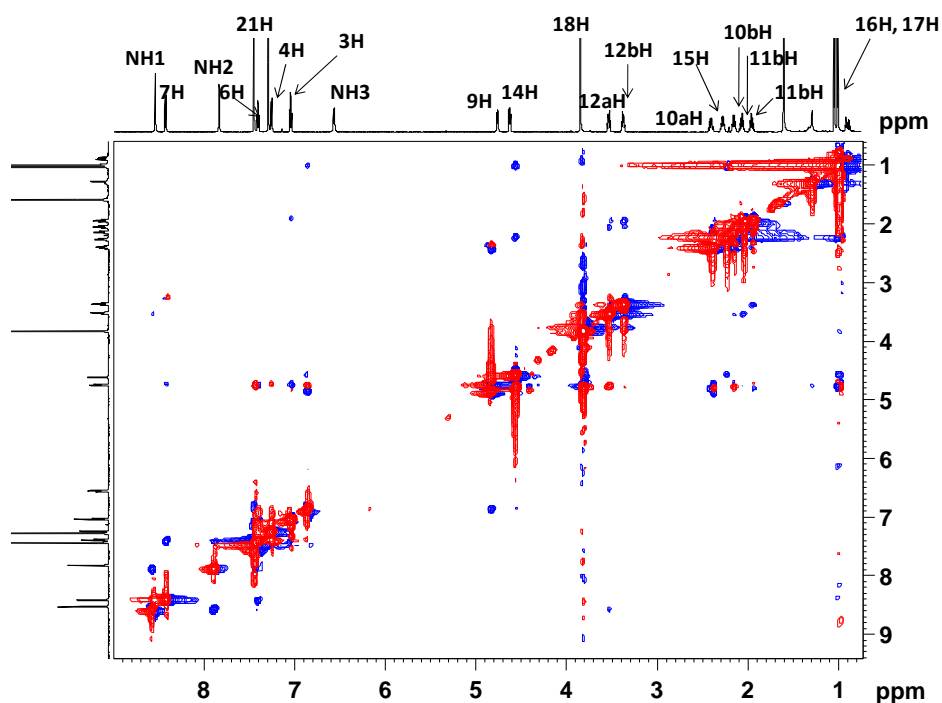


Figure 2.31 ROESY spectrum of **4** (10 mM, CDCl<sub>3</sub>, 700MHz)

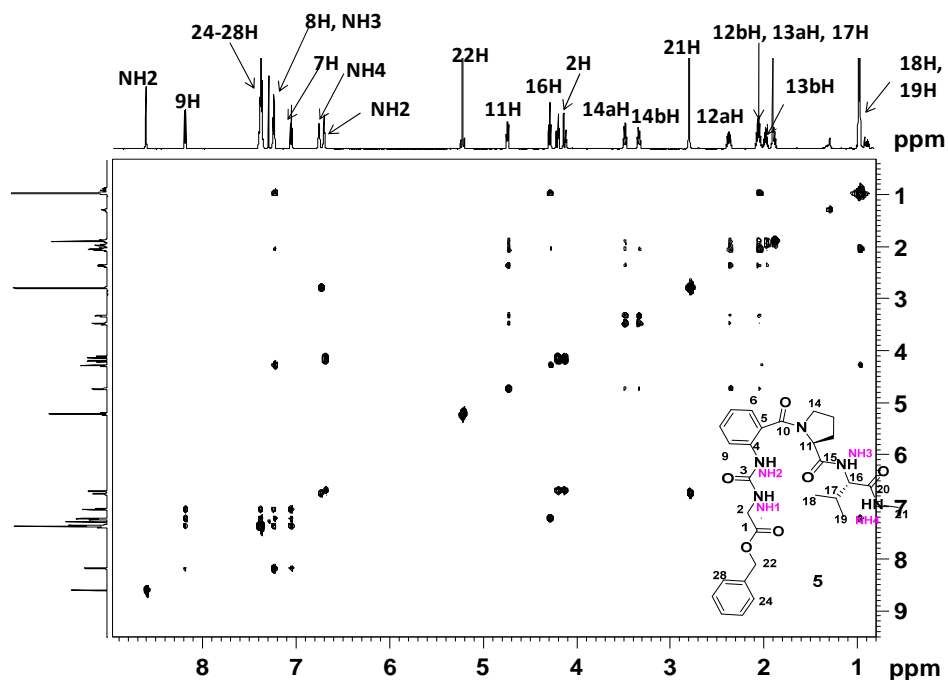


Figure 2.32 TOCSY spectrum of **5** (20 mM, CDCl<sub>3</sub>, 500MHz)

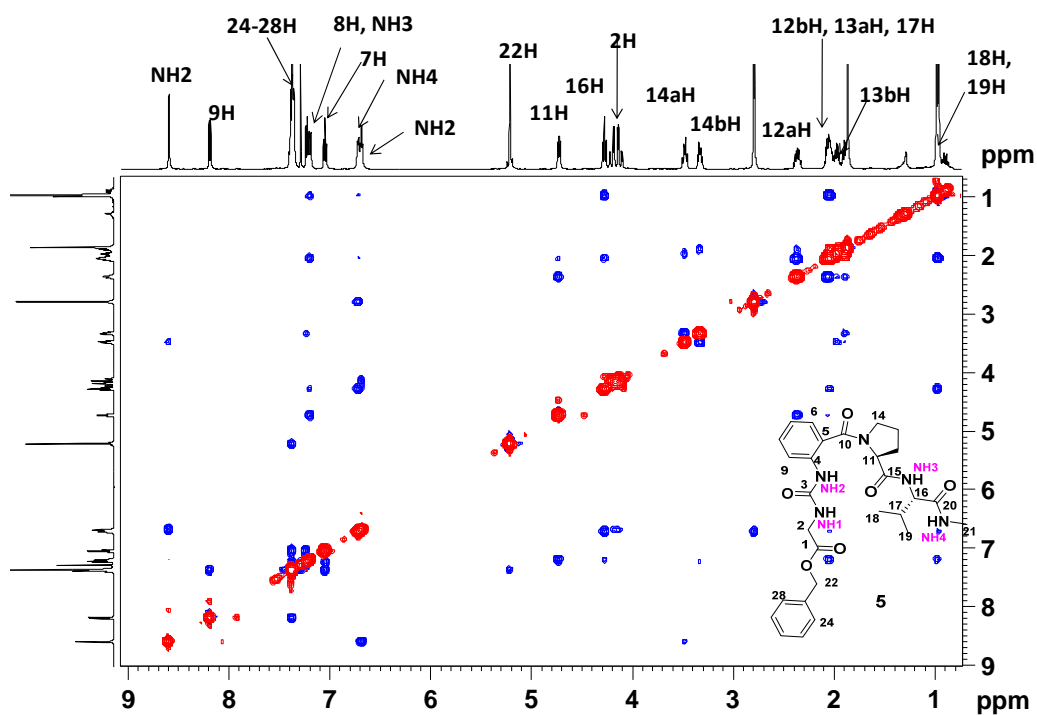


Figure 2.33 NOESY spectrum of **5** (20 mM, CDCl<sub>3</sub>, 500MHz)

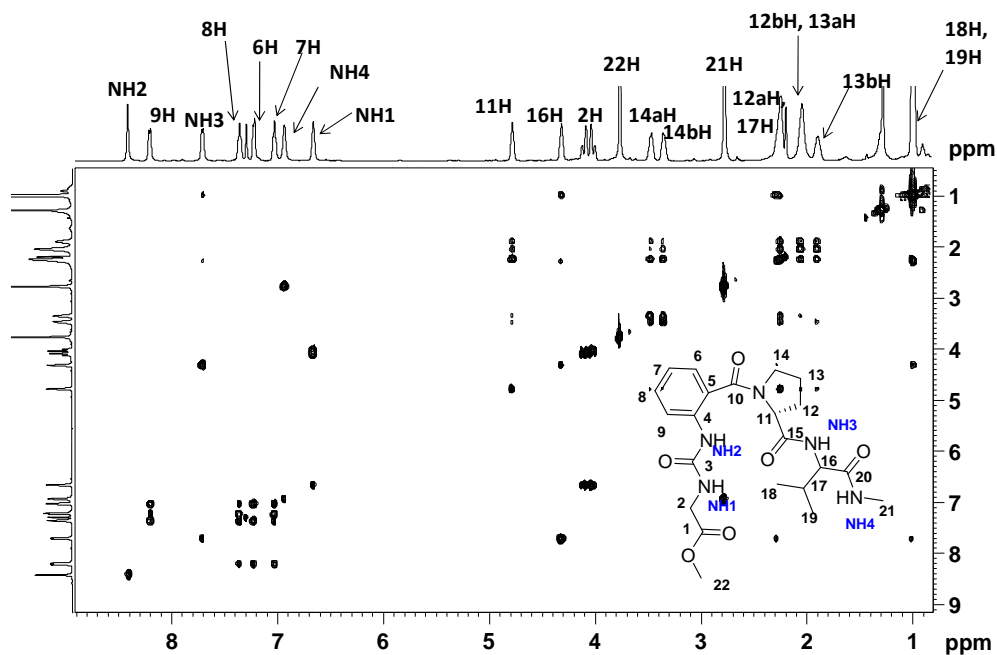


Figure 2.34 TOCSY spectrum of **6** (20 mM, CDCl<sub>3</sub>, 500MHz)

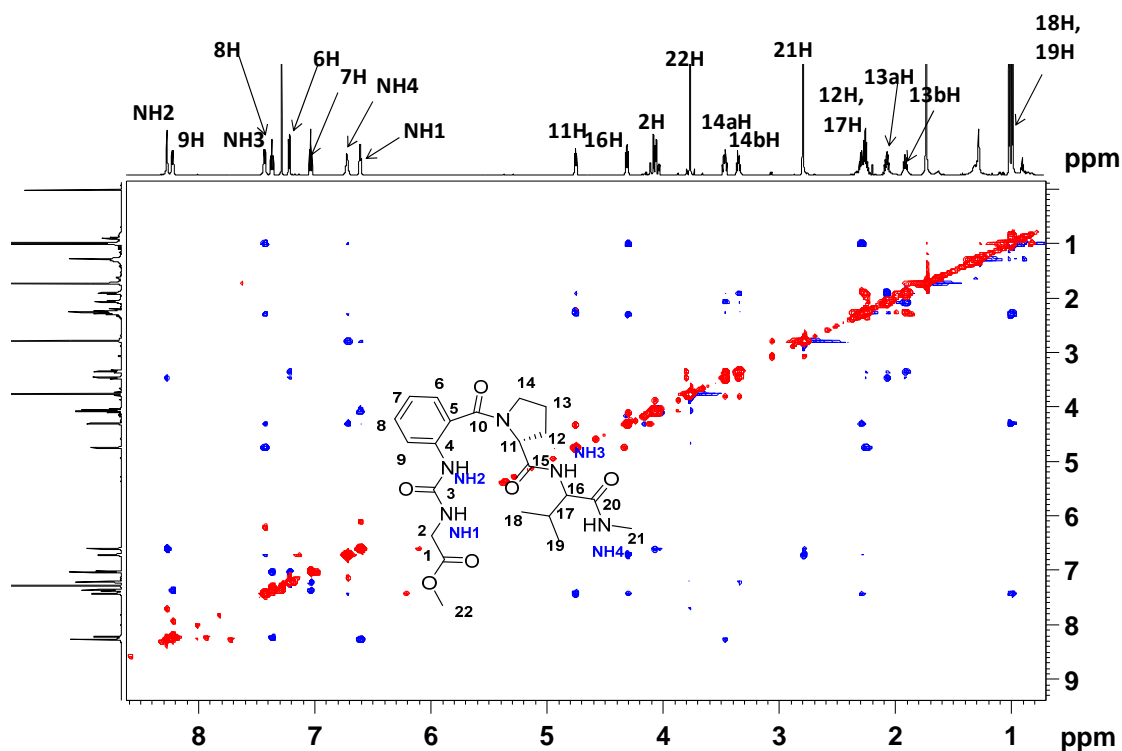


Figure 2.35 NOESY spectrum of **6** (20 mM, CDCl<sub>3</sub>, 700MHz)

**Chapter II: Design, Synthesis & Conformational Investigation of “Ant-Pro Urea”  
Based Foldamers**

**Table 2.9** ROESY restraints used for MD simulation studies of **4**

(F2) [ppm]	(F1) [ppm]	Upper Bound	Lower Bound	Between
8.3995	7.3584	2.68	2.2	7H/6H
8.9524	8.2401	2.55	2.09	NH1/NH2
8.9474	3.4233	4.07	3.33	NH2/12aH
8.2451	7.5029	2.8	2.29	NH1/21H
8.3497	4.9376	3.16	2.59	NH3/9H
8.3397	4.5441	3.55	2.91	NH3/14H
8.3497	1.0224	4.16	3.4	NH3/16H
7.2538	3.3436	4.14	3.39	4H/12bH
4.9475	2.3972	3.06	2.5	9H/10aH
4.9525	2.1232	3.5	2.86	9H/10bH
4.5241	1.0074	3.07	2.51	14H/16H
3.4482	1.9289	3.35	2.74	12aH/11aH
3.3685	1.919	3.28	2.68	12bH/11bH

**Table 2.10** NOESY restraints used for MD simulation studies of **5**

(F2) [ppm]	(F1) [ppm]	Upper Bound	Lower Bound	Between
7.364	7.0332	2.68	2.2	7H/8H
8.1788	7.3552	2.62	2.14	9H/8H
8.5912	6.6809	2.38	1.95	NH1/NH2
8.5962	3.4706	3.11	2.54	NH2/14aH
8.5962	7.2244	4.64	3.8	NH2/NH3
7.359	5.2016	2.44	1.99	22H/24H
7.2282	0.9647	2.74	2.24	NH3/19H,18H
7.2282	2.0315	2.79	2.29	NH3/17H
7.2232	3.3196	3.11	2.55	6H/14H
7.2282	4.7235	2.6	2.13	NH3/11H
6.7454	0.9597	3.23	2.65	NH4/18,19H
6.7403	2.7762	2.66	2.18	NH4/21H
6.7454	2.0265	4.36	3.57	NH4/17H
6.7454	4.2656	2.45	2.01	NH4/16H
6.685	4.1952	2.82	2.31	NH1/2aH
6.675	4.0895	3.77	3.08	NH1/2bH
4.7235	2.3485	2.46	2.02	11H/12aH
4.7235	2.0466	3.29	2.69	11H/12bH
4.2709	0.9547	2.36	1.93	16H/19,18H
4.2709	2.0265	2.84	2.33	16H/17aH
3.4712	1.961	2.82	2.31	14bH/13bH
3.3254	1.956	3.3	2.7	14aH/13aH
3.3254	1.8654	2.86	2.34	14bH/13bH
2.0328	0.9547	2.07	1.69	17H/18,19H
2.3597	2.0365	2.08	1.7	12aH/12bH
2.3597	1.8755	3.17	2.6	12aH/13aH



**Table 2.11** NOESY restraints used for MD simulation studies of **6**

(F2) [ppm]	(F1) [ppm]	Upper Bound	Lower Bound	Between
7.364	7.0281	2.68	2.2	7H/8H
8.219	7.3552	2.65	2.17	8H/9H
8.2592	6.6004	2.36	1.93	NH1/NH2
8.2693	3.4605	3.24	2.65	NH2/14aH
8.2643	3.3448	5.06	4.14	NH2/14bH
7.4243	0.9899	2.7	2.21	NH3/18,19H
7.4243	2.273	3.08	2.52	NH3/12H
7.4243	4.3009	3.3	2.7	NH3/16H
7.4243	4.7437	2.55	2.08	NH3/11H
7.4243	6.7111	3.48	2.85	NH3/NH4
7.2131	3.3448	3.25	2.66	6H/14bH
7.2131	3.4605	3.67	3.01	6H/14aH
6.7102	0.9949	3.46	2.83	NH4/18,19H
6.7102	2.2831	3.62	2.96	NH4/17H
6.7051	2.7863	2.66	2.18	NH4/21H
6.5995	2.7812	3.68	3.01	21H/NH1
6.7102	4.3009	2.66	2.18	NH4/16H
6.5945	4.0694	2.82	2.31	NH1/2aH
6.6046	4.0392	2.89	2.36	NH1/2bH
6.6046	4.3009	4.04	3.3	NH1/16H
4.7437	2.2529	2.5	2.04	11H/12H
4.7437	1.9057	3.65	2.99	11H/13aH
4.3011	0.9949	2.58	2.11	16H/18,19H
4.3011	2.2831	2.75	2.25	16H/17H
3.3455	1.9007	2.95	2.42	14bH/13bH
3.4612	1.9057	3.67	3	14aH/13BH
3.4612	2.0667	2.95	2.41	14aH/13aH
2.2893	0.9949	2.24	1.83	17H/18,19H

## **2.7 References and notes**

(1) (a) J. L. Crawford, W. N. Lipscomb and C. G. Schellman, *Proc. Natl. Acad. Sci. U. S. A.*, 1973, **70**, 538. (b) A. M. C. Marcelino and L. M. Gierasch, *Biopolymers*, 2008, **89**, 380; (c) J. D. Puglisi, L. Chyen, S. Blanchard and A. D. Frankel, *Science*, 1995, **270**, 1200; (d) W. S. Somers and S. E. Phillips, *Nature*, 1992, 359, 387; (e) P. Prabakaran, J. Gan, Y.-Q. Wu, M.-Y. Zhang, D. S. Dimitrov and X. Ji, *J. Mol. Biol.*, 2006, **357**, 82;

(2) (a) D. R. M Hughes and M. L Waters, *Curr. Opin. Struct. Biol.*, 2006, **16**, 514; (b) C. E. Stotz and E. M. Topp, *J. Pharm. Sci.*, 2004, **93**, 2881; (c) C. Ritter, M-L. Maddelein, A. B. Siemer, T. Luhrs, M. Ernst, B. H. Meier, S. J. Saupe and R. Riek, *Nature*, 2005, **435**, 844; (e) T. A. Petkova, Y. Ishii, J. J. Balbach, O. N. Antzutkin, R. D. Leapman, F. Delaglio and R. Tycko, *Proc. Natl. Acad. Sci. U.S.A.*, 2002, **99**, 16742.

(3) (a) C. M. Rufo, Y. S. Moroz, O. V. Moroz, J. Stohr, T. A. Smith, X. Hu, W. F. De Grado and I. V. Korendovych, *Nat. Chem.*, 2014, **6**, 303; (b) F. Bachle, J. Duschmale, C. Ebner, A. Pfaltz and H. Wennemers, *Angew. Chem. Int. Ed.*, 2013, **52**, 12619; (c) K. W. Fiori, A. L. A. Puchlopek and S. J. Miller, *Nat. Chem.*, 2009, **1**, 630; (d) E. A. C. Davie, S. M. Mennen, Y. Xu and S. J. Miller, *Chem. Rev.*, 2007, **107**, 5759; (e) Scott J. Miller, *Acc. Chem. Res.*, 2004, **37**, 601. (f) D. R. Kelly and S. M. Roberts, *Biopolymers (Pept. Sci.)*, 2006, 84, 74; (g) A. Berkessel, B. Koch, C. Toniolo, M. Rainaldi, Q. B. Broxterman and B. Kaptein, *Biopolymers (Pept. Sci.)*, 2006, **84**, 90.

(4) (a) P. J. Knerr, M. C. Branco, R. Nagarkar, D. J. Pochan and J. P. Schneider, *J. Mater. Chem.*, 2012, **22**, 1352. (b) C. M. Micklitsch, S. H. Medina, T. Yucel, K. J. Nagy-Smith, D. J. Pochan and J. P. Schneider, *Macromolecules*, 2015, **48**, 1281;

(5) (a) E. Lacroix, T. Kortemme, M. L. de la Paz and L. Serrano, *Curr. Opin. Struct. Biol.*, 1999, **9**, 487, (b) S. H. Gellman, *Curr. Opin. Chem. Biol.*, 1998, **2**, 717.

(6) G. Wagner and M. Feigel, *Tetrahedron*, 1993, **49**, 10831.

- (7) M. J. Winningham and D. Y. Sogah, *J. Am. Chem. Soc.*, 1994, **116**, 11173.
- (8) H. Diaz and J. W. Kelly, *Tetrahedron Lett.*, 1991, **32**, 5725.
- (9) J. S. Nowick, E. M. Smith and G. Noronha, *J. Org. Chem.*, 1995, **60**, 7386.
- (10) D. Ranganathan, V. Haridas, S. Kurur, A. Thomas, K. P. Madhusudanan, R. Nagaraj, A. C. Kunwar, A. V. S. Sarma and I. L. Karle, *J. Am. Chem. Soc.*, 1998, **120**, 8448.
- (11) (a) M. G. Woll, J. R. Lai, I. A. Guzei, S. J. C. Taylor, M. E. B. Smith and S. H. Gellman, *J. Am. Chem. Soc.*, 2001, **123**, 11077; (b) J. M. Langenhan, I. A. Guzei and S. H. Gellman, *Angew. Chem. Int. Ed.*, 2003, **42**, 2402.
- (12) F. Freire, J. D. Fisk, A. J. Peoples, M. Ivancic, I. A. Guzei and S. H. Gellman, *J. Am. Chem. Soc.*, 2008, **130**, 7839.
- (13) F. Freire and S. H. Gellman, *J. Am. Chem. Soc.*, 2009, **131**, 7970.
- (14) S. Chowdhury, G. Schatte, H.-B. Kraatz, *Angew. Chem. Int. Ed.*, 2008, **47**, 7056.
- (15) A. K. Medda, C. M. Park, A. Jeon, H. Kim, J.-H. Sohn and H.-S. Lee, *Org. Lett.*, 2011, **13**, 3486.
- (16) C. R. Jones, M. K. N. Qureshi, F. R. Truscott, S. T. D. Hsu, A. J. Morrison and M. D. Smith, *Angew. Chem. Int. Ed.*, 2008, **47**, 7099.
- (17) C. R. Jones, G. D. Pantos, A. J. Morrison and M. D. Smith, *Angew. Chem. Int. Ed.*, 2009, **48**, 7391.
- (18) (a) P. Prabhakaran, S. S. Kale, V. G. Puranik, P. R. Rajamohanam, O. Chetina, J. A. K. Howard, H. J. Hofmann, and G. J. Sanjayan *J. Am. Chem. Soc.*, 2008, **130**, 17743. (b) S. S. Kale, A. S. Kotmale, A. K. Dutta, S. Pal, P. R. Rajamohanam and G. J. Sanjayan *Org. Biomol. Chem.*, 2012, **10**, 8426. (c) K. N. Vijayadas, R. V. Nair, R. L. Gawade, A. S. Kotmale, P. Prabhakaran, R. G. Gonnade, V. G. Puranik, P. R.

***Chapter II: Design, Synthesis & Conformational Investigation of “Ant-Pro Urea”  
Based Foldamers***

---

Rajamohanam and G. J. Sanjayan, *Org. Biomol. Chem.*, 2015, **13**, 3064. (d) V. H. Thorat, T. S. Ingole, K. N. Vijayadas, R. V. Nair, S. S. Kale, V. V. E. Ramesh, H. C. Davis, P. Prabhakaran, R. G. Gonnade, R. L. Gawade, V. G. Puranik, P. R. Rajamohanam and G. J. Sanjayan, *Eur. J. Org. Chem.* 2013, **17**, 3529.

***Chapter 3: Synthesis of Novel  
Antibacterial & Anticancer Agents***

***Part A - Self Assembly In  
Designed  $\beta$ -Lactam Antibiotics***



## Introduction

### 3.1.1 $\beta$ -lactam antibiotics

In 1928, Sir Alexander Fleming isolated the antibiotic substance penicillin from the fungus *penicillium notatum*,<sup>1</sup> for which he shared a Nobel Prize in 1945. Penicillin is an antibiotic used in the treatment of bacterial infections. It belongs to a class of antibiotic agents containing beta-lactam ring in their molecular structure and are known as  $\beta$ -lactam antibiotics. These are broad-spectrum antibiotics and are the most widely used group of antibiotics. This includes penicillin derivatives (penams), cephalosporins (cephems), monobactams, and carbapenems. They work, by inhibiting the cell wall biosynthesis of the bacterial organism.  $\beta$ -Lactam antibiotics are used for prevention and treatment of bacterial infections caused by susceptible organisms. Initially,  $\beta$ -lactam antibiotics were mainly used against only Gram-positive bacteria, but recent development of broad-spectrum  $\beta$ -lactam antibiotics active against various Gram-negative organisms has increased their effectiveness.

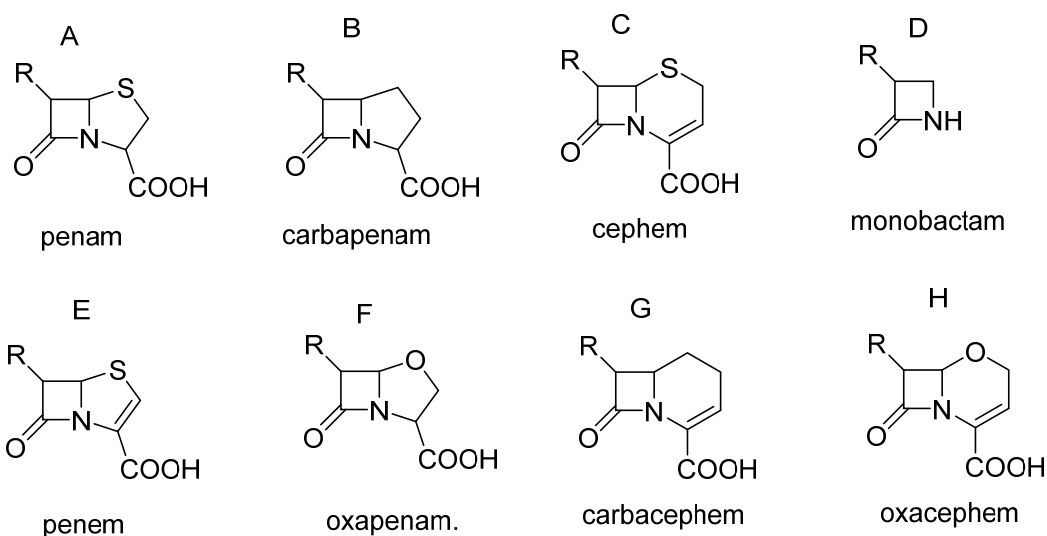


**Figure 3.1**  $\beta$ -Lactams are classified according to their core ring structures.<sup>2</sup>

### 3.1.2 Mode of action

Most of the  $\beta$ -lactam antibiotics work by inhibiting cell wall biosynthesis of the bacterial organism. They inhibit the synthesis of peptidoglycon layer containing *N*-acetylglucosamine (NAG) and *N*-acetylmuramic acid (NAM) connected by penicillin binding proteins (PBP).<sup>3</sup> Penicilins act on PBP and thus inhibit the synthesis of peptidoglycon.<sup>4</sup>

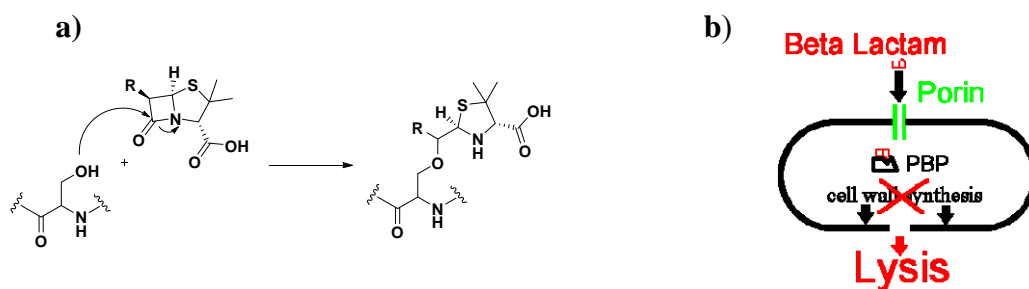


**Figure 3.2** Interaction between the  $\beta$ -lactam antibiotics and the active site serine of the PBP, formation of a stable acyl-enzyme complex (a). The beta lactam enters the bacterium through the porin and which binds to the PBP, inhibiting cell wall synthesis and thus the bacterium dies (b).

### 3.1.3 Categories of Beta-lactam antibiotics

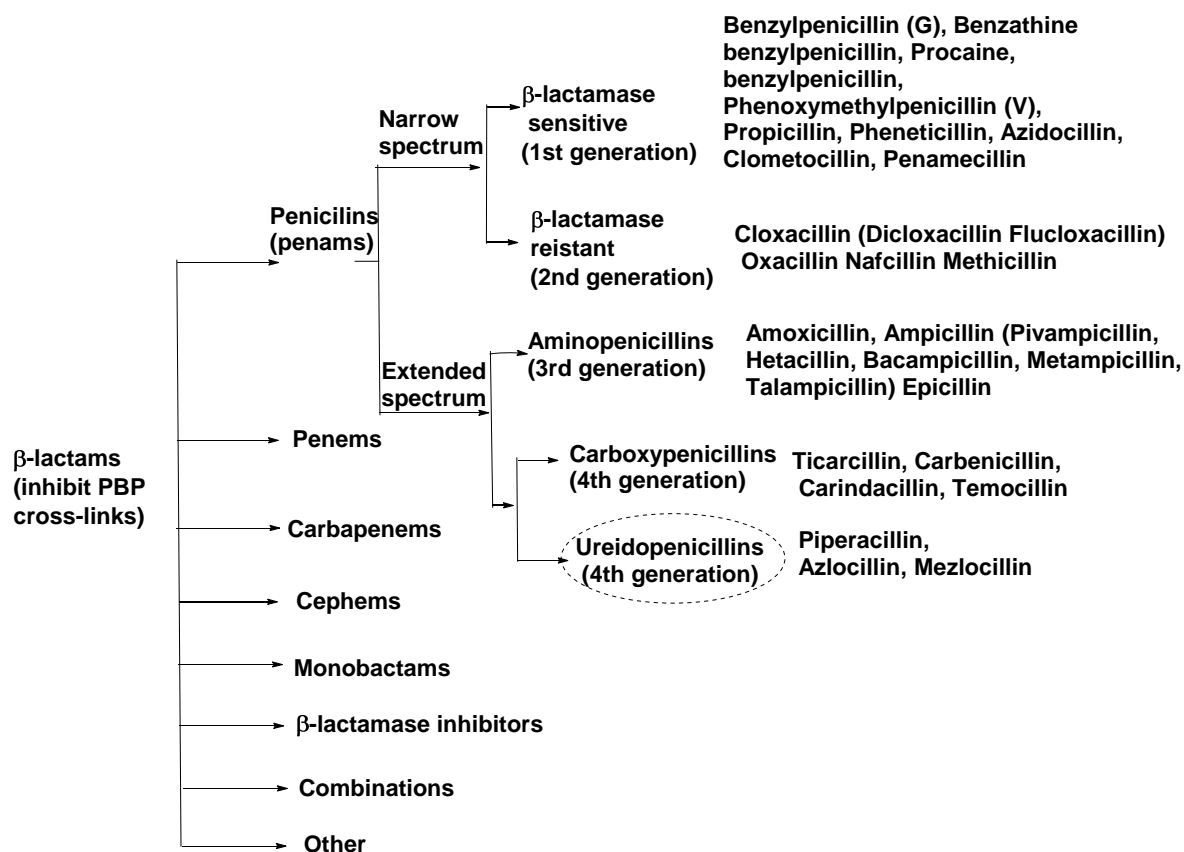


**Figure 3.3:** Classification of  $\beta$ -lactam antibiotics, specifically for penicilin (generation wise) with an examples of drugs. Highlighted ureidopenicillins are the area of interest of the present work.



### 3.1.4 Resistance:

In 1940, Abraham and Chain, showed that the resistance developed by *E Coli* bacteria to penicillins.<sup>5</sup> During the 1950's, resistance became a serious problem as some bacteria had built up resistance to penicillins via selection of penicillin  $\beta$ -lactamase-producing strains. Bacteria have several strategies to diminish the antibiotic activity such as enzymatic destruction, target site (PBP) alterations, diminished permeability for the drug to enter the cell, and active efflux systems that pump the drug out of the cell.<sup>6</sup> Bacteria utilises all these to fight  $\beta$ -lactams, but the most common and well-known mechanism is the enzymatic destruction via synthesis of  $\beta$ -lactamases. This group of enzymes hydrolyse the essential  $\beta$ -lactam ring (Figure 3.4), thus it prevent further reactions with PBPs.

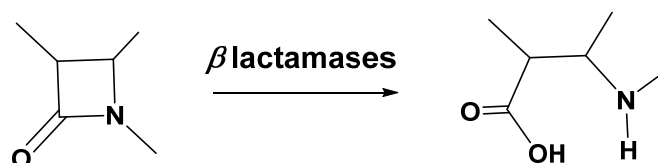


**Figure 3.4:** Enzymatic hydrolysis of the  $\beta$ -lactam ring in the penicillin

The  $\beta$ -lactamases are secreted into the periplasm in Gram-negative bacteria and to the outer medium in Gram-positive species to destroy  $\beta$ -lactam antibiotics before they can reach the PBP targets in the cytoplasmic membrane.

During the years, two main strategies have been employed to avoid the resistance caused by  $\beta$ -lactamases. The first strategy is based on alterations of the structure of the  $\beta$ -lactam core to produce new variants not recognized by the  $\beta$ -lactamases. But, it is usually only a question of time until a new mutation allows a modified  $\beta$ -lactamase to recognize and hydrolyse the new compound. The second strategy involves inhibition of the  $\beta$ -lactamases. An example is of clavulanic acid, a naturally occurring  $\beta$ -lactam that has little antibacterial activity in itself but binds the  $\beta$ -lactamases irreversibly and is used together with  $\beta$ -lactam antibiotics.

### 3.1.5 Ureidopenicillins

The ureidopenicillins<sup>7</sup> are a group of extended  $\beta$ -lactam penicillins which are generally active against gram negative bacteria such as *Pseudomonas aeruginosa*. Few examples of ureidopenicillins in clinical use are Azlocillin, Piperacillin, Mezlocillin etc. (Depicted in Figure 3.5). Generally, ureidopenicillins are derived from ampicillin or

amoxicillin. It is speculated that the extra side chain interact with the peptidoglycan chain, more effectively than ampicillin, and thus would bind more easily to the penicillin-binding proteins.<sup>8, 9</sup> Moreover, ureidopenicillins are not resistant to beta-lactamases, therefore, they are used in combination with the beta-lactamase inhibitor such as tazobactam.<sup>10</sup>

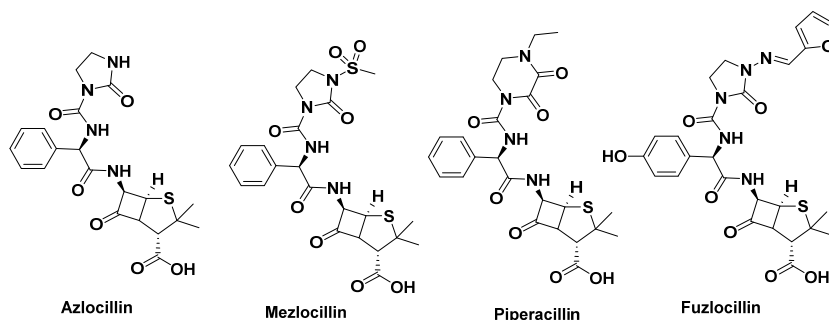


**Figure 3.5** Molecular structures of ureidopenicillins in use.

### 3.1.6 Pyrimidinones:

Derivatives of pyrimidone are the basis of many biological molecules, including, nucleobases, such as cytosine, barbiturates, such as metharbital which is used in the treatment of epilepsy.

### 3.1.7 Ureidopyrimidones:

Meijer and coworkers used ureidopyrimidones in designing of quadruple hydrogen bonded AADD or DDAA type self assembling systems (A= Hydrogen bond acceptor, D= Hydrogen bond donor).<sup>11</sup> Later, many group showed applications of ureidopyrimidones self assembly in material science, supramolecular science<sup>12</sup> and also in biomedical applications.<sup>13, 14</sup>

### 3.1.8 Tautomeric and Dimeric forms of ureidopyrimidinones

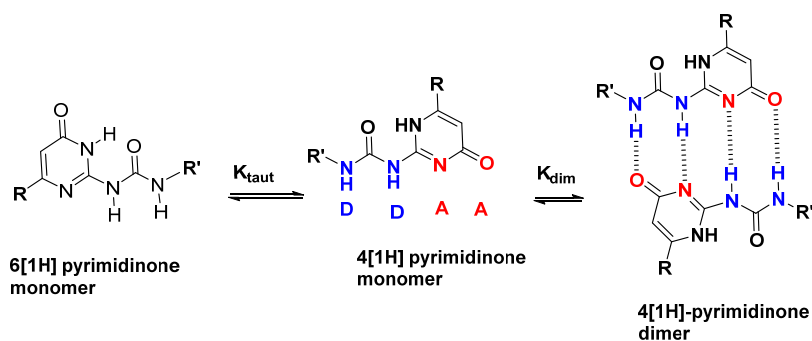


**Figure 3.6** Equilibria of the tautomeric and dimeric forms of ureidopyrimidinones

Ureidopyrimidinones are exists in the two different tautomeric forms (Figure 3.6). These tautomeric forms result in the formation of either discrete monomeric species (6[1*H*]- pyrimidinone) or dimeric species via pre-organised DDAA (4[1*H*]-pyrimidinone). G. Cooke and co-workers proved that 4[1*H*]-pyrimidinone tautomer exist in the non polar solvents such as chloroform while 6[1*H*]-pyrimidinone tautomer exist in the polar solvents such as DMSO, using NMR spectroscopy and cyclic voltammetry studies.<sup>15</sup>

### 3.1 Objective of present work

The aim of the present work is to design and synthesize ureidopyrimidone conjugated with beta lactam antibiotics such as ampicillin, amoxicillin, cephalexin etc, and also to examine the antimicrobial activity of synthesised compound.

### 3.2 Design strategy

$\beta$ -Lactam antibiotics are among the most frequently used antibiotics for the treatment of bacterial infections. The designing of extended beta lactam antibiotics is of interest because they binds more effectively to PBP as compared to ampicillin, therefore we designed the following acylated penicillins containg pyrimidinone conjugated to ureidopenicillins, derived from ampicillin, amoxicillin and cephalexin (Figure 3.7).

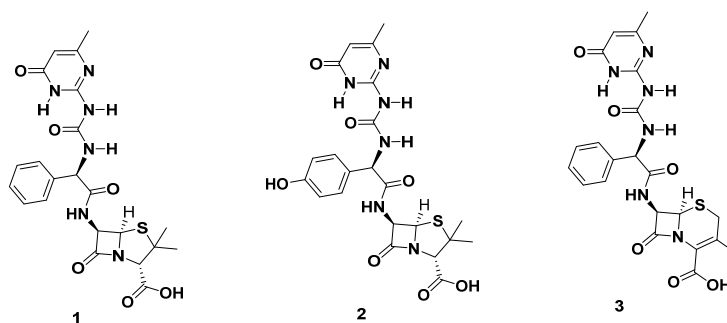
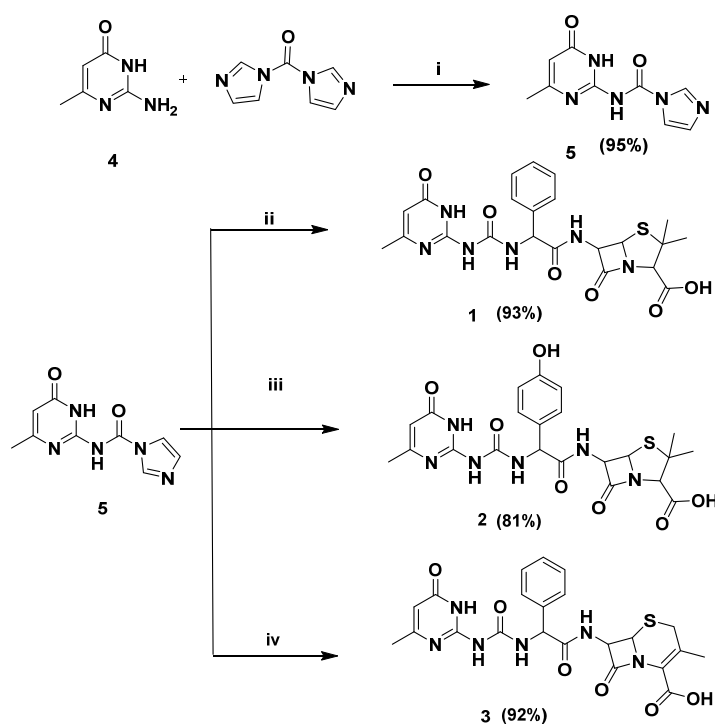


**Figure 3.7** Designed pyrimidinone ureidopenicillins.

### 3.4 Synthesis

The synthesis of the designed ureidopenicillins was started with the coupling of 2-amino-6-methylpyrimidin-4(3*H*)-one and carbonyldiimidazole to form CDI coupled compound **5**. This intermediate compound **5** was used for next reaction with ampicillin, amoxicillin and cephalexin respectively, to get the desired conjugated product.

Scheme 3.1: Synthetic scheme for ureidopenicillins



**Reagents and conditions:**(i) DMSO, 60°C, 2h; (ii) DIEA, DMF, RT, 2h; (iii) DIEA, drops of water, DMF, RT, 2h.

### 3.5 Result and Discussion

#### 3.5 a) Duplex Formation

Ureidopyrimidones are well known for the duplex formation in the non polar solvents. Here, the designed pyrimidinone ureidopenicillin were also shown to have their self assembled duplex form which was confirmed from the  $[2M+1]$  in the ESI HRMS (Figure 3.8).

AK-501 #94 RT: 0.42 AV: 1 NL: 6.49E8  
T: FTMS + p ESI Full ms [100.00-1500.00]

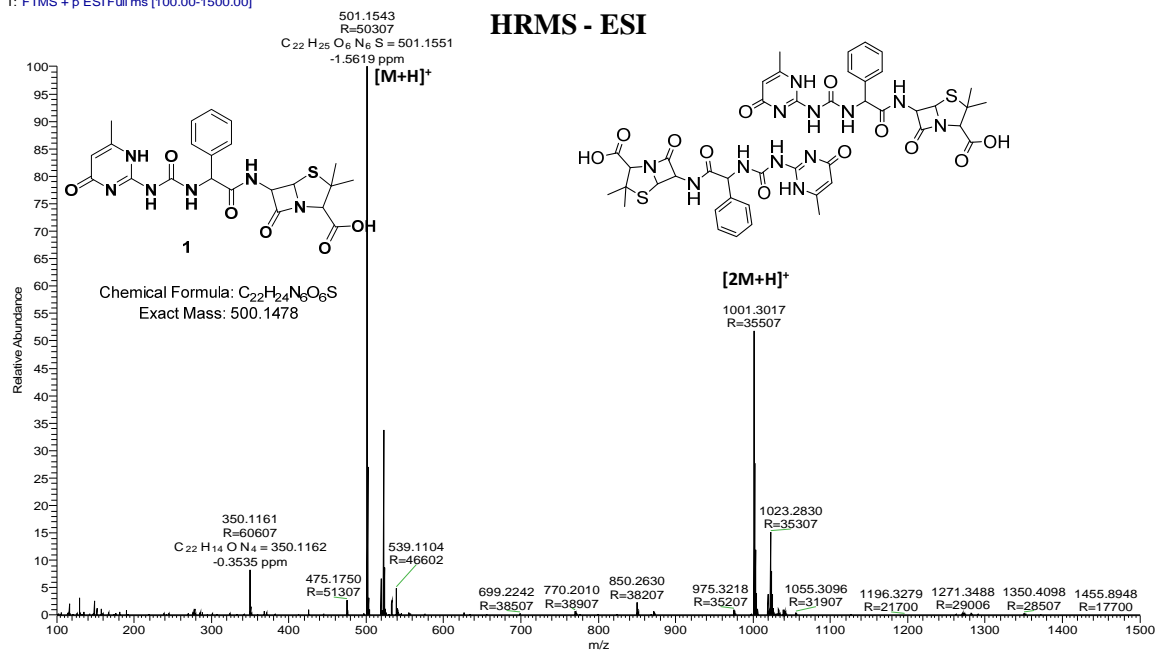


**Figure 3.8** HRMS of monomeric form and dimeric form of ureidopyrimidinones containing the ampicillin.

### 3.5b) 6[1H] pyrimidone monomeric form in polar solvent:

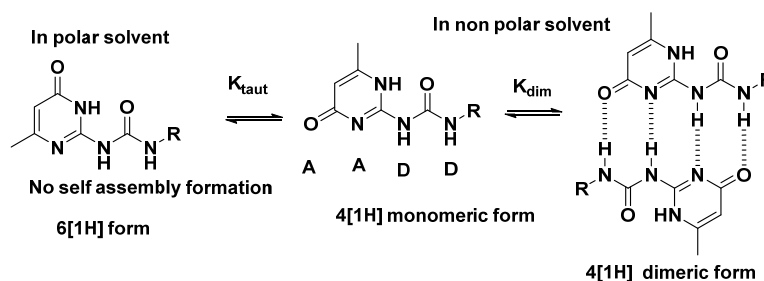


**Figure 3.9** The tautomeric form and dimeric form of ureidopyrimidinones containing the penicillins.<sup>15</sup>

In polar solvents such as DMSO, this system is present in the 6[1H] monomeric form<sup>15</sup> (Figure 3.9), since DMSO solvent is hydrogen bond breaker. Therefore, the synthesized compounds **1-3** are present in the 6[1H] monomeric form in DMSO-*d*<sub>6</sub>, which also confirmed from the broad signals of NH's in the amide region of <sup>1</sup>H NMR spectra.

### 3.6 Antibacterial studies

All the three ureidopenicillin analogs **1-3** synthesized were tested against gram positive bacteria such as *Staphylococcus aureus* and *Bacillus subtilis* as well as gram negative bacteria such as *Escherichia coli* and *Pseudomonas aeruginosa*. The IC<sub>50</sub> and MIC values in µg/mL (for screening all compounds were taken in DMSO) of each synthetic and parent analogs were shown in Table 3.1. All the synthesized ureidopenicillin analogues showed equipotent antibacterial activity as compared to their parent penicillins.

**Table 3.1** The values of IC<sub>50</sub> and MIC (µg/mL) of synthetic and parent analogs.

	<b>S. aureus</b>		<b>Bacillus subtilis</b>		<b>E. coli</b>		<b>P. aeruginosa</b>	
	<b>IC<sub>50</sub></b>	<b>MIC</b>	<b>IC<sub>50</sub></b>	<b>MIC</b>	<b>IC<sub>50</sub></b>	<b>MIC</b>	<b>IC<sub>50</sub></b>	<b>MIC</b>
<b>Compound 1</b>	0.161	0.283	0.185	0.581	5.45	10.01	>10	>10
<b>Compound 2</b>	0.224	0.615	0.215	0.948	6.25	>10	9.31	>10
<b>Compound 3</b>	0.283	3.484	0.229	3.56	>10	>10	>10	>10
<b>Ampicillin</b>	0.156	0.288	0.156	0.288	0.224	0.884	>10	>10
<b>Amoxicillin</b>	0.156	0.298	0.156	0.322	0.156	0.322	>10	>10
<b>Cefalexin</b>	0.77	2.399	0.254	1.876	3.684	4.945	>10	>10

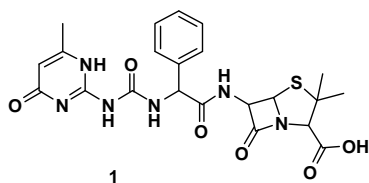
### 3.7 Conclusions

The novel uridopenicillins i.e. pyrimidone conjugated with penicillins such as ampicillin, amoxicillin and cephalixin were successfully synthesized. All synthetic ureidopenicillin analogues showed equipotent antibacterial activity with parent penicillins against tested bacteria.

### 3.8 Experimental Section

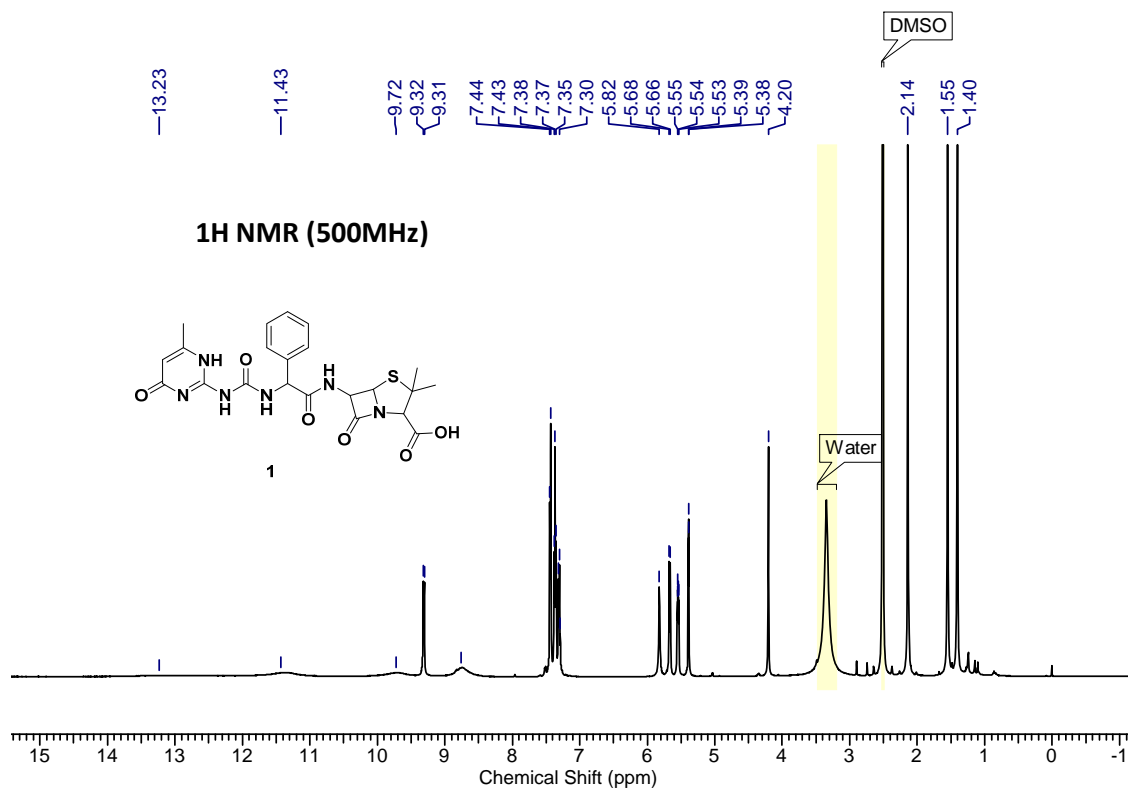
Compounds **5** was synthesized as per the reported procedure.<sup>16</sup>

**Compound 1:** To a solution of Ampicillin (0.239 g, 0.593 mmol, 1.3 equiv.) in DMF, DIEA (0.24 ml, 1.36 mmol, 3 equiv.) was added and reaction mixture was stirred for 5

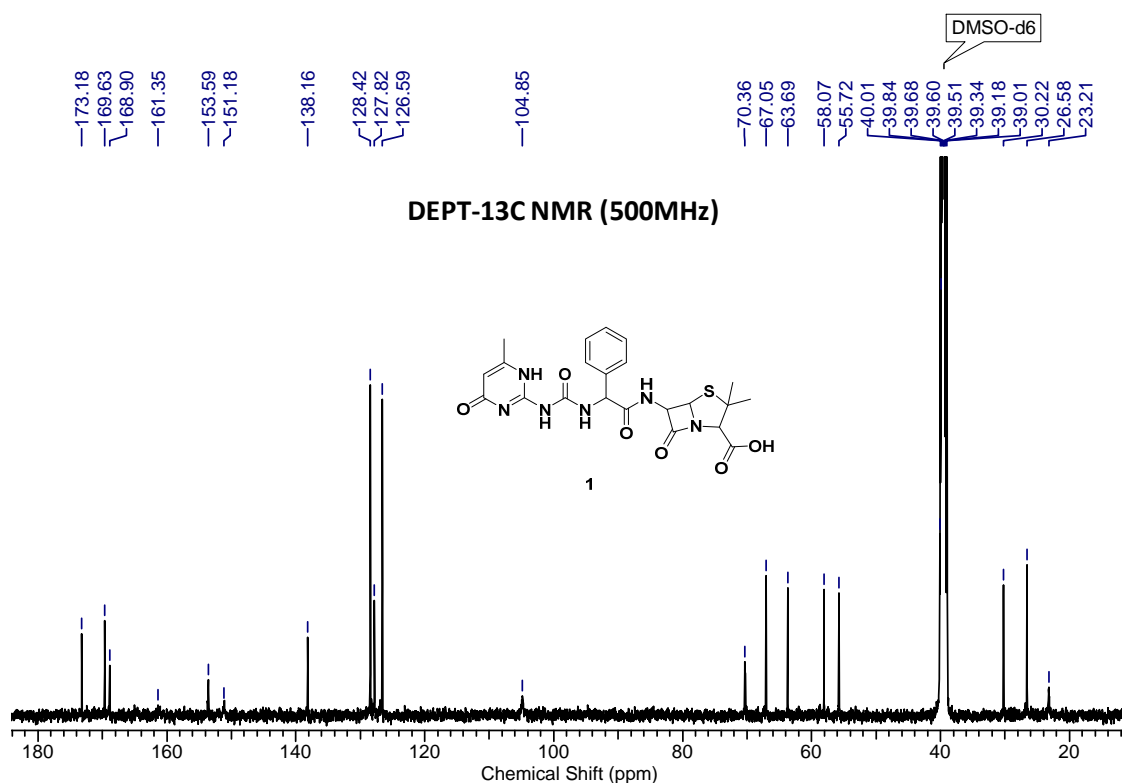


min at room temperature, followed by addition of dry **5** (0.1 g, 0.456 mmol, 1. equiv.). After stirring the reaction mixture for 2 h, it was poured into cold water which was slightly acidified by formic acid. The precipitated product was filtered under suction and washed with plenty of water and later kept in P<sub>2</sub>O<sub>5</sub> containing desiccator for vacuum drying. This yielded the pure product **1** (0.2 g, 93%) as white solid, mp: 92-94 °C; IR (Nujol)  $\nu$  (cm<sup>-1</sup>): 3338.76, 3207.87, 1774.35, 1660.90, 1517.43, 1308, 1221.61; <sup>1</sup>H NMR (500MHz, DMSO-d<sub>6</sub>)  $\delta$  = 13.12 (bs, 1 H), 11.43 (bs, 1 H), 9.27 (bs, 1 H), 9.31 (d,  $J$  = 7.6 Hz, 1 H), 8.76 (bs, 1 H), 7.44 (d,  $J$  = 7.6 Hz, 2 H), 7.37 (t,  $J$  = 7.4 Hz, 2 H), 7.30 (t,  $J$  = 7.25 Hz 1 H), 5.82 (bs, 1 H), 5.67 (d,  $J$  = 8.0 Hz, 1 H), 5.54 (dd,  $J$  = 3.8, 7.6 Hz, 1 H), 5.39 (d,  $J$  = 3.8 Hz, 1 H), 4.20 (s, 1 H), 2.14 (s, 3 H), 1.55 (s, 3 H), 1.40 (s, 3 H); <sup>13</sup>C NMR (125MHz, DMSO-d<sub>6</sub>)  $\delta$  = 173.2, 169.7, 168.9, 161.3, 153.7, 151.2, 138.2, 128.4, 127.8, 126.6, 104.7, 70.3, 67.0, 63.7, 58.1, 55.7, 30.2, 26.6, 23.2; HRMS (ESI) calculated [M+H]<sup>+</sup> for C<sub>22</sub>H<sub>25</sub>N<sub>6</sub>O<sub>6</sub>S: 501.1478, found 501.15438, calculated [2M+H]<sup>+</sup> for C<sub>44</sub>H<sub>49</sub>N<sub>12</sub>O<sub>12</sub>S<sub>2</sub>: 1001.2956 found 1001.3017.

a)



b)



c)

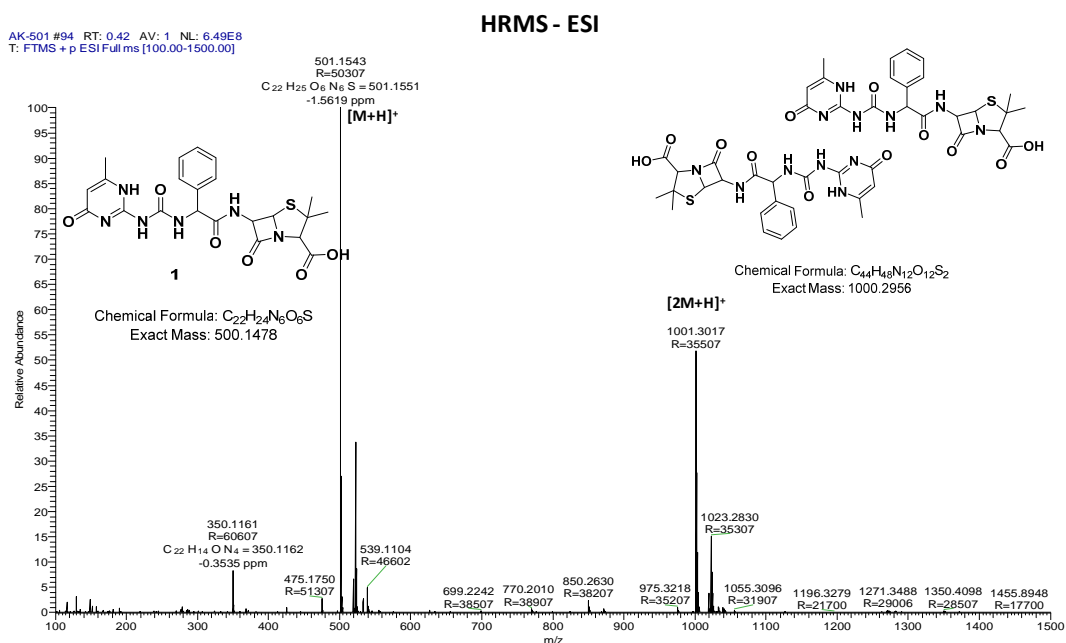
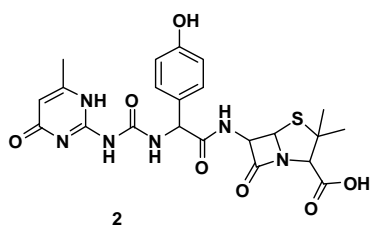


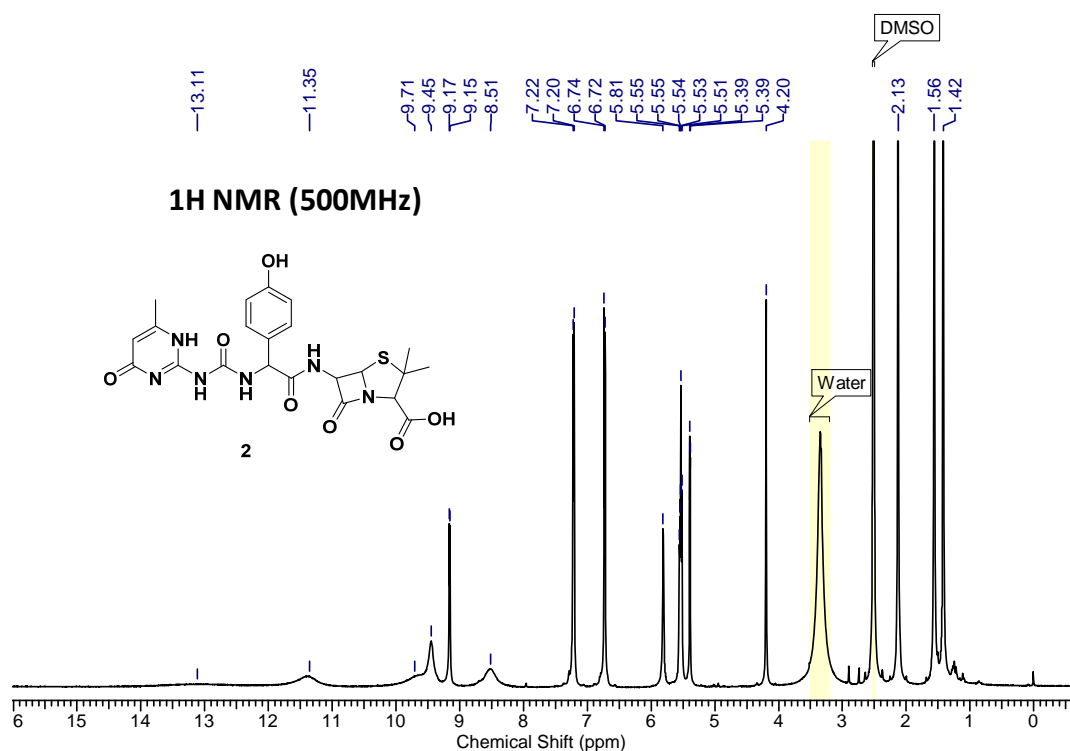
Figure 3.10 a)  $^1H$ , b)  $^{13}C$  and c) HRMS spectra of **1**



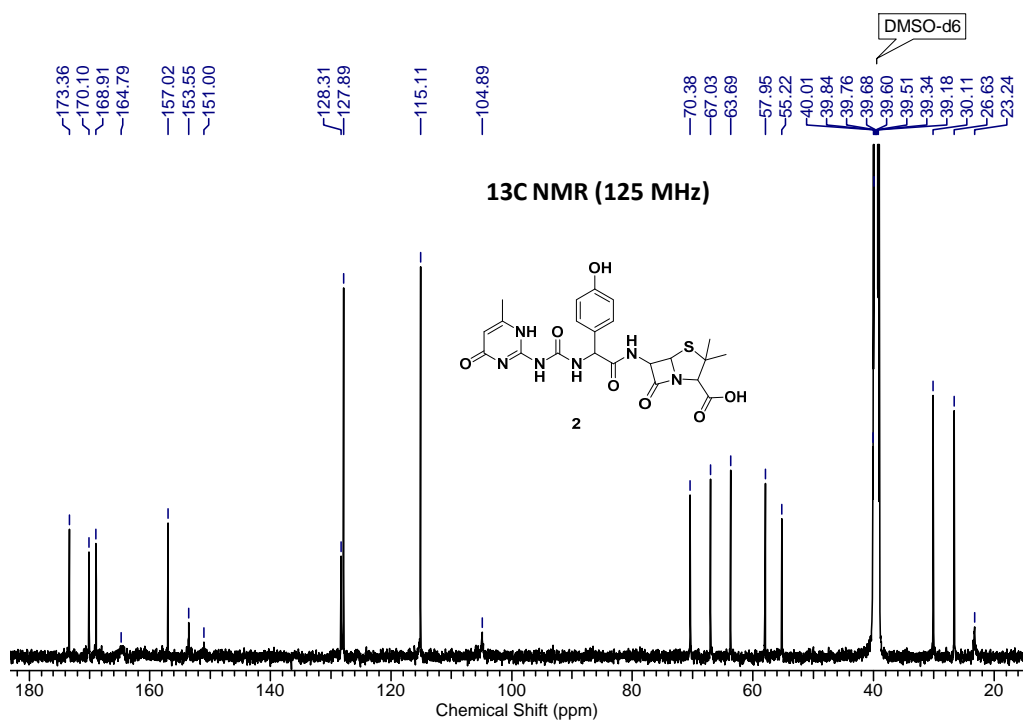


**Compound 2:** Following the procedure for synthesis of compound **1** and using Amoxicillin (0.433 g, 1.23 mmol, 1.3 equiv.), compound **2** was synthesized (0.365 g, 81%) as a white solid; mp 194-196 °C; IR (Nujol)  $\nu$  (cm<sup>-1</sup>): 3350, 3182.68, 2728.25, 1769.45, 1657.27, 1513.24, 1229.90, 1041.66; <sup>1</sup>H NMR (500 MHz, DMSO-d<sub>6</sub>)  $\delta$  = 13.11 (bs, 1 H), 11.35 (bs, 1 H), 9.71 (bs, 1 H), 9.45 (bs, 1 H), 9.16 (d,  $J$  = 7.6 Hz, 1 H), 8.51 (bs, 1 H), 7.21 (d,  $J$  = 8.4 Hz, 2 H), 6.73 (d,  $J$  = 8.4 Hz, 2 H), 5.81 (bs, 1 H), 5.57 - 5.49 (m, 2 H), 5.39 (d,  $J$  = 3.8 Hz, 1 H), 4.20 (s, 1 H), 2.13 (s, 3 H), 1.56 (s, 3 H), 1.42 (s, 3 H); <sup>13</sup>C NMR (125MHz, DMSO-d<sub>6</sub>)  $\delta$  = 173.4, 170.1, 168.9, 164.5, 160.8, 157.0, 153.5, 150.9, 128.3, 127.9, 115.1, 104.9, 70.4, 67.0, 63.7, 58.0, 55.2, 30.1, 26.6, 23.2; HRMS (ESI) calculated [M+H]<sup>+</sup> for C<sub>22</sub>H<sub>25</sub>N<sub>6</sub>O<sub>7</sub>S: 517.1427, found 517.1500, calculated [2M+H]<sup>+</sup> for C<sub>44</sub>H<sub>49</sub>N<sub>12</sub>O<sub>14</sub>S<sub>2</sub>: 1033.2854 found 1033.2931.

a)



b)



c)

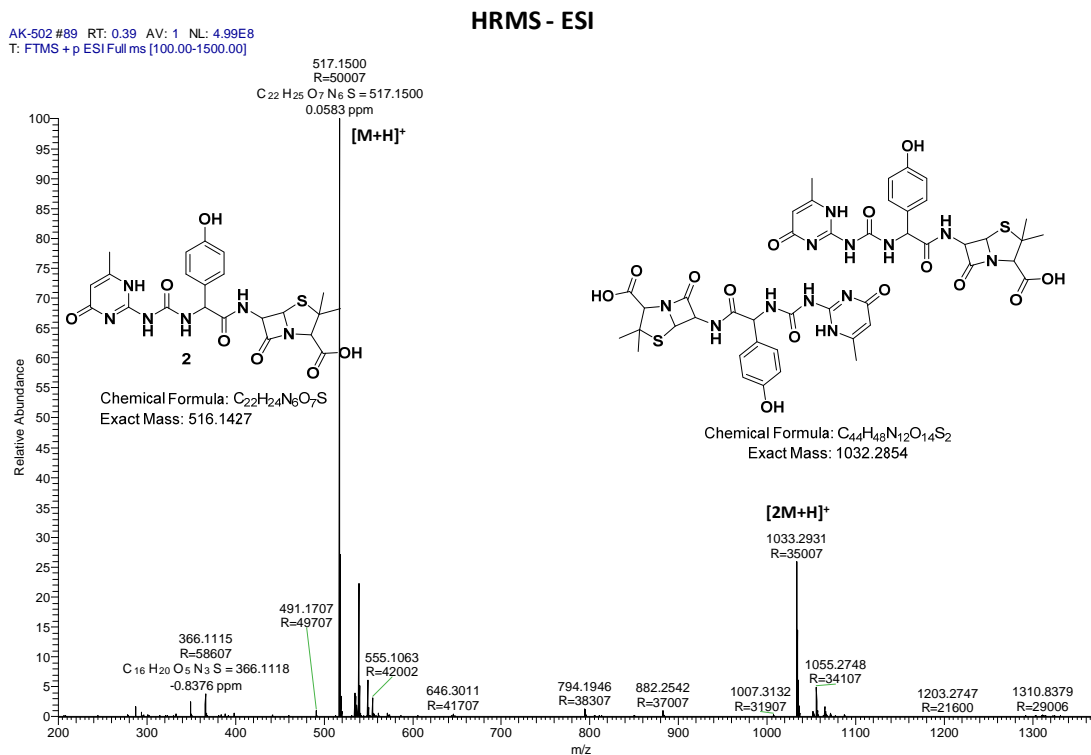
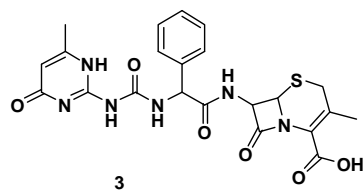


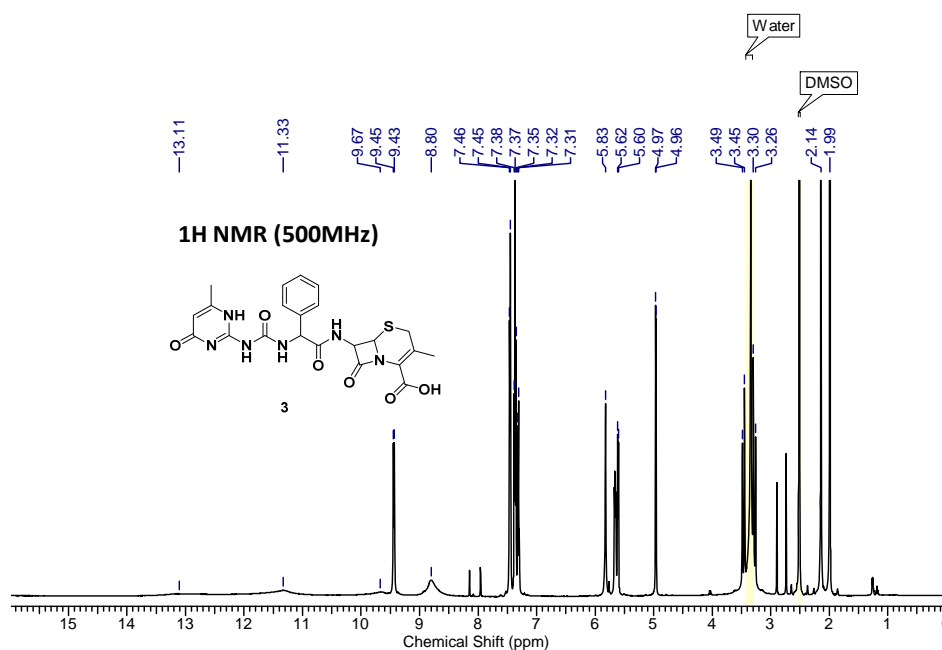
Figure 3.11 a) <sup>1</sup>H, b) <sup>13</sup>C and c) HRMS spectra of 1

**Compound 3:** To a solution of Cefalexin (0.412 g, 1.18 mmol, 1.3 equiv.) in DMF, at room temperature, DIEA (0.47 ml, 2.74 mmol, 3 equiv.) and few drops of water (for making clear solution) were added and reaction mixture was stirred for 5 min at 0°C, then to this reaction mixture compound **5** (0.2 g, 0.913 mmol, 1. equiv.) was added. After stirring the reaction for 2

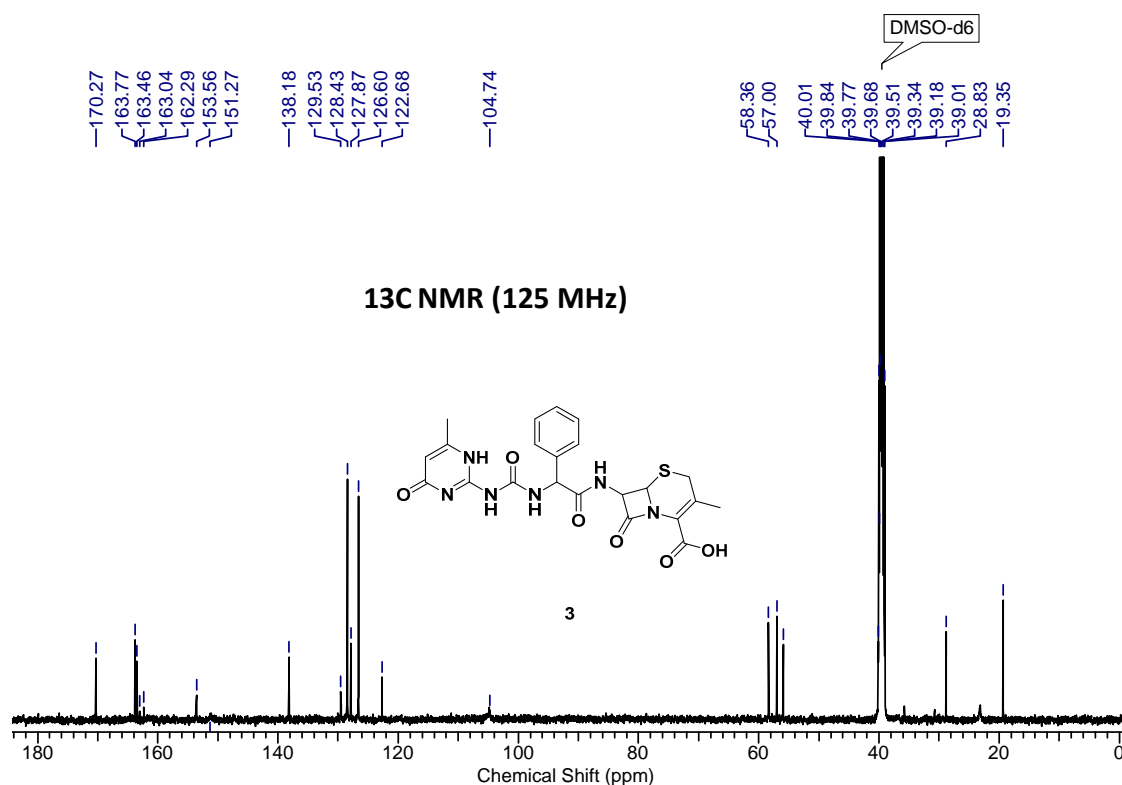


h, it was poured in cold water which was slightly acidified by formic acid, and the product was precipitated out. This precipitate was filtered using suction pump and washed with plenty of water and later kept in P<sub>2</sub>O<sub>5</sub> containing desiccator for vacuum drying. This gave pure product **3** (0.42 g, 92%) as a white solid; mp 198-200 °C; IR (Nujol)  $\nu$  (cm<sup>-1</sup>): 3368, 3267.13, 3179.13, 2724.81 1765.44, 1658.76, 961.79; <sup>1</sup>H NMR (500MHz, DMSO-d<sub>6</sub>)  $\delta$  = 13.08 (bs, 1 H), 11.35 (bs, 1 H), 9.67 (bs, 1 H), 9.44 (d,  $J$  = 8.4 Hz, 1 H), 8.80 (bs, 1 H), 7.46 (d,  $J$  = 7.6 Hz, 2 H), 7.37 (t,  $J$  = 7.4 Hz, 2 H), 7.31 (t,  $J$  = 7.25 Hz 1 H), 5.83 (s, 1 H), 5.66 (dd,  $J$  = 4.8, 7.8 Hz, 1 H), 5.61 (d,  $J$  = 7.6 Hz, 1 H), 4.96 (d,  $J$  = 4.6 Hz, 1 H), 3.47 (d,  $J$  = 18.3 Hz, 1 H), 3.28 (d,  $J$  = 18.3 Hz, 1 H), 2.14 (s, 3 H), 1.99 (s, 3 H); <sup>13</sup>C NMR (125MHz, DMSO-d<sub>6</sub>)  $\delta$ : 170.8, 164.3, 163.9, 163.5, 162.8, 154.1, 151.6, 138.7, 130.0, 128.9, 128.4, 127.1, 123.2, 105.3, 58.8, 57.5, 56.4, 29.3, 23.7, 19.8; HRMS (ESI) calculated [M+H]<sup>+</sup> for C<sub>22</sub>H<sub>23</sub>N<sub>6</sub>O<sub>6</sub>S: 499.1322, found 499.1398, calculated [2M+H]<sup>+</sup> for C<sub>44</sub>H<sub>45</sub>N<sub>12</sub>O<sub>12</sub>S<sub>2</sub>: 997.2643 found 997.2726.

a)



b)



c)

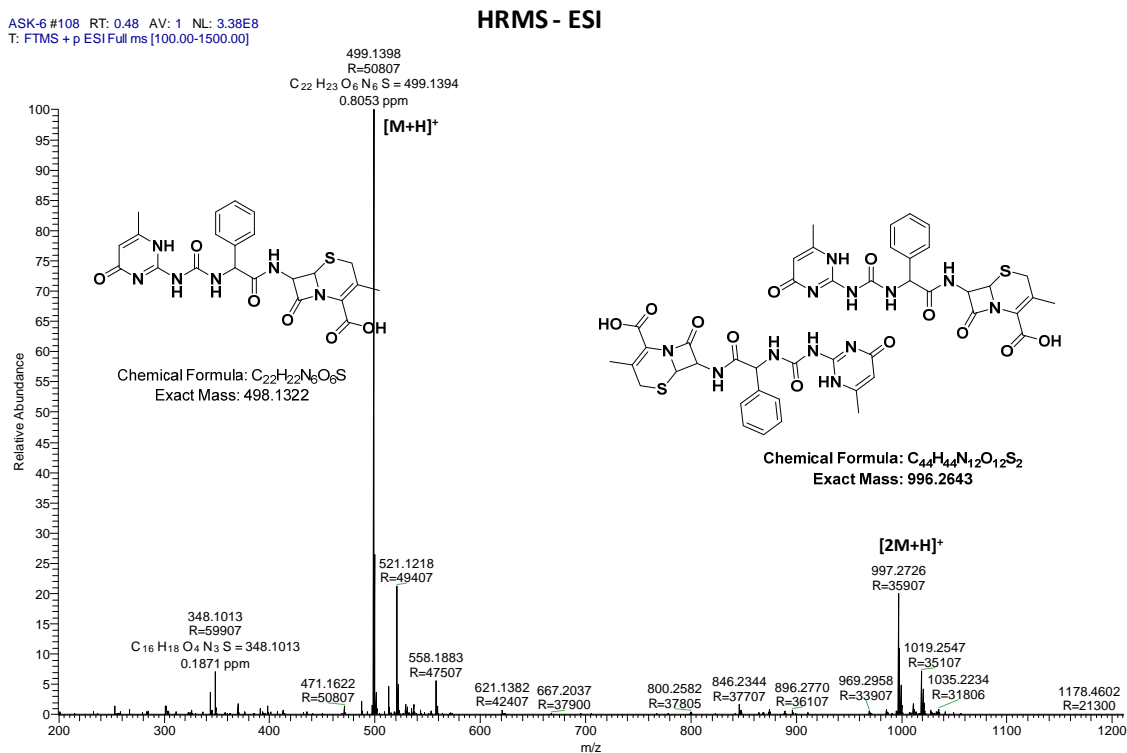
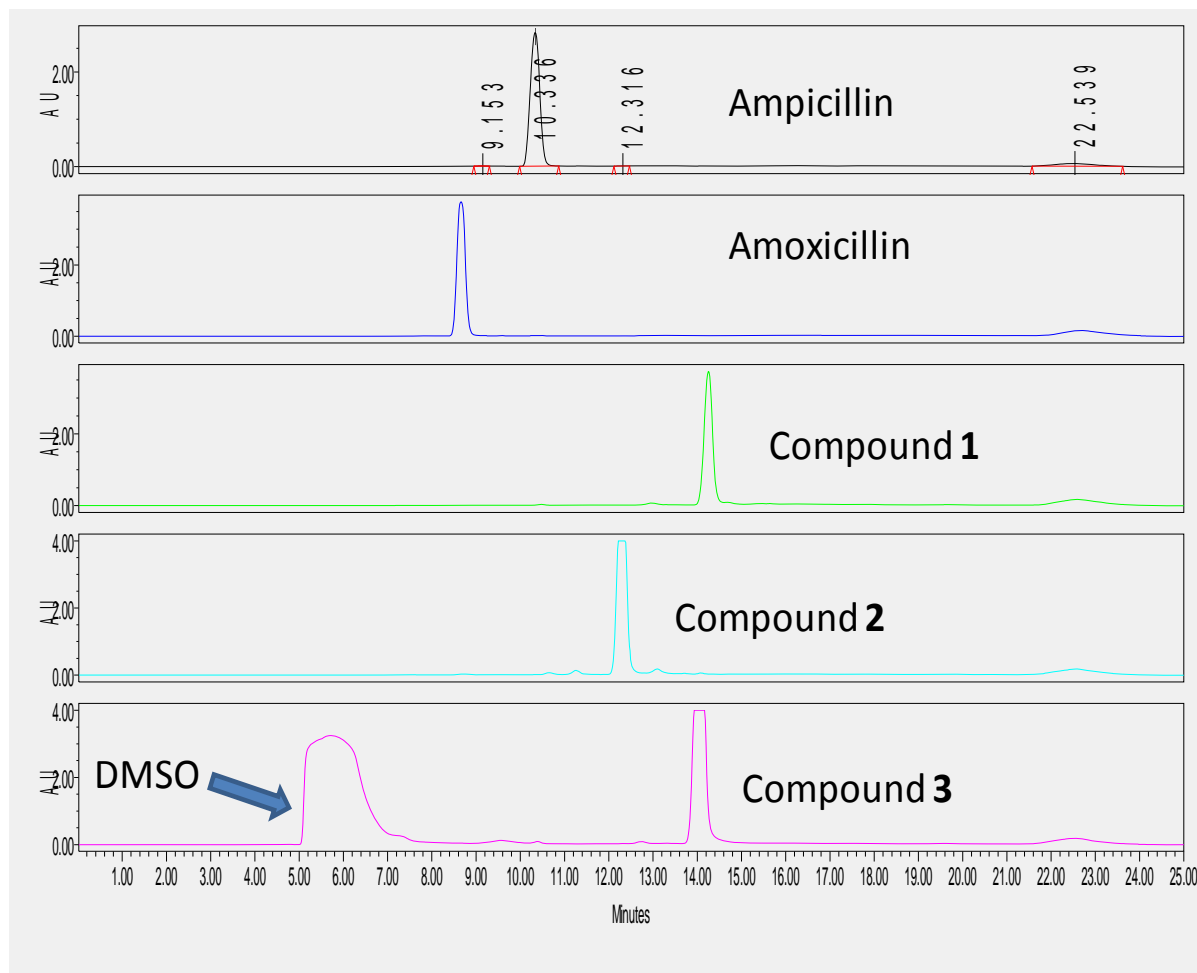


Figure 3.12 a) <sup>1</sup>H, b) <sup>13</sup>C and c) HRMS spectra of 1

**HPLC Data:**

Purity was examined using reverse phase HPLC (Figure 3.13) using DELTA PAK column, SB-C18, 300 \* 3.9 mm, specially used for penicillin like structures, Mobile phase A=0.025 M KH<sub>2</sub>PO<sub>4</sub> in water (pH=3), B= acetonitrile. Injection volume 5 μL, Flow rate 1 mL/min, Gradient of 5% to 65% of B in 25 min. UV detector 214 nm wavelength.



**Figure 3.13** stacked plots of HPLC spectra of compounds **1-3** and standard compound ampicillin and amoxicillin (taken in methanol/ water). Note-Compound **3** was taken in DMSO solvent; hence the highlighted peak is from DMSO.

### 3.9 References and Notes:

1. A. Fleming, *Brit. J. Exp. Pathol.*, 1929, **10**, 226.
2. A. Dalhoff, N. Janjic, R. Echols, "Redefining penems". *Biochemical Pharmacology*. 2006, **71** (7), 1085.
3. A. Matagne, A. Dubus, M. Galleni, J.-M. Frere, 1999, *Nat. Prod. Rep.* **16**, 1.
4. M.R. Salton, K. S. Kim Baron S, Structure. In: *Baron's Medical Microbiology*, 1996.
5. E. P. Abraham, E. B. Chain, 1940, *Nature* **146**, 837.
6. C. Walsh, 2000, *Nature*, **406**, 775.
7. a) G. M Eliopoulos, R. C. Moellering Jr., *Ann Intern Med.*, 1982, **97**(5), 755. b) G. L. Drusano, S. C. Schimpff, W. L. Hewitt, *Rev Infect Dis.*, 1984, **6** (1), 13.
8. L. VERBIST *Antimicrob Agents Chemother.*, 1979, **16**(2), 115.
9. K. Kong, L. Schneper and K. Mathee, *APMIS*, 2009, **118**, 1–36.
10. Y. Yang, B. A. Rasmussen, D. M. Shlaes, *Pharmacol Ther*, 1999, **83**, 141.
11. F. H. Beijer, R. P. Sijbesma, H. Kooijman, A. L. Spek and E. W. Meijer, *J. Am. Chem. Soc.*, 1998, **120**, 6761.
12. B. J. B. Folmer, R. P. Sijbesma, H. Kooijman, A. L. Spek, E. W. Meijer, *J. Am. Chem. Soc.* 1999, **121**, 9001.
13. a) J. H. Ky Hirschberg, F. H. Beijer, H. A. vanAert, P. C. M. M. Magusin, R. P. Sijbesma, E. W. Meijer, *Macromolecules* 1999, **32**, 2696; b) B. J. B. Folmer, R. P. Sijbesma, R. M. Versteegen, J. A. J. vander Rijt, E.W. Meijer, *Adv. Mater.* 2000, **12**, 874.
14. (a) A. J. Wilson, *Soft Matter*, 2007, **3**, 409; (b) R. P. Sijbesma and E. W. Meijer, *Chem. Commun.*, 2003, **1**, 5; (c) C. Schmuck and W. Wienand, *Angew. Chem., Int. Ed.*, 2001, **40**, 4363.

- 15.** A. M. Alexander, M. Bria, G. Brunklaus, S. Caldwell, G. Cooke, J. F. Garety, S. G. Hewage, Y. Hocquel, N. McDonald, G. Rabani, G. Rosair, B. O. Smith, H. Wolfgang Spiess, V. M. Rotello and P. Woisel, *Chem. Commun.*, 2007, **22**, 2246.
- 16.** A. T. ten Cate, P. Y. W. Dankers, H. Kooijman, A. L. Spek, R. P. Sijbesma, and E. W. Meijer, *J. Am. Chem. Soc.* 2003, **125**, 6860.





## ***Chapter 3***

***Part B- Unusual three residual cyclization in the AVPI peptides.***



### 3.10 Preamble

#### 3.10.1 Apoptosis

Apoptosis is a programmed cell death that occurs in multicellular organisms to carry out the normal development and homeostasis.<sup>1</sup> Modern cancer therapies, such as radiation therapy, chemotherapy, and immune therapy work by inducing apoptosis in cancer cells.<sup>2</sup> Cancer cells resist apoptosis if the process is discontinued by any reason which lead to many human immune diseases such as autoimmune diseases, neurodegenerative disorders including cancer.<sup>3</sup> Apoptosis occurred *via* two distinct pathways namely intrinsic and extrinsic pathway (Figure 3.14). In extrinsic pathway, death ligands such as TRAIL (TNF-Related Apoptosis Inducing Ligand), TNF $\alpha$  (Tumor Necrosis Factor  $\alpha$ ), or FasL (Fas Ligand) undergo ligation with the death receptor and leads to the formation of FADD (Fas-Associated Death Domain), which later activates caspase-8 and caspase-10 (caspase: cysteine-aspartic proteases).<sup>4</sup> Finally, apoptosis is accomplished by caspase-3 and caspase-7. In intrinsic pathway, due to external factors such as radio or chemotherapy, Bcl-2 family protein such as Bax (Bcl-2 associated X protein) causes the release of cytochrome c from the mitochondria into the cytosol.<sup>5</sup> Cytochrome c then binds to Apaf-1 (Apoptotic Protease Activating Factor-1) to form the apoptosome complex, caspase-9 then induces the activation of the effectors, caspase-3 and caspase-7 to achieve apoptosis.

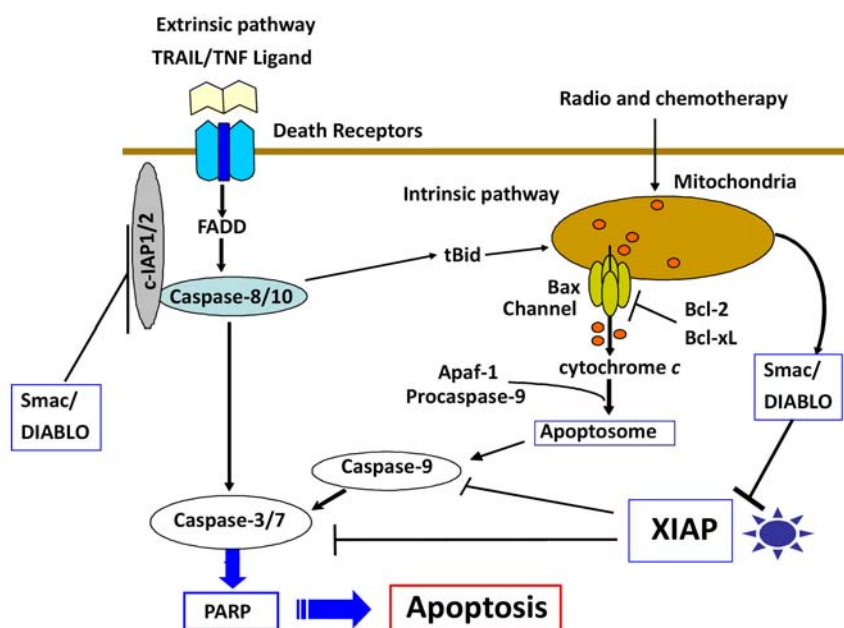


**Figure 3.14** A simplified schematic representation of apoptosis pathway.<sup>6</sup>

### **3.10.2 Inhibitor of Apoptosis Proteins (IAP)**

IAPs (Inhibitors of Apoptosis Protein) are kind of proteins which can inhibit apoptosis process particularly in cancer cells.<sup>7</sup> There are many IAPs known, some of them are listed here:

- XIAP (X-chromosome linked Inhibitor of Apoptosis Protein)
- c-IAP1 (cellular IAP 1)
- c-IAP2 (cellular IAP 2)
- Cp-IAP
- Op-IAP
- Survivin
- NAIP

Each IAP member contains three BIR (Baculovirus IAP Repeat) domains which are the important characteristic functional domain of apoptosis inhibition.<sup>8</sup> XIAP binds to the effector caspase-3 or caspase-7, with BIR2 domain and the initiator caspase-9, with its BIR3 domain.<sup>9</sup> So, these caspases remain unavailable for apoptosis and hence strategies targeting XIAP can be an useful method for reducing the resistance of cancer cells towards apoptosis.<sup>10</sup>

### **3.10.3 Smac/DIABLO**

Smac (Second Mitochondria-derived Activator of Caspase), or DIABLO (Direct IAP Binding protein with Low pI), is a protein released from mitochondria that potentiates apoptosis.<sup>11</sup> 55 Residues out of 239 residues are removed during translocation to yield active Smac. Figure 3.15, shows the terminal amino- tetrapeptide in Smac, Ala-Val-Pro-Ile (residue 56 to 59) which is homologous with the exposed terminal amino-tetrapeptide of caspase-9 (Ala-Thr-Pro-Phe). Smac binds with the BIR3 domain of XIAP and releases caspase-9 for apoptosis. It also binds with BIR2 domain and makes caspase-3 and caspase-7 accessible for apoptosis.<sup>12</sup> This tetrapeptide AVPI segment is equipotent with the Smac protein ( $K_d = 0.4 \mu\text{M}$ ). Hence, it is possible to mimic this tetrapeptide AVPI in order to get potent synthetic analogs of Smac peptides which can further enhance the bioactivity by binding to BIR2 and BIR3 domains of XIAP effectively and thus releasing caspase-9, caspase-3 and caspase-7 for the apoptosis. The structure of Smac peptide complexes with XIAP-BIR3 domain is comprehensively studied using X-ray

crystallography and NMR spectroscopy.<sup>13</sup> Figure 3.15 shows the interaction of the Smac peptide with the XIAP BIR3 domain.<sup>13a</sup>

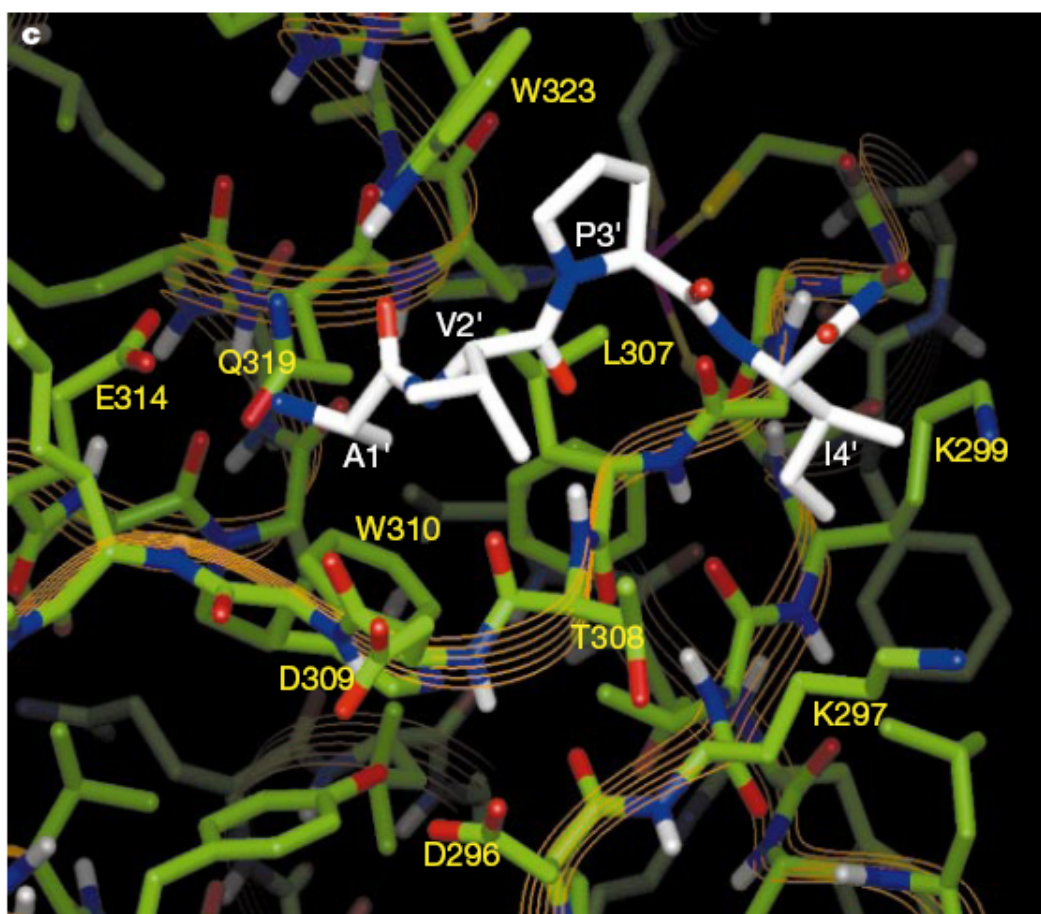


**Figure 3.15** Structure of XIAP BIR3 and Smac peptide (AVPI) complex.<sup>13a</sup>

#### 3.10.4 Structure Activity Relationship of Smac mimetics:

The structure activity relationships (SAR) of small molecular Smac mimetics have been extensively explored by many groups and the general SAR profile is shown *vide infra* in Figure 3.16.<sup>14</sup>

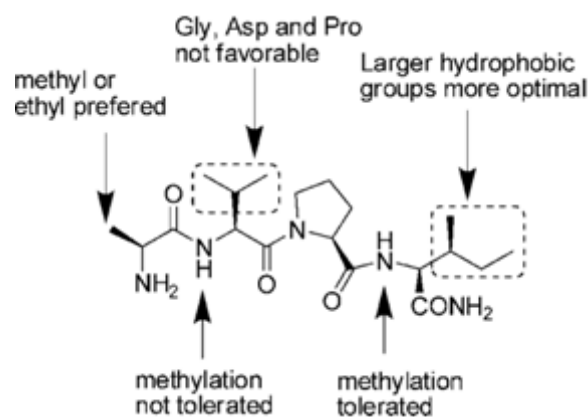
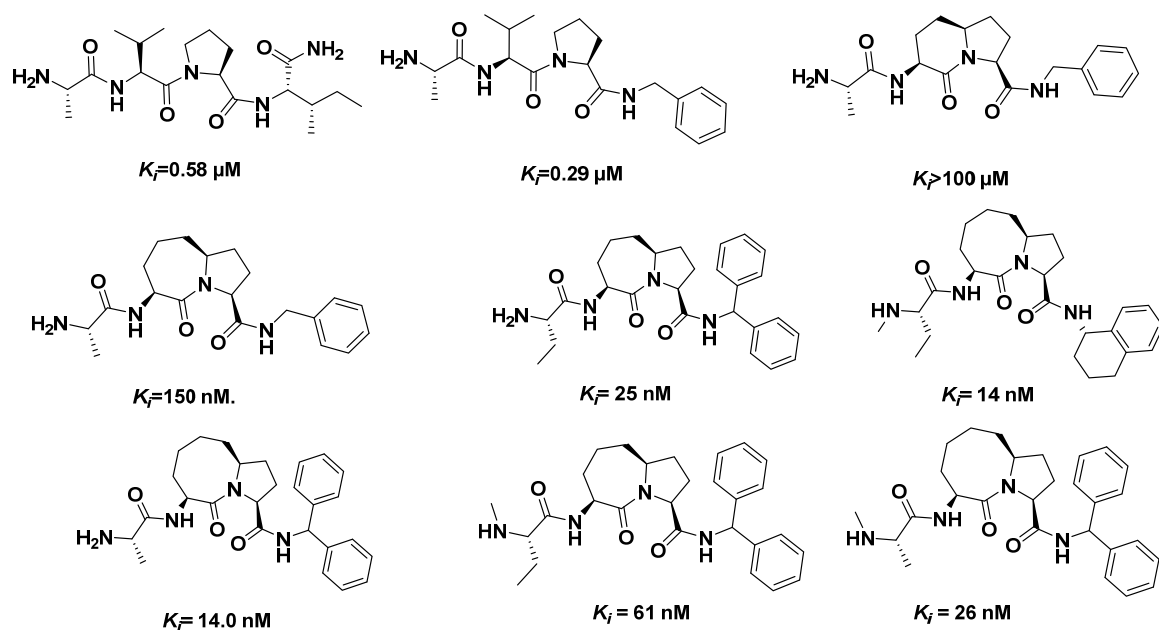


**Figure 3.16** Summary of structure-activity relationship of Smac mimetics.<sup>15</sup>

From N-terminus, it has been observed that the methyl group (Me) of Alanine residue can be replaced with ethyl (Et) but, higher alkyl groups are shown to have an adverse effect on the binding with BIR domains and activity.<sup>13-16</sup> Valine residue at second position has been replaced with many amino acids except glycine (Gly), aspartic acid (Asp) and Proline (Pro) along with some D- amino acids such as D-Ala, D-Val and D-Phe. *N*-methylation of the amide NH's at position 2 is not tolerated. Proline at position 3 is essential for the bioactivity which keep the molecule at the right conformation. Fourth placed Isoleucine (Ile) has been replaced by many other groups and it has been observed that large hydrophobic groups have been well tolerated because of the presence of large hydrophobic pocket formed by lysine 297 and lysine 299 of the XIAP BIR3 domain. These structural studies have helped many researchers to design diverse class of Smac mimetics with improved efficacy.<sup>17</sup>

### 3.10.5 Smac mimetics and their binding affinities to XIAP protein:

The Wang group from the University of Michigan was first to report the design and binding activity of conformationally constrained Smac mimetics.<sup>18</sup> Figure 3.17 shows the different Smac analogs with their binding affinity ( $K_i$ , competitive inhibition constant) towards XIAP BIR3.<sup>18, 19</sup> Note, lesser the  $K_i$  value more the binding with XIAP BIR3 and more active compound.



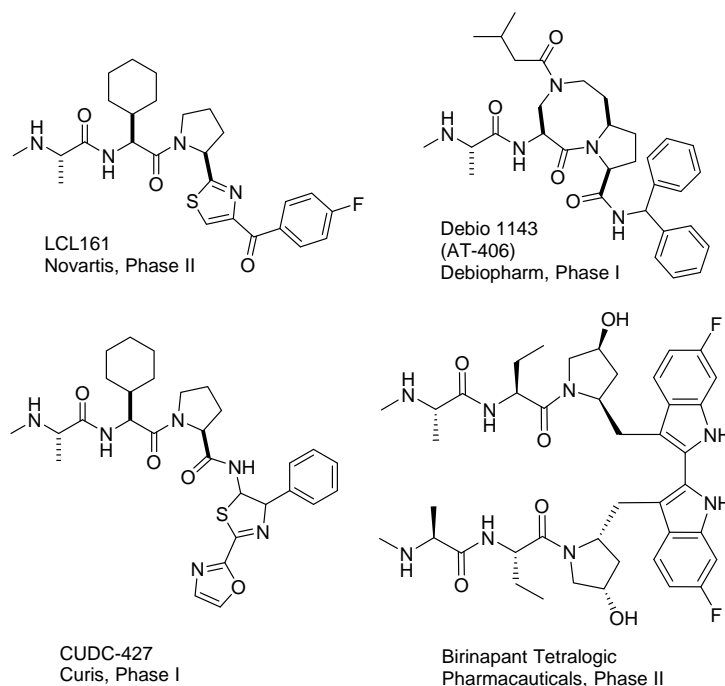
**Figure 3.17** Conformationally constrained Smac mimetics; Val and Pro residues have been fused together to form reverse turn like structures which are several fold active than the Smac tetrapeptide.<sup>18,19</sup>

Figure 3.17 also shows the structure of highly active Smac mimetics containing fused bicyclic ring system. It has been observed that with increasing the ring size of the fused ring system, there is an increase in the binding affinity and hence there is a constant decrease in the competitive inhibition constant  $K_i$  value. ( $K_i = 150$  nM to 14 nM). The increase in the size of the hydrophobic group at the C-terminus have a favorable effect on the binding affinity of the Smac mimetics.<sup>19</sup>

Many studies showed that Smac mimetics inhibits cell growth and help in inducing apoptosis in cancer cells.<sup>20, 21</sup> These Smac mimetics were found active against various cancer cells which include breast cancer cell lines BT-549 and MDA-MB-231, leukemia cell line HL-60, melanoma cell line SK-MEL-5, renal cancer cell line RXF-393, ovarian cancer cell line SK-OV-3, and non-small-cell lung cancer cell lines NCI-H23 and NCI-H522.

### 3.10.6 Examples of Smac mimetics which are in clinical trials

Structures of some of the Smac mimetics are depicted in Figure 3.18.



**Figure 3.18** Examples of IAP antagonists in clinical development.<sup>20</sup>

### 3.11 Objective of the present work

Objective of this part of the thesis is synthesis of cyclic AVPI or cyclic Smac mimetics, and also to find out the correct mode of cyclization (Figure 3.19), whether it is forming cyclic compound A (three residual 9 member unusual cyclization) or compound B (four residual 12 member cyclization).

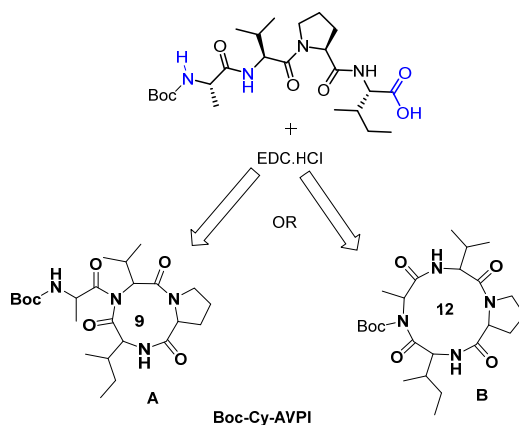


**Figure 3.19** Reaction of Boc-AVPI-OH with EDC.HCl, producing cyclic AVPI either 9 member or 12 member cyclic system.



### 3.12 Design and strategy

The unusual cyclization in the AVPI peptides and synthesis of new cyclic AVPI analogues have been investigated to generalize the unusual cyclization. For cyclization, the C-terminus was made free acid and the N-terminus was protected either with Boc or Cbz protecting group, and was subjected for cyclization in the presence of EDC. HCl. The cyclic tetra peptide with *N*-Methylated alanine (Boc NMe Cy-AVPI) and cyclic tri peptide (Boc-Cy VPI), strongly suggest that the A ring products (cyclic nine member ring compounds) were forming exclusively. The molecular structures of the designed cyclic AVPI peptide analogues are depicted in Figure 3.20. The structures of three residual cyclic products were also investigated by using 2D NMR spectra (Figures 3.31 to 3.34).

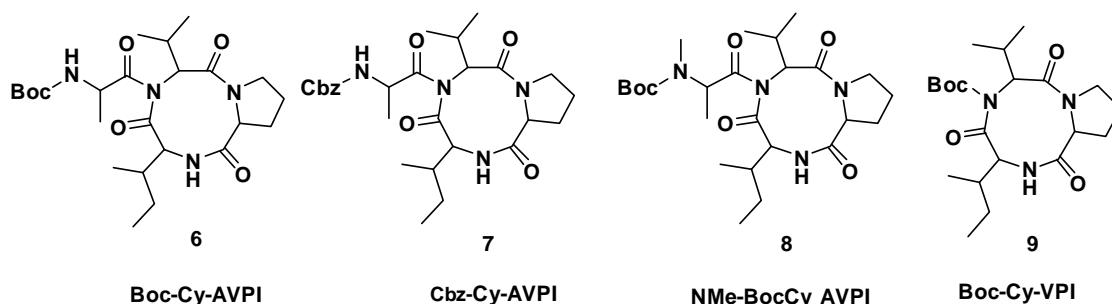
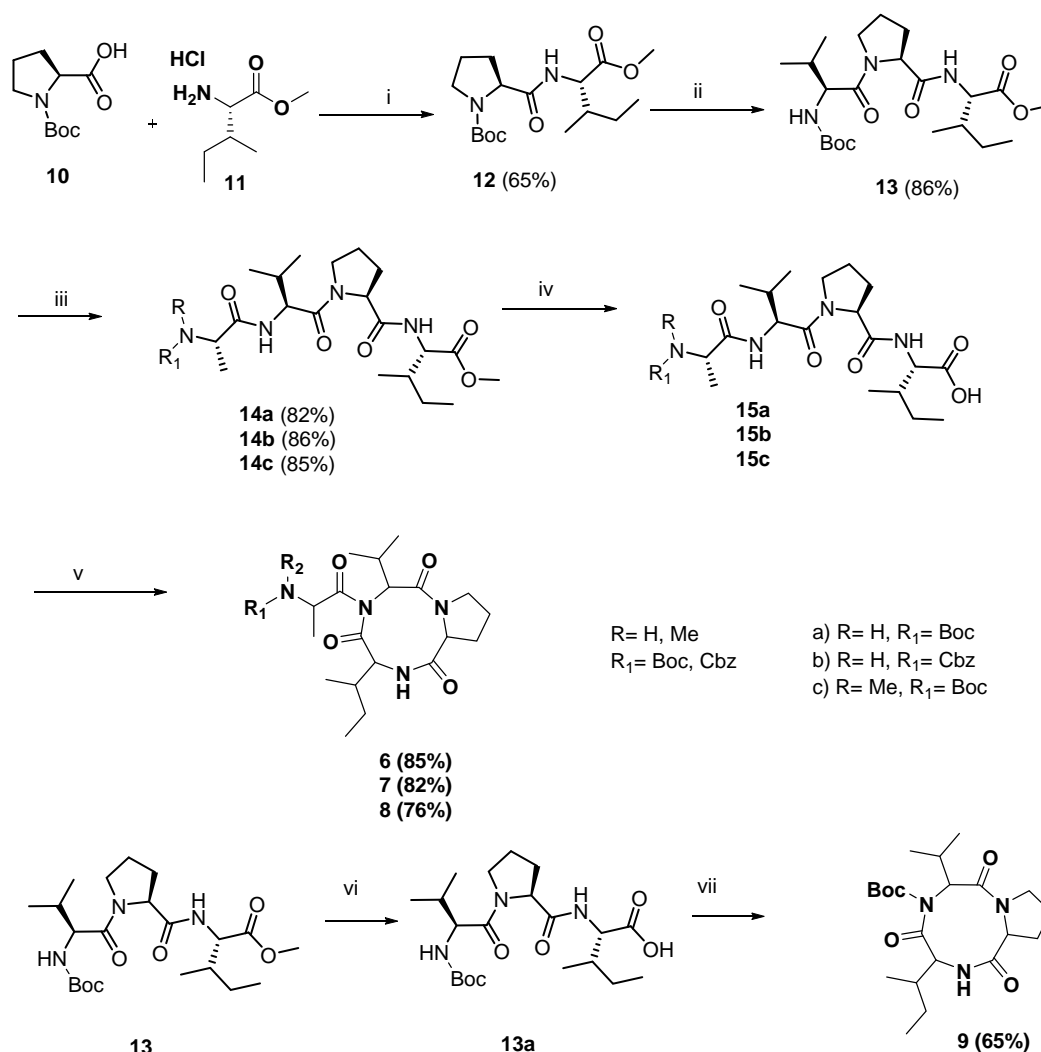


**Figure 3.20** Designed analogues of cyclic AVPI peptides.

### 3.13 Syntheses

The cyclic tetrapeptide AVPI analogues were synthesized in the solution phase using Boc peptide coupling strategy. The synthesis is shown in Scheme 3.2. Boc-<sup>L</sup>Pro-OH was coupled with HCl.H-<sup>L</sup>Ile-OMe using HBTU, to give the dipeptide **12**, which was converted to tripeptide **13** by deprotecting the Boc group of **12** and coupling with Boc-<sup>L</sup>Val-OH. Using similar reaction sequences, tripeptide was converted to tetrapeptide **15** using different protected alanine. These tetra peptides on hydrolysis and reaction with EDC.HCl yielded the cyclic tetra peptides. Similarly, cyclic tri peptide Val-Pro-Ile was synthesized from linear tri peptide **13**, which showed occurrence of an unusual cyclization in the three residues in which NH of Val residue and free acid of Ile residue taking part in the cyclization.

Scheme 3.2: Synthesis of cyclic AVPI analogues.



**Reagents and conditions:** (i) TBTU, HOBt, DIEA, ACN, rt, 8 h; (ii) (a) TFA, DCM, rt, 30 min; (b) Boc-L-Val-OH, HBTU, HOBt, DIEA, ACN, rt, 8 h; (iii) (a) TFA, DCM, rt, 30 min; (b) Boc-L-Ala-OH, HBTU, DIEA, DCM, rt, 8 h; (iv) LiOH.H<sub>2</sub>O, aq. MeOH rt; (v) EDC.HCl, DCM, 8h. (vi) LiOH.H<sub>2</sub>O, aq. MeOH rt; (vii) EDC.HCl, DCM, 8h.

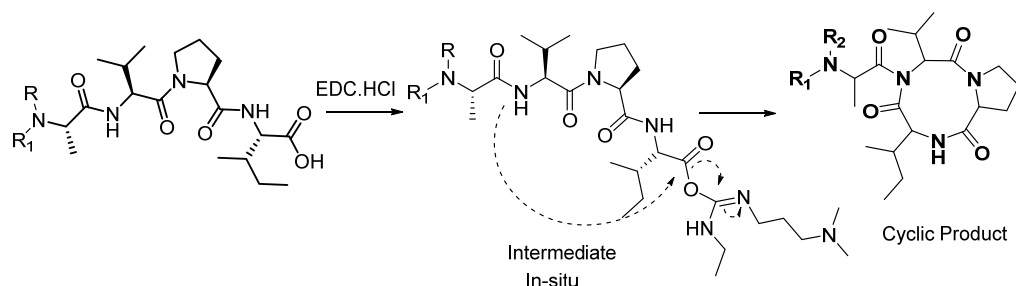


Figure 3.21 Possible reaction path for unusual cyclization

The reaction of N terminal protected AVPI-OH with EDC. HCl, forms an active ester with 1-Ethyl-3-(3-dimethylaminopropyl) carbodiimide which undergo amide bond formation with NH of Val residue leading to formation of a bisacylated cyclic product (Figure 3.21).

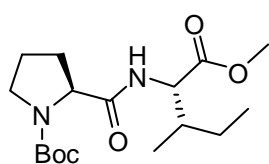
### 3.14 Conclusions

In conclusion, formation of an unusual nine membered, three residual cyclization in the AVPI peptide on treatment with EDC. HCl, was observed. The synthesis of few more cyclic AVPI analogues were carried out, in order to generalize the unusual cyclization. These unusual cyclic bisacylated products are not stable in polar protic solvents.

### 3.15 Experimental Section :

#### Synthetic procedure and data

#### Compound 12: Boc-<sup>L</sup>Pro-<sup>L</sup>Ile-OMe

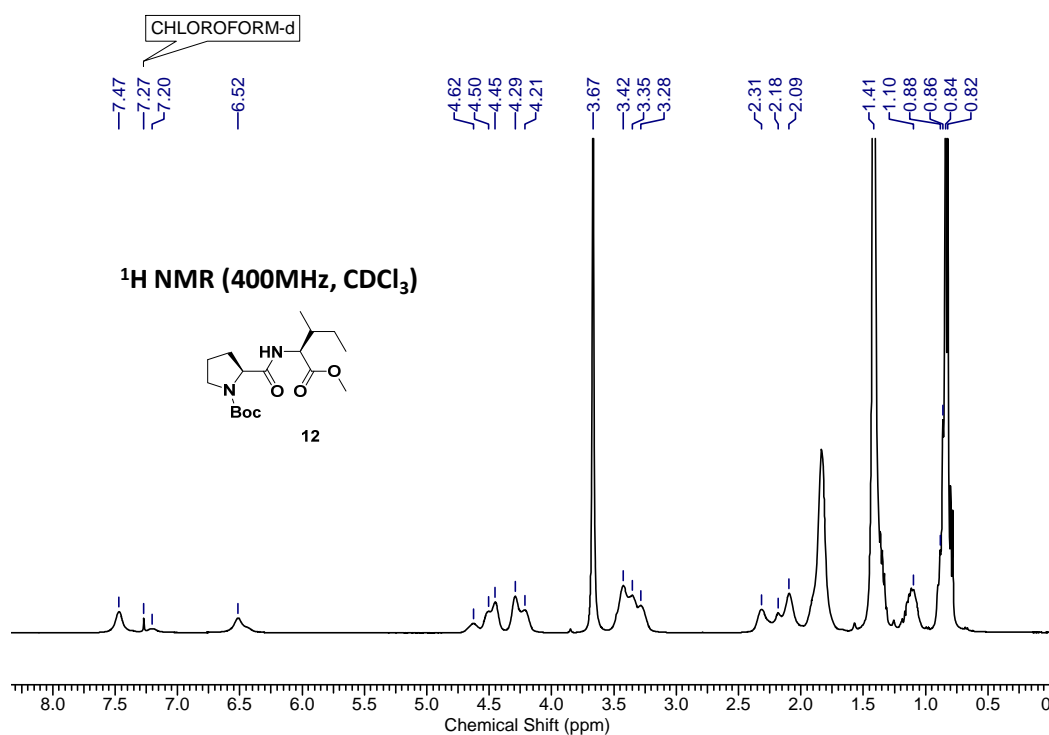


**12** (65%)

To a solution of HCl.<sup>L</sup>Ile-OMe (6 g, 33.03 mmol, 1.5 equiv.) and DIEA (11.47 mL, 66.12 mmol, 3 equiv.) in ACN (50 mL), Boc-<sup>L</sup>Pro-OH (4.73 g, 22.02 mmol, 1 equiv.) was added, followed by addition of TBTU (10.59 g, 33.01 mmol, 1.5 equiv.) and HOBT (catalytic amount). This mixture was stirred at room temperature for 8 h. After completion of reaction, ACN was removed under reduced pressure and then the compound was taken into ethyl acetate. The combined organic layers were washed sequentially with saturated solutions of KHSO<sub>4</sub>, NaHCO<sub>3</sub> and brine. Organic layer was then dried over Na<sub>2</sub>SO<sub>4</sub> and was evaporated under vacuum. The crude product was purified by column chromatography (eluent 20% AcOEt/pet. Ether, R<sub>f</sub>: 0.3) to furnish **12** (6.12 g, 65 %) as a pasty material;  $[\alpha]^{26.8}_D = -91.73$  ( $c = 0.135$ , CHCl<sub>3</sub>); IR (CHCl<sub>3</sub>)  $\nu$  (cm<sup>-1</sup>): 3407.78, 3318.89, 2969.82, 2935.13, 2879, 1743.65, 1254.86, 1205.87, 1031.34, 772.05<sup>1</sup>H NMR (400 MHz, CDCl<sub>3</sub>)  $\delta = 7.47$  (bs, rota H), 6.52 (bs, rota H), 4.5 (m, 1 H), 4.29 (m, 1 H), 3.67 (s, 3 H), 3.35 (m, 2 H), 2.31 (bs, 1 H), 2.09 (m, 3 H), 1.84 (bs, 3 H), 1.41 (s., 9 H), 1.35 (m, 1 H), 1.10 (m., 1 H), 0.82 (m, 6 H); <sup>13</sup>C NMR (175 MHz, CDCl<sub>3</sub>)

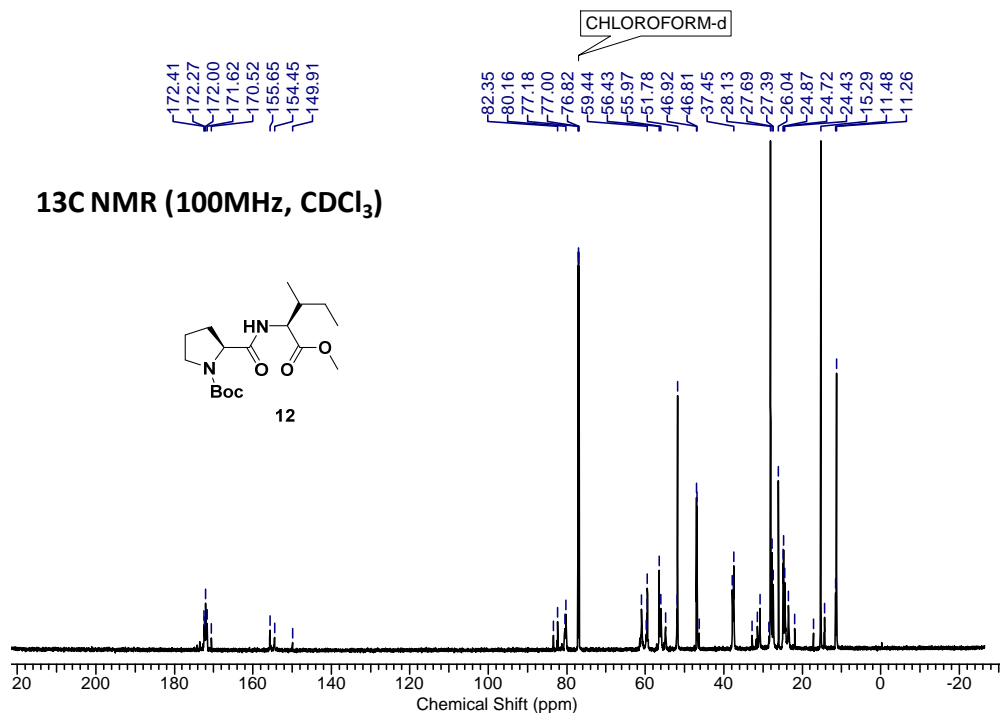
$\delta = 172.5$  (rota), 172.4 (rota), 172.1(rota), 171.8(rota), 155.8(rota), 154.6 (rota), 80.7 (rota), 80.3(rota), 61.1(rota), 59.6 (rota), 56.6 (rota), 56.1 (rota), 55.0 (rota), 51.9 (rota), 47.0 (rota), 37.9 (rota), 37.6 (rota), 30.9 (rota), 28.3, (rota), 27.5 (rota), 24.7 (rota), 23.6, 15.4 (rota), 14.5 (rota), 11.5 (rota); HRMS  $[M+H]^+$   $C_{17}H_{31}N_2O_5$  Calculated: 343.2155, Found: 343.2223,  $[M+Na]^+$   $C_{17}H_{30}N_2NaO_5$  Calculated: 365.2052, Found: 365.2042.

a)



**NOTE:** Extra signals and / or signal broadening are seen due to rotamer (minor conformer) formation at N-terminus of proline residue (*Chem. Eur. J.* **2008**, *14*, 6192).

b)



**NOTE:** Extra signals and / or signal broadening are seen due to rotamer formation (*Chem. Eur. J.* **2008**, *14*, 6192).

c)

101\_170323140539 #160 RT: 0.71 AV: 1 NL: 1.37E9  
T: FTMS + p ESI Full ms [100.00-1500.00]

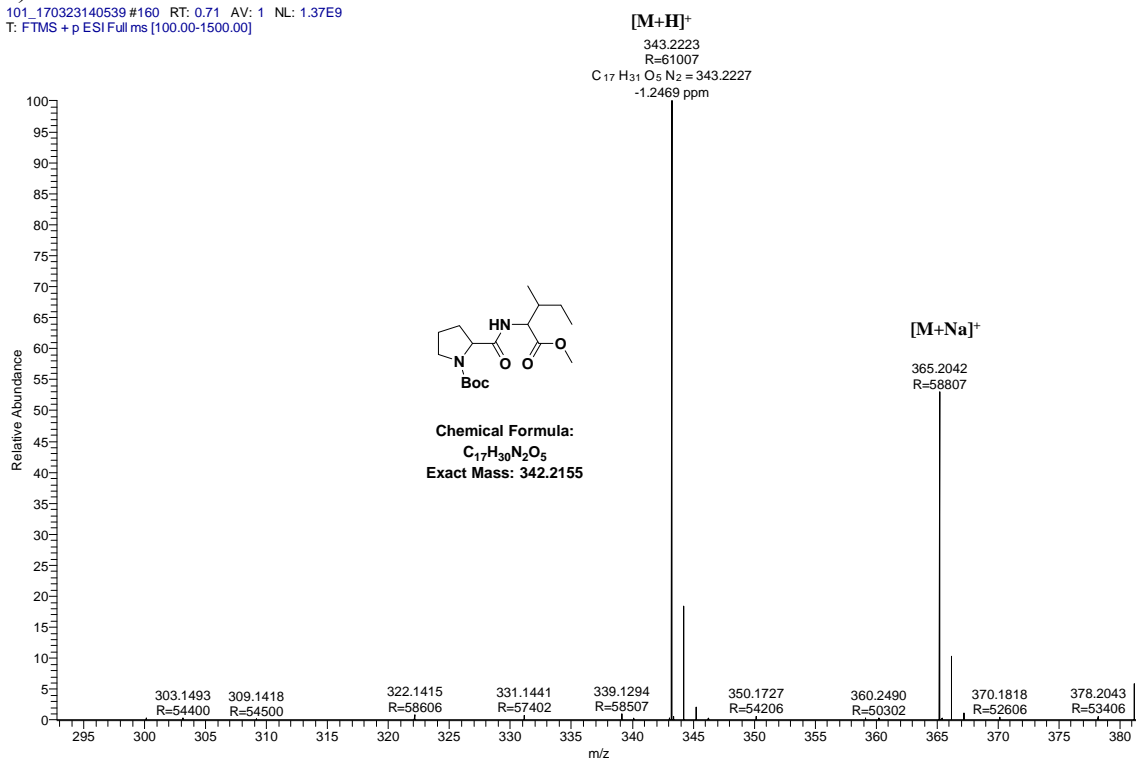
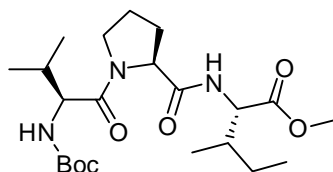


**Figure 3.22** a) <sup>1</sup>H, b) <sup>13</sup>C and c) HRMS spectra of **12**

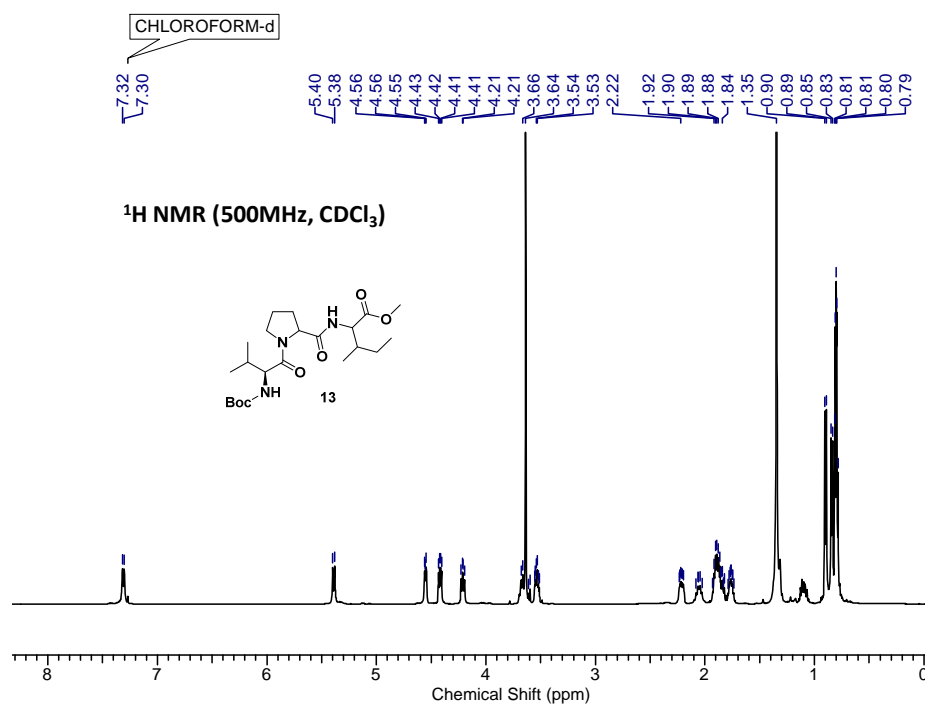
## Compound 13: Boc-L-Val-L-Pro-L-Ile-OMe



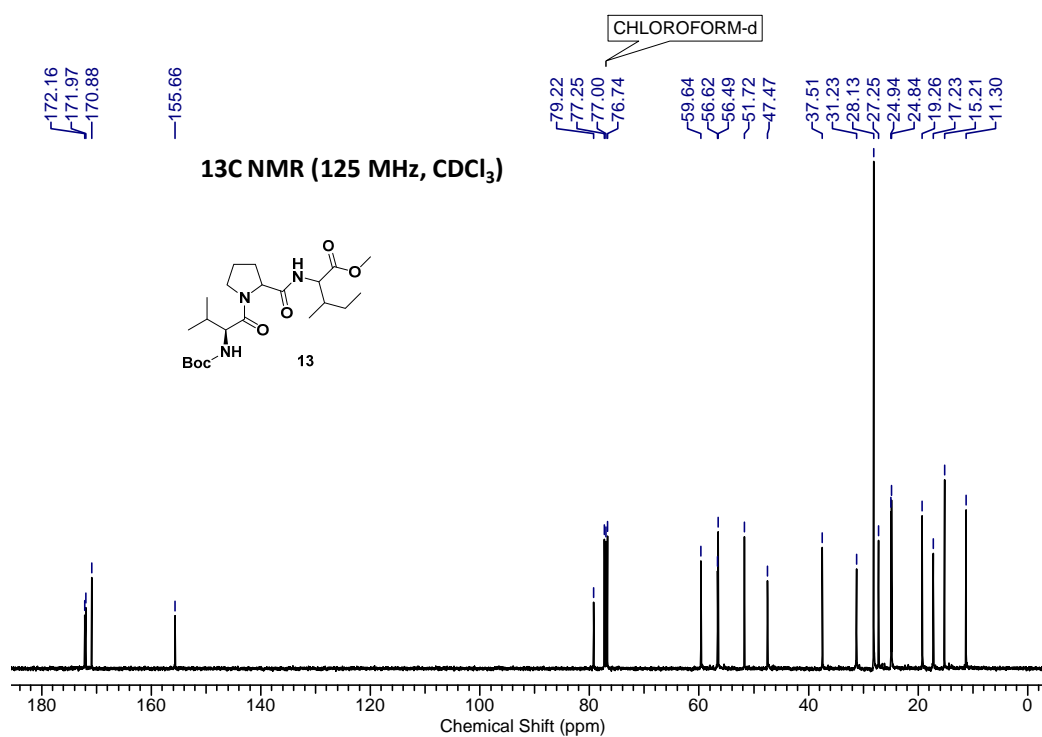
13

To a solution of TFA salt  $\cdot\text{H-L-Pro-L-Ile-OMe}$  (6 g, 16.85 mmol, 1.2 equiv.) and DIEA (7.32 mL, 42.1 mmol, 3 equiv.) in ACN (40 mL), Boc-L-Val-OH (3.04 g, 14.04 mmol, 1 equiv.) was added, followed by addition of TBTU (6.76 g, 21.06 mmol, 1.5 equiv.) and HOBt (catalytic amount). This mixture was stirred at room temperature for 8 h. After completion of reaction, ACN was evaporated under reduced pressure and then the compound was taken into ethyl acetate. The combined organic layers were washed sequentially with saturated solutions of  $\text{KHSO}_4$ ,  $\text{NaHCO}_3$  and brine. Organic layer was then dried over  $\text{Na}_2\text{SO}_4$  and was evaporated under vacuum. The crude product was purified by column chromatography (eluent 35 % AcOEt/pet. Ether,  $R_f$ : 0.3) to furnish **13** (7.52 g, 86 %) as a colorless pasty material;  $[\alpha]^{26.9}_D$ : -124.0 ( $c = 0.1$ ,  $\text{CHCl}_3$ ); IR ( $\text{CHCl}_3$ )  $\nu$  ( $\text{cm}^{-1}$ ): 3310.36, 2968.85, 2935.68, 2877.53, 1741.00, 1687.58, 1632.55, 1367.07, 1092.88, 1016.41, 756.04;  $^1\text{H}$  NMR (500 MHz,  $\text{CDCl}_3$ )  $\delta$  = 7.31 (d,  $J = 8.2$  Hz, 1 H), 5.39 (d,  $J = 9.5$  Hz, 1 H), 4.55 (m, 1 H), 4.42 (dd,  $J = 4.9, 8.2$  Hz, 1 H), 4.21 (dd,  $J = 6.6, 9.0$  Hz, 1 H), 3.67 (m, 1 H), 3.64 (s, 3 H), 3.53 (m, 1 H), 2.22 (m, 1 H), 2.06 (m, 1 H), 1.89 (m, 3 H), 1.76 (m, 1 H), 1.35 (s, 9 H), 1.31 (m, 1 H), 1.10 (m, 1 H), 0.90 (d,  $J = 6.7$  Hz, 3 H), 0.84 (d,  $J = 6.7$  Hz, 3 H), 0.80 (m, 6 H);  $^{13}\text{C}$  NMR (125 MHz,  $\text{CDCl}_3$ )  $\delta$  = 172.2, 172.0, 170.9, 155.7, 79.2, 59.6, 56.6, 56.5, 51.7, 47.5, 37.5, 31.2, 28.1, 27.3, 24.9, 24.8, 19.3, 17.2, 15.2, 11.3; HRMS  $[\text{M}+\text{H}]^+$   $\text{C}_{22}\text{H}_{40}\text{N}_3\text{O}_6$  Calculated: 442.2839, Found: 442.2911,  $[\text{M}+\text{Na}]^+$   $\text{C}_{22}\text{H}_{39}\text{N}_3\text{NaO}_6$  Calculated: 464.2737, Found: 464.2726.

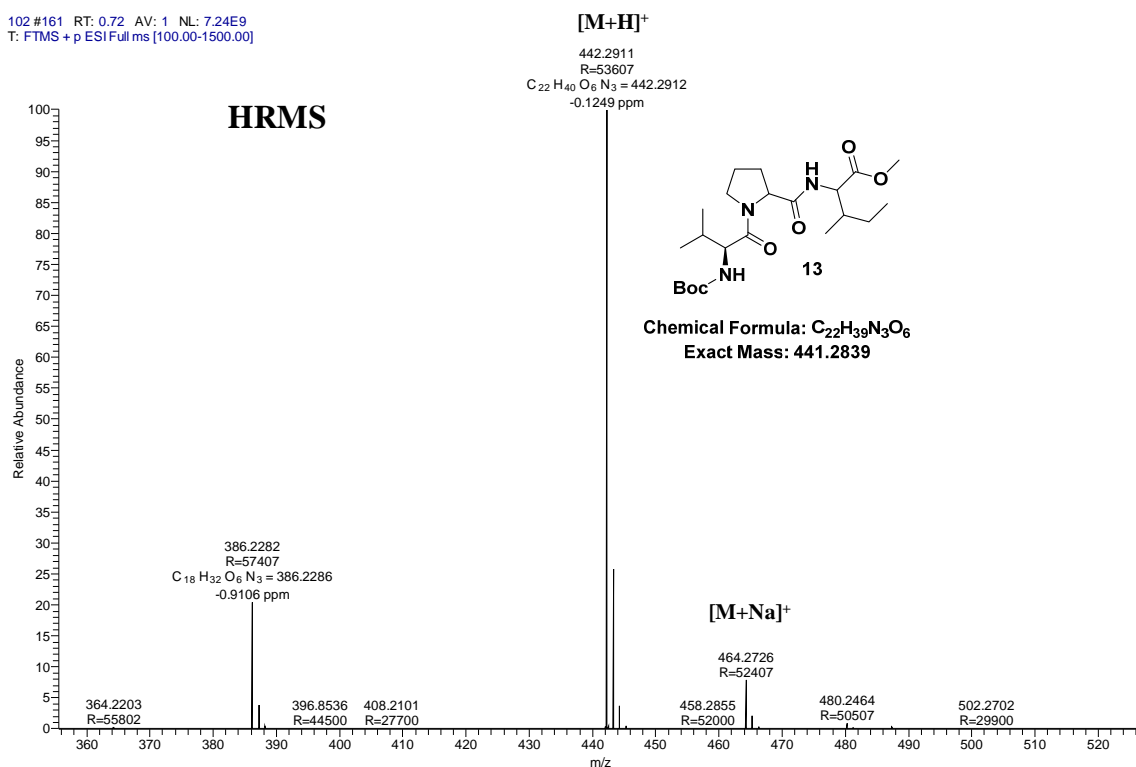
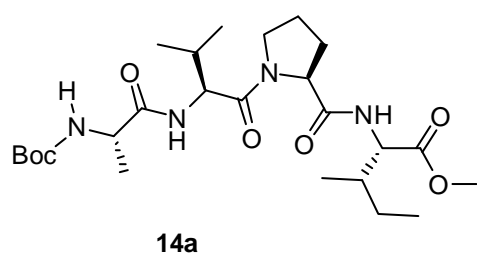
a)



b)



c)

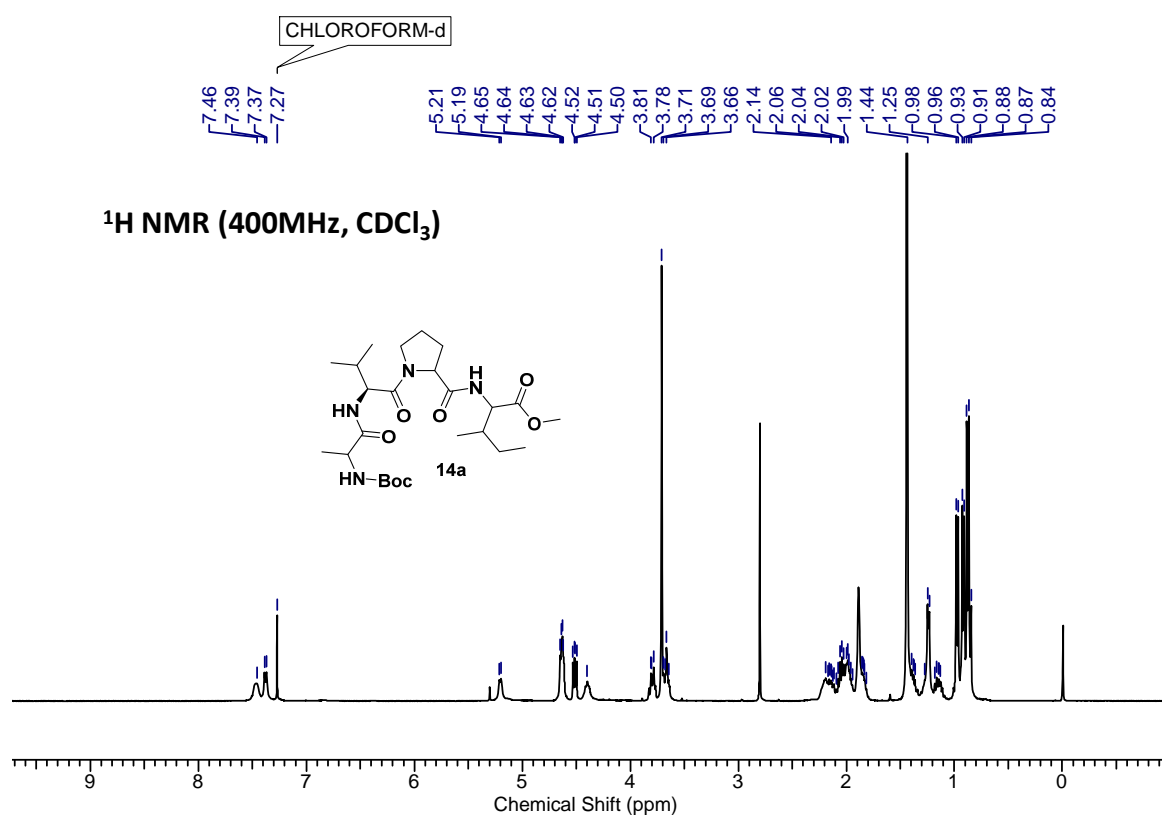
Figure 3.23 a) <sup>1</sup>H, b) <sup>13</sup>C and c) HRMS spectra of **13****Compound 14a: Boc-L-Ala-L-Val-L-Pro-L-Ile-OMe**

To a solution of TFA salt .H-L-Val-L-Pro-L-Ile-OMe (2.5 g, 5.49 mmol, 1.2 equiv.) and DIEA (3.18 mL, 18.31 mmol, 4 equiv.) in DCM (40 mL), Boc-L-Ala-OH (0.865 g, 4.57 mmol, 1 equiv.) was added, followed by addition of TBTU (2.2 g, 6.86 mmol, 1.5 equiv.) and HOBT (catalytic amount). This mixture was stirred at room temperature for 8 h. After completion of reaction, the reaction mixture was diluted with DCM. The DCM solution was washed sequentially with saturated solutions of KHSO<sub>4</sub>, NaHCO<sub>3</sub> and brine. Organic layer was then dried over Na<sub>2</sub>SO<sub>4</sub> and was evaporated under vacuum. The crude product was purified by column chromatography (eluent 50 % AcOEt/pet. Ether, R<sub>f</sub>: 0.3) to furnish **14a** (2.12 g, 82 %) as a white sticky solid; mp 57 °C; [α]<sup>26.8</sup><sub>D</sub> = - 139.84 (c = 0.05, CHCl<sub>3</sub>); IR (CHCl<sub>3</sub>) ν (cm<sup>-1</sup>): 3428.94, 3322.44, 3018.57, 2971.91, 2935.41, 2878.60, 1738.65, 1670.75, 1628.37, 1216.44, 1163.09, 1052.77; <sup>1</sup>H

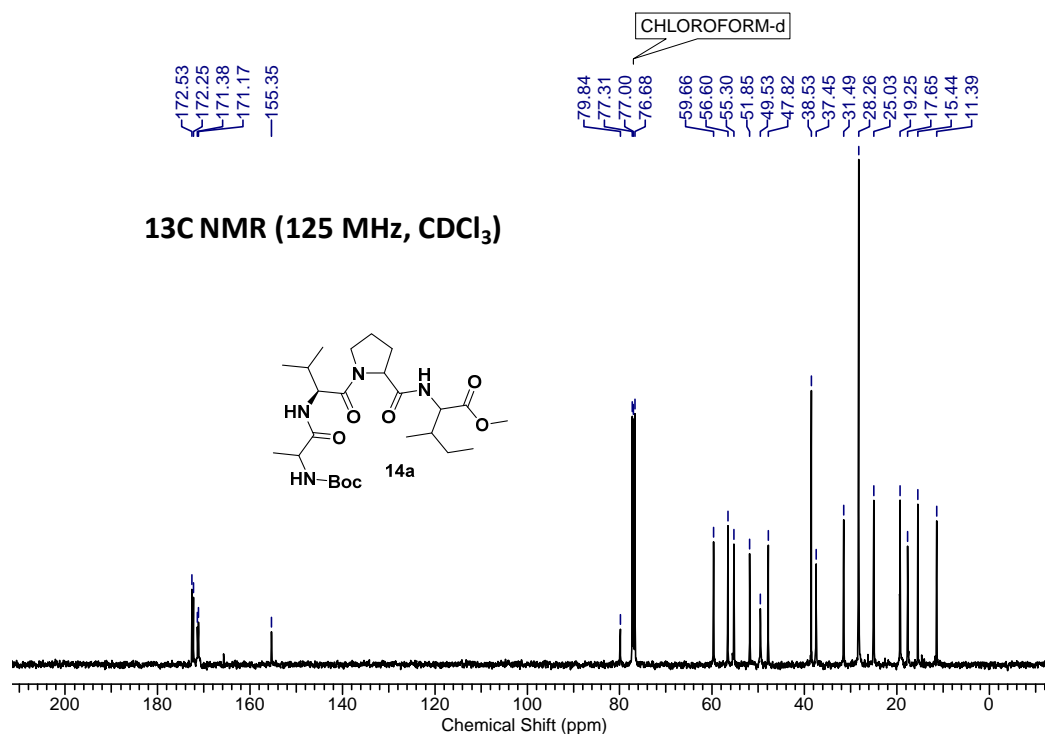


NMR (400MHz, CDCl<sub>3</sub>)  $\delta$  = 7.46 (bs., 1 H), 7.38 (d,  $J$  = 8.1 Hz, 0 H), 5.20 (d,  $J$  = 7.3 Hz, 1 H), 4.64 (m, 1 H), 4.51 (dd,  $J$  = 5.3, 8.4 Hz, 1 H), 4.40 (m., 1 H), 3.78 (m, 1 H), 3.71 (s, 3 H), 3.66 (m, 1 H), 2.2 (m, 2 H), 1.95 (m, 2 H), 1.89 (bs., 2 H), 1.85 (m, 1 H), 1.44 (s, 9 H), 1.38 (m, 1 H), 1.25 (d,  $J$  = 6.38 Hz 3 H), 1.14 (m, 1 H), 0.97 (d,  $J$  = 6.8 Hz, 3 H), 0.92 (d,  $J$  = 6.6 Hz, 3 H), 0.87 (m, 6 H); <sup>13</sup>C NMR (100 MHz, CDCl<sub>3</sub>)  $\delta$  = 172.6, 172.3, 171.4, 171.2, 155.4, 79.9, 59.7, 56.7, 55.4, 51.9, 49.6, 47.9, 38.6, 37.5, 31.6, 28.3, 25.1, 25.0, 19.5, 19.3, 17.7, 15.5, 11.4; HRMS [M+H]<sup>+</sup> C<sub>25</sub>H<sub>45</sub>N<sub>4</sub>O<sub>7</sub> Calculated: 513.3210, Found: 513.3283, [M+Na]<sup>+</sup> C<sub>25</sub>H<sub>44</sub>N<sub>4</sub>NaO<sub>7</sub> Calculated: 535.3108, Found: 535.3097.

a)



b)



c)

103\_170323141201 #133 RT: 0.59 AV: 1 NL: 6.12E9  
T: FTMS + p ESI Full ms [100.00-1500.00]

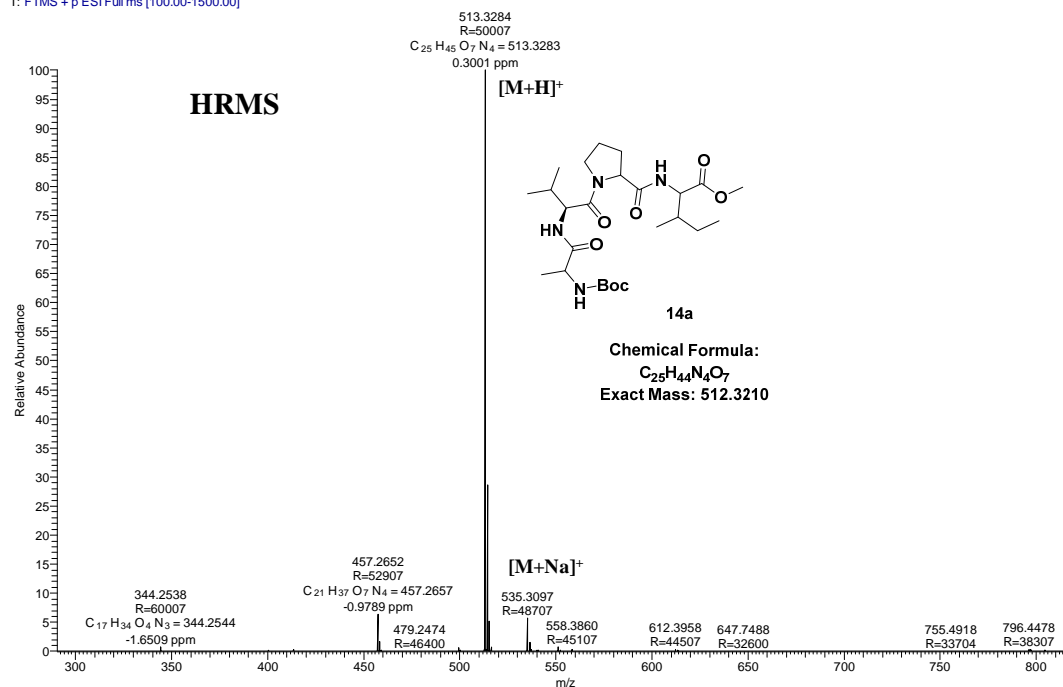
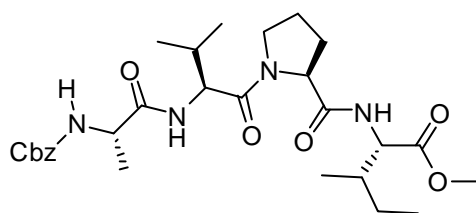


Figure 3.24 a) <sup>1</sup>H, b) <sup>13</sup>C and c) HRMS spectra of **14a**

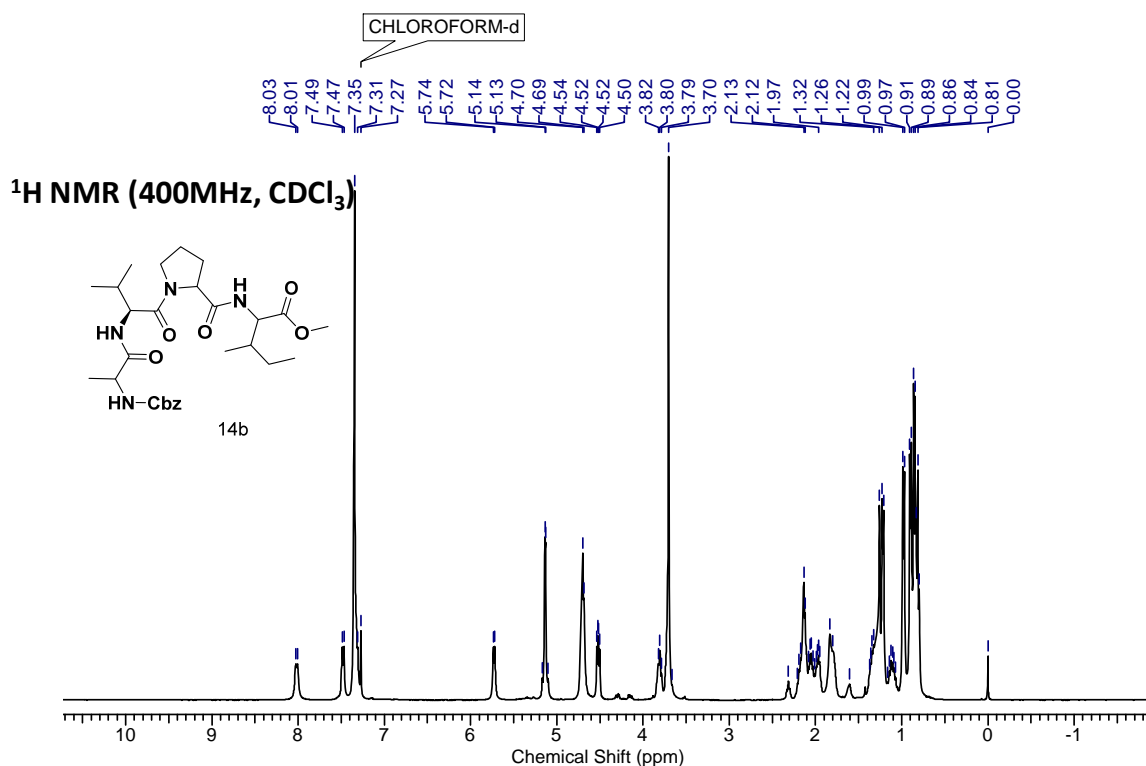
Compound **14b**: Cbz-<sup>L</sup>Ala-<sup>L</sup>Val-<sup>L</sup>Pro-<sup>L</sup>Ile-OMe**14b**

Compound **14b** was synthesized using same synthetic procedure of **14a**. The, compound **14b** was yielded (0.36 g, 86 %) as a white solid; mp 58-60 °C,  $[\alpha]^{27.1} = -140.84^\circ$  ( $c = 0.15$ ,  $\text{CHCl}_3$ );

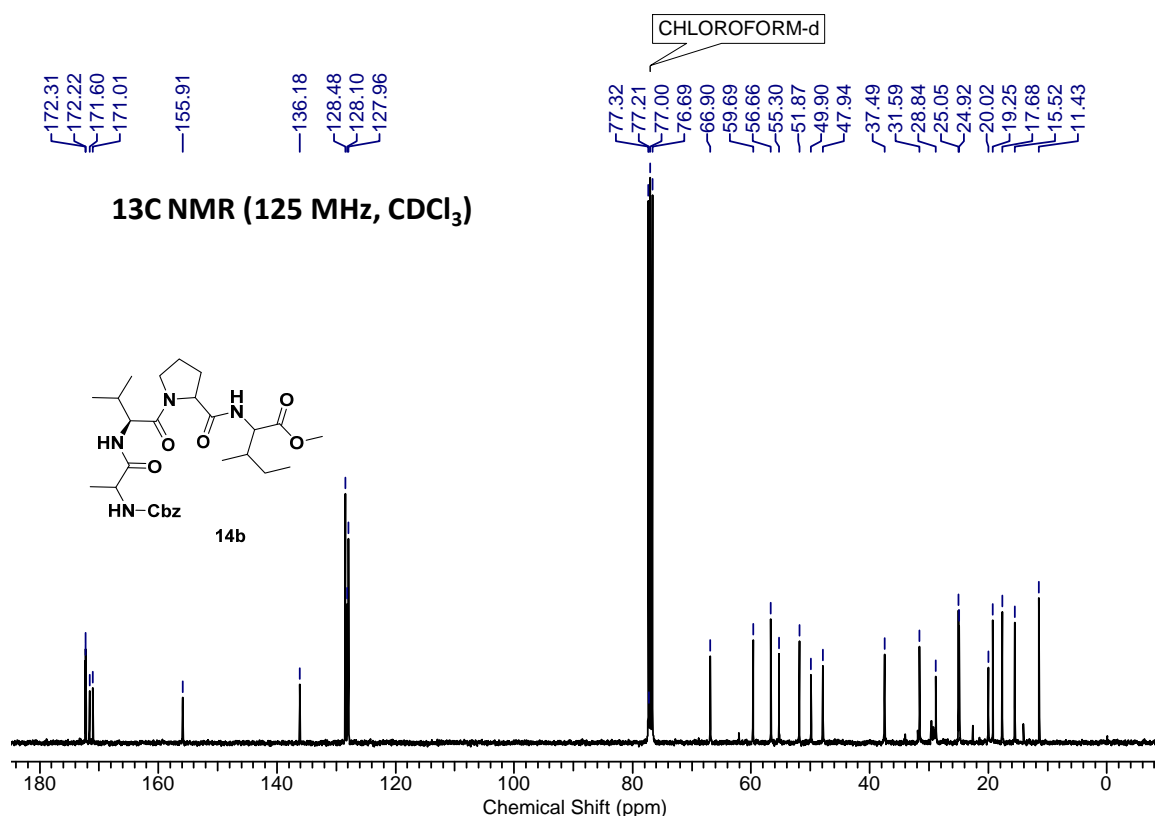
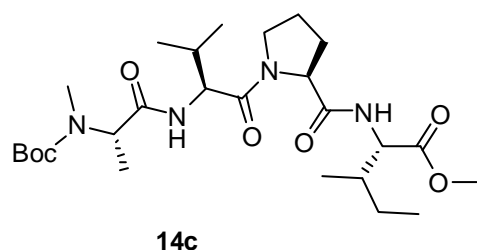
IR ( $\text{CHCl}_3$ )  $\nu$  ( $\text{cm}^{-1}$ ): 3450.0, 3311.44, 3018.02,

2968.60, 2933.36, 1739.26, 1704.92, 1673.24, 1504.76, 1216.27, 1053.71;  $^1\text{H}$  NMR (400 MHz,  $\text{CDCl}_3$ )  $\delta = 8.02$  (d,  $J = 8.3$  Hz, 1 H), 7.48 (d,  $J = 8.3$  Hz, 1 H), 7.35 (m, 5 H), 5.73 (d,  $J = 7.3$  Hz, 1 H), 5.15 (m, 2 H), 4.69 (m, 3 H), 4.52 (dd,  $J = 5.4, 8.3$  Hz, 1 H), 3.8 (m, 1 H), 3.73 (m, 1 H), 3.70 (s, 3 H), 2.20 (m, 1 H), 2.13 (m, 2 H), 2.05 (m, 1H), 1.97 (m, 1 H), 1.83 (m, 1 H), 1.35 (m, 1 H), 1.22 (d,  $J = 6.4$  Hz, 3 H), 1.11 (m, 1 H), 0.98 (d,  $J = 6.4$  Hz, 3 H), 0.90 (d,  $J = 6.4$  Hz, 3 H), 0.84 (m, 6 H)  $^{13}\text{C}$  NMR (100 MHz,  $\text{CDCl}_3$ )  $\delta = 172.3, 172.3, 171.6, 171.1, 155.9, 136.2, 128.5, 128.1, 128.0, 66.9, 59.7, 56.70, 55.3, 51.91, 49.94, 48.0, 37.5, 31.6, 28.9, 25.1, 25.0, 20.1, 19.3, 17.7, 15.6, 11.5$ ; LCMS  $[\text{M}+\text{H}]^+$   $\text{C}_{28}\text{H}_{43}\text{N}_4\text{O}_7$  Calculated: 547.3053, Found: 547.3131,  $[\text{M}+\text{Na}]^+$   $\text{C}_{28}\text{H}_{42}\text{N}_4\text{NaO}_7$  Calculated: 569.2951, Found: 569.2941.

a)



b)

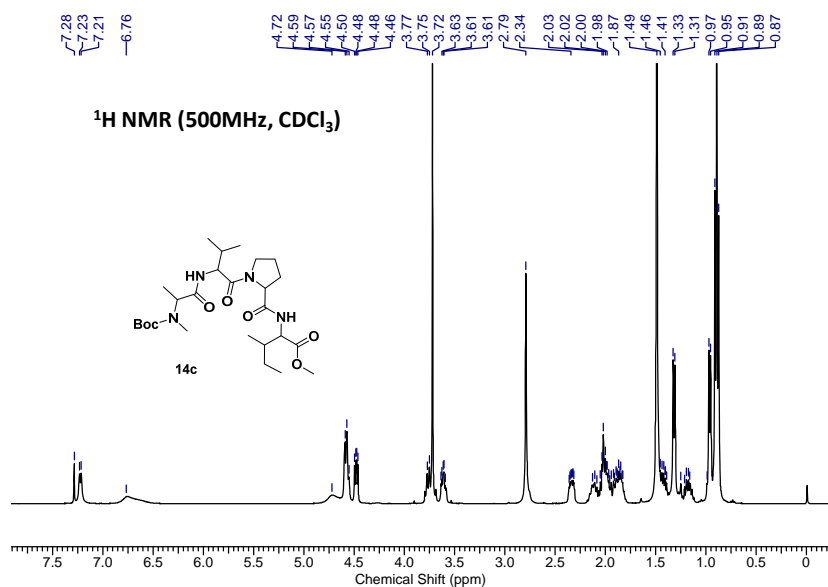
Figure 3.25 a) <sup>1</sup>H and b) <sup>13</sup>C spectra of **14b****Compound 14c: Boc-NMe<sup>L</sup>Ala-<sup>L</sup>Val-<sup>L</sup>Pro-<sup>L</sup>Ile-OMe**

Compound **14c** was synthesized using *N*-methylated Boc-Ala-OH by following the same synthetic procedure of **14a**. Compound **14c** was yielded (0.24 g, 85 %) as a pasty material,  $[\alpha]_{D}^{26.98}$

$D = -108.26^\circ$  ( $c = 0.2$ , CHCl<sub>3</sub>); IR (CHCl<sub>3</sub>)  $\nu$  (cm<sup>-1</sup>): 3415.20, 3319.00, 3017.01, 2970.84, 2935.96, 2878.85, 1738.93, 1679.57, 1631.87, 1516.43, 1439.19, 1322.85, 1215.92, 863.19; <sup>1</sup>H NMR (400 MHz, CDCl<sub>3</sub>)  $\delta$  = 7.22 (d,  $J$  = 7.8 Hz, 1 H), 6.76 (bs, 1 H), 4.72 (bs, 1 H), 4.57 (m, 2 H), 4.48 (dd,  $J$  = 5.0, 8.2 Hz, 1 H), 3.76 (m, 1 H), 3.72 (s, 3 H), 3.61 (m, 1 H), 2.79 (s, 3 H), 2.33 (m, 1 H), 2.11 (m, 1 H), 2.02 (m, 2 H), 1.87 (m, 2 H), 1.49 (s, 9 H), 1.42 (m, 1 H), 1.32 (d,  $J$  = 6.8 Hz, 3 H), 1.17 (m, 1 H), 0.96 (d,  $J$  = 6.6 Hz, 3 H), 0.89 (t,  $J$  = 7.1 Hz, 9 H); <sup>13</sup>C NMR (101 MHz, CDCl<sub>3</sub>)  $\delta$  = 172.0, 171.7, 171.4, 170.7, 156.2, 80.6, 59.87 (rota), 59.82 (rota), 56.71 (rota), 56.69

(rota), 55.33, (rota) 55.29, (rota) 53.4, 51.9, 47.7, 37.6, 31.3, 29.8, 28.3, 27.1, 25.1, 25.0, 19.5, 17.6, 15.4, 13.49, 11.5; LCMS  $[M+H]^+$   $C_{26}H_{47}N_4O_7$  Calculated: 527.3366, Found: 527.3443,  $[M+Na]^+$   $C_{26}H_{46}N_4NaO_7$  Calculated: 549.3264, Found: 549.3256.

a)



NOTE: Extra signals and / or signal broadening are seen due to rotamer formation (*Chem. Eur. J.* **2008**, *14*, 6192).

b)

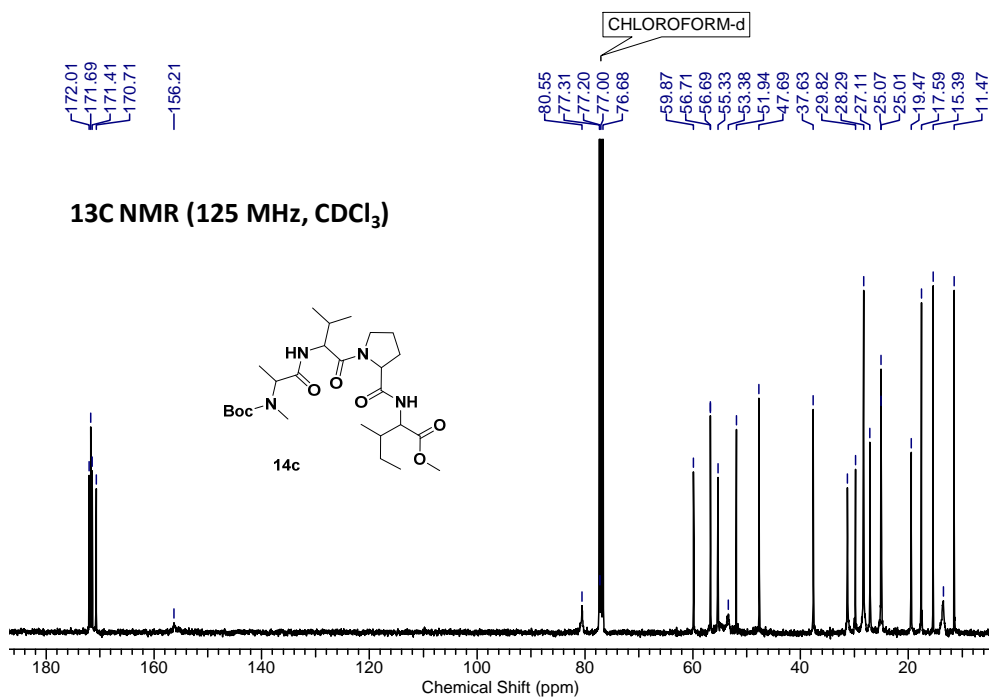
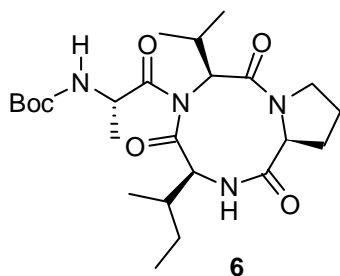


Figure 3.26 a)  $^1H$ , and b)  $^{13}C$  spectra of **14c**

Hydrolysis of the compounds **15a-c** and **13** was done using LiOH:H<sub>2</sub>O in aq. Methanol.

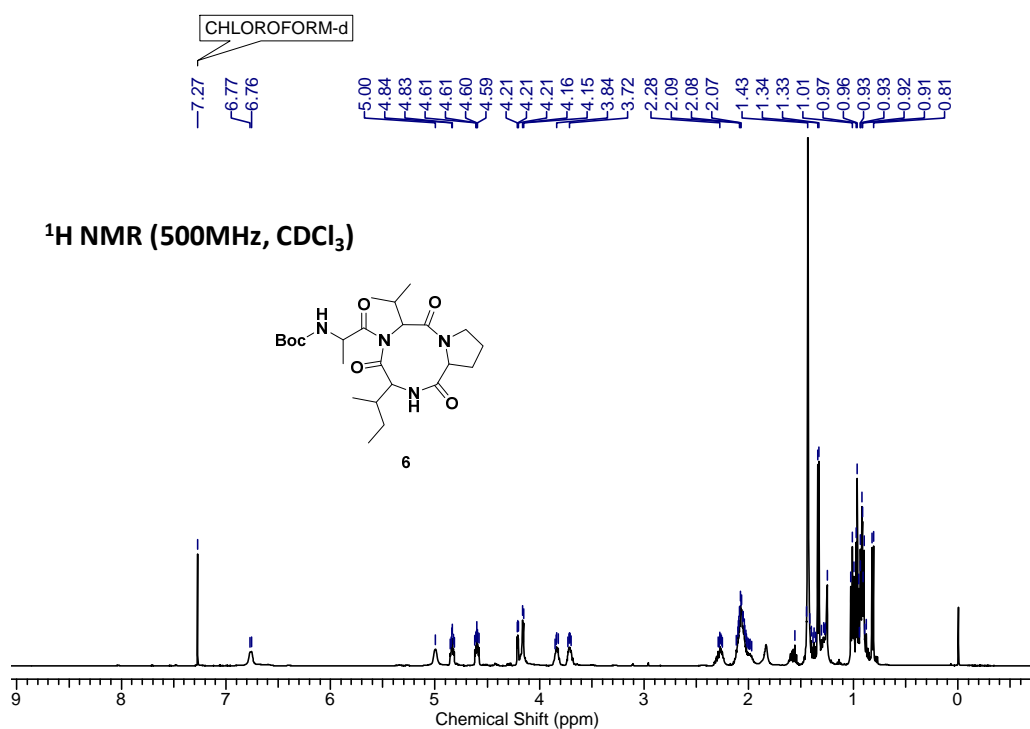
**Compound 6: Boc-<sup>L</sup>Ala-<sup>Cy</sup>-<sup>L</sup>Val-<sup>L</sup>Pro-<sup>L</sup>Ile**



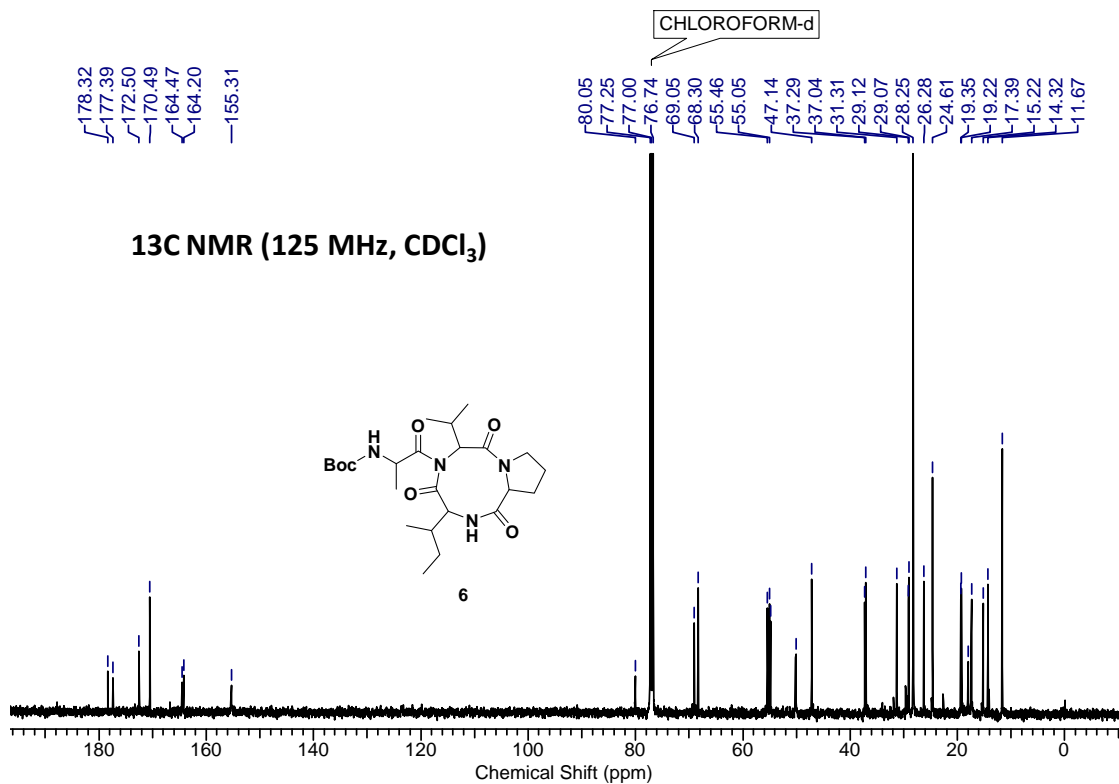
To a solution of **15a** (1.6 g, 3.2 mmol, 1 equiv.) in DCM (40 mL), EDC.HCl (1.3 g, 6.4 mmol, 2 equiv.) was added and the reaction mixture was stirred at room temperature for 5-6 hr. After completion of reaction, the mixture was diluted with DCM. The organic layer then washed with NaHCO<sub>3</sub>, KHSO<sub>4</sub> and brine solution, later the organic layer was dried over

Na<sub>2</sub>SO<sub>4</sub> and evaporated under reduced pressure. The crude product was purified by column chromatography (eluent 50 % AcOEt/pet. Ether, R<sub>f</sub>: 0.3) to furnish **6** (1.31 g, 85 %) as a white sticky solid; mp 70 °C; [α]<sup>26.85</sup><sub>D</sub> = -94.26 (*c* = 0.175, CHCl<sub>3</sub>); IR (CHCl<sub>3</sub>) ν (cm<sup>-1</sup>): 3431.4, 3308.89, 3019.06, 2972.00, 2935.38, 1826.17, 1705.54, 1676.96, 1645.64, 1450.9, 1166.07, 1043.65; <sup>1</sup>H NMR (500 MHz, CDCl<sub>3</sub>) δ = 6.76 (d, *J* = 6.1 Hz, 1 H), 5.00 (bs, 1 H), 4.88 (m, 2 H), 4.60 (m, 2 H), 4.16 (dd, rota, 1 H), 3.84 (m, 1 H), 3.72 (m, 1 H), 2.28 (m, 1 H), 2.07 (m, 4 H), 1.56 (m, 1 H), 1.43 (s, 9 H), 1.38 (m, 1 H), 1.34 (d, *J* = 7.2 Hz 3 H), 1.29 (m, 1 H), 1.01 – 0.91 (m, 11 H), 0.82 (d, *J* = 7.0 Hz, rota, 1 H). <sup>13</sup>C NMR (125 MHz, CDCl<sub>3</sub>) δ = 178.4 (rota), 177.4 (rota), 172.5, 170.5, 164.5 (rota), 164.2 (rota), 155.4, 80.1, 69.1 (rota), 68.3 (rota), 55.50 (rota), 55.49 (rota), 55.1 (rota), 54.9 (rota), 50.2 (rota), 47.19 (rota), 47.18 (rota), 37.3 (rota), 37.1 (rota), 31.4 (rota), 31.3 (rota), 29.2 (rota), 29.1 (rota), 28.3, 26.3, 24.68 (rota), 24.65 (rota), 19.4 (rota), 19.3 (rota), 18.12 (rota), 18.07(rota), 17.4, 15.3 (rota), 14.4 (rota), 11.7; HRMS [M+H]<sup>+</sup> C<sub>24</sub>H<sub>41</sub>N<sub>4</sub>O<sub>6</sub> Calculated: 481.2948, Found: 481.3021, [M+Na]<sup>+</sup> C<sub>24</sub>H<sub>40</sub>N<sub>4</sub>NaO<sub>6</sub> Calculated: 503.2846, Found: 503.2850.

a)



b)



**NOTE:** Extra signals and / or signal broadening are seen due to rotamer formation (*Chem. Eur. J.* **2008**, *14*, 6192).

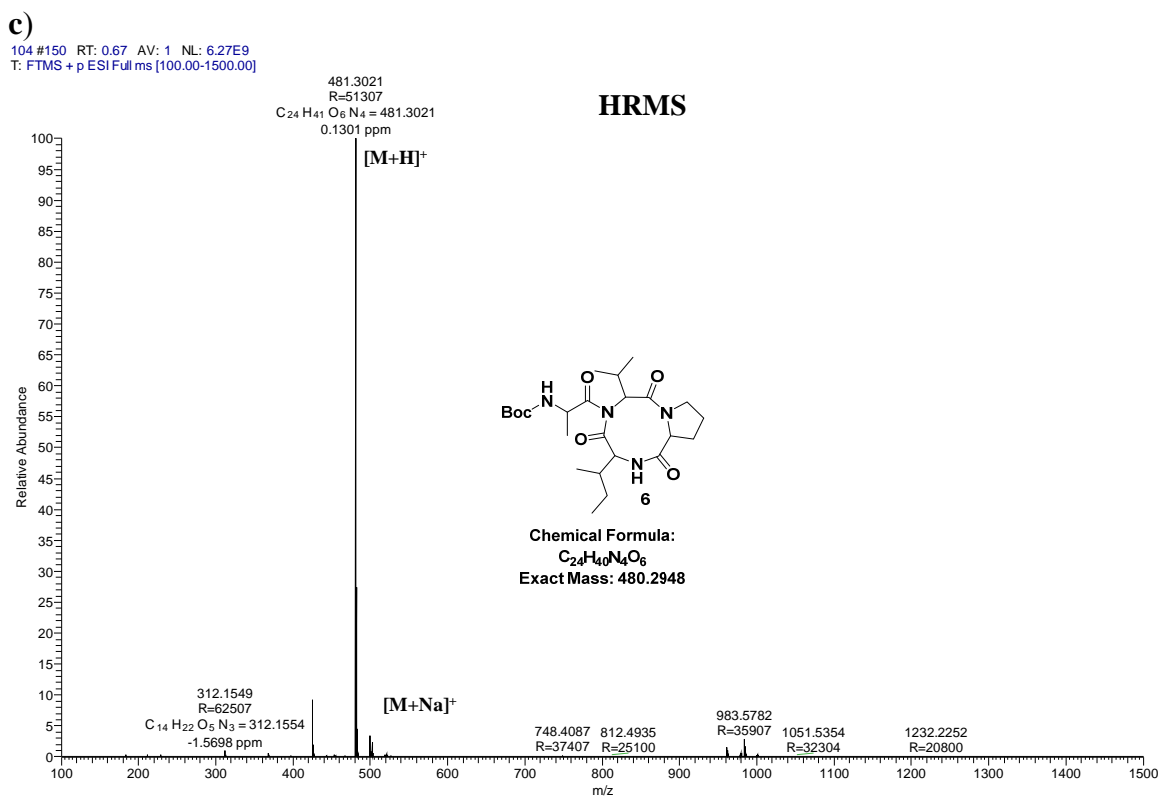
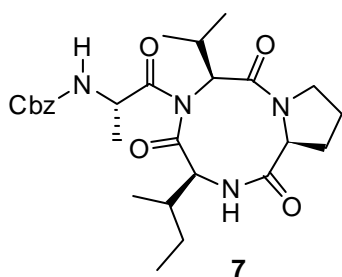


Figure 3.27 a) <sup>1</sup>H, b) <sup>13</sup>C and c) HRMS spectra of **6**

### Compound 7: Cbz-<sup>L</sup>Ala-<sup>Cy</sup>-<sup>L</sup>Val-<sup>L</sup>Pro-<sup>L</sup>Ile



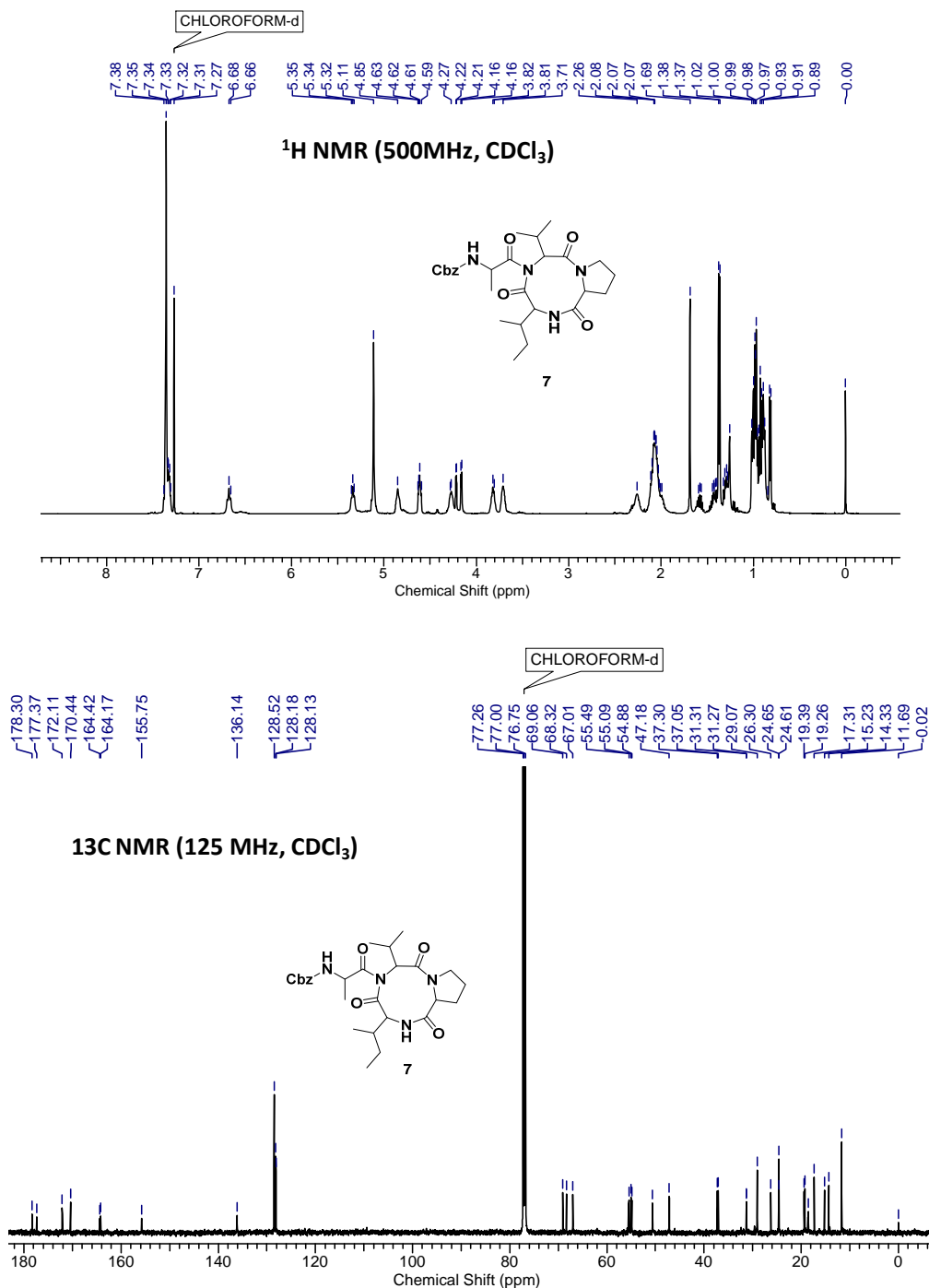
Compound **7** was prepared using same synthetic procedure of

compound **6** as a white sticky solid; mp 72-74 °C;  $[\alpha]_{D}^{26.9} = -100.2$  ( $c = 0.16$ , CHCl<sub>3</sub>); IR (CHCl<sub>3</sub>)  $\nu$  (cm<sup>-1</sup>): 3450.0, 3310.44, 3019.02, 2970.60, 1739.26, 1704.92, 1673.24, 1504.76, 1220.27, 1055.71; <sup>1</sup>H NMR (500 MHz, CDCl<sub>3</sub>)  $\delta$  = 7.31 (m, 5 H), 6.69 (t,  $J = 8.9$  Hz, 1 H), 5.35 (t,  $J = 7.6$  Hz, 1 H), 5.13 (s, 2 H), 4.87 (m, 1 H), 4.63 (m, 1 H), 4.29 (m, 1 H), 4.23 (d,  $J = 3.4$  Hz, rota, 0.5 H), 4.18 (d,  $J = 4.0$  Hz, rota 0.5 H), 3.83 (m, 1 H), 3.73 (m., 1 H), 2.28 (m, 1 H), 2.17 - 1.88 (m, 4 H), 1.60 (m, 1 H), 1.43 (m, 1 H), 1.39 (d,  $J = 7.0$  Hz, 3 H), 1.31 (m, 1 H), 1.07 - 0.87 (m, 11 H), 0.84 (d,  $J = 7.0$  Hz, 2 H); <sup>13</sup>C NMR (125 MHz, CDCl<sub>3</sub>)  $\delta$  = 178.3 (rota), 177.4 (rota), 172.2 (rota), 172.1 (rota), 170.5 (rota), 164.5 (rota), 164.2 (rota), 155.8 (rota), 136.1 (rota), 128.6, 128.2, 128.2, 69.1 (rota), 68.4 (rota), 67.0 (rota), 55.6 (rota), 55.5 (rota), 55.1 (rota), 54.9 (rota), 50.6 (rota), 47.2 (rota), 47.2 (rota), 37.3 (rota), 37.1 (rota), 31.35 (rota), 31.31 (rota), 29.1 (rota), 26.3, 24.7 (rota), 24.7 (rota), 19.4 (rota), 19.3



(rota), 18.7 (rota), 18.6 (rota), 17.4, 15.3 (rota), 14.4 (rota), 11.7; HRMS  $[M+H]^+$   $C_{27}H_{39}N_4O_6$  Calculated: 515.2791, Found: 515.2781,  $[M+Na]^+$   $C_{27}H_{38}N_4NaO_6$  Calculated: 537.2689, Found: 537.2678.

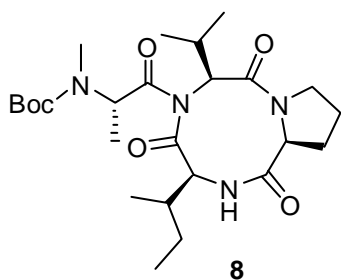
a)



NOTE: Extra signals and / or signal broadening are seen due to rotamer formation (*Chem. Eur. J.* **2008**, *14*, 6192).

Figure 3.28 a)  $^1H$ , and b)  $^{13}C$  spectra of 7

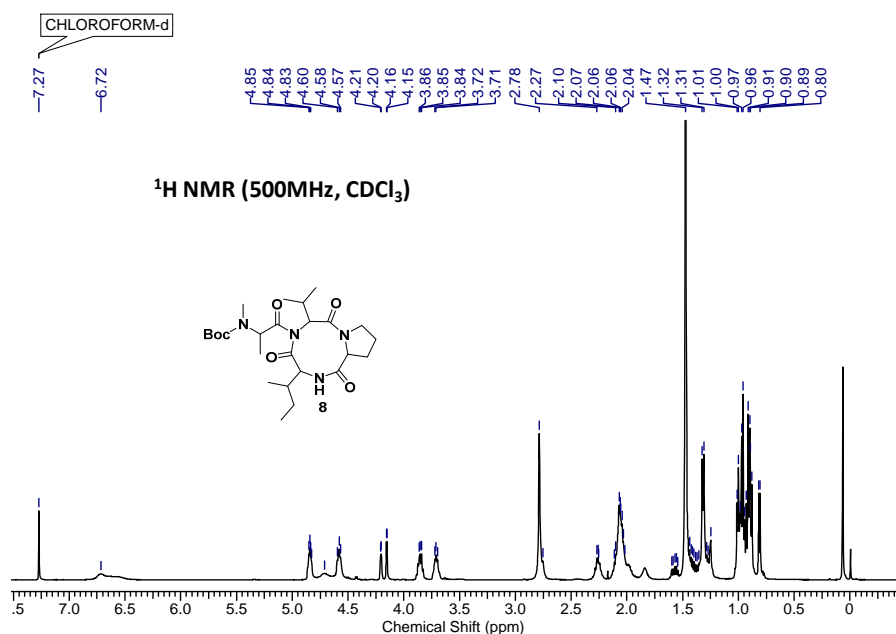
## Compound 8: Boc-NMe-L-Ala-Cy-L-Val-L-Pro-L-Ile



Compound **8** was prepared using same synthetic procedure of compound **6**. Compound **8** is yielded as a white solid; mp 121-123 °C;  $[\alpha]_D^{26.9} = -88.92$  ( $c = 0.2$ ,  $\text{CHCl}_3$ ); IR ( $\text{CHCl}_3$ )  $\nu$  ( $\text{cm}^{-1}$ ): 3412.42, 3332.45, 3019.96, 2969.93, 2935.19, 1678.30, 1648.77, 1826.22, 1548.77, 1155.51, 928.04;  $^1\text{H}$  NMR (500 MHz,  $\text{CDCl}_3$ )  $\delta = 6.71$ (bs, 1 H), 4.84 (m, 1 H), 4.72 (bs, 1 H),

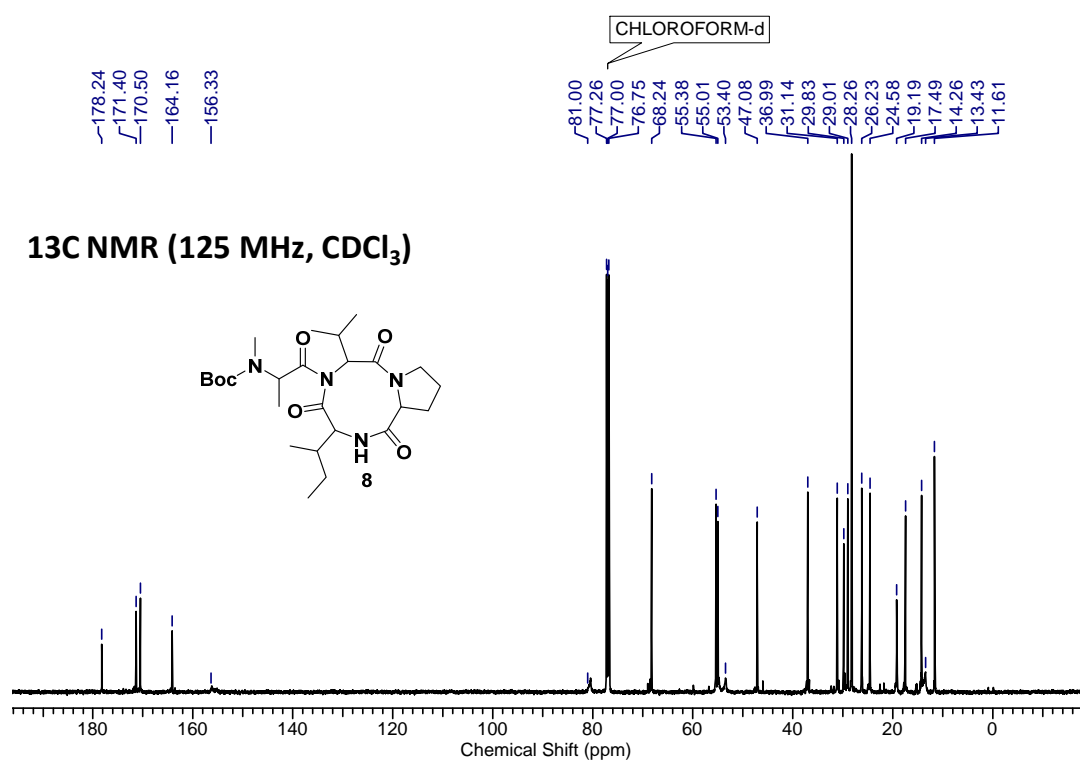
4.58 (t,  $J = 7.3$  Hz, 1 H), 4.20 (d,  $J = 2.7$  Hz, rota 0.5 H), 4.15 (d,  $J = 4.0$  Hz, rota 0.5 H), 3.85 (m, 1H), 3.71 (m, 1H), 2.78 (s, 3 H), 2.26 (m, 1 H), 2.14 - 1.94 (m, 5 H), 1.58 (m, 1 H), 1.47 (s, 9 H), 1.40 (m, 1 H), 1.32 (d,  $J = 6.7$  Hz, 3 H), 1.03 - 0.86 (m, 12 H), 0.81 (d,  $J = 6.7$  Hz, 1 H);  $^{13}\text{C}$  NMR (125 MHz,  $\text{CDCl}_3$ )  $\delta = 178.4$  (rota), 177.5 (rota), 171.5, 170.57 (rota), 170.55 (rota), 164.5 (rota), 164.2 (rota), 156.3, 80.6, 69.1 (rota), 68.4 (rota), 55.4, 55.1 (rota), 54.8 (rota), 47.2, 37.3 (rota), 37.1 (rota), 31.3, 30.0 (rota), 29.9 (rota), 29.2 (rota), 29.1 (rota), 28.4, 26.3, 24.7 (rota), 24.6 (rota), 19.4 (rota), 19.3 (rota), 17.6, 15.3, 14.4, 13.5, 11.7; HRMS  $[\text{M}+\text{H}]^+$   $\text{C}_{25}\text{H}_{43}\text{N}_4\text{O}_6$  Calculated: 495.3104, Found: 495.3104,  $[\text{M}+\text{Na}]^+$   $\text{C}_{25}\text{H}_{42}\text{N}_4\text{NaO}_6$  Calculated: 517.3002, Found: 517.3002.

a)



**NOTE:** Extra signals and / or signal broadening are seen due to rotamer formation (*Chem. Eur. J.* **2008**, *14*, 6192).

b)



NOTE: Extra signals and / or signal broadening are seen due to rotamer formation (*Chem. Eur. J.* **2008**, *14*, 6192).

c)

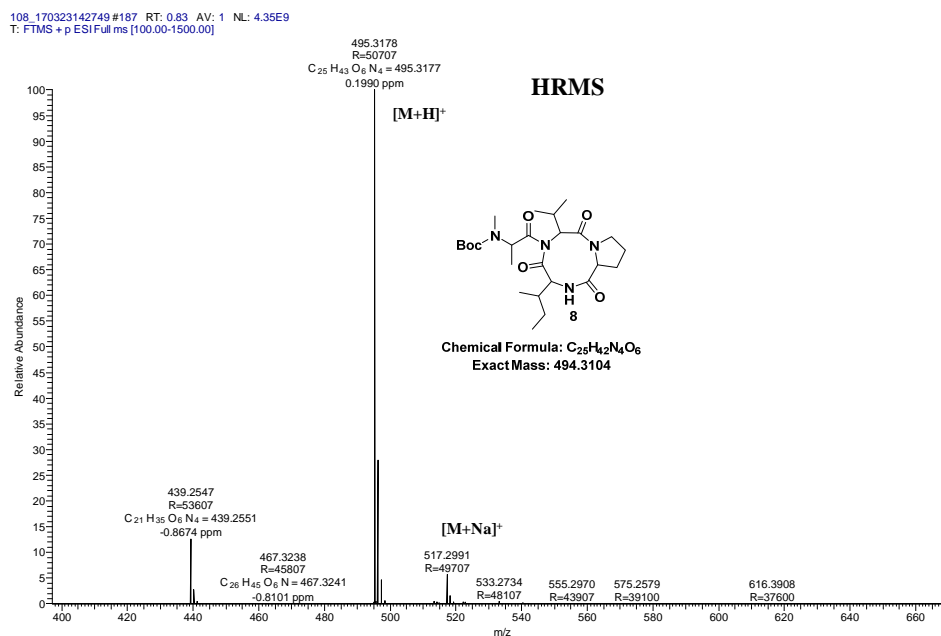
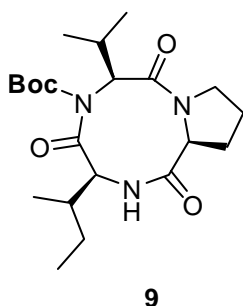
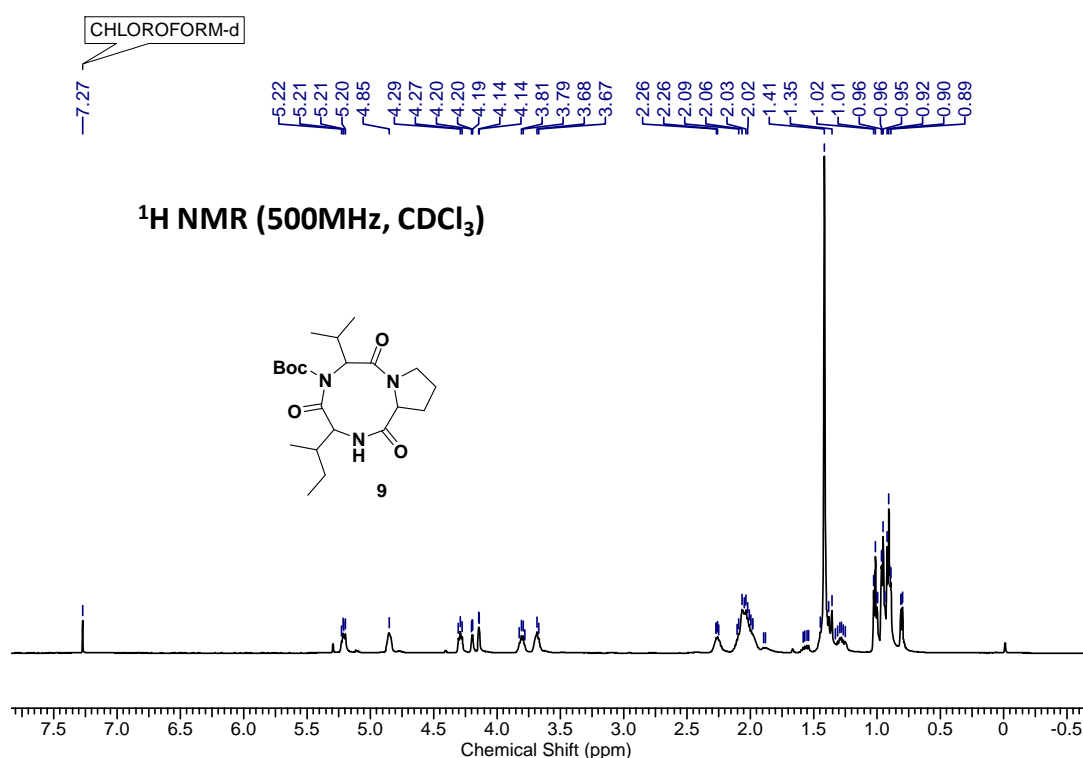


Figure 3.29 a) <sup>1</sup>H, b) <sup>13</sup>C and c) HRMS spectra of 8

Compound 9: Boc-Cy<sup>L</sup>Val<sup>L</sup>Pro<sup>L</sup>Ile

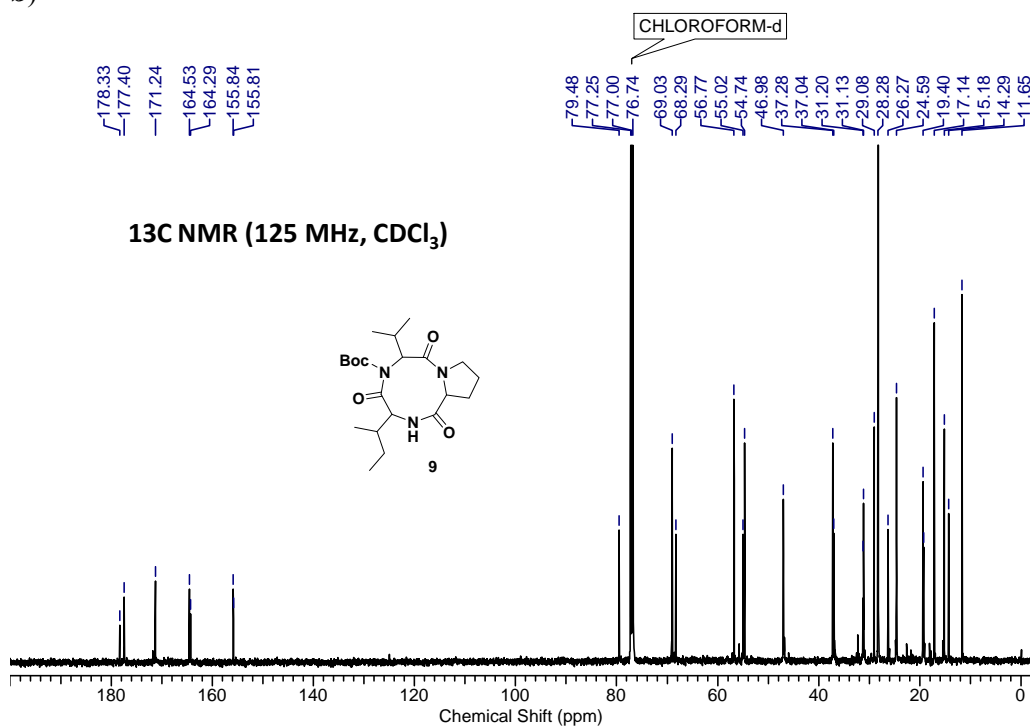
Compound **9** was prepared from Boc-<sup>L</sup>Val-<sup>L</sup>Pro-<sup>L</sup>Ile-OH, using same procedure of **7**. Compound **9** is yielded as colourless pasty material.  $[\alpha]^{27.01}_D = -82.34$  ( $c = 0.15$ , CHCl<sub>3</sub>); IR (CHCl<sub>3</sub>)  $\nu$  (cm<sup>-1</sup>): 3434.96, 3316.22, 3018.45, 2970.55, 2930.0, 1704.16, 1684.68, 1636.99, 1505.00, 1216.01, 1095.94; <sup>1</sup>H NMR (500 MHz, CDCl<sub>3</sub>)  $\delta$  = 5.21 (m, 1 H), 4.85 (m, 1 H), 4.29 (m, 1 H), 4.20 (m, rota, 0.5 H), 4.14 (m, rota, 0.5 H), 3.81 (m, 1 H), 3.68 (m, 1 H), 2.26 (m, 1 H), 2.06 (m, 5 H), 1.41 (s, 9 H), 1.28 (m, 2 H), 1.05 - 0.86 (m, 11 H), 0.80 (m, 1 H); <sup>13</sup>C NMR (125 MHz, CDCl<sub>3</sub>)  $\delta$  = 178.4 (rota), 177.5 (rota), 171.3 (rota), 171.3 (rota), 164.6 (rota), 164.3 (rota), 155.9 (rota), 155.9 (rota), 79.5, 69.1 (rota), 68.3 (rota), 56.8, 55.1 (rota), 54.8 (rota), 47.1 (rota), 47.0 (rota), 37.3 (rota), 37.1 (rota), 31.3 (rota), 31.2 (rota), 29.14 (rota), 29.12 (rota), 28.3, 26.3 (rota), 24.7 (rota), 24.68 (rota), 24.6 (rota), 19.5 (rota), 19.3 (rota), 17.2, 15.2 (rota), 14.3 (rota), 11.7; HRMS [M+H]<sup>+</sup> C<sub>21</sub>H<sub>36</sub>N<sub>3</sub>O<sub>5</sub> Calculated: 410.2577, Found: 410.2649.

a)



**NOTE:** Extra signals and / or signal broadening are seen due to rotamer formation (*Chem. Eur. J.* **2008**, *14*, 6192).

b)



**NOTE:** Extra signals and / or signal broadening are seen due to rotamer formation (*Chem. Eur. J.* **2008**, *14*, 6192).

c)

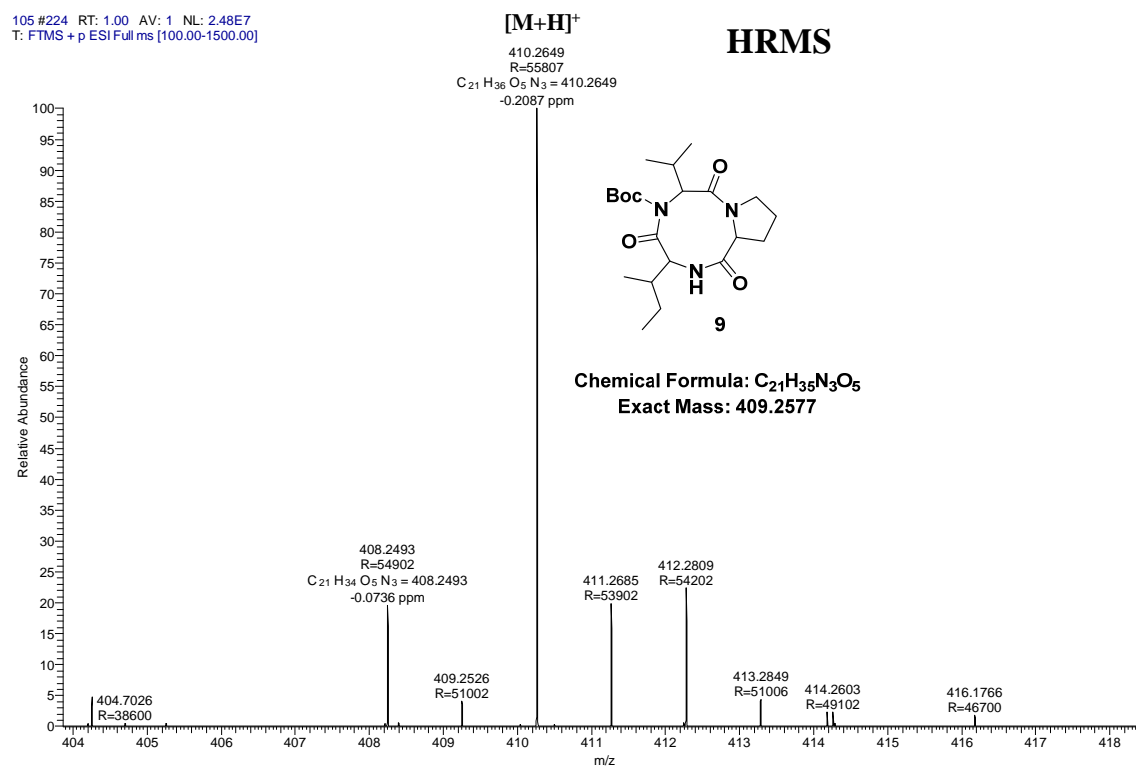


**Figure 3.30** a) <sup>1</sup>H, b) <sup>13</sup>C and c) HRMS spectra of **9**

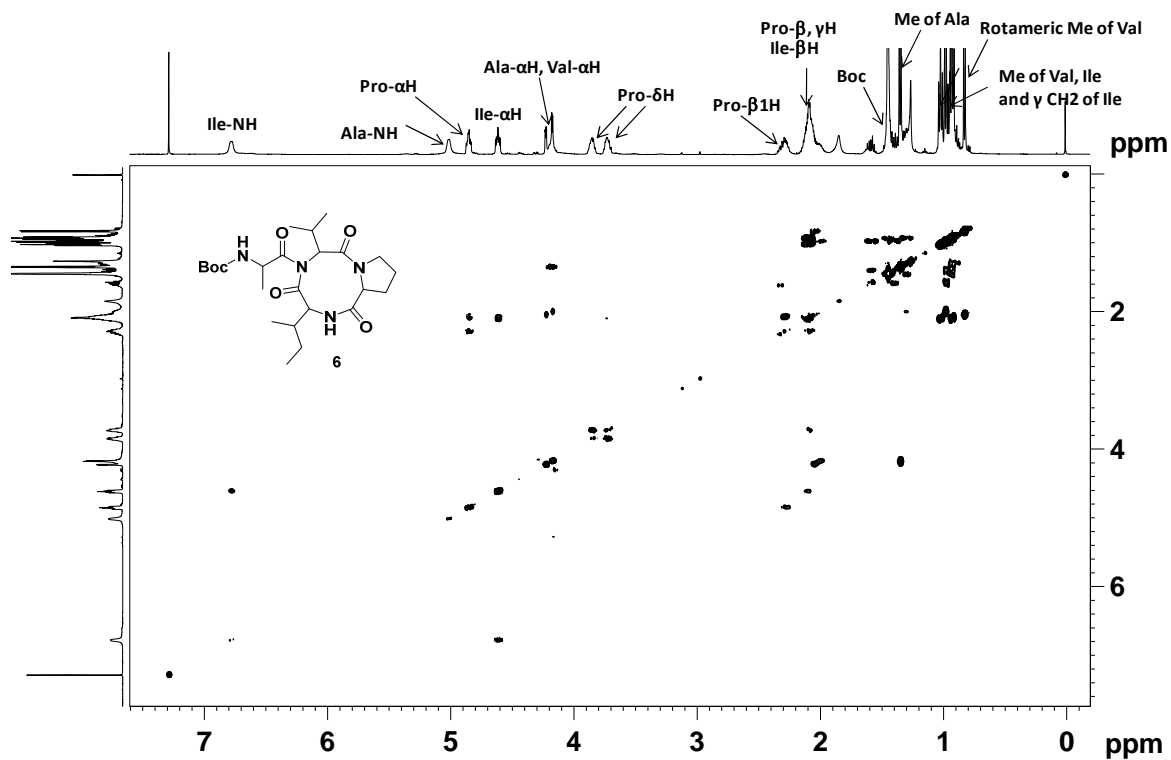


Figure 3.31 COSY spectrum of **6** (CDCl<sub>3</sub>, 500 MHz)

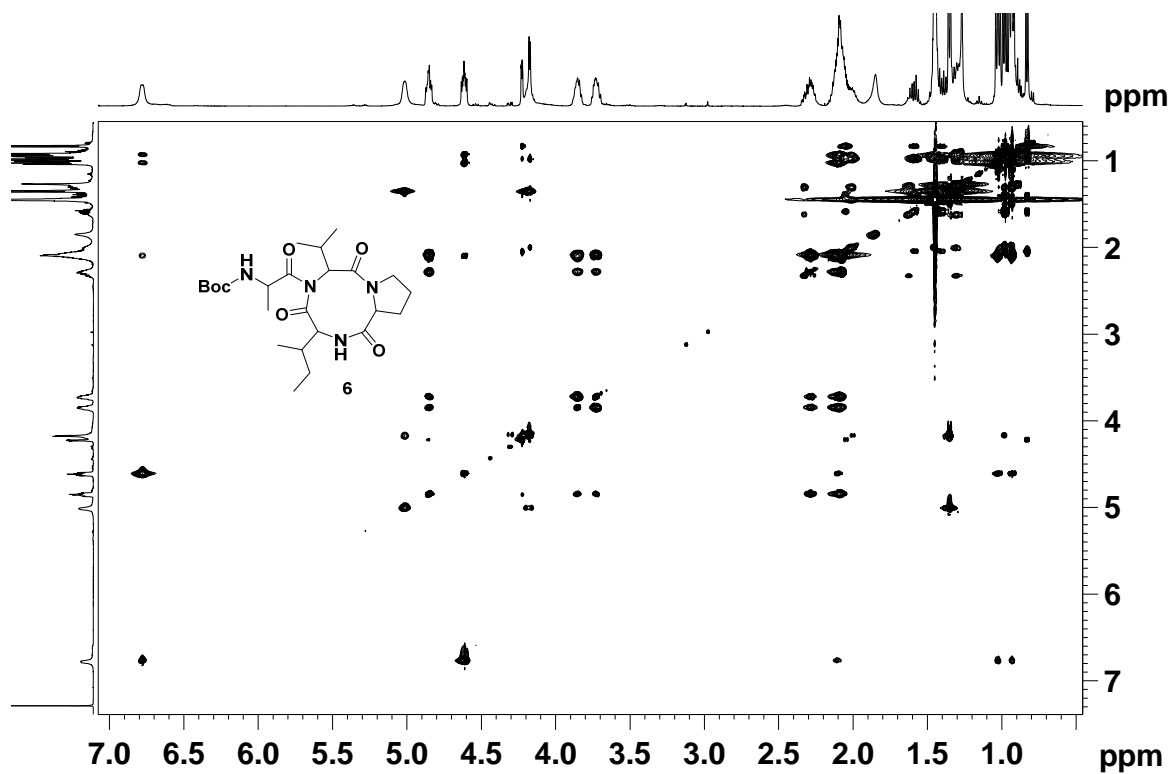


Figure 3.32 TOCSY spectrum of **6** (CDCl<sub>3</sub>, 500 MHz)

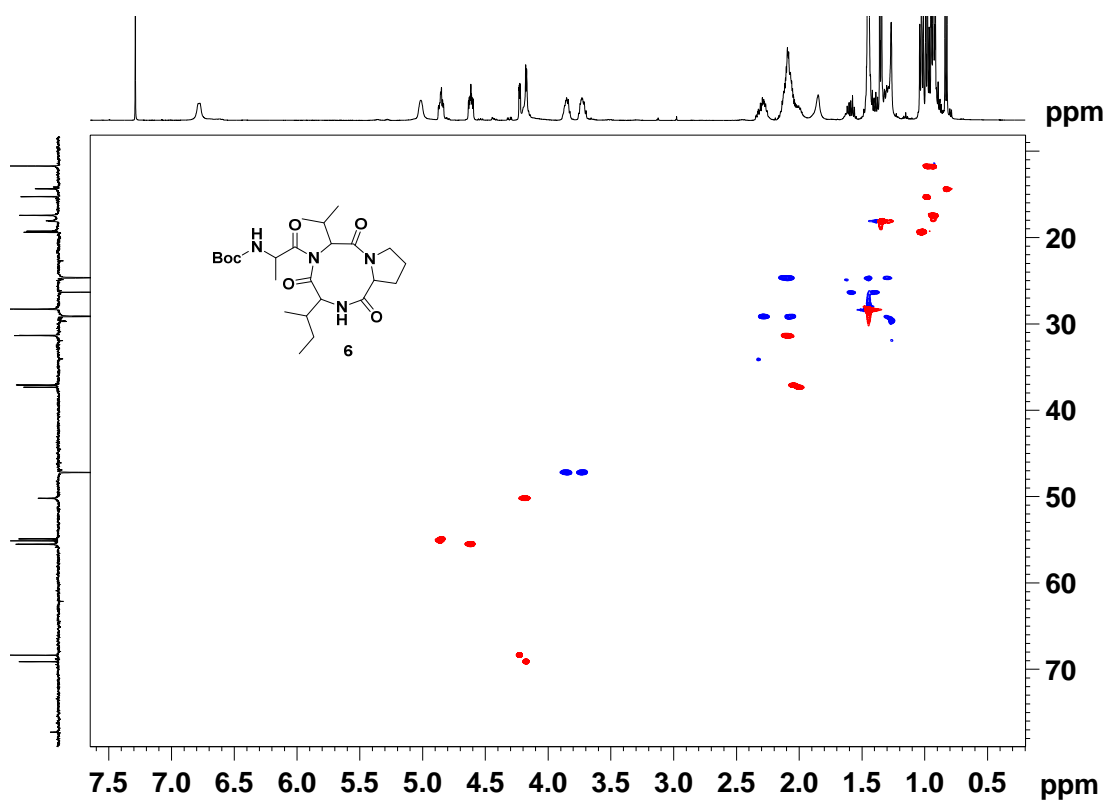


Figure 3.33 HSQC spectrum of **6** (CDCl<sub>3</sub>, 500 MHz)

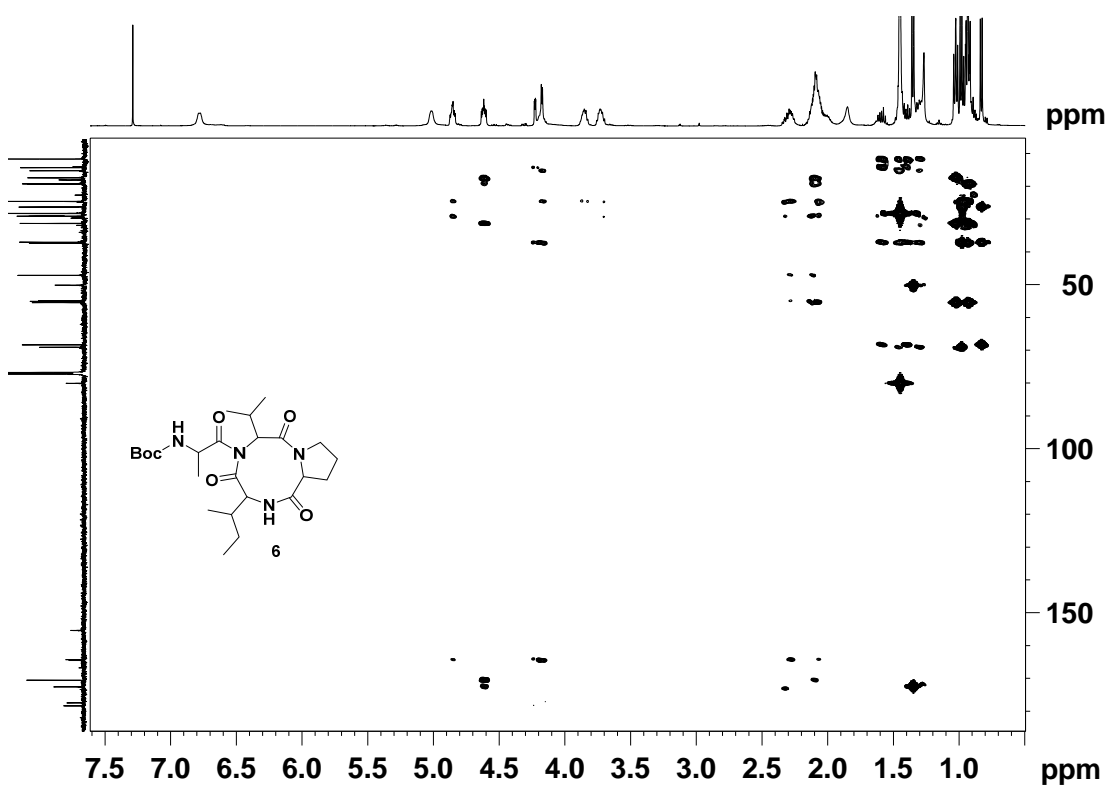


Figure 3.34 HMBC spectrum of **6** (CDCl<sub>3</sub>, 500 MHz)

### 3.16 References and Notes:

1. (a) S. W. Lowe, and A. W. Lin, *Carcinogenesis* 2000, **21**, 485. (b) G. T. Williams, *Cell*, 1991, **65**, 1097. (c) N. Modjtahedi, F. Giordanetto, F. Madeo, and G. Kroemer, *Trends Cell Biol.* 2006, **16**, 264.
2. (a) D. W. Nicholson, *Nature* 2006, **407**, 810. (b) B. A. Ponder, *Nature*, 2001, **411**, 336. (c) X.W. Meng, S.H. Lee, S. H. Kaufmann, *Curr. Opin. Cell Biol.* 2001, **18**, 66.
3. (a) P. Hersey, and X. D. Zhang, *J Cell Physiol.* 2003, **196**, 9. (b) P. Hersey, X. D. Zhang, N. Mhaidat, *Adv Exp Med Biol.* 2008, **615**, 105. (c) S. Inoue, T. Salah-EldTsuruo, M. Naito, A. Tomida, N. Fujita, T. Mashima, H. Sakamoto, N. Haga, *Cancer Sci.* 2003, **94**, 15.
4. (a) F. C. Kischkel, S. Helbardt, I. Behrmann, M. Germer, M. Pawlita, P. H. Krammer, M. E. Peter, *EMBO J.* 1995, **14**, 5579. (b) S. Fulda, K. M. Debatin, *Oncogene* 2006, **25**, 4798.
5. R. M. Kluck, E. Bossey Wetzels, D. R. Greenand, D. D. Newmeyer, *Science* 1997, **275**, 1132.
6. H. Sun, Z. Nikolovska-Coleska, J. Lu, J. L. Meagher, C.Y. Yang, S. Qiu, Y. Tomita, Y. Ueda, S. Jiang, K. Krajewski, P. P. Roller, J. A. Stuckey, S. Wang, *J. Am. Chem. Soc.* 2007, **129**, 15279. (Image courtesy for Figure 10)
7. (a) Q. L. Devraux, and J. C. Reed, *Genes Dev.* 1999, **13**, 239. (b) M. Holick, H. Gibson, R. G. Korneluk, *Apoptosis* 2001, **6**, 253. (c) S. J Martin, *Cell* 2002, **109**, 793. (d) A. M. Verhagen, D. L. Vaux, *Apoptosis* 2002, **7**, 163.
8. (a) A. M. Verhagen, E. J. Coulson, D. L. Vaux, *Genome Biology*, 2001, **2**, 3009. (b) T. Samuel, K. Welsh, T. Lober, S. H. Togo, J. M. Zapata, J. C. Reed, *J. Biol. Chem.* 2006, **281**, 1080. (c) H. Shin, M. Rensatus, B. P. Eckelman, V. A. Nunes, C. A. Sampaio, G. S. Salvesen, *Biochem. J.* 2005, **385**, 1.
9. a) R. Takahashi, Q. L. Deveraux, I. Tamm, K. Welsh, A. N. Munt, G. S. Salvesen, J. C. Reed, *J. Biol. Chem.* 1998, **273**, 7787. (b) E. Asselin, G. B. Mills, B. K. Tsang, *Cancer Res.* 2001, **61**, 1862.
10. (a) Q. L. Deveraux, R. Tahashi, G. S. Salvesen, J. C. Reed, *Nature* 1997, **388**, 300. (b) Q. L. Deveraux, E. Leo, H. R. Stennicke, K. Welsh, G. S. Salvesen, J. C. Reed, *EMBO J.* 1999, **18**, 5242. (b) H. A. Rajapakse, *Curr. Top. Med. Chem.* 2007, **7**, 966.
11. (a) C. Du, M. Fang, Y. Li, L. Li, X. Wang, *Cell* 2000, **102**, 33. (b) A. M. Verhagen, P. G. Kkert, M. Pakusch, J. Silke, L. M. Connolly, G. E. Reid, R. L. Moritz, R. J. Simpson, D. L. Vaux, *Cell*, 2000, **102**, 43.
12. P. G. Ekert, J. Silke, C. J. Hawkins, A. M. Verhagen, and D. L. Vaux, *Cell Biol.* 2001, **152**, 483.



13. (a) Z. Liu, C. Sun, E. T. Olejniczak, R. P. Meadows, S. F. Betz, T. Oost, J. Herrmann, J. C. Wu, S. K. Fesik, *Nature* 2000, **408**, 1004. (Image courtesy for Figure 11) (b) G. Wu, J. Chai, T. L. Suber, J. W. Wu, C. Du, X. Wang, Y. Shi, *Nature* 2000, **408**, 1008.
14. R. A. Kipp, M. A. Case, A. D. Wist, C. M. Cresson, M. Carrell, E. Griner, A. Wiita, P. A. Albinak, J. Chai, Y. Shi, M. F. Semmelhack, G. L. McLendon, *Biochemistry* 2002, **41**, 7344.
15. H. Sun, Z. N. Coleska, C. Y. Tang, D. Qian, J. Lu, S. Qiu, L. Bai, Y. Peng, Q. Cai, S. Wang, *Acc. Chem. Res.* 2008, **41**, 1264. (Image courtesy for Figure 12)
16. T. K. Oost, et. al. *J. Med. Chem.* 2004, **47**, 4417.
17. (a) I. Monfardini, J. W. Huang, B. Beck, J. F. Cellitti, M. Pellicchia, A. Domling *J. Med. Chem.* 2011, **54**, 890. (b) Y. Peng, H. Sun, J. Lu, L. Lin, Q. Cia, R. Shen, C. Y. Yang, Yi, S. Wang, *J. Med. Chem.* 2012, **55**, 106. (c) H. Sun, J. Stuckey, Z. N. Coleska, D. Quin, J. Meagher, S. Qiu, J. Lu, C. Y. Yang, N. G. Saito, S. Wang, *J. Med. Chem.* 2006, **49**, 7916.
18. H. Sun, Z. N. Coleska, C. Y. Yang, L. Xu, M. Liu, Y. Tomita, H. Pan, Y. Yoshioka, K. Krajewski, P. P. Roller, S. Wang, *J. Am. Chem. Soc.* 2004, **126**, 16686
19. H. Sun, Z. N. Coleska, C. Y. Tang, D. Qian, J. Lu, S. Qiu, L. Bai, Y. Peng, Q. Cai, S. Wang, *Acc. Chem. Res.* 2008, **41**, 1264. (b) H. Sun, J. Stuckey, Z. N. Coleska, D. Quin, J. Meagher, S. Qiu, J. Lu, C. Y. Yang, N. G. Saito, S. Wang, *J. Med. Chem.* 2006, **49**, 7916.
20. (a) L. Bai, D. C. Smith, S. Wang, *Pharmacol. Ther.* 2014, **144**, 82. (b) H. L. Perez, C. Chaudhry, S. L. Emanuel, C. Fanslau, J. Fagnoli, J. Gan, K. S. Kim, M. Lei, J. G. Naglich, S. C. Traeger, R. Vuppugalla, D. D. Wei, G. D. Vite, R. L. Talbott, R. M. Borzilleri, *J. Med. Chem.*, 2015, **58**, 1556.

## *Chapter 4*

### *Detailed NMR studies of Zipper peptides*



## 4.1 Introduction

### 4.1.1 Structure Determination

The molecular structures of organic compounds are determined mainly by single crystal *X-ray* and nuclear magnetic resonance (NMR) spectroscopy. In addition to these techniques there are many spectroscopic methods such as Mass spectrometry, Infrared (IR) spectroscopy, Circular Dichroism (CD), Raman spectroscopy, Ultra Violet (UV) spectroscopy, Fluorescence spectroscopy etc, that give the information about the structural and molecular property of the organic molecules. For peptides and proteins, X-ray and NMR spectroscopy are the most widely used techniques. Although X-ray diffraction provides precise structural information of proteins and peptides, it has some limitations such as difficulties associated with crystallization and also, it gives only a snapshot of image which is in static form. On the contrary, the NMR spectroscopy provides information about the structure as well as the dynamics of proteins and peptides. Using NMR spectroscopy one can carry out the detailed structural studies of any bio-molecules dissolved in aqueous solution, which is similar to the physiological condition and thus it provides insight into the structural and dynamics over the wide range of time scales.

### 4.1.2 One dimensional NMR spectroscopy:

One dimensional NMR spectrum is commonly used for routine analysis of compounds, this includes regular ( $^1\text{H}$ ) Proton,  $^{13}\text{C}$  Carbon and 1D spectrum of other NMR active nuclei.

**Regular 1D experiment:** It consists of two parts, *viz.* preparation and detection (Figure 4.1).<sup>1,2</sup>

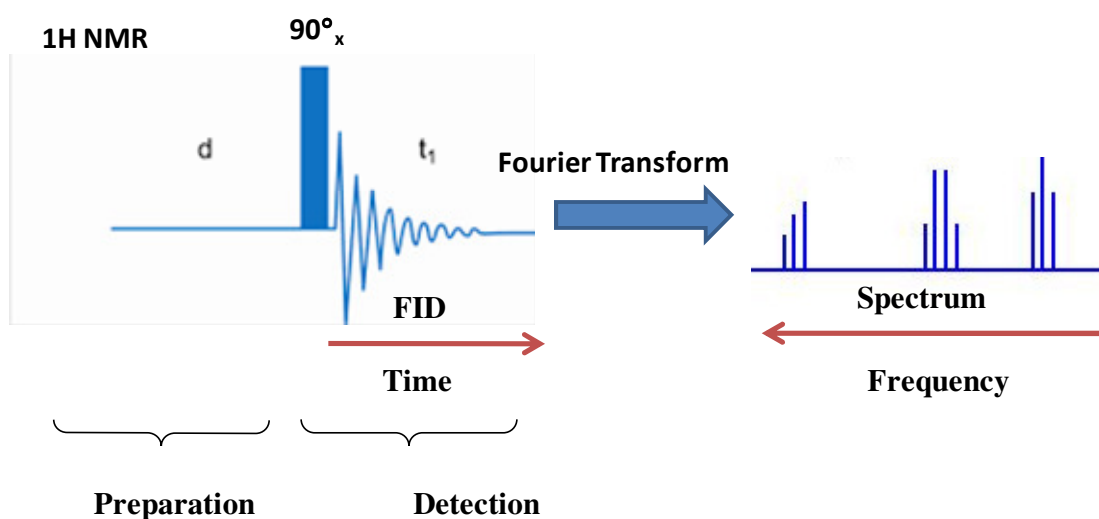


**Figure 4. 1** Schematic representation of 1D NMR

During preparation period the spin systems are in thermal equilibrium state, an rf signal of sufficient power (near to 50 W) is transmitted (pulse) for a short period (a few microseconds), in order to move the magnetization vector from the z-axis to the x,y-plane. After applying a  $90^\circ$  pulse all magnetization are placed in the transverse plane. The signal that evolves due to precession of the magnetization vector is measured after the pulse during the detection period and the signal also decays with time (Free induction decay, FID) due to  $T_2$  relaxation. During this process, the vector also returns to equilibrium on the z-axis (due to  $T_1$  relaxation). The measured FID is the variation of magnetization with time and it is incomprehensible. Therefore, to make it understandable, the FID is converted into readable frequency domain spectrum, using a mathematical process called the Fourier transformation (FT). Usually, the experiments is repeated several times and summed up the data to increase the signal height or to get better signal to noise ratio (S/N).

The spectral parameters such as the chemical shift ( $\delta$  in ppm), the indirect dipole-dipole coupling or scalar coupling (J coupling), relaxation times, longitudinal ( $T_1$ ) and transverse ( $T_2$ ) can be determined from 1D NMR studies.

#### 4.1.3 Two dimensional NMR spectroscopy

Early NMR studies of biomacromolecules were performed on relatively simple low molecular weight model systems using one-dimensional (1D) methods, however higher molecular weight systems are difficult to interpret due to signal overlapping.

Multidimensional NMR techniques provide elegant tools for unambiguous resonance signal assignment for biomacromolecules such as proteins, peptides and sugars. Two dimensional NMR was first proposed by Jean Jeener in 1971,<sup>3</sup> later Ernst in 1976 developed and demonstrated two dimensional NMR.<sup>4,5</sup> These 2D NMR techniques give the data plotted in a space defined by two frequency axes, and it is easier to interpret and often more informative. To obtain structural information from the NMR spectral parameters, a variety of 2D experiments have been developed.

In two-dimensional NMR, the signal is recorded as a function of two time variables,  $t_1$  (evolution time) and  $t_2$  (detection time) and the resulting data is Fourier transformed twice to yield a spectrum which is a function of two frequency variables. All 2D NMR experiments have the same four stages (Figure 4.2), *viz.* preparation period, evolution period ( $t_1$ ), mixing period and detection period ( $t_2$ ).



**Figure 4.2** General pulse scheme of any 2D NMR experiment

During preparation period, the sample is excited by one or more pulses. The resulting magnetization is allowed to evolve for the first time variable  $t_1$  followed by another period, called the mixing time, which consists of a further pulse or pulses. After the mixing period the signal is recorded as a function of the second time variable,  $t_2$ , the detection or acquisition time. Recording of a 2D data set involves repeating of the pulse sequence for increasing values of  $t_1$  and recording free induction decay as a function of  $t_2$  for each value of  $t_1$ .

#### 4.1.4 Types of 2D NMR spectroscopy

a) Homonuclear:

Through bond: COSY, TOCSY

Through Space: NOESY, ROESY

b) Heteronuclear correlation

One-bond correlation: HSQC, HMQC

Long-range correlation/Multiple bond correlation: HMBC.

#### 4.1.5 Correlation Spectroscopy (COSY):

COSY<sup>7</sup> is the simplest 2D NMR experiment. It correlates one proton to another proton *via* J coupling that generated from 2-bond or 3-bond.

#### 4.1.6 Total Correlation Spectroscopy (TOCSY):

TOCSY<sup>8</sup> is useful for large molecules with many separated coupling networks such as peptides, proteins, oligosaccharides and polysaccharides. It is a homonuclear experiment, used to establishment of connectivity between remote nuclei belonging to the same spin system. It differs from COSY at the mixing pulse; here spin lock ( $90^\circ$ - $\tau$ - $180^\circ$ - $\tau$ - $90^\circ$ ) pulse train MLEV-17 is used.<sup>9, 10</sup>

#### 4.1.7 Heteronuclear Correlation Spectroscopy:

Coherence transfer between unlike spins example  $^{13}\text{C}$  or  $^{15}\text{N}$  and  $^1\text{H}$  can be observed in 2D heteronuclear- correlation experiments. In the HETCOR experiments,<sup>11</sup> the spectrum maps the chemical shift of each X nucleus ( $^{13}\text{C}$  or  $^{15}\text{N}$ ) to the chemical shift of directly attached protons (HSQC<sup>12</sup> experiment) or indirectly attached protons (protons attached to different carbons by three/two bonds in HMBC<sup>13</sup> experiment).

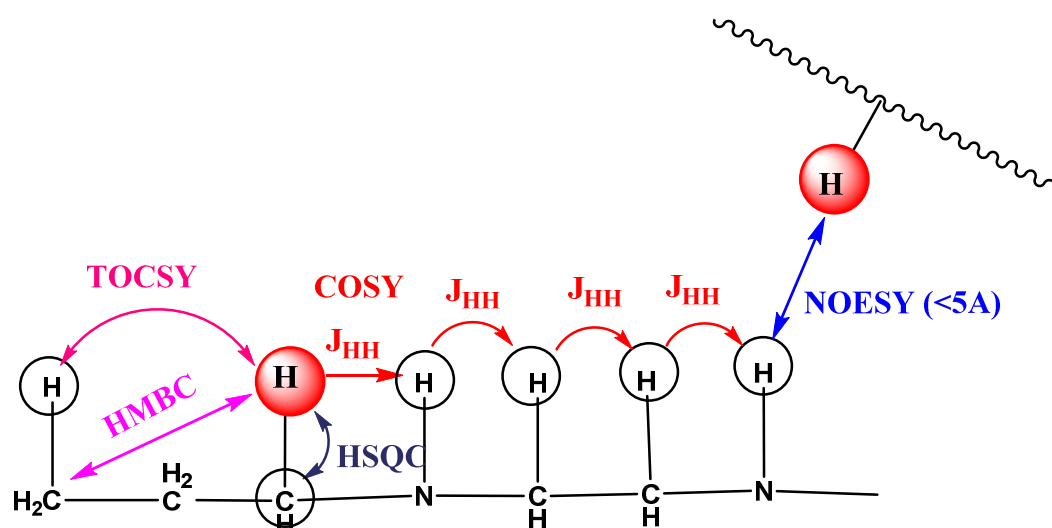


**Figure 4.3** Information extracted from different 2D NMR Experiments.

#### **4.1.6 Nuclear Overhauser Effect Spectroscopy (NOESY)**

The NOESY spectrum uses the nuclear Overhauser effect (nOe) to provide information about the spatial proximity of nuclei (typically  $^1\text{H}$ ). This spectroscopy is the most powerful technique for obtaining structural information of molecules in solution. The NOESY experiment<sup>14</sup> is used for defining molecular geometry, stereochemistry, conformation, and biomolecular structure and interactions. The nuclear Overhauser effect (nOe) is the cross-relaxation of spin polarization from one spin to another induced by dipole-dipole interaction. Therefore, this method is used for investigation of cross-relaxation and chemical exchange processes. Since its amplitude depends on the separation of the two spins, it can be used to measure the distance between them. The nuclear Overhauser enhancement can be positive or negative, depending on the correlation time of the molecules. It is positive for small molecules and negative for large molecules (macromolecules). The nOe for molecules of intermediate size are usually weak but, it can also be zero (Figure 4.4)

#### **4.1.7 Rotating-frame Overhauser Spectroscopy (ROESY)**

In ROESY experiment,<sup>15</sup> cross-relaxations measurements are carried out in the rotating-frame with spin-locked magnetization and it means that NOE in the transverse plane (ROE) is always positive (no nulling condition as in NOESY-type experiments) and, in addition, chemical exchange can always be distinguished which is negative.

#### **4.1.8 Molecular Weight and Maximum NOE/ ROE**

The maximum attainable peak intensities or peak volumes depend on the molecular size and the frequency of the spectrometer.



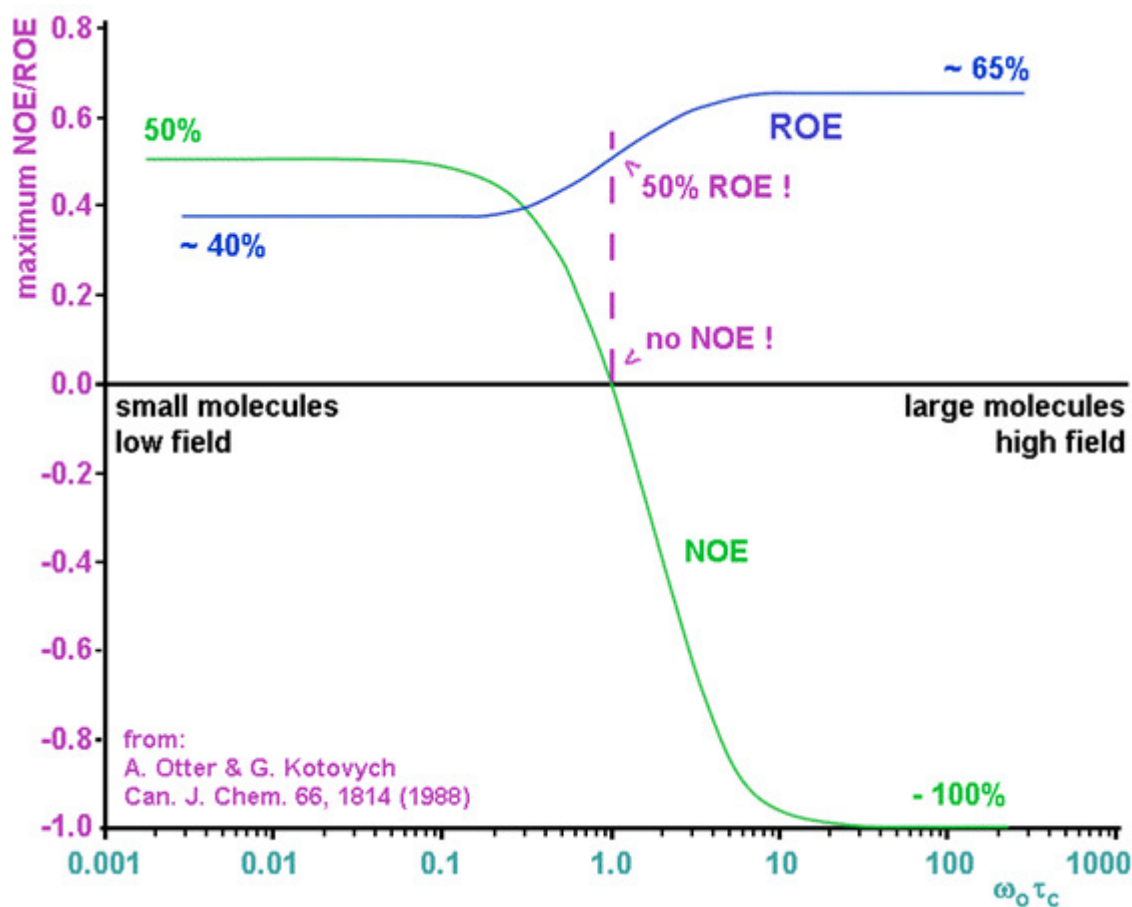


**Figure 4.4** Comparison of ROESY and NOESY build up with molecular weight or product of the field of the magnet ( $\omega$ ) and the correlation time of the compound ( $\tau_c$ )

The diagram (Figure 4.4) illustrates that for certain combinations of field (e.g.  $\omega_0 = 700$  MHz) and molecular size (expressed in the correlation time  $\tau_c$ ), the nOe can be zero even when the protons are very close in space. In this case ROESY experiment is useful for getting the good and precise data.

#### 4.1.9 Constraints Generation:

NMR is the only technique that can determine peptide and protein structures in solution. The inter-nuclear distances and dihedral angles are the most often used constraints for generating a three dimensional structure of peptides and proteins.

##### 4.1.9.1 Distance Constraint

In contrast to X-ray crystallography, NMR primarily measures data that locally describe the position of atoms relative to each other. Most important parameter for the

determination of 3D structures of peptides and proteins is inter proton distance calculated from the nuclear Overhauser enhancement (nOe). Comparison of the cross-peak volume integrals in a quantitative NOESY/ ROESY is used for measurement of the distance between the protons. The strength of the nOe or rOe signal is inversely proportional to the sixth power of the distance between the atoms. Generally, a distance of 1.8 Å between the geminal (methylene) protons or 2.44 Å between the vicinal protons for aromatic protons are taken as standard reference ( $r_{\text{ref}}$ ) with standard intensity of cross peaks ( $\eta_{\text{ref}}$ ). All distant constraints ( $r_{\text{obs}}$ ) can be calculated using following equation.

$$\eta_{\text{ref}} / \eta_{\text{obs}} = (r_{\text{obs}} / r_{\text{ref}})^6$$

$\eta_{\text{ref}}$  = Volume integral of reference cross peak

$\eta_{\text{obs}}$  = Volume integral of observed cross peak

This relationship between cross peak intensity and the distance is not exact, therefore, upper and lower bound are calculated for providing distance constraints by adding or subtracting 10% to the calculated distance  $r_{\text{obs}}$ . These calculated NOE depended distances are divided into Strong (1.8-2.5 Å), Medium (2.5-3.5 Å), and Weak (3.5-5 Å).

#### 4.1.9.2 Angle Constraints

The three bond (vicinal)  $J$ -coupling constant is depended on the torsion angles ( $\theta$ ) between the coupled spins. The Karplus equation<sup>16</sup> provides a relation between  $J$  and  $\theta$  as shown in the following equation.

$${}^3J = A \cos^2(\theta) + B \cos(\theta) + C$$

Where A, B and C are constants and which are empirically derived parameters whose values depend on the atoms and substituent's involved. Particularly, for the peptides the Karplus curve (Figure 4.5) is derived as follows.

$${}^3J_{\text{NH-C}\alpha\text{H}} = 6.4 \cos^2 |\Phi-60| + 1.4 \cos |\Phi-60| + 1.9$$

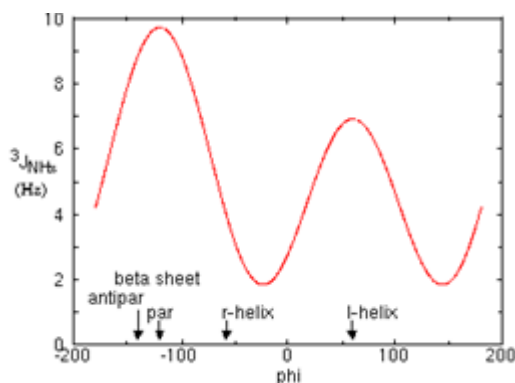


**Figure 4.5** Karplus curve showing relation between dihedral angle vs  $^3J$  values.

#### 4.1.10 Hydrogen bonding

Hydrogen bonding<sup>17</sup> is an important constituent for stabilizing the secondary and tertiary structure of proteins and peptides. There are two types of hydrogen bonds, intermolecular hydrogen bond (H-bond present between two atoms of two different molecules) and intra molecular hydrogen bond (H-bond present between two atoms of the same molecule or within the molecule). For peptides, the amide protons are generally involved in the hydrogen bonding. To verify the involvement of amide NH in the intra molecular H-bonding, NMR experiments such as variable temperature studies (in non polar or polar solvent), DMSO- $d_6$  titration studies, time dependent methanol (MeOD) exchange or deuterium ( $D_2O$ ) exchange studies, and dilution studies, in which chemical shift change of amide proton is measured with the concentration of the peptide entity, are employed. The smaller chemical shift change (VT, Dilution and DMSO titration studies) or the more exchange time (Deuterium exchange) for amide protons suggests the involvement of strong intra molecular hydrogen bonding.

#### 4.1.11 Molecular Dynamics

Molecular dynamics<sup>18</sup> is the most versatile computational method to calculate the time dependent behaviour of a bio-molecular system. MD simulations can provide detailed information of the fluctuations and conformational changes of proteins, peptides

nucleic acids. This method is used to investigate the structure, dynamics, thermodynamics of molecules and their complexes.

The steps involved in the MD simulations are as follows:

Step1- Start with extended structure

Step2- Minimize using restraints (or simulated annealing process)

Step3- Start MD simulation using minimized structure

Step4- Equilibration and Dynamics simulation

Step4- Collection of the trajectories for further analysis

#### **4.1.12 Ant–Pro zipper peptides:**

A new class of synthetic Ant–Pro ( $\alpha\beta_n$ ) based zipper peptide which showed its three-dimensional zipper like structures stabilized by hydrogen bonding, aromatic stacking, and backbone chirality (Figure 4.6).<sup>20</sup> Structural studies were carried out in both solid and solution state confirmed the zipper-like structural architecture assumed by the synthetic peptide which makes use of unusually remote inter-residual hydrogen-bonding and aromatic stacking interactions to attain its shape. The effect of chirality modulation and the extent of noncovalent forces in the structure stabilization have also been comprehensively explored *via* single-crystal X-ray diffraction and solution-state NMR studies.

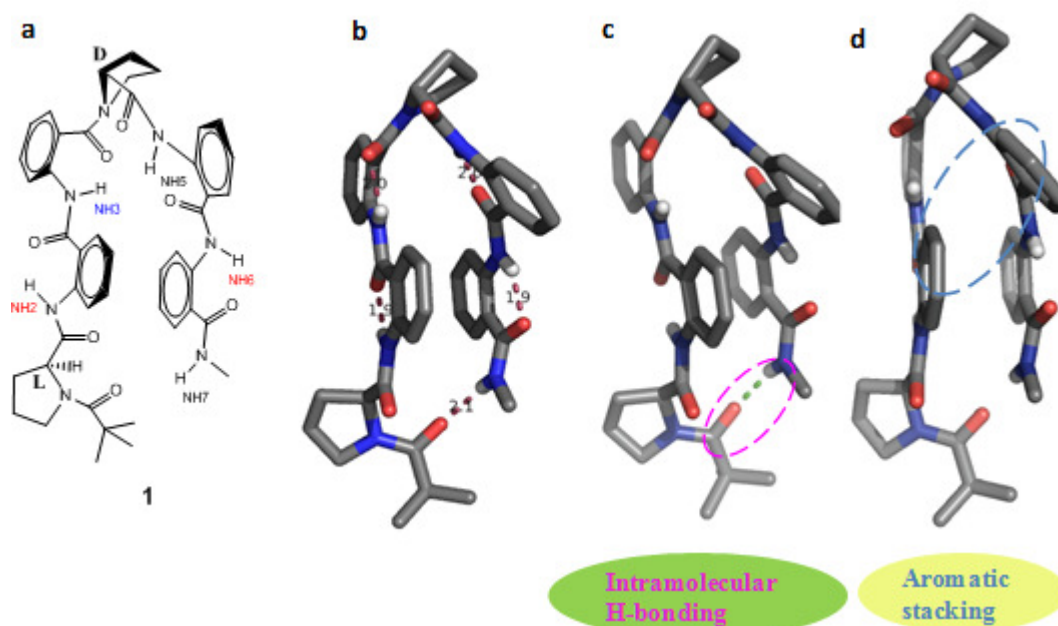


**Figure 4.6** a) Molecular structure, b) Crystal structure of **1**. The non covalent forces which stabilize the zipper architecture, c) Highlighted the long ranged 26 member, terminal hydrogen bonding and d) *Edge to face* aryl stacking.<sup>20, 21</sup>

## 4.2 Objective

The objective of this chapter is to carry out structural studies of Ant-Pro based zipper architectural peptides in solution state. First part of this chapter was to study the effect of ratio variation of Pro:Ant from 1:2 to 1:4 (decamer **2**) and in absence of C-terminal amide (hexamer **3**) on their conformation, using solution state NMR and MD simulation studies (Figure 4.7a). The second part of this work was the solution state NMR studies on replacement of N-terminus proline by flexible (Ala) and constrained (Aib) amino acid residues in the Ant-Pro zipper motif (Figure 4.7b).

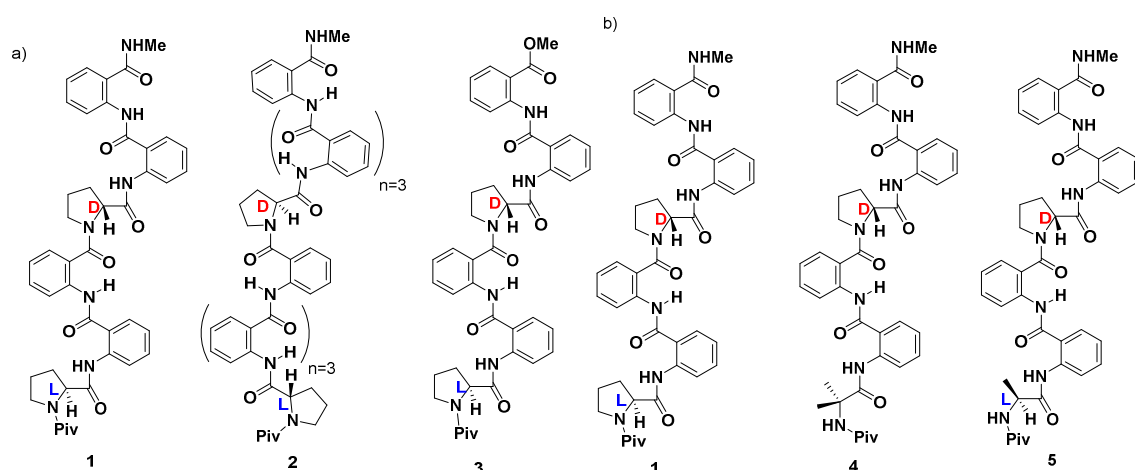


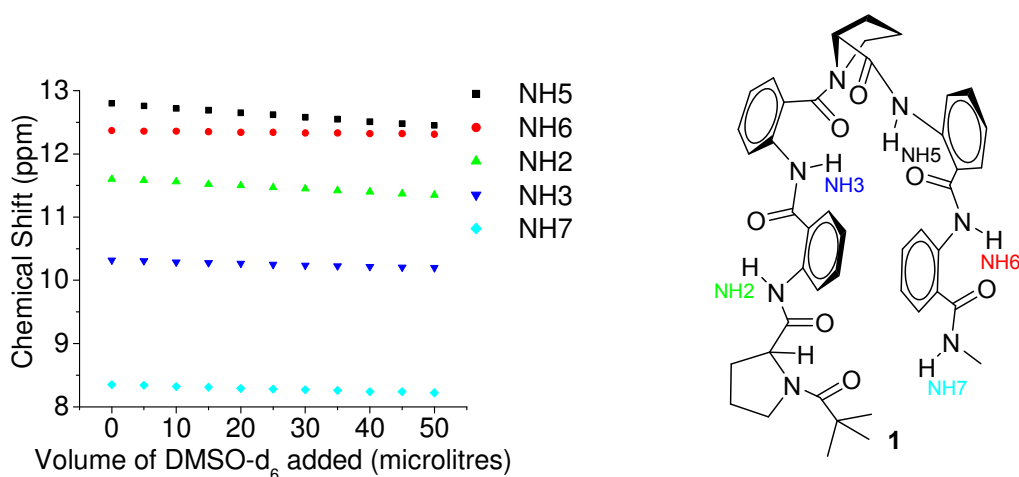
**Figure 4.7** Structures of zipper peptides which are under taken for solution state conformational studies. a) Solution state NMR studies of oligomers 1, 2 and 3; b) Comparative NMR studies of oligomers 2 and 3 with 1.

### Part A: Solution state conformational investigation of 1, 2 and 3

#### 4.3 NMR studies of 1, 2 and 3:

We carried out DMSO- $d_6$  titration studies, variable temperature studies and deuterium (MeOD) exchange studies were carried out for evaluating the *intra* molecular hydrogen bonds in the following peptides 1, 2 and 3 (Figure 4.8 to 4.10 and Tables 4.1 to 4.3).

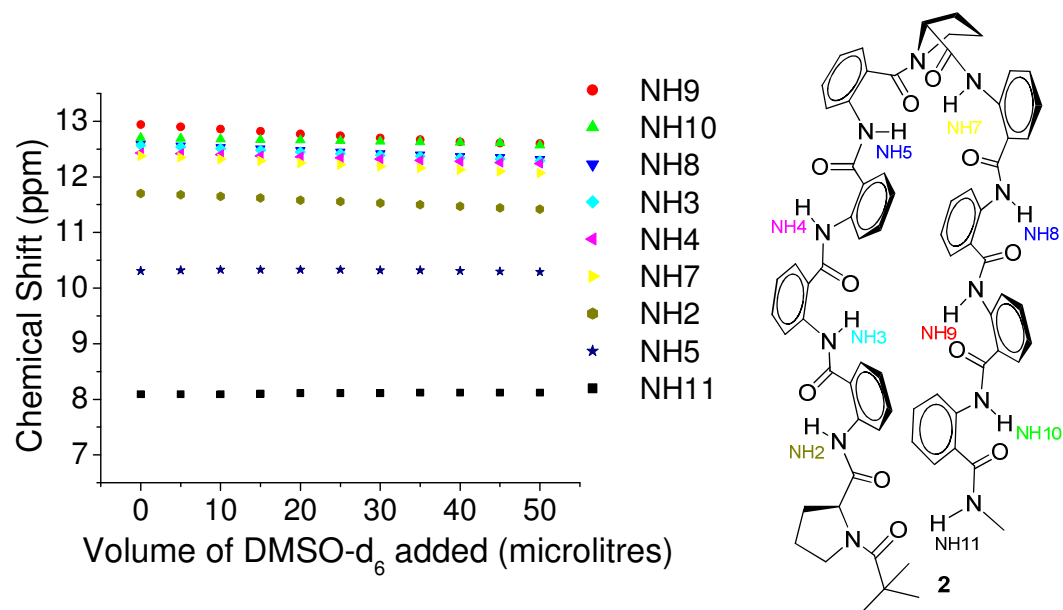
##### 4.3.1 Titration studies of 1, 2 and 3



**Figure 4.8** Titration study plot (chemical shift vs volume of DMSO- $d_6$  added) of hexapeptide 1 (5 mM, 400 MHz)

**Table 4.1** Titration study of hexapeptide 1 in CDCl<sub>3</sub> (5mM) with DMSO-*d*<sub>6</sub>.

Amide protons	NH5	NH6	NH2	NH3	NH7
Chemical Shift Change after addition of 50 $\mu$ l of DMSO- <i>d</i> <sub>6</sub>	0.35	0.06	0.25	0.12	0.13

**Figure 4.9** Titration study plot (chemical shift vs volume of DMSO-*d*<sub>6</sub> added, See Table 4.5 experimental section) of decapeptide 2 (5 mM, 400 MHz)**Table 4.2** Titration study of decapeptide 2 in CDCl<sub>3</sub> (5mM) with DMSO-*d*<sub>6</sub>

Amide protons	NH2	NH3	NH4	NH5	NH7	NH8	NH9	NH10	NH11
Chemical Shift Change after addition of 50 $\mu$ l of DMSO- <i>d</i> <sub>6</sub>	0.42	0.23	0.19	0.02	0.31	0.27	0.32	0.13	0.03

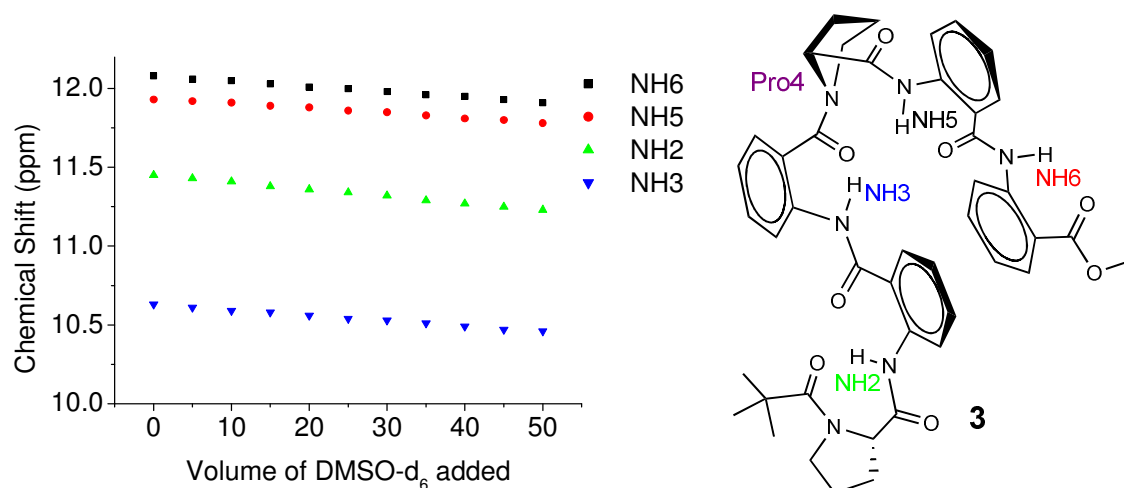


**Figure 4.10** Titration study plot (chemical shift vs volume of DMSO- $d_6$  added, See Table 4.6 experimental section) of hexapeptide **3** (5 mM, 400 MHz)

**Table 4.3** Titration study of hexapeptide **3** in CDCl<sub>3</sub> (2mM) with DMSO- $d_6$

Amide protons	NH2	NH3	NH4	NH5
Chemical shift change after addition of 50 $\mu$ l of DMSO- $d_6$	0.22	0.17	0.17	0.15

### 4.3.2 Temperature variation study

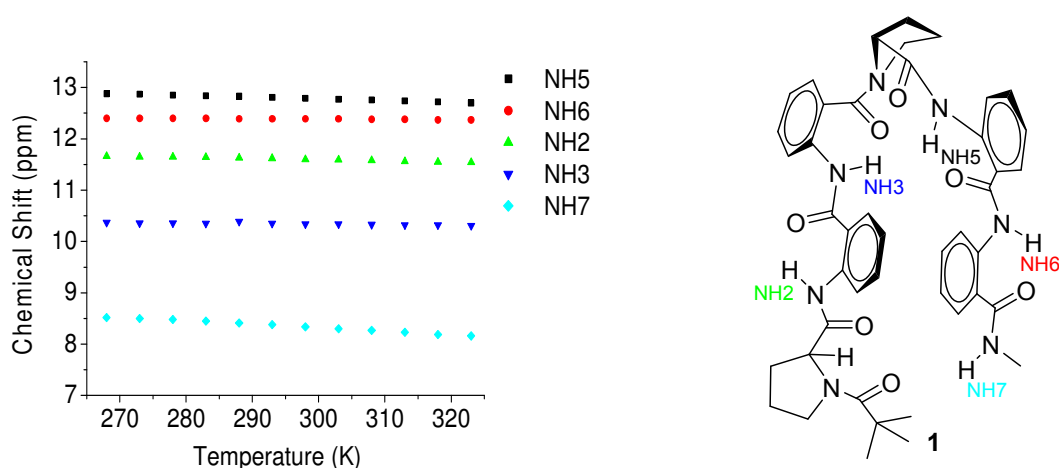


**Figure 4.11** Temperature variation study plot (chemical shift vs temperature, Table 4.7, experimental section) of hexapeptide **1** (5 mM, 400 MHz)



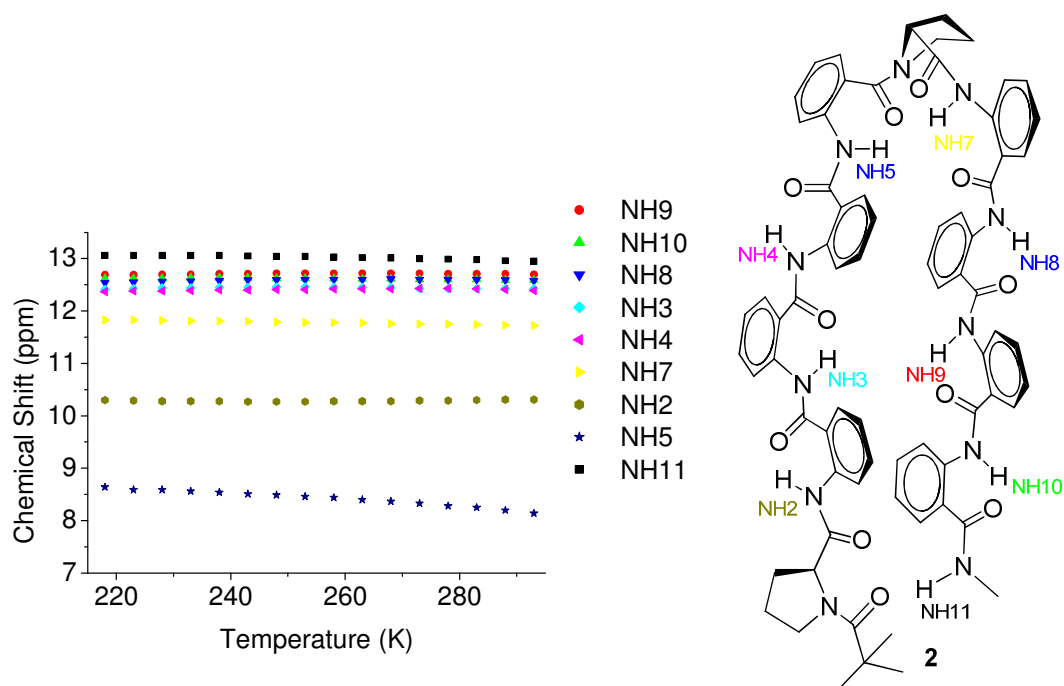


**Figure 4.12** Plot of Temperature vs Chemical shift (Table 4.8, experimental section) of amide protons in the oligomer **2**

The small chemical shift change in the amide protons in DMSO- $d_6$  and V.T studies suggests all amide protons are involved in the *intra*-molecular hydrogen bonding in these systems.

#### 4.3.3 H/D exchange studies study in Methanol- $d_4$ :

Deuterium exchange of the amide protons (NH/D) in **1**, **2** and **3** was studied by dissolving the compound in  $\text{CDCl}_3$  (0.4 ml) and methanol- $d_4$  (0.1 ml) at 400 MHz. The experiment was started instantly after the dissolution of compound using the following parameters: number of transients = 16, relaxation delay = 1 sec, flip angle =  $30^\circ$  and temperature at 298 K. A stacked plot of partial (amide region)  $^1\text{H}$  NMR spectra at different time intervals is shown *vide infra*.

The amide protons could not be completely exchanged even after prolonged time (>22 h), (Figure 4.13 to 4.15) which suggests the strong confirmation for the *intra*-molecular nature of H-bonding present in all oligomer **1**, **2** and **3**.

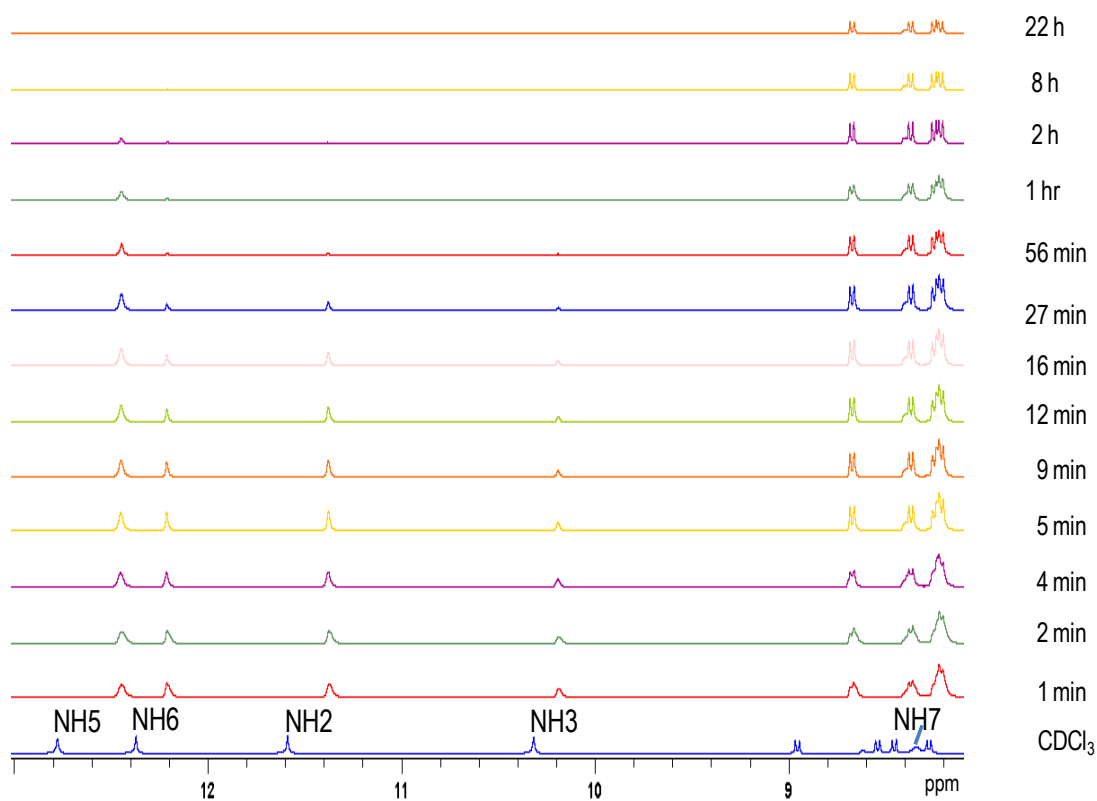


Figure 4.13 H/D Exchange of hexapeptide 1 (400MHz,  $\text{CDCl}_3$  + methanol- $d_4$ ).

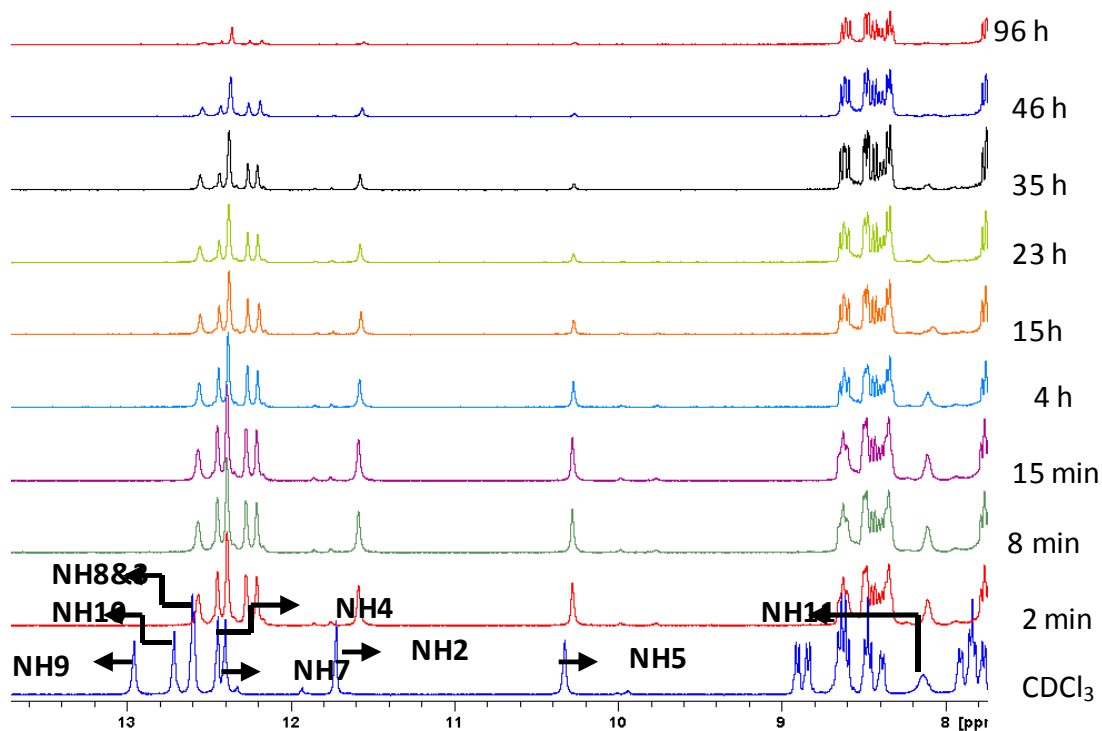
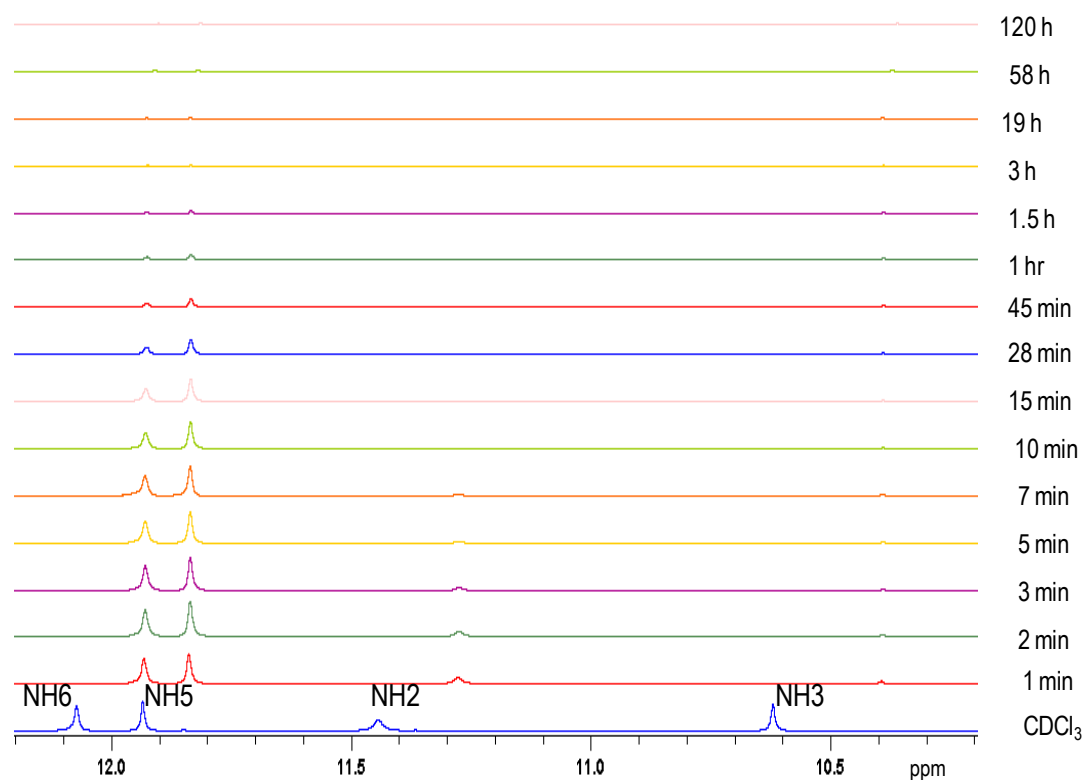


Figure 4.14 H/D Exchange of hexapeptide 2 (400MHz,  $\text{CDCl}_3$  + methanol- $d_4$ ).



**Figure 4.15** H/D Exchange of hexapeptide **3** (400MHz, CDCl<sub>3</sub> + methanol-*d*<sub>4</sub>).

### 4.3.4 2D NOESY/ ROESY analysis

To evaluate the solution-state NMR based structure, the signals were assigned using a combination of 2D experiments such as COSY, HSQC, HMBC, TOCSY and NOESY/ ROESY (See experimental section of this chapter).

#### 4.3.4.1 2D NOESY Spectral analysis of 1

The characteristic long-range inter-residual nOes are observed between the groups placed at the termini (C42H/C40H and C42H/NH7) are some of the diagnostic dipolar coupling interactions that clearly indicated the fact that the fully folded conformation in the solid-state is clearly prevailed in the solution-state as well. Other characteristic nOes which support the folded conformations were the dipolar interactions between amide NH3/NH5, P1 $\alpha$ H/C35H, C10H/C40H, C10H/NH5 and C10H/NH6. Solution-state NMR also supported an *edge-to-face*<sup>19</sup> stacking interaction faced by C10H (Ant2) causing the

proton to appear relatively up field at  $\delta$  6.1 ppm. Distinctive nOes that validate the stacking interactions are between C10H/C30H and C31H (Figure 4.16).

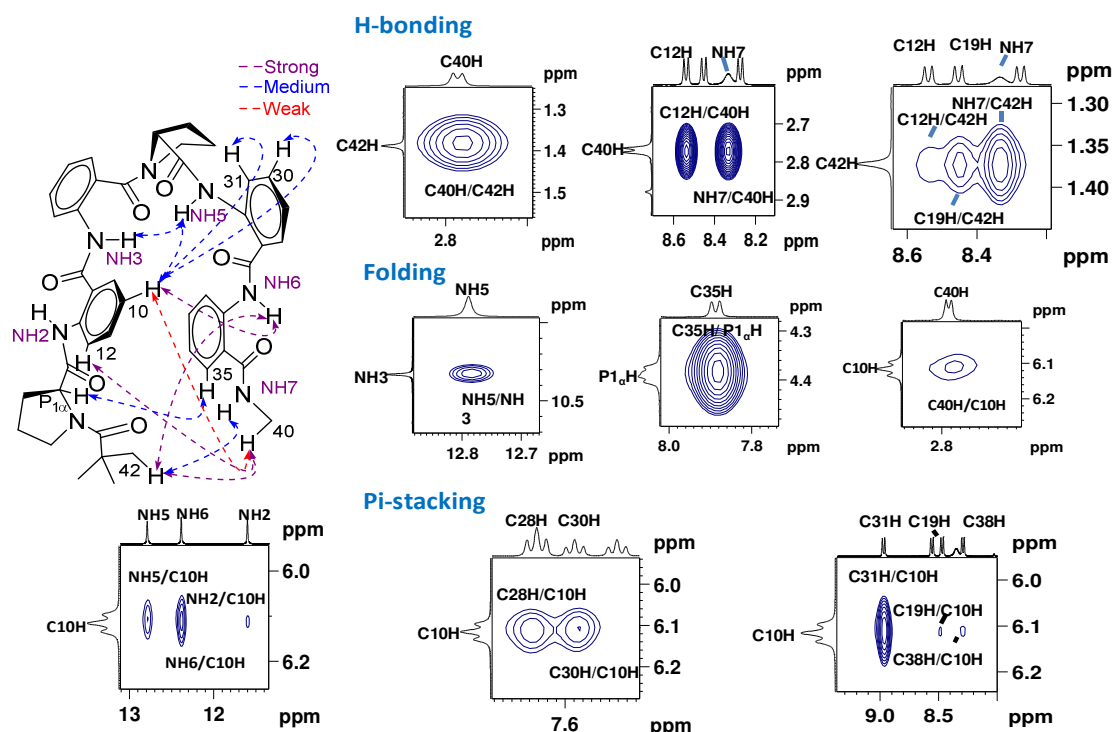


**Figure 4.16** 2D NOESY extracts of **1** (500 MHz, CDC13). The full NOESY spectrum is given in Figure 4.31, Experimental section

#### 4.3.4.2 2D ROESY Spectral analysis of **2**

The distinctive long-range inter-residual nOes are observed between the termini groups C68H/C70H and NH11/C70H (Figure 4.17a,b) and are some of the characteristic dipolar coupling interactions which unambiguously confirmed its long range *inter-residual* 42 membered terminal hydrogen bonding and folded zipper architecture in the solution-state. The folded confirmations are further supported by the characteristic nOe interactions between C12H/C68H, NH2/C68H and C63H/P1 $\alpha$ H (Figure 4.17d,e,f). Aromatic stacking (*edge-to-face*) interactions were also supported by solution-state NMR studies. In the  $^1\text{H}$  NMR spectrum, two aryl protons appear comparatively up field at  $\delta$  6.88 ppm and 6.48 ppm for C10H and C24H respectively owing to stacking interactions.

The diagnostic nOes that authenticate the stacking interactions between NH10/C10H and C45H/C24H (Figure 4.17k,l).

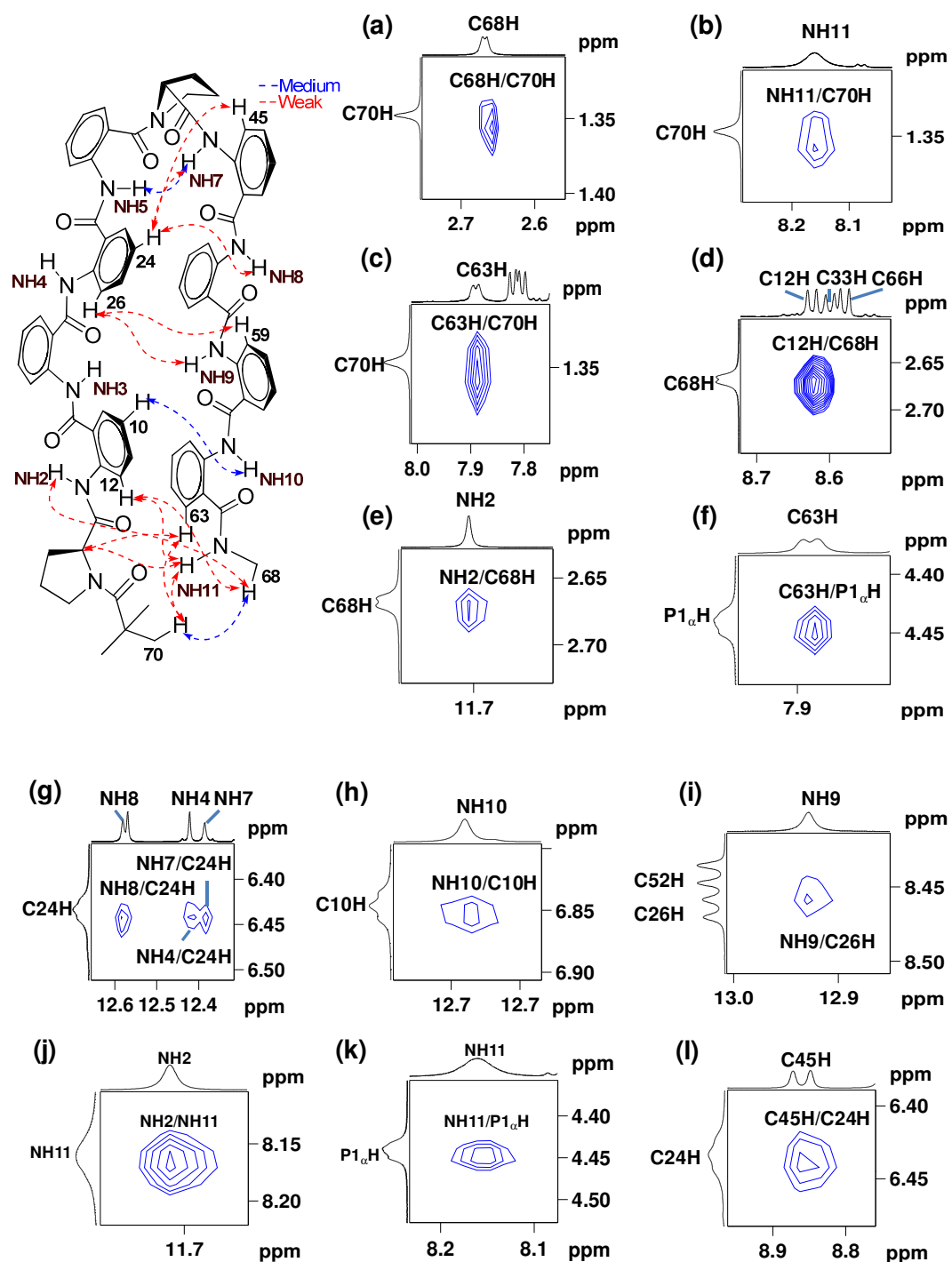


**Figure 4.17** 2D ROESY extracts of **2** (700 MHz, CDCl<sub>3</sub>). The full ROESY spectrum is given in Figure 4.36 Experimental section

## 4.3.4.3 2D NOESY Spectral analysis of 3

Remarkably, the diagnostic terminal nOe interactions which were present in **1** and **2** were clearly absent in **3**, which suggest fraying of the termini (Figure 4.18). The pivaloyl group attached to Pro1 experienced fraying, and it was confirmed from the strong nOe it experiences with C19H (Ant3). Folding induction at Ant-Pro segment remained intact similar to **1** and **2**, leading to similar diagnostic nOe between NH3/NH5 (Figure 4.18). Another strange nOe interaction that supported the staggered conformation of the structures is C16H/C38H. The effect of aromatic interactions remains noticeable in **3**, as weak nOe cross peak was observed between C10H/C31H, which suggests presence of stacking effect in **3**. This result demonstrated that the existence of weak *edge-to-face* aromatic interactions failed to bring remote H-bonding sites into proximity, consequently evading the zipper architecture.

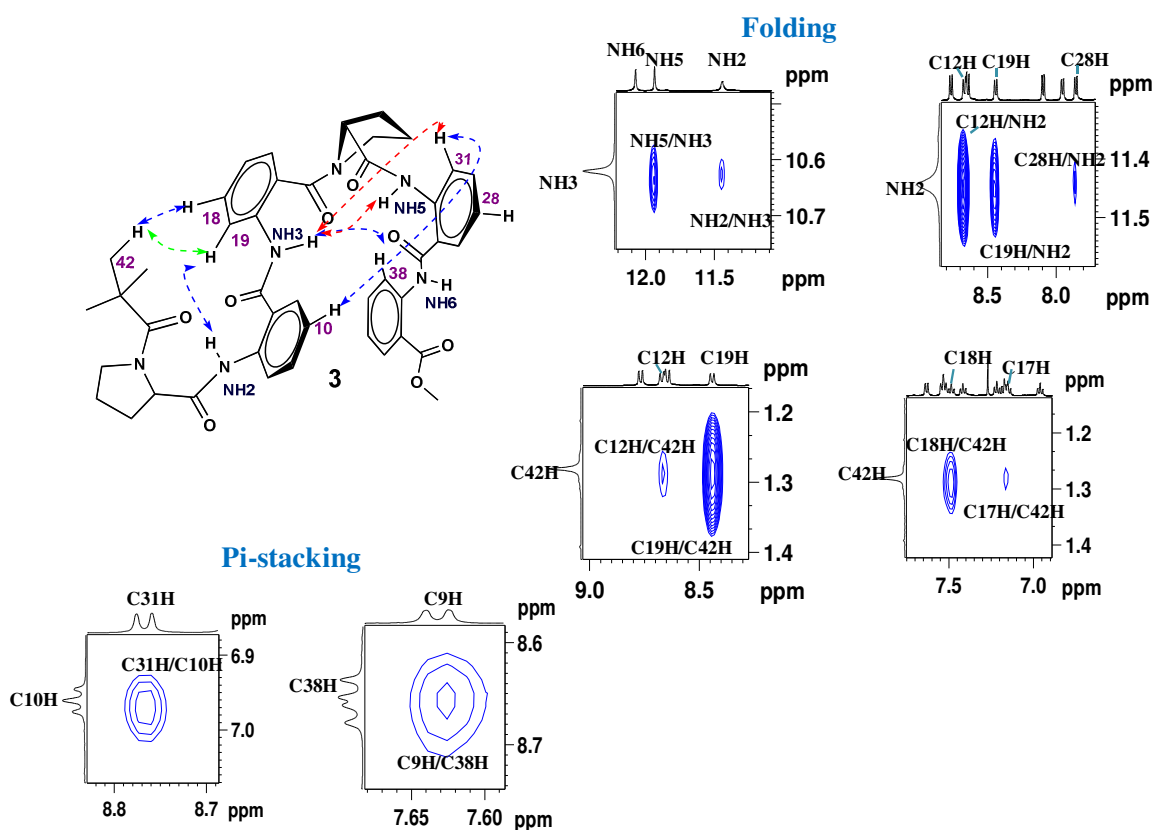


**Figure 4.18** NOESY extracts of **3** (500 MHz, CDCl<sub>3</sub>). The full NOESY spectrum is given in Figure 4.41, Experimental section

#### 4.4 MD simulation studies

MD simulations of **2** and **3** were done using Insight II (97.0)/Discover program on a Silicon Graphics Octane workstation. MD simulations were employed all the restraints, excluding the H-bond restraint using a simulated annealing protocol. Minimization of structures was done with steepest decent, then using conjugate gradient methods for 10,000 iterations each. The energy minimized structures were then used to MD simulations.

##### 4.4.1 MD simulation studies of **2**

For deca-peptide **2**, the minimum energy structures were equilibrated for 50,000 ps and molecular dynamics was later carried out for 50,000 ps at 300 K, with a step size of 50,00,000 fs with dielectric constant for CDCl<sub>3</sub> as 4.7. The superimposed structures were displayed low RMSD values (<0.2 Å). Distance constraints used in MD calculations for decamer **2** derived from ROESY experiment are given in Table 4.11.

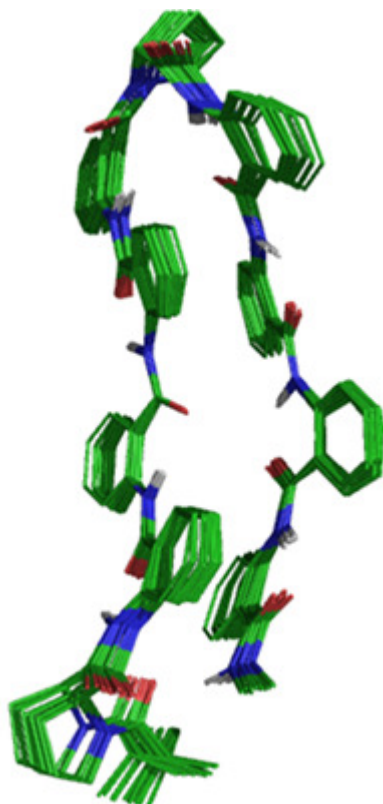


**Figure 4.19** Stereo view of superimposed MD simulated 20 minimum energy structures for deca peptide **2**. (Hydrogens, except the polar amide hydrogens are omitted for clarity).

#### 4.4.2 MD simulation studies of **3**

For hexa peptide **3**, the minimum energy structures were equilibrated for 10,000 ps and molecular dynamics was carried out for 10,000 ps at 300 K, with a step size of 1,00,000 fs. Distance restraints were used in MD calculations for hexamer **3** derived from NOESY experiment are given in Table 4.12.

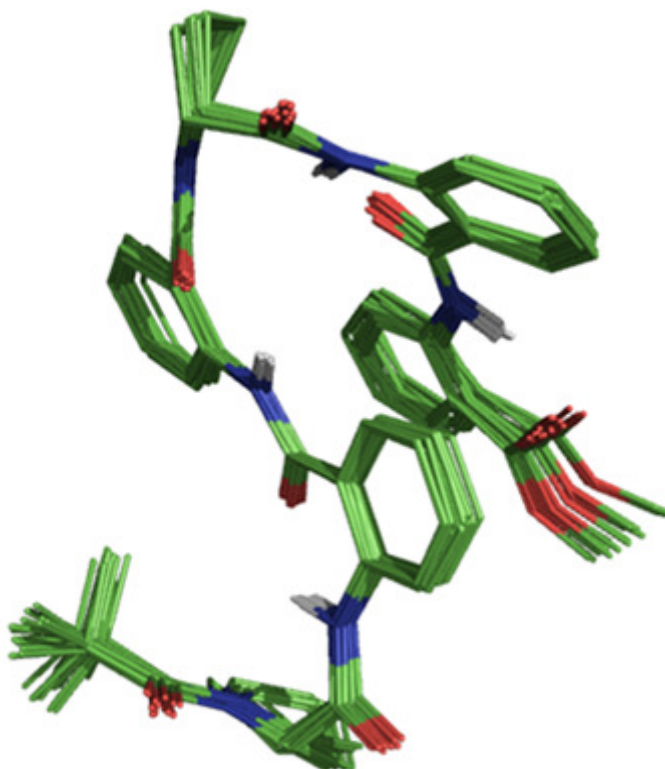


**Figure 4.20** Stereoview of superimposed MD simulated 20 minimum energy structures for peptide **3** (Hydrogens, except the polar amide are omitted for clarity).

#### 4.5 Conclusion of NMR studies of **1**, **2** and **3**

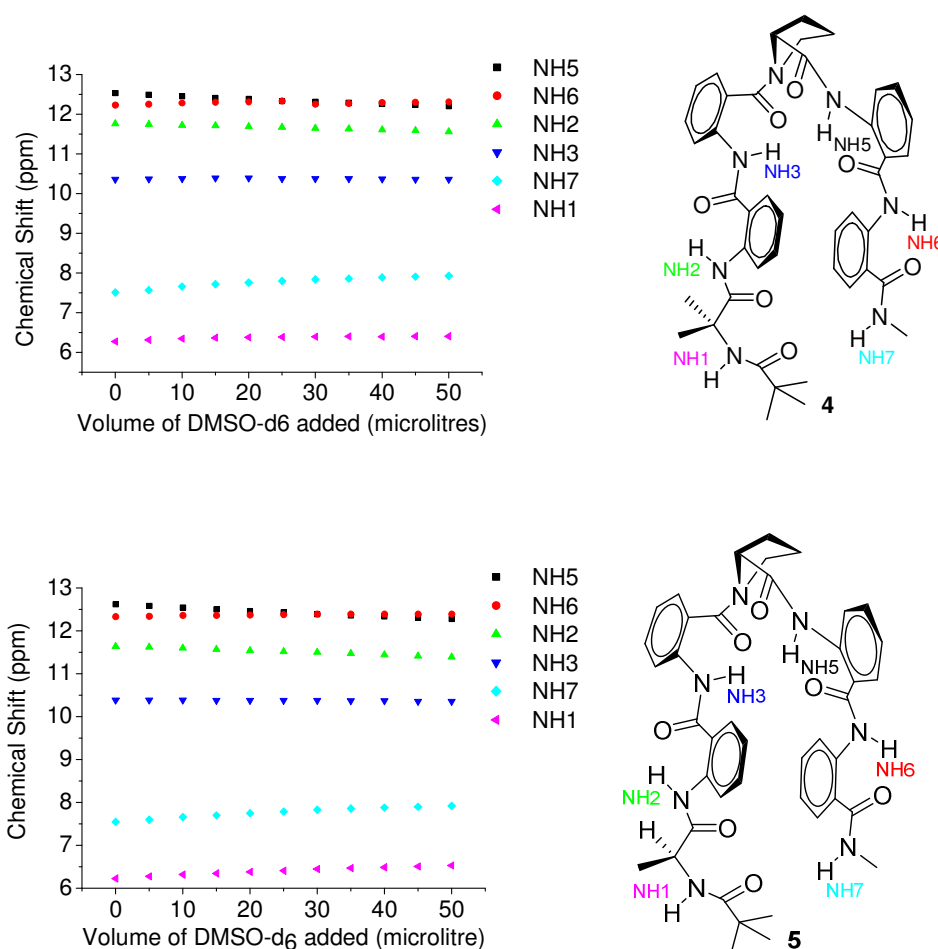
This solution state structural study reveals the presence of folded architecture stabilized by complementary aromatic interactions and typically large remote inter-residual H-bonding interactions completely coequal the solid state conformation (crystal structure of **1**). In the higher oligomer, peptide **2** exhibits a folded conformation involving 46-membered remote H-bond. While in the absence of hydrogen bond donor (in peptide **3**) folded architecture remains unchanged but fraying of the termini betided.<sup>20</sup>



## Part B: Comparative NMR studies of 4 and 5 with 1

## 4.6 NMR studies of 4 and 5

For evaluating the presence of *intra* molecular hydrogen bonds in the peptides 4 and 5, DMSO- $d_6$  titration studies (Figure 4.21) and deuterium (MeOD) exchange studies (Figure 4.22 and 4.23) were performed.

4.6.1 DMSO- $d_6$  titration studies of 4 and 5

**Figure 4.21** DMSO- $d_6$  titration studies (Tables 4.9 and 4.10, experimental section) of 4 (above) and 5 (below)

This DMSO- $d_6$  titration experiment (Figure 4. 21) suggests the presence of weaker terminal *intra*-molecular hydrogen bonding interaction as revealed by the larger chemical shift variation for NH7 about 0.42 ppm and 0.37 ppm for hexapeptide 4 and 5

respectively, which was 0.17 ppm for the peptide **1**. Therefore, it can be concluded that the long range terminal H-bonding in **1** having N-terminus Pro residue is stronger than in **4** and **5** containing N- terminus Aib and Ala residues respectively.

#### 4.6.2 H/D exchange studies of **4** and **5**

Deuterium exchange of the amide protons (NH/D) in the oligomer **4** and **5** (Figure 4.22 and 4.23) was performed under similar condition of oligomer **1** (Figure 4.13).

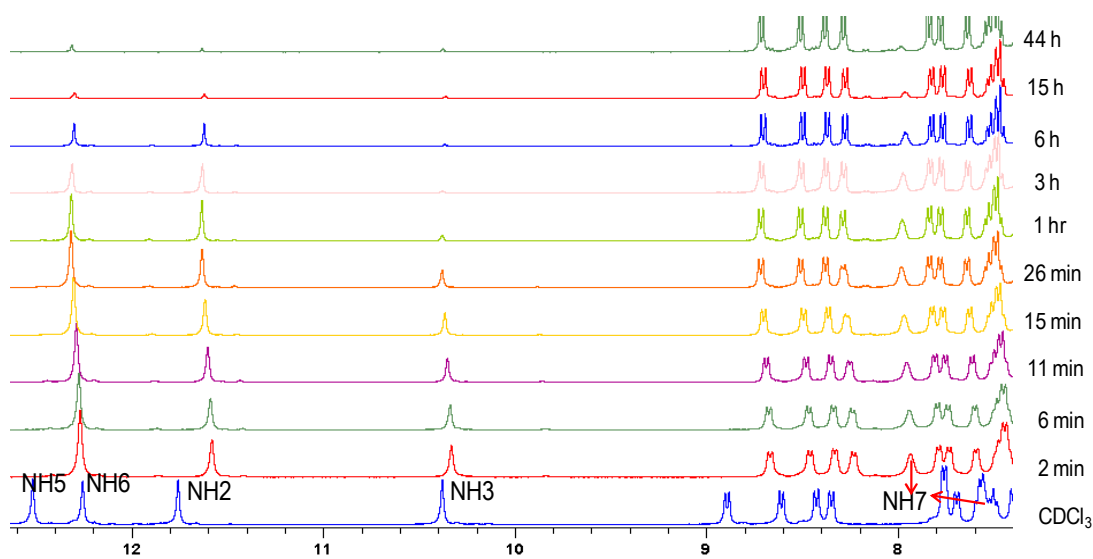


**Figure 4** Deuterium exchange study of **4** (400MHz,  $\text{CDCl}_3$  + methanol- $d_4$ ).

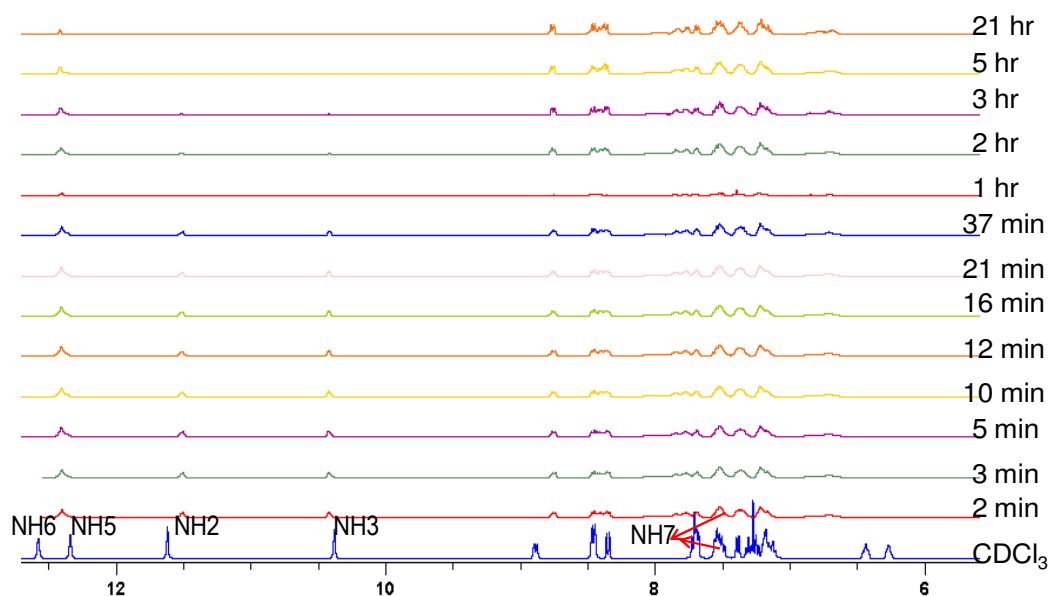


**Figure 4.23** Deuterium exchange study of **5** (400MHz,  $\text{CDCl}_3$  + methanol- $d_4$ ).

The slow H/D exchange rate in MeOD (more than 21h) experiment suggests the presence of *intra*-molecular long-range hydrogen bonding in **4** and **5** as in the case of **1**.

#### 4.6.3 NOESY spectral analysis of **4**

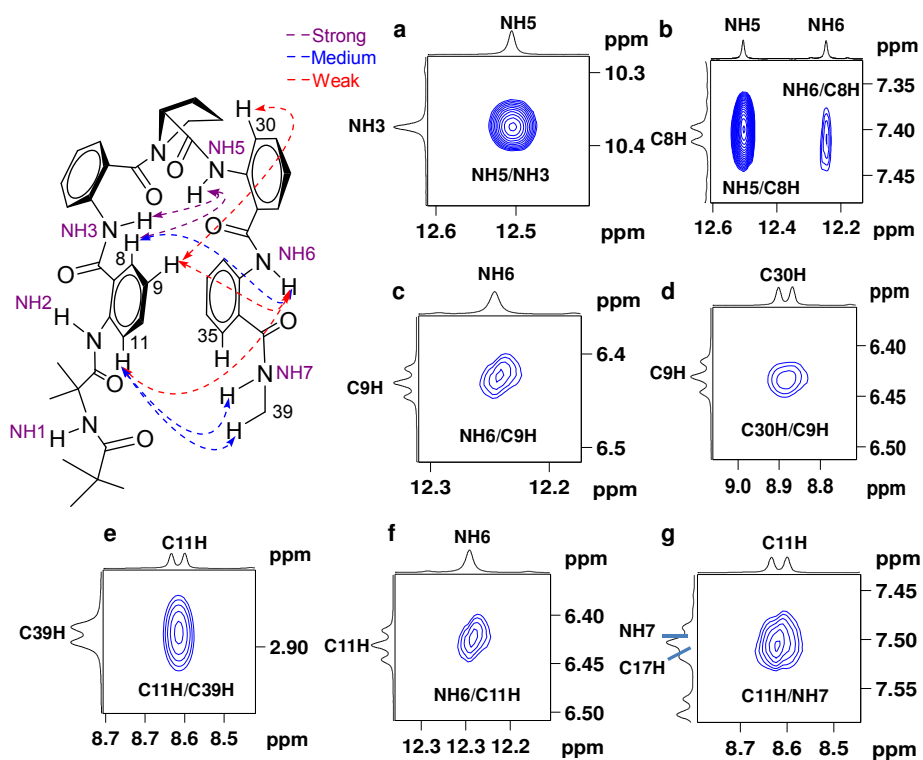


**Figure 4.24** 2D NOESY excerpts of **4** (500 MHz, CDCl<sub>3</sub>). The full NOESY spectrum is given in Figure 4.46, Experimental section.

Similar to compound **1**, aromatic stacking effect in **4** was clearly evidenced from C9H proton of Ant2 as it appeared up field chemical shift at  $\delta = 6.4$  ppm in the <sup>1</sup>H-spectrum of **4**, which showed diagnostic nOe between C9H/C30H. An unambiguous proof for folding feature was obtained from the strong dipolar coupling (nOe) between C11H/C39H (*vide supra* Figure 4.24).

#### 4.6.4 NOESY spectral analysis of **5**

The oligomer **5** with N-terminus Ala showed diagnostic long-range inter-residual nOes observed between the termini groups C38H/C40H and C10H/C38H. The aromatic

stacking effect in **5** was clearly verified from C8H proton of Ant2 as it appeared at  $\delta=6.42$  ppm in the  $^1\text{H}$  NMR spectrum, which also confirmed from the diagnostic dipolar nOe between C8H/C29H (Figure 4.25). Comparison of the analogues **1** and **5** revealed that the overall zipper architecture remains preserved in both the cases.

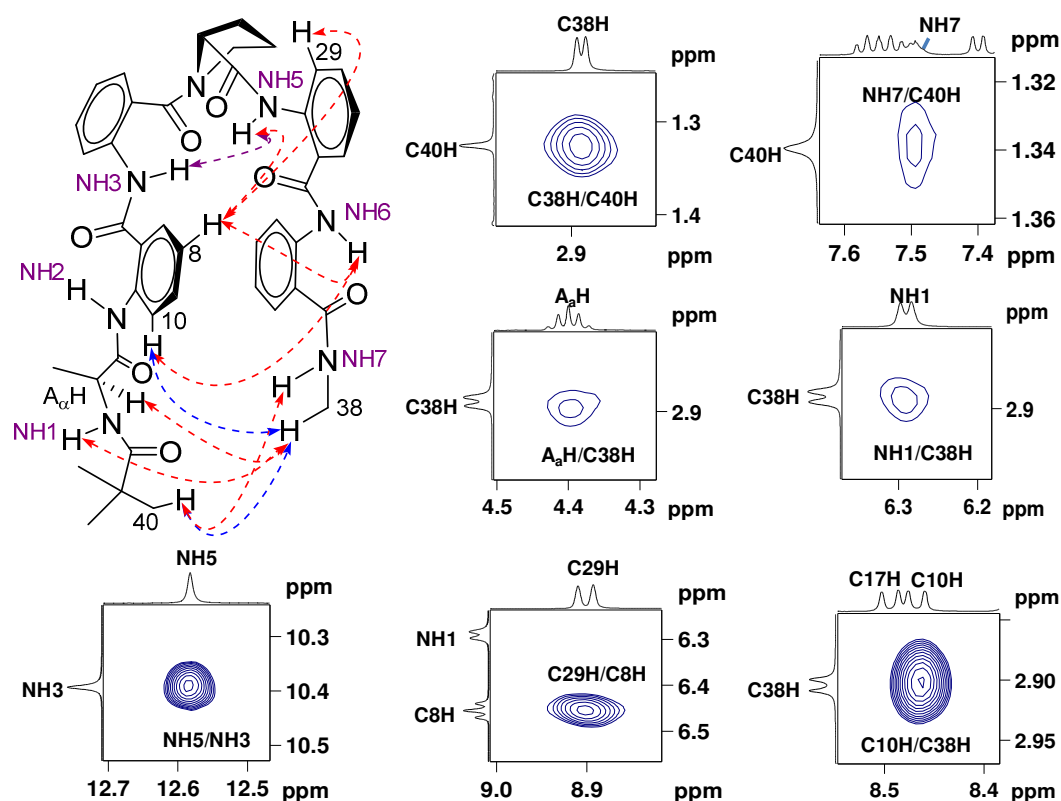


**Figure 4.25** 2D NOESY excerpts of **5** (500 MHz,  $\text{CDCl}_3$ ). The full NOESY spectrum is given in Figure 4.51, Experimental section.

#### 4.7 MD simulation studies of **4** and **5**

MD simulated structures of compound **4** and **5** (Figure 4.26a, 4.26b) were derived from nOe cross peaks (given in Table 4.13 and 4.14, experimental section) by using Maestro v9.3.518 from Schrödinger. The MD simulated twenty lowest-energy superimposed structures of compound **4** and **5** showed RMSD of  $0.15 \pm 0.06$  Å and  $0.20 \pm 0.06$  Å, respectively.

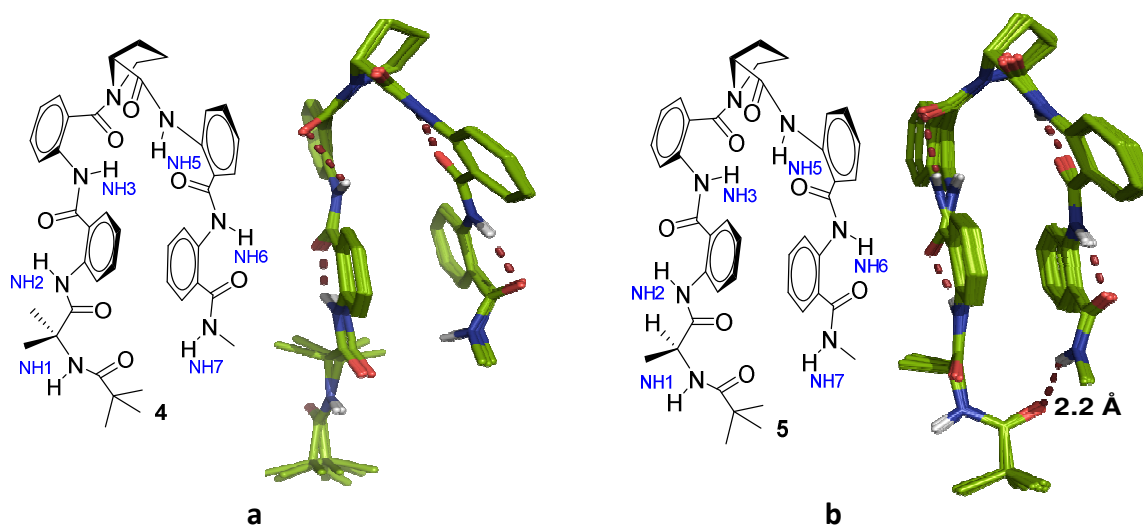


**Figure 4.26** Stereo views of MD simulated 20 superimposed minimum energy structures of peptides 4 and 5. (Hydrogens, except the polar amide hydrogens have been removed for clarity).

## 4.8 Conclusions

A study of comparative assessment of the three residues (Pro, Aib and Ala) at the N-terminus of zipper architecture motif was undertaken. This study reveals that the substitutions at the N-terminus with Aib or <sup>L</sup>Ala support zipper architecture, but considerably weaker terminal H-bonding interaction indicates the interplay of dihedral constraints in stability of these unique structures.

## 4.9 Experimental section

**Table 4.4** Titration study of hexapeptide **1** in CDCl<sub>3</sub> (5 mM) with DMSO-*d*<sub>6</sub>

Vol. of DMSO- <i>d</i> <sub>6</sub> added (μl)	Chemical shift (in ppm)				
	NH5	NH6	NH2	NH3	NH7
0	12.8	12.37	11.6	10.32	8.35
5	12.76	12.36	11.58	10.31	8.34
10	12.72	12.36	11.56	10.29	8.32
15	12.69	12.35	11.52	10.28	8.31
20	12.65	12.34	11.5	10.27	8.29
25	12.62	12.34	11.47	10.25	8.28
30	12.58	12.33	11.45	10.24	8.27
35	12.55	12.33	11.42	10.23	8.26
40	12.51	12.32	11.4	10.22	8.24
45	12.48	12.32	11.37	10.21	8.24
50	12.45	12.31	11.35	10.2	8.22

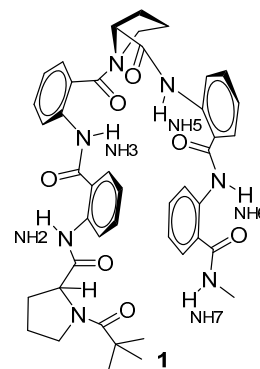


**Table 4.5** Titration study of decapeptide **2** in CDCl<sub>3</sub> (2 mM) with DMSO-*d*<sub>6</sub>

Vol. of DMSO- <i>d</i> <sub>6</sub> added (μl)	Chemical Shift (in ppm)								
	NH2	NH3	NH4	NH5	NH7	NH8	NH9	NH10	NH11
0	11.70	12.57	12.43	10.31	12.38	12.59	12.94	12.70	8.09
5	11.68	12.54	12.42	10.32	12.35	12.56	12.90	12.69	8.09
10	11.65	12.51	12.40	10.33	12.32	12.53	12.86	12.68	8.09
15	11.62	12.48	12.38	10.33	12.29	12.51	12.82	12.67	8.10
20	11.58	12.45	12.36	10.33	12.25	12.48	12.77	12.66	8.11
25	11.56	12.42	12.34	10.33	12.22	12.45	12.74	12.65	8.11
30	11.53	12.39	12.32	10.32	12.19	12.42	12.70	12.64	8.11
35	11.50	12.37	12.30	10.32	12.16	12.40	12.67	12.63	8.12
40	11.47	12.34	12.28	10.31	12.13	12.37	12.63	12.62	8.12
45	11.44	12.32	12.26	10.30	12.10	12.35	12.61	12.61	8.12
50	11.42	12.29	12.24	10.29	12.07	12.32	12.60	12.57	8.12

**Table 4.6** Titration study of hexapeptide **3** in CDCl<sub>3</sub> (2 mM) with DMSO-*d*<sub>6</sub>

Vol. of DMSO- <i>d</i> <sub>6</sub> added (μl)	Chemical shift (in ppm)			
	NH5	NH6	NH2	NH3
0	12.08	11.93	11.45	10.63
5	12.06	11.92	11.43	10.61
10	12.05	11.91	11.41	10.59
15	12.03	11.89	11.38	10.58
20	12.01	11.88	11.36	10.56
25	12.0	11.86	11.34	10.54
30	11.98	11.85	11.32	10.53
35	11.96	11.83	11.29	10.51
40	11.95	11.81	11.27	10.49
45	11.93	11.80	11.25	10.47
50	11.91	11.78	11.23	10.46

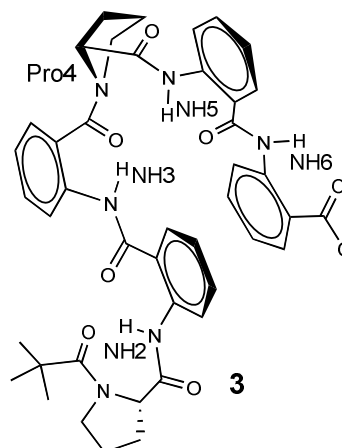


**Table 4.7** Temperature variation study of hexamer **1** (20 mmol, 400 MHz, CDCl<sub>3</sub>)

Temperature (K)	Chemical shift (in ppm)				
	NH5	NH6	NH2	NH3	NH7
218	12.98	12.38	11.71	10.4	8.74
223	12.97	12.38	11.71	10.4	8.72
228	12.96	12.38	11.71	10.4	8.71
233	12.95	12.38	11.71	10.39	8.68
238	12.94	12.38	11.7	10.39	8.67
243	12.93	12.38	11.7	10.39	8.65
248	12.92	12.38	11.69	10.38	8.63
253	12.91	12.38	11.68	10.38	8.61
258	12.9	12.38	11.67	10.37	8.59
263	12.89	12.38	11.66	10.36	8.58
268	12.88	12.38	11.65	10.35	8.57

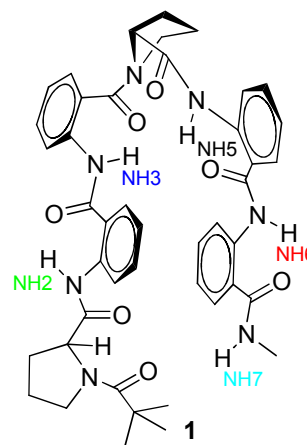
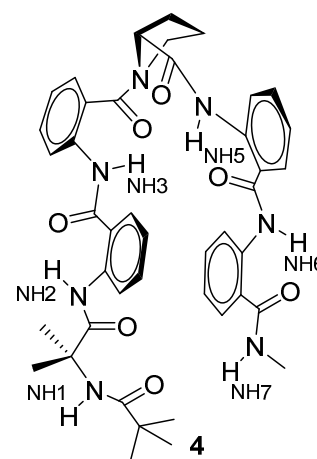


**Table 4.8** Temperature variation study of decamer 2 (20 mmol, 400 MHz, CDCl<sub>3</sub>)

Temperature (K)	Chemical Shift (in ppm)								
	NH2	NH3	NH4	NH5	NH7	NH8	NH9	NH10	NH11
213	13.06	12.68	12.61	12.52	12.4	12.36	11.84	10.31	8.64
218	13.06	12.69	12.62	12.54	12.41	12.37	11.83	10.3	8.64
223	13.06	12.69	12.62	12.55	12.43	12.38	11.83	10.29	8.59
228	13.06	12.7	12.62	12.56	12.44	12.38	11.82	10.28	8.59
233	13.06	12.7	12.63	12.57	12.44	12.39	11.81	10.28	8.56
238	13.06	12.71	12.63	12.58	12.45	12.4	11.81	10.28	8.54
243	13.05	12.71	12.63	12.59	12.45	12.4	11.8	10.27	8.51
248	13.04	12.72	12.62	12.59	12.46	12.41	11.79	10.27	8.49
253	13.04	12.72	12.62	12.6	12.46	12.41	11.78	10.27	8.46
258	13.03	12.72	12.62	12.6	12.45	12.42	11.78	10.28	8.44
263	13.02	12.72	12.61	12.6	12.45	12.42	11.77	10.28	8.4
268	13.01	12.72	12.61	12.61	12.45	12.42	11.76	10.28	8.37
273	13	12.72	12.6	12.6	12.43	12.43	11.75	10.29	8.33
278	12.99	12.71	12.6	12.6	12.43	12.43	11.75	10.29	8.28
283	12.98	12.71	12.6	12.6	12.43	12.42	11.74	10.3	8.25
288	12.96	12.71	12.59	12.59	12.43	12.41	11.73	10.31	8.2
293	12.95	12.7	12.59	12.58	12.43	12.39	11.72	10.31	8.14

**Table 4.9** Titration study of hexamer 4 in CDCl<sub>3</sub> (5mM) with DMSO-*d*<sub>6</sub>

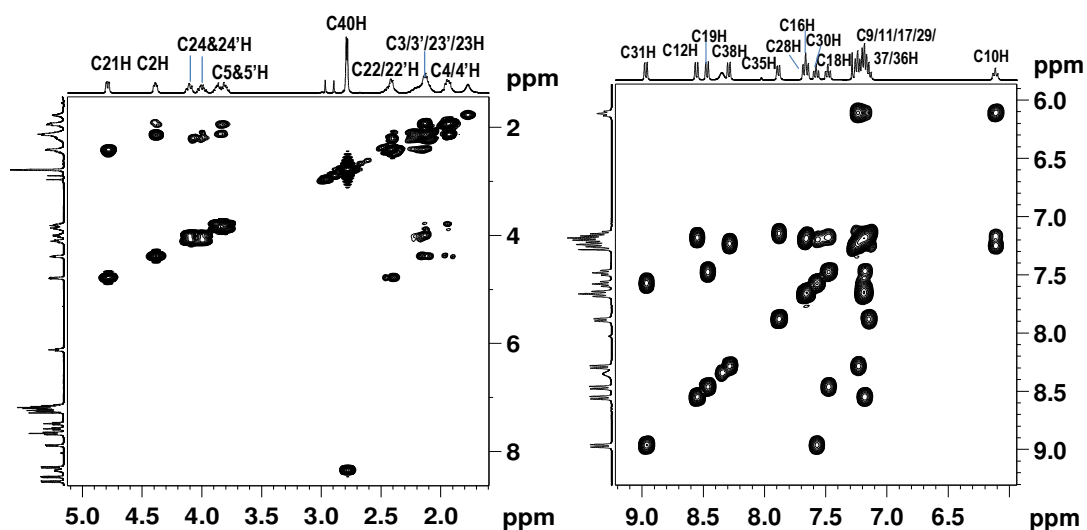
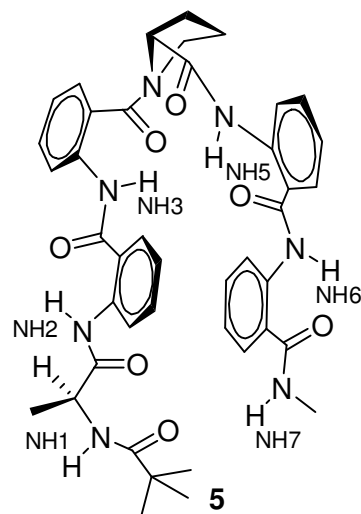
Vol. of DMSO- <i>d</i> <sub>6</sub> added (μl)	Chemical shift (in ppm)					
	NH5	NH6	NH2	NH3	NH7	NH1
0	12.53	12.23	11.76	10.36	7.51	6.28
5	12.49	12.25	11.74	10.37	7.57	6.32
10	12.45	12.28	11.72	10.38	7.66	6.35
15	12.41	12.3	11.71	10.39	7.72	6.37
20	12.38	12.31	11.69	10.39	7.76	6.38
25	12.33	12.33	11.67	10.38	7.8	6.39
30	12.31	12.25	11.65	10.38	7.84	6.4
35	12.29	12.27	11.63	10.38	7.86	6.405
40	12.26	12.29	11.61	10.37	7.89	6.41
45	12.23	12.3	11.59	10.36	7.91	6.41
50	12.2	12.31	11.56	10.36	7.93	6.41





**Table 4.10** Titration study of hexamer **5** in CDCl<sub>3</sub> (5mM) with DMSO-*d*<sub>6</sub>

Vol. of DMSO- <i>d</i> <sub>6</sub> added (μl)	Chemical shift (in ppm)					
	NH5	NH6	NH2	NH3	NH7	NH1
0	12.62	12.33	11.64	10.39	7.55	6.23
5	12.58	12.34	11.62	10.39	7.6	6.28
10	12.54	12.36	11.6	10.39	7.66	6.32
15	12.5	12.36	11.57	10.38	7.7	6.35
20	12.46	12.37	11.54	10.38	7.75	6.38
25	12.43	12.38	11.52	10.38	7.79	6.41
30	12.39	12.39	11.5	10.38	7.83	6.45
35	12.36	12.39	11.47	10.37	7.86	6.47
40	12.34	12.39	11.44	10.37	7.88	6.49

**Figure 4.27** Partial COSY spectra of hexapeptide **1** (CDCl<sub>3</sub>, 400 MHz): Aliphatic (left) and aromatic region (right).

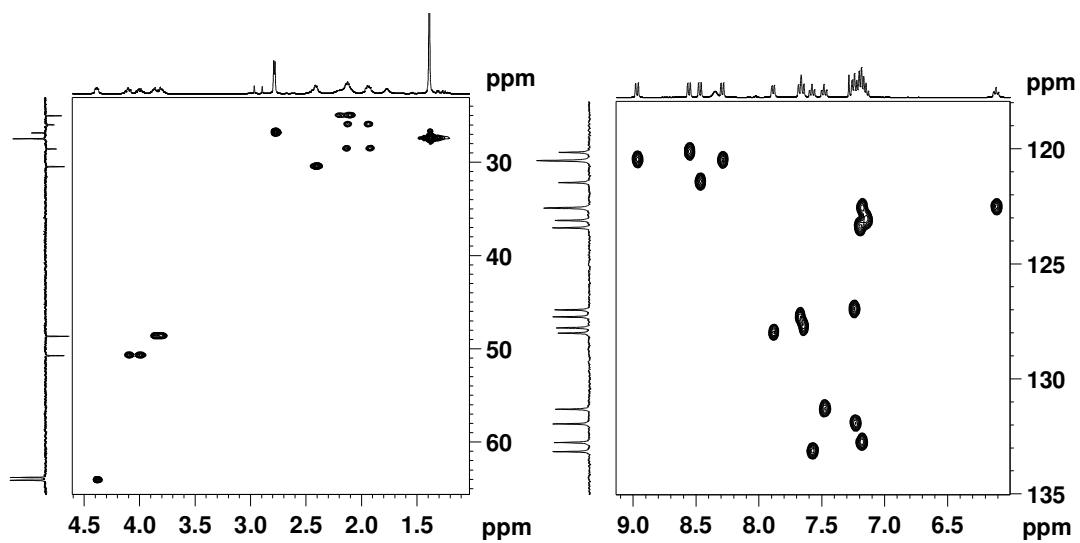


**Figure 4.28** Partial HSQC spectra of **1** ( $\text{CDCl}_3$ , 400 MHz): Aliphatic (left) and aromatic region (right).

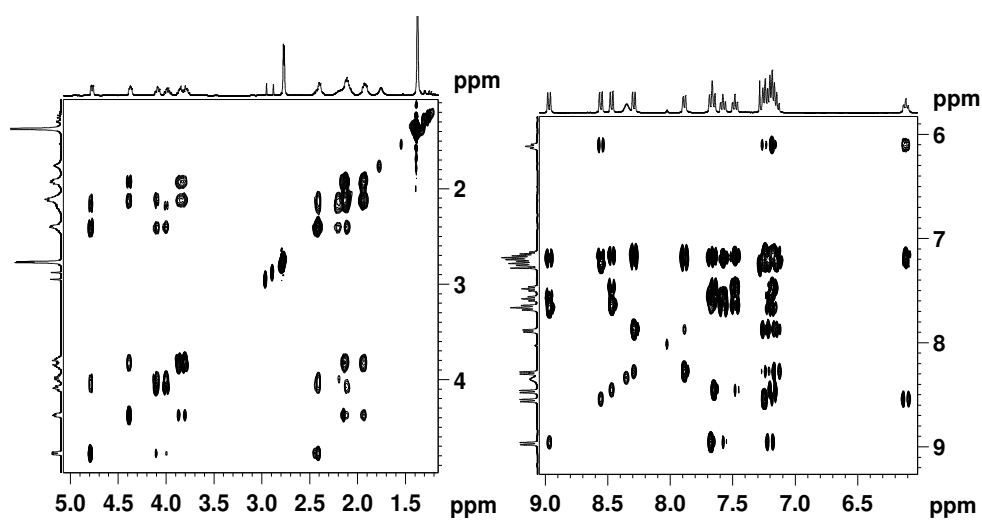


**Figure 4.29** Partial TOCSY spectra of **1** ( $\text{CDCl}_3$ , 400MHz): Aliphatic (left) and aromatic region (right).

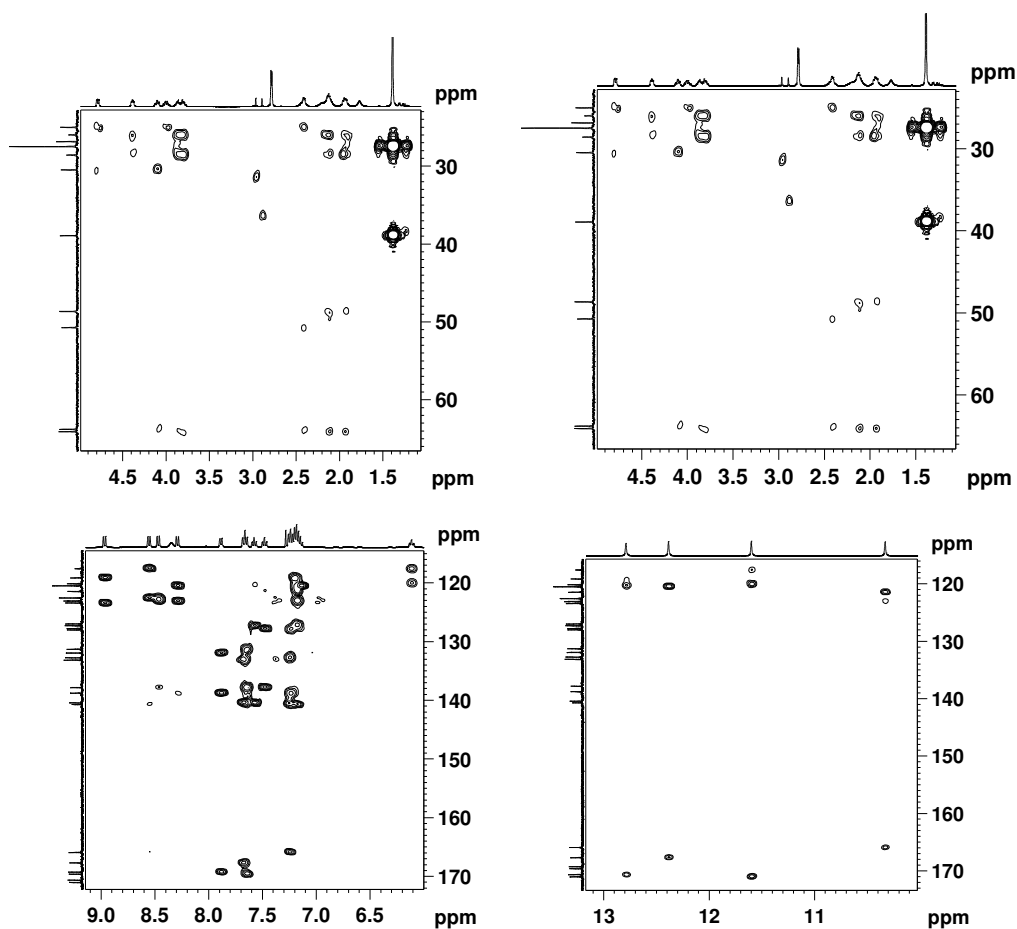


Figure 4.30 Partial HMBC spectra of 1 (CDCl<sub>3</sub>, 400MHz)

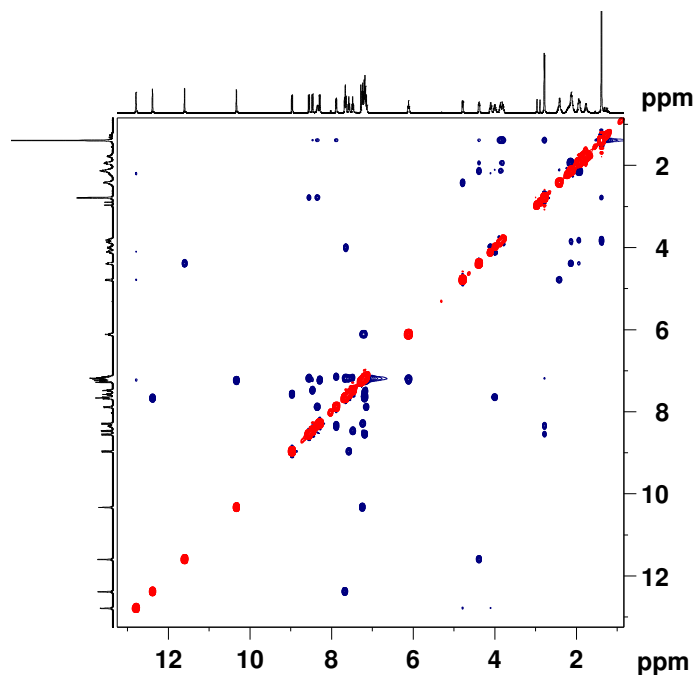
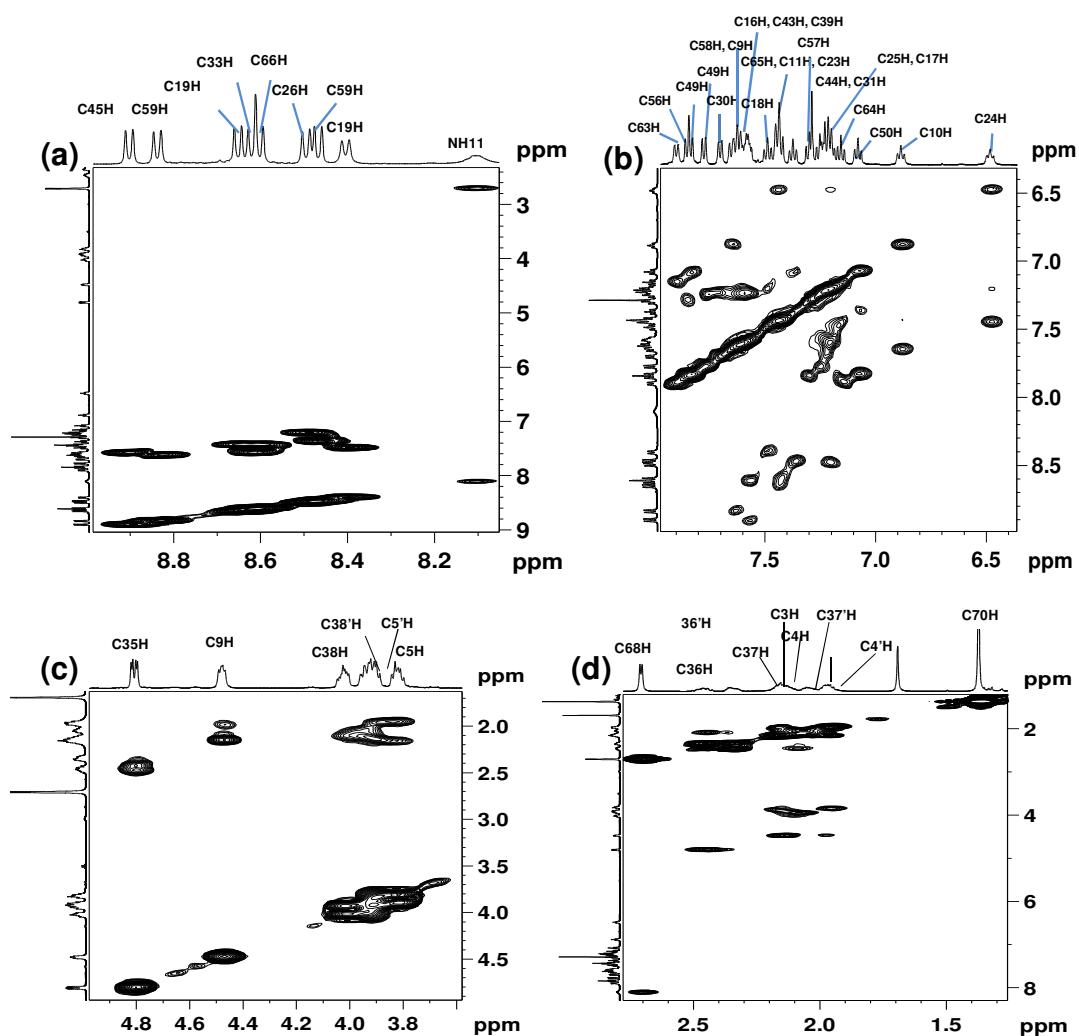
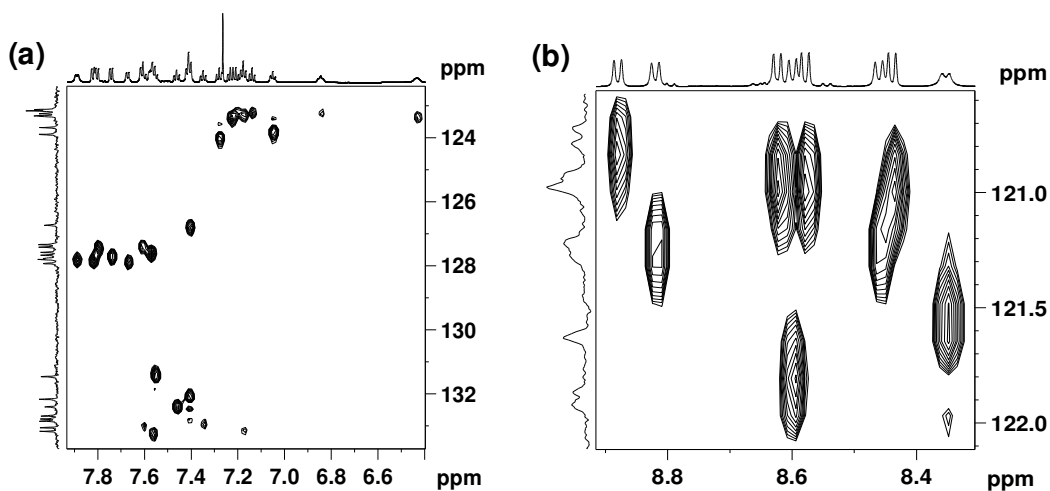
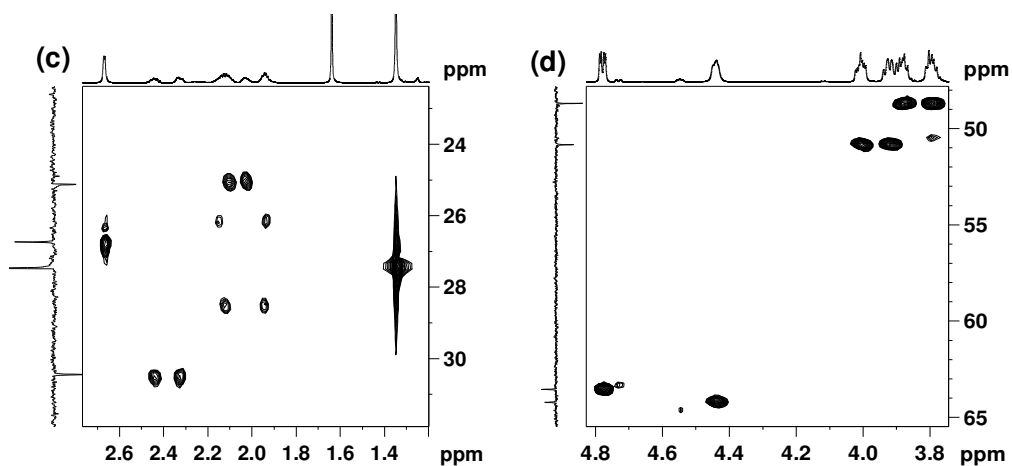


Figure 4.31 NOESY spectrum of 1 (CDCl<sub>3</sub>, 400MHz)



**Figure 4.32** Partial COSY spectra of decapeptide 2 ( $\text{CDCl}_3$ , 700MHz): Aromatic (a, b) and aliphatic region (c, d).





**Figure 4.33** Partial HSQC spectra of **2** ( $\text{CDCl}_3$ , 700 MHz): Aromatic (**a**, **b**) and aliphatic regions (**c**, **d**).

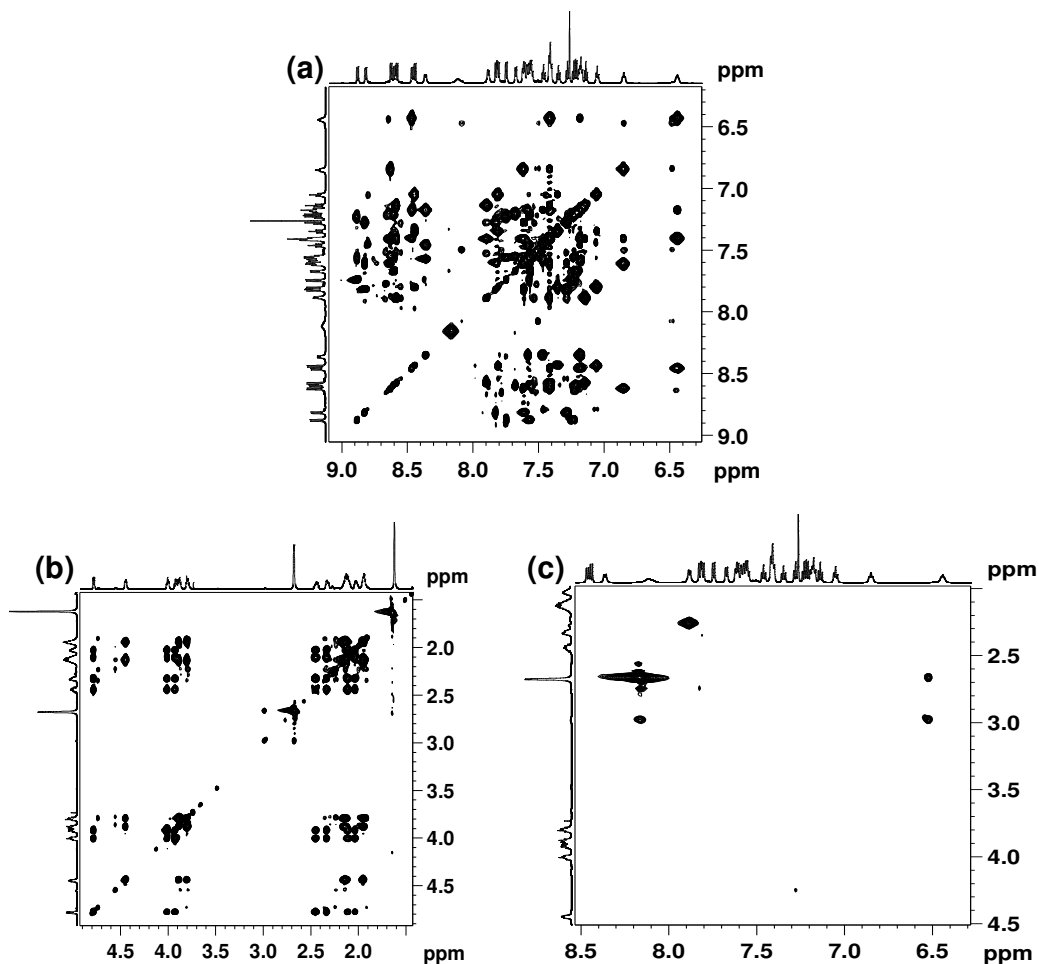


**Figure 4.34** Partial TOCSY spectra of **2** ( $\text{CDCl}_3$ , 700 MHz): Aromatic (**a**) aliphatic (**b**) and aliphatic vs aromatic regions (**c**).

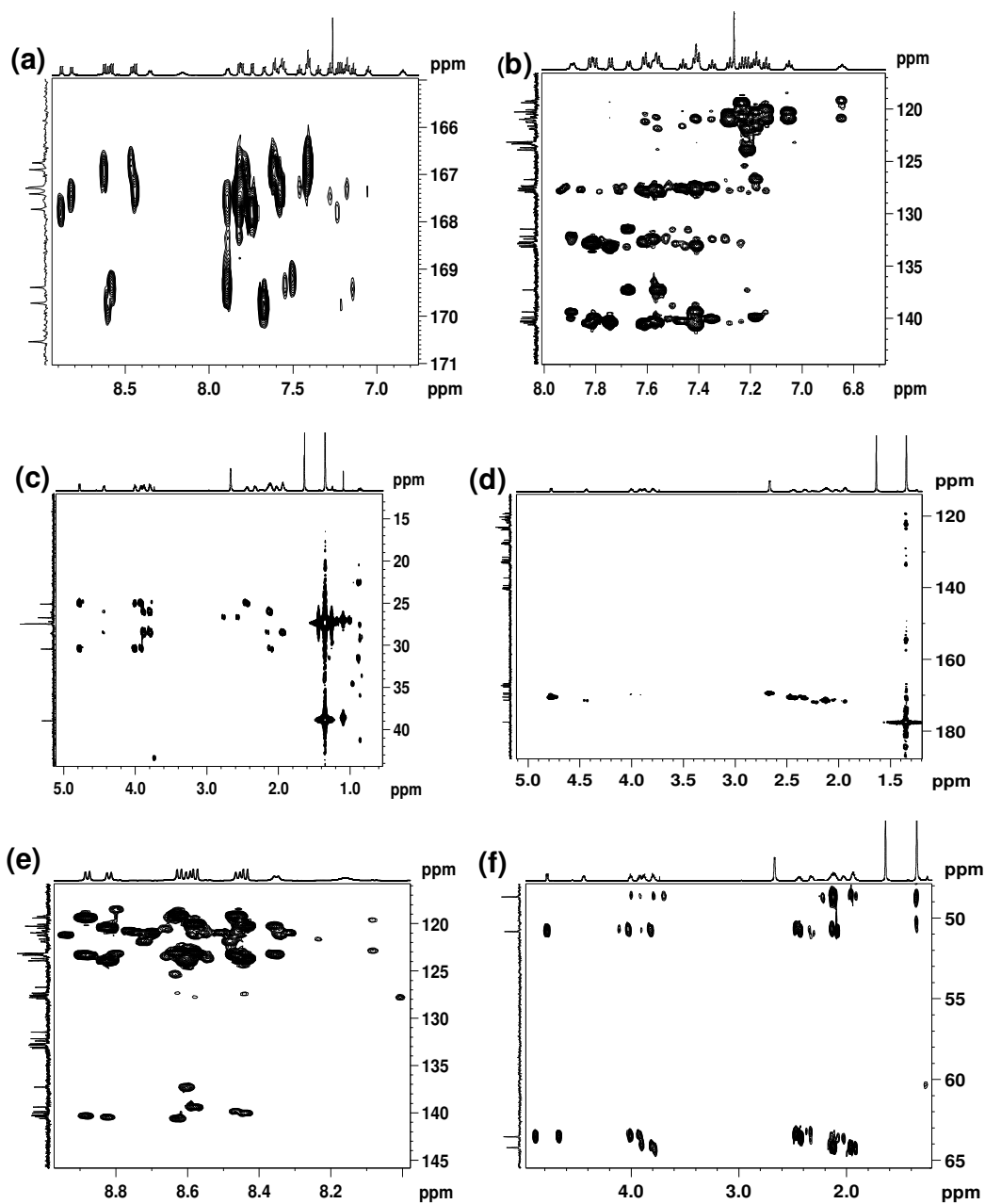


**Figure 4.35** Partial HMBC spectra of **2** ( $\text{CDCl}_3$ , 700 MHz): Aromatic (**a,b,e**) and aliphatic region (**c,d,f**).

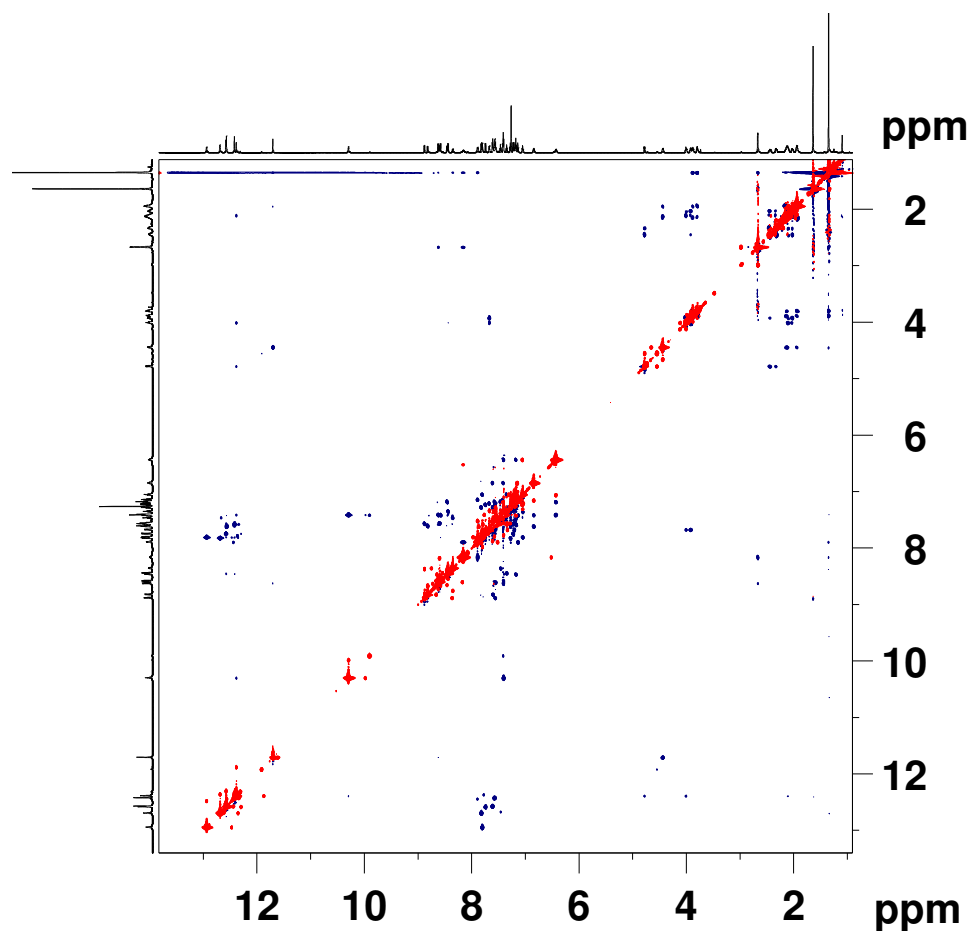


**Figure 4.36** Full ROESY spectrum of decamer **2** ( $\text{CDCl}_3$ , 700 MHz).

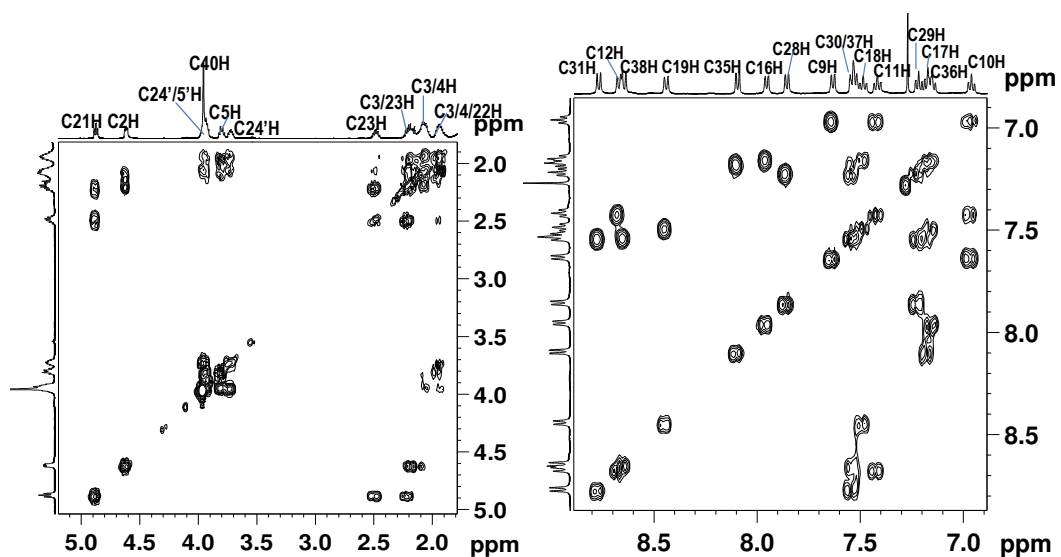


**Figure 4.37** Partial COSY spectra of hexapeptide **3** ( $\text{CDCl}_3$ , 500 MHz): Aliphatic (left) and aromatic region (right).

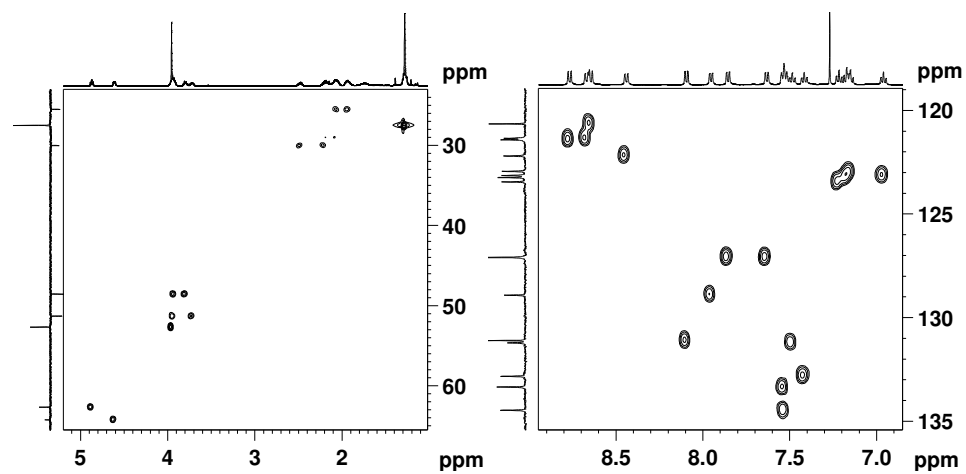


**Figure 4.38** Partial HSQC spectra of **3** (CDCl<sub>3</sub>, 500 MHz): Aliphatic (left) and aromatic regions (right).

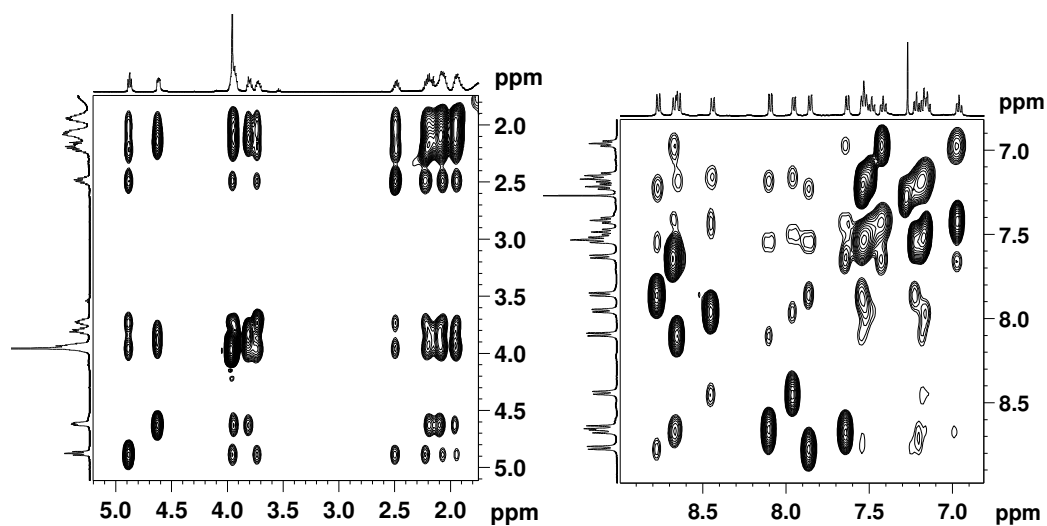


**Figure 4.39** Partial TOCSY spectra of **3** (CDCl<sub>3</sub>, 500 MHz): Aliphatic (left) and aromatic regions (right).



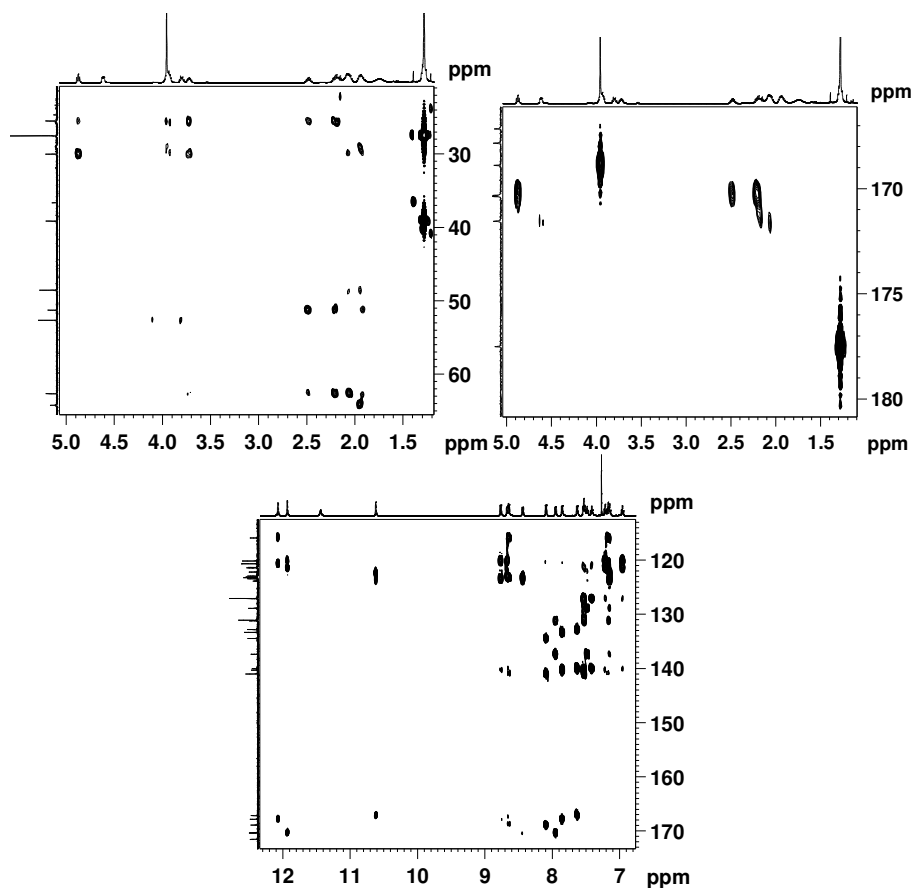


Figure 4.40 Partial HMBC spectra of **3** (CDCl<sub>3</sub>, 500 MHz).

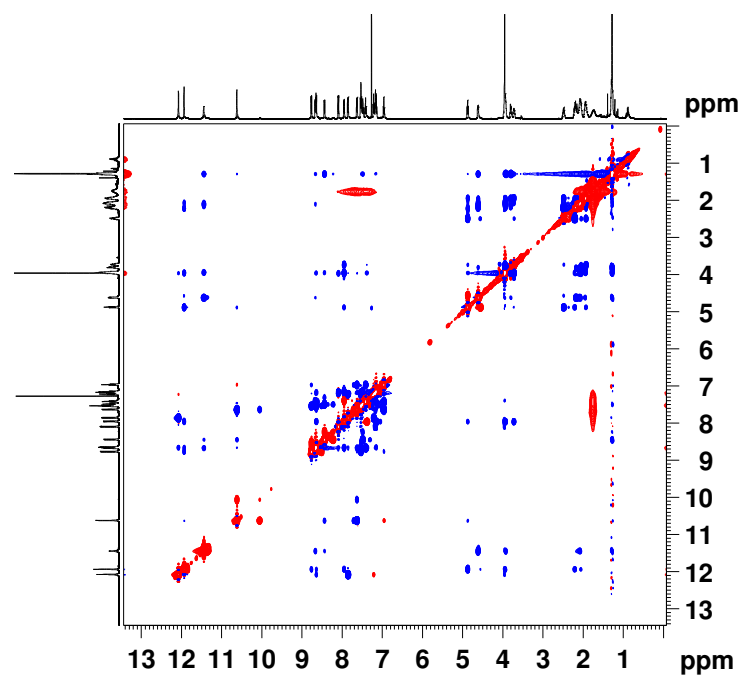
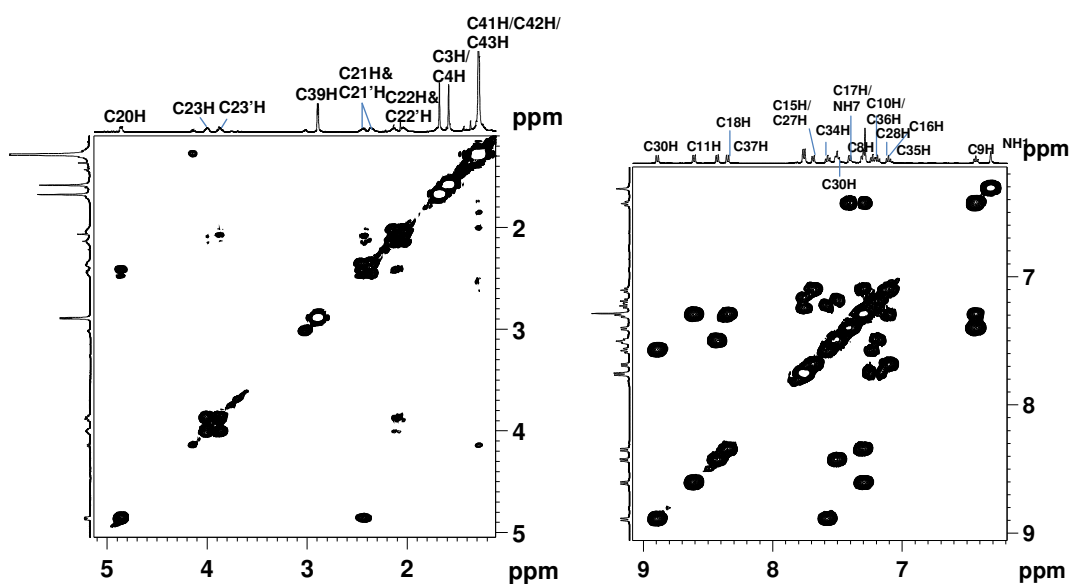
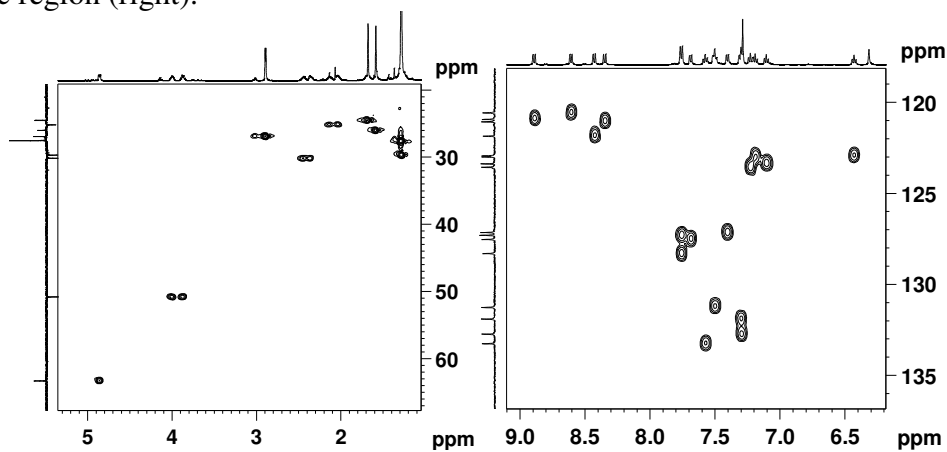


Figure 4.41 NOESY spectrum of **3** (CDCl<sub>3</sub>, 500 MHz).



**Figure 4.42** Partial COSY spectra of hexamer 4 ( $\text{CDCl}_3$ , 500 MHz): Aliphatic (left) and aromatic region (right).



**Figure 4.43** Partial HSQC spectra of hexamer 4 ( $\text{CDCl}_3$ , 500 MHz): Aliphatic (left) and aromatic region (right).

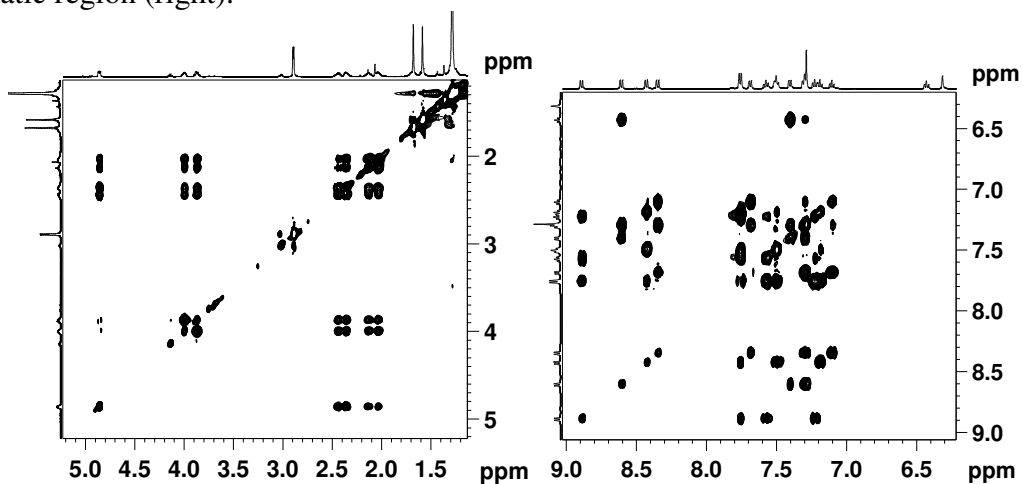


**Figure 4.44** Partial TOCSY spectra of hexamer 4 ( $\text{CDCl}_3$ , 500 MHz): Aliphatic (left) and aromatic region (right).

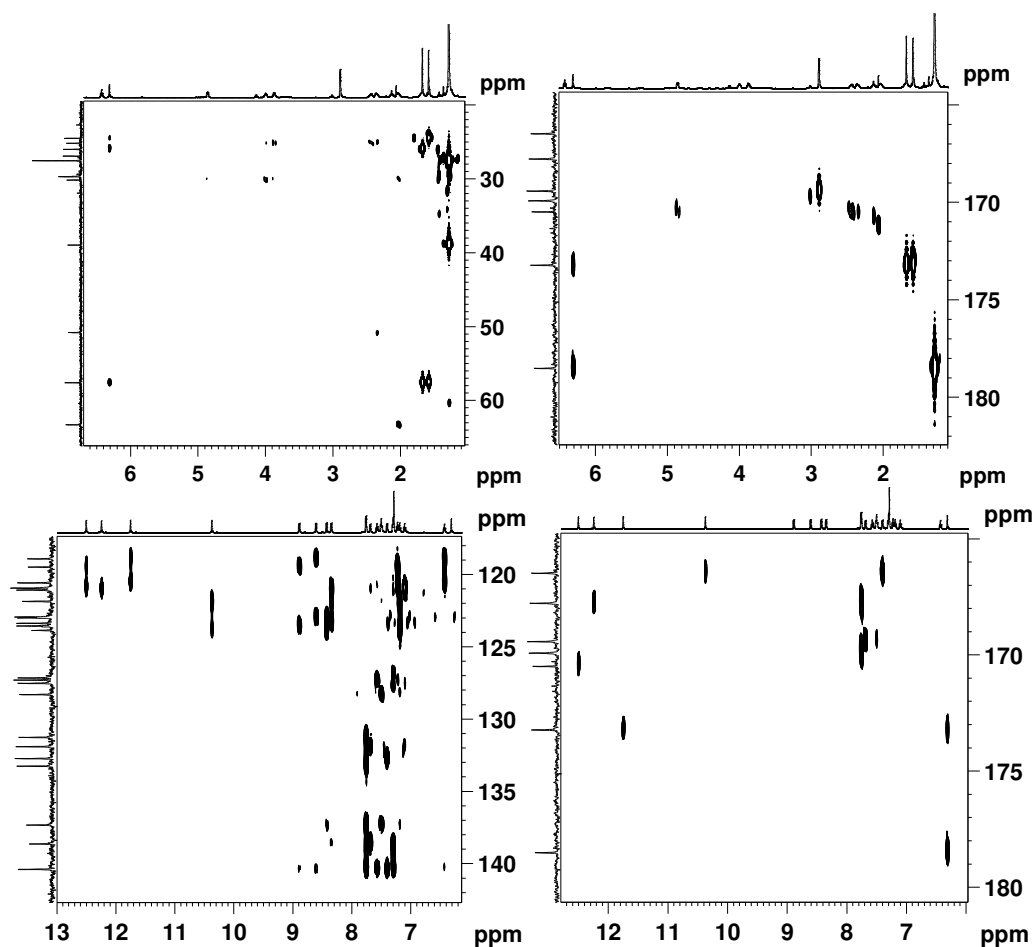


**Figure 4.45** Partial HMBC spectra of hexapeptide **4** ( $\text{CDCl}_3$ , 500 MHz): aliphatic (a, b), aromatic (c,d).

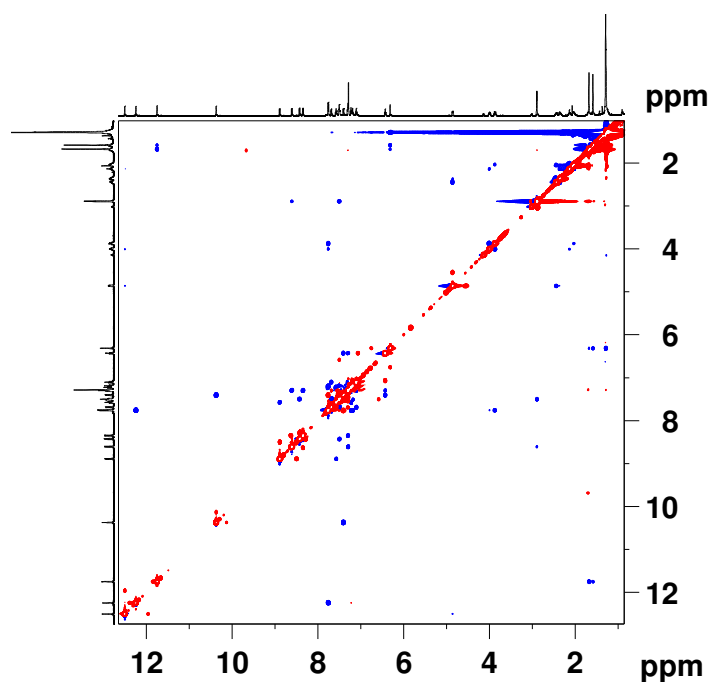


**Figure 4.46** NOESY spectrum of hexapeptide **4** ( $\text{CDCl}_3$ , 500 MHz).

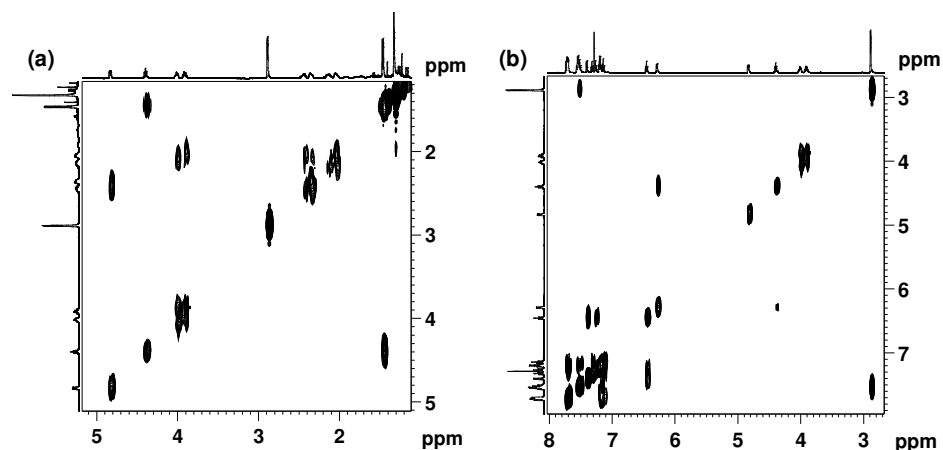


**Figure 4.47** Partial COSY spectra of hexamer **5** ( $\text{CDCl}_3$ , 500 MHz): aliphatic (a), methylamide  $-\text{CH}_3$  and aromatic region (b).

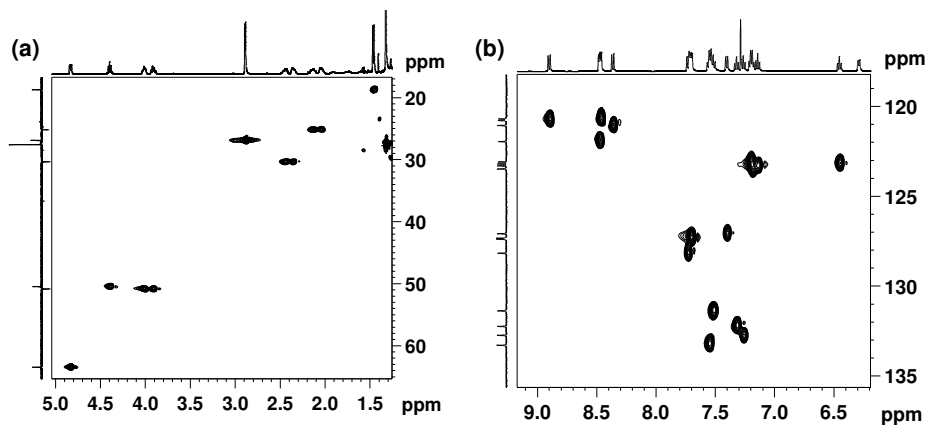


**Figure 4.48** Partial HSQC spectra of hexamer **5** ( $\text{CDCl}_3$ , 500 MHz): aliphatic (a) and aromatic regions (b).

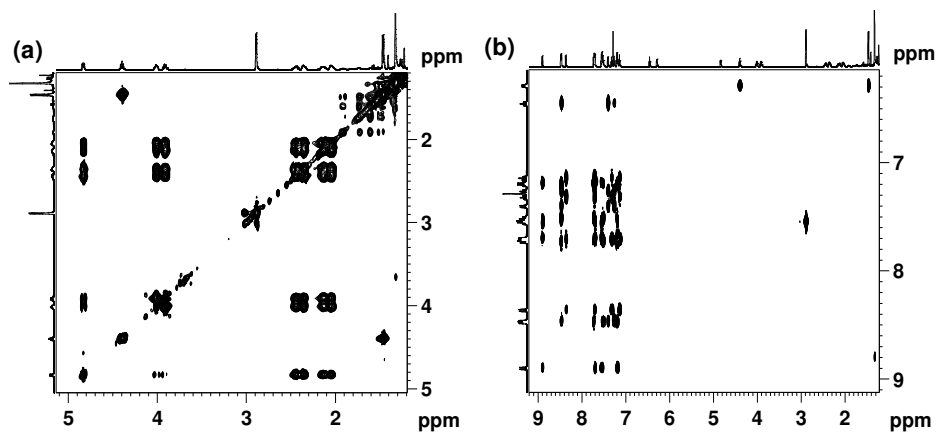


**Figure 4.49** Partial TOCSY spectra of hexamer **5** ( $\text{CDCl}_3$ , 500 MHz): aliphatic (a) and aromatic regions (b).

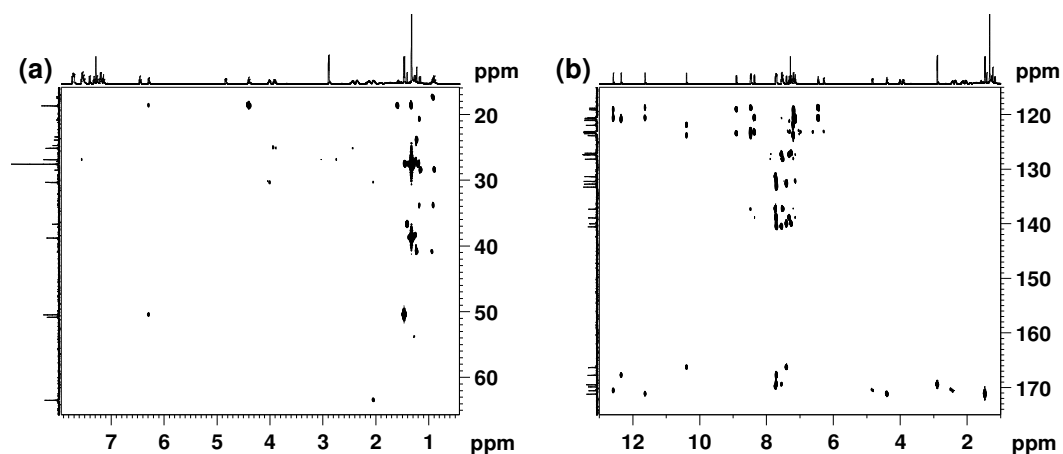


**Figure 4.50** Partial HMBC spectra of hexapeptide **5** (CDCl<sub>3</sub>, 500 MHz): Aliphatic (a), aromatic and amide -NH regions (b).

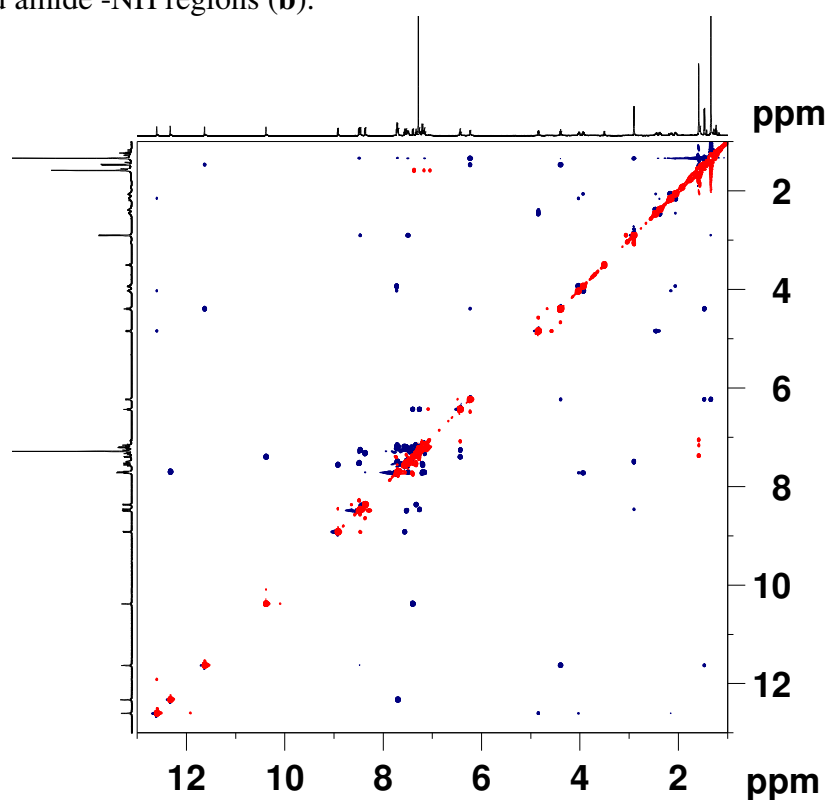


**Figure 4.51** NOESY spectrum of **5** (CDCl<sub>3</sub>, 500 MHz)

**Table 4.11** Distance restraints used in MD calculations for decamer **2** derived from ROESY experiment.

Residue	Atom	Residue	Atom	Lower Bound	Upper Bound
Ant 4	C4H	Ant7	C6H	3.905672	4.773599
Ant 5	NH5	Ant 4	NH4	3.899387	4.765918
Ant 5	NH5	Ant 7	NH7	2.985797	3.649308
Ant 9	NH9	Ant 9	C6H	3.719821	4.546448
Ant 9	NH9	Ant 10	C6H	3.733473	4.563133
Ant 9	NH9	Ant 4	C6H	4.391102	5.366903
Ant 9	NH9	Ant 8	C3H	1.830166	2.23687
Ant 8	NH8	Ant 7	C3H	1.839096	2.247783
Ant 4	NH4	Ant 4	C6H	3.351444	4.09621
Ant 7	NH7	Ant 8	C6H	3.715348	4.540981
Ant 7	NH7	Ant 4	C3H	3.326146	4.06529
Ant 7	NH7	Pro 5	CH $\alpha$	3.0008	3.684659
Ant 7	NH7	Pro 5	CH $\beta$ 1	2.763406	3.377497
Ant 7	NH7	Pro 5	CH $\beta$ 2	3.965646	4.846901
Ant 2	NH2		Piv	4.08223	4.989392
Ant 2	NH2		Me	4.206407	5.141164
Ant 2	NH2	Pro 2	CH $\square$ $\square$	3.575435	4.369977
Ant 2	NH2	Pro 2	CH $\alpha$	2.139394	2.614815
Ant 2	NH2	Ant 10	C4H	5.051629	6.174214
Ant 2	NH2	Ant 10	C3H	3.823587	4.673273
Ant 2	NH2		NH11	3.640704	4.449749
Ant 2	NH2	Ant 3	C6H	3.857282	4.714456
Ant 2	NH2	Ant 2	C6H	3.511528	4.291868
Ant 5	NH5	Pro 6	CH $\square$ 1	4.239147	5.18118
Ant 5	NH5	Pro 6	CH $\alpha$	4.451287	5.440462
Ant 5	NH5	Ant 4	C3H	1.821805	2.226651
Ant 5	NH5	Ant 8	C3H	3.733473	4.563133
Ant 5	NH5	Ant 5	C6H	3.607037	4.408601
Ant 3	C6H		Piv	3.508536	4.288211
	NH11		Piv	3.069646	3.75179
Ant 10	C3H		Piv	2.937536	3.590322
Pro 1	CH $\alpha$		Piv	3.08635	3.772206
Pro 1	CH $\square$ 1		piv	2.158095	2.637671
pro 1	CH $\square$ 2		Piv	2.102789	2.570075
	NH11		Piv	2.476976	3.027415
Ant 7	C6H	Pro 6	CH $\square$ 1	4.882115	5.967029
Ant 8	C6H	Pro 6	CH $\square$ 1	3.233282	3.951789
Ant 8	C6H	Pro 6	CH $\square$ 2	4.745809	5.800433
Ant 10	NH10		Me	4.108655	5.021689

Ant 2	C6H		Me	2.738412	3.346948
Ant 10	C3H		Me	3.857282	4.714456
Ant 9	C3H		Me	3.93154	4.805216
Ant 2	C5H		Me	3.353614	4.098862
Ant 2	C4H		Me	4.797133	5.863162
Ant 7	NH7	Pro 6	CH $\beta$ 1	4.297976	5.253081
Ant 7	NH7	Pro 6	CH $\beta$ 2	3.457533	4.225873
Ant 7	NH7	Pro 6	CH $\square$ 1	2.798581	3.420487
Ant 7	NH7	Pro 6	CH $\square$ 2	3.93154	4.805216
Ant 2	NH2	Pro 2	CH $\beta$ 1	3.207097	3.919785
Ant 2	NH2	Pro 2	CH $\beta$ 2	3.311987	4.047984
Ant 7	C6H	Pro 6	CH $\beta$ 2	4.108655	5.021689
Ant 5	NH5	Ant 8	NH8	4.517767	5.521716
Ant 8	NH8	Ant 8	C6H	3.578852	4.374152
Ant 7	NH7	Ant 7	C6H	3.607037	4.408601
Ant 4	NH4	Ant 5	C6H	3.771678	4.609829
Ant 10	NH10	Ant 10	C6H	3.719821	4.546448
Ant 3	NH3	Ant 3	C6H	3.189924	3.898796
Ant 9	NH9	Ant 2	C3H	3.766751	4.603807
Ant 4	NH4	Ant 3	C3H	1.83026	2.236985
Ant 10	NH10	Ant 9	C3H	1.852265	2.26388
Ant 3	NH3	Ant 2	C3H	1.839583	2.248379
Ant 7	NH7	Ant 5	2CH	3.83459	4.686721
Ant 7	C6H	Pro 6	CH $\alpha$	4.451287	5.440462
Pro 1	CH $\alpha$		NH11	4.297976	5.253081
Pro 1	CH $\alpha$	Ant 10	C3H	3.493837	4.270245
Pro 1	CH $\alpha$	Ant 10	C4H	3.715348	4.540981
Ant 5	C3H	Pro 6	CH $\alpha$	4.009481	4.900477
Ant 4	C3H	Pro 6	CH $\alpha$	4.108655	5.021689
Ant 5	C3H	Pro 6	CH $\square$ 2	2.074502	2.535502
Ant 5	C3H	Pro 6	CH $\square$ 1	2.436845	2.978366

**Table 4.12** Distance restraints used in MD calculations for hexamer **3** derived from NOESY experiment

Residue	Atom	Residue	Atom	Lower Bound	Upper Bound
Pro 1	CH $\delta$ 1		Piv	2.21685	2.709484
Pro 1	CH $\delta$ 1		Piv	2.129175	2.602325
Ant 3	C5H		Piv	3.559215	4.350152
Ant 3	C6H		Piv	3.152493	3.853047
Ant 2	2NH		Piv	3.34715	4.090961
Pro 1	CH $\alpha$		Piv	2.87397	3.51263

Ant 6	6NH		Me	4.127999	5.045332
Pro 1	CH $\alpha$	Ant 2	2NH	2.702904	3.303549
Pro 4	CH $\alpha$	Ant 5	5NH	2.903594	3.548837
Pro 4	CH $\alpha$	Ant 3	C3H	4.001898	4.891209
Ant 2	C6H	Ant 2	2NH	4.161209	5.085922
Ant 5	C6H	Ant 5	5NH	3.712527	4.537533
Ant 5	5NH	Ant 6	C6H	4.143353	5.064098
Ant 6	C6H	Ant 6	6NH	3.848684	4.703947
Ant 3	C6H	Ant 3	3NH	3.92252	4.794191
Ant 3	C3H	Ant 5	5NH	3.338956	4.080946
Ant 5	C3H	Ant 6	6NH	1.983915	2.424785
Ant 2	C3H	Ant 3	3NH	2.088579	2.552708
Ant 3	C3H	Ant 6	C6H	3.213983	3.928202
Ant 2	C3H	Ant 6	C6H	3.13627	3.833219

**Table 4.13** Distance restraints used in MD calculations for hexamer **4** derived from NOESY experiment

Residue	AtomI	Residue	AtomII	Lower Bound	Upper Bound
Ant 3	NH3	Ant 5	NH5	3.165592894	3.869057982
Ant 5	NH5	Ant 5	30H	3.611599715	4.41417743
Ant 5	NH5	Ant 6	37H	4.076698791	4.982631856
Ant 5	NH5	Ant 3	15H	4.38711944	5.362034871
Ant 5	NH5	Ant 2	8H	3.010650548	3.679684003
Ant 5	NH5	Pro 4	20H	2.822345517	3.44953341
Ant 5	NH5	Pro 4	23aH	2.754629584	3.366769491
Ant 5	NH5	Pro 4	22aH	2.736498951	3.34460983
Ant 5	NH5	Pro 4	21aH	3.640284719	4.449236879
Ant 6	NH6	Ant 5	27H	1.795542826	2.194552342
Ant 6	NH6	Ant 6	237H	3.742275843	4.573892697
Ant 2	NH2	Aib 1	3H	2.55661634	3.124753305
Ant 2	NH2	Aib 1	4H	2.076008994	2.537344326
Ant 2	NH2	Aib 1	NH1	3.698144574	4.51995448
Ant 2	NH2		NH7	4.049426332	4.94929885
Ant 2	NH2	Ant 3	18H	3.868379751	4.728019696
Ant 2	NH2	Ant 2	11H	3.661788878	4.47551974
Ant 3	NH3	Ant 2	8H	1.812456081	2.215224099
Ant 3	NH3	Ant 5	27H	3.343186166	4.086116425
Ant 3	NH3	Ant 6	37H	3.527260703	4.311096415
Ant 3	NH3	Ant 3	18H	3.757837025	4.592911919
Ant 3	NH3	Pro 4	23bH	4.754769136	5.8113845
Ant 2	9H	Ant 5	29H	4.402872705	5.381288861
Ant 5	21bH	Pro 4	21bH	4.630372695	5.659344405
NHMe	39H	Ant 2	11H	2.507537593	3.064768169
Ant 6	37H	Pro 4	23aH	3.345513483	4.088960923



Ant 2	11H		NH7	3.307418163	4.042399977
Ant 3	15H	Pro 4	23aH	2.072312582	2.532826489
Ant 3	15H	Pro 4	23bH	2.5106514	3.068573933
NHMe	39H		NH7	2.235901355	2.732768322
Aib 1	NH1	Piv	41H	2.132819494	2.606779382
Aib 1	NH1	Aib 1	3H	2.305230272	2.817503666
Aib 1	NH1	Aib 1	4H	2.594749148	3.171360069
Pro 4	20H	Pro 4	21aH	2.565239278	3.135292451
Pro 4	20H	Pro 4	21bH	2.073211899	2.533925655
Pro 4	22aH	Pro 4	23aH	2.448016454	2.99202011
Pro 4	22bH	Pro 4	23bH	2.464102681	3.011681055
Pro 4	23aH	Pro 4	21aH	3.233834807	3.952464764

**Table 4.14** Distance restraints used in MD calculations for hexamer **5** derived from NOESY experiment

Residue	Atom I	Residue	Atom II	Lower Bound	Upper Bound
Ant 5	NH5	Ant 3	NH3	3.237294406	3.956693163
Ant 5	NH5	Ant 6	36H	3.812211486	4.659369594
Ant 5	NH5	Ant 2	7H	3.203385131	3.915248494
Ant 5	NH5	Pro 4	19H	2.839000134	3.469889052
Ant 5	NH5	Pro 4	22aH	2.8502677	3.483660523
Ant 5	NH5	Pro 4	21aH	2.81350174	3.438724349
Ant 5	NH5	Pro 4	20aH	3.674814535	4.491439987
Ant 6	NH6	Ant 6	36H	3.685607213	4.504631038
Ant 6	NH6	Ant 5	26H	1.867053803	2.281954648
Ant 6	NH6	NHMe	38H	4.356036917	5.32404512
Ant 2	NH2	Ant 2	10H	3.095988369	3.783985785
Ant 2	NH2		NH7	4.404725355	5.383553212
Ant 2	NH2	Ala 1	NH1	3.27547644	4.003360093
Ant 2	NH2	Ala 1	2H	2.188153091	2.674409333
Ant 2	NH2	Ala 1	3H	2.634474893	3.219913759
Ant 3	NH3	Ant 3	17H	3.640365042	4.449335051
Ant 3	NH3	Ant 6	36H	3.586586591	4.383605834
Ant 3	NH3	Ant 2	7H	1.903456917	2.326447343
Ant 3	8H	Ant 5	29H	3.880787705	4.743184973
Ant 2	10H	Piv	40H	3.180799408	3.887643721
Ant 2	10H	Ala 1	3H	3.704101328	4.527234957
Ant 2	10H	NHMe	38H	2.696863384	3.296166358
Ant 2	10H	Ala 1	2H	5.034943583	6.153819934
Ant 6	36H	Pro 4	22aH	3.466771324	4.237164951
Pro 4	19H	Ant 3	14H	3.768020128	4.605357934
Pro 4	22aH	Ant 3	14H	2.596602631	3.173625437

## Chapter IV: Detailed NMR studies of Zipper peptides

---

Pro 4	22bH	Ant 3	14H	2.17573976	2.659237484
Ala 1	2H	Ant 6	33H	3.200669241	3.911929073
Ala 1	2H		NH7	3.291668774	4.023150724
NHMe	38H		NH7	2.3032811	2.815121345
Piv	40H	Ant 6	33H	3.532488454	4.317485888
Piv	40H		NH7	3.56024275	4.351407806
Ala 1	2H	Ant 6	34H	3.493527609	4.269867077
Piv	40H	Ant 2	9H	3.637042017	4.445273576
Piv	40H	Ala 1	NH1	2.187115268	2.673140883
Ala 1	3H	Ala 1	NH1	2.407393137	2.942369389
Ala 1	2H	Ala 1	NH1	2.716973722	3.32074566
Ala 1	2H	Ala 1	3H	2.147548893	2.624781981
Pro 4	19H	Pro 4	22aH	2.515209568	3.074145027
Pro 4	19H	Pro 4	22bH	2.238350808	2.735762098
Pro 4	22aH	Pro 4	21aH	2.621531505	3.204094061
Pro 4	22bH	Pro 4	20bH	3.322296645	4.060584788
Pro 4	22bH	Pro 4	21bH	2.626248352	3.209859097
Pro 4	22aH	Pro 4	21bH	3.891319241	4.75605685
Piv	40H	NHMe	38H	3.34546797	2.723473658

---

#### 4.10 References and Notes:

1. J. Keeler, “*Understanding NMR Spectroscopy*”, John Wiley & Sons Ltd, Chichester, 2005
2. a) J. Schraml, J. M. Bellama, “*Two Dimensional NMR Spectroscopy*”, John Wiley and sons, New York., b) Horst Friebolin "Basic One- and Two-Dimensional NMR Spectroscopy", 5th Edition, 2010, Wiley-VCH, Weinhiem.
3. J. Jenner, *Adv. Magn. Reson.* 1968, **3**, 205
4. W. P. Aue, E. Bartholdi, R. R. Ernst, *Journal of Chemical Physics.*, 1976, **64**, 2229.
5. R. R. Ernst, W. S., *Rev. Sci. Instrum.*, 1996, **37**, 93
6. G. E Martin, A. S. Zekter, “*Two-Dimensional NMR Methods for Establishing Molecular Connectivity*”. New York: VCH Publishers, Inc. 1988.
7. a) J. Jeener, B. H. Meier, P. Bachmann, R. R. Ernst, *J. Chem. Phys.*, 1979, **71**, 4546.; b) A. Bax, R. Freeman, *J. Mag. Reson.*, 1977, **44**, 542., c) G. Bodenhausen, R. Freeman, *J. Mag. Reson.*, 1977, **28**, 471., d) H. Kessler, M. Gehrke, C. Griesinger, *Angew. Chem. Int. Ed. Engl.* 1988, **27**, 490.
8. L. Braunschweiler, R. R. Ernst, *J. Mag. Reson.*, 1983, **53**, 521.
9. M. H. Levitt, R. Freeman, T. A. Frenkiel, *J. Mag. Reson.*, 1982, **47**, 328., b) A. Bax, D. G. Davies, *J. Mag. Reson.*, 1985, **65**, 355.
10. M. L. Remerowski, S. J. Glaser, G. P. Drony, *Mol. Phys.* 1989, **68**, 1191.
11. a) G. Bodenhausen, R. Freeman, *J. Am. Chem. Soc.* 1978, **100**, 320., b) A. Bax, S. K. Sarkar, *J. Mag. Reson.*, 1984, **60**, 170.
12. a) G. Bodenhausen, D. Ruben, *J. Chem, Phs. Lett.* 1980, **69**, 185., b) A. Bax, M. Ikura, L. E. Kay, D. A. Torchia, R. Tschudin, *J. Mag. Reson.*, 1990, **86**, 304.
13. a) T. J. Norwood, J. Boyd, J. E. Heritage, N. Soffe, I. D. Chapbell, *J. Mag. Reson.*, 1990, **87**, 488., b) A. Bax, M. F. Summers, *J Am. Chem. Soc.* 1986, **108**, 2093.

14. a) A. W. Overhauser, *Physical Review*, 1953, **92**, 411., b) W. A. Anderson, R. Freeman, *J. Chem. Phys.*, 1962, **37**, 411.c) R. Kaiser, *The Journal of Chemical Physics*. 1962, **39**, 2435. d) T. R. Carver, C. P Slichter, *Physical Review*, 1953 **92**, 212
15. a) A. A. Bothner-By, R. L. Stephens, J. Lee, C. D. Warren, R. W. Jeanlog, *J Am. Chem. Soc.* 1984, **106**, 811., b) A. Bax, D. G. Davies, *J. Mag. Reson.*, 1985, **63**, 207.
16. a) M. Karplus, *J. Phys. Chem.*, 1959, **30**, 11., b) P. D. Thomas, V. J. Basus, T. L. James, *Proc. Natl. Acad. Sci. USA*, 1991, **88**, 1237.
17. T. Phil Pitner, D. W. Urry, *J Am. Chem. Soc.* 1972, **94**, 1399.
18. a)A. Rahman, *Physical Review*, 1964, **136**, 405, b) J. A. Mc Cammon, B. R. Gelin, M. Karplus, *Nature*, 1977, **267**, 585.
19. C. D. Tatko, M. L. Waters, *J. Am. Chem. Soc.*, 2002, **124**, 9372.
20. R. V. Nair, S. Kheria, S. Rayavarapu, A. S. Kotmale, B. Jagadeesh, R. G. Gonnade, V. G. Puranik, P. R. Rajamohanan and G. J. Sanjayan, *J. Am. Chem. Soc.*, 2013, **135**, 11477.
21. S. Kheria, R. V. Nair, A. S. Kotmale, P. R. Rajamohanan and G. J. Sanjayan; *New J. Chem.*, 2015, **39**, 3327.

